

Synthetic and Mechanistic Studies of Ruthenium Catalyzed C-C, C-N and C-O Bond Activation Reactions

Nishantha Kumara Kalutharage
Marquette University

Recommended Citation

Kalutharage, Nishantha Kumara, "Synthetic and Mechanistic Studies of Ruthenium Catalyzed C-C, C-N and C-O Bond Activation Reactions" (2015). *Dissertations (2009 -)*. Paper 506.
http://epublications.marquette.edu/dissertations_mu/506

**SYNTHETIC AND MECHANISTIC STUDIES OF RUTHENIUM CATALYZED
C-C, C-N AND C-O BOND ACTIVATION REACTIONS**

By

Nishantha Kalutharage, B.Sc. (Hons)

A Dissertation Submitted to the Faculty of the Graduate School,
Marquette University,
in Partial Fulfillment of the Requirements for
the Degree of Doctor of Philosophy

Milwaukee, Wisconsin

May 2015

ABSTRACT

SYNTHETIC AND MECHANISTIC STUDIES OF RUTHENIUM CATALYZED C-C,
C-N AND C-O BOND ACTIVATION REACTIONS

Nishantha Kalutharage, B.Sc. (Hons)

Marquette University, 2015

Transition metal catalyzed selective C-C, C-N and C-O bond activation reactions are fundamentally important in organometallic chemistry and organic synthesis. Catalytic C-C, C-N and C-O activation are highly valuable for reforming processes of crude oils. Significant research has been devoted to transition metal mediated C-C, C-N and C-O bond cleavage reactions to form new compounds as these processes are expected to provide novel ways to transformation of inexpensive hydrocarbons into more commercially valuable products such as pharmaceuticals, agrochemicals and polymers.

A few examples of transition metal catalyzed cross coupling reactions involving C-N bond cleavage have been reported. A well-defined Ru catalytic system has been developed for oxidative alkylation of alcohol by deaminative coupling reactions of amines to form alkylated ketones. The catalytic method was successfully applied to the decarboxylative and deaminative coupling of amino acids with ketones.

Reductive deoxygenation of aldehydes and ketones has attracted considerable attention due to its many applications in fine-chemical synthesis and biofuel production. Classical methods for the deoxygenation of carbonyl compounds are generally associated with harsh reaction conditions and the use of stoichiometric amounts of toxic reagents, and poor functional-group tolerance. A well-defined Ru-H catalyst was found to mediate the reductive deoxygenation of carbonyl compounds to produce aliphatic compounds. Two different mechanistic pathways have been investigated in detail to probe the electronic nature of the catalysts and ligands.

Reductive etherification of ketones/aldehydes and alcohols have been studied intensively as cheaper and greener ways to synthesize ethers. A method for the reductive coupling of carbonyl compounds with alcohols has been developed, which involved a highly chemoselective formation of unsymmetrically substituted ether products. The catalytic etherification method employs cheaply available molecular hydrogen as the reducing agent, tolerates a number of common functional groups, and uses environmentally benign water as the solvent.

ACKNOWLEDGMENTS

Nishantha Kalutharage, B. Sc (Hons)

I would like to express my special appreciation and thanks to my advisor, Professor Chae S. Yi, for his tremendous guidance during study at Marquette University. I would like to thank him for encouraging my research and for allowing me to grow as a research scientist. I would also like to thank my committee members Professors Adam Fiedler and Christopher Dockendoff, for their encouragement, insightful comments, and support. My special thanks goes to Professor William Donaldson who was on my thesis committee but is on sabbatical at the present time. I would like to thank my group members, Dr. Kwang-Min Choi, Junghwa Kim and Hanbin Lee, for being such good friends, and former group members as mentors Dr. Dong-Hwan Lee and Dr. Ki-Hyeok Kwon, for their support and valuable conversations during my first year.

I thank my teachers and colleagues at the Ruhuna University, especially Dr. Sarath Wanniarachchi, who gave me precious help during my first year at Marquette. Two professors, Ruchira Cumaranatunga and Hema Pathirana, have inspired and encourage me choose chemistry as my future. My deepest gratitude goes to my parents for their unflagging love and support throughout my life. They have sacrificed their lives to provide the best possible environment for me to get the education. Most of all, I want to thank my wife Sugandhi Wasana for her love, sacrifice, and kind indulgence. To my beloved son Sandaru and daughter Hawanya, I would like to express my thanks for being such good children always cheering up, inspiring and astonishing me every day. I would like to thank

all of my friends who have been helping me to keep my mind peacefully under difficult situations, especially Mohamed El-Mansy and Wei Hu.

My gratefulness to the countless technical support from Dr. Sheng Cai (for his support and his help running special NMR studies) and Dr. Sergey Lindeman (for providing single crystal diffraction analysis data).

I am extremely appreciative of the financial assistance and the research assistantship given by Marquette University, the Arthur J. Schmitt Foundation, and the National Science Foundation which provided me with more time to focus on my research. Also, I would like to thank the Graduate School and all of the Marquette University administration.

DEDICATION

I dedicate this work to my wife, son, daughter and my mother, for their patience and support. Thank you for your understanding and your love.

TABLE OF CONTENTS

ACKNOWLEDGEMENT.....	i
DEDICATION.....	iii
LIST OF TABLES.....	iv
LIST OF FIGURES.....	viii
LIST OF SCHEMES.....	xvi
CHAPTER 1	1
INTRODUCTION	1
1.1 C-C Bond Activation of Hydrocarbon Molecules.....	1
1.1.1 Stoichiometric C-C Bond Activation Reaction.....	3
1.1.2 Catalytic C-C Bond Activation Reactions	4
1.1.2.1 C-C Bond Activation of Strained Molecules.....	4
1.1.2.2. Catalytic C-C Activation of Unstrained Molecules.....	7
1.1.2.3. Chelate Assisted C-C Bond Activation Reactions of Unstrained Molecules.....	8
1.1.2.4 Alkene/Alkyne Insertion Reactions via C-C Bond Cleavage.....	12
1.2. Catalytic C-N Bond Activation Reactions	14
1.2.1 Heterogeneous Hydrodenitrogenation of Nitrogen Heterocycles	14

1.2.1 Hydrodenitrogenation Reactions Catalyzed by Soluble Metal Complexes.....	14
1.2.2. Catalytic Deaminative C-N Cleavage Reactions.....	18
1.2.2.1 C-N Bond Cleavage of Allylic Amines.....	18
1.2.2.2 C-N Cleavage of Arylamines.....	22
1.2.2.3 C-N Cleavage of Secondary and Tertiary Amines.....	23
1.2.2.4 Biochemical Deamination Reactions.....	25
CHAPTER 2: PART 1: Transition Metal Catalyzed C-O Bond Activation Reactions....	31
2.1 Transition Metal Catalyzed Hydrogenolysis of Carbonyl Compounds.....	31
2.1.1 Classical Carbonyl Reduction Methods.....	31
2.1.2 Wolff-Kishner Reduction.....	31
2.1.2.1 Catalytic Modification to Wolff-Kishner Reduction.....	32
2.1.3 Clemmensen Reduction.....	33
2.1.4 Reduction of ketone/aldehydes using aluminum, silane etc.....	35
2.1.5 Homogeneous Catalytic Reduction Methods.....	36
2.1.6 Reductive Deoxygenation of Ester, Amide, and other Carbonyl Compounds.....	38
2.1.7 Hydrogenolysis of C-O Bonds.....	43

2.1.7.1 Hydrogenolysis of Aryl Ethers	43
CHAPTER 2: PART 2: Transition Metal Catalyzed Ether Synthesis	53
2.2.1 Introduction	53
2.2.2 Classical Methods	54
2.2.2.1 O-Alkylation.....	54
2.2.2.2 Mitsunobu Etherification.....	54
2.2.2.3 Etherification by Using DialkylPhosphites	55
2.2.3 Cross-coupling Reactions.....	57
2.2.3.1 Ullman Reaction	57
2.2.4 Catalytic Etherification Methods	60
2.2.5 Etherification by [IrCl ₂ Cp*(NHC)] Catalyst	63
2.2.6 dehydrative Etherification of Alcohols	70
2.2.7 Additions to Unsaturated Bonds	72
2.2.7.1 Wacker-type Reaction	72
2.2.7.2 Hydroetherification of Unactivated Aliphatic Alkenes.....	74
2.2.8 Dehydrative Coupling of Alcohols by Sodium Bisulfite.....	76
2.2.9 Reductive Etherification	77

CHAPTER 3: Synthesis and Mechanistic Studies of Deaminative Coupling Reactions of Amines with Alcohols.....	78
3.0. Introduction	84
3.1 Results and Discussion.....	90
3.1.1 Synthesis and Mechanistic Studies of Deaminative Coupling Reactions of Amines.....	84
3.1.2 Optimization Study.....	86
3.1.2.1 Catalytic Survey.....	86
3.1.2.2 Solvent and Temperature Effect Studies.....	87
3.1.3 Reaction Scope	89
3.1.4 Mechanistic Study	96
3.1.4.1 H/D exchange experiment.....	96
3.1.4.2 Hammett Study	97
3.1.4.3 Carbon Isotope Effect Study.....	99
3.1.4.4 Proposed Mechanism.....	101
3.2 Synthetic and Mechanistic Studies of Decarboxylative and Deaminative Coupling Reactions of Amino Acids with Ketones.....	105
3.2.1 Optimization of Reaction Conditions.....	106
3.2.1.1 Catalytic Survey	106

3.2.1.2 Solvent and Temperature Effects	107
3.2.1.3 Catalyst Loading.....	109
3.2.2 Reaction Scope.....	110
3.2.3 Mechanistic Studies.....	116
3.2.3.3 H/D exchange Experiments.....	116
3.2.3.4 ¹³ C-Kinetic Isotope Effect	117
3.2.3.5 Hammett Study	119
3.2.3.6 Formation of Intermediate Products	120
3.2.4 Proposed Mechanism	120
3.2.5 Conclusion:	123
 CHAPTER 4: Synthetic and Mechanistic Studies of Reductive Deoxygenation and Hydrogenolysis of Aldehydes and Ketone and Hydrogenolysis of Alcohols.....	 124
4.0 Introduction	124
4.1 Results and Discussion.....	126
4.2 Optimization studies.....	128
4.2.1 Catalyst, Ligand and Solvent Screening.....	128
4.1.1.1 Catalytic Loading and Solvent Effect.....	130
4.3 Reaction Scope.....	131

4.4 Mechanistic Studies	136
4.4.1 Hammett Study.....	136
4.4.2 Kinetic Isotope Effect.....	138
4.4.3 Deuterium Isotope Effect.....	138
4.4.4 Carbon Isotope Effect.....	145
4.4.5 Deuterium Labeling Study.....	148
4.4.6 Determination of Empirical Rate Law.....	152
4.4.6.1 Catalyst Concentration Dependence.....	152
4.4.6.2 Dependence of Substrate Concentration.....	153
4.4.6.3 Effect of Hydrogen Pressure.....	154
4.5 Isolation and Characterization of Catalytically Relevant Ruthenium Complexes.....	157
4.5.1 Catalyst Concentration Dependence Study.....	164
4.6 Determination of pKa of Ru-H complexes.....	166
4.7 Proposed Mechanism.....	168
4.8 Conclusion.....	175
 CHAPTER 5: Synthetic and Mechanistic Studies of Ruthenium Catalyzed Reductive Etherification of Carbonyl Compounds and Alcohols.....	 176
5.0 Introduction.....	176

5.1 Result and Discussion	178
5.1.1 Optimization Studies.....	178
5.1.1.1 Catalyst Screening	178
5.1.1.2 Solvent and Temperature Effects.....	180
5.1.2 Optimization of Turnover Number (TON) and Turnover Frequency (TOF).....	181
5.2 Reaction Scope.....	182
5.2.1 Reaction Scope of Synthesis of unsymmetrical Ether by Ruthenium Catalyzed Reductive Etherification of Carbonyl Compounds and Alcohols.....	182
5.2.2 Reaction Scope of Synthesis of Unsymmetrical Ethers from the Dehydrative Coupling of Highly Functionalized Bioactive Alcohols.....	186
5.3 Determination of X-ray Crystallography	188
5.4 Mechanistic Studies.....	188
5.4.1 Hammett Study.	188
5.4.2 Solvent Isotope Effect.....	189
5.4.3 H/D Exchange Experiment	193
5.4.4 Carbon Isotope Effect	196
5.4.5 Identification of Catalytic Active Intermeditaes.....	199
5.5 Proposed Mechanism	203

5.6 Conclusion:	205
CHAPTER 6: EXPERIMENTAL SECTION.....	206
6.0 General Information.....	206
6.1. Synthesis and Mechanistic Studies of Deaminative Coupling Reactions of Amines with Alcohols	207
6.1.1 General Procedure for the Coupling Reaction of an Amine with an Alcohol.	207
6.1.2 Synthesis of Ru catalysts	221
6.1.3 Synthesis of $[(\eta^6\text{-C}_6\text{H}_6)\text{RuH}(\text{CO})(\text{PCy}_3)]^+\text{BF}_4^-$ (2).....	207
6.1.4 Catalyst Screening for the Alkylation of 2-Butanol with 3-methoxybenzylamine.....	207
6.1.5 Deuterium Labeling Study.....	209
6.1.6. Carbon Isotope Effect Study.....	209
6.1.7 Hammett Study.....	210
6.1.8 Characterization of Organic Products.....	210
6.2 Synthesis and Mechanistic studies of Decarboxylative and Deaminative Coupling Reactions of Amino Acids with Ketones.....	224
6.2.1 Catalyst Screening for the Alkylation of 4-methoxyacetophenone with L-leucine.....	224
6.2.2. General Procedure for the Coupling Reaction of an Amino Acid with a Ketone.....	224

6.2.3. H/D Exchange Reaction of Acetophenone- d_8 with (<i>S</i>)-Leucine.	225
6.2.4 Carbon Isotope Effect Study.....	225
6.2.5 . Hammett Study.	226
6.2.6 . Characterization Data of the Products.	227
6.3. Scope and Mechanistic Analysis for Chemoselective Hydrogenolysis of Carbonyl Compounds Catalyzed by a Cationic Ruthenium-Hydride Complex with Tunable Phenol Ligands	243
6.3.1. Experimental Procedures.	243
6.3.2 Ligand Screening and Optimization Study.....	244
6.3.2 Hammett Study	246
6.3.3 Deuterium Isotope Effect Study.	247
6.3.4 Carbon Isotope Effect Study.....	249
6.3.5 Deuterium Labeling Study.....	251
6.3.6 Empirical Rate Measurements: Catalyst Concentration Dependence.	254
6.3.7 Catalyst Dependence Study.	257
6.3.8 Ketone Substrate Dependence Study.....	258
6.3.9 Hydrogen Pressure Dependence.	260
6.3.10 Isolation and Characterization of Catalytically Relevant Ruthenium Complexes.....	264

6.3.11 X-Ray Crystallographic Determination of 8a , 8c , 8e , 10 and 11 .	266
6.3.12 Characterization Data of the Products.	272
6.3.13 X-Ray Data:	287
6.4 Synthetic and Mechanistic Studies of Ruthenium Catalyzed Reductive Etherification of Carbonyl Compounds and Alcohols	294
6.4.2 Experimental Procedures	294
6.4.3 Catalyst Screening Study.	295
6.4.4 Determination of TON.	296
6.4.5 Hammett Study.	296
6.4.6 Solvent Isotope Effect Study.	297
6.4.7 H/D Exchange Reaction of 4-Methoxybenzaldehyde with 1-Butanol in D ₂ O.	299
6.4.8 Carbon Isotope Effect Study.	300
6.4.9 Generation and Synthesis of the Alcohol and Aqua Complexes 7 , 8 and 9 .	302
6.4.10 X-Ray Crystallographic Determination of 3d , 3e , 3f , 9 , 10 and 11 .	303
6.4.10 Characterization Data of the Products.	308
6.4.11 X-Ray Data:	324
BIBLIOGRAPHY	329

LIST OF TABLES

Table 3.1: Catalyst Survey on the Reaction of Coupling Product 14 of 3-methoxybenzylamine with 2-butanol.....	88.
Table 3.2: Solvent Effect on the Reaction of 3-Methoxybenzylamine and 2-Butanol.....	89.
Table 3.3: Deaminative Coupling of Amines with Alcohol.....	91.
Table 3.4: Deaminative Coupling of Secondary Amines and Biologically Active Compounds.	94.
Table 3.5: Calculated Average ¹³ C KIE from Virgin (<i>R</i> ₀) and Recovered (<i>R</i>) Samples of Octanophenone.	100.
Table 3.6: Catalyst Screening for the Coupling of 4-methoxyacetophenone with L-leucine.	107.
Table 3.7: Solvent Effect on the Reaction of Leucine with 4-Methoxyacetophenone.....	108.
Table 3.8: Catalyst Loading Effect on the Reaction of Leucine with 4-Methoxyacetophenone.....	109.
Table 3.9: Decarboxylative and Deaminative Coupling of α -Amino Acids with Ketones.....	111.
Table 3.10: Decarboxylative and Deaminative Coupling of β -Amino Acids with Ketone.....	114.
Table 3.11: Decarboxylative and Deaminative Coupling Reaction of Biologically Important Ketones and Peptides.....	115.

Table 3.12: Average ^{13}C Integration of the Product 14k at High Conversion (R_0 ; 96 % conversion), at Low Conversion (R ; avg 18 % conversion) and the Calculated ^{13}C KIE.....	118.
Table 4.1: Ligand Screening for the Hydrogenolysis Reaction of 4-Methoxyacetophenone.....	129
Table 4.2: Reaction Scope of Catalytic Hydrogenolysis of Aldehydes and Ketones.....	132
Table 4.3: Deoxygenation of Biological active Ketone/Aldehyde Compounds.....	135
Table 4.4: Deuterium Isotope Effect Study for the Reaction of 4-Methoxyacetophenone with H_2/D_2 with $p\text{-X-C}_6\text{H}_4\text{OH}$ as the Ligand.....	142
Table 4.5: Average ^{13}C Integration of the Product 6j-[c1] at High Conversion (Virgin, R_0 ; 96 % conversion), at Low Conversion (R ; avg 18 % conversion) and the Calculated ^{13}C KIE using 4-Methoxyphenol as the Ligand.....	147
Table 4.6: Average ^{13}C Integration of the Product 6j-[c2] at High Conversion (Virgin, R_0 ; 96 % conversion), at Low Conversion (R ; avg 18 % conversion) and the Calculated ^{13}C KIE using 4-Trifluoromethylphenol as the Ligand.....	148
Table 4.7: Selected Spectroscopic Data for Complexes 8a-g	158
Table 4.8: Selected Physical Parameters of Complexes 5, 8a and 8f	160
Table 4.9: Summary of Kinetic Parameters for the Hydrogenolysis of Aryl ketone Catalyzed by 4 / $p\text{-X-C}_6\text{H}_4\text{OH}$ ($\text{X} = \text{OMe}, \text{CF}_3$).....	170
Table 5.1: Catalyst Survey for the Reaction of 4-Methoxybenzaldehyde with 1-Butanol ^a	179
Table 5.2: Solvent Effect on the Reaction of 4-Methoxybenzaldehyde with 1-Butanol.....	180

Table 5.3: Synthesis of Unsymmetrical Ethers from the Dehydrative Coupling of Alcohols.....	183
Table 5.4: Synthesis of Unsymmetrical Ethers from the Reductive Coupling of Carbonyl Compounds with Alcohols.....	187
Table 5.5: Calculated Average ^{13}C KIE from Virgin (R_0) and Recovered (R) Samples of 2f	197
Table 6.1: Ligand Screening for the Hydrogenolysis Reaction of 4-Methoxyacetophenone.....	245
Table 6.2: Average ^{13}C Integration of the Product 6j at High Conversion (Virgin, R_0 ; 96% conversion), at Low Conversion (R ; avg 18% conversion) and the Calculated ^{13}C KIE using 4-OMeC ₆ H ₄ OH as the ligand.....	250
Table 6.3: Average ^{13}C Integration of the Product 6j at High Conversion (Virgin, R_0 ; 96% conversion), at Low Conversion (R ; avg 18% conversion) and the Calculated ^{13}C KIE using 4-CF ₃ -C ₆ H ₄ OH as the ligand.....	250
Table 6.4: Crystal Data and Structure Refinement for 8a	287
Table 6.5: Crystal Data and Structure Refinement for 8a'	288
Table 6.6: Crystal Data and Structure Refinement for 8c	289
Table 6.7: Crystal Data and Structure Refinement for 8e	290
Table 6.8: Crystal Data and Structure Refinement for 10	291
Table 6.9: Crystal Data and Structure Refinement for 11	192
Table 6.10: Crystal Data and Structure Refinement for 14	293
Table 6.11. Catalyst Survey for the Coupling Reaction of 4-Methoxybenzaldehyde with 1-Butanol.	295

Table 6.12. Calculated Average ^{13}C KIE from Virgin (R_0) and Recovered (R) Samples of 2k	301
Table 6.13: Crystal Data and Structure Refinement for 9	324
Table 6.14: Crystal Data and Structure Refinement for 3e	325
Table 6.15: Crystal Data and Structure Refinement for 3f	326
Table 6.16: Crystal Data and Structure Refinement for 11	327
Table 6.17: Crystal Data and Structure Refinement for 10	328

LIST OF FIGURES

Figure 1.1: Combination of D-amino acid Oxidase and L-glutamate Dehydrogenase (Glu-DH).	26
Figure 1.2: Balancing the Supply of Nitrogen for Urea Cycle when Aspartate in Excess.	27
Figure 2.1. 2-Aryloxy-1-Arylethanol Approximate the Functionality in β -[O]-4'-Glycerolaryl Ethers.	45
Figure 2.2: Selective Cleavage of Aryl-Oxygen Bond in Different Conditions	49
Figure 2.3: Some Natural Products and Drugs Containing Ether Bond.	53
Figure 2.4. Natural Products Synthesized by Ullman Coupling	58
Figure 2.5: Natural Product from Wacker-type Oxidation	68
Figure 3.1. ^1H and ^2H NMR Spectra of the Reaction Mixture of 3-Methoxybenzyl Amine with 2-Propanol- d_8 at 80 °C.	97
Figure 3.2. Hammett Plot of p-X-C ₆ H ₄ CH ₂ NH ₂ (X = OCH ₃ , CH ₃ , H, Cl, Br) with 1-Phenyl-1-ethanol.	97
Figure 3.3. ^1H and ^2H NMR Spectra of 14m-d Obtained from the Reaction of Acetophenone- d_8 with (S)-Leucine.	117
Figure 3.4. Hammett Plot of p-X-C ₆ H ₄ COCH ₃ (X = NH ₂ , CH ₃ , H, Cl, Br, CN) with (S)-Leucine.	117
Figure 3.5: Transition state of alkyl-ruthenium enolate complex.	119
Figure 4.1: Some Biologically Active Ketone Compounds	124

- Figure 4.2.** Hammett Plot of 4-Methoxyacetophenone with p-X-C₆H₄OH (X = ^tBu, Cl, CF₃, Et, F, H, Me, OMe). 138
- Figure 4.3:** Deuterium Isotope Effect Study for the Reaction of 4-Methoxyacetophenone with H₂/D₂ with 4-OMe-C₆H₄OH as the Ligand. 139
- Figure 4.4:** Deuterium Isotope Effect Study for the Reaction of 4-Methoxyacetophenone with H₂/D₂ with 4-Ethylphenol as the Ligand 140
- Figure 4.5:** Deuterium Isotope Effect Study for the Reaction of 4-Methoxyacetophenone with H₂/D₂ with 4-CF₃-C₆H₄OH as the Ligand 141
- Figure 4.6.** Deuterium Isotope Effect Study for the Reaction of 4-Methoxyacetophenone with H₂/D₂ with 4-Cl-C₆H₄OH as the Ligand..... 141
- Figure 4.7.** Deuterium Isotope Effect Study for the Reaction of 4-Methoxyacetophenone with H₂/D₂ with 4-F-C₆H₄OH as the Ligand. 142
- Figure 4.8:** ¹H and ²H NMR Spectra for the Hydrogenolysis of 4-Methoxyacetophenone with D₂ Catalyzed by 4/4-CF₃C₆H₄OH..... 149
- Figure 4.9:** ¹H and ²H NMR Spectra for the Hydrogenolysis of 1-(4-Methoxyphenyl)ethanol with D₂ Catalyzed by 4/4-CF₃C₆H₄OH..... 150
- Figure 4.10:** ¹H and ²H NMR Spectra for the Hydrogenolysis of 4-Methoxyacetophenone with D₂ Catalyzed by 4/4-OMeC₆H₄OH..... 150
- Figure 4.11:** ¹H and ²H NMR Spectra for the Hydrogenolysis of 1-(4-Methoxyphenyl)ethanol with D₂ Catalyzed by 4/4-OMeC₆H₄OH. 151
- Figure 4.12:** (A) The Formation of 1-Ethyl-4-methoxybenzene vs Time. (B) Initial Rate of the Formation 1-Ethyl-4-methoxybenzene vs at Different Catalyst Concentrations of 4/HBF₄·OEt₂/4-OMe-C₆H₄OH (**8a**)..... 152
- Figure 4.13:** (A) The Formation of 1-Ethyl-4-methoxybenzene vs Time. (B) Initial Rate of the Formation 1-Ethyl-4-methoxybenzene vs at Different Catalyst Concentrations of 4/HBF₄·OEt₂/4-CF₃-C₆H₄OH (**8f**). 152

Figure 4.14: (A) The Formation of 1-Ethyl-4-methoxybenzene vs Time. (B) Initial Rate of the Formation 1-Ethyl-4-methoxybenzene vs at Different 4-Methoxyacetophenone Concentrations for the Catalyst **4**/HBF₄·OEt₂/4-OMe-C₆H₄OH (**8a**)..... 153

Figure 4.15: (A) The Formation of 1-Ethyl-4-methoxybenzene vs Time. (B) Initial Rate of the Formation 1-Ethyl-4-methoxybenzene vs at Different 4-Methoxyacetophenone Concentrations for the catalyst **4**/HBF₄·OEt₂/4-CF₃-C₆H₄OH (**8f**) 154

Figure 4.16: (A) The Formation of 1-Ethyl-4-methoxybenzene vs Time. (B) Initial Rate of the Formation 1-Ethyl-4-methoxybenzene vs at Different [H₂] (C) Inverse rate vs [H₂] for the Catalyst **4**/HBF₄·OEt₂/4-OMe-C₆H₄OH (**8a**) 155

Figure 4.17: (A) The Formation of 1-Ethyl-4-methoxybenzene vs Time. (B) Initial Rate of the Formation 1-Ethyl-4-methoxybenzene vs at Different [H₂] for the Catalyst **4**/HBF₄·OEt₂/4-CF₃-C₆H₄OH (**8f**) 156

Figure 4.18: ORTEP Diagram of Complex **8c** (H atoms and Solvent Molecules Removed for Clarity) 158

Figure 4.19: ORTEP Diagram of Complex **8a** (H atoms and Solvent Molecules Removed for Clarity) 158

Figure 4.20 : ORTEP Diagram of Complex **8a'** (H atoms and Solvent Molecules Removed for Clarity) 159

Figure 4.21: ORTEP Diagram of Complex **8e** (H atoms and Solvent Molecules Removed for Clarity).....160

Figure 4.22: ORTEP Diagram of Complex **10** (H atoms and Solvent Molecules Removed for Clarity) 162

Figure 4.23: ORTEP Diagram of Complex **11** (H atoms and Solvent Molecules Removed for Clarity) 163

Figure 4.24: A) Plot of [2'-Hydroxyethylbenzene] vs Time at Different Catalyst **17** Concentrations (4μM-16μM). B) Initial Rate of Formation 2'-Hydroxyethylbenzene vs Different Catalytic **17** Loading 164

Figure 4.25: ORTEP Diagram of Complex 14 (H atoms and Solvent Molecules Removed for Clarity)	166
Figure 4.26: The Plot of pH vs $\text{Log}([A^-]/[HA])$	167
Figure 4.27: Acidic and Hydridic Nature of Ruthenium Phenol Bifunctional Catalyst	168
Figure 5.1: X-ray Crystal Structure of (A) 3d (B) 3e (C) 3f	188
Figure 5.2: Hammett Plot from the Reaction of p-X-C ₆ H ₄ CHO (X = OMe, Me, H, F, Cl) with 2-Butanol.	189
Figure 5.3: First Order Plot of the 4-Methoxybenzaldehyde (S) with 2-Butanol in H ₂ O (circle) and in D ₂ O (triangle).	191
Figure 5.4: First Order Plot of the 4-Methoxybenzaldehyde with 2-Propanol (triangle) and in 2-Propanol-d ₁ (circle).	192
Figure 5.5: Transition State of Ruthenium Alkoxy Species	192
Figure 5.6: ¹ H and ² H NMR Spectra of the Product 2f Isolated from the Reaction of 4-Methoxybenzaldehyde with 1-Butanol in D ₂ O.	193
Figure 5.7: ¹ H and ² H NMR Spectra of the Product 6-[D] Isolated from the Reaction of 4-Methoxybenzaldehyde with 2-propanol-d ₈ in H ₂ O.	194
Figure 5.8: ¹ H and ² H NMR Spectra of the Reaction Mixture of 4-methoxybenzaldehyde-d ₁ with H ₂ O at 110 °C.	195
Figure 5.9: ¹ H NMR Spectra of the Reaction Mixture of iPrOH with D ₂ O at 110 °C. .	296
Figure 5.10: ¹ H NMR Spectra of the Reaction of 1 with 1-Butanol.	197
Figure 5.11: ¹ H NMR Spectra of the Reaction of 5 with H ₂ O.	201
Figure 5.12: ORTEP Diagram of Comlex 9 (H Atoms Reomoved for Clarity)	201

Figure 5.13: ORTEP Diagram of Complex 10 (H Atoms Removed for Clarity)	202
Figure 5.14: ORTEP Diagram of Complex 11 (H Atoms Removed for Clarity)	202
Figure 6.1. Hammett Plot of 4-Methoxyacetophenone with <i>p</i> -X-C ₆ H ₄ OH (X = OMe, <i>t</i> -Bu, Me, Et, H, F, Cl, CF ₃).	247
Figure 6.2. First Order Plots from the Hydrogenolysis Reaction of 4-Methoxyacetophenone with H ₂ (triangle) and D ₂ (circle) Catalyzed by 4/4-X-C ₆ H ₄ OH (X = OMe, Et, Cl, F, CF ₃).	248
Figure 6.3. ¹ H and ² H NMR spectra for the Hydrogenolysis of 4-Methoxyacetophenone with D ₂ Catalyzed by 4/4-CF ₃ C ₆ H ₄ OH.....	252
Figure 6.4. ¹ H and ² H NMR spectra for the Hydrogenolysis of 1-(4-Methoxyphenyl)ethanol with D ₂ Catalyzed by 4/4-CF ₃ C ₆ H ₄ OH.....	252
Figure 6.5. ¹ H and ² H NMR spectra for the Hydrogenolysis of 4-Methoxyacetophenone with D ₂ Catalyzed by 4/4-OMeC ₆ H ₄ OH.....	253
Figure 6.6. ¹ H and ² H NMR spectra for the Hydrogenolysis of 1-(4-Methoxyphenyl)ethanol with D ₂ Catalyzed by 4/4-OMeC ₆ H ₄ OH.....	253
Figure 6.7: The Formation of 1-Ethyl-4-Methoxybenzene vs Time at Different Catalyst Concentrations of 4/HBF ₄ ·OEt ₂ /4-OMe-C ₆ H ₄ OH.....	255
Figure 6.8: Initial Rate of the Formation 1-Ethyl-4-Methoxybenzene vs Catalyst Concentration of 4/HBF ₄ ·OEt ₂ /4-OMe-C ₆ H ₄ OH.....	255
Figure 6.9: The Formation of 1-Ethyl-4-Methoxybenzene vs Time at Different Catalyst Concentrations of 4/HBF ₄ ·OEt ₂ /4-CF ₃ -C ₆ H ₄ OH.....	256
Figure 6.10: Initial Rate of the Formation 1-Ethyl-4-Methoxybenzene vs Catalyst Concentration of 4/HBF ₄ ·OEt ₂ /4-CF ₃ -C ₆ H ₄ OH.....	257
Figure 6.11: The Formation of 2'-hydroxyethylbenzene vs Time at Different Catalyst Concentrations of 10 (4μM-16μM).	258

- Figure 6.12:** Initial Rate of the Formation 2'-Hydroxyethylbenzene Vs Catalyst Concentration of **10**..... 258
- Figure 6.13:** The Formation of 1-Ethyl-4-Methoxybenzene Vs Time at Different Concentration of 4-Methoxyacetophenone for the Catalyst 4/HBF₄·OEt₂/4-OMe-C₆H₄OH. 258
- Figure 6.14:** Initial Rate of Formation 1-Ethyl-4-Methoxybenzene Vs Concentration of 4-Methoxyacetophenone for the Catalyst 4/HBF₄·OEt₂/4-OMe-C₆H₄OH. 259
- Figure 6.15:** The Formation of 1-Ethyl-4-Methoxybenzene Vs Time at Different Concentration of 4-Methoxyacetophenone for the Catalyst 4/HBF₄·OEt₂/4-CF₃-C₆H₄OH. 259
- Figure 6.16:** Initial Rate of Formation 1-Ethyl-4-Methoxybenzene Vs Concentration of 4-Methoxyacetophenone for the Catalyst 4/HBF₄·OEt₂/4-CF₃-C₆H₄OH. 260
- Figure 6.17:** The Formation of 1-Ethyl-4-Methoxybenzene Vs Time at Different Hydrogen Pressure for the Catalyst 4/HBF₄·OEt₂/4-OMe-C₆H₄OH. 261
- Figure 6.18:** Initial Rate of the Formation 1-Ethyl-4-Methoxybenzene vs Time at Different Hydrogen Pressure for the Catalyst 4/HBF₄·OEt₂/4-OMe-C₆H₄OH. 261
- Figure 6.19:** Initial Rate of the Formation 1-Ethyl-4-Methoxybenzene (1/ N₀) vs Time at Different Hydrogen Pressure for the Catalyst 4/HBF₄·OEt₂/4-OMe-C₆H₄OH. 262
- Figure 6.20:** (A) Plot of Initial Rate of Formation 1-Ethyl-4-Methoxybenzene Vs Time at Different Hydrogen Pressure when 4-Methoxyphenol is used. (Inset) (1/ v₀) Vs Time at Different Hydrogen Pressure for the Catalyst 4/HBF₄·OEt₂/4-OMe-C₆H₄OH 262
- Figure 6.21:** The Formation of 1-Ethyl-4-Methoxybenzene vs Time at different hydrogen pressure for the catalyst 4/HBF₄·OEt₂/4-CF₃-C₆H₄OH. 263
- Figure 6.22:** Initial Rate of the Formation 1-Ethyl-4-Methoxybenzene vs time at different hydrogen pressure for the catalyst 4/HBF₄·OEt₂/4-CF₃-C₆H₄OH. 263
- Figure 6.23.** Molecular Structure of **8a**..... 269

Figure 6.24: X-ray Structure of Complex 8a'	269
Figure 6.25. Molecular Structure of 8c	270
Figure 6.26. Molecular Structure of 8e	270
Figure 6.27. Molecular Structure of 10	270
Figure 6.28. Molecular Structure of 11	271
Figure 6.29: X-ray structure of complex 14	271
Figure 6.30: Hammett Plot from the Reaction of <i>p</i> -X-C ₆ H ₄ CHO (X = OMe, Me, H, F, Cl) with 2-Butanol.	297
Figure 6.31: First Order Plot of the 4-Methoxybenzaldehyde with 2-Butanol in H ₂ O (triangle) and in D ₂ O (circle).	298
Figure 6.32. First Order Plot of the 4-Methoxybenzaldehyde with 2-Propanol (triangle) and in 2-Propanol- <i>d</i> ₁ (circle).	299
Figure 6.33: ¹ H and ² H NMR Spectra of the Product 2f Isolated from the Reaction of 4-Methoxybenzaldehyde with 1-Butanol in D ₂ O.	300
Figure 6.34. ¹ H NMR Spectra of the Reaction of 5 with 1-Butanol. Indicate Time and Temp For Each Spectrum.	302
Figure 6.35: X-ray Crystal Structure of 3d	305
Figure 6.36: X-ray Crystal Structure of 3e	306
Figure 6.37: X-ray Crystal Structure of 3f	306
Figure 6.38: Molecular Structure of 9	306

Figure 6.39: X-ray structure of complex **10** (H atoms removed for clarity) 307

Figure 6.40: X-ray structure of complex **11** 307

LIST OF SCHEMES

Scheme 1.1: Microscopic Reversibility of C-C Bond Activation.....	2
Scheme 1.2: C-C Bond Activation of Propane by Cp*Rh(PMe ₃)(H) ₂	3
Scheme 1.3: C-C Bond Activation of Pincer-Type Ligands.....	3
Scheme 1.4: C-C Bond Activation of Propane by (PPh ₃) ₃ RhCl.....	5
Scheme 1.5: Rh Catalyzed C-C Activation of Cyclobutanone.	5
Scheme 1.6: Proposed Mechanism of Pd Catalyzed Arylation of <i>tert</i> -cyclobutanol.....	6
Scheme 1.7: Ruthenium-Catalyzed Deallylation of Unstrained Homoallylic Alcohol.	7
Scheme 1.8: Proposed Mechanism for the α -C-C Bond Cleavage of 8-Quinolinyl Alkyl Ketone.....	9
Scheme 1.9: Proposed Mechanism Decarbonylative C–C Bond Activation of Oxazolidine.....	10
Scheme 1.10: Proposed Mechanism for Chelate Assisted C-C Bond Activation Catalyzed by (PPh) ₃ RhCl.....	11
Scheme 1.11: Proposed Mechanism for C-C Bond Cleavage of Secondary Benzyl Alcohol.....	12
Scheme 1.12: Postulated Mechanism for the Ni-Catalyzed Intermolecular Alkyne Insertion into Cyclobutanone.....	13
Scheme 1.13: Proposed Mechanism for Denitrogenation of N-heterocycle by Ti Catalyst.....	19

Scheme 1.14: Allylic Isomerization Promoted by a Combination of Palladium and Protic Acid.....	19
Scheme 1.15: Plausible Reaction Mechanism Pd Catalyzed Allylic Alkylation.	20
Scheme 1.16: Proposed Mechanism for Rh/Cu Catalyzed Anulation of Benzimide and Alkyne.....	24
Scheme 1.17: Proposed Repair Mechanism for AlkB-family Proteins.....	28
Scheme 1.18: Mechanism of Aspartate Deamination by Lyases.	35
Scheme 2.1: Zinc Promoted Reduction of Ketone and Ozonolysis of Alkene	36
Scheme 2.2: Reduction of Carboxylic Acid into Alkane.....	37
Scheme 2.3: Mechanism of Ga(OTf) ₃ Catalyzed Reduction of Ketone by Silane.	40
Scheme 2.4: Proposed Mechanism for Ru Catalyzed Hydrogenolysis of Esters	40
Scheme 2.5: Proposed the Reaction Mechanism for the Zinc Catalyzed Amide.....	42
Scheme 2.6: C-O Cleavage of Aryl-OMe Ether by Rh.....	44
Scheme 2.7: Proposed Mechanism for the Hydrogenolysis of Aryl Ether Catalyzed By Ru Catalyst.	47
Scheme 2.8: Oxidation of Phenolic Ligand Model Compound with Vanadium Catalysts	50
Scheme 2.9: Tentative Mechanism for the Rhodium-Catalyzed Rearrangement of 2-(Aryloxy) Benzaldehydes to 2-Hydroxybenzophenones.....	52
Scheme 2.10: Mechanism of Etherification of Cholesterol, ROH= Cholesterol.....	56

Scheme 2.11: Mechanism of Rhenium (I) Catalytic Etherification Cycle.....	61
Scheme 2.12: Mechanism of In (III) Catalyzed Deoxygenation of Esters.....	62
Scheme 2.13: Proposed Mechanism of Synthesis of Unsymmetrical Ether by Iridium Catalyst	64
Scheme 2.14: Working Mechanistic Hypothesis for Unsymmetrical Ether Formation...	66
Scheme 2.15: Proposed Mechanism for Ir Catalyzed Hydroetherification of Phenol and Alkene	70
Scheme 2.16: Proposed Generation of Active Catalyst.....	74
Scheme 2.17: Proposed Simplified Catalytic Cycle with TESOTf as Active Catalyst....	74
Scheme 2.18: Synthetic Raoute for the Synthesis of (-)-Exiguolide.....	75
Scheme 2.19: Proposed Mechanism for the Zn Catalyzed Etherification.....	77
Scheme 3.1: Pyridoxal Derivatives and Cu ²⁺ ion Catalyzed Oxidative Deamination of Amino Acids.	82
Scheme 3.2: Synthesis of Cationic Ruthenium Hydride Complex 5	84
Scheme 3.3: Generation of Cationic Ru-Alkenyl Species 9	102
Scheme 3.4: Proposed Mechanism for Deaminative Coupling of Amines with Alcohol.	104
Scheme 3.5: Proposed Mechanism for the Decarboxylative and Deaminative Coupling of Amino Acids with Ketone.....	121
Scheme 4.1: Electronic Effect of Ru-H (8) Catalyzed H ₂ Activation	145

Scheme 4.2: ^{13}C KIE data for the 6-Methoxy-1,2,3,4-tetrahydronaphthalene (A) for the in-situ Generated Catalyst 8a (B) for the in-situ Generated Catalyst 8f .	146
Scheme 4.3: Deuterium Incorporation pattern of 1-Ethyl-4-methoxybenzene Product when (a) 4-Methoxyacetophenone and 4-(Trifluoromethyl)phenol (b) 1-(4-Methoxyphenyl)ethanol and 4-(Trifluoromethyl)phenol (c) 4-Methoxyacetophenone and 4-Methoxyphenol (d) 1-(4-Methoxyphenyl)ethanol and 4-Methoxyphenol is used.	148
Scheme 4.4: Keto Enol Tautomerization and Formation of Ru-enolate Complex	161
Scheme 4.5: Synthetic Routes for the Complex 9	164
Scheme 4.6: Possible Intermediates from the Reaction of Complex 10 with H_2	164
Scheme 4.7: Synthetic Route for the Complex 14	165
Scheme 4.8: Catalytic Cycle of Noyori Catalyst via a Concerted Six-membered Transition State	169
Scheme 4.9: Outer-sphere Mechanism for the Hydrogenation of Ketones to Alcohols	170
Scheme 4.10: Proposed Mechanism of Ruthenium Catalyzed Hydrogenolysis of 1-Phenethanol to Ethyl Benzene for the Catalyst 8a ($\text{X} = \text{OMe}$)	172
Scheme 4.11: Proposed Mechanism of Ruthenium Catalyzed Hydrogenolysis of 1-Phenethanol to Ethyl Benzene for the Catalyst 8f ($\text{X} = \text{CF}_3$)	174
Scheme 5.1: Synthesis of Complex 7 , 8 and 9	199
Scheme 5.2: Proposed Mechanism for the Catalytic Reductive Coupling of Carbonyl Compound with Alcohols	204

CHAPTER 1

TRANSITION METAL CATALYZED C-C AND C-N BOND ACTIVATION REACTIONS

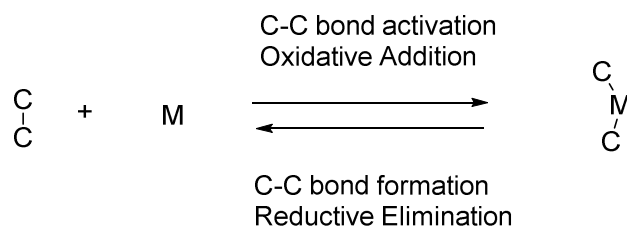
1.0 INTRODUCTION

Transition metal catalyzed selective C-C^{1, 3-5} and C-N² bond activation reactions are fundamentally important in organometallic chemistry and organic synthesis as well as petrochemical refining processes. Designing selective catalytic C-C and C-N bond activation for the reforming processes of organic feedstocks is very challenging because they are thermodynamically less favored than C-H activation. During the last few decades, significant research attention has been focused on the transition metal mediated C-C bond and C-N bond cleavage reactions to form new compounds, as these processes are expected to provide novel processes for the transformation of inexpensive hydrocarbons into more commercially valuable products such as pharmaceuticals, agrochemicals and polymers. Catalytic C-C and C-N activation are also highly valuable for hydro-reforming and hydrodenitrogenation processes of crude oils to make high quality fuels.³ The main focus of this chapter is to survey synthetic and mechanistic aspects of transition metal mediated C-C and C-N bond cleavage reactions.

1.1 C-C Bond Activation of Hydrocarbon Molecules

Catalytic C-C bond cleavage process is fundamentally important for obtaining complex organic compounds from petroleum feedstocks. In petroleum cracking processes, heterogeneous catalysts are used to convert heavy petroleum into lighter hydrocarbons, but

harsh conditions such as high temperature $>500\text{ }^{\circ}\text{C}$ gives low selectivity on forming C-C cleavage products.^{4,6} Designing catalytic C-C bond activation processes is one of the most challenging problems in the field of organometallic chemistry and homogeneous catalysis. Examples of C-C bond activation reactions using homogeneous catalysts are very rare because the oxidative addition of C-C bond is thermodynamically less favored than the C-H activation for substituted hydrocarbon compounds.

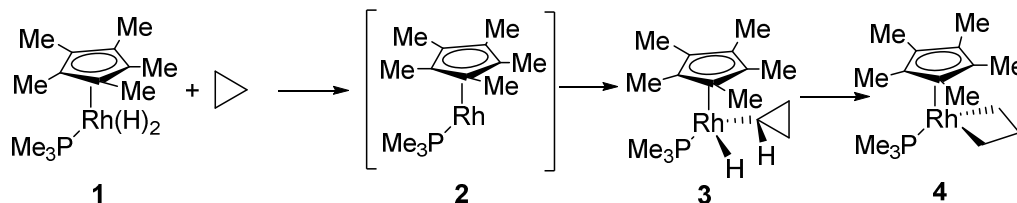


Scheme 1.1: Microscopic Reversibility of C-C Bond Activation.

Selective C-C bond activation process of unstrained hydrocarbons which is reverse of the C-C bond formation, has been rarely achieved because it forms two weak M-C bonds (20 kcal/mol each) by breaking a relatively strong C-C bond (90 kcal/mol) (Scheme 1.1). Two basic strategies have been applied to facilitate the C-C activation reactions. One is to increase the energy of starting material, and the other is to lower the energy of C-C bond cleaved products.^{1c} The first strategy is used for high energy starting materials such as strained 3- or 4-membered cycloalkane compounds. To overcome unstable ring strain of these cycloalkane compounds, metal complexes can affect the C-C bond activation by making more stable ring expanded metallocycle through metal insertion into the strained C-C bond.

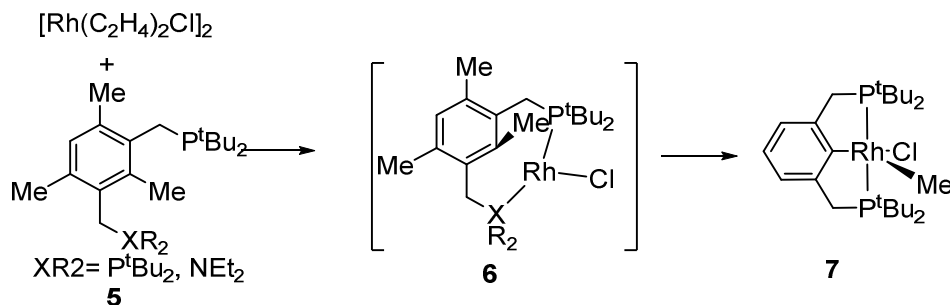
1.1.1 Stoichiometric C-C Bond Activation Reactions

In a pioneering study, Bergman has shown that UV irradiation of Rh complex **1** generates 16 electron species **2** which reacts with cyclopropane to give the C-H activated product **3**, which upon heating leads to formation of 4-membered heterocycle **4**.⁷



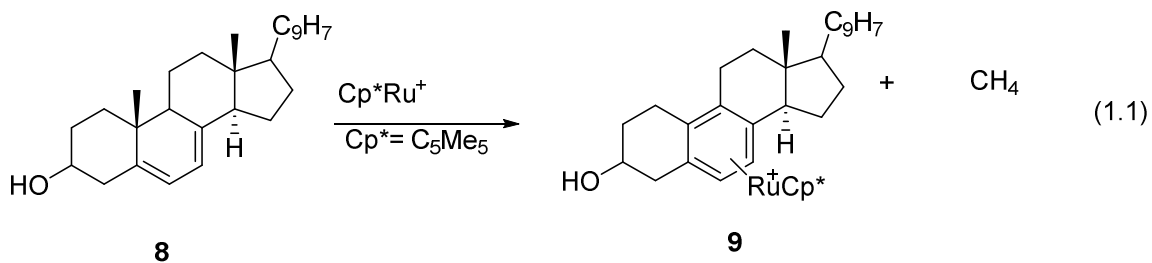
Scheme 1.2: C-C Bond Activation of Propane by Cp*Rh(PMe₃)(H)₂.

Milstein has shown that the formation of 5-membered metallocycles with pincer type ligands provided the driving force for the C-C bond activation.⁸ Since then, reactions of pincer-type model compounds and various transition metal complexes have been achieved for C-C bond activation reactions under mild reaction conditions.⁸ The C-C bond activation of **5** by Rh(I) is thermodynamically and kinetically favored over the C-H activation due to stable 5-membered metallocyclic structure. The direct observation of intermediate **6** (when X = NEt₂), confirmed the single step C-C activation in formation of the product **7**.



Scheme 1.3: C-C Bond Activation of Pincer-Type Ligands.

Crabtree has shown that the C-C bond activation of unstrained molecules by Cp^*Ru^+ ($\text{Cp}^* = \text{C}_5\text{Me}_5$) can be explained by especial stabilization of lower energy states products. Elimination of methyl group in a series of steroid compounds such as ergosterol **8**, which forms stable products by the aromatic stabilization of ring B of product **9** [eq. (1.1)].⁹

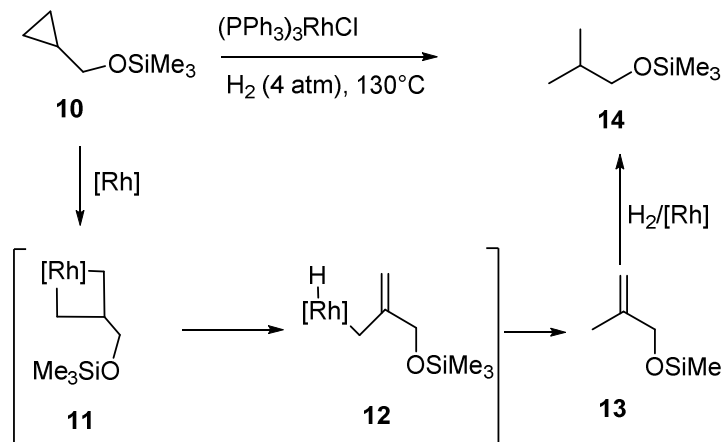


1.1.2 Catalytic C-C Bond Activation Reactions

Only few examples of catalytic C-C activation reactions have been reported with limited substrate scope. Two common strategies oxidative addition of a strained C-C bond and via β -carbon elimination have been utilizing for homogeneous catalytic C-C activation reactions.

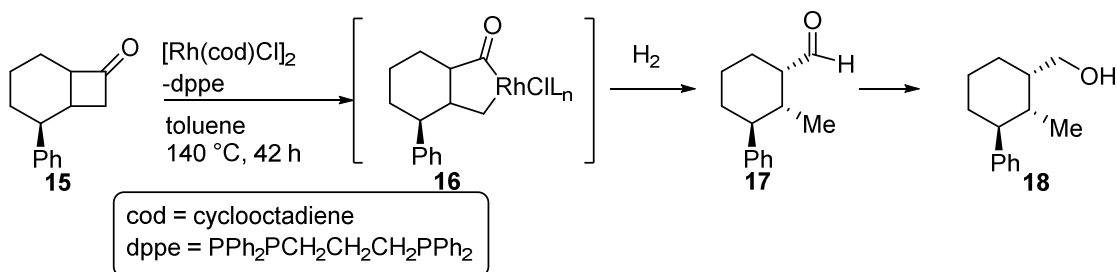
1.1.2.1 C-C Bond Activation of Strained Molecules

A number of transition metal catalyzed direct C-C bond cleavage of strained molecules such as cyclopropane have been reported. Both Bart and Chirik reported a selective C-C activation of cyclopropane using a Rh(I) catalyst.¹⁰ Sterically hindered C-C bond of cyclobutane **10** is cleaved by formation of rhodacyclobutane **11**, by the reaction of $\text{Rh}(\text{PPh}_3)\text{Cl}$ and β -H elimination followed by reductive elimination of branch alkenes **13** which react with H_2 to produce **14**.



Scheme 1.4: C-C Bond Activation of Propane by $(\text{PPh}_3)_3\text{RhCl}$.

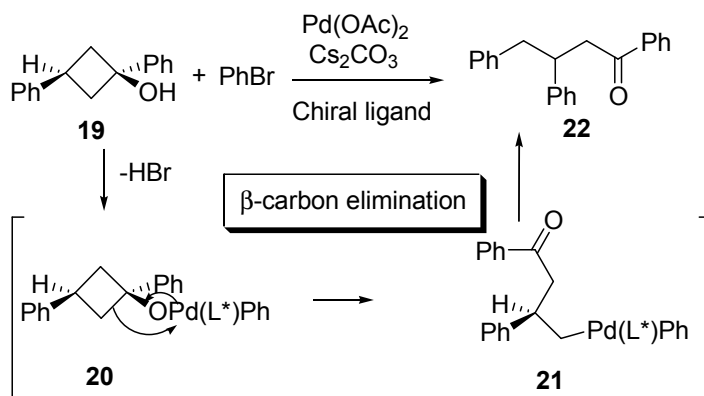
Murakami et al reported a similar kind of regio and stereo-selective C-C activation of cyclobutanone by using a Rh(I) catalyst.¹¹ They successfully used this method to synthesize lactams using O-phenols and O-styryl cyclobutanone as starting materials. They proposed that cyclobutanone **15** oxidatively added to Rh(I) (complex **17**) and ring opened stereoselectively to give ring opened alcohol **18** through aldehyde **17** (Scheme 1.5).



Scheme 1.5: Rh Catalyzed C-C Activation of Cyclobutanone.

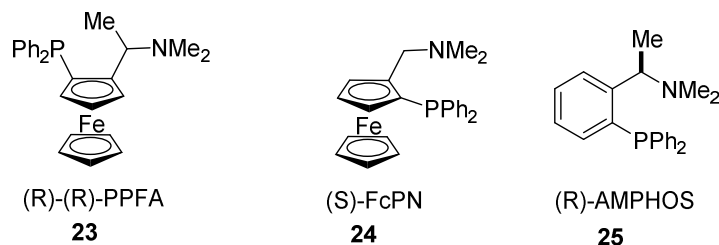
Another way to promote C-C bond activation of strained molecules is via β -alkyl elimination. When a strained molecule is bonded to a metal through a C, N, O atom, β -alkyl elimination can occur to give ring opened alkyl-metal intermediates. Uemura and coworkers reported that Pd catalyzed C-C bond cleavage of tert-cyclobutanol to produce

optically active α -arylated ketone.¹² In these reactions, *tert*-cyclobutanol **19** and arylating reagent PhBr in the presence of Pd(II) forms Pd(II) alcohol complex **20**, and the β -alkyl elimination gives α -arylated ketone **22** in excellent yield. In this reaction, chiral bidentate ligand controls the enantio-selectivity of the product (Scheme 1.6).



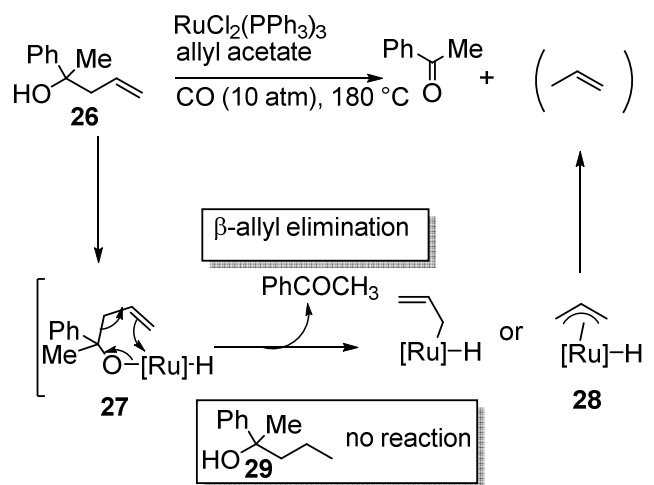
Scheme 1.6: Proposed Mechanism of Pd Catalyzed Arylation of *tert*-Cyclobutanol.

Different type of chiral N, P ligands, (R)- (R)-PPFA (**23**), (S)-FcPN (**24**) and (R)-AMPHOS (**25**) were used for enantioselective reaction. They also published that palladium(0)-catalyzed β -alkyl elimination of strained molecules such as reaction of cyclobutanone *O*-acyloximes leading to various nitriles.¹³ Ito proposed that spirocyclobutanone oxidatively added to Rh(I) prior to β -alkyl elimination to produce cyclohexanones.^{14b} Osakad et al reported that the palladium catalyzed ring opening of methylenecyclopropane associated with CO could be applied to the polymerization reactions.^{14a} Pd(OAc)₂ catalyst was successfully used to ring opening of *tert*-cyclobutanol under oxygen atmosphere.



1.1.2.2. Catalytic C-C Activation of Unstrained Hydrocarbons

As described above, the β -alkyl elimination is an effective method to promote the C-C activation for the ring strained molecules. However, even with unstrained molecules it is possible to cleave the C-C bond through β -alkyl elimination by generating more stable products. Tertiary homoallylic alcohols have been successfully used for selective C-C bond cleavage. Mitsudo et al achieved a ruthenium-catalyzed deallylation of unstrained homoallylic alcohol **26**, via the oxidative addition of a hydroxyl group and subsequent β -allyl elimination of **27** to afford acetophenone and propene (Scheme 1.7).¹⁵



Scheme 1.7: Ruthenium-Catalyzed Deallylation of Unstrained Homoallylic Alcohol.

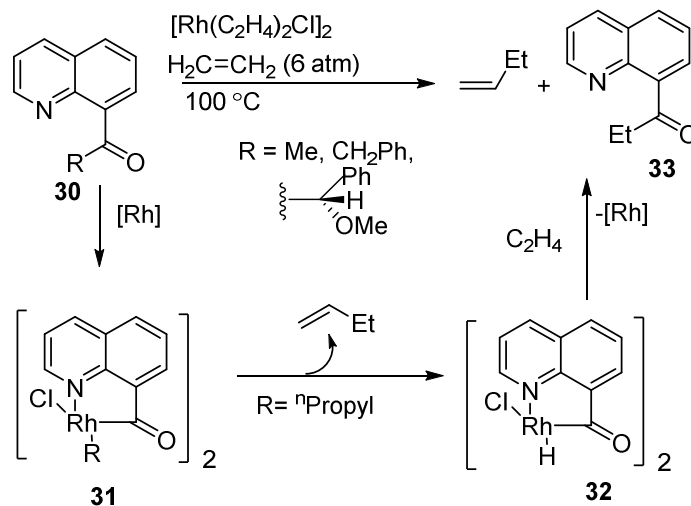
The formation of a stable η^3 -allyl ruthenium(II) species **28** served as the forward driving force of this reaction, because the tertiary alcohol **29** bearing no homoallylic functionality did not give any C–C bond cleaved product.

1.1.2.3. Chelate Assisted C-C Bond Activation Reactions of Unstrained Molecules

The cyclometallation via the chelate assistance is one of the promising methods for promoting C-C bond activation of unstrained molecules. Suggs and Jun developed activation of α -C-C bond to the carbonyl group in 8-quinolnyl alkyl ketone **30**.¹⁶ When the reaction of 8-quinolnyl butyl ketone and ethylene was carried out using the $[\text{Rh}(\text{C}_2\text{H}_4)_2\text{Cl}]$ catalyst, 8-quinolnyl ethyl ketone **33** and 1-butene were obtained. They proposed a reaction mechanism, coordination of the nitrogen to ruthenium provides the metal with a more nucleophilic character, as well as bringing it close to the ketonic carbon (Scheme 1.8). In this reaction, β -hydrogen elimination occurs in the acylrhodium(III) butyl complex **31**, generated from the cleavage of the α -C–C bond, to give an acylrhodium (III) hydride **32** and 1-butene. Further reaction of the acylrhodium(III) hydride with ethylene leads to 8-quinolnyl ethyl ketone product **33**.

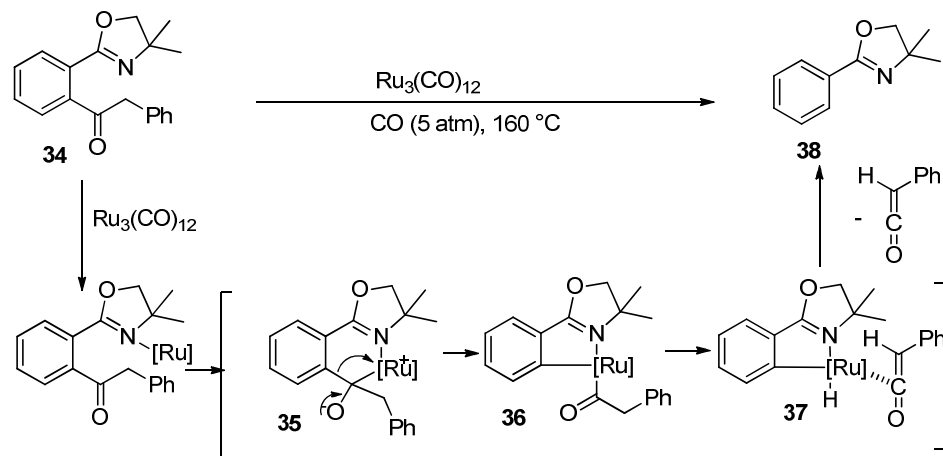
Murai et al¹⁷ demonstrated a similar type of decarbonylative C–C bond activation of the ketone **34**, bearing an oxazoline group as a directing group for a facile C–C bond activation. In this reaction, the removal of the acyl group might take place via β -hydrogen elimination and reductive elimination of the resulting ruthenium (II) hydride complex **37**, and removal of ketene resulted in the formation of decarbonylated oxazolidone **38**. The coordinated ruthenium attacks the carbonyl group to generate **35**, the first C-C bond cleavage to form **36**. An aryl group rearranges in **35**, then the five-membered metallacycle

36, is formed. The Ru-alkyl intermediate **36** undergoes β -hydrogen elimination, followed by reductive elimination, to give **38** and ketene.

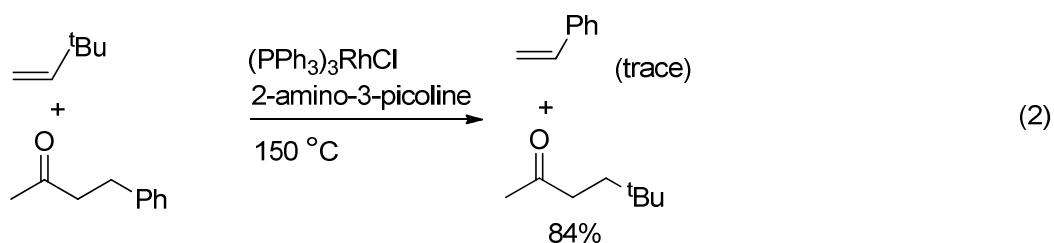


Scheme 1.8: Proposed Mechanism for the α -C-C Bond Cleavage of 8-Quinolinylyl Alkyl Ketone.

Jun reported a Rh-catalyzed C–C bond activation of unstrained ketones utilizing a chelation-assisted protocol, developed in the course of studies on a chelate-assisted hydroacylation using 2-amino-3-picoline **39** as a temporary chelating auxiliary.¹⁸ Interestingly, benzylacetone reacted with excess olefin, *tert*-butylethylene, under co-catalysts of Wilkinson’s complex and 2-amino-3-picoline to give an alkyl group-exchanged ketone and a trace of styrene [eq. (2)].

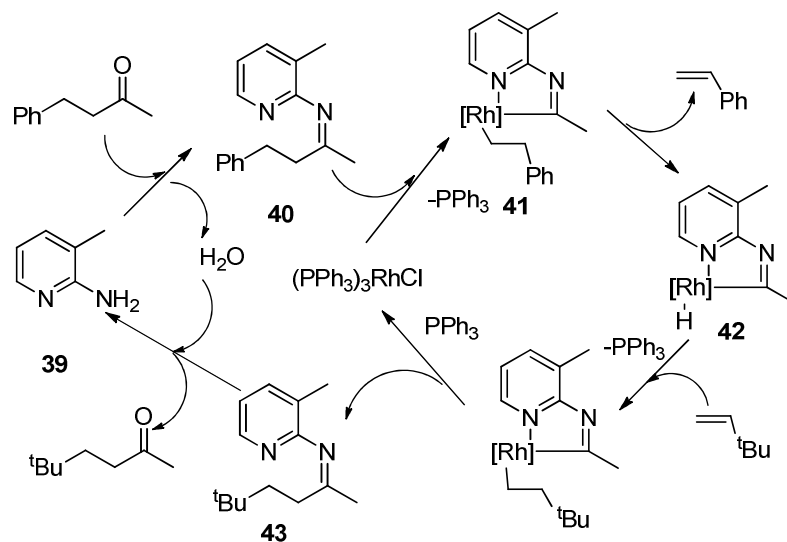


Scheme 1.9: Proposed Mechanism Decarbonylative C–C Bond Activation of Oxazolidine.



The first step involves the formation of ketimine **40** by the condensation of ketone and 2-amino-3-picoline **39** (Scheme 1.10).¹⁸ Then, the C–C bond of ketimine **40** is cleaved by the Rh(I) complex to generate an (iminoacyl)rhodium(III) phenethyl **41**, which undergoes β -hydrogen elimination giving an (iminoacyl)rhodium(III) hydride **42** and styrene. At high temperature, styrene is polymerized. The hydrometallation of into *tert*-butylethylene and the subsequent reductive elimination afford ketimine **43**. Hydrolysis of ketimine **43** by H_2O formed during the initial condensation step leads to the formation of ketone with regeneration of ligand **39**. The formation of a stable 5-membered ring metallacyclic complex is the driving force for this catalytic reaction, which undergoes

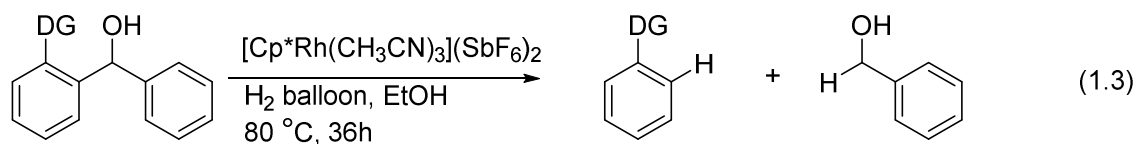
further energy release by β -hydrogen elimination and subsequent hydride insertion of **41** into 1-alkene.



Scheme 1.10: Proposed Mechanism for Chelate Assisted C-C Bond Activation Catalyzed by $(\text{PPh}_3)_3\text{RhCl}$.

Since the reaction is a thermodynamic equilibrium, the polymerization of styrene, one of the products, might drive a forward reaction.

Very recently, Shi¹⁹ reported reductive cleavage of the $\text{Csp}^2\text{-Csp}^3$ bond of secondary benzyl alcohol by Rh catalyst directed by pyridine and imidazole directing groups. [eq. (1.3)].

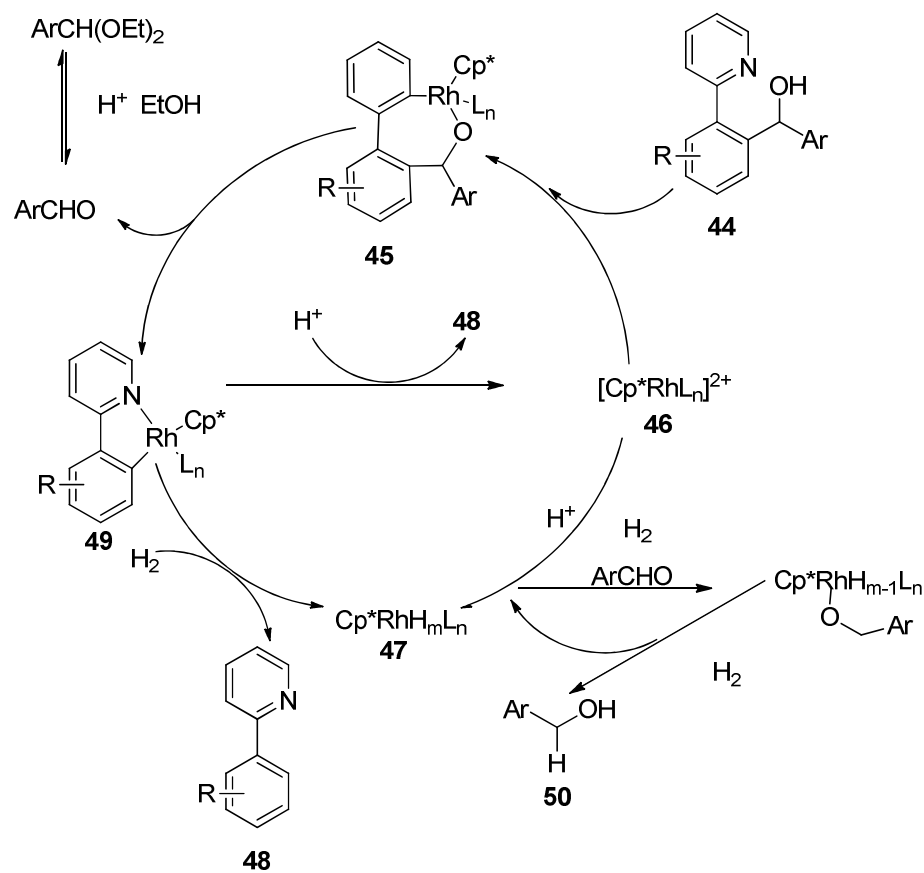


A possible mechanism is proposed in Scheme 1.11. First, the C-C bond of **45** is cleaved with the assistance of Rh(III) and thus the C-Rh species **49** is generated. The intermediate **49** could then be cleaved by H_2 to generate **48** and the Rh (III) hydride species **47**, which reduces the aldehyde to the alcohol **50**. Alternatively, **46** could undergo

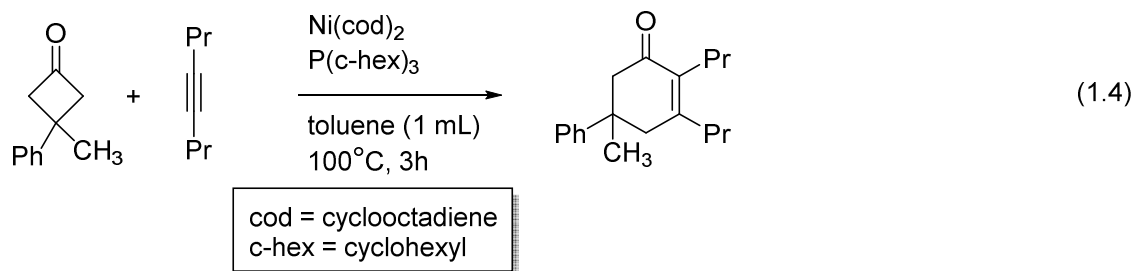
protonation with H^+ to regenerate the cationic Rh(III) species **49** for the C-C catalytic cycle. At this stage, they cannot exclude the conversion of the cationic Rh (III) precursor **49** into the Rh(III) hydride species **47**. The Rh(III) hydride species **47** could then promote both the C-C bond cleavage and reduction of the aldehyde in the same catalytic cycle.

1.1.2.4 Alkene/Alkyne Insertion Reactions via C-C Bond Cleavage

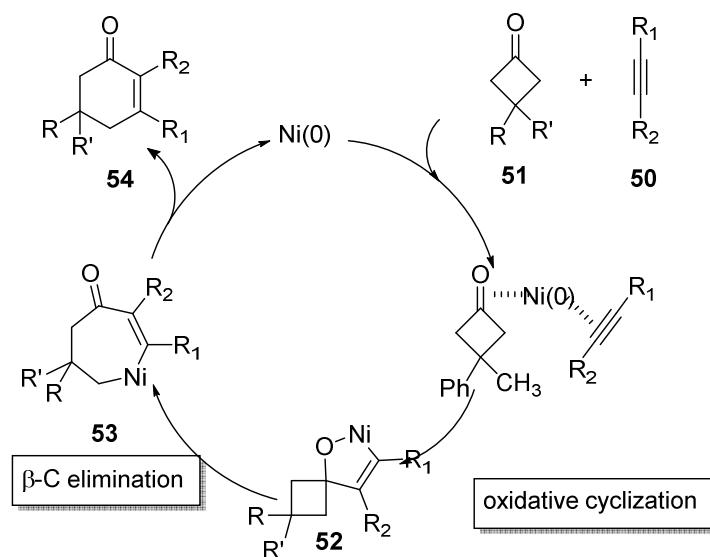
Matsuda group have been reported rhodium-catalyzed intra-molecular alkene insertion reaction using cyclobutanone derivatives.²⁰ Also they have been reported that the Nickel catalyzed intermolecular insertion of alkyne into cyclobutanones that achieves ring expansion of four membered ring skeletons by two carbons, producing substituted 2-cyclohexanones [eq. (1.4)]²¹.



Scheme 1.11: Proposed Mechanism for C-C Bond Cleavage of Secondary Benzyl Alcohol.



They proposed a mechanism that Oxanickelacyclopentene **52** is initially formed by oxidative cyclization of the carbonyl group of cyclobutanone **51** and an alkyne **50** with Ni(0). The 4-membered ring is then opened by β -carbon elimination, resulting in ring expansion to form seven membered nickelacycle **53**. Finally reductive elimination gives the product **54** with regeneration the species of Ni(0).



Scheme 1.12: Postulated Mechanism for the Ni-Catalyzed Intermolecular Alkyne Insertion into Cyclobutanone.

Despite such remarkable advances, chelate assisted catalytic C–C bond cleavage of arylsubstituted alcohols, ketones and nitriles,²² and Pd-catalyzed decarboxylation methods,²³ selective sp^3 - sp^3 C–C bond activation of unstrained aliphatic compounds is still remained as an enigmatic problem in homogeneous catalysis,²⁴ because the C–C bond

activation of unstrained saturated hydrocarbons is kinetically less favored than that of the C–H bonds.²⁵

1.2. Catalytic C-N Bond Activation Reactions

1.2.1 Heterogeneous Hydrodenitrogenation of Nitrogen Heterocycles

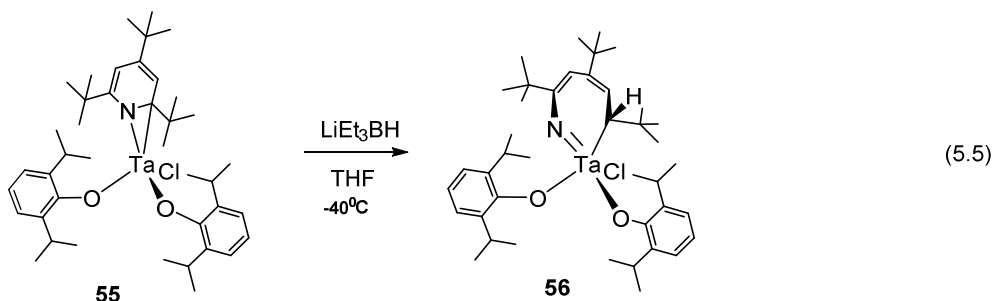
Catalytic hydrodenitrogenation (HDN) process, which removes nitrogen from petroleum feedstocks in the form of NH₃, provides more processable and environmentally compatible liquid fuels. Nitrogen removal is required to maintain NO_x emissions below regulatory levels due to maintain fuel stability.^{26,27}

Industrial HDN is generally affected over sulfided CoMo/ γ -Al₂O₃ or NiMo/ γ -Al₂O₃ under rather severe hydrogenation conditions (e.g. 350- 500 °C and 200 atm H₂) that ultimately remove the nitrogen as NH₃. Several non-molybdenum catalysts have also been used in HDN such as vanadium,²⁸ ruthenium sulfide,²⁹⁻³⁰ NiW/Al₂O₃ and NiW/zeolite,³¹ molybdenum nitrides.^{26b} Since most of the HDN studies were done by using metal catalyzed heterogeneous catalytic systems, the mechanisms of simple metal catalyzed HDN reactions are not well understood. In HDN reactions, most of the unsaturated N-heterocyclic compounds are converted to saturated N-heterocycles and amino compounds and finally to hydrocarbons by C-N bond cleavage.

1.2.1 Hydrodenitrogenation Reactions by Soluble Metal Complexes

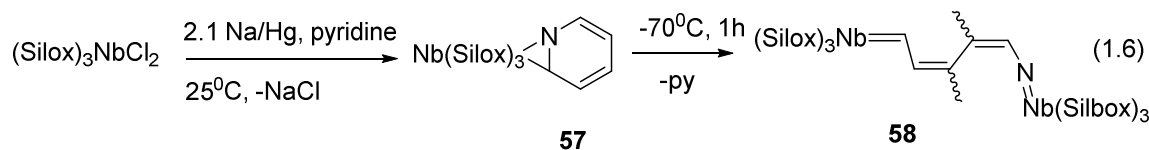
Hydrotreating and HDN is a principal H₂ consumer since achieving nitrogen removal typically occurs only after complete hydrogenation of all aromatic rings at heterocycles. As a result, HDN reactions are non-selective and lead to lower the quality of fuel. Homogeneous model studies have been prepared to address this question.²⁷ The goal

of C-N cleavage without prior hydrogenation of nitrogen containing heteroarenes was achieved by with substituted pyridine.^{27d, 32-34}

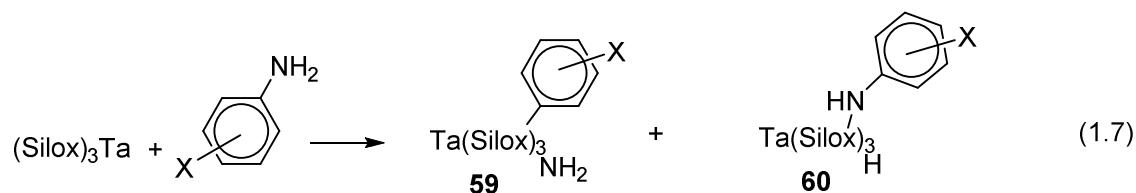


Upon reacting $\eta^2(\text{N,C})$ coordinated tris(*t*-butyl)pyridine ligand in starting complex **55** with 1 equiv of LiEt_3BH (THF, 20 h, room temperature), red crystalline **56** can be isolated in low yield after appropriate workup. Spectroscopic data consistent with hydride addition occurring at the metal-bound carbon of the $\eta^2(\text{N,C})$ -pyridine ligand as shown in eq. (1.5). Several of these complexes with Ta-R group has been isolated and fully characterized.^{27d} The formation of Ta=N multiple bond provides the driving force for the C-N bond cleavage of these reactions.

Wolczanski and co-workers have reported a remarkably selective pyridine C-N bond cleavage reaction.^{27c} Reduction of $(\text{Silox})_3\text{NbCl}_2$ (Silox= Bu^t_3SiO) with Na/Hg in the presence of pyridine [eq. (1.6)] gives $\eta^2(\text{N,C})$ -pyridine complex **57** followed by thermolysis gives ring opened product **58** in which the cleave C=N forms a Nb=C alkylidene complex with one Nb and Nb=N imido complex with the other. Isomerization of C=C double bond gives four different isomers. Although the mechanism is not known, this reaction suggested a new way to think C-N cleavage without first hydrogenation.



Wolczanki have been reported reactions of $(\text{Silox})_3\text{Ta}$ with series of substituted anilines [eq. (1.7)] to give products resulting from either C-N **59** or N-H **60** oxidative addition.³⁴ C-N oxidative addition product is favored by EWG whereas EDG gives exclusively N-H oxidative addition product. It is important that in these reactions cleavage of C-N even though the HDN of aniline requires hydrogenation of the arene ring before C-N cleavage occurs.



Parkin^{27f} reported the reactivity of $\text{Mo}(\text{PMe}_3)_6$ towards Pyrrole, indole and quinoline. They have observed the reaction of $\text{Mo}(\text{PMe}_3)_6$ three different coordination models (η^1 , η^5 and η^6) molecular structure of $(\eta^6\text{-indolyl})\text{Mo}(\text{PMe}_3)\text{H}$ has been characterized by X-ray diffraction. The observation of $\eta^6\text{-indolyl}$ is particularly interesting because indolyl ligand typically binds either η^1 - through N or η^5 -manner through 5-membered heterocycle. Even for heterocyclic compounds like quinoline with $\text{Mo}(\text{PMe}_3)_6$ forms $[\eta^6\text{-(C}_5\text{N)-quinoline}]\text{Mo}(\text{PMe}_3)$ which react with H_2 at 80°C to give inter alia $\text{Mo}(\text{PMe}_3)\text{H}_4$ and release 1,2,3,4-tetrahydroquinoline, the product of selectively hydrogenating heterocyclic ring^{27e}

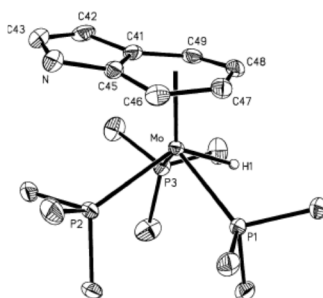
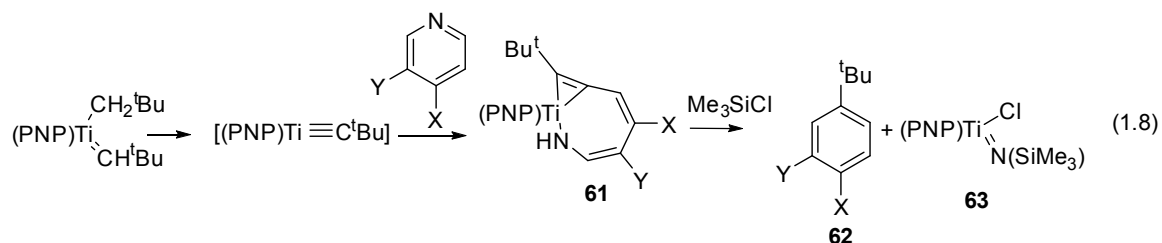
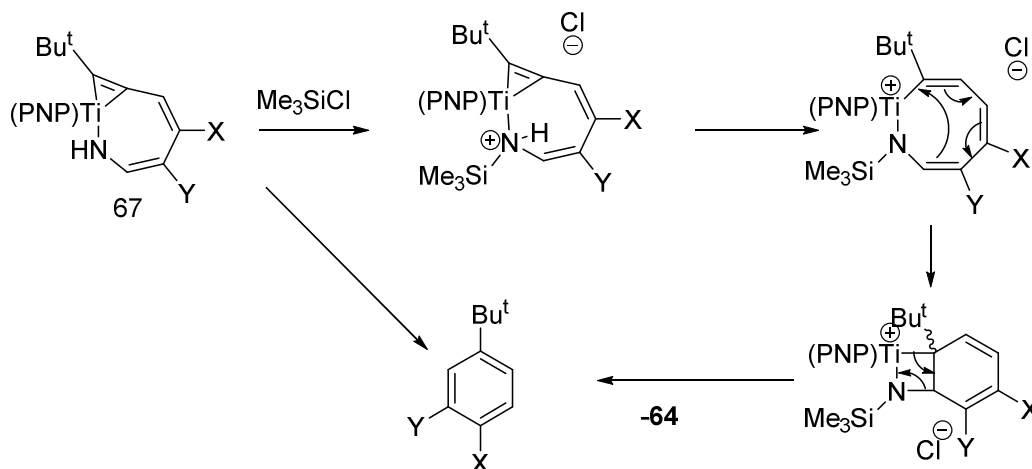


Fig 1: X-ray Structure of (η^6 -Indolyl)Mo(PMe₃)H Adapted from Reference 27(f).

Mindiola recently found that (PNP)Ti=CH^tBu(CH₂^tBu) (PNP = N[2-P(CHMe₂)₂-4-methylphenyl]₂) can ring-open both pyridine and picoline at room temperature over 12h to afford azametallabicyclic system **61** of type (PNP)Ti(C-(Bu^t)CC₄H₃RNH). They have reported that pyridine nitrogen of complex (**61**) can be denitrogenated under mild conditions and in a cyclic manner when treated with electrophile such as Me₃SiCl. [eq. (1.8)]



They proposed a mechanism of denitrogenation reaction (Scheme 1.13). The first step of **65** has been proposed to occur first by silylation of α -nitrogen composing to azametallabicyclic ring, followed by a ring expansion applying a 1,3-hydrogen shift to afford the eight membered ring intermediate. And then ring contract to generate bicyclic system and [2+2] retrocyclo-extrude the substituted arene product **64** as shown in Scheme 1.13.



Scheme 1.13: Proposed Mechanism for Denitrogenation of N-heterocycle by Ti Catalyst.

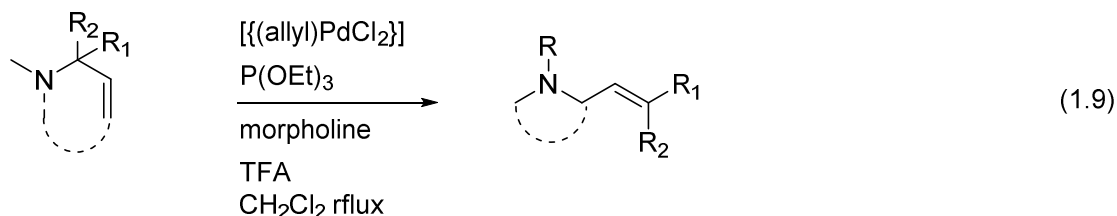
1.2.2. Catalytic Deaminative C-N Cleavage Reactions

The nitrogen containing compounds such as amines, amides, enamines and imines are valuable and commercially important precursors for organic synthesis and medicinal chemistry. Therefore making and breaking of sp^3 C-N bond in the construction of functional molecules are important steps in the synthesis of pharmaceutical and polymers.^{35,2} C-N bonds are generally quite inert towards strong acid, base, metal salts and most of synthetic reagents including oxidants and reductants.³⁵ The synthetic application of breaking or cleavage of C-N bond to form C-C or C-heteroatom bond is one of the challenging topics in organic synthesis. Catalytic breaking of C-N had a long history and the past years have been significant research attention focused on breaking C-N bond to form new compounds.²

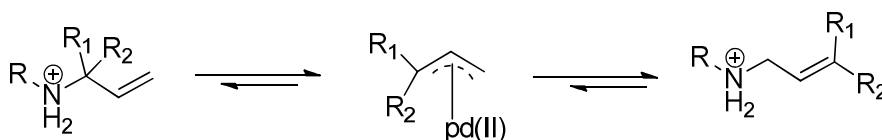
1.2.2.1 C-N Bond Cleavage of Allylic Amines

In an early study it has shown that the C-N bond of porphyrin is susceptible to cleavage by $Ru_3(CO)_{12}$.³³ Recent work have shown that transition metal complexes³⁴, as well as Bronsted acids³⁵, and Lewis acids³⁶ were able to facilitate C-N bond cleavage,

where amino or amide group has been served as leaving groups towards a range of nucleophiles. Recently, Zhang has reported Tsuji-Trost type Pd-catalyzed allylic alkylation of cyclohexanone by breaking very strong C-N bond of allylic amines.³⁷ Hirao and Yamamoto reported that Pd-catalyzed allylic alkylation of allylic amine using allylic ammonium cation as a lacy intermediate.³⁸ Aggawal and Trost adopted a vinyl aziridine to cleavage of C-N bond of allylic amine by means of minicyclic tension.³⁹ More recently, Tian reported that cross coupling of primary allylic amines with Boronic acid and boronates through Pd catalyzed C-N bond cleavage.⁴⁰⁻⁴¹ Yudin showed that Pd catalyzed ring contraction and ring expansion of cyclic allyl amines. In this isomerization reactions $[\{(allyl)PdCl\}_2]$ used as the catalyst for C-N bond cleavage, $P(OEt)_3$ as ligand, presence of TFA, 10% morpholine and CH_2Cl_2 as solvent [eq. (1.9)].⁴²

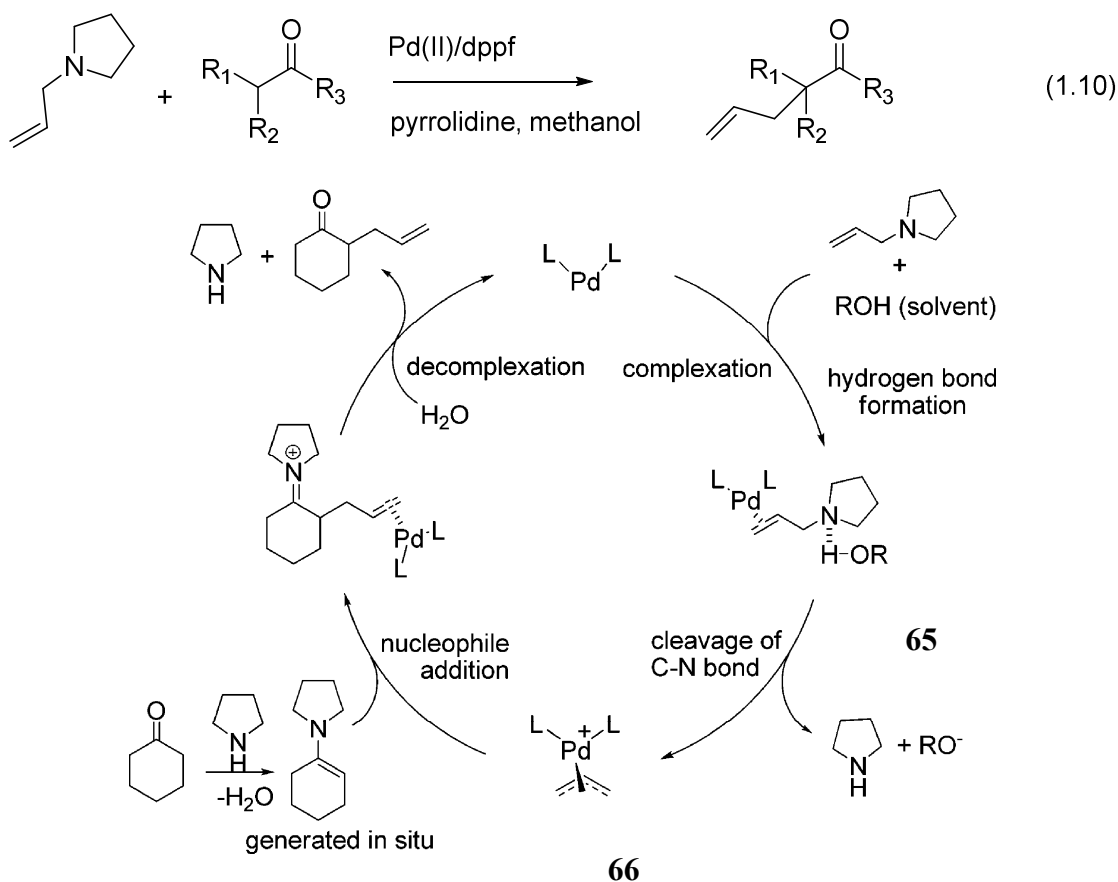


They have shown several examples of ring-contraction reactions of seven and eight membered allylic amines and ring expansion of allylic aziridine. It is envisioned straight forward access to complex allylic amine by skeletal isomerization of readily accessible cyclic allylamine sinfolds (Scheme 1.14)



Scheme 1.14: Isomerization of Allylic Amine Promoted by a Combination of Palladium and Protic Acid.

Zhang group reported that the hydrogen bond promoted C-N bond cleavage at allyl amines using Pd(II) as the catalyst. They have used very mild conditions (only alcohol as the solvent) [eq. (1.10)].³⁷ They used 6 mol % of dppf and 2.5 mol % $[\text{Pd}(\eta^3\text{-C}_3\text{H}_5)\text{Cl}]_2$ as catalyst and pyrrolidine which supposed to be hydrogen bonded and generates enamines insitu as nucleophiles (Scheme 1.15).

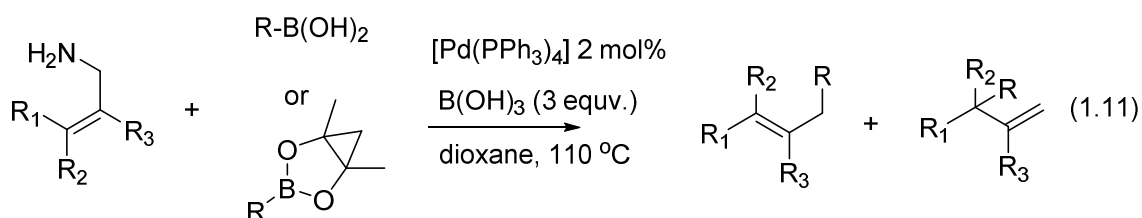


Scheme 1.15: Plausible Reaction Mechanism Pd Catalyzed Allylic Alkylation.

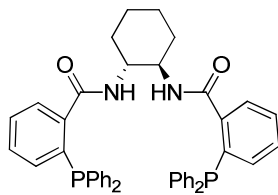
The proposed mechanism begins with coordination of the Pd-catalyst to the allyl double bond to form a Pd-olefin complex **65**. At the same time a hydrogen bond forms between N-atom of N-allylpyrrolidine and the H atom at the alcohol solvent. The C-N bond of N-allylpyrrolidine is thus activated by this hydrogen bond action, resulting in cleavage

of the C-N bond and subsequent formation of Pd allylic complex **66**. The complex is then attacked by the enamine generated insitu, followed by removal of the Pd catalyst to give the C-C bond product.

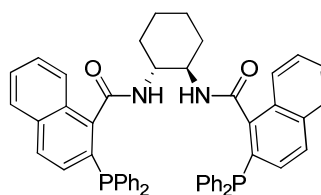
Recently Tian reported ⁴⁰ regio- specific cross coupling of primary allylic amine with boronic acids which involves amino group as the leaving group. They used 5 mol% of Pd(OAc)₂ or [Pd(PPh₃)₂Cl₂] catalyst, B(OH)₃ additive and dioxane as the solvent.[eq. (1.11)]



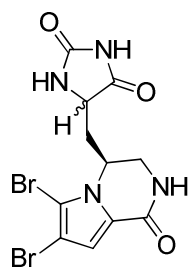
In the presence of 2 mol% of [Pd₂(dba)₃] and 8 mol% of TMEDA, a range of α -chiral primary allylic amines smoothly couple with boronic acid to give optically active alkenes in moderate yields. The proposed a reaction pathway, which the NH₂ group of amine activated by boronic acid and the allylic C-N bond is cleaved by Pd(0) catalyst with inversion of configuration to give π -allylpalladium. Dong ⁴¹ and coworkers also successfully used Pd(0) catalyst to synthesis biologically active indole and pyrroles using chiral ligands **L1** and **L2**. They have shown that vinylaziridines and pyrroles or indole derivatives can be used to synthesis alkaloids such as cyclocordin, agesamide A and Cyclooroidin.



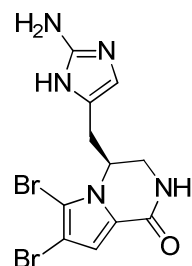
(R,R)-L1



(R,R)-L2



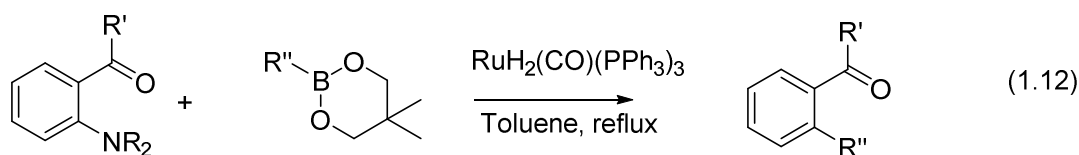
Agesamide A



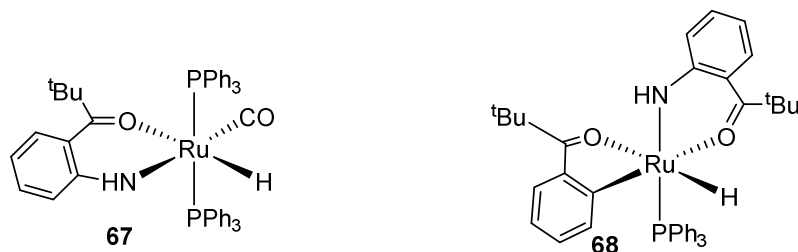
cyclooroidin

1.2.2.2. C-N Cleavage of Arylamines

MacMillan and coworkers documented the first Suzuki cross-coupling of aryltrimethylammonium salts. $\text{Ni}(\text{cod})_2$ catalyst was used in the presence of IMes.HCl as the ligand in dioxane as the solvent at 50°C .⁴⁴ In 2009, Kakiuchi reported the cleavage of C-N bond in aniline derivatives using ruthenium complex as catalyst. O-arylanilines were used as substrate and coupling reactions with various organoboronic acid esters proceeded using $\text{RuH}_2(\text{CO})(\text{PPh}_3)_3$ as a catalyst. [eq. (1.12)]⁴³

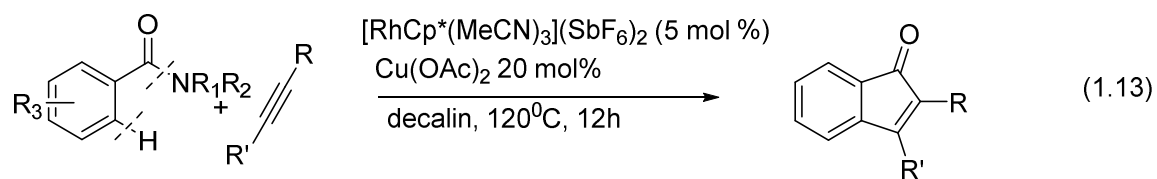


As they proposed in mechanism this is the first reported oxidation of arene C-N bond. And then trans metallation between the Ru amide complex and organoboronate and finally reductive elimination to form C-C bond. They were able identify isolate and characterized C-N oxidatively added intermediates **67** and **68**.



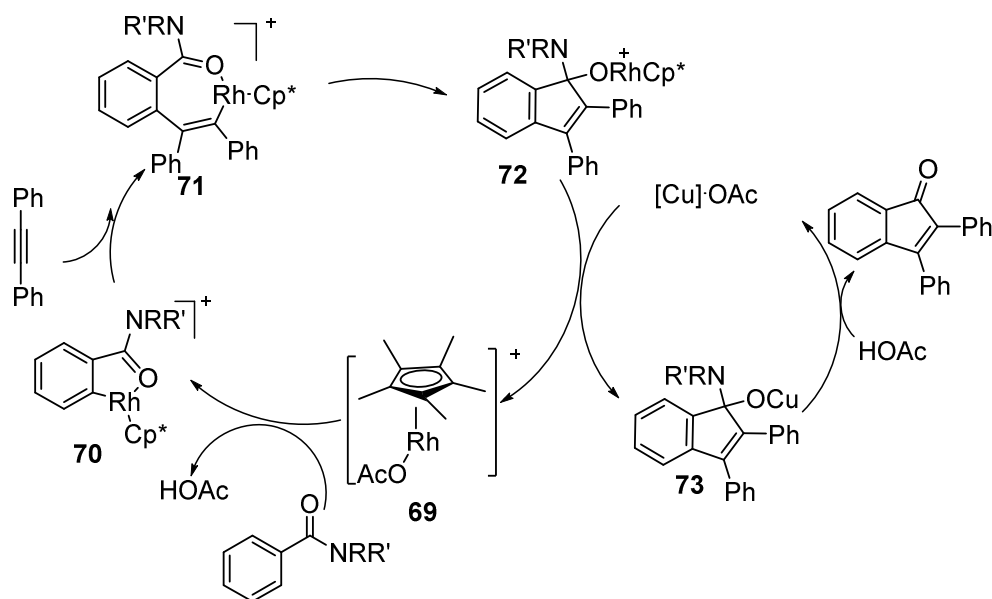
1.2.2.3 C-N Bond Cleavage of Secondary and Tertiary Amines

Catalytic free alkylation of sulfinic acid with sulfonamide via sp^3 C-N bond cleavage was reported by Tian⁴⁵, and also α -alkylation of ketone and aldehyde with N-benzylic sulfonamide through C-N bond cleavage was reported.⁴⁶ In 2010 Tian published⁴⁶ iron catalyzed regioselective synthesis of indene derivatives from N-benzylic sulfonamides and disubstituted alkynes. And also very recently Shi and coworkers established similar reaction with a rhodium(III)-catalyzed annulations of benzimides with alkynes for the synthesis of indenones which involves an uncommon acylation of organorhodium(III) with an imide motif [eq. (1.13)].⁴⁸



Only few transition metal catalyzed C-N bond cleavage reactions in amides or imides have been reported. Shi reported that the reaction of an organometallic reagent with ester or amide generates a ketone product which is typically more reactive than the starting material. They have successfully used oxazolidone as the best amide leaving group. Different substituent on aromatic rings, alkynes are used and electron-donating groups at the *para*-position of the aryl ring slightly decreased the yield, presumably because of the decreased electrophilicity of the imide which slows the addition of the C-Rh intermediate

to the carbonyl group. Functional groups such as methoxy and halide groups on alkyne were tolerated. An aryl alkyl alkyne, however, exhibited lower reactivity. Coordination of benzimide to the cationic rhodium species **69** and subsequent C-H cleavage forms the five-membered rhodacycle **70**. (Scheme 1.16) Then alkyne insertion gives the seven-membered intermediate **71**, which undergoes an intramolecular insertion of the carbonyl group into the vinyl-Rh bond. Transmetalation between copper acetate and the rhodium alkoxide **72** takes place to regenerate the catalyst with formation of the copper alkoxide **73**, which decomposes to form the product and release the copper species. The beneficial effect of copper salt may also originate from the increased electrophilicity of imide moiety upon coordination with copper, thus facilitating the insertion of the carbonyl group into the C-Rh bond.

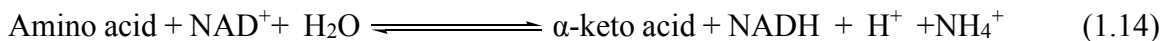
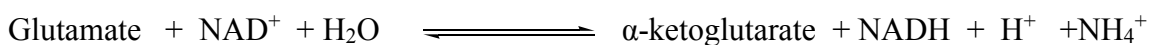
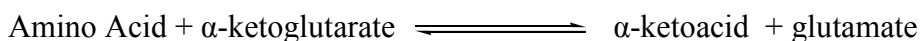


Scheme 1.16: Proposed Mechanism for Rh/Cu Catalyzed Anulation of Benzimide and Alkyne.

Hu and coworkers⁴⁹ reported Pd-C catalyzed N-debenzylation of benzylamines. Benzylamines are major protective group for amines in multistep synthesis, where N-debenzylation is an essential conversion for the deprotection and to remove auxiliary residues from the induced molecule. Lactams also responsible for C-N bond cleavage under catalytic conditions. Aube⁵⁰ reported that reductive cleavage of C-N bond of seven membered twisted amides by using Pd/C as the catalyst. None of the product resulting from reaction of the C-N bond in six membered rings was observed. The result was obtained once they used Pearlman's catalyst (Pd(OH)₂) in ethanol.

1.2.2.4. Biochemical Deamination Reactions.

The first step of amino acid catabolism in biological system is deamination which is removal of amino group of α -amino acids. One of the deamination methods in biological system is trans-amination with α -ketoglutarate to form α - keto acids and glutamate. The glutamate is oxidized to α -ketoglurate and ammonia by action of mitochondrial glutamate dehydrogenase. ([eq. (1.14)], Fig 2)⁵¹



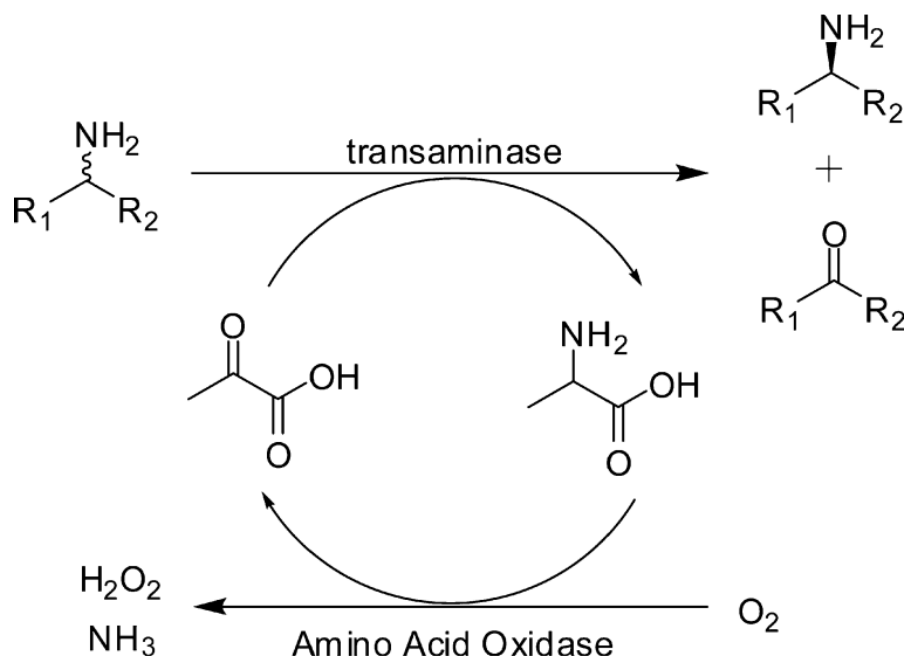


Figure 1.1: Combination of D-amino acid Oxidase and L-glutamate Dehydrogenase (Glu-DH).

The amide group of Gln and Asn are hydrolyzed by specific enzymes glutaminase and Asparaginase respectively to produce NH₃ and corresponding dicarboxylic acid Glu and Asp. Ammonia formed from amide and amino group that is not used for synthetic reactions is excreted as urea in most terrestrial animals and as NH₃ in aquatic animal.⁵⁰

Oxidative deamination of amines can be catalyzed by a number of different enzymes including monoamine oxidase, horse radish peroxidase, hemoglobin cytochrome P450.⁵² Korzekwa proposed the mechanism of oxidative dealkylation of substituted N,N-dimethyl anilines by Cyt-P450.⁵³ Lap established Oxidative N-dealkylation of tertiary amines.⁵⁴ Lippard reported oxidative N-dealkylation of a carboxylate bridged diiron(II) precursor complex by reaction of oxygen affords the elusive {Fe(μ-OH)₂(μ-O₂CR)}³⁺ core of soluble methane monooxygenase hydrogenase.⁵⁵

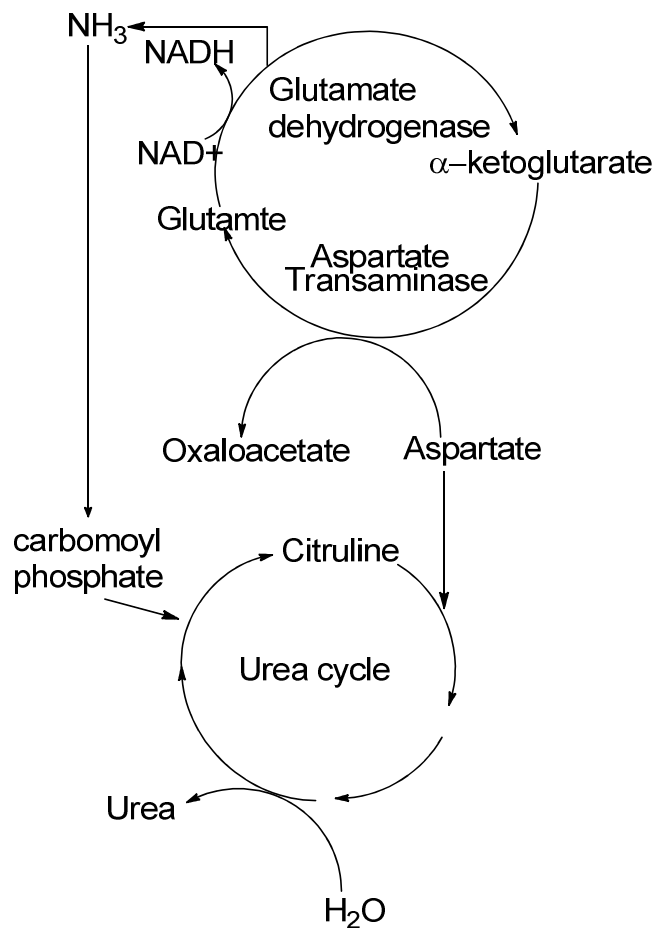
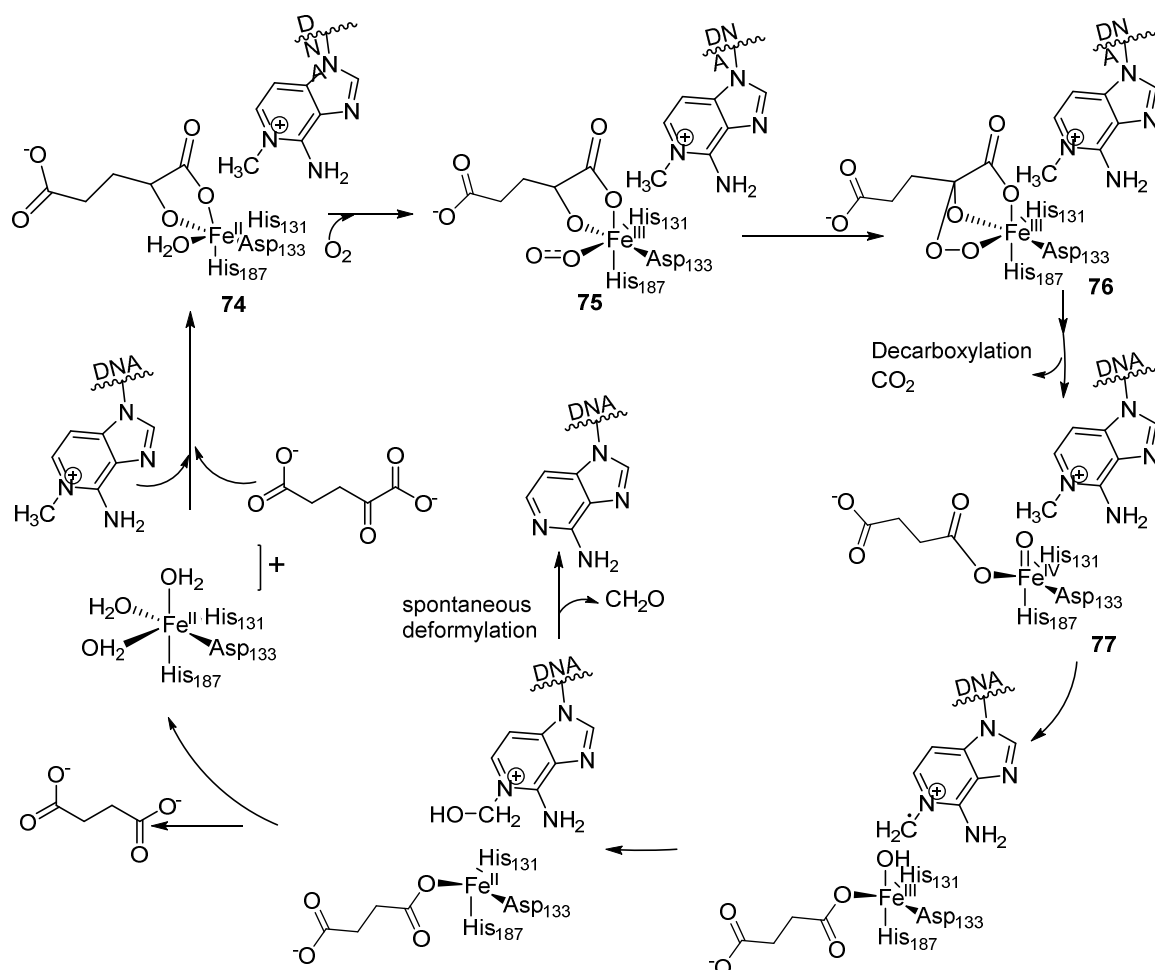


Figure 1.2: Balancing the Supply of Nitrogen for Urea Cycle when Aspartate in Excess.

Aberrant DNA methylation can be led to cytotoxic or mutagenesis consequences.⁵⁶ A DNA repair protein in *E. coli*, AlkB, corrects some of the unwanted methylations in which methyl carbon is liberated as formaldehyde. He reported that mechanism of oxidative demethylation of DNA base lesions. 1-methyl adenine and 3-methylcytosine by AlkB Fe(II). AlkB uses a non heme-mononuclear iron (II) **74** and cofactor α -ketoglutarate and dioxygen to effect oxidative demethylation of DNA base lesions 1-methyladenine (1-meA), 3-methylcytosine (3-meC), 1-methylguanine (1-meG) and 3-methylthymine (3-meT). In the event of oxidation reactions, AlkB utilizes an

iron(II) site, which is coordinated by the conserved His2/Asp motif, to activate the dioxygen molecule for oxidation of the inert C-H bond.

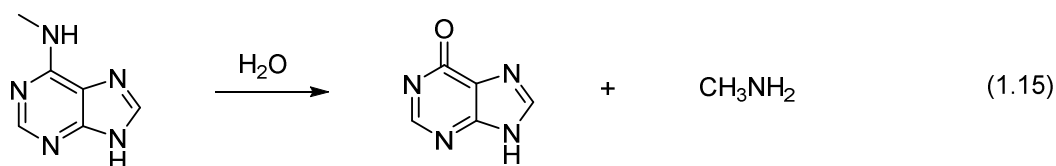


Scheme 1.17: Proposed Repair Mechanism for AlkB-family Proteins.

A possible mechanism involves formation of a superoxo radical anion (O₂⁻) bound to iron(III) 75, a subsequent bridged peroxo intermediate 76 produced by the attack of the superoxide to the R-keto carbon of an iron-bound 2-KG, and a speculated high-valent iron(IV)-oxo 77 intermediate that hydroxylates the C-H bond of the methyl lesion. One of

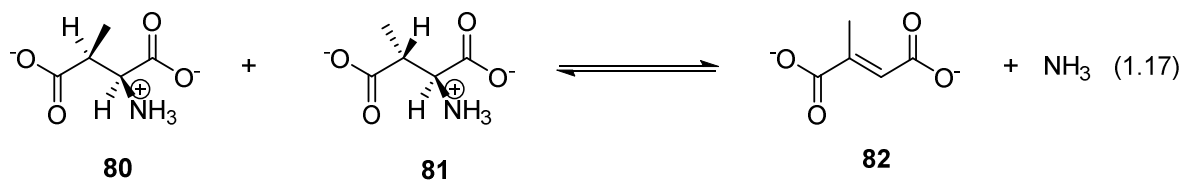
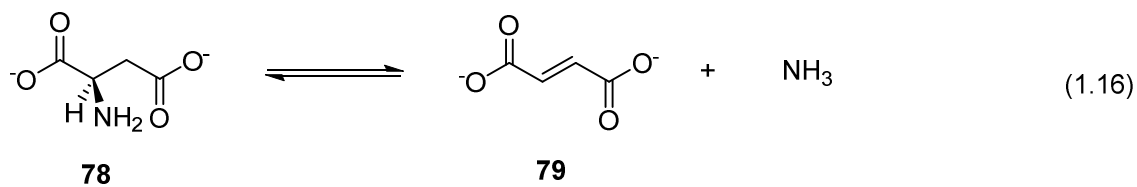
the oxygen atoms from the dioxygen cofactor is incorporated into succinic acid and the other becomes the oxygen of the hydroxyl product (Scheme 1.17). In the case of AlkB, the initial hydroxylation at the methyl group on the N¹-position of adenine or N³-position of cytosine leads to the heterocleavage of C-N bonds, which gives the unmodified base and formaldehyde.

Several deamination enzymes from biologically systems have been identified and characterized well.⁵⁷ Raushel has been reported that 6-N-methyladenine can be deaminase to produce adenine and methylamine by the enzyme N-6-Methyladenine deaminase (6-MAD) [eq. (1.15)] but the mechanism is unresolved.⁵⁹

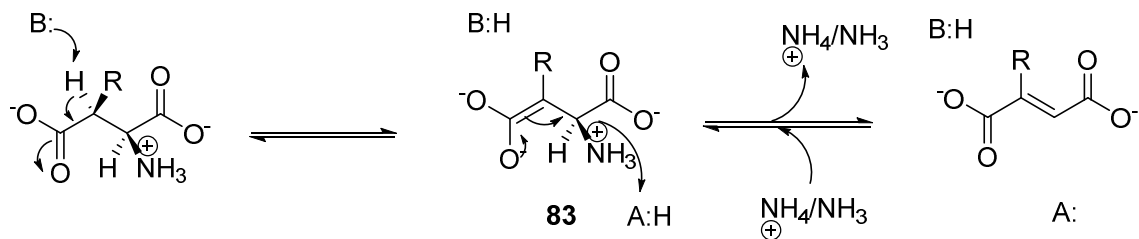


Also deamination of isoguanine to xanthene by Isoguanine demainase⁵⁸ and deamination of isoxanthopterin to 7-oxylumazine by isoxanthopterin deaminase were reported.^{51a}

Ammonia lyases are another kind of deamination enzymes found in biological system.⁶⁰ These are capable of cleaving C-N bonds without employing any hydrolysis or oxidation mechanism. Among various lyases found in nature three types of are specific for aspartate or its derived substrates. They are Aspartate ammonia lyase (aspartase), methyl aspartate ammonia lyase (MAL), and 3-hydroxyaspartate ammonia lyase.⁶¹ Aspartate ammonia lyase is very important in nitrogen metabolism of microbes by catalyzing the reversible deamination of L-aspartate **78** into fumarate **79** and ammonia [eq. (1.16)]. 3-Methylaspartate ammonia lyase (MAL) catalyses the reversible α , β -elimination of ammonia from L-threo-3-methylaspartate **80** and L-erythro-3-methylaspartate **81** to mesaconate **82** [eq. (1.17)].



General acid base reaction mechanism was proposed for aspartates (Scheme 1.18). The active site general base abstracts the pro-R proton from the C3 position of **81** resulting in a carbanion, which is stabilized as an aci-carboxylate intermediate (**83**). This proposed enolate anion intermediate can rearrange to eliminate ammonia and form the product, fumarate (**82**). The rate-determining step is the cleavage of the C α -N bond, which may be facilitated by a general acid that donates a proton to the leaving group (NH₃) to form an ammonium ion.



Scheme 1.18: Mechanism of Aspartate Deamination by Lyases.

CHAPTER 2

TRANSITION METAL CATALYZED C-O BOND ACTIVATION REACTIONS

2.1 Transition Metal Catalyzed Hydrogenolysis of Carbonyl Compounds.

2.1.1 Classical Carbonyl Reduction Methods

The elimination of oxygen functional groups is a highly valuable transformation in fine chemicals synthesis. In particular, the carbonyl to methylene conversion is especially useful for converting polyfunctional natural products into useful building blocks or into bioactive molecules. There is a great need for new methodologies for promoting selective deoxygenation because such methods are useful for the conversion of polyfunctional natural products to useful building blocks and bioactive molecules. A few classical methods Clemmensen¹ or Wolff-Kishner reduction,² have been developed but for carbonyl deoxygenation methods to aliphatic compounds both of which require very harsh reaction conditions.

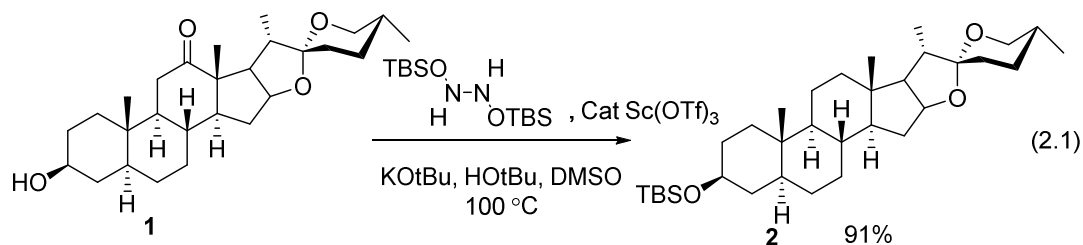
2.1.2 Wolff-Kishner Reduction

Wolff-Kishner reaction requires condensation of the carbonyl compound with hydrazine forms the hydrazone, and treatment with strong base induces the reduction of the carbon coupled with oxidation of the hydrazine to gaseous nitrogen, to yield the corresponding aliphatic product. Even though the Wolff-Kishner reduction used harsh conditions, it has been successfully applied to the total synthesis of several organic molecules such as morphine,³ aspidospermidine,^{4,5} and dysidiolide.⁶ Several modifications

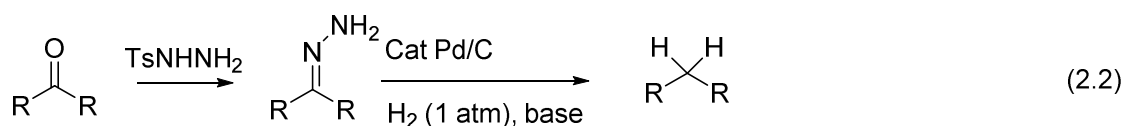
have been made to Wolff-Kishner reduction over the decades. Huang-Minlon reported a modified procedure for the Wolff-Kishner reduction of ketones in which excess hydrazine and water were removed by distillation after hydrazone formation.⁷ Significantly reduced reaction times and improved yields have been obtained by using this modification. Cram has modified the reaction condition by slow addition of preformed hydrazones to potassium *tert*-butoxide in DMSO as reaction medium instead of glycols allows hydrocarbon formation to be conducted successfully at temperatures as low as 23 °C.⁸ Treatment of tosylhydrazones with hydride reagents to obtain the corresponding alkanes is known as the Caglioti reaction.⁹

2.1.2.1 Catalytic Modification to Wolff-Kishner Reduction

In 2004, Myers and coworkers developed a novel catalytic method for the preparation of *N-tert*-butyldimethylsilylhydrazones from carbonyl-containing compounds.¹⁰ These products can be used as a superior alternative to hydrazones in the transformation of ketones into alkanes. The advantages of this procedure compare to Wolff-Kishner method are considerably milder reaction conditions and higher efficiency as well as operational convenience. The condensation of 1,2-bis(*tert*-butyldimethylsilyl)-hydrazine with aldehydes and ketones with Sc(OTf)₃ as catalyst is rapid and efficient at ambient temperature. Formation and reduction of *N-tert*-butyldimethylsilylhydrazones were conducted in a one pot procedure to give the product in high yield. As shown in eq. 18, steroidal ketone **1** can be converted to TBS protected alcohol contained steroid **2** in high yield [Eq. (2.1)].



They showed a broad substrate scope including benzylic aldehyde, benzylic ketone, aliphatic aldehyde, aliphatic ketone, protected sugar and unsaturated aldehyde contained double bonds without reducing C=C double bond. However, the use of freshly prepared dry solvents, the risk of detonation during the distillation of anhydrous TBSHs, and the tenuous operations might limit its applications in large scale synthesis.



Jianbo Wang group 2013 added a modification to the Wolf-Kishner reduction.¹¹

They were able to develop a catalytic method to deoxygenate ketones and aldehydes by using a mild and efficient method. The reaction is mediated by N-tosylhydrazine with H₂ (1 atm) as the reductant and 10% Pd/C as the catalyst [Eq. (2.2)].

This reaction involved a one-pot, two-step deoxygenation of carbonyl to methyl or methylene, which involve hydrogen as a clean reductant. Carboxylic acids, aromatic amines, benzylic alcohols, ethers, esters and halides are tolerated for these conditions. But they also were unable to avoid use of hydrazine.

2.1.3 Clemmensen Reduction

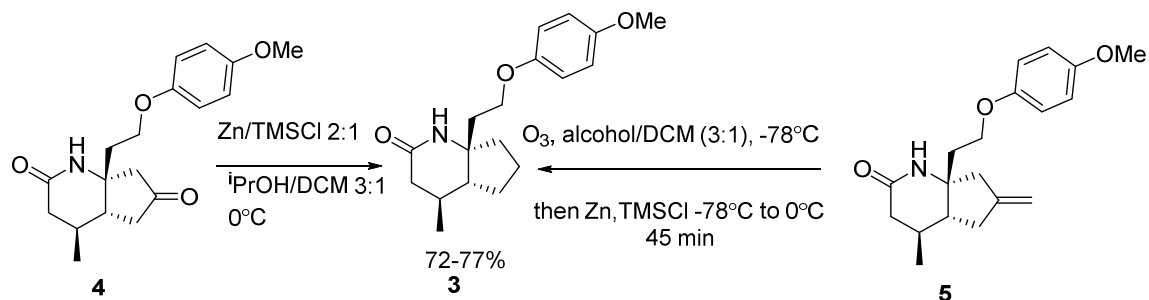
The well-known Clemmensen reduction is a general method in which aryl alkyl ketones are readily converted to the corresponding hydrocarbons by using amalgamated zinc and hydrochloric acid. However, it is not particularly effective, with alicyclic and

aliphatic ketones. and less reliable for unconjugated ketones. Normally reaction runs with hot conc. HCl in ethanolic solvent [Eq. (2.3)].



The Clemmensen reduction is particularly effective for reducing aryl-alkyl ketones.¹² With aliphatic or cyclic ketones, zinc metal reduction is much more effective.¹² Clemmensen reduction is a historically important reaction. However, because of its original harsh conditions (aqueous HCl, reflux) and use of toxic Hg reagent, it is seldom applied in the modern organic synthesis but few examples are available in recent literature.¹³ In late 1960s, Yamamura *et al.* developed an excellent modification of the Clemmensen reduction with a very mild condition (activated zinc, saturated HCl in Et₂O at 0 °C), which avoids the utility of toxic Hg.¹⁴

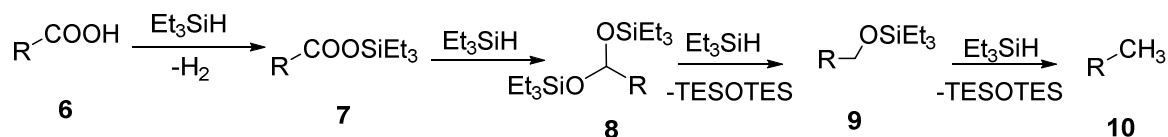
Arimoto in 2010 developed the most recent modification to the Clemmensen reduction.^{13a} They used TMSCl with the combination of Zn in in alcoholic solvents for the reduction. They were able to reduce steroidal carbonyl compounds to corresponding methylene by using milder conditions. Also they used the similar protocol to ozonolysis and reduce exocyclic double bond to methylene (Scheme 2.1). They were able to reduce ketone **3** to methylene compound **4** and also able to synthesis the same molecule by ozonolysis of **5**.



Scheme 2.1: Zinc Promoted Reduction of Ketone and Ozonolysis of Alkene

2.1.4 Reduction of Ketone/Aldehydes Using Aluminum, Silane Reagents

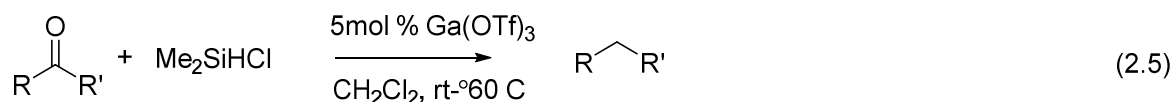
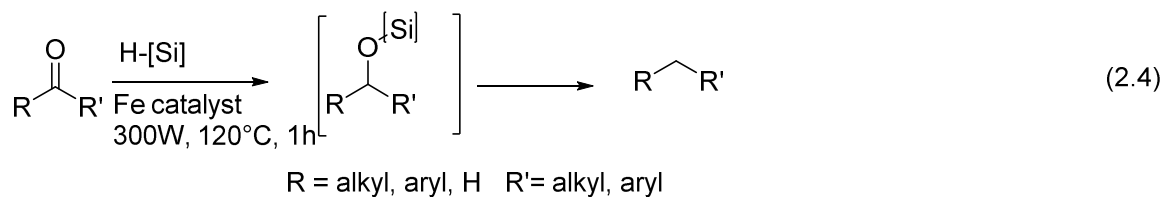
Tashiro *et al* in 2003, reported the reduction of carbonyl group to corresponding methylene with Ni-Al alloy in water.¹⁴ Dixon *et al*¹⁵ (1959) reported hydrogenolysis of 6-hexylbenzanthrone using LiAlH_4 as the reducing agent. Boleslawski¹⁶ in 1992 reported reductive deoxygenation of ketone and secondary alcohols by organoaluminum Lewis acids. Few of the carbonyl reduction articles are reported using organosilanes as the reducing agents.¹⁷ Yamamoto *et al*^{17a} reported the first examples of an efficient direct transformation of the aliphatic carboxylic acid, aldehyde, acyl chloride and ester function into the methyl group by using HSiEt_3 in the presence of a catalytic amount of $\text{B}(\text{C}_6\text{F}_5)_3$. An exhaustive reduction of aliphatic carbonyl groups into the hydrocarbons and partial reduction of their aromatic counterparts, as well as aromatic carboxylic acids, have been developed. Carboxylic acid **6** reacts with triethylsilane to produce triethylsilyl ester **7** and triethyl silyl acetal **7** by further reacting with one more molecule of triethylsilane. **8** react with another silane molecule and removal of di(triethylsilyl) ether produces alkyl silyl ether **9**. **9** further react with triethyl silane produces alkane **10** by removing another molecule of di(triethylsilyl)ether. (Scheme 2.2)



Scheme 2.2: Reduction of Carboxylic Acid into Alkane

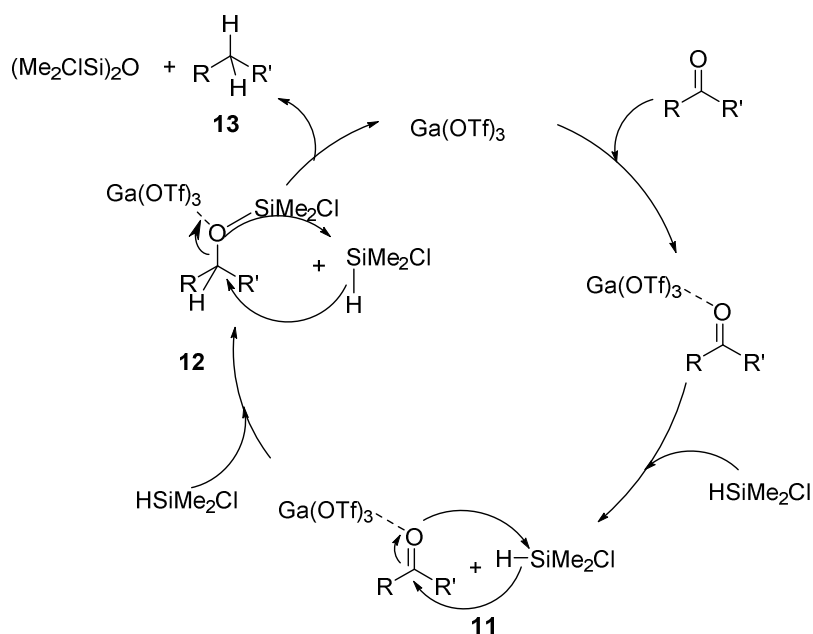
2.1.5 Homogeneous Catalytic Reduction Methods

Campagne group established a method to reduce ketones and aldehydes to alkane compounds using FeCl_3 Lewis acid as a catalyst (10 mol %) in the presence of PMHS as the reducing agent at 120 °C microwave irradiation.¹⁸ They believe that the reduction goes through the Lewis acid character of iron salts promotes the reduction of intermediate O-silyl ether [Eq. (2.4)]. Olah has been reported similar method using $\text{Ga}(\text{OTf})_3$ as the catalyst¹⁹ to deoxygenate aromatic ketones [Eq. (2.5)]. Both cases mechanisms are similar (Scheme 2.3).

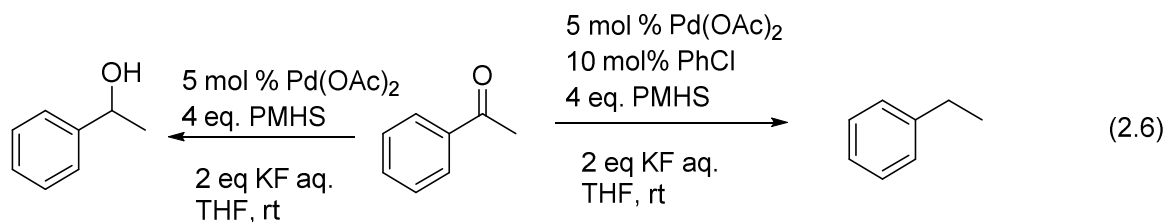


In 2010, Morris Bullock²⁰ reported a homogeneous Ru catalyzed reduction of aryl ketone to methylene compounds. In the presence of 1.5 mol% of $\{[\text{Cp}^*\text{Ru}(\text{CO})_2]_2(\mu\text{-H})\}^+\text{OTf}$ in CD_2Cl_2 under 4 atm H_2 heat at 85 °C for 4 days, acetophenone was cleanly converted to ethylbenzene. The substrate scope only limited to acetophenone and other ketones gives corresponding alcohols.

Most recently, Maleczka²¹ reported C-O hydrogenolysis catalyzed by Pd-PMHS nanoparticles in the accompany of chlorobenzene. Catalyst Pd(OAc)₂ and polymethylhydrosiloxane (PMHS), in conjunction with aqueous KF, and a catalytic amount of an aromatic chloride, led to the chemo-, regio-, and stereoselective deoxygenation of benzylic oxygenated substrates at room temperature. Preliminary mechanistic experiments suggest that the process involved palladium–nanoparticle-catalyzed hydrosilylation followed by C-O reduction. The chloroarene additive appears to facilitate the hydrogenolysis process through the slow controlled release of HCl. Substrate scope is limited to benzylic ketones.



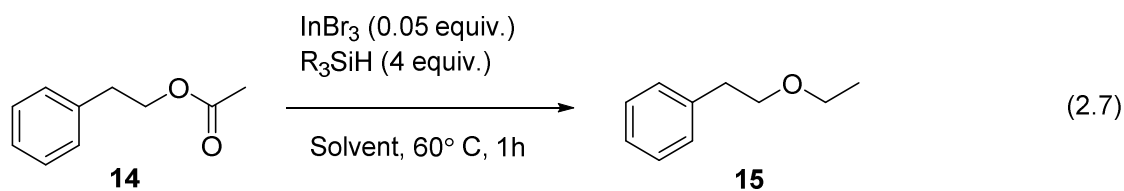
Scheme 2.3: Mechanism of Ga(OTf)₃ Catalyzed Reduction of Ketone by Silane.



They have shown that without chlorobenzene acetophenone converted to 1-phenylethanol under same reaction condition [Eq. (2.6)].

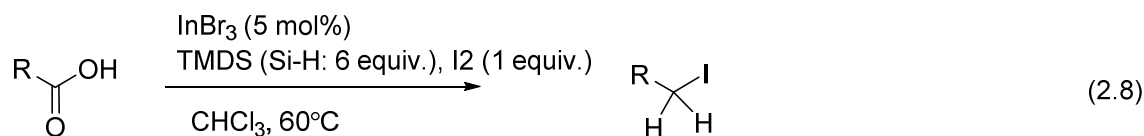
2.1.6 Reductive Deoxygenation of Ester, Amide, and other Carbonyl Compounds

The development of homogeneous catalysts capable of hydrogenating esters has lagged way behind the research on hydrogenation of other carbonyl substrates such as aldehydes and ketones. This is mainly due to the fact that the carbonyl group in esters is less electrophilic than that in aldehydes and ketones. A few publications of catalytic reductive deoxygenation of ester²² amide²³ and carboxylic acids²⁴ are reported. Sakai group established an efficient one-pot synthesis of unsymmetrical ethers by direct reductive deoxygenation of esters using an $\text{InBr}_3/\text{Et}_3\text{SiH}$ catalyst system.^{23c} They were able to convert ester into corresponding ether by combination of 0.05 equivalence of InBr_3 and 4 equivalence of Et_3SiH in chloroform at 60°C . As shown in eq. 2.7, ester **14** can be converted to ether **15** catalyzed by InBr_3 .

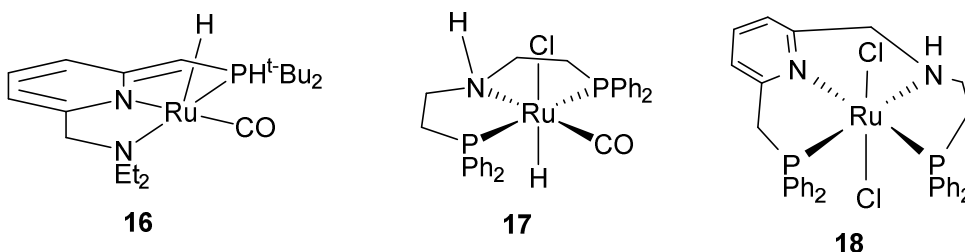


Under similar conditions they were unable to deoxygenate thioester, amides, or ketones. Carboxylic acid results corresponding alcohols but low yields and also ketones

results symmetric ethers. Very recently the same group published a paper to convert carboxylic acid into alkyl halides by reductive deoxygenation [Eq. (2.8)].²⁵

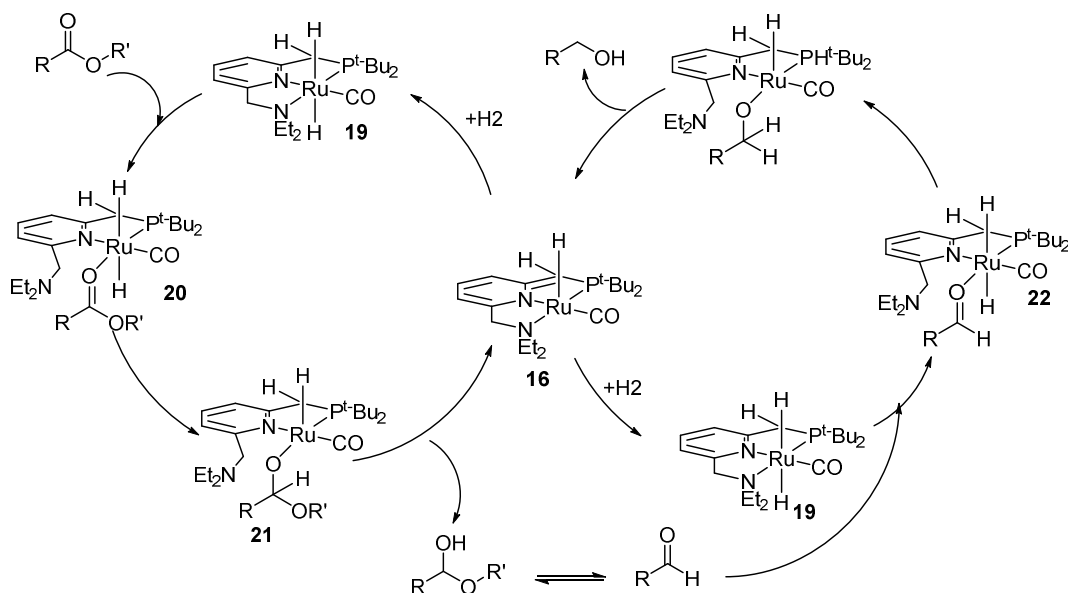


Catalytic reduction of esters into alcohols using hydrogen is much more common than true deoxygenation of esters.²⁶ Although great efforts have been made in the past decades, homogeneous hydrogenation of esters had been confined to special substrates under harsh conditions,²⁶ until significant breakthrough was made by Milstein,²⁷ Saudan,²⁸ Kuriyama,²⁹ Gusev,³⁰ *et al*³¹. The common feature Milstein's, Takasago's and Zhang³² catalyst is ruthenium catalysts feature a tridentate ligand and a CO ligand. (Complex **16**, **17** and **18**).



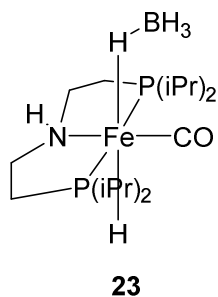
The mechanism of ester hydrogenolysis using above catalysts are similar. Milstein proposed a mechanism based on ligand aromatization and dearomatization (Scheme 2.4). Initially, dihydrogen addition to complex **16** resulted in aromatization, to form the coordinatively saturated, trans-dihydride complex **19**. Dissociation of amine ligand can provide a site for ester coordinate to ruthenium center, to give the intermediate **20**. A hydride ligand subsequently transfers to the carbonyl group of ester, followed by O-H elimination of hemiacetal and regeneration of complex **16** via intermediate **21**. The

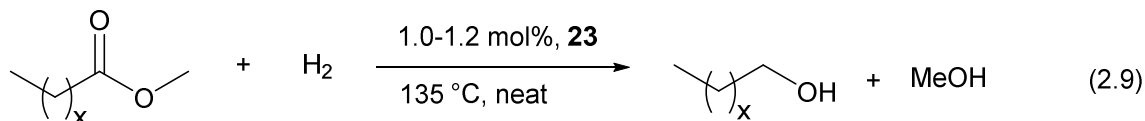
hemiacetal is equilibrium with aldehyde, which is readily hydrogenated following similar catalytic cycle via intermediate **22** to form the corresponding alcohol.



Scheme 2.4: Proposed Mechanism for Ru Catalyzed Hydrogenolysis of Esters

Very recently Guan³³ reported an iron-based catalytic method to hydrogenation of esters into corresponding alcohols. In the presence of catalyst (3 mol %) **23**, 150-230 psi H₂ gas in toluene at 115°C successfully converted esters into corresponding alcohols. The mechanism they proposed is similar to scheme 2.4 above. Using the same protocol they were able to syntheses fatty alcohols from industrial samples of fatty acids esters [Eq. (2.9)].





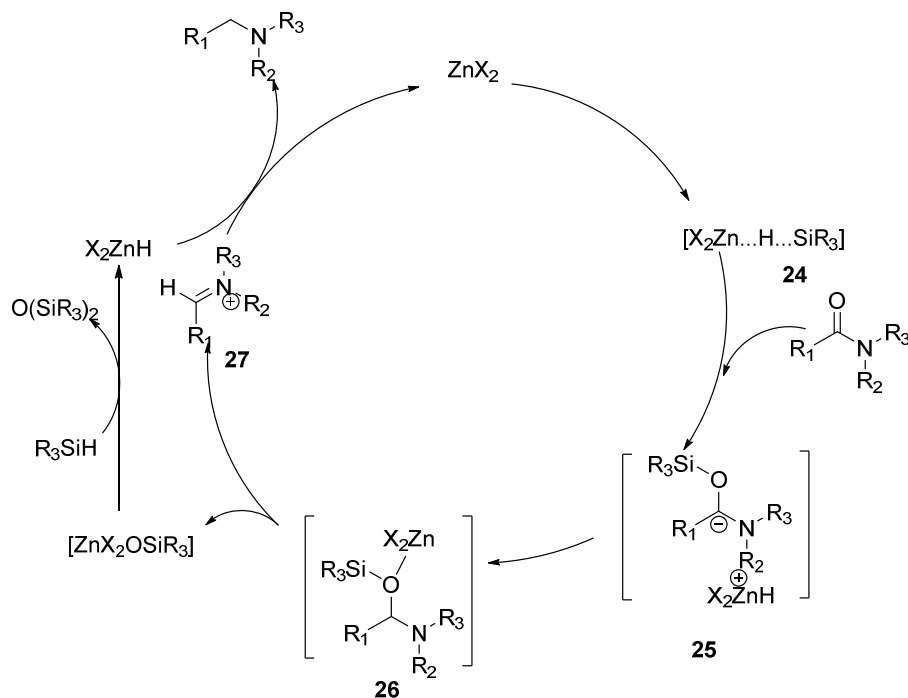
mixture of C10-C16 esters

($x = 8, 10, 12, \text{ and } 14$)

Several traditional methods available for the deoxygenation of amides. Mainly used of highly active agents such as LiAlH_4 , boranes and NaBH_4 .³³ Usually NaBH_4 does not react with amides, but it can be modified with either inorganic or organic materials to increase its reductive strength to reduce amide to amine. ZnBH_4 under reflux conditions will reduce aromatic amides to amines in high yield.³⁴

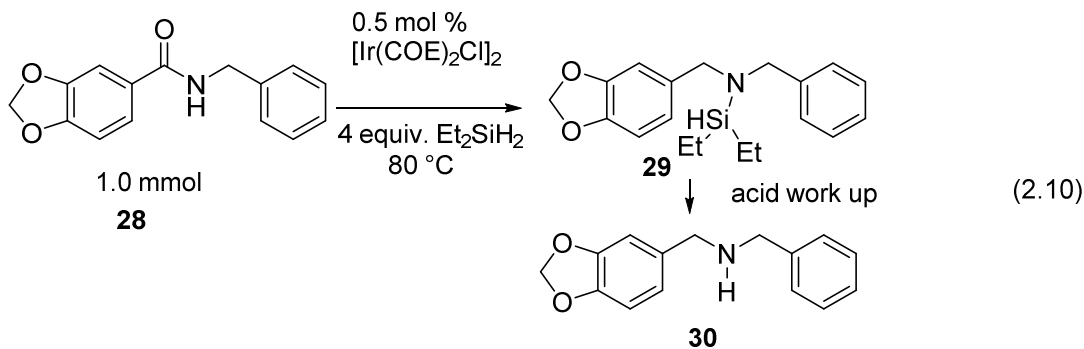
Beller³⁶ reported for the first time the efficient reduction of tertiary amides using convenient zinc catalysts with excellent chemo-selectivity and unique functional group tolerance. They found that in the presence of 10 mol % zinc acetate and 3 equiv. of triethoxysilane *N,N*-dimethylbenzamide reduction took place at room temperature leading to the corresponding amine in 97% yield. Comparing differently substituted benzamides, they observed that the introduction of electron-withdrawing groups at the *para*-position of the benzene ring resulted in faster reduction than in the case of those bearing electron-donating groups. Notably, amide reduction took place chemo-selectively even in the presence of a ketone group, which is known to be much more active.

Based on these observations, they proposed the reaction mechanism shown in Scheme 2.5. Zinc acetate reacts with triethoxysilane at room temperature and forms an activated species **24**. Next, the amide is coordinated to the metal center in **24** and generates the corresponding *N,O*-acetal **C** via **25**. Release of the anionic zinc ether **26** led to the iminium species **27**. Finally, another equivalent of the silane converts the iminium ion to the product and the siloxane.



Scheme 2.5: Proposed the Reaction Mechanism for the Zinc Catalyzed Amide

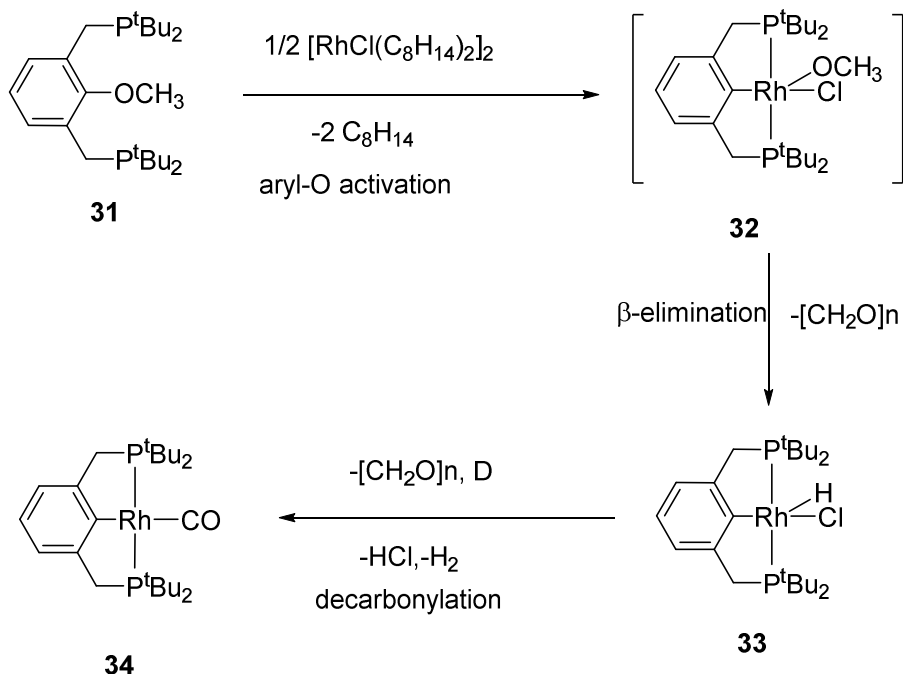
Kaneda *et al* found a hydroxyapatite supported gold nanoparticles (Au/HAP) efficiently catalyzed the deoxygenation of amide to amines using silanes as reductants.³⁷ Brookhart³⁸ in 2012 reported that iridium catalyzed reduction of secondary amides to secondary amine and imine by diethylsilane. They found that amides can be reduced to amines by 4 equivalence of Et_2SiH_2 in the presence of $Ir(COE)_2Cl_2$ (0.5 mol %) at room temperature in nonpolar solvents such as benzene or CH_2Cl_2 . Compound **28** initially react with diethylsilane to form N-Silyl compound **29** and acid work up let to form amine compound **30** [Eq. (2.10)].



2.1.7 Hydrogenolysis of C-O bond of Ethers

2.1.7.1 Hydrogenolysis of Aryl Ethers

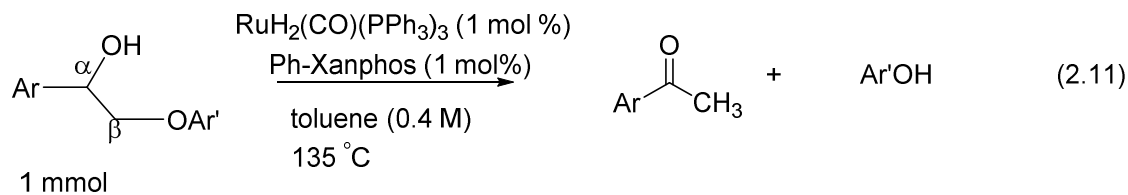
Because of the strength and stability of these linkages, selective hydrogenolysis of aryl carbon-oxygen (C-O) bonds is challenging.³⁹ This process is important for the conversion of oxygen-rich lignocellulosic plant biomass to deoxygenated fuels and fine chemicals.⁴⁰ The aromatic C-O bonds in lignin cannot be cleaved by hydrolysis and dehydration using common processes used to hydrolyse the aliphatic C-O bonds because those are resisted selective cleavage by hydrogen.^{39a,c} Method for reductive cleavage of unactivated aromatic C-O bonds would expand the utility of alkoxy and aryloxy substituents as removable directing groups that can influence synthetic transformations of aromatic systems. In contrast to hydrogenolysis of benzyl ethers, which proceeds selectively under mild conditions over heterogeneous catalysts, the cleavage of C-O bonds in aryl ethers requires high temperatures and pressures (over 250°C and 30 bar), which led to poor selectivities.^{39, 40a} The C-O cleavage methods of aryl ethers require stoichiometric alkali metals⁴¹ or electro-catalytic hydrogenolysis,⁴² both of which are expensive and difficult to conduct on a large scale. In 1998 Milstein group published a Rh catalyzed for selective, reductive cleavage of various aromatic C-O bonds of Ar-OCH₃ with hydrogen under mild conditions (scheme 2.6).⁴¹



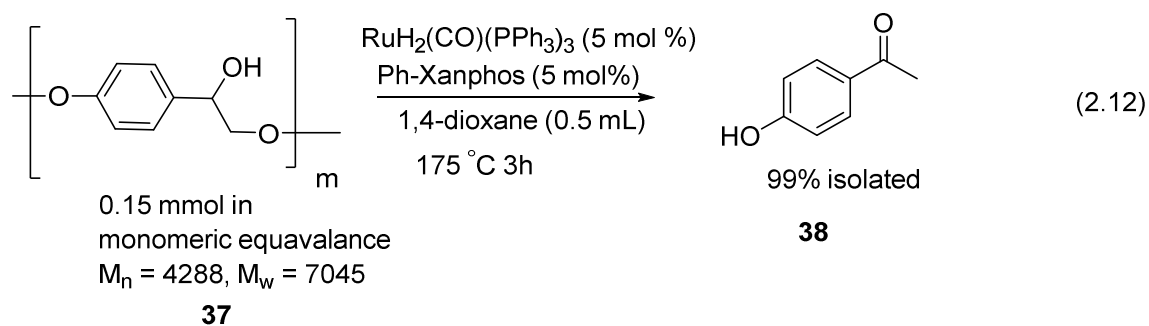
Scheme 2.6: C-O Cleavage of Aryl-OMe Ether by Rh

Reaction of the complex $[\text{RhCl}(\text{C}_8\text{H}_{14})_2]_2$ (C_8H_{14} = cyclooctene) with 2 equivalence of **31** in C_6D_6 at 85°C for 3 h (in a sealed vessel) resulted in quantitative formation of the known Rh(III) hydride complex **33**, which was unambiguously identified by various NMR techniques and by comparison to an authentic sample (Scheme 2.6). The presumably formed (unobserved) Rh(III)-OCH₃ intermediate **32** undergoes readily β -hydrogen elimination to afford complex **34** and formaldehyde.

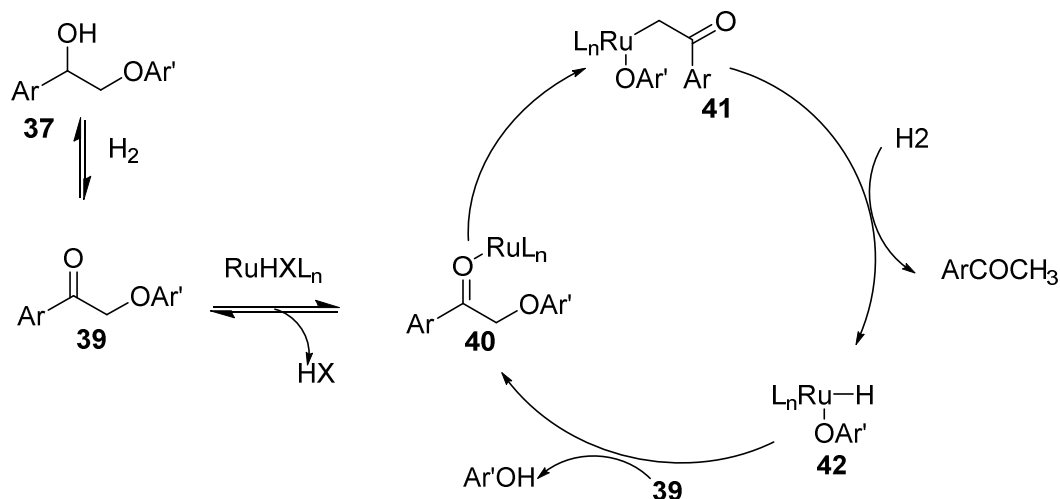
To realize a selective hydrogenolysis of aromatic C-O bonds, Hartwig envisioned a reaction that involves insertion of a discrete transition metal complex into the aromatic C-O bond and reaction of the resulting intermediate with hydrogen to yield arene and alcohol. They anticipated that the low reactivity of homogeneous catalysts toward hydrogenation of aromatic rings⁴² would prevent competitive formation of cycloalkanes and cycloalkanols from such a process.



For the depolymerization of lignin based polymer they used the catalytic system with high catalytic loading [Eq. (2.12)].

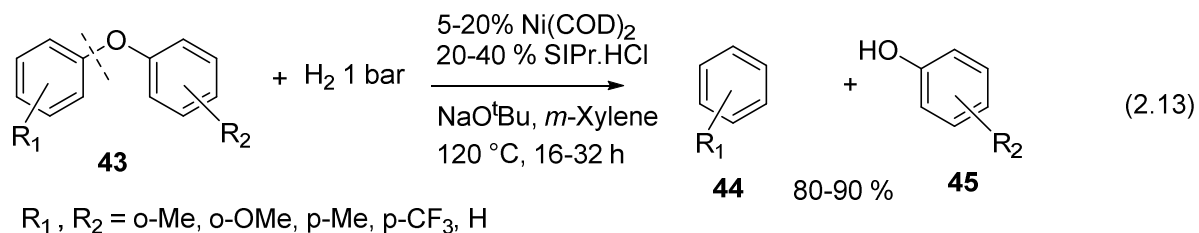


Based on the experimental evidence they proposed the mechanism for the transformation as shown in Scheme 2.7. It begins with a well-known Ru-catalyzed dehydrogenative equilibrium between a benzylic alcohol and the corresponding aryl ketone. This is followed by loss of HX from the catalyst precursor and formation of Ru(0) complex **40**. C-O activation in **40** leads to Ru-enolate (**41**). Hydrogenation of **41** yields a Ru-alkoxide (**42**) followed by reductive elimination of phenol and association with **40** to close the cycle.

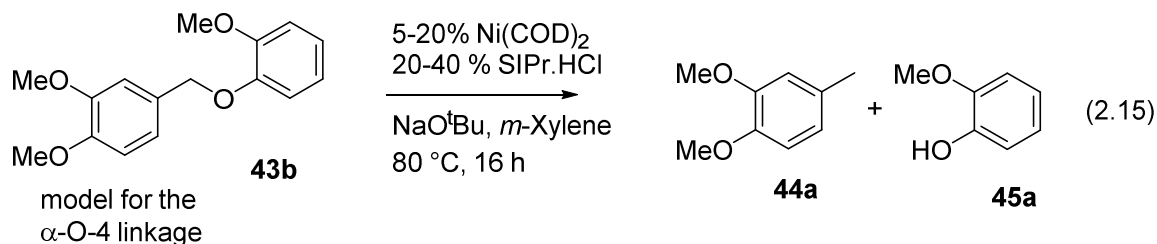
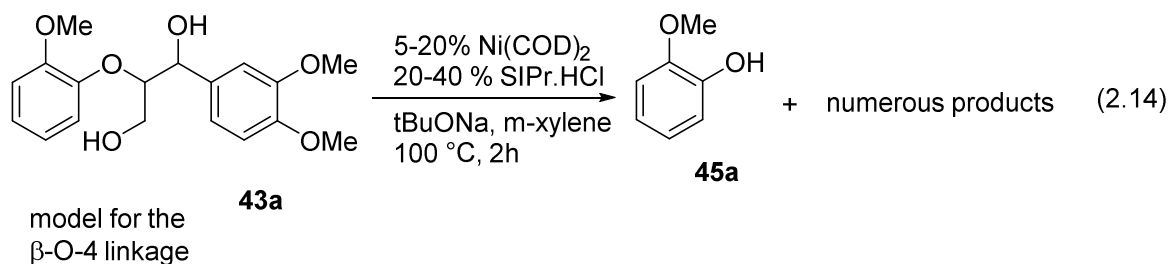


Scheme 2.7: Proposed Mechanism for the Hydrogenolysis of Aryl Ether Catalyzed By Ru Catalyst.

In 2011 Hartwig group published a seminal report, on the nickel-catalyzed hydrogenolysis of C-O bond of aryl ether.⁴⁸ Using Ni(0)–NHC complexes as unusually active catalysts for the cleavage of a range of aryl and benzyl ethers with main group hydride donors, they explored the use of hydrogen a cheaper, cleaner, and milder reagent for the reduction of aryl ethers. Indeed, the combination of Ni(COD)₂ and 1,3-Bis(2,6-diisopropylphenyl)imidazolium Chloride (SIPr·HCl, 20 mol %) as catalyst and NaO^tBu (2.5 equiv.) as base effected the selective hydrogenolysis of various diaryl ethers **43**, with only 1 bar pressure of H₂ in *m*-xylene to give the corresponding arenes **44** and phenols **45** in good to excellent yields [Eq. (30)]. The scope of the reaction encompasses both electron-rich and electron-poor diaryl ethers. Hydrogenolysis occurred faster with unsubstituted diphenyl ether and diaryl ethers bearing an electron-withdrawing trifluoromethyl group than with diaryl ethers bearing electron-donating alkyl or methoxy substituents. Reactions with the less reactive diaryl ethers required substantial catalyst loadings (20%) but occurred to high conversions [eq. (2.13)].



He was able demonstrate C-O bond cleavage of several lignin model compounds using the same protocol. Model compound that represent β -O-4-linkage **43a**, and α -O-4-linkage **43b**, were cleave by the nickel catalyst in excellent yield to products **45a**, and **44a** [Eq. (2.14) & (2.15)].



In 2012, Hartwig group published a further developed method to cleave the aryl C-O bond.⁴⁹ A heterogeneous nickel catalyst have been used for the selective hydrogenolysis of aryl ethers to arenes and alcohols generated without an added dative ligand. The catalyst is formed *in situ* from the well-defined soluble nickel precursor $\text{Ni}(\text{COD})_2$ or $\text{Ni}(\text{CH}_2\text{TMS})_2(\text{TMEDA})$ in the presence of a base additive, such as $t\text{BuONa}$. The catalyst selectively cleaves $\text{C}_{\text{Ar}}\text{-O}$ bonds in aryl ether models of lignin without hydrogenation of aromatic rings, and it operates at loadings down to 0.25 mol % at 1 bar of H_2 pressure. The

selectivity of this catalyst for electronically varied aryl ethers differs from that of the homogeneous catalyst reported previously, implying that the two catalysts are distinct from each other.

They were able to change the selectivity of aryl ether bond of unsymmetrical ether by changing the reaction conditions. As shown in Figure 2.2, the ligandless nickel catalyst cleaved the C_{Ar}-O bond adjacent to the most electron-rich arene ring of 4-hydroxy diphenyl ether, **46** to form 2 equivalence of phenol as the sole product. In contrast, the SiPr-Ni catalyst preferentially cleaved the C_{Ar}-O bond adjacent to the more electron-deficient ring to form predominantly hydroquinone (67%) and benzene (48%). These results on both inter- and intramolecular competition experiments clearly indicate that the catalytic species generated without added ligand is distinct from the species generated with added SiPr ligand.

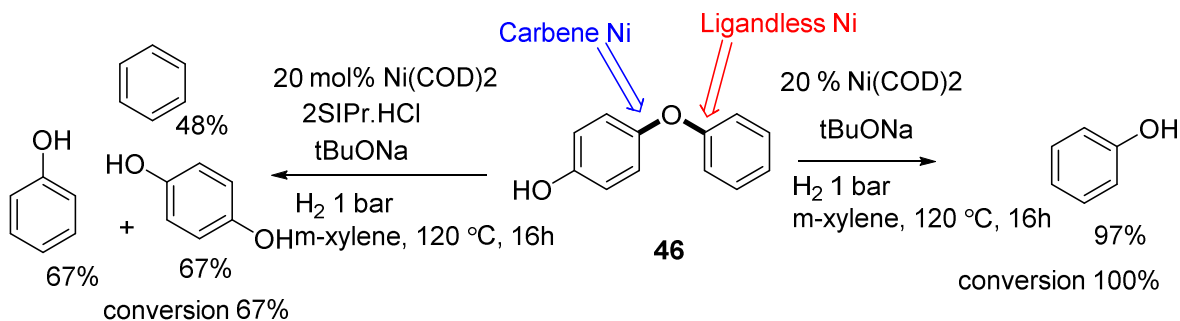
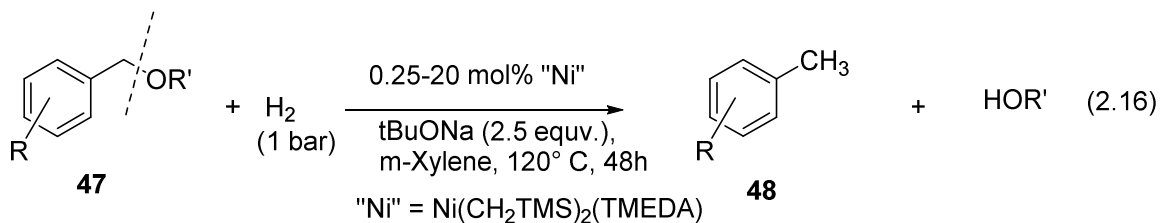


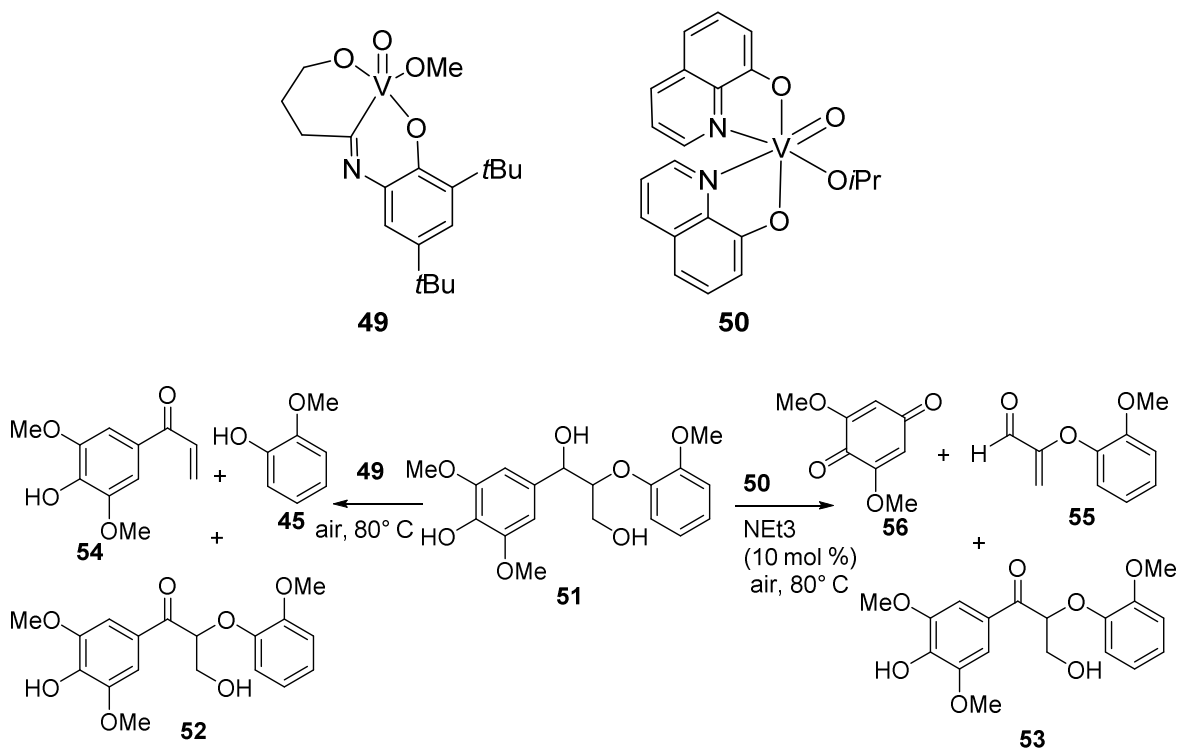
Figure 2.2: Selective Cleavage of Aryl-Oxygen Bond in Different Conditions

The ligandless nickel system also catalyzes the hydrogenolysis of benzyl aryl and benzyl methyl ether, **47** which are two additional types of linkages in lignin. Benzyl aryl ethers were converted to methyl-substituted arenes, **48** and phenols in excellent yields in the presence of 0.25–2 mol % of the nickel catalyst [Eq. (2.16)]. Benzyl methyl ether, **47**

was unreactive under standard reaction conditions, but full conversion could be achieved in the presence of 1 equivalence of AlMe₃.



Hanson *et. al*⁵⁰ in 2012 found that C-O bond cleavage in phenolic lignin model compounds using vanadium catalyst. They used aerobic oxidation of lignin model compounds using two different vanadium catalysts (**49** and **50**) which has different selectivity.

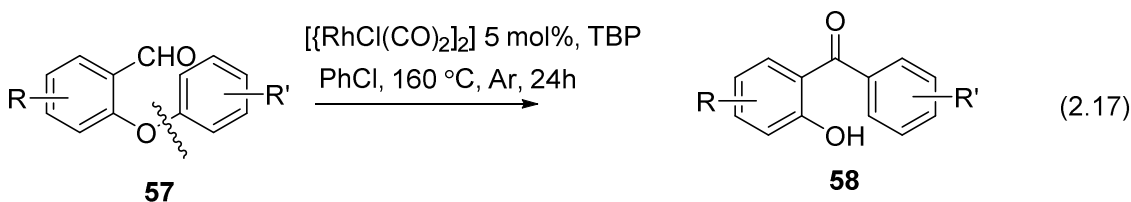


Scheme 2.8: Oxidation of Phenolic Ligand Model Compound with Vanadium Catalysts

Remarkably, the two vanadium catalysts show different selectivity for the aerobic oxidation of **49**. Vanadium catalyst **50** mediates a new type of reaction in which the C-C

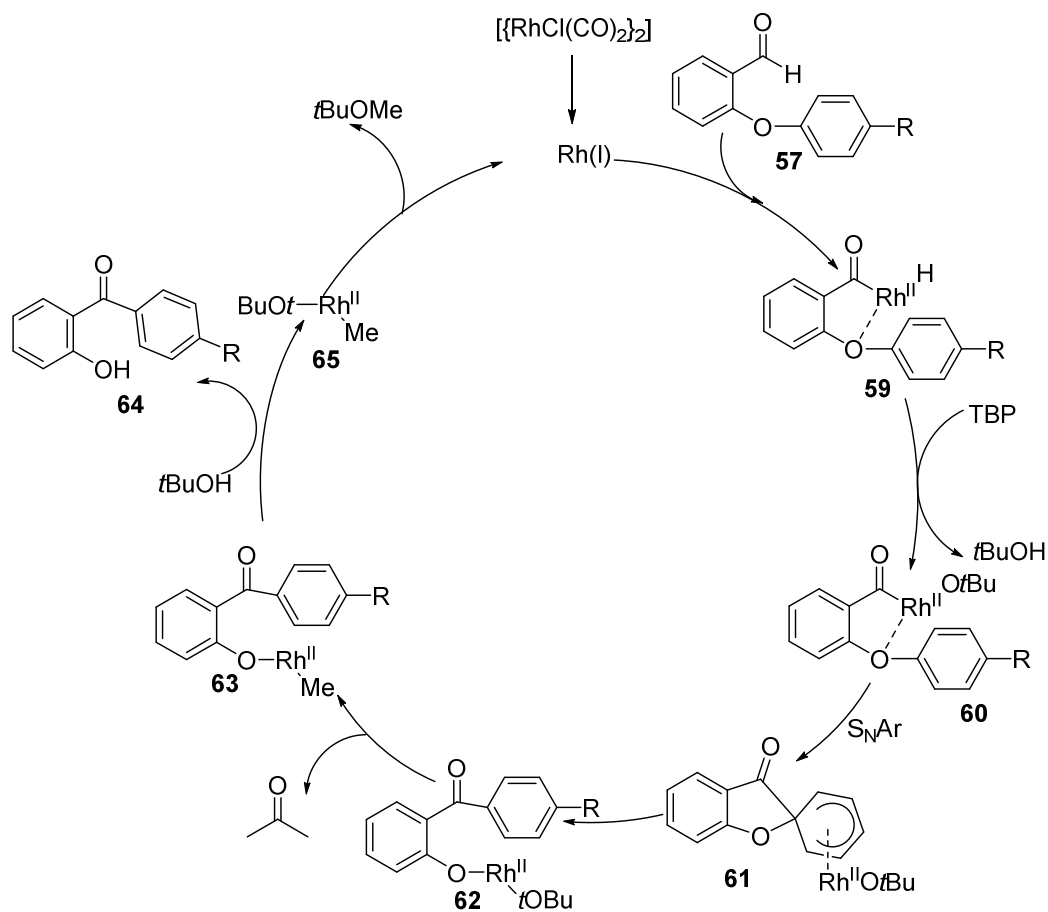
bond between the aryl ring and the adjacent alcohol group is broken to give 2, 6-dimethoxybenzoquinone, **56** and acrolein derivative **135**, and ketone **53**. In contrast, catalyst **49** affords C-O bond cleavage products **128** and **52**, and ketone **54**. The significant difference in selectivity between the two catalysts underscores the potential of homogeneous catalysts for controlling the selectivity in the aerobic oxidation of lignin. But they did not explore the reactivity towards the other lignin compounds (Scheme 2.7).

Li⁵¹ also investigate rhodium catalyzed aryl ether bond cleavage of 2-aryloxybenzaldehyde **57** and rearrangement to 2-hydroxybenzophenone **58**. They used $[\{\text{RhCl}(\text{CO})_2\}_2]$ (5 mol %) as the catalyst, tributyl phosphine (TBP) in chlorobenzene at 160 °C [Eq. (2.17)]. Based on their experimental evidence they proposed the following mechanism Scheme 2.9.



Initially, the chelating aldehyde C-H insertion of 2-(aryloxy)benzaldehydes **57** by Rh^{I} generates the Rh^{III} hydride species **59**. Upon reaction with TBP, the Rh^{III} complex **59** is formed, thus liberating one molecule of *t*BuOH. Then complex **59** may undergo an intramolecular $\text{S}_{\text{N}}\text{Ar}$ process to afford the complex **60** upon heating to 160 °C, thereby generating the Rh^{III} complex **61** (an alternative process through 1, 4-elimination of $\text{Ar}-\text{Rh}-t\text{OBu}$ from **62** with subsequent conjugate addition of $\text{Ar}-\text{Rh}-t\text{OBu}$ to the resulting enone species may be excluded based on the result of the cross-experiment), which could release one molecule of acetone (detected by GC-MS) to afford the $\text{Rh}^{\text{III}}/\text{Me}$ complex **63**. Finally, reaction of the previously formed *t*BuOH with complex **63** can release one molecule of the

desired product **58** and form $[\text{Rh}^{\text{III}}(\text{Me})(t\text{OBu})]$ (**65**), which could regenerate the Rh^{I} catalyst through a reductive elimination process by releasing $t\text{BuOMe}$



Scheme 2.9: Tentative Mechanism for the Rhodium-Catalyzed Rearrangement of 2-(Aryloxy) Benzaldehydes to 2-Hydroxybenzophenones.

2.2: Transition Metal Catalyzed Ether Synthesis

2.2.1 Introduction

Ether bonds are prevalent in many natural and unnatural products that exhibit diverse biological activity (figure 2.3)⁵² and also drugs as well as many industrially important intermediate. Paxil (Parotin), **66** is active ingredient of drug used to treat major depressive disorder. Fluoxetine **67**, (also known by the trade names Prozac, Sarafem, Ladose and Fontex, among others) is an antidepressant of the selective serotonin reuptake inhibitor (SSRI) class.

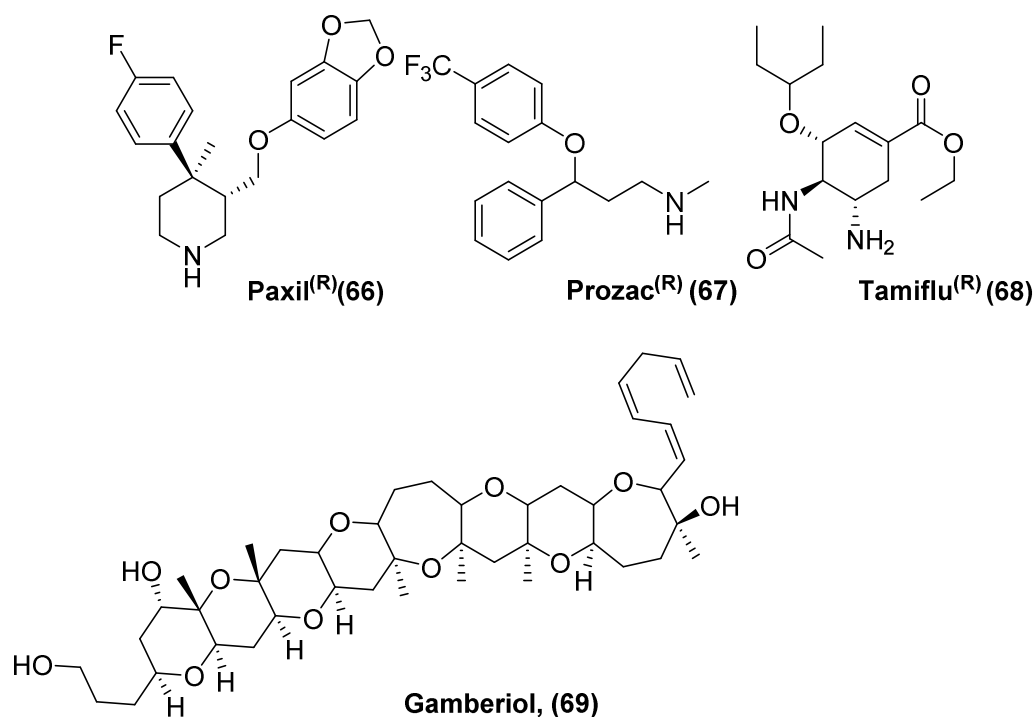


Figure 2.3: Some Natural Products and Drugs Containing Ether Bond.

Oseltamivir **68**, marketed under the trade name Tamiflu, is an antiviral medication used to prevent and treat influenza A and influenza B (flu). Gambierol **69**, is a marine polycyclic ether toxin a polyether ladder toxin derived from the marine dinoflagellate

Gambierdiscus toxicus. The physiological activity of these products are, at times, critically dependent on the stereochemistry adjacent to the C-O bonds within the framework of the molecule, which provides a strong impetus to the stereoselective synthesis of C-O bonds.

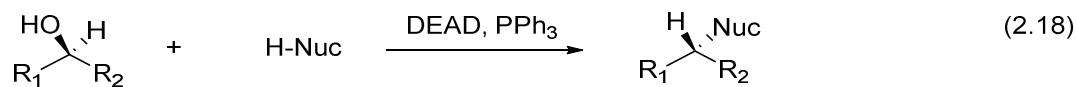
2.2.2 Classical Methods

Williamson ether synthesis is powerful method of forming ether bond linkages.⁵³ It involves an S_N2 reaction between an alkaline metal alkoxide and a suitable electrophile such as an alkyl halide to form unsymmetrical ethers.⁵⁴ The Williamson ether synthesis is often complicated by competing elimination reactions and racemization of stereochemically intricate starting materials, making it difficult to be incorporated into the synthesis of complex molecules. In fact, the scope of the Williamson ether synthesis is primarily relegated to primary alcohols and alkyl halides. In an attempt to find more temperate alternatives to the Williamson ether synthesis much research has been conducted in search of transition metal mediated processes. In this part of the chapter, many transition metal-catalyzed methods developed as an alternative to the Williamson ether synthesis are discussed.

2.2.2.1 O-Alkylation Method

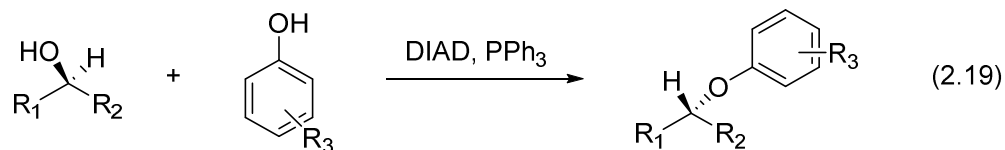
2.2.2.2 Mitsunobu Etherification

In 1967, Mitsunobu and co-workers initially introduced the Mitsunobu reaction. Since its discovery, the reaction has become a useful tool in organic synthesis due to its effectiveness and versatility⁵⁵. The reaction is starting with the conversion of a hydroxyl group into a potent leaving group that is able to be displaced by a wide variety of nucleophiles which require pK_a less than 15 [Eq. (2.18)]. Using phenol as a nucleophile can be used to synthesis unsymmetrical ethers.



Nuc = carboxylic acid, amine, amide, azides, ester, phenol, hydrazoic acid

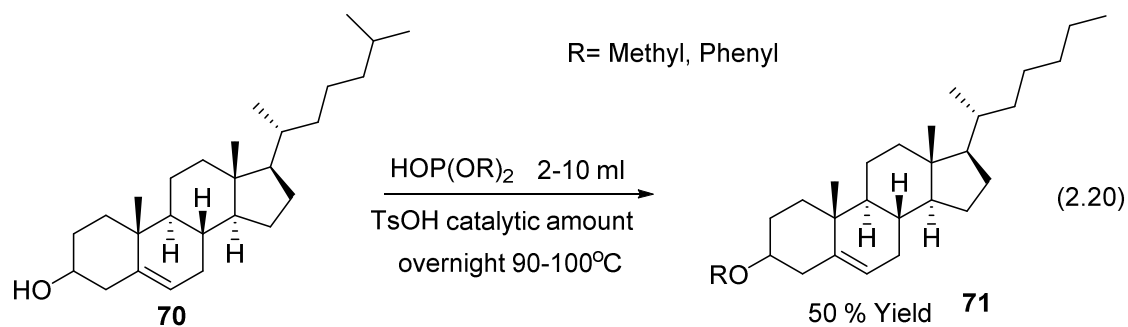
Mitsunobu reaction has been widely used in pharmaceutical and natural product synthesis particularly for inversion of a chiral center. However, there are a couple of limitations to be overcome in Mitsunobu reaction. The coupling between bulky alcohols is not efficient in terms of yield and reaction time, the use of explosive diethyl azodicarboxylate (DEAD) and separation problem, and the use of which phosphonium oxide and hydrazine which complicate purification process in order to isolate its product. Shi et al. reported the etherification reaction of tertiary alcohol with various phenols via Mitsunobu reaction which is more electron rich diisopropylazodicarboxylate (DIAD) is used instead of diethyl azodicarboxylate (DEAD) [Eq. (2.19)].⁵⁶



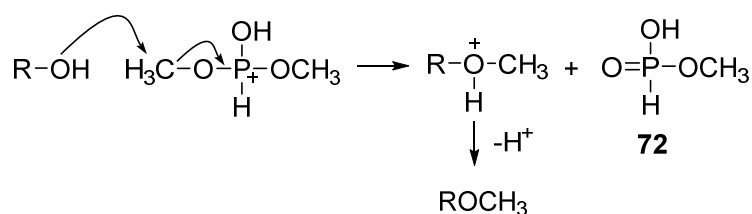
2.2.2.3 Etherification by Using Dialkylphosphites

In 1971, Kashmann⁵⁷ reported etherification reaction of cholesterol with dialkyl- or diaryl-phosphite by using a catalytic amount of TsOH (Scheme 2.10). This method is able to produce cholesteryl phenyl ethers (**70**) by a one step reaction of cholesterol (**71**) [Eq.

(2.20)].



The first step of the mechanism involves the protonation of dialkyl phosphite by catalytic amount of acid (TsOH). Nucleophilic hydroxyl of cholesterol attacks methoxy carbon of phosphite and forms carbocation and **72**. The deprotonation of carbocation by TsO^- forms unsymmetrical ethers (Scheme 2.10).



Scheme 2.10: Mechanism of Etherification of Cholesterol, ROH= Cholesterol

Cholesterol and excess amount of dimethyl or diphenylphosphite are required to synthesize unsymmetrical ethers⁵⁸. Excess amount of alkyl or aryl phosphite are consumed and the yield of reaction is relatively low (50 %) based on cholesterol. The only functional tolerance groups are alkene and carbonyl groups. Also excess of phosphite **72** is formed as a waste (Scheme 2.10). Etherification of cholesterol is a very impressive result from first large molecular etherification in a one step, but the reaction is not efficient as described above.

2.2.3 Cross-Coupling Reactions

Cross-coupling reactions of alkyl halide and phenols represents one of the simplest transition metal-mediated etherification methods. These reactions often include Cu or Pd as a mediator, a phenolic nucleophile, and an aryl halide or boronic acid. Due to the challenges associated with this type of cross-coupling process, these reactions are often bypassed in natural product synthesis. Among the major challenges are the often low reactivity of the electrophile and highly coordinative ability of the alcohols with the transition metal causing harsh reactions conditions such as high temperatures or high metal loading. However, examples have been shown where the cross-coupling approach successfully constructs the ether linkages that are otherwise difficult to form.

2.2.3.1 Ullman Reaction

Since its introduction in 1903, the Ullman coupling reaction between aryl halides and alcohols mediated by Cu has become a standard reaction in organic synthesis.⁵⁹ its emergence in many total syntheses is due in large part to the incidence of biaryls ether bonds found in many biological active natural products. Unlike typical nucleophilic aromatic substitution (S_NAr)⁶⁰ the Ullman reaction does not require, additional activating groups. Limitations associated with the Ullman reaction includes necessity of high reaction temperatures and often superstoichiometric amounts of Cu. Even though catalytic versions of this reaction is rare, this reaction is the standard by which most other metal-catalyzed etherification reactions are compared. Many examples employing the Ullman or Ullman-type reactions can be found in total syntheses of natural products.

Many instances of Ullman coupling usage in total synthesis revolve around intramolecular ring closing reactions. The power of this form of coupling reaction is

evident in a few examples shown in Figure 2.4, where challenging etherification reactions have been accomplished. (+)-Hirsutellone B (**73**), isolated from the insect pathogenic fungus *Hirsutella nivea* BCC 2594, shows good activity against *Mycobacterium tuberculosis*. Tejedine (**74**) is a seco-bisbenzyltetrahydroisoquinoline isolated in 1998 as a minor component from *Berberis vulgaris*.

Boger and co-workers reported a particularly striking application of the Ullman coupling is in the intramolecular ring closing etherification incorporated in the total synthesis potent antitumor antibiotic Bouvardin (**74**) [Eq. (2.21)].⁶¹ Aryl iodide **75** coupled with phenol in the same molecule to synthesis of cyclic intermediate **76** for the synthesis of **74** by copper catalyzed Ullman coupling.

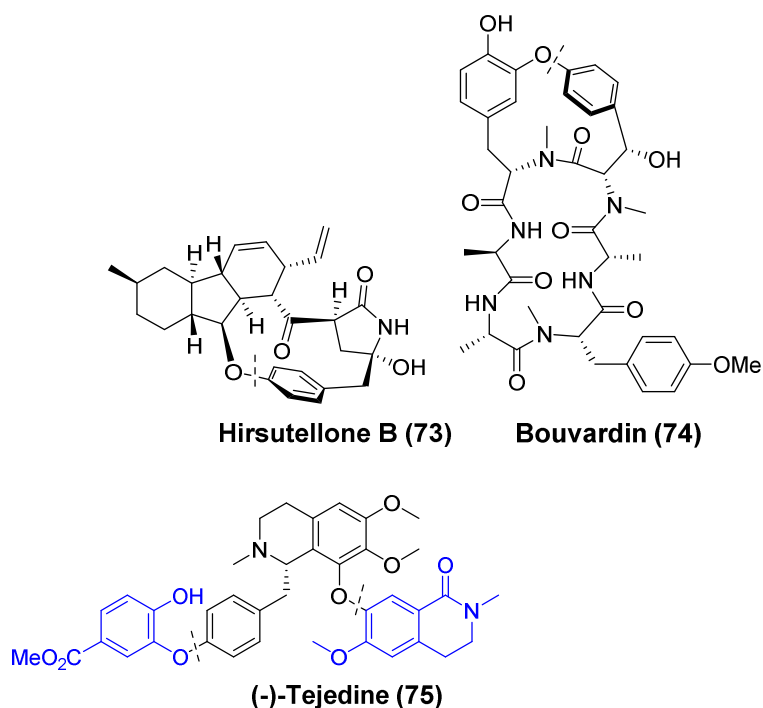
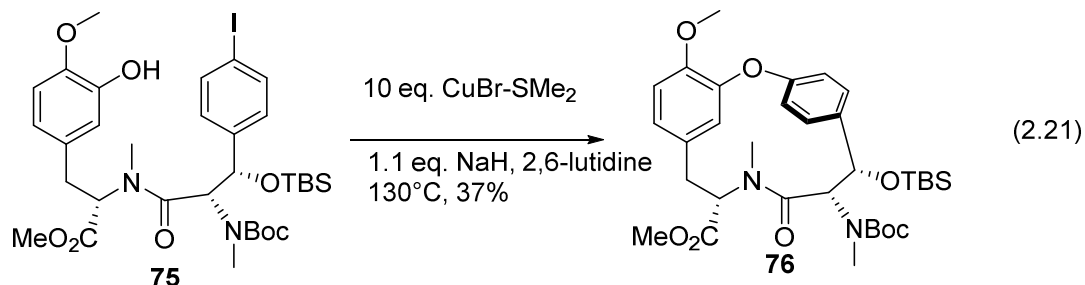
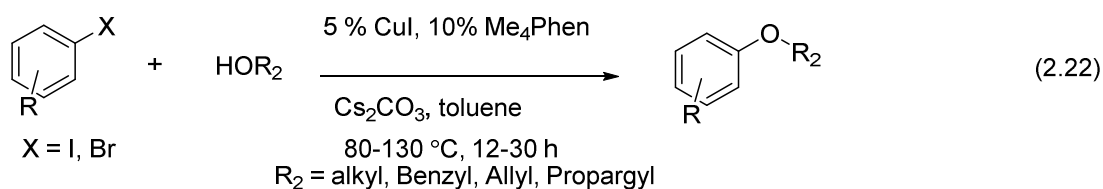


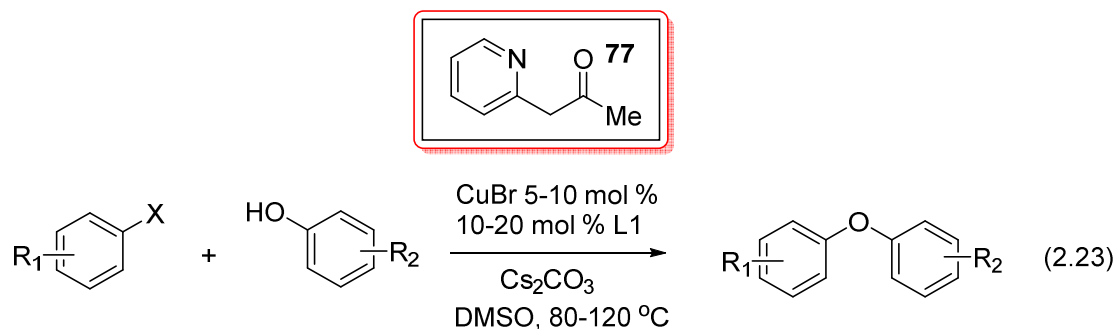
Figure 2.4. Natural Products Synthesized by Ullman Coupling



Buchwald group developed an improved Cu(I)-based catalytic system for the reaction of alcohol and aryl halide for syntheses of alkyl aryl ethers [Eq. (2.22)].⁶² The use of 3,4,7,8-tetramethyl-1,10-phenanthroline (Me₄-Phen) as a ligand improved the Cu-catalyzed cross-coupling reactions of aryl iodides and bromides with primary and secondary aliphatic, benzylic, allylic, and propargylic alcohols. Most importantly, by employing this catalyst system, the need for an excessive quantity of the alcohol coupling partner is alleviated. The relatively mild conditions, short reaction times, and moderately low catalyst loading allow for a wide array of functional groups to be tolerated on both the electrophilic and nucleophilic coupling partners.



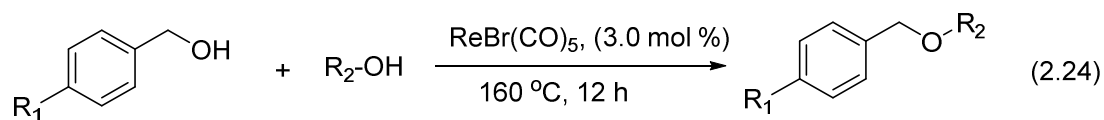
Zhang et al added a good modification to Ullmann etherification by Employing (2-pyridyl) acetone, **77** as a new supporting ligand, the copper-catalyzed coupling reactions of aryl chlorides, aryl bromides, and aryl iodides with various phenols successfully proceeded in good yields under mild conditions. This reaction displays great functional groups compatibility and excellent reactive selectivity [Eq. (2.23)].⁶³



Even in advanced Ullmann reactions, the Ullmann reaction still requires expensive or rare halogenated starting materials and excess amount of base, which forms stoichiometric amounts of halogenated byproducts.

2.2.4 Catalytic Etherification Methods

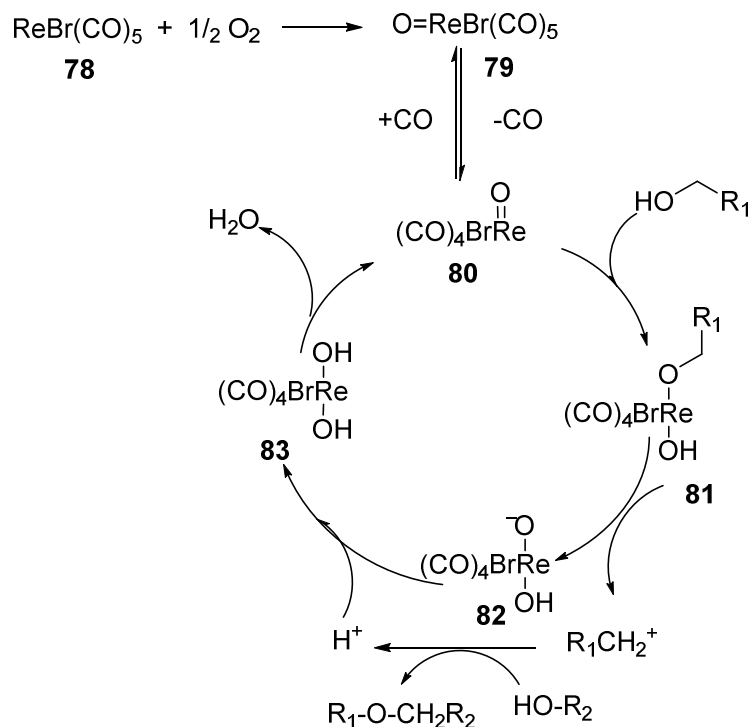
The developments of a new catalytic etherification methods are needed to eliminate many of the disadvantages associated with these stoichiometric reactions. Qiu,⁶⁴ and co-workers reported a method to syntheses of unsymmetrical benzyl ether using rhenium (I) catalyst. Benzyl alcohol (1.0 mmol) and 1-butanol (5.0mmol) with $\text{ReBr}(\text{CO})_5$ (0.03mmol) were autoclaved at 160 °C for 12 h [Eq. (2.24)].



R_1 = hydrogen, methyl, chloride, R_2 = aliphatic

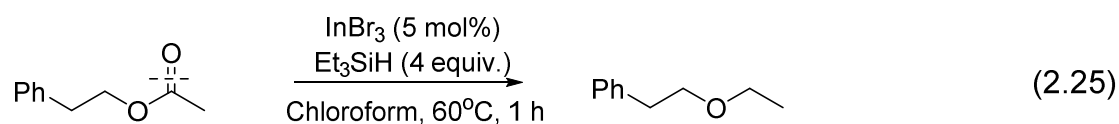
The substrate scope was limited to benzylic alkyl ethers. They proposed the following mechanism based on their experimental evidence (Scheme 2.11). $\text{Re}(\text{I})$ complex **78** reacts with oxygen to give $\text{Re}(\text{III})$ oxide **79**. Decarboxylation of $\text{Re}(\text{III})$ oxide **80** affords the intermediate $\text{Re}(\text{III})$ complex **80**. Benzyl alcohol is added to **80** via an oxidative

addition. Alpha hydrogen addition to oxygen forms Re(III) complex **81**. Re(III) complex **81** released carbocation and Re(III) complex **82**. Benzyl cation reacted with another alcohol produces the ethers. Dehydration of dihydroxo-rhenium(III) **83** is regenerated to **80**. However, the reaction has less functional group tolerance.

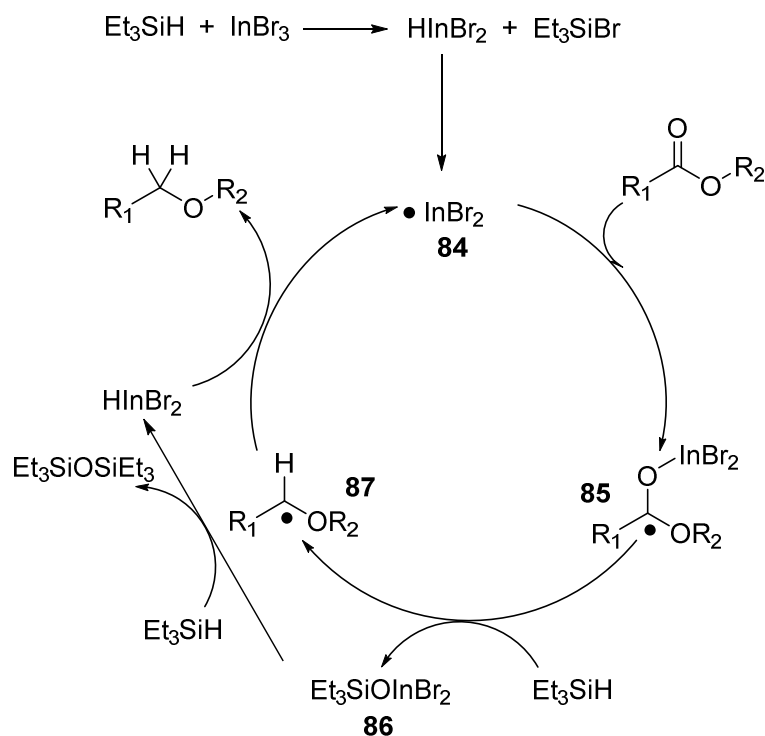


Scheme 2.11: Mechanism of Rhenium (I) Catalytic Etherification Cycle

In 2009, Sakai *et al*⁶⁵ developed a method for selective deacetoxylation of several organic compounds using the InBr₃-Et₃SiH system, remarkably it was found that, the InBr₃-Et₃SiH reducing system causes the reduction of the carbonyl function of esters under milder conditions, resulting in the preparation of unsymmetrical ethers [Eq. (2.25)].



Synthesis of ether by reduction of ester is a completely different method than the previous explained methodology. Catalytic amounts of Indium complex are used to eliminate waste and the reaction condition is mild for functional group tolerance. This different method eliminates waste problems, selectivity issues, relatively modest yields and still the use of excess of Et_3SiH are the common drawbacks.

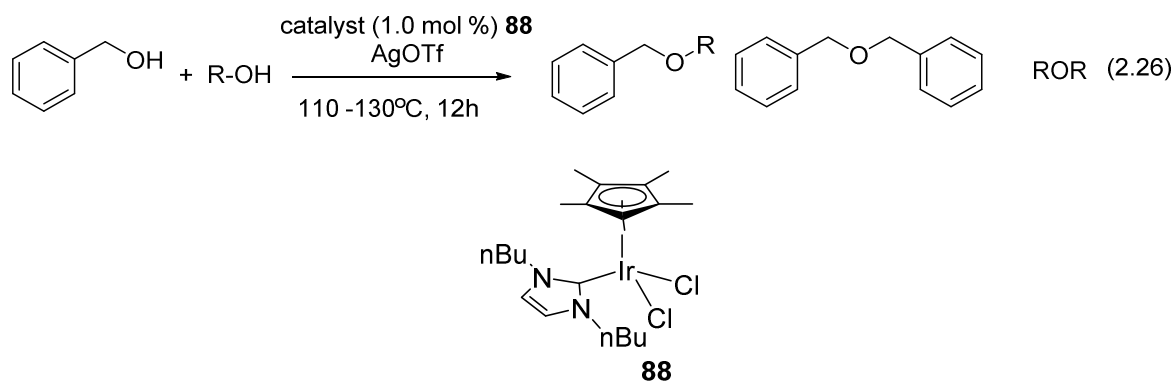


Scheme 2.12: Mechanism of In (III) Catalyzed Deoxygenation of Esters

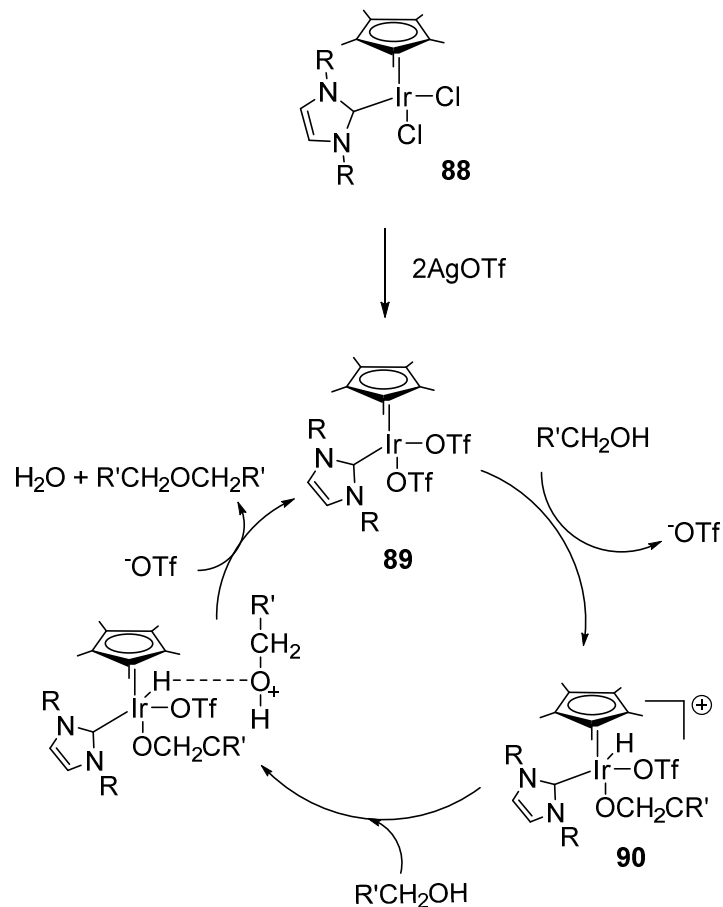
A plausible mechanism for the reaction is shown in Scheme 2.12. The reaction path involves the following steps: (i) transmetalation between Et_3SiH and InBr_3 as an initial step to generate **84**, (ii) a consecutive abstraction of hydrogen by the radical intermediate **85** and the formation of an ether product, and (iii) finally, the regeneration of an indium radical species **84**.

2.2.5 Etherification by [IrCl₂Cp*(NHC)] Catalyst

Peris et al has shown that [IrCl₂Cp*(NHC)] catalyst is effective for the cross coupling of benzyl alcohol with primary and secondary alcohols to form unsymmetrical ethers.⁶⁶ It displays a high selectivity to the unsymmetrical ethers. Only for the homocoupling of benzyl alcohol they obtained a very low yield in the formation of benzyl ether because the dehydrogenation to form benzaldehyde is a highly favorable process for this alcohol [Eq. (2.26)].



Plausible mechanism was proposed in Scheme 2.13. Initially, AgOTf activated Ir(III) complex **88** to generate Activated Ir(III) complex **89**. Alcohol is added to the Ir(III) center via oxidative addition to form Ir(V) hydride **90**. The key complex of the reaction is the formation of Ir(V) hydride species **90**. Ir(V) hydride complex **90** acts as a Brønsted acid and activates another alcohol. Coupling of the alkyl group of activated alcohol to the coordinated alkoxide produces water as a byproduct and ethers as a product. Main drawbacks of this reaction are limited substrate scopes and excess of aliphatic alcohol for high selectivity

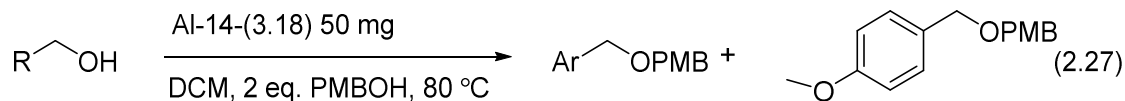


Scheme 2.13: Proposed Mechanism of Synthesis of Unsymmetrical Ether by Iridium Catalyst

2.2.6 Dehydrative Etherification of Alcohols

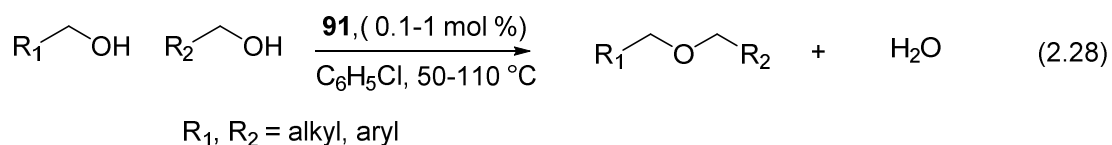
The dehydrative etherification of alcohols is the most efficient way of synthesis of ether compounds in both industrial and academic laboratory settings.^{67,68} But the synthesis of unsymmetrical ether from two different alcohols selectively is challenging. Very recently two major papers were published based on metal catalyzed dehydrative coupling of alcohols to make ethers. The first, Graham group reported a nanoporous aluminosilicate-

mediated synthesis of ether by dehydrative etherification approach [Eq. (2.27)].^{67a}



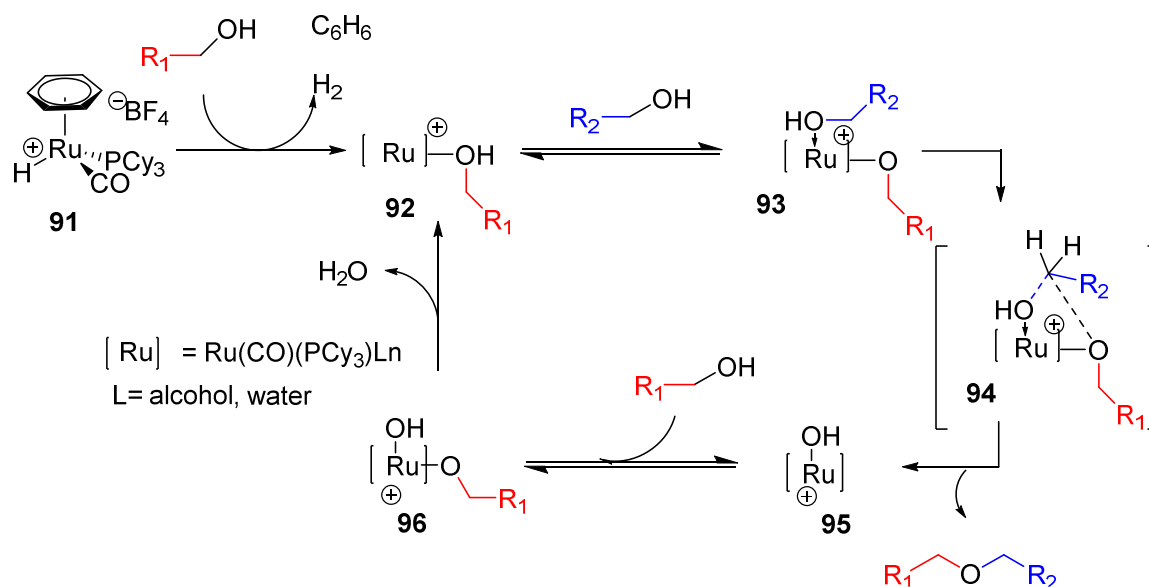
The Al-14-(3.18) catalyst (50 mg) was added to a mixture of benzyl alcohol (1 mmol) and PMBA (2 mmol) in dimethyl carbonate (2 mL) and heated to 80 °C with vigorous stirring. The substrate scope was limited to PMB ethers and they have selectivity problem unresolved. The Al-14-(3.18) is consist of Si/Al ratio 14:1 and the pore size 3.18 nm.

Very recently, we reported an efficient and selective synthesis of unsymmetrical ether from dehydrative coupling of two different alcohols catalyzed by cationic ruthenium hydride complex **91**.⁶⁹ The catalytic method exhibits a broad substrate scope while tolerating a range of heteroatom functional groups in forming unsymmetrical ethers, and it is successfully used to directly synthesize a number of highly functionalized chiral nonracemic ethers [Eq. (2.28)].



On the basis of these observations, mechanistic hypothesis was proposed for the selective formation of unsymmetrical ethers (Scheme 2.13). They proposed that a cationic Ru-alkoxy species **91**, initially generated from the deprotonation of the alcohol substrate, is the key intermediate species for the etherification reaction. They suggest a S_{NI} type of nucleophilic displacement mechanism for the formation of α-chiral ethers. Also the acidity of alcoholic substrate may be an important factor in promoting the formation of Ru-alkoxy species **92** from the deprotonation of a less reactive, more basic alcohol substrate. The

coordination of another alcohol substrate to form complex **93** and the liberation of water byproduct through intermediate **94** would facilitate the regeneration of the alkoxy species **92** via the Ru-hydroxy intermediates **95** and **96**. Still, many aspects on how the catalyst can mediate a high degree of selectivity remain unresolved.



Scheme 2.14: Working Mechanistic Hypothesis for Unsymmetrical Ether Formation

2.2.7 Additions to Unsaturated Bonds

Addition of nucleophiles to double bonds via transition metal-mediated catalysis has become a fundamental process in organic synthesis.⁷¹ The addition of alcohols to carbon-carbon double and triple bonds are two of the most utilized transition metal catalyzed ether bond-forming reactions in natural product synthesis. These methods have become attractive due to their flexibility and generality that has been shown over the years. Copious amounts of studies have shown the addition process to proceed in very predictable ways, establishing the feasibility of the formation of the ether bond with high stereocontrol.

2.2.7.1 Wacker-type Reaction

The Wacker reaction offers a convenient method for oxidizing a C-C double bond to a ketone. An adjustment to this reaction using alcohols in place of water gives way to a method of forming C-O ether bonds.^{68,72} This process offers an approach to ether formation which utilizes simple Pd catalysis that can lead to further tandem reaction after the initial addition of the alcohol. This way of functionalizing a double bond could have great use when planning out a synthesis from the simplest starting materials.

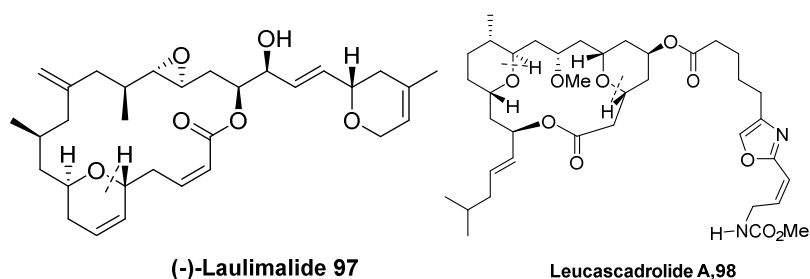
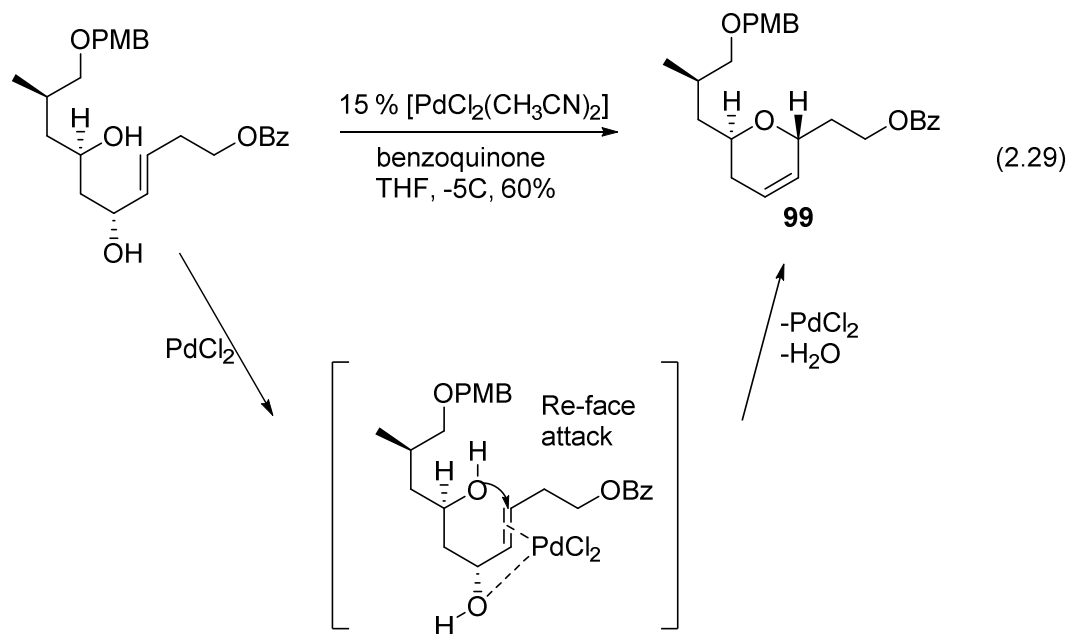


Figure 2.5: Natural Products from Wacker-type Oxidation

This Wacker-type reaction has found great use in the total syntheses of many natural products. In particular, the capability of the alkyl-Pd intermediates to undergo further reactions has been shown to be of broad utility. A few of these examples are shown (Figure 2.5).



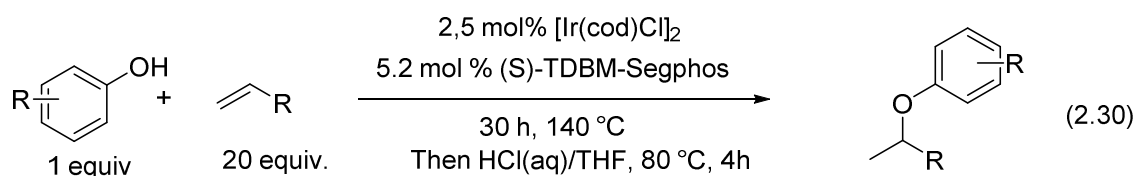
In the synthesis of microtubulin-stabilizer (-)-lulimalide (**97**),⁷² Uenishi and Ohmi showed that a Wacker-type reaction could be used to synthesize the chiral α,α' -dihydropyran moiety **99** [Eq. (2.29)]. The installment of a chiral allylic alcohol helps to direct the Pd-coordination in order to block the *Si*-face of the olefin leaving the *Re*-face open for attack of the nucleophile alcohol in a 6-*endo*-trig fashion.⁷² Then, β -hydroxide elimination provided the dihydropyran the potential for alkyl-Pd intermediates to undergo additional functionalization.

2.2.7.2 Hydroalkoxylation of Unactivated Aliphatic Alkenes

Metal catalyzed hydroetherification (the addition of an O-H bond across an unsaturated C-C bond) is much less developed. The ether products of hydroetherification are more often formed by substitution reactions than addition reactions.⁷⁴ The electrophiles in substitution reactions are typically prepared by a multistep sequence that includes

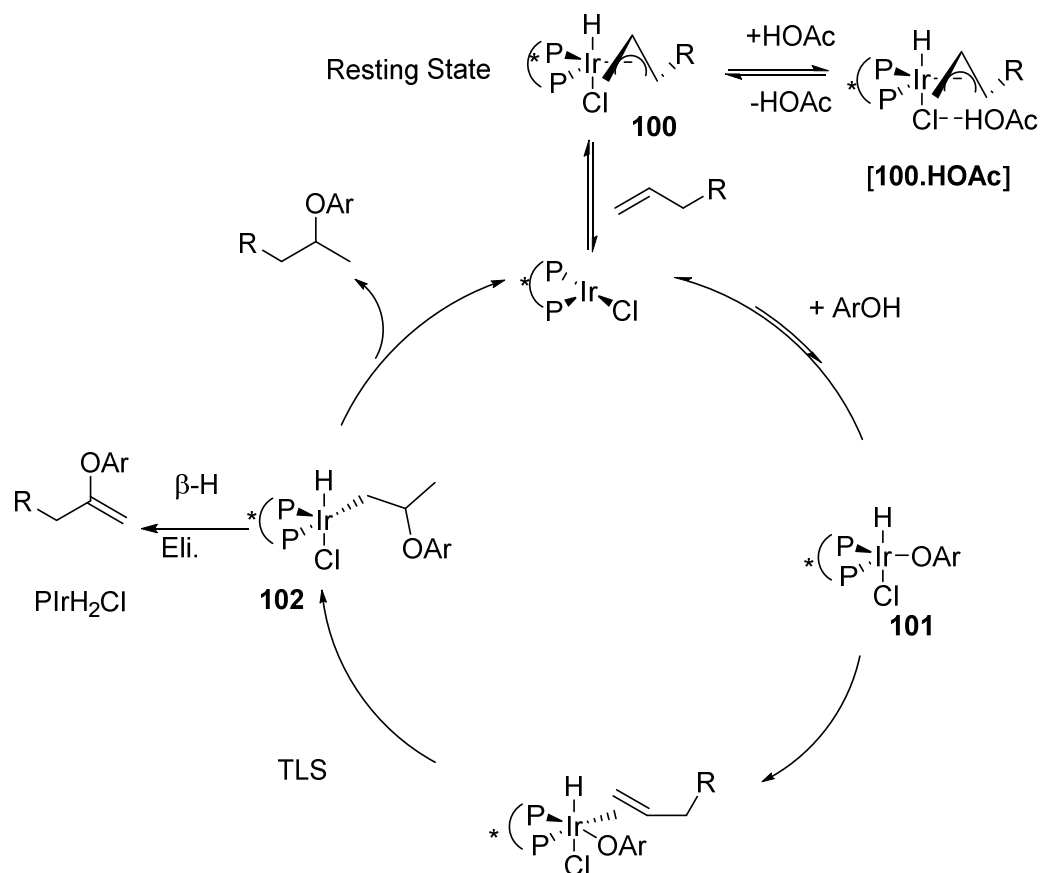
oxidation or reduction and functional group interconversion or activation of an alcohol. Moreover, these substitution reactions generate salt byproducts. Alternatively, ethers are formed by acid-catalyzed additions of alcohols to alkenes.⁷⁵ However, these additions often require strong acids and high temperatures, form side products from isomerization of carbocationic intermediates, and occur without control of the product stereochemistry. Moreover, acid-catalyzed additions of phenols to alkenes occur with competitive reaction of the alkene at the O-H bond and at an *ortho* or *para* C-H bond.⁷⁶ Metal-catalyzed hydroetherification would exploit the abundance and stability of alkene starting materials and could overcome many of the limitations of the classical syntheses of ethers.

In 2013 Hartwig group⁷⁷ reported one of the seminal intermolecular, metal-catalyzed additions of phenols to unactivated α -olefins in good yields. The measurable enantioselectivity and lack of reaction in the presence of acid but the absence of the metal show that the iridium complex rather than a proton catalyzes the addition reaction. Mechanistic studies imply that the reaction proceeds by reversible oxidative addition of the O-H bond of the phenol followed by turnover-limiting insertion of the alkene [Eq. (2.30)].



These mechanistic data are consistent with the proposed catalytic cycle shown in Scheme 2.23. In this mechanism, the (allyl) iridium hydride resting state **100**, which equilibrates with hydrogen-bonded [**100**·HOAr], undergoes C-H bond-forming reductive

elimination to release the olefin and form an Ir(I) complex that can undergo reversible, endergonic oxidative addition of the O-H bond of the phenol to form **101**.



Scheme 2.15: Proposed Mechanism for Ir Catalyzed Hydroetherification of Phenol and Alkene

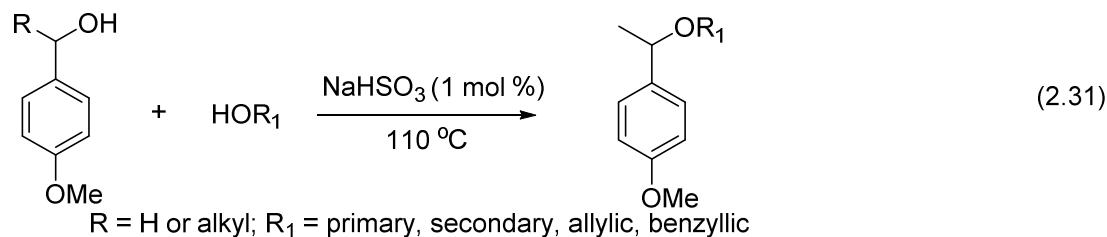
Subsequent olefin coordination and turnover-limiting insertion into the Ir-O bond forms an alkyl-Ir complex **101**. C-H bond-forming reductive elimination would then release the ether product, whereas β -H elimination from the same intermediate would form the enol ether side product. This mechanism is consistent with the observed zeroth-order dependence of the rate on the concentration of alkene because the alkene is released and added prior to the turnover-limiting step. This mechanism is also consistent with the fractional-order dependence with respect to the alcohol because a significant fraction of

the resting state exists as the alcohol adduct [$100 \cdot \text{HOAr}$]. The alcohol dissociates and adds prior to the turnover-limiting step of a reaction initiated from [$100 \cdot \text{HOAr}$]

2.2.8 Dehydrative Coupling of Alcohols by Sodium Bisulfite

Dehydrative coupling of two different alcohols are commonly used to synthesize symmetrical ethers because of low selectivity. Additionally, Elimination reaction competes with dehydration of the alcohol. With consideration of this selectivity issue, the synthesis of unsymmetrical ethers by using two different alcohols is not desired.

Liu⁷⁸ and coworkers showed more effective ways to synthesize unsymmetrical ethers by using two different alcohols in catalytic amount of sodium bisulfite (Scheme 2.24)⁷⁹ The substrate scopes of this coupling reaction were limited to benzyl alcohol derivatives with various aliphatic alcohols with moderate yield [Eq. (2.31)].

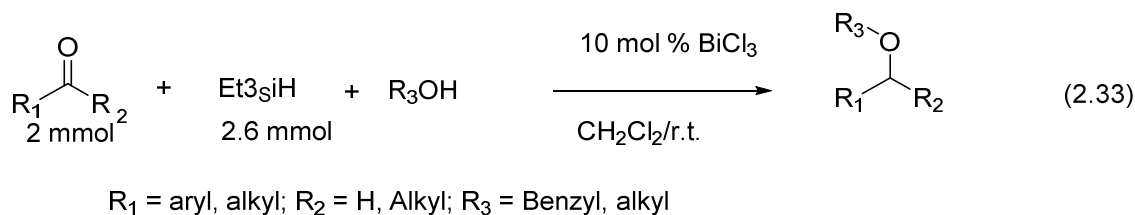
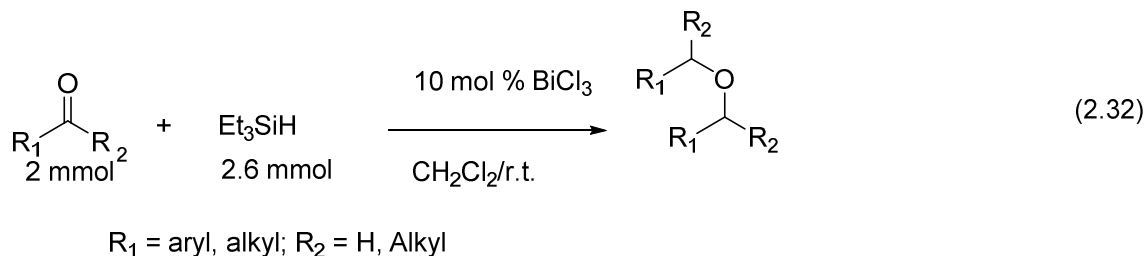


In the presence of 1 mol % of NaHSO₃ benzylic alcohols (1 mmol) reacts with aliphatic alkyl alcohol (8.0 mmol) to generate asymmetric product ether at 110 °C.

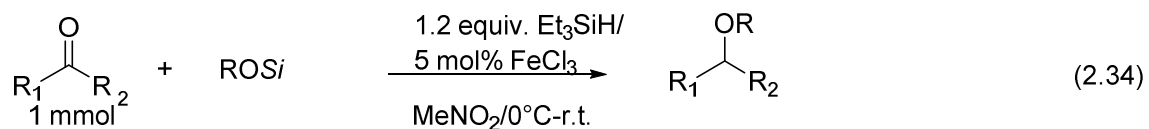
2.2.9 Reductive Etherification of Carbonyl Compounds

Reductive etherification of carbonyl compounds is known as an alternative method of the Williamson ether synthesis. In 1972, Doyle et al. reported the synthesis of ethers by the reduction of carbonyl compounds with triethylsilane in alcohol in the presence of

excess amounts of sulfuric acid or trifluoroacetic acid.⁸⁰ Nicolaou et al. demonstrated the formation of the oxepane ring from hydroxy ketone using 10 equiv. of triethylsilane and a stoichiometric amount of TMSOTf.⁸¹ In 2005, Izumi and Fukase described a reductive benzylolation of hydroxy functions by using the combination of benzaldehyde, triethylsilane, and quite an excess molar TMSCl.⁸² On the other hand, some methods have been reported for reductive etherification of carbonyl compounds with triethylsilane and alkoxytrimethylsilane under the influence of Lewis acids.⁸³ However, these reactions require an annoying step-by-step procedure or a longer reaction time. Although Wada et al. reported a reductive etherification of carbonyl compounds with alcohols promoted by bismuth(III) chloride under mild reaction conditions,⁷⁹ this involves some substrate limitation; the yields of the ether products from aliphatic aldehydes and ketones are unsatisfactory [Eq. (2.32) and (2.33)].



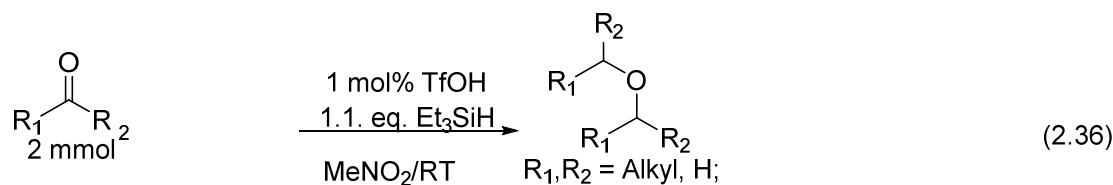
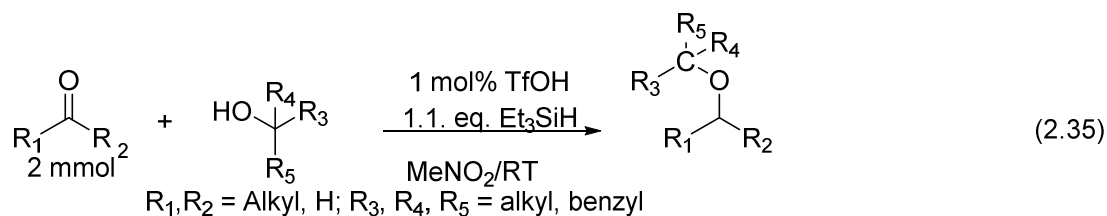
While exploring the reactions promoted by iron(III) chloride,⁸³ Iwanami *et al* have developed a highly efficient reductive etherification of carbonyl compounds with alkoxytrialkylsilane and triethylsilane catalyzed by iron(III) chloride [Eq. (2.34)].⁸⁴



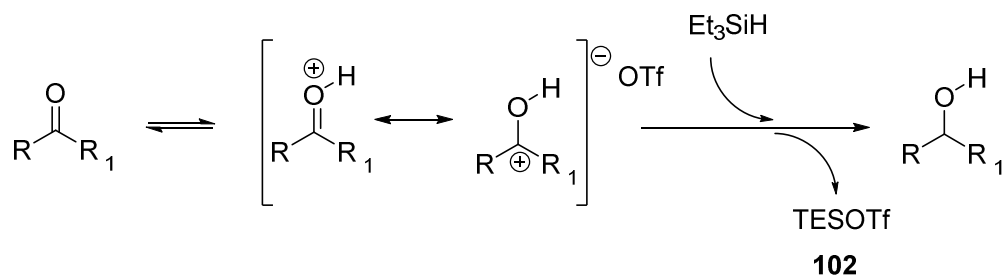
$\text{R}_1 = \text{aryl, alkyl}; \text{R}_2 = \text{H, Alkyl}; \text{Si} = \text{TMS, TES, TBS}$

This includes some striking features: 1) extremely short reaction time is needed in contrast to the known methods, 2) not only trimethylsilyl (TMS) ether but also triethylsilyl (TES) and t-butyldimethylsilyl (TBS) ethers can be used as the parent silyl ether, 3) various ethers are obtained from a wide range of aldehydes and ketones, and 4) high-yielding process. Etherification of carbonyl compounds with the parent alcohol, not alkoxytrialkylsilane, is more straightforward and promising. Therefore, they applied this reductive etherification into the naked and unmodified alcohols.

In 2011, Roth⁸⁵ has reported a general metal-free method for the direct reductive synthesis of symmetrical ethers, unsymmetrical ethers, and thioethers from carbonyl compounds through the use of organosilanes. The reaction was performed under one set of reaction conditions with triflic acid (1-5 mol %) as the catalyst and capable of being carried out in an open flask without any exclusion of moisture or air [Eq. (2.35) and (2.36)].

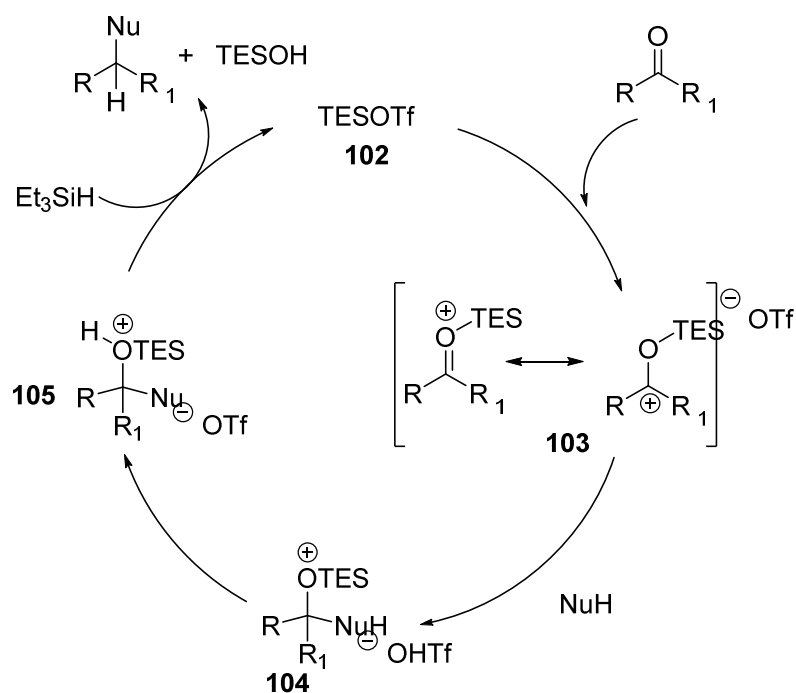


They proposed that in an initial step TESOTf **102**, is formed as the active catalyst from triflic acid, triethylsilane and the carbonyl substrate (Scheme 2.24).



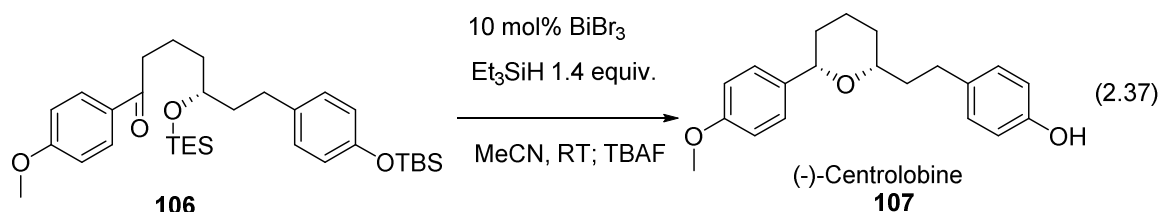
Scheme 2.16: Proposed Generation of Active Catalyst

The catalyst generated in situ then activates the carbonyl compound for a nucleophilic attack (**104**). Proton transfer and reduction gives the coupled product and silanol byproduct. The catalyst is regenerated and the catalytic cycle is completed (Scheme 2.17).

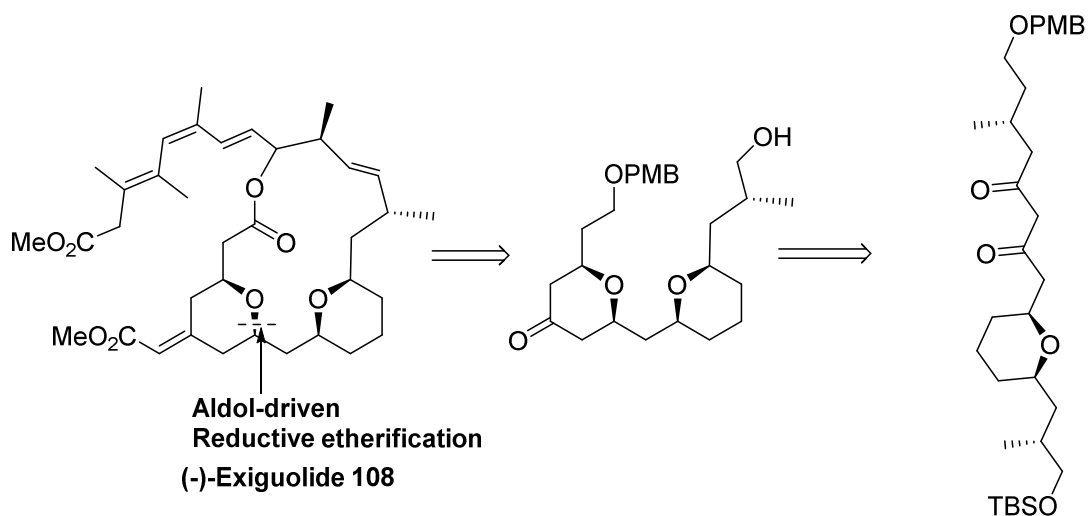


Scheme 2.17: Proposed Catalytic Cycle Based on TESOTf as Active Catalyst.

Few examples of application reductive etherification in synthesis of natural products.⁸⁶ Evans used the BiCl₃ catalyzed reductive etherification to synthesize the natural product (-)-Centrolobin ds_≥99:1 with 93% yield [Eq. (2.37)].

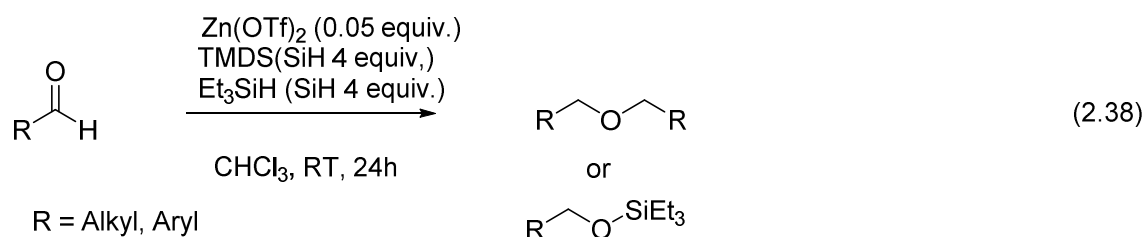


Reddy and coworkers described the formal total synthesis of (-)-exiguolide through the chiral-pool approach.⁸⁷ The major methylene *bis*-tetrahydropyran fragment was achieved in a convergent manner from L-glutamic acid and L-aspartic acid involving the *oxa*-Michael reaction and an aldol-driven reductive etherification as key steps for the formation of a tetrahydropyran ring. HF (40 %) in CH₃CN at room temperature is used for reductive etherification.

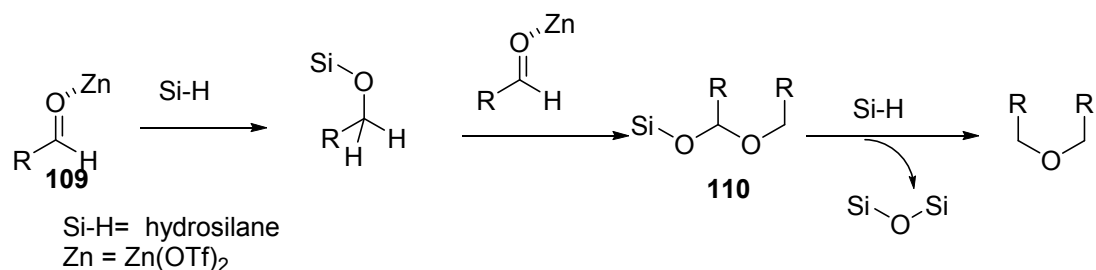


Scheme 2.18: Synthetic Route for the Synthesis of (-)-Exiguolide, **108**

In 2013, Sakai⁸⁸ reported an efficient reductive etherification of aromatic or aliphatic aldehydes using a reducing system that combines $\text{Zn}(\text{OTf})_2$ with either TMDS or Et_3SiH . This reducing system can also be applied to the hydrosilylation of aromatic aldehydes having either a strong electron-withdrawing group or a pyridine ring [Eq. (2.38)].



On the basis of these results, a plausible reaction path for the etherification they proposed is shown in Scheme 2.26. As with the etherification using a conventional reducing system, the reaction of the silyl ether, which was formed by hydrosilylation, with an activated aldehyde **109** initially produced a silylated hemiacetal **110**, followed by a second reduction of the acetal with another hydrosilane to afford the corresponding symmetric ether. Further, for the formation of the silyl ether, the introduction of a strong electron withdrawing group on the benzene ring remarkably lowered the nucleophilicity of the in situ formed silyl ether, which led to the preclusion of a subsequent addition.



Scheme 2.19: Proposed Mechanism for the Zn Catalyzed Etherification

CHAPTER 3

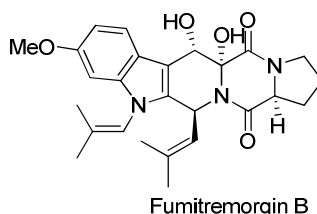
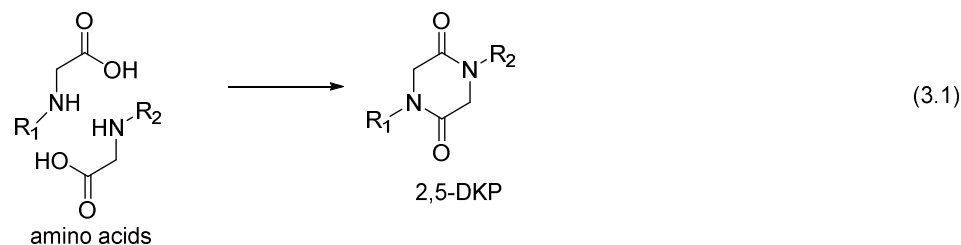
SYNTHESIS AND MECHANISTIC STUDIES OF DEAMINATIVE COUPLING REACTIONS OF AMINES WITH ALCOHOLS AND AMINO ACIDS WITH KETONES.

3.0. Introduction

Carbon-nitrogen (C-N) bond is commonly present in numerous organic compounds including amines, amino acids, proteins, drugs and natural toxins. Direct C-N cleavage coupling reactions are rare in organometallic chemistry due to strong C-N bond and poor leaving group ability of the amino group. Transition metal catalyzed cross coupling reactions involving C-N bond cleavage are rarely investigated. Trost¹⁻², Tian³ and Zhang⁴ reported catalytic examples of cross coupling of allylic amines. Very recently, Tian reported decarboxylative alkylation of β -keto acids by electron withdrawing group-activated alkylamines including C-N bond cleavage.³ Considerable research effort has been devoted Pd-catalyzed allylic alkylation reactions via the C-N bond cleavage of allylic amines.⁴ Hu established Pd catalyzed N-debenzylation of benzylamines in the presence of 1,1,2-trichloroethane.⁵ Very recently, Tian reported the Pd catalyzed cross coupling of primary allylic amine with boronic acid.⁶ Only few approaches have been reported on catalytic sp^3 C-N bond cleavage of tertiary reactions of amines. Although many organic transformations via sp^3 C-N bond cleavage have been widely encountered and investigated, simple and practical protocols for selective sp^3 C-N bond cleavage of primary and secondary amines have been found to be difficult because they are unreactive under strong acidic and basic conditions.

Amino acids are one of the major classes of compounds containing C-N bond. Amino acids play central role as both building blocks for proteins and as intermediates in metabolic cycles. The 22 natural α -amino acids that are found in proteins convey a vast array of chemical versatility in biological functions. Amino acids also perform critical biological roles outside proteins including neurotransmitters and ion transport.⁷ Non-protein amino acids also have important roles as metabolic intermediates, such as in the biosynthesis of the neurotransmitter γ -aminobutyric acid. Some non-standard amino acids are used as defenses against herbivores in plants.⁸

In organic synthesis, naturally occurring α -amino acids are commonly utilized as chiral reagents and also employed in the asymmetric synthesis of complex chiral molecules.⁹ One of the major uses of amino acids are as chiral auxiliaries in transition metal based enantioselective organic synthesis.¹⁰ Peptide synthesis is also very important in synthesis of number of bioactive molecules.¹¹ In typical peptide coupling reactions, the carboxylic acid moiety of the amino acid is first activated by an appropriate peptide coupling reagent, and then reacted with amine moiety of the other amino acid to produce desired peptides.¹² Synthesis of 2,5-diketopiperazines (2,5-DKP) [eq. (3.1)] is also very important in synthesis of various bioactive natural products and pharmaceuticals. Amine-protected and carboxylic acid protected amino acids are usually used for these coupling reactions. As an example fumitremorgin B, which is caused DNA damage in human lymphocytes is caused by amino acids Pro, Leu, Thr and Tyr.⁸ Optical active N-protected α -amino aldehydes which are derived from amino acids are extensively used in organic synthesis.¹³⁻¹⁴

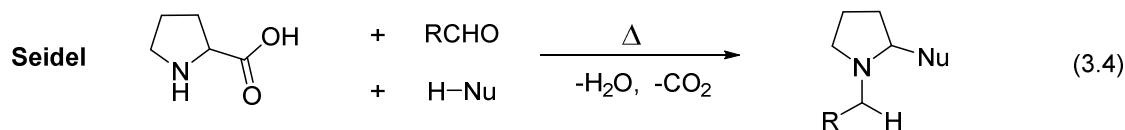
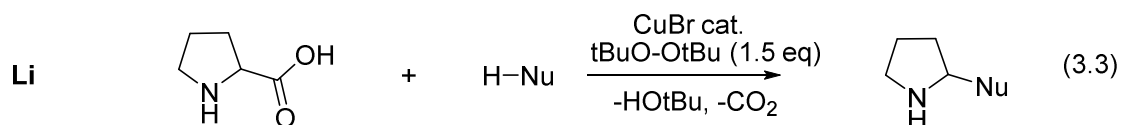
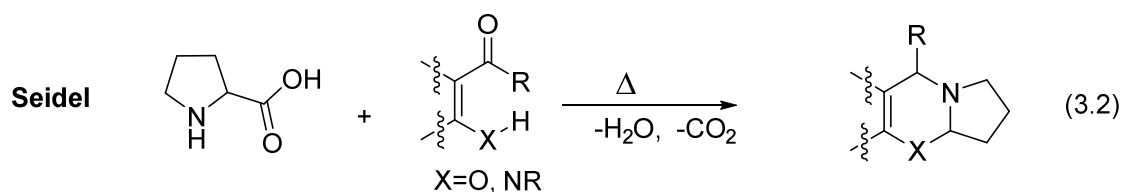


Decarboxylation of amino acids has been found to be one of the effective methods for obtaining a number of important amines. Transition-metal-catalyzed decarboxylative coupling reactions hold considerable promise among novel carbon-carbon bond formations owing to their potential advantages, such as high efficiency, selectivity, and convenience.^{16,17} For example, Goossen,¹⁸ Myers,¹⁹ and Tunge²⁰ groups have reported transition-metal-catalyzed intermolecular and intramolecular decarboxylative couplings of amino acids.

Few catalytic decarboxylative methods have been reported including catalytic peroxide or ketone in high boiling solvents, irradiation with UV light and heating in diphenylmethane solvents. Aoki reported decarboxylation of amino acids catalyzed by 2-cyclohexene-1-one.²¹ Decarboxylation of amino acids by microbes such as *Lactobacillus curvatus* CTC273 was reported²² Golding reported NBS catalyzed decarboxylation of α -amino acids into corresponding amines.²³

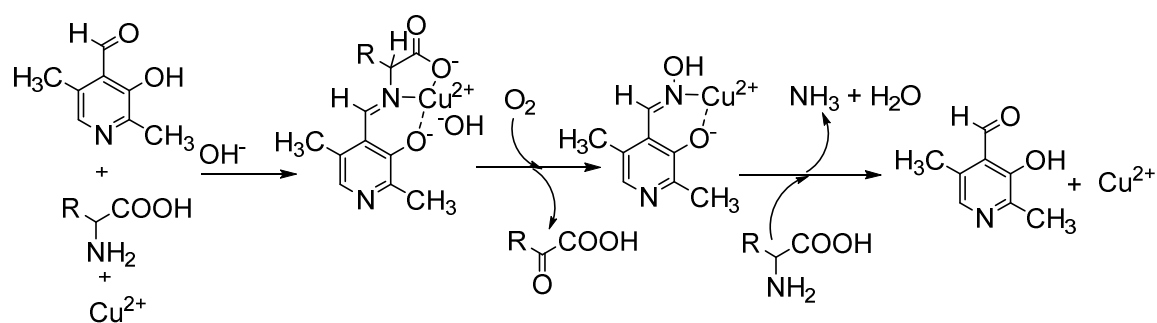
Li's research group reported a C-C bond-forming reaction based on a copper- or iron-catalyzed oxidative decarboxylative coupling of sp^3 -hybridized carbons with N-benzylproline.²⁴ Wang have reported copper iodide catalyzed aldehyde induced tandem

decarboxylation-coupling of natural α -amino acids and phosphites or secondary phosphine oxide.²⁵ Seidel and coworkers reported that decarboxylative Strecker reaction of amino acids with aldehyde coupling.²⁶ These new reactions expand the scope and synthetic utility of the catalytic decarboxylative coupling reactions previously developed. However, this method still suffers from drawbacks as in these methods need other oxidants²⁴ or transition metals²⁵ besides copper to facilitate the reaction. In 2010, Li's group [eq. (3.3)] and Seidel [eq. (3.2)] successfully improved the method involving a new reaction pathway, respectively, and they both reported an interesting aldehyde-induced intermolecular tandem decarboxylation-coupling of secondary α -amino acids with alkynes to afford propargylic amino derivatives, releasing H₂O and CO₂ as the only byproducts^{26,27} and also α -amination of N-heterocycle by using amino acid to make amins [eq. (3.4)]²⁸ In these methods, the carboxylic acids provide the possibility for site-specific functionalization of the α -amino acids skeletons, using decarboxylative coupling reactions to generate amine derivatives.



Deamination of amino acids is another way to use amino acids in organic synthesis due to the fact that selective C-N bond cleavage is more energetically disfavored than

decarboxylation. But in biological system deamination of amino acids are more common.³⁰ However few catalytic examples of deamination of amino acids are reported but those also similar to biological molecules. Diorganotin(IV) promoted deamination of amino acids by pyridoxal was reported by Varela.³⁰ Martel has reported molecular oxygen with pyridoxal derivatives and metal ion catalyzed oxidative deamination of amino acids.³¹ In all these cases, in the presence of Cu^{2+} and 3,5'-pyridoxal or pyridoxal 5'-phosphate react with amino acid to form Cu(II) complex of Schiff base intermediate, which reacts with O_2 to form oxidative deaminated product α -keto acid (Scheme 3.1). All of the literature explained above have limited substrate scope to proline and also high temperature $> 200^\circ\text{C}$. Furthermore, these reactions are limited to either decarboxylation or deamination of amino acids.



Scheme 3.1: Pyridoxal Derivatives and Cu^{2+} ion Catalyzed Oxidative Deamination of Amino Acids.

α -Alkylation of ketone is one of the most important reactions in organic synthesis. Traditionally ketones are transferred to metal enolates^{29a} or enamines,³² which are ready to react with carbon electrophile to give α -alkylated ketones. All these methods require stoichiometric amount of base or other reagents. In recent years, transition metal catalyzed α -alkylation of ketones has been developed.³³ Shim and coworkers reported that $\text{RuCl}_2(\text{PPh}_3)_3$ can catalyze R-alkylation of ketones with primary alcohols.³⁴ Ishii and co-

workers found that $[\text{IrCl}(\text{cod})]_2$ is an excellent catalyst for the R-alkylation of ketones with primary alcohols.³⁵ Very recently, the α -alkylation reaction of ketones with primary alcohols to make α -alkylated ketones was achieved using $\text{RuHCl}(\text{CO})(\text{PPh}_3)_3$ as a catalyst in the presence of Cs_2CO_3 as a base was reported by Ryu.³⁶

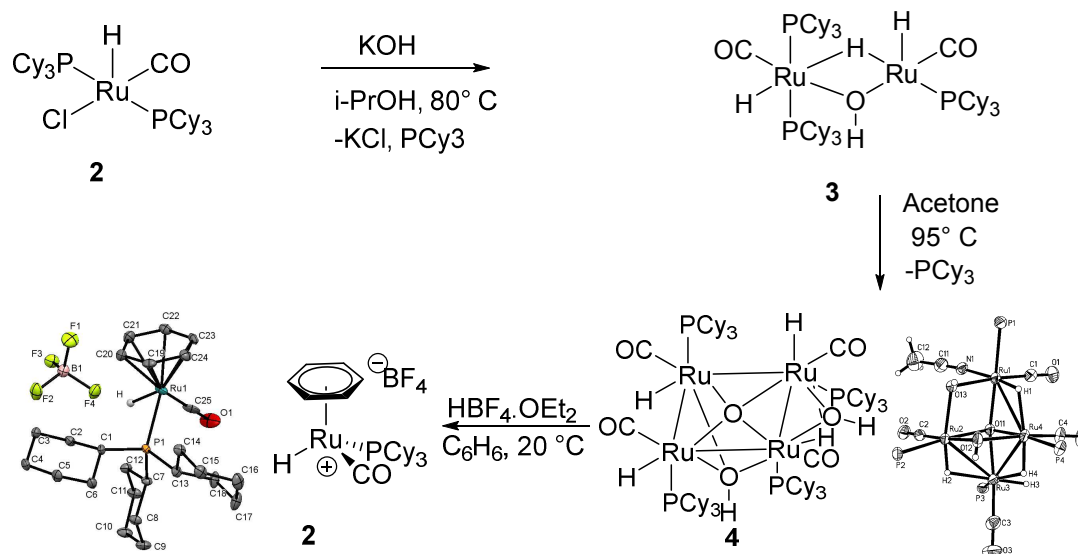
In general, classical alkylation reactions have been described with numerous strong bases which makes it necessary to use an excess of one of the reagents in the presence of promoters, such as stoichiometric strong bases or acids which generate salts as byproducts. In this context, recent advances have focused on methods able to develop catalytic, group-tolerant, environmentally benign, and mild reaction conditions. Development of catalytic alkylation methods to make complex molecules starting from readily available amino acids is beneficial from synthetic and environmental points of view. We developed a catalytic system for oxidative C-H alkylation of alcohol by deaminative coupling reactions of amines which involve C-N bond activation of amine primary or secondary amines and byproduct as ammonia. The catalytic method was successfully applied to the decarboxylative and deaminative coupling of amino acids with ketones. This chapter devotes the synthesis and mechanistic studies of deaminative coupling of amines with alcohols and deaminative and decarboxylative coupling of amine acid with ketones.

3.1. Results and Discussion

3.1.1 Synthesis and Mechanistic Studies of Deaminative Coupling Reactions of Amines

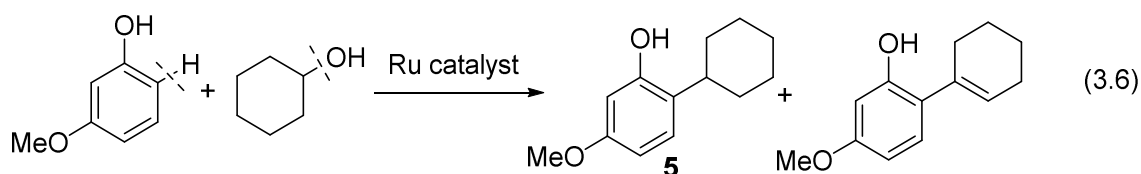
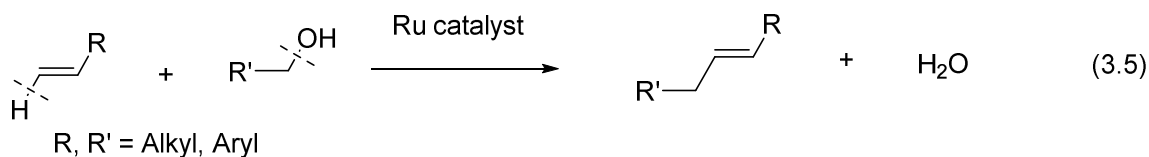
Recently, our research group developed a convenient method to synthesize a cationic ruthenium-hydride complex $[(\eta^6\text{-C}_6\text{H}_6)(\text{PCy}_3)(\text{CO})\text{RuH}]^+\text{BF}_4^-$ (**1**) from the protonation reactions of tetrameric ruthenium complex $\{[(\text{PCy}_3)(\text{CO})\text{RuH}]_4(\mu\text{-O})(\mu\text{-OH})_2\}$, which was synthesized in two steps from ruthenium hydride complex $(\text{PCy}_3)_2(\text{CO})\text{RuHCl}$ (**2**) (Scheme 3.2).³⁷ Reaction of **3** with KOH in 2-propanol produced the bimetallic complex **3**, which was isolated in 85 % yield after recrystallization in hexane. The subsequent treatment of **2** with acetone at 95 °C yielded complex **4** in 84 % yields as brown-red solid. Thus the treatment of tetrameric ruthenium complex **4** (200 mg, 0.12 mmol) with $\text{HBF}_4\cdot\text{OEt}_2$ (64 μL) in C_6H_6 at room temperature cleanly afforded the cationic ruthenium hydride complex **1**, which was isolated as ivory-colored solid in 95 % yield (Scheme 3.2). The ruthenium-hydride signal was observed at δ -10.39 (d, $J_{\text{P-H}} = 25.9$ Hz) by ^1H NMR spectroscopy of **1** in CD_2Cl_2 , and a single phosphine signal was detected at δ 72.9 ppm by $^{31}\text{P}\{^1\text{H}\}$ NMR spectroscopy. The molecular structure of the ruthenium complex **1**, as determined by X-ray crystallography, showed a three legged piano-stool geometry, which is capped by a η^6 benzene moiety.

We also reported selective catalytic C-H alkylation of alkenes with alcohols^{38a} [eq. (3.5)] and dehydrative C-H alkylation and alkenylation of phenol with alcohols to produce product **5** [eq. (3.6)].^{38b-39} In these reactions, alcohols were used as the alkylating agent to promote C-O bond cleavage which generate H_2O as the only byproduct.

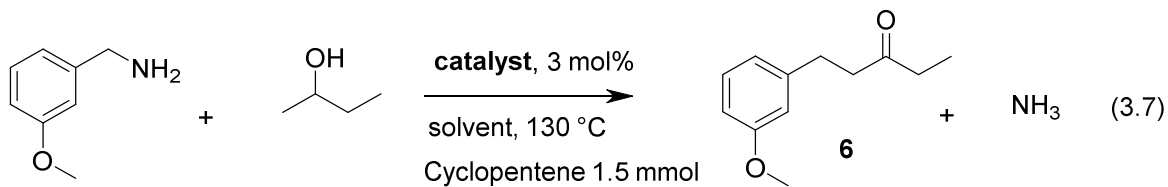


Scheme 3.2: Synthesis of Cationic Ruthenium Hydride Complex **1**.

Yi and Kwon^{37c} reported chelate assisted oxidative coupling reactions of aryl amides and unactivated alkene catalyzed by the same catalyst **1**.



Having well defined cationic ruthenium-hydride complex **1** in hand, we next explored its catalytic activity for the deaminative coupling reactions of amines with secondary alcohols. Initially, we found that **1** is an effective catalyst for the coupling of 3-methoxybenzylamine with 2-butanol in toluene at 130 °C to give (6-(3-methoxyphenyl)hexan-3-one) **6** in 89 % yield [eq. (3.7)].



This catalytic method efficiently produced deaminative coupling product **6** from the coupling of 3-methoxybenzylamine with 2-butanol which was isolated by simple silica gel chromatography. The structure of **6** was completely established by spectroscopic techniques [eq. (3.7)]. From both environmental and economic points of view, alcohol substrates constitute a highly attractive class of organic compounds because they are inexpensive and often easily derived from natural sources. As will be presented below, the catalytic method employs environmentally friendly and cheaply available alcohols, and exhibits a broad substrate scope and high chemoselectivity towards C-N bond cleavage reactions without employing any reactive agents.

3.1.2 Optimization Studies

3.1.2.1 Catalytic Survey

The catalytic activity of **1** was initially screened for the coupling reaction of 3-methoxybenzylamine with 2-butanol (Table 3.1). Thus, the treatment of 3-methoxybenzylamine (0.5 mmol) and with 2-butanol (0.6 mmol) with an excess amount of alkene (1.5 mmol) in the presence of the metal catalyst (3 mol %) in toluene at 130 °C was analyzed by GC-MS after 12 h reaction time. Among the surveyed ruthenium catalysts, complex **1** exhibits a uniquely high activity for the deaminative coupling reaction in the presence of cyclopentene additive. In the absence of cyclopentene as an additive, the

product yield is about 10 %. But none of them showed activity or gave product in low yield. All the other catalysts were investigated in the presence of cyclopentene.

3.1.2.2 Solvent and Temperature Effects

A number of different solvents were examined for the coupling reaction of amine and alcohol (Table 3.2). The treatment of 3-methoxybenzylamine (0.5 mmol) and 2-butanol (0.5 mmol) with excess amount of alkene (1.5 mmol) in the presence of ruthenium hydride catalyst **1** (3 mol %) in different solvents at 130 °C was analyzed by GC-MS after 12 h reaction time. Both chlorobenzene and toluene were found to be the most suitable for the amine coupling reaction among screened solvents (entry 1 and 2). Acetonitrile strongly coordinates to the ruthenium center and inhibits the catalytic activity (entry 6). Coordinative solvents such as dioxane and THF also coordinate to Ru center and are less effective for the catalytic reaction (entry 3, 5).

The temperature effect was investigated by running reactions at different temperatures (entry 7-9). The deaminative coupling reaction of amines requires relatively high temperatures at 130 °C, as no reaction was observed below 110 °C. No considerable increase in product yield was observed when temperature was increased to 140 °C. Therefore, 130 °C was chosen to be the most optimal temperature for the coupling reaction.

Table 3.1: Catalyst Survey for the Production **6** from 3-Methoxybenzylamine and 2-Butanol.^a

Entry	Catalyst	Additive	Yield (%) ^b
1	{[(PCy ₃)(CO)RuH] ₄ (μ-O)(μ-OH) ₂ }	Cyclopentene	0
2	1	Cyclopentene	89
3	1	-	10
4	RuHCl(CO)(PCy ₃) ₂	Cyclopentene	0
5	RuCl ₂ (PPh ₃) ₂	Cyclopentene	0
6	RuCl ₃ ·3H ₂ O	Cyclopentene	0
7	[Ru(p-cymene)Cl ₂] ₂	Cyclopentene	0
8	(PPh ₃) ₃ (CO)RuH ₂	Cyclopentene	0
9	Ru ₃ (CO) ₁₂	Cyclopentene	0
10	PCy ₃	Cyclopentene	0
11	HBf ₄ ·OEt ₂	Cyclopentene	0

^aReaction conditions: 2-butanol (0.6 mmol), 3-methoxybenzylamine (0.5 mmol), cyclopentene (2.5 mmol), catalyst (3 mol %) in toluene (2 mL) at 130 °C, 12 h. ^b The conversion of alcohol was determined by GCMS analysis using C₆Me₆ as an internal standard.

The coupling reaction was run with different amounts of catalytic loading. It was found that 3 mol % was the optimal catalytic loading as 1 mol % -1.5 mol % was less active), while the yield has not systematically increased at 5 mol %. From these optimization studies, we found that the optimum conditions for the coupling reaction are 3 mol % catalytic loading, 10 mol % cyclopentene, at 130 °C and 8-14 h reaction time and toluene as the solvent.

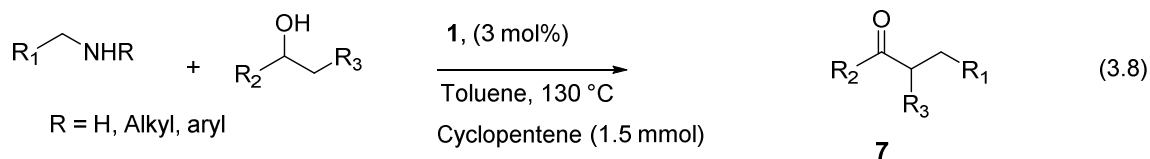
Table 3.2: Solvent Effect on the Reaction of 3-Methoxybenzylamine and 2-Butanol.^a

Entry	Solvent	Temp/°C	Yield(%) ^b
1	Toluene	130	89
2	Chlorobenzene	130	90
3	Dioxane	130	0
4	Methanol	120	<2
5	THF	120	22
6	CH ₃ CN	120	0
7	Toluene	110	<10
8	Toluene	120	75
9	Toluene	140	93

^aReaction conditions: 2-butanol (0.6 mmol), 3-methoxybenzylamine (0.5 mmol) , cyclopentene (1.5 mmol) , Ru-H catalyst **1** (3 mol %) in solvent (1 mL) at different temperatures °C, 12 h. ^b the conversion of ketone was determined by GCMS analysis using C₆Me₆ as an internal standard.

3.1.3 Reaction Scope

We found that catalyst **1** catalyzes deaminative coupling of amines and with alcohol to afford product **7** in high yield. [Eq. (3.8)] Addition of excess amount of cyclopentene (1.5 mmol) was found to promote the coupling reaction. Scope of the coupling reaction was investigated by the catalyst **1**.



Simple aliphatic amines such as propylamine smoothly react with 2-butanol to produce deaminative coupling product **7a**, which was analyzed by GC and GC-MS (Table 3.3, entry 1). Excess amine (5 equiv.) was used because *n*-propylamines has a low boiling point, and the products were analyzed by GC-MS method. *n*-Propylamine with aromatic substituted alcohols like 4-phenyl-2-butanol and 1-phenyl-1-ethanol also gave the corresponding coupling products, in high yield, in which the alkylation produced regioselectively to less sterically hindered side of alcohol (Table 3.3, entry 2 and 3). 1-Phenyl-1-ethanol with long chain primary aliphatic amines like 1-hexylamine also gives 90 % yield product **7d** (Table 3.3, entry 4).

To investigate diastereoselectivity of coupling reaction, the reaction of propylamine with a cyclic aliphatic alcohol such as cyclohexanol and cyclopentanol was examined (Table 3.3, entry 5-6). Propylamine with 2-methylcyclohexanol gave 1:1 ratio of diastereomeric coupling product by GC-MS yield (Table 3.3, entry 7). Cyclic aliphatic amines like cyclohexyl amine with 3-methoxyphenethanol led to the formation of coupling product in 68 % yield (Table 3.3, entry 8).

We investigated benzylamines with different aliphatic secondary alcohols. Benzylamines with 2-butanol, 1-phenylethanol gave the coupling products in high yield (Table 3.3, entry 9-10). Interestingly, 3-methoxybenzyl amine with 2-propanol, 2-pentanol and 1-phenylethanol provided coupling product in reasonable yield (Table 3.3, entry 11-13). Next, we explored the reactivity of benzylamine with aliphatic cyclic alcohols such as cyclopentanol, cyclohexanol, and cyclodecanol which gave moderately high yield of coupling products **7n**, **7o**, and **7q** (Table 3.3, entry 14-17). Also the coupling reaction with 3-methoxybenzyl amine with cycloheptanol produced 71 % of coupling product **7p**. The

coupling reaction of 2-methylcyclohexanol is with benzylamine exclusively formed a diastereoselective *cis* product (Table 3.3, entry 18).

Table 3.3: Deaminative Coupling of Amines with Alcohol.^a

entry	amine	alcohol	product(s)	time (h)	yield (%)
1				12	64
2	n = 1	R = Et	7a	8	91
3	n = 1	R = CH ₂ CH ₂ Ph	7b	8	82
4	n = 1	R = Ph	7c	8	89
	n = 3	R = Ph	7d		
5	n = 1			12	75
6	n = 2	R = H	7e	12	78
7	n = 2	R = Me	7f	12	69
			7g	dr(1:1)	
8	c-C ₆ H ₁₁ -NH ₂			12	82
			Ar = 3-OMeC ₆ H ₄		
			7h		
9				8	89
10	X = H	R = n-Pr	7i	8	84
11	X = H	R = Ph	7j	12	97
12	X = OMe	R = Me	7k	8	92
13	X = OMe	R = n-Bu	7l	8	90
	X = OMe	R = Ph	7m		
14				8	87
15	X = H, n = 1	R = H	7n	8	68
16	X = H, n = 2	R = H	7o	12	71
17	X = OMe, n = 3	R = H	7p	12	63
18	X = H, n = 6	R = H	7q	12	74
	X = OMe, n = 2	R = Me	7r	dr (>20:1)	

^aReaction conditions: alcohol (1.2 mmol), amine (1 mmol), cyclopentene (1.5 mmol), Ru-H catalyst **1** (3 mol %) in toluene (1 mL) at 130 °C.

Table 3.3 Cont.....

entry	amine	alcohol	product(s)	time (h)	yield (%)
19				10	81
20		X = OMe, R = Et X = OMe, R = Ph		10	89
21				12	62
		X = OMe	dr > 20:1		
22				8	88
23		R = H R' = Et		8	92
24		R = H R' = Ph		8	84
25		R = Me R' = n-Pr		8	89
		R = Me R' = Ph			
26				8	87
27		n = 1 n = 2		8	82
28				8	84
29				8	87
30				8	81

^aReaction conditions: alcohol (1.2 mmol), amine (1 mmol), cyclopentene (1.5 mmol), Ru-H catalyst **1** (3 mol %) in toluene (1 mL) at 130 °C.

We investigated the reaction of secondary benzylamines such as N-methyl-3-methoxybenzylamine with 2-butanol and 1-phenyl-1-ethanol selectively gave the coupling products **7s** and **7t**, which involved the cleavage of benzylic C-N over N-CH₃ bond (Table 3.3, entry 19, 20). Same amine with 2-methylcyclohexanol produces extremely cis diastereoselective of **7r** (Table 3.3, entry 21). Highly deactivated benzylamines such as 3, 5-dimethoxybenzyl amine with 2-butanol and 1-phenyl-1-ethanol also produced the coupling products **7u** and **7v** in 88 % and 92 % yield respectively (Table 3.3, entry 22, 23). Same amine with 3-hexanol gave exclusively regioselectively coupled at less hindered β -carbon of alcohol in 84 % yield as a racemic mixture **7w** (Table 3.3, entry 24). 1-Phenyl-1-propanol with 3, 5-dimethoxybenzyl amine produced corresponding ketone **7x** with a chiral center (Table 3.3, entry 25). Cyclic aromatic alcohols such as 1, 2, 3, 4-Tetrahydro-1-naphthol and 1-indanol react with 3, 5-dimethoxybenzylamine yielding 87 % and 82 % coupling products **7y** and **7z** (Table 3.3, entry 26, 27). Then we explored the scope to 3-methoxyphenethylamine with 1-phenyl-1-ethanol, 2-butanol, which formed coupling products and cyclopentanol in high yield (Table 3.3, entry 28-30).

We explored the synthetic utility of coupling of alcohols by using biologically active amines and chiral and heterocyclic amines (Table 3.4). Ethyl 3-benzylaminopropionate which is a β -alanine derivative also led to selective deamination of benzyl C-N bond coupling with alcohols (Table 3.4, entry 1). Chiral amines such as (R)-2-phenyl-1-propylamine react with 1-(4-methoxyphenyl) ethanol leading to formation of chiral ketone **8b** in 60 % yield with stereoselectively (Table 3.4, entry 2).

The reaction with 1-acenaphthenol gave the coupling product **8c** with 3:2 diastereomeric ratio in 90 % yield (Table 3.4, entry 3) and with cyclic alcohol such as

cyclopentanol with high diastereoselectivity 10:1 ratio in 85 % yield (Table 3.4, entry 46). Next we tried to expand the scope to α,β -unsaturated ketone substrate such as 1-acetyl-1-cyclohexene with benzylamine which led to formation of saturated coupling product **8e** (Table 3.4, entry 4). Then we expanded the scope for biologically active alcohol and ketone compounds.

Table 3.4: Deaminative Coupling of Various Amines and Biologically Active Compounds.

entry	amine	alcohol	product(s)	time (h)	yield (%)
1				12	85
2				12	75
3				12	60
4				12	85
5				12	68
6				12	65

Table 3.4: Cont....

entry	amine	alcohol	product(s)	time (h)	yield (%)
7			 2:1	12	70
8			 (23:1 d.r.)	12	52
9			 (>20:1 d.r.)	12	54
10				12	54
11				12	80
12				12	70

^aReaction conditions: alcohol (1.2 mmol), amine (1.0 mmol), cyclopentene (1.5mmol), Ru-H catalyst **1** (3 mol %) in toluene (1 mL) at 130 °C.

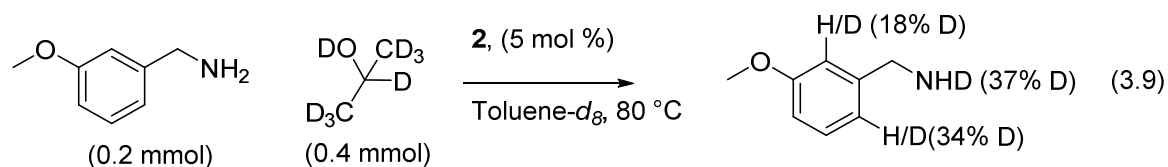
The case of 3-methoxybenzylamine with progesterone led to the formation of selective alkylation of 2-benzyl progesterone **8f** in *cis:trans* (3:1) diastereomeric mixture in 65 % yield (Table 3.4, entry 5). When 3-methoxybenzylamine coupled with estradiol led to formation of selective alkylation of 16'-aryl progesterone **8g** in *cis:trans* (2:1) diastereomeric mixture in 70 % yield (Table 3.4, entry 6). In both cases, *cis* diastereomer is the major product. Benzylamine with cholesterol led to formation of 2-

benzylcholetenone with high regio- and stereoselective dr >20:1, 3- α product **8h**. Benzylamine with benzyl deoxycholic acid ester produces 3- β product selectively **8i**. Heterocyclic benzyl amines such as 2-aminomethylpyridine and 2-aminomethylfuran with 1-phenylethanol produces corresponding ketone product in high yield (Table 3.4, entry 10-12)

3.1.4 Mechanistic Study

3.1.4.1 H/D exchange experiment

The following kinetic experiments were performed to gain mechanistic insights into catalytic C-N bond cleavage reaction of amines. To examine H/D exchange pattern of benzylamine, the reaction of 3-methoxybenzyl amine (0.2 mmol) with 2-propanol- d_8 (0.4 mmol, 99 % D) in the presence of **1** (4 mg, 3 mol %) in toluene- d_8 (0.4 mL) at 80 °C was seen for 1 h [eq. (29)]. The reaction progress was monitored by both ^1H and ^2H NMR.



A substantially higher amount of deuterium incorporation to the arene *para* to the methoxy group (34 %) was observed than to the hydrogen to the *ortho* to methoxy group (18 %) (Figure 3.1). The results indicate that the meta-electron releasing group promotes *ortho*-metallation of benzylamine substrate.

The results are not consistent with a possible mechanism through imine formation.³⁹ But in H/D exchange experiment none of H/D exchange was observed at benzylic C-H of 3-methoxybenzylamine. If the mechanism is going through imine formation, it should exchange D at benzylic position of benzylamine [eq. (3.10)].

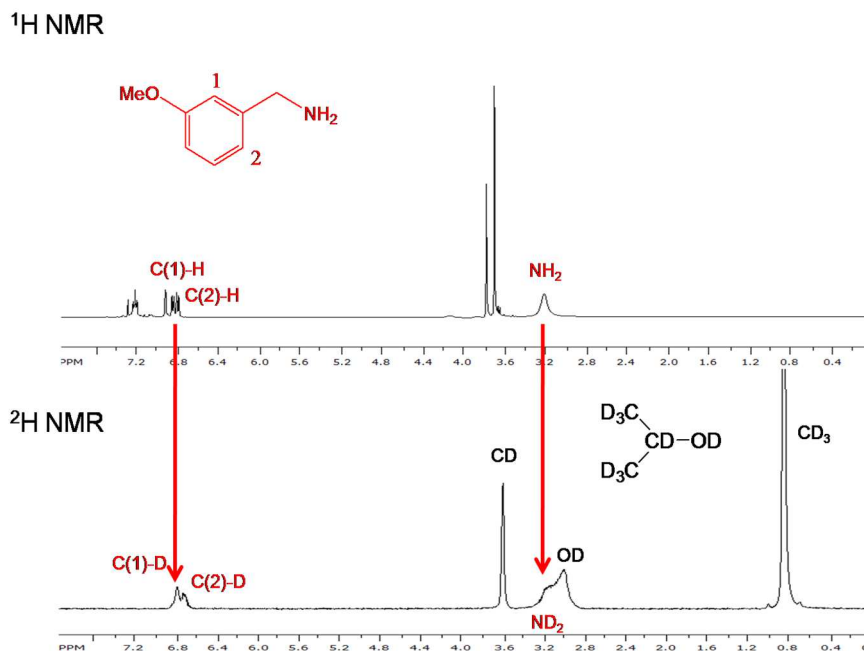
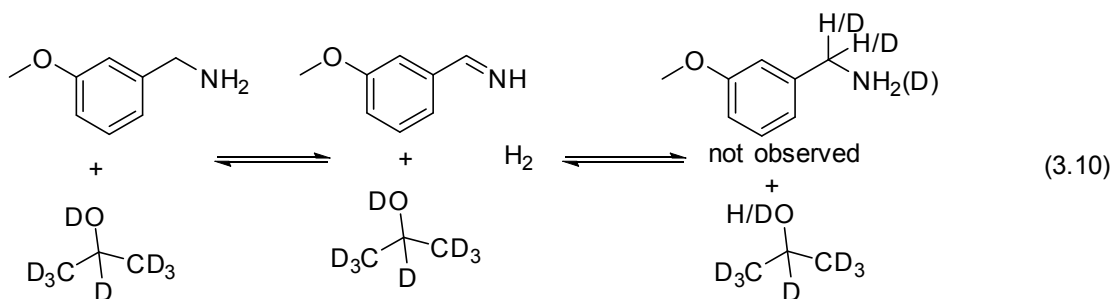


Figure 3.1. ¹H and ²H NMR Spectra of the Reaction Mixture of 3-Methoxybenzyl Amine with 2-Propanol-*d*₈ at 80 °C.



3.1.4.2 Hammett Study

Hammett studies of *para*-substituted benzylamine substrates were performed to determine the electronic effects on arylalketone substrate during C-N bond cleavage reaction. *Para*-substituted benzylamines, *p*-X-C₆H₄CH₂NH₂ (X = OCH₃, CH₃, H, Cl) (1.0

mmol), 1-phenylethanol (1.5 mmol), cyclopentene (0.05 mmol) and complex **1** (3 mol %) were dissolved in toluene (2 mL) in six separate 25 mL Schlenk tubes in a glove box. The tubes were brought out of the glove box, and stirred in an oil bath set at 120 °C. Each reaction tube was taken out of the oil bath in 30 minute intervals, and was immediately cooled and analyzed by ^1H NMR using hexamethyl benzene as the internal standard. The k_{obs} was determined from a first-order plot of $-\ln([p\text{-X-C}_6\text{H}_5\text{CH}_2\text{NH}_2]_t/[p\text{-X-C}_6\text{H}_5\text{CH}_2\text{NH}_2]_0)$ vs. time. The Hammett plot of $\log(k_X/k_H)$ vs. σ_p is shown in Fig. 3.2. The reaction rate was found to be considerably accelerated by benzylamine containing electron donating groups.

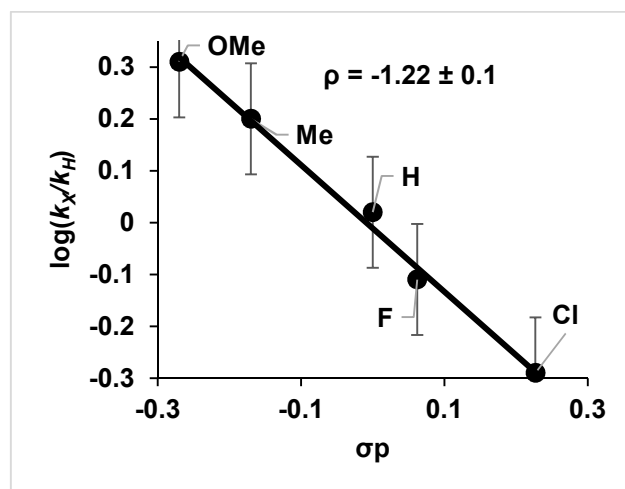
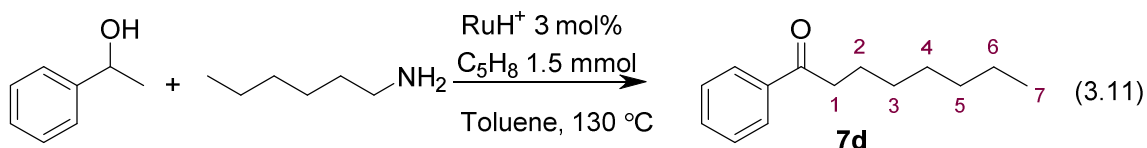


Figure 3.2. Hammett Plot of $p\text{-X-C}_6\text{H}_4\text{CH}_2\text{NH}_2$ (X = OCH₃, CH₃, H, Cl, Br) with 1-Phenyl-1-ethanol.

The Hammett correlation of *para*-substituted benzylamine substrates ($p\text{-X-C}_6\text{H}_4\text{CH}_2\text{NH}_2$ (X = OMe, CH₃, H, F, Cl)) led to $\rho = -1.2 \pm 0.1$ (Figure 3.2). Thus, a relatively electron rich Ru catalyst with electron-donating group should promote the binding and the activation of C-N bond. The negative value of ρ indicates considerable cationic character

in the transition state of the ruthenium complex which is generated from keto-enol tautomerization of ketone. We believe that a highly electrophilic ruthenium enolate complex is formed during the reaction and C-N bond cleavage is the rate determine step (Scheme 3.4).



3.1.4.3 Carbon Isotope Effect Study.

The following ¹³C KIE experiment was performed to established rate- determine step of the catalytic reaction. In a glove box, 1-phenylethanol (1.5 g, 1.5 mmol), 1-hexylamine (1.6 g, 12 mmol), cyclopentene (70 mg, 1 mmol) and complex **1** (180 mg, 3 mol %) were dissolved in toluene (30 mL) in 3, 100 mL Schlenk tubes equipped with a Teflon screw cap stopcock and a magnetic stirring bar. The tube was brought out of the box, and stirred for 4h, 4.5h, and 5 h respectively, in an oil bath which was preset at 120 °C. Compound 1-phenyl-1-octanone (**7d**) was isolated by a column chromatography on silica gel (hexanes/EtOAc = 40:1 to 10:1) separately after filtering through a short silica gel column eluting with CH₂Cl₂ (20 mL), and each solution was analyzed by GC (15, 18 and 20 % conversion). The commercially available authenitc sample was used as the virgin sample.

The ¹³C{¹H} NMR analysis of the recovered and virgin samples of 1-phenyl-1-octanone was performed by following Singleton's ¹³C NMR measurement technique.⁴⁰ The

NMR sample of virgin and recovered 1-phenyl-1-octanone was prepared identically by dissolving (100 mg) in CDCl_3 (0.5 mL) in a 5 mm high precision NMR tube. The $^{13}\text{C}\{^1\text{H}\}$ NMR spectrum was recorded with H-decoupling and 45 degree pulse. A 60 s delay between pulses was imposed to minimize T_1 variations (d1 = 60 s, at = 5.0 s, np = 245098, nt = 704).

The data are summarized in Table 3.6.

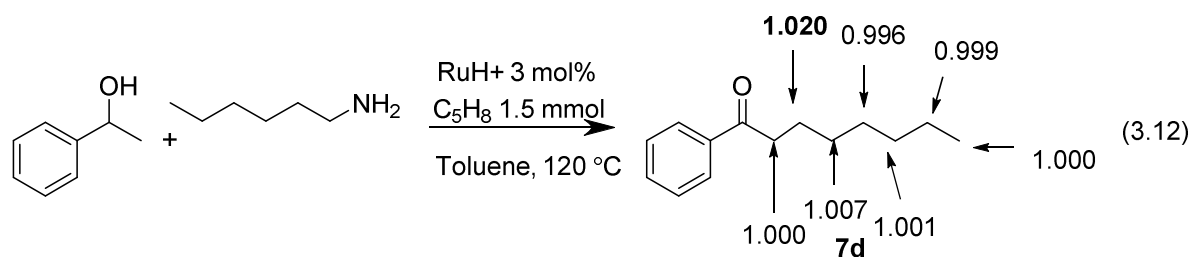


Table 3.5: Calculated Average ^{13}C KIE from Virgin (R_0) and Recovered (R) Samples of Octanophenone.

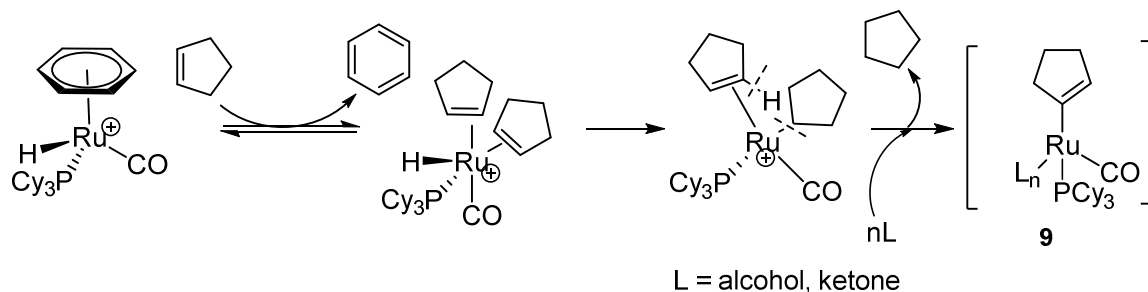
Carbon no.	Authentic sample (R_0)	Low conversion 7d (R)	R_0/R	^{13}C KIE
1	1.000(0)	0.995(0)	1.005	1.000
2	1.000(3)	0.977(5)	1.023	1.023
3	1.000(1)	0.9998(3)	1.002	1.002
4	0.998(9)	1.001(3)	0.997	0.997
5	1.003(3)	1.002(1)	1.002	1.001
6	1.000(1)	1.000(2)	1.000	1.000
7	1.000(0)	1.000(0)	1.000	1.000

As shown in Equation 3.12, the most pronounced carbon isotope effect was observed on the β -carbon atom of **7d** when the ^{13}C ratio of product at average 18 % conversion was compared to that of the virgin sample ($^{13}\text{C}(\text{low conversion})/^{13}\text{C}(\text{virgin})$) at

$C_{\beta} = 1.020$, average of three runs). Using the equations developed by Melander and Saunderson,⁴¹ the $^{12}\text{C}/^{13}\text{C}$ isotope effects are calculated as summarized in Table 3.5. NMR measurement gave KIEs which are relative to some reference atom C(8), which has KIE 1.000 by definition. C8 was chosen as the reference atom of **7d** because it is the carbon atom furthest from the site of alkylation. We observed that a significantly lower incorporation of ^{13}C at the C(3) = 1.020 of the product **7d** due to slower rate of C-N bond cleavage. C(3) of the product is from the C-N bond of amines. This results consistency with the C-N bond cleavage is much slower than the other steps of the alkylation reaction. If the C-C bond formation or enolate formation is the rate limiting step ^{13}C KIE should be higher on C2.

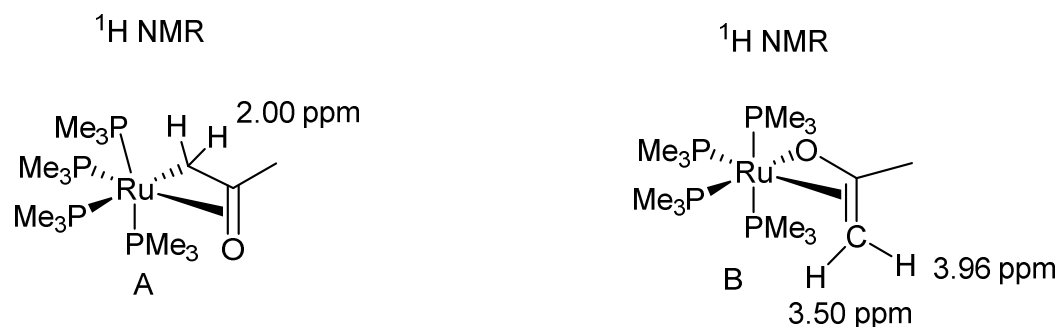
3.1.4.4 Proposed Mechanism

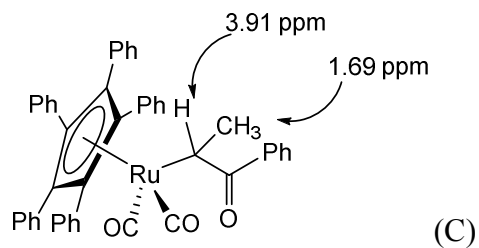
Although details of the reaction mechanism remain unclear, we present a working hypothesis involving ruthenium enolate as a mechanistic rationale for the cleavage of C-N bond and formation of product **7**, as illustrated in Scheme 3.3. Dehydrogenation of alcohol to carbonyl compounds are known for the tetrameric ruthenium catalyst,³⁷ and ketone from alcohol dehydrogenation was detected by GC-MS of crude mixture. Therefore, we propose that the first step would be the formation of ketone from alcohol. On the basis of similar reactivity pattern^{38a}, we propose a mechanism involving a cationic Ru-alkenyl species **9**, which is initially formed from the reaction of **1** with two equivalents of cyclopentene substrate via the vinylic C-H activation and an alkane elimination step (Scheme 3.3).³⁹



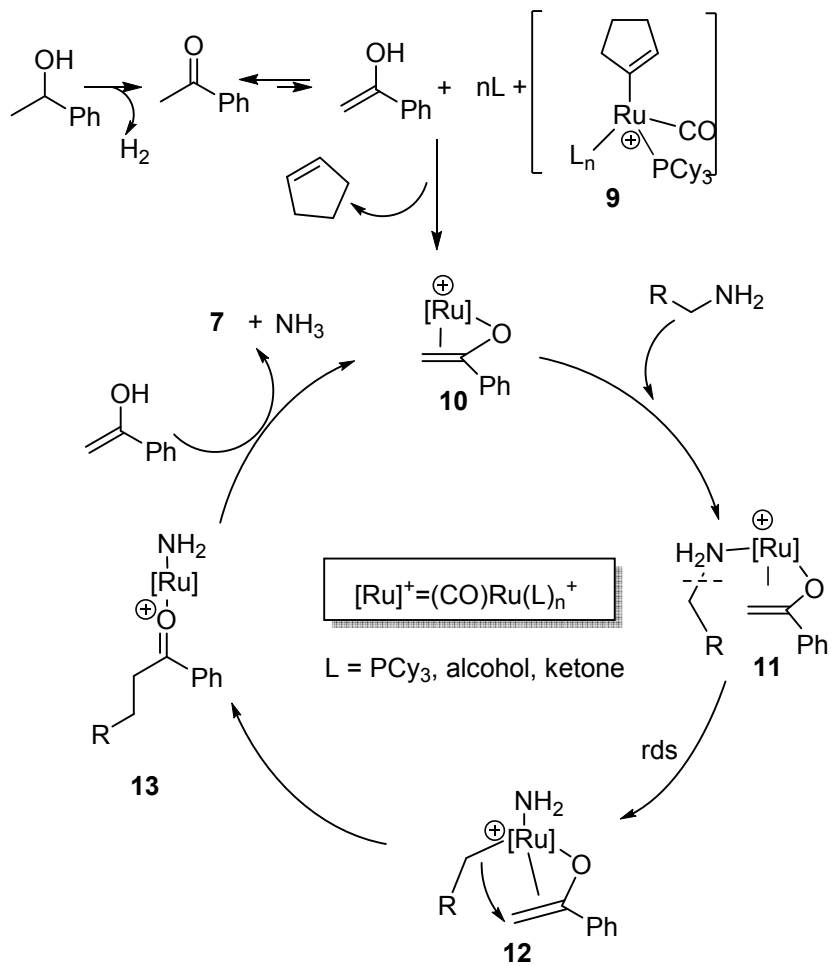
Scheme 3.3: Generation of Cationic Ru-Alkenyl Species **9**.

Next we attempt to generate catalytically relevant ruthenium enolate complex **10**, which could be formed from complex **9** with reaction of enol form of the ketone and cyclopentene act as a hydrogen acceptor in this step.⁴³ Hartwig et al have been identified and characterized O-bound (A) or C-bound Ruthenium enolates (B).^{43g-1} Very recently, Martín-Matute also identified C-bound Ru enolate (C), and they proposed that is not the catalytically active species in the reaction of β -hydroxy ketone from allylic alcohol catalyzed by $\text{Ru}(\eta^5\text{-C}_5\text{Ph}_5)(\text{CO})_2\text{Cl}$. Their attempts were not successful to identify Ru O-bound enolate species and they proposed the Ru O-bound enolate is the catalytically active intermediate.^{43f}





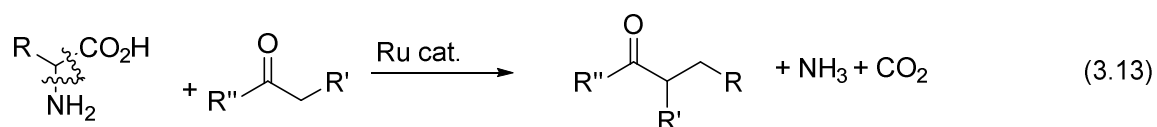
We also proposed that the O-bound ruthenium enolate **10** will be catalytically active species in the amine coupling reaction generated from active ruthenium species **9**, because C-bound enolate stable 18e complex and O-bound enolate is in equilibrium with η^1 and η^3 which has coordination site for another molecule. Then the amine coordinates to the active Ru species **10** (Scheme 3.4). Though the exact mechanism of the C–N cleavage step is not clear at the present time, one possible pathway involves the oxidative addition of the C–N bond to form a cationic Ru(IV)-alkenyl-alkyl species **11** (similar complexes for C–O bond has been proposed).^{40a} High negative Hammett value suggest that the cationic character in the rate limiting step of the reaction. We proposed that is due to formation of highly electrophilic ruthenium enolate species **10** is involved in the reaction. Therefore we propose that the oxidative addition of amine C–N bond will be the rate determine step as described under ¹³C KIE study. The next step is insertion of alkyl group to the enol to form ketone coupled product.⁴³ Catalytically active species **9** is regenerated by reacting another enol and release of product **7** and NH₃. Ammonia was detected from the crude reaction mixture giving white fumes with concentrated HCl.



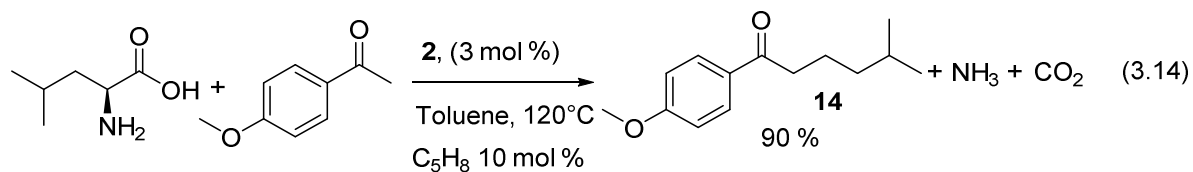
Scheme 3.4: Proposed Mechanism for Deaminative Coupling of Amines with Alcohol.

3.2 Synthetic and Mechanistic Studies of Decarboxylative and Deaminative Coupling Reactions of Amino Acids with Ketones.

From both environmental and economic points of view, amino acids constitute a highly attractive class of alkylating reagent because they are inexpensively derived from natural sources and ammonia and carbon dioxide is the only by-product resulting from the associated coupling reaction. We developed catalytic system for decarboxylative and deaminative coupling reactions of α - and β -amino acids ketones. The coupling reaction involves C-C and C-N bond activation of amino acids with linear alkyl chain also and for more functionalized amino acids. The byproducts of this reaction are ammonia and carbon dioxide which are removed from the reaction mixture. To the best of our knowledge this is the first example of catalytic C-C and C-N bond cleavage of amino acids by metal ion catalysis [eq. (3.13)].



Having well defined cationic ruthenium-hydride complex **1** in hand, we explored its catalytic activity for decarboxylative and deaminative coupling reaction of amino acids with ketones. For example, L-Leucine (1.2 mmol), 4-methoxyacetophenone (1 mmol), cyclopentene (10 mmol) and complex **1** (17 mg, 3 mol %) were dissolved in toluene (2 mL) and was stirred in an oil bath set at 120 °C for 12 h to obtain coupling product with 90 % yield [eq. (3.14)]. This catalytic method efficiently produces decarboxylative and deaminative coupling product **14** from the reaction of L-leucine with 4'-methoxyacetophenone which was isolated by simple silica gel chromatography and the structure was completely established by spectroscopic techniques [eq. (3.14)].



3.2.1 Optimization of Reaction Conditions

3.2.1.1 Catalytic Survey

To assess the feasibility of the deaminative coupling reaction, we initially screened a number of ruthenium catalysts for the coupling reaction of (L)-leucine with 4'-methoxyacetophenone under the reaction conditions stipulated in Equation (14). Among screened catalysts, the catalyst **1** shows distinctively high activity in forming the coupling product 1-(4-methoxyphenyl)-5-methylhexan-1-one (**14**). Moreover, the catalyst mediates highly regioselective alkylation to the sterically less demanding α -ketone carbon atom in forming the product **14**.

Following the previously developed protocol for generating an active ruthenium vinyl species,^{38c} we have been able to promote the catalytic activity of **5** by adding a substoichiometric amount of an alkene (10 mol %). We have also been able to trap both ammonia and carbon dioxide byproducts by chemically converting them into isolable forms. Thus, carbon dioxide is readily converted into BaCO₃ (82% CO₂) with Ba(OH)₂, while the treatment of the crude reaction mixture with HCl (aq.) is used to estimate the formation of ammonia (79 % NH₃) by following a literature procedure.⁴⁵⁻⁴⁷

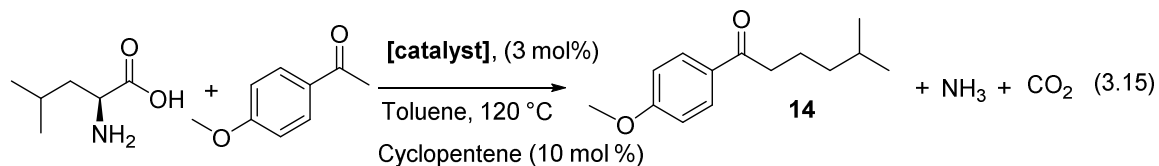


Table 3.6: Catalyst Screening for the Coupling of 4-Methoxyacetophenone with L-leucine.^a

Entry	Catalyst	Additive	Yield (%) ^b
1	1		90
2	[RuH(CO)(PCy ₃) ₄ (O)(OH) ₂]		5
3	[RuH(CO)(PCy ₃) ₄ (O)(OH) ₂]	HBF ₄ ·OEt ₂	55
4	RuHCl(CO)(PCy ₃) ₂	HBF ₄ ·OEt ₂	0
5	RuCl ₃ ·3H ₂ O		0
6	RuCl ₂ (PPh ₃) ₃	HBF ₄ ·OEt ₂	0
7	RuH ₂ (CO)(PPh ₃) ₃	HBF ₄ ·OEt ₂	<5
8	[RuH(CO)(PCy ₃) ₂ (CH ₃ CN) ₂] ⁺ BF ₄ ⁻		10
9	[(<i>p</i> -cymene)RuCl ₂] ₂		0
10	Ru ₃ (CO) ₁₂	NH ₄ PF ₆	0
11	HBF ₄ ·OEt ₂		0

^aReaction conditions: L-Leucine (0.6 mmol), 4-methoxyacetophenone (0.5 mmol), cyclopentene (10 mol %), catalyst (3 mol %) in toluene (2 mL) at 120 °C, 12 h. ^b The product yield was determined by GC and GC-MS using C₆Me₆ as an internal standard.

3.2.1.2 Solvent and Temperature Effects

The solvent effect on the activity was examined for the coupling reaction of amino acid with ketone [Eq. (3.16)]. The treatment of L-Leucine (0.6 mmol) and 4-methoxyacetophenone (0.5 mmol) with substoichiometric amount of alkene (10 mol %) in the presence of metal catalyst **1** (3 mol %) in different solvents at 120 °C was analyzed by

GC-MS after 12 h reaction time. It was found that the nature of the solvent considerably affects the activity of coupling reaction.

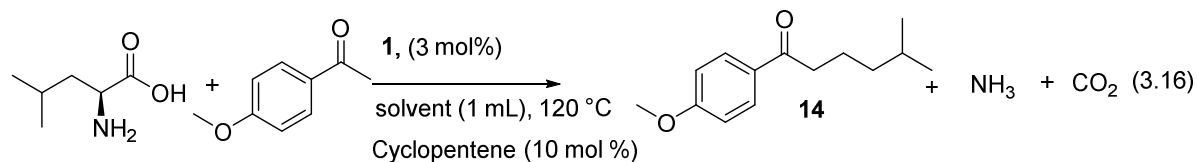


Table 3.7: Solvent Effect on the Reaction of Leucine with 4-Methoxyacetophenone.^a

Entry	Solvent	Temp/°C	Yield(%) ^b
1	Toluene	120	90
2	Chlorobenzene	120	88
3	Dioxane	120	18
4	Methanol	120	<5
5	THF	120	15
6	CH ₃ CN	120	0
7	Toluene	100	<2
8	Toluene	110	35
9	Toluene	135	95

^aReaction conditions: L-Leucine (0.6 mmol), 4-methoxyacetophenone (0.5 mmol), cyclopentene (10 mol %), catalyst (3 mol %) in solvent (1 mL), time 12 h. ^b the conversion of ketone was determined by GCMS analysis using C₆Me₆ as an internal standard.

Non-protic, non-coordinating solvents such as chlorobenzene or toluene were found to be the most suitable for the amine and alcohol coupling reaction among screened solvents (Table 3.7, entry 1 and 2). Acetonitrile strongly coordinates to the ruthenium center and inhibits the catalytic activity (Table 3.7, entry 6). Coordinating solvents such as dioxane and THF are also less effective for the catalytic reaction, which could be due to coordination ability to the Ru center (Table 3.7, entry 3, 5).

The temperature effect was investigated by running reaction at different temperatures in toluene (Table 3.7, entry 7-9). It was observed that high temperature such as 120 °C is needed for decarboxylation and deamination of amino acids. At 100 °C no reaction was observed and less active at 110 °C. Once temperature increased up to 135 °C no considerable increment of yield was observed. Therefore 120 °C was found to be the best temperature for the reaction.

3.2.1.3 Catalyst Loading

Table 3.8: Catalyst Loading Effect on the Reaction of Leucine with 4-Methoxyacetophenone.^a

Entry	Catalytic loading / (mol %)	Yield (%) ^b
1	1	65
2	1.5	71
3	2	80
4	3	90
5	5	92

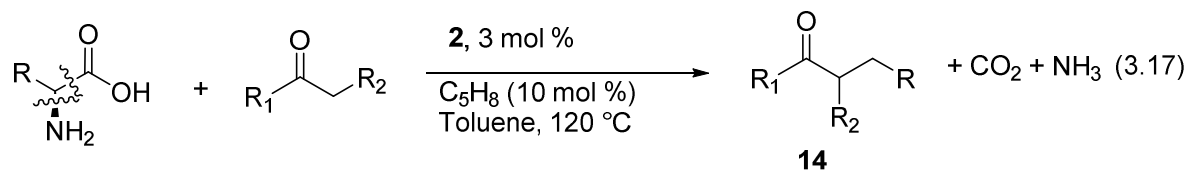
^aReaction conditions: L-Leucine (0.6 mmol), 4-methoxyacetophenone (0.5 mmol) , cyclopentene (10 mol %) , catalyst (3 mol %) in toluene (1 mL) at different 120 °C, 12 h. ^b the conversion of ketone was determined by GCMS analysis using C₆Me₆ as an internal standard.

The coupling reaction was optimized by using different amount of catalyst (Table 3.8). It was found to be 3 mol % was the best catalytic loading for the coupling reaction (Table 3.8, entry 4). 1 mol % -1.5 mol % of **5** was less active (Table 3.8, entry 1-3) and also 5 mol % of **5** has not increased (Table 3.8, entry 5) the yield by significant amount. We

found that the optimum conditions for the coupling reaction are 3 mol % catalytic loading, 10 mol % cyclopentene, at 120 °C and 12 h reaction time in toluene as the solvent.

3.2.2 Reaction Scope

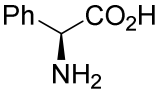
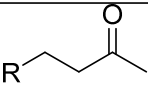
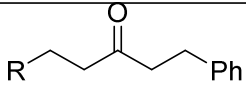
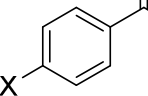
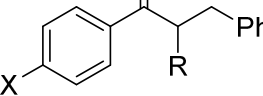
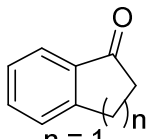
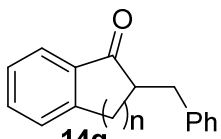
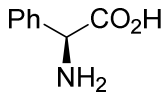
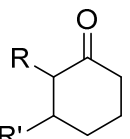
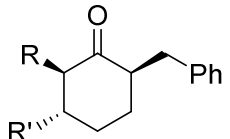
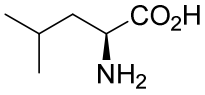
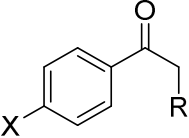
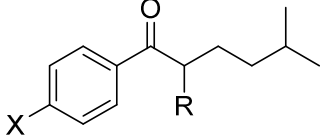
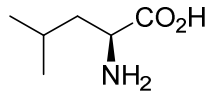
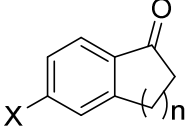
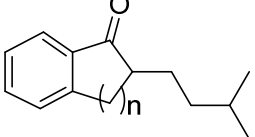
We found that catalyst **1** catalyzed decarboxylative and deaminative coupling of amino acids with ketone to afford product **14** in high yield [eq. (3.17)]. Addition of substoichiometric amount of cyclopentene (10 mol %) was found to promote the coupling reaction. Protected amino or carboxylic groups are generally used in coupling reactions, but in this case both amine and carboxylic acid groups are used as leaving groups.



Having established the optimized conditions at hand, we then surveyed the scope of the present α -alkylation of ketones, and the results are summarized in Table 3.9.

In general, α -amino acids with both aliphatic and aryl side chains readily react with aliphatic ketones (Table 3.9, entry 1-2) and also acetophenone type ketones (Table 3.9, entry 3-6) to form the α -alkylated ketone products **14a-14f**. The coupling of (*S*)-phenylglycine with indanone and tetralone also produced coupling products high yield (Table 3.9, entry 7-8). The coupling of (*S*)-phenylglycine with both 2- and 3-methylcyclohexanone result in a highly diastereoselective formation of the α -alkylated products **14i** and **14j**, respectively (entries 9 and 10).

Table 3.9: Decarboxylative and Deaminative Coupling of α -Amino Acids with Ketones.^a

entry	amino acid	ketone	product(s)	time (h)	yield (%)
1					
2		R = H R = Et	14a 14b	12	90
3				12	88
4		X = H R = H	14c	12	79
5		X = OMe R = H	14d	12	90
6		X = OMe R = Me X = H R = Ph	14e 14f	8 8	80 76
7				8	95
8		n = 1 n = 2	14g 14h	8	89
9					
10		R = H, R' = Me R = Me R' = H	14(±)-2i (dr > 20:1) 14(±)2j (dr > 20:1)	12 12	83 85
11				12	90
12		X = OMe R = H	14k	12	80
13		X = OMe R = Me	14l	12	80
14		X = H R = H	14m	12	74
15		X = Cl R = H	14n	12	80
16		X = CN R = H	14o	12	74
17		X = NH ₂ R = H X = NC ₄ H ₈ O R = H	14p 14q	12 12	90 92
18				8	90
19		X = H n = 1	14r	8	82
20		X = OMe n = 1 X = H n = 2	14s 14t	8 8	82 89

^aReaction conditions: amino acid (1.2 mmol), ketone (1 mmol), cyclopentene (10 mol %), catalyst (3 mol%) in toluene (1 mL) at 120 °C.

Table 3.9: Cont...

entry	amino acid	ketone	product(s)	time (h)	yield (%)
21				12	93
22				8	88
23		X = H, R = Me	14v	12	90
24		X = H, R = i-Pr	14w	12	75
25		X = OMe, R = Bn	14x	12	80
26		X = OMe, R = CH ₂ OBn	14y	10	75
27		X = H, R = CH ₂ CO ₂ Me	14z	12	95
		X = H, R = CH ₂ Cy	14aa		

^aReaction conditions: amino acid (1.2 mmol), ketone (1 mmol), cyclopentene (10 mol %), catalyst (3 mol %) in toluene (1 mL) at 120 °C.

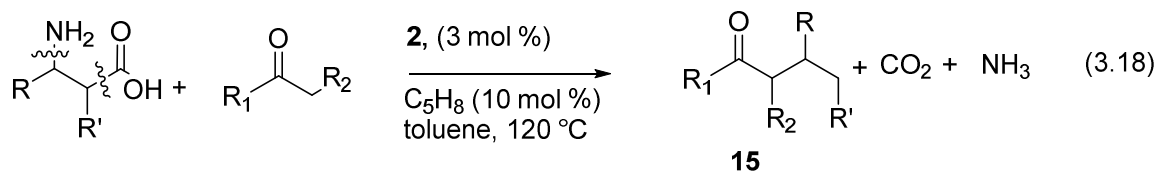
A number of oxygen and nitrogen groups are tolerated in the coupling with aryl-substituted ketone substrates (entries 11-17). Aliphatic amino acid such as L-leucine coupled with both tetralone and indanone to produce alkylated ketone products **14r-14t** (Table 3.9, entry 18-20). The coupling of an amino acid having a chiral substituent, L-isoleucine, with 4-methoxyacetophenone directly forms an optically active product (+)-**14u** (Table 3.9, entry 21). α -Amino acids such as L-alanine, L-Valine, and L-phenyl alanine smoothly react with indanone to produce alkylated products **14v-14x** (Table 3.9, entry 22-24). Protected α -amino acids having oxygenated side chains such as L-serine and L-aspartic acid derivatives smoothly afford the coupling products **14y** and **14z**, respectively (entries 25 and 26). In most cases, racemic *d,l*-amino acids can be used without any significant change in the product yields, but a secondary amino acid, L-proline, does not yield any coupling products. We also compared the analogous coupling of aliphatic and benzylic amines with ketones, and in these cases, similar alkylation products are formed

but with considerably lower yield because of the formation of imine and other side products resulting from the homocoupling of amines. To the best of our knowledge, the catalytic method represents a unique set of examples on using bio-based amino acids as the alkylating agent for the C-C coupling reaction.

Heteroatom functionalized α -amino acids such as lysine, serine, threonine, cystine; guanine did not give coupling products because alcohol, primary amines and guanidine functionalities are known to prefer Ru coordination. But the serine which was alcohol group of protected by benzyl group was coupled with 5-methoxy-1-indanone in 80% yield (Table 3.9, entry 16). Also γ -carboxylic acid protected L-glutamic acid 5-methyl ester coupled with 1-indanone in 75 % yield (Table 3.9, entry 26). In an effort to extend its synthetic utility, we next inspected the coupling reaction of β -amino acids with ketones (Table 3.10, [eq. (3.18)]).

In the coupling of (*S*)-3-amino-2-methylpropanoic acid with aryl-substituted ketones, the *n*-propyl group is regioselectively alkylated to form the coupling products **15a-f** (entries 1-6). The coupling reaction with 2-phenylcyclohexanone leads to the diastereoselective formation of **15g** (Table 3.10, entry 7). In contrast, a modestly diastereoselective formation of the ethylated product **15h** is observed from the coupling of 3-aminopropanoic acid with 2-phenylcyclohexanone (Table 3.10, entry 9).

Generally, the coupling reaction with branched β -amino acids is quite sluggish, thus leading to the decomposition products predominantly. Despite such difficulties, we have been able to effect the coupling reaction of the branched β -amino acids such as 3-aminobutanoic acid and 3-amino-3-phenylpropanoic acid with acetophenone and indanone substrates to form the alkylated products **15i-k** (entries 10-12).

**Table 3.10:** Decarboxylative and Deaminative Coupling of β -Amino Acids with Ketones.^a

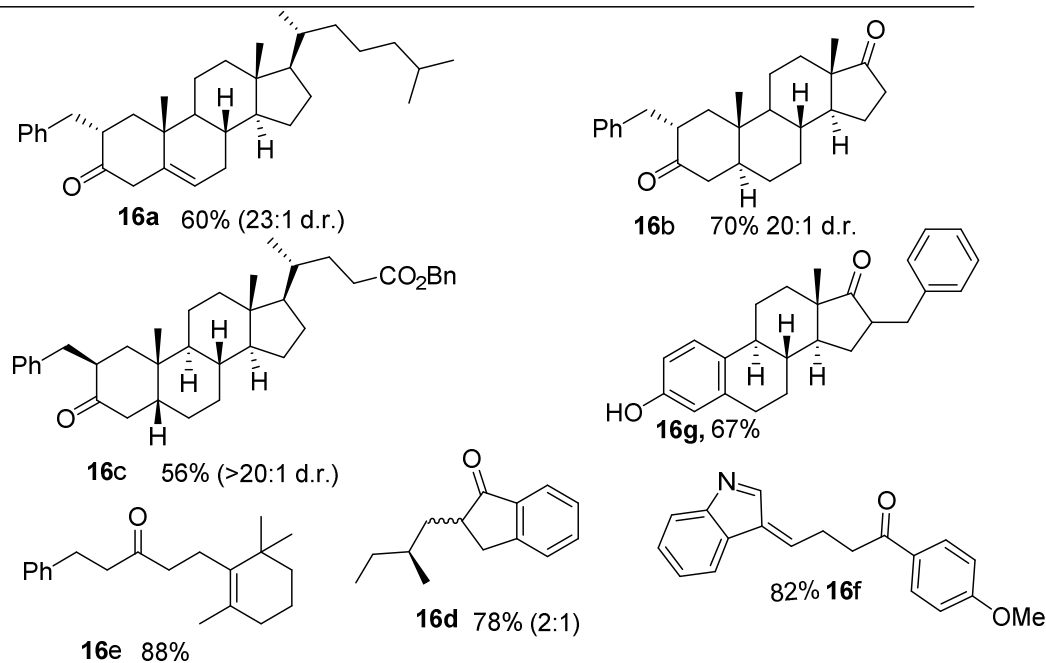
entry	amino acid	ketone	product(s)	time (h)	yield (%)
1				12	80
2		X = H R = H	15a	12	85
3		X = OMe R = H	15b	8	78
4		X = OMe R = Me	15c	8	90
5		X = H R = Ph	15d		
6				8	90
7				16	83
8				12	90
9			15g dr = 10:1		
10				12	89
11		X = OMe	15h	12	83
12		X = H	15i (dr = 3:2)		
13				12	81
14			15j	12	78
15			15k		
16				12	80
17			15l		

^aReaction conditions: Amino acid (1.2 mmol), ketone (1 mmol), cyclopentene (10 mol %), catalyst (3 mol %) in toluene (1 mL) at 120 °C.

Our attempts to couple with α and δ amino acids with ketone were not successful indicating that chelation of amine and carboxylic acid to ruthenium catalyst with stable 5- or 6-membered ring structure prior to the decarboxylation.

To further demonstrate synthetic versatility of the catalytic coupling method, we employed a number of bioactive ketone substrates to probe chemo- and stereoselectivity patterns on the alkylation products (Table 3.11). The alkylation of cholesterol (which readily undergoes alcohol dehydrogenation under the reaction conditions) and *trans*-androsterone with (*S*)-phenylglycine occurs in a highly regio- and stereoselective manner to give the *anti*-selective alkylation products, (+)-**16a** and (+)-**16b**, respectively. In contrast, the *cis*-fused deoxycholic acid benzyl ester with (*S*)-phenylglycine leads to the *syn*-selective alkylation product (+)-**16c**.

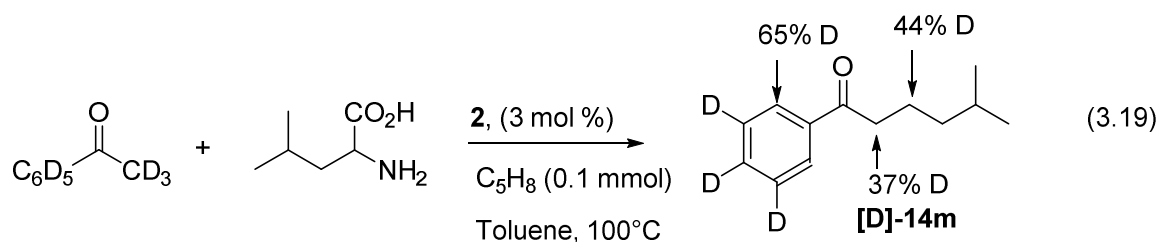
Table 3.11: Decarboxylative and Deaminative Coupling Reaction of Biologically Important Ketones and Peptides.^a



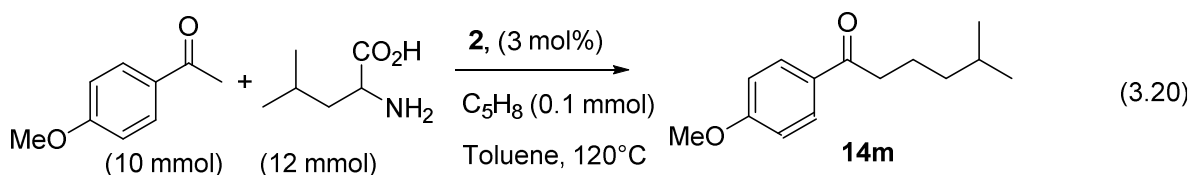
^aReaction conditions: amino acid (1.2 mmol), ketone (1 mmol), cyclopentene (10 mol %), catalyst (3 mol %) in toluene (1 mL) at 120 °C.

The alkylation of L-isoleucine with indanone leads to a modestly diastereoselective formation of the coupling product 16d (d.r. =2:1). The coupling reaction of (*S*)-phenylglycine with dihydro- β -ionone proceeds in a regioselective fashion to give 16e, while the coupling of L-tryptophan with 4-methoxyacetophenone yields the coupling product 16f, thus resulting from the dehydrogenation of indole moiety. The regio- and diastereoselective formation of these alkylation products can readily be explained from imposing a sterically least hindered ruthenium enolate species.

3.2.3 Mechanistic Studies



3.2.3.3 H/D exchange Experiments



We performed the following experiments to gain mechanistic insights into the coupling reaction. First, the treatment of $C_6D_5COCD_3$ with L-leucine leads to substantial deuterium incorporation at both α - and β -carbon atoms on the coupling product [D]-**14m** [Eq. (38)]. The observed hydrogen-deuterium exchange pattern is consistent with a facile

keto-enol tautomerization of the ketone substrate and the *ortho*-arene C-H exchange. The extensive deuterium incorporation on the β -carbon atom can be interpreted as an amine-imine hydrogenation/dehydrogenation of the amino acid substrate under the reaction conditions.

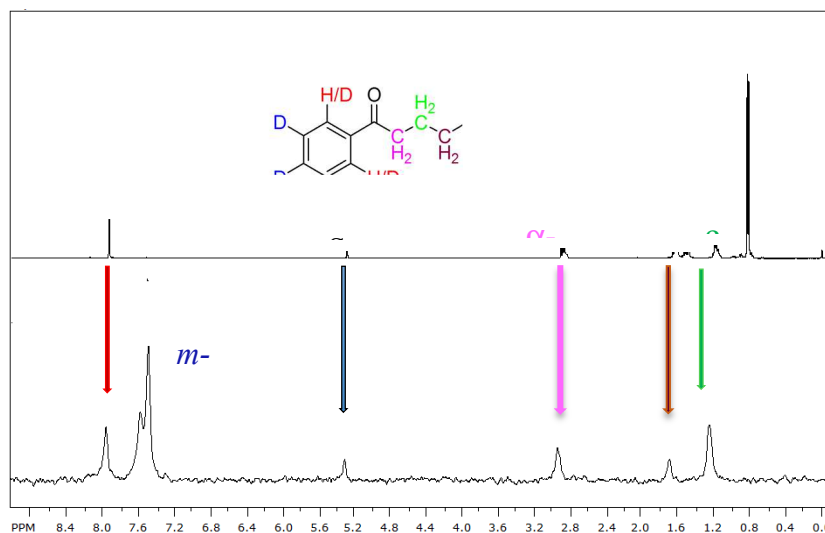


Figure 3.3. ^1H and ^2H NMR Spectra of **14m-d** Obtained from the Reaction of Acetophenone- d_8 with (*S*)-Leucine.

3.2.3.4 ^{13}C -Kinetic Isotope Effect

Second, the NMR technique reported by Singleton and co-workers is used to measure the $^{12}\text{C}/^{13}\text{C}$ kinetic isotope effect (KIE) from the coupling reaction of 4-methoxyacetophenone with L-leucine [Eq. (3.20)]. The most pronounced carbon KIE is observed for the β -carbon atom of **14 k**, when the $^{12}\text{C}/^{13}\text{C}$ ratio of the product at 7 % conversion is compared to that of the product obtained at a low conversion (KIE on C3=1.024; average of 3 runs; see Table 3.12).⁴⁰

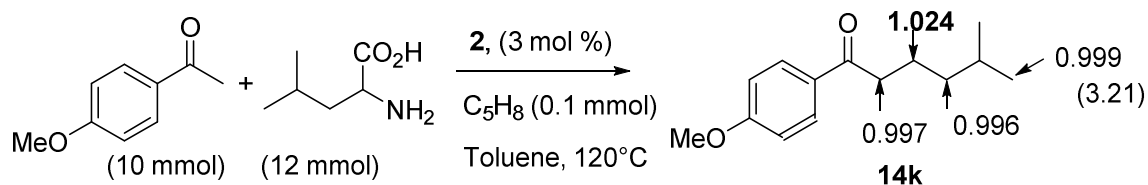
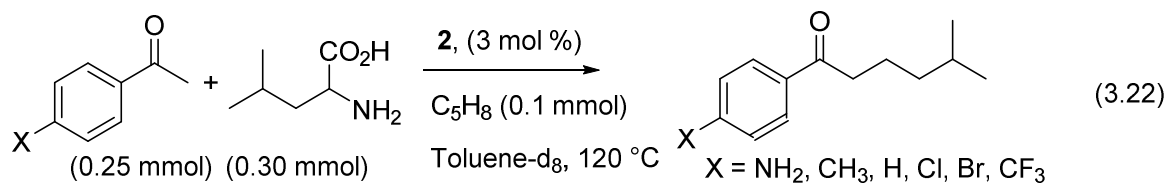


Table 3.12: Average ^{13}C Integration of the Product **14k** at High Conversion (R_0 ; 96 % conversion), at Low Conversion (R ; avg 18 % conversion) and the Calculated ^{13}C KIE.

Carbon no.	High conversion 14k (R_0)	Low conversion 14k (R)	R_0/R	KIE
1(ref)	1.000(0)	1.000(0)	1.000	1.000
2	1.000(5)	0.997(1)	0.997	0.997
3	1.000(1)	1.023(6)	1.024	1.024
4	0.997(9)	1.001(3)	0.996	0.996
5	1.003(3)	1.002(1)	1.001	1.001
6	0.996(1)	0.998(2)	0.999	0.999

β -Carbon of the product **14k** is α -carbon of the starting amino acid. The higher incorporation of ^{12}C at β -carbon of **14k**, suggest that the C-N bond cleavage or decarboxylation step is intimately involved in the turnover limiting step of the coupling reaction. But as we observed the amine formation by decarboxylation of amino acid is the first step and faster than C-N cleavage step decarboxylation step is not the rate limiting step. Also as we explained earlier if Ru-enolate formation is the rate determine step, we should observe high ^{13}C at α -carbon. Gathering all information we propose that the C-N bond cleavage step is the rate limiting step of the alkylation reaction.



3.2.3.5 Hammett Study

To further probe electronic effect of the ketone substrate, a Hammett plot is constructed from the reaction of a series of p -X-C₆H₄CO₂Me (X=NH₂, OCH₃, CH₃, H, Cl, CN) with L-leucine [Eq. (3.22)]. A linear correlation from the relative rate versus the Hammett σ_p is observed with a positive slope ($\rho=+1.2\pm 0.2$; see Figure 3.4). Strong promotional effects by *para*-electron-withdrawing groups suggests a substantial build-up of cationic character on the α -carbon atom of the ketone substrate, and the results can be explained by the formation of a cationic ruthenium enolate species.

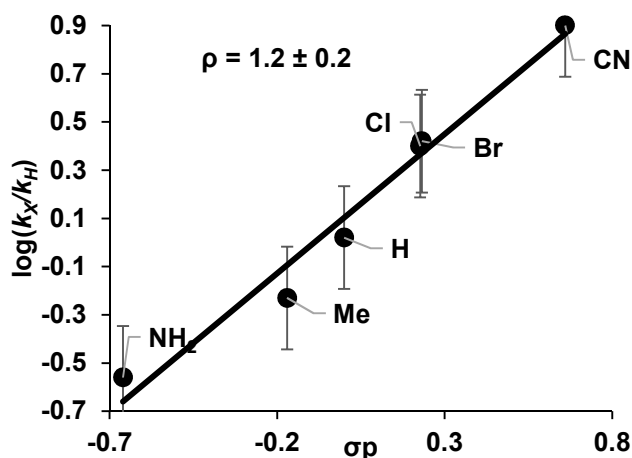
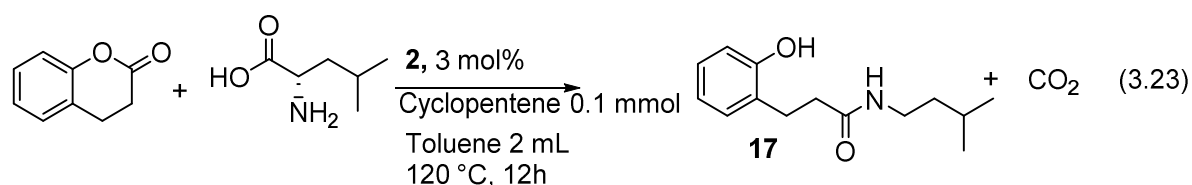


Figure 3.4. Hammett Plot of p -X-C₆H₄COCH₃ (X = NH₂, CH₃, H, Cl, Br, CN) with (*S*)-Leucine.

3.2.3.6 Formation of Intermediate Species

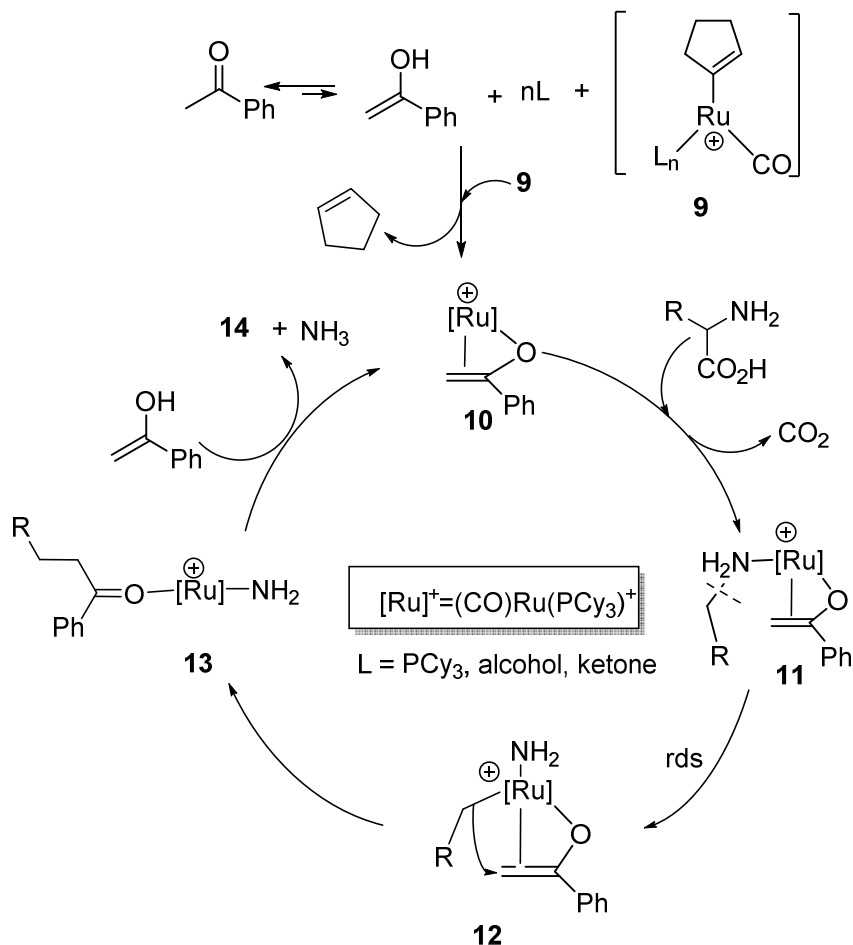
To probe the deamination versus decarboxylation sequence, we surveyed a number of different carbonyl substrates with L-leucine. The trapped amide product **17** is successfully obtained from the treatment of dihydrocoumarin with L-leucine [Eq. (3.23)]. The selective formation of the amide product **17** supports a preferential decarboxylation over the deamination step for the amino acid substrate. Transition metal catalyzed decarboxylative coupling methods have been successfully employed for the synthesis of complex organic molecules.⁴⁶



3.2.4 Proposed Mechanism

Although details still remain unclear, we propose a working mechanistic hypothesis for the coupling reaction on the basis of these experimental results (Scheme 3.5). By considering the first step of the mechanism is decarboxylation of amino acid evidenced by [Eq. (3.23)], we propose that the cationic ruthenium(II) enolate species **10**, initially generated from the keto-enol tautomerization and dehydrogenation steps, is the key species for the coupling reaction. The observed deuterium exchange pattern on the coupling product [D]-**14 m** is consistent with a facile and reversible enolization of the ketone substrate via the ruthenium enolate species **10**.⁴⁸ Late transition metal/enolate complexes have been well known to mediate a variety of C=C coupling reactions, including Michael-

type conjugate addition and nucleophilic addition reactions. We also showed that the ruthenium hydride complex effectively catalyzes the formation of silyl enol ethers from the coupling reaction of ketones and vinylsilanes. Though the trapping experiment supports for a preferential decarboxylation, we do not have any direct mechanistic evidence for the decarboxylation process at the present time



Scheme 3.5: Proposed Mechanism for the Decarboxylative and Deaminative Coupling of Amino Acids with Ketone.

If the enolate formation is rate determine step Hammett value should be positive value because electron withdrawing groups contained ketones stabilizes keto-enol tautomirization. Decarboxylation of amino acid would be the next step and decarboxylated

amine acid coordinates to the ruthenium complex **10**. By correlating with Hammett studies shown in Chapter 2, rate-determine step would be generating positive charge on Ru complex. Therefore we propose oxidative addition of amine C-N bond in complex **11** to form complex **12** is the rate determine step. Then the insertion of alkyl group from amine to enolate double bond produces the expected ketone. Reaction of another enol form of ketone with complex **13** generates active Ru-enolate by releasing product **14** and NH_3 .

Phenylglycine with 2-methylcyclohexanone yielded *cis* diastereomer product as high diastereoselective product (Table 3.9, entry 11). Active species of Ru catalyst coordinates to opposite side of the methyl group of enol form of 2-methyl-1-cyclohexanone due to steric repulsion. Therefore bulky group contain Ru and PCy_3 blocks the one side of enolate intermediate. Alkylation of enolate could occur opposite to the high steric catalyst which is same side of methyl group. Therefore *cis*-diastereomer is the major product of this alkylation reaction (Fig. 3.5).

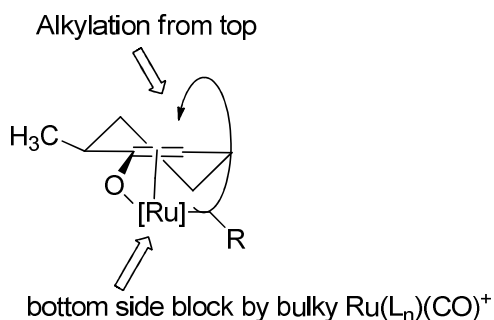


Figure 3.5: Transition State of Alkyl-Ruthenium Enolate Complex.

After the initial decarboxylation, the resulting amine substrate proceeds to the C-N bond-cleavage step either by a direct oxidative addition/reductive coupling mechanism or by the formation of an imine and the subsequent coupling with the enolate substrate. In either

case, the observed carbon KIE data provides support for the C-N cleavage as the rate-limiting step in leading to the formation of the alkylated product **14**. The regio- and stereoselective formation of the alkylation product can be readily rationalized from the preferential formation of the sterically least demanding ruthenium enolate complex and an intramolecular addition of the alkyl group. Finally, the extrusion of ammonia byproduct provides the driving force for the regeneration of the ruthenium enolate complex **10**.

This work was published in Kalutharage, N. and Yi, C. S. (2013), Deaminative and Decarboxylative Catalytic Alkylation of Amino Acids with Ketones. *Angew. Chem. Int. Ed.*, 52: 13651-13655. doi: 10.1002/anie.201307766.

3.2.5 Conclusion:

In conclusion, we have successfully developed a novel catalytic C-N bond cleavage method of saturated amines from the dehydrogenative coupling reactions with alcohols with high substrate scope. The catalytic method employs environmentally friendly and cheaply available alcohols and exhibit a broad substrate scope and high chemoselectivity.

Also we have successfully developed a novel catalytic alkylation method using readily available amino acid substrates as a bio-based alkylation agent. The salient features of the catalytic method are that it achieves direct C-C and C-N bond cleavage of biomass-derived amino acid substrates, exhibits a broad range of substrate scope, as well as high regio- and stereoselectivity, and it does not require any reactive reagents or pre-functionalization of the substrates in forming the α -alkylated ketone products.

CHAPTER 4

**SYNTHETIC AND MECHANISTIC STUDIES OF REDUCTIVE
DEOXYGENATION AND HYDROGENOLYSIS OF ALDEHYDES AND
KETONES**

4.0 Introduction

Ketones and aldehydes are commonly present in many natural organic compounds and pharmaceutical agents. A variety of biological functions are associated with aldehydes and ketones including flavors and fragrances (e.g. vanillin, cinnamaldehyde, etc.), and hormones (e.g. estrone, testosterone, etc.). Some are essential vitamin precursors, while the others may be drugs such as tetracycline and plant flavonoids naringin.

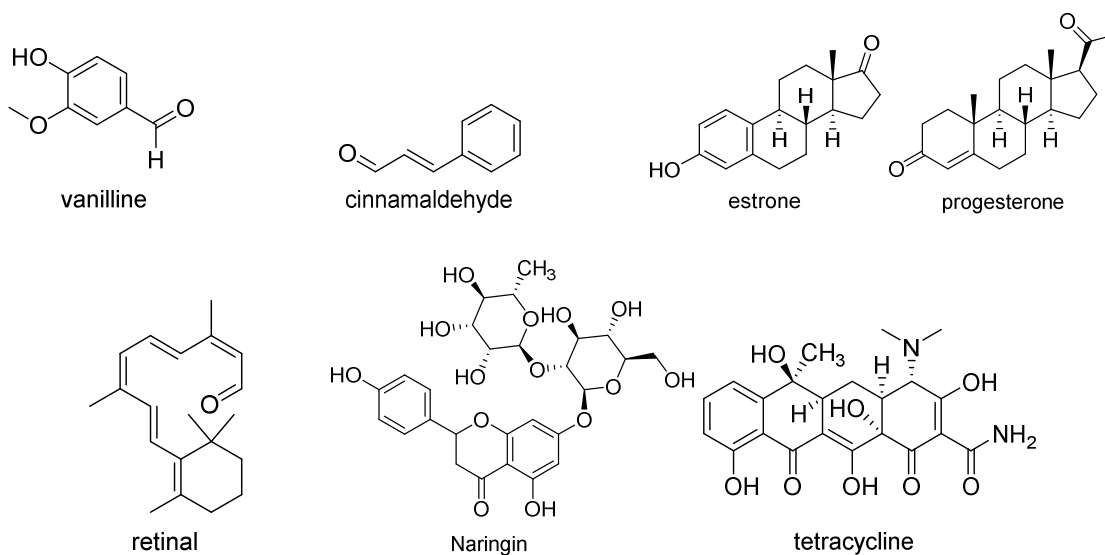


Figure 4.1: Some Biologically Active Aldehydes and Ketone Compounds

The depletion of fossil fuels has led to increasing interest toward the use of biomass feedstock as a sustainable source for chemicals and biofuels.¹ Since fossil fuels are the major source of greenhouse gases, the challenge of producing the next generation of

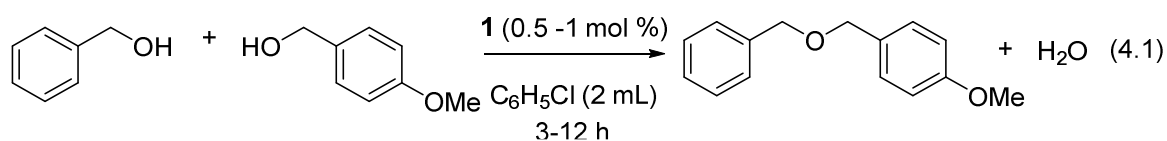
biofuels that can effectively function as “drop-in” replacements for fossil fuels has led to renewed interests in conversion and utilization of cheaply and readily available alcohols and other oxygenated biomass precursors. Reductive deoxygenation of aldehydes and ketones to the corresponding saturated compounds has attractive features, given its many applications in fine-chemical synthesis² and biofuel production.³ Unfortunately, classical deoxygenation methods of carbonyl compounds, such as those based on either the Barton–McCombie,⁴ Clemmensen,⁵ or Wolff–Kishner⁶ methodologies, are generally associated with harsh reaction conditions and the use of stoichiometric amounts of toxic reagents, as well as poor functional-group tolerance.

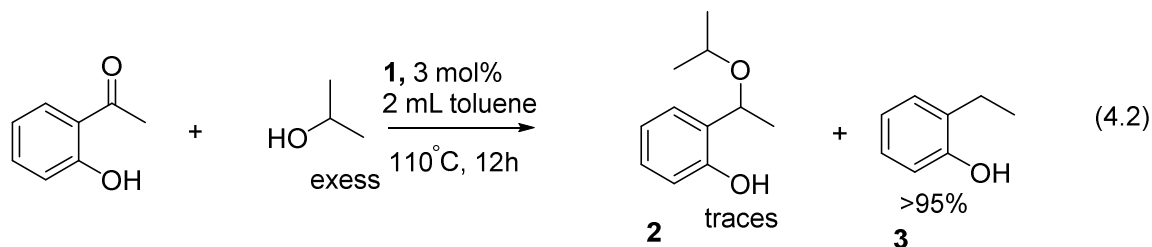
Wolff and Kishner first developed via hydrazone or semicarbazone cleavage in basic media.⁶ Clemmensen reduction method uses stoichiometric reducing agents Zn-Hg in strongly acidic media.⁵ The original Wolff–Kishner reduction procedure was to mix the carbonyl compound with 100 % H_2NNH_2 and potassium hydroxide in a sealed tube and heat the mixture at high temperature (160–200 °C) for days. Over the decades, the Wolff–Kishner–Huang Minlon reduction method has been widely used in organic synthesis. For example, Huang–Minlon modified procedure employs 85 % $\text{H}_2\text{NNH}_2 \cdot \text{H}_2\text{O}$ in a high boiling point solvent (ethylene glycol).^{6d} In the meantime, the original procedures have been modified in order to make the reaction conditions milder and more efficient.^{8–9} Other reduction methods involving the use of metal hydrides,^{9–12} with a combination of protic acids or Lewis acids have been well studied. From for the consideration of green chemistry and atom economy aspects, catalytic methods utilizing molecular hydrogen as a clean hydrogen source would be highly desired for the reduction of carbonyl compounds to hydrocarbons.

Currently, there are a number of catalytic protocols for the deoxygenation of carbonyl compounds by employing molecular hydrogen (H₂).¹⁴ Although H₂ constitutes the most atom-efficient and green reducing agent, its use is generally associated with high pressure, special equipment, and safety precautions to minimize the explosion risk.¹⁵ From an experimental point of view, it is very important to develop a catalytic method that avoids the use of highly active reagents, toxic starting materials, and minimize the formation of unwanted byproducts. Exploring the use of molecular hydrogen as a sustainable source for the reduction of carbonyl compounds is an important research field for obtaining valuable hydrocarbon source from readily available alcohols sources. This chapter describes development of synthetic and mechanistic aspects of ruthenium catalyzed deoxygenation of carbonyl compounds by using molecular hydrogen.

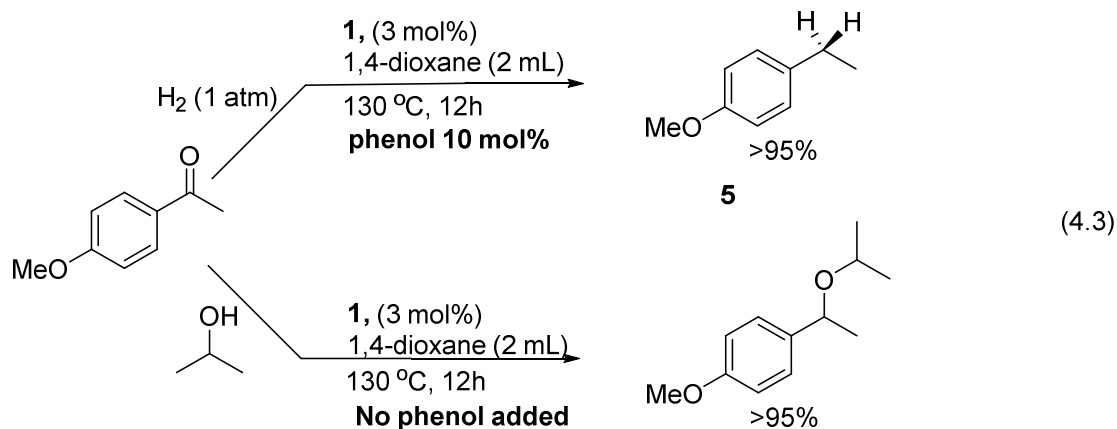
4.1 Results and Discussion

Our research group previously reported a selective catalytic C-H alkylation of alkenes with alcohols¹⁵ [Eq. (4.1)] from chap 4) and dehydrative C-H alkylation and alkenylation of phenol with alcohols [Eq. (26)] chapter 4).¹⁵ Very recently, we also reported a selective catalytic synthesis of unsymmetrical ethers from the dehydrative coupling of two different alcohols.¹⁶ [Eq. (4.1)]. In these cases, dehydrative C-O bond cleavage of alcohols has been utilized as the driving force for the C-C coupling reactions.





In an effort to extend the scope of catalytic C-O cleavage reactions, we next explored its catalytic activity for reductive etherification of carbonyl compounds with alcohols to form the corresponding unsymmetrical ethers. Initially, we found that $[(\eta^6\text{-C}_6\text{H}_6)(\text{PCy}_3)(\text{CO})\text{RuH}]^+\text{BF}_4^-$ (**1**) in the presence of phenol as a ligand could catalyze hydrogenolysis of 4-methoxyacetophenone with $i\text{PrOH}$ in 1,4-dioxane at 130°C to give the product 1-ethyl-4-methoxybenzene **3** in >95 % yield [Eq. (4.3)]. From the reaction of 2-hydroxyacetophenone in the presence of excess amount of isopropanol did not produce the expected ether product, **2**. Instead the reaction produced the ketone hydrogenolysis product 2-hydroxyethylbenzene **3** [eq. (4.2)]. In contrast, the coupling reaction produced unsymmetrical ether **2** as the major product in the absence of phenol [eq. (4.3)]. This catalytic method efficiently produces hydrogenolysis product **3** of 4-methoxyacetophenone with 2-propanol, which was isolated by simple silica gel chromatography and its structure was completely established by spectroscopic techniques [Eq. (4.3)]. The catalytic method employs environmentally friendly and cheaply available H_2 and exhibits high chemoselectivity towards C-O bond cleavage reactions. This reaction employs H_2 , does not use any reactive agents and produces H_2O as the only byproduct.



4.2 Optimization Study

4.2.1 Catalyst, Ligand and Solvent Screenings

To ascertain the ligand effect on the hydrogenolysis reaction, we screened a number of oxygen and nitrogen donor ligands as well as ruthenium catalysts to optimize the hydrogenolysis of carbonyl compounds (Table 4.1). Initially, 4'-methoxyacetophenone (160 mg, 1 mmol), complex **1** (3 mol %) and ligand (10 mol %) were dissolved in dioxane (2 mL) in a 25 mL Schlenk tube equipped with a Teflon stopcock and a magnetic stirring bar. The tube was brought out of the glove box, and cooled in liquid nitrogen and degased under vacuum. Then the Schlenk tube was filled with hydrogen gas (~2 atm), and the reaction mixture was stirred in an oil bath set at 130 °C for 12 h [Eq. (4.4)].

The preliminary survey showed that the Ru complex **1** with phenol ligand exhibited distinctively high activity for the hydrogenolysis of 4-methoxyacetophenone among screened ruthenium catalysts and the oxygen and nitrogen containing ligands (entry 1-10). Also, both the isolated complex **1** and in-situ formed from the reaction of tetranuclear ruthenium complex **4**/H⁺ showed nearly identical activity for the hydrogenolysis.

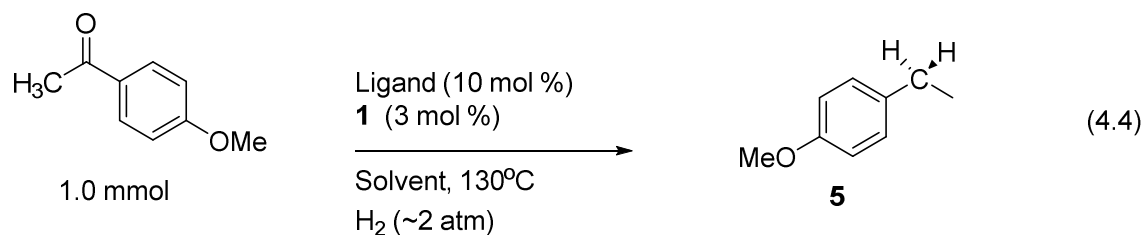


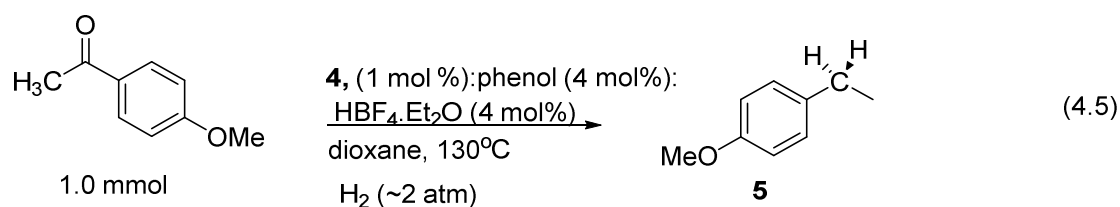
Table 4.1: Ligand Screening for the Hydrogenolysis Reaction of 4-Methoxyacetophenone.^a

	Catalyst	Ligand	Solvent	Yield
1	1	phenol	dioxane	>95
2	1	phenol	PhCl	89
3	1	aniline	PhCl	<5
4	1	2-NH ₂ PhCOMe	PhCl	35
5	1	benzamide	PhCl	<5
6	1	1,2-catechol	toluene	73
7	1	1,1'-BINOL	toluene	54
8	1	1,2-C ₆ H ₄ (NH ₂) ₂	toluene	<5
9	4	phenol	dioxane	<5
10	4/H⁺	phenol	dioxane	95
11	[Ru(cod)Cl ₂] _x	phenol	dioxane	0
12	RuCl ₃ ·3H ₂ O	phenol	dioxane	0
13	Ru ₃ (CO) ₁₂	phenol	dioxane	0
14	(PPh ₃) ₃ (CO)RuH ₂	phenol	dioxane	0
15	[(PCy ₃) ₂ (CO)(CH ₃ CN) ₂ RuH]BF ₄	phenol	dioxane	30

^a Reaction conditions: 4-methoxyacetophenone (160 mg, 1 mmol), solvent (2 ml), catalyst (3 mol %), ligand (10 mol %), H₂ (2 atm), 130 °C, 12 h. ^b The product yield of **5** was determined by ¹H NMR using methyl benzoate as an internal standard.

4.2.1.1.1 Catalytic Loading and Solvent Effect.

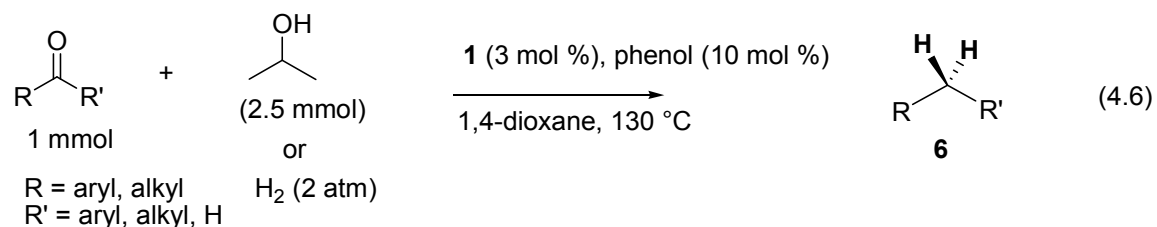
The hydrogenolysis reaction was screened with different amounts of catalyst loading and different solvents in order to optimize the reaction conditions. It was found that 3 mol % was the best amount of catalytic loading. The catalyst loading 1 mol % -1.5 mol % was less active, while the yield has dramatically increased when polar solvents such as 1,4-dioxane are used. Aliphatic ketones and aldehydes gave a low yield on the product under the similar reaction conditions. We believe that the phenol coordinated catalyst is active for the hydrogenolysis reaction. We ran those reactions using in situ generated phenol coordinated catalyst [Eq. (4.5)].



The following procedure was used to generate the phenol-coordinated cationic ruthenium hydride complex. Tetrameric ruthenium complex **4** (17 mg, 1 mol %) and phenol (4 mg, 4 mol %) were reacted with $\text{HBF}_4 \cdot \text{OEt}_2$ (6.6 μL , 4 mol %) in CH_2Cl_2 (1 mL) in a 25 mL Schlenk tube. The mixture was stirred about 15 min at room temperature. The carbonyl compound (1 mmol) and dioxane (2 mL) was added to the tube and the tube was filled with H_2 gas (1 atm) via vacuum line. The tube was stirred in an oil bath set at 130 $^\circ\text{C}$ for 12 h. Analytically pure product **5** was isolated by a simple column chromatography on silica gel (280-400 mesh, hexanes/EtOAc).

4.3 Reaction Scope

We found that the Ru-H catalyst **1** with phenol ligand efficiently catalyzes the hydrogenolysis of ketones and aldehydes to afford the alkane product **6** in high yield either by using either *i*PrOH or H₂ as the hydrogen source. [Eq. (4.6)] Addition of in situ generated phenol coordinated Ru-H catalyst also showed identical activity for the hydrogenolysis reaction. We surveyed the scope of the hydrogenolysis reaction by using the isolated catalyst **1**.



The hydrogenolysis of simple aromatic aldehydes such as 4-hydroxybenzaldehyde, vanillin and 3-phenoxybenzaldehyde gave the corresponding toluene product **6a**, **6b** and **6c** in high yields (Table 4.2, entry 1-3). Interestingly, aliphatic unsaturated aldehydes such as *cis*-11-hexadecenal produces 74 % of hydrogenolysis product **6d** without affecting the alkene bond (Table 4.2, entry 4).

Table 4.2: Reaction Scope of Catalytic Hydrogenolysis of Aldehydes and Ketones^a.

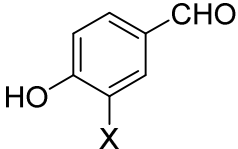
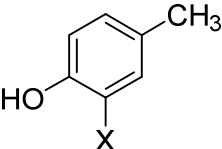
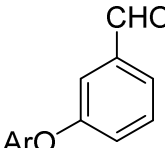
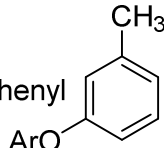
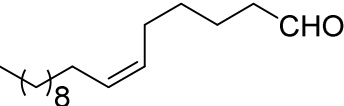
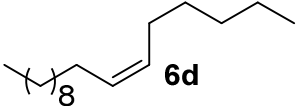
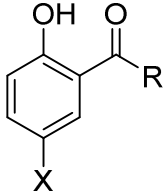
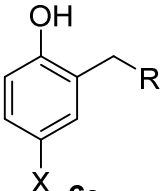
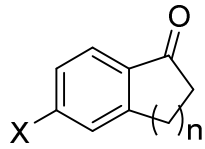
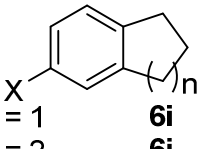
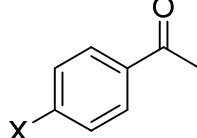
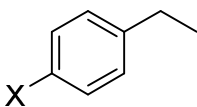
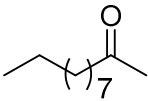
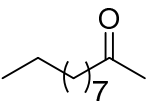
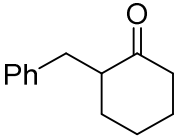
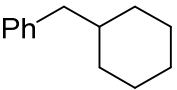
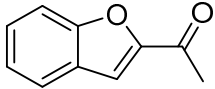
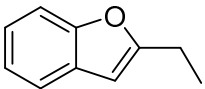
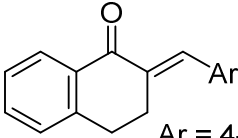
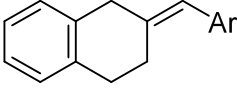
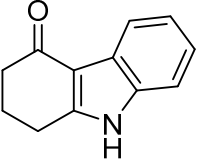
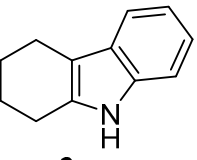
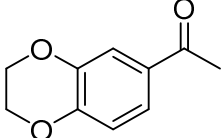
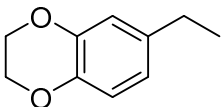
entry	carbonyl compound	product(s)	method	time (h)	yield (%) ^b
1			A	12	90
2		X = H 6a X = OMe 6b	B	12	95
3		Ar = 4-methoxyphenyl 	A	8	92
4			A	12	72
5			A	8	94
6		X = H R = Me 6e	B	8	91
7		X = H R = Et 6f	A	8	92
8		X = H R = CH ₂ CH ₂ Ph 6g X = F R = Et 6h	B	8	91
9			A	16	90
10		X = H n = 1 6i X = OMe n = 2 6j	A	16	88
11			A	12	79
12		X = H 6k X = Cl 6l	B	12	81
13		X = Me 6m	A	12	92
14		X = OMe 6n	B	12	95

Table 4.2: Cont..

entry	carbonyl compound	product(s)	method	time (h)	yield (%) ^b
15		 6o	A	24	65
16		 6p	A	24	54
17		 6q	A	24	54
18	 Ar = 4-methoxyphenyl	 6r	A	24	54
19		 6s	B	24	54
20		 6t	A	12	85

^a Reaction Conditions: (A) ketone/aldehyde (1 mmol), *i*PrOH (2 mL), catalyst **1** (3 mol %), 4-OMe-C₆H₄OH (10 mol %) 130 °C, (B) ketone/aldehyde (1 mmol), dioxane (2 mL), catalyst **1** (3 mol %), 4-OMeC₆H₄OH (10 mol %), H₂ (~2 atm) 130 °C, 12 h. ^bIsolated yields.

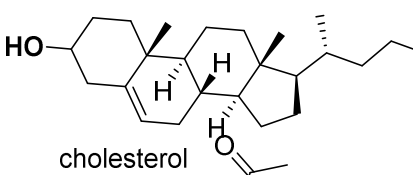
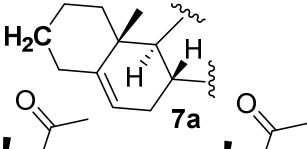
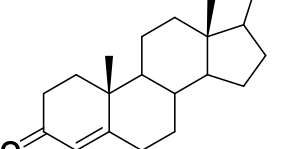
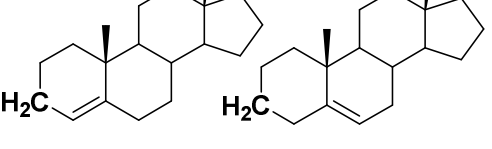
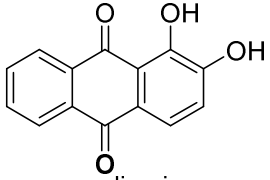
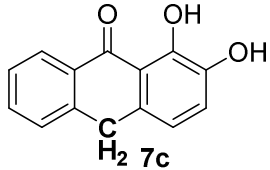
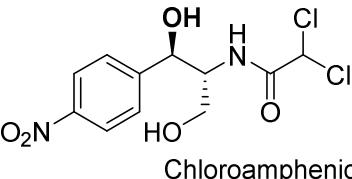
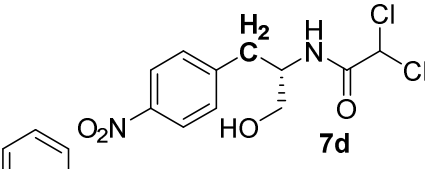
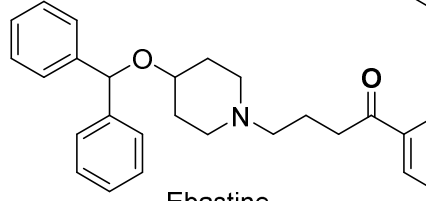
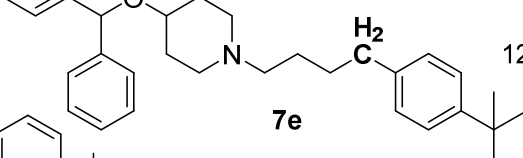
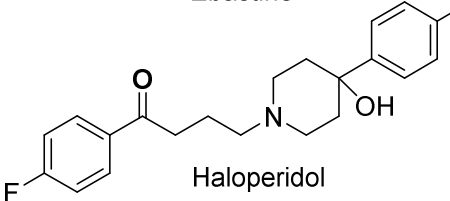
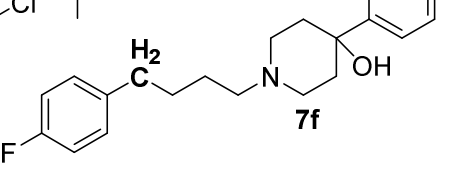
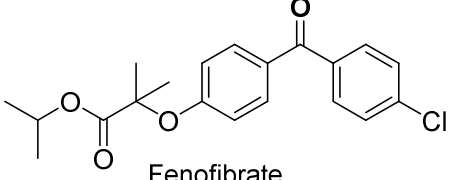
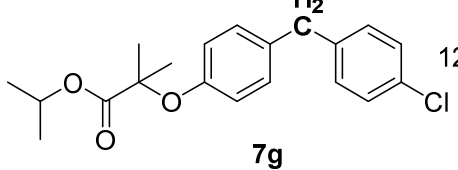
4-Hydroxyphenone derivatives such as 4-hydroxyacetophenone, 4-hydroxypropiophenone, 1-(4-hydroxyphenyl)-3-phenyl-1-propanone yielded >90 % of the aliphatic product **6e-6g**, which was believed to be produced via a chelate assisted pathway (Table 4.2, entry 5-7). 1-(5-Fluoro-4-hydroxyphenyl)-1-propanone produced in 91 % yield of the product **6h** (Table 4.2, entry 8). Cyclic benzylic ketones such as indanone and 6-

methoxy-1-tetralone also afforded 90 % and 88 % yield of the hydrogenolysis product **6i** and **6j**, respectively (Table 4.2, entry 9-10).

To investigate the electronic effect on the *para* substituent of aromatic ketones, we ran the reaction of several *p*-substituted acetophenones which *p*-X-C₆H₄COMe (X = H, Cl, Me and OMe). All substrates gave over 80 % yield of hydrogenolysis products **6k-6m**, but slightly higher yield of the products was obtained for electron donating group such Me and OMe (Table 4.2, entry 11-14). Simple aliphatic ketones such as 4-undecanone produced methylene product in 65 % yield **6o** when the reaction runs 24 h at 3 atm of H₂ gas (Table 4.2, entry 15). Cyclic aliphatic ketones also produced methylene product in 54 % yield under similar reaction conditions. Oxygen containing aromatic ketones such as 1-(1-benzofuran-2-yl)ethanone gave methylene product **6q** in 95 % yield (table 4.2, entry 17).

Selective hydrogenolysis of 2-(4-methoxybenzylidene)-1-tetralone afforded the corresponding methylene product **6r**, in chemoselective formation towards carbonyl group over the exocyclic double bond (Table 4.2, entry 18). A ketone with an indole functional group, 1, 2, 3, 9-tetrahydro-4H-carbazol-4-one, also led to the product **6s** (Table 4.2, entry 19). Glycol protected phenolic aromatic ketones such as 1-(2, 3-dihydro-1, 4-benzodioxin-6-yl)ethanone produced 85 % of methylene compounds **6t** (Table 4.2, entry 20).

Table 4.3: Deoxygenation of Biological Active Ketone/Aldehyde Compounds^a

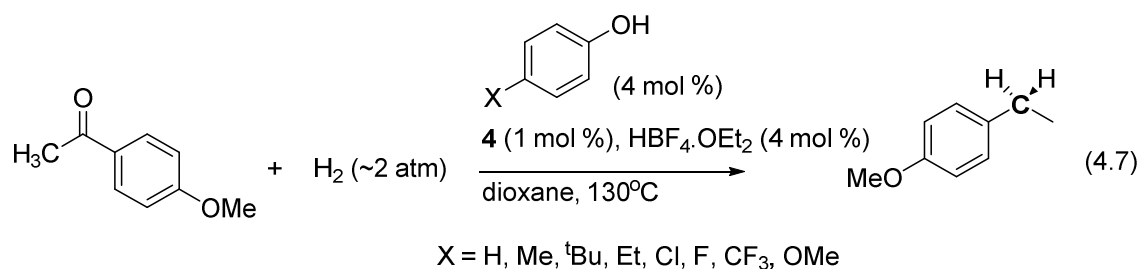
entry	carbonyl compound	product(s)	time (h)	yield (%) ^b
1	 cholesterol	 7a	12h	67
2	 progesterone	 7b (1:1)	12h	52
3	 alizarin	 7c	12h	71
4	 Chloroamphenicol	 7d	12h	45
5	 Ebastine	 7e	12h	84
6	 Haloperidol	 7f	12h	68
7	 Fenofibrate	 7g	12h	72

^a Reaction Conditions: ketone/aldehyde (1 mmol), catalyst **1** (3 mol %), dioxane (2 mL), 4-OMeC₆H₄OH (10 mol %), 130 °C, H₂ (~2 atm), 130 °C, 12 h. ^b Isolated yields.

To further demonstrate its synthetic utility, we examined the hydrogenolysis of highly functionalized, biologically active alcohol and carbonyl substrates (Table 4.3). The treatment of cholesterol and progesterone led to the chemoselective hydrogenolysis of alcoholic and ketone groups formed the corresponding methylene products **7a** and **7b**, respectively. In case of progesterone, a 1:1 mixture of olefin isomerization products was obtained. The chemoselective hydrogenolysis of benzylic alcohol is observed over aliphatic alcohol and amide groups for chloroamphenicol **7d**, while the hydrogenolysis occurred regioselectively at the 9 position for alizarin **7c**. The hydrogenolysis of ebastatine, haloperidol and fenofibrate cleanly yielded the corresponding methylene products **7e**, **7f** and **7g** without the formation of any alcoholic products.

The catalytic method exhibits high selectivity toward the hydrogenolysis of benzylic alcoholic and ketone groups while tolerating common oxygen and nitrogen functional groups such as amide, amine and ester.

4.4 Mechanistic Study



4.4.1 Hammett Study.

To probe electronic effects of the phenolic ligand on the catalyst activity, we compared the relative rates of the hydrogenolysis of ketones by using a series of *para*-substituted phenol derivatives *p*-X-C₆H₄OH (X = OMe, *t*-Bu, Et, Me, H, F, Cl, CF₃) [Eq. (4.5)]. The rate of the hydrogenolysis of 4-methoxyacetophenone with H₂ (2 atm) in the presence of **5** (3 mol %) and a phenol ligand (4 mol %) in dioxane was monitored by ¹H NMR. The

appearance of the product peak was normalized against an internal standard (methyl benzoate) in 30 min intervals, and k_{obs} of the each catalytic reaction was determined from a first-order plot of $-\ln[(4\text{-methoxyacetophenone})_t/(4\text{-methoxyacetophenone})_0]$ vs time. The Hammett plot of $\log(k_X/k_H)$ vs σ_p is shown in Figure 4.2.

Two opposite electronic substituents effects were observed as depicted in the Hammett plot (Fig. 4.2). A linear correlation with highly negative linear slope was obtained from the phenols with electron-donating group $\rho = -3.3 \pm 0.3$ ($X = \text{OCH}_3, t\text{-Bu, Et, Me}$)¹⁷, while a positive linear slope was successfully fitted from the phenols with electron withdrawing group $\rho = +1.5 \pm 0.1$ ($X = \text{F, Cl, CF}_3$). Looking at the right side of the Hammett plot in Fig. 18, one can observe that electron withdrawing group such CF_3 and Cl on phenol increase the reaction rate with the Hammett value of $\rho = +1.5 \pm 0.1$. In case of electron donating groups ($X = \text{OMe, Me, etc}$), the hydrogenolysis rate from the Ru catalyst with an electron donating group **4**/*p*-OMe- $\text{C}_6\text{H}_4\text{OH}$ was found to be several times faster than the rate from the catalyst **4**/PhOH. This V-shaped Hammett relationship is indicative of changing mechanism on either side of the vertex.¹⁷ The observation of two opposing slopes clearly indicates different operating reaction mechanistic pathways between electron-donating and withdrawing groups.¹⁷ The Hammett study showed that the hydrogenolysis reaction is promoted by two opposing electronic factors. The results suggest that a relatively electron rich Ru center promotes the binding of H_2 for the reaction catalyzed by electron-donating group, in which the activation of H_2 may be involved in the rate-limiting step. On the other hand, a relatively electron-poor metal center should promote the binding of ketone and alcohol substrates, and the rate-enhancement by phenol with electron withdrawing group may be resulted from a strong coordination of these oxygenate substrates.

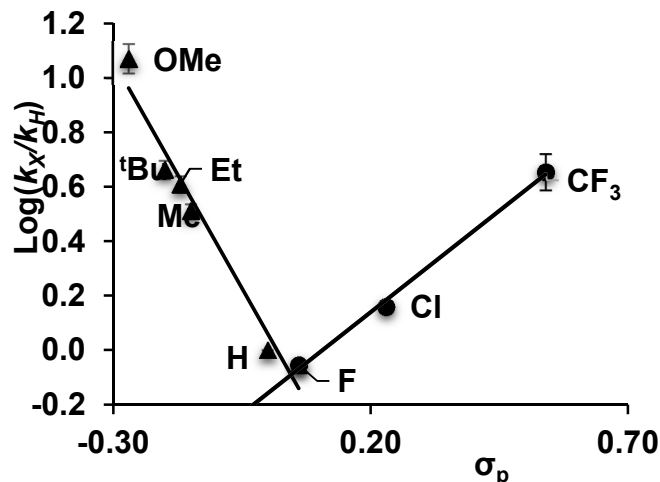
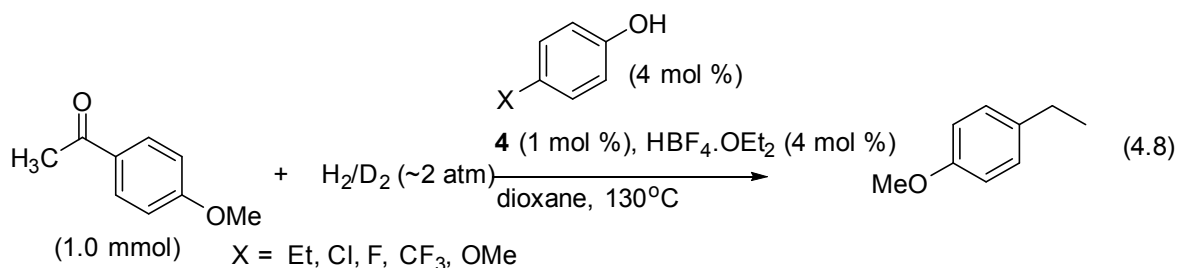


Figure 4.2. Hammett Plot of Hydrogenolysis of 4-Methoxyacetophenone Catalyzed by 4/*p*-X-C₆H₄OH (X = ^tBu, Cl, CF₃, Et, F, H, Me, OMe).

4.4.1 Kinetic Isotope Effects



4.4.1.1 Deuterium Isotope Effect Study

To probe electronic effects on the H-H bond activation, we measured the deuterium isotope effect for the catalytic hydrogenolysis reaction catalyzed by the complex **4** with phenol ligands with both electron donating and withdrawing groups. Thus, the rate of hydrogenolysis of 4-methoxyacetophenone with H₂ (2 atm) and with D₂ (2 atm) in the presence of **4** (1 mol %)/HBF₄ and a *para*-substituted phenol (4 mol %) was measured by monitoring the appearance of the product signals on ¹H and ²H NMR, which were normalized against the peak of an internal standard (methyl benzoate). The *k*_{obs} was

determined from a first-order plot of $-\ln[(4\text{-methoxyacetophenone})_t / (4\text{-methoxyacetophenone})_0]$ vs time (Figure 4.3). The k_H/k_D was calculated from the ratio of the first order plots. To check the pattern shown in the Hammett plot the same experiment was repeated for the hydrogenolysis of 4-methoxyacetophenone for five different *para*-substituted phenolic ligands $p\text{-X-C}_6\text{H}_4\text{OH}$ (X = OMe, Et, CF₃, Cl, CF₃), and the k_H/k_D for each case was obtained from the first order plots (Figure 4.3-4.7).

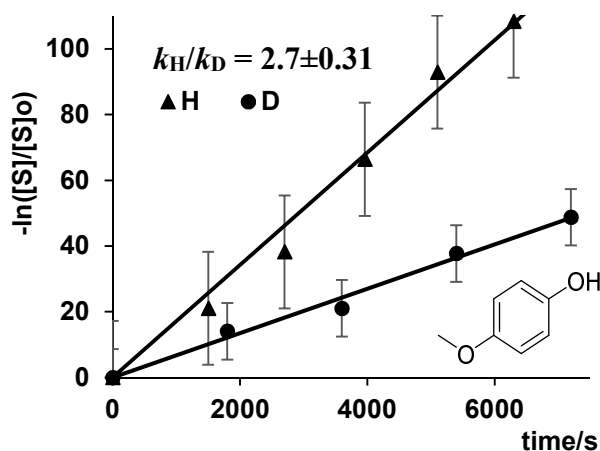


Figure 4.3: Deuterium Isotope Effect Study for the Reaction of 4-Methoxyacetophenone with H₂/D₂ with 4-OMe-C₆H₄OH as the Ligand.

Under first order condition, 4/HBF₄ with 4-methoxyphenol as the ligand, the plot of $-\ln[(4\text{-methoxyacetophenone})_t / (4\text{-methoxyacetophenone})_0]$ vs time yielded a straight line with the slope of $1.79 \times 10^{-5} \text{ s}^{-1}$ for H₂ and $6.73 \times 10^{-6} \text{ s}^{-1}$ for D₂. The experimentally determined kinetic isotope value (k_H/k_D), = 2.7 ± 0.3 (Figure 4.3) was obtained from the slope of graph.

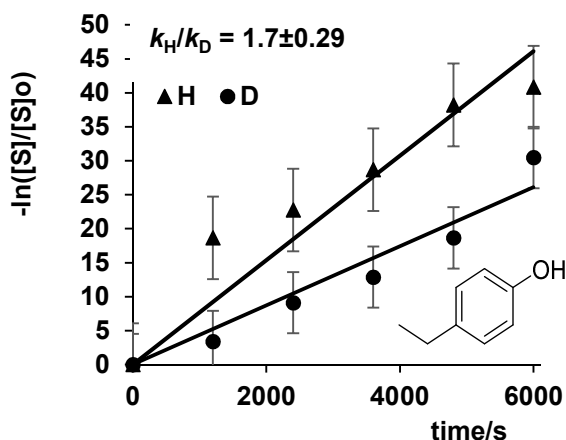


Figure 4.4: Deuterium Isotope Effect Study for the Reaction of 4-Methoxyacetophenone with H₂/D₂ with 4-Ethylphenol as the Ligand

With 4/HBF₄ 4-ethylphenol as the ligand, the plot of $-\ln[(4\text{-methoxyacetophenone})_t/(4\text{-methoxyacetophenone})_0]$ vs time yielded a straight line with the slope of $6.40 \times 10^{-6} \text{ s}^{-1}$ for H₂ and $3.84 \times 10^{-6} \text{ s}^{-1}$ for D₂. The deuterium isotope effect (k_H/k_D) of 1.8 ± 0.3 was obtained from the slope of the graph (Figure 4.4). Also with (4-Trifluoromethyl)phenol as the ligand, the plot of $-\ln[(4\text{-methoxyacetophenone})_t/(4\text{-methoxyacetophenone})_0]$ vs time yielded a straight line with the slope of $(6.92 \pm 0.03) \times 10^{-6} \text{ s}^{-1}$ for H₂ and $1.12 \times 10^{-5} \text{ s}^{-1}$ for D. The deuterium isotope effect (k_H/k_D) of 0.6 ± 0.1 which is inverse kinetic isotopic effect (Figure 4.5) was obtained from the slope of the graph. With 4-chlorophenol as the ligand, the plot of $-\ln[(4\text{-methoxyacetophenone})_t/(4\text{-methoxyacetophenone})_0]$ vs time yielded a straight line with the slope of $2.2 \times 10^{-6} \text{ s}^{-1}$ for H₂ and $3.32 \times 10^{-6} \text{ s}^{-1}$ for D₂. The deuterium isotope effect (k_H/k_D) of 0.8 ± 0.1 was obtained which is inverse kinetic isotopic effect (Figure 4.6).

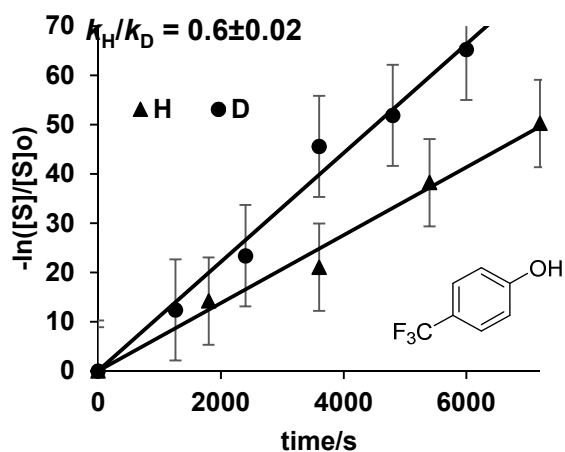


Figure 4.5: Deuterium Isotope Effect Study for the Reaction of 4-Methoxycetophenone with H_2/D_2 with 4- $CF_3-C_6H_4OH$ as the Ligand

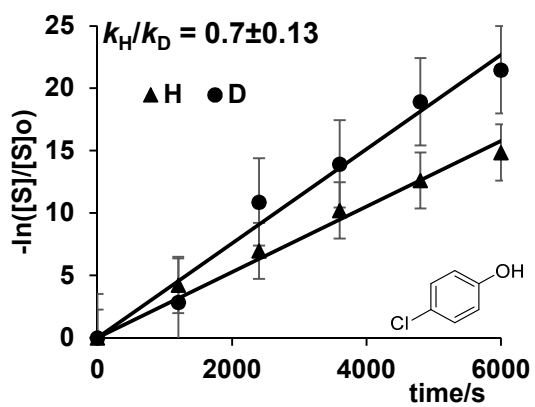


Figure 4.6. Deuterium Isotope Effect Study for the Reaction of 4-Methoxycetophenone with H_2/D_2 with 4- $Cl-C_6H_4OH$ as the Ligand.

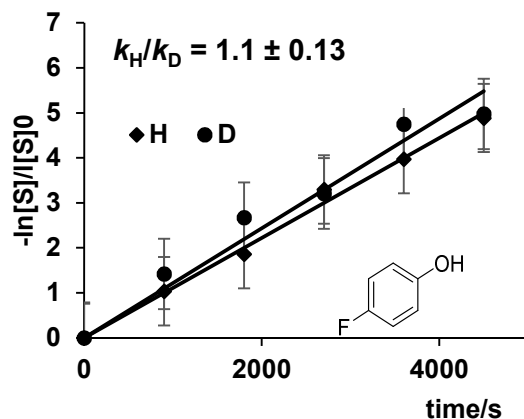
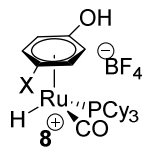


Figure 4.7. Deuterium Isotope Effect Study for the Reaction of 4-Methoxyacetophenone with H_2/D_2 with 4-F- C_6H_4OH as the Ligand.

Table 4.4: Deuterium Isotope Effect Study for the Reaction of 4-Methoxyacetophenone with H_2/D_2 with p-X- C_6H_4OH as the Ligand.

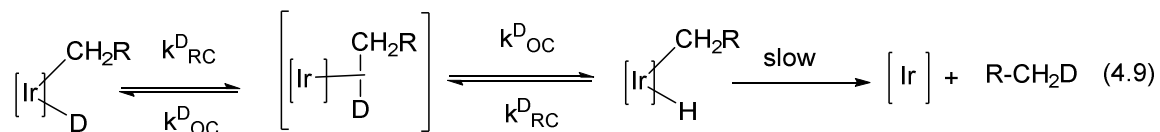


Complex	X	k_H/k_D	σ_p
8a	OMe	2.7 ± 0.3	-0.28
8b	Et	1.7 ± 0.3	-0.14
8c	H	1.2 ± 0.1	0.00
8d	F	1.1 ± 0.1	+0.15
8e	Cl	0.7 ± 0.1	+0.24
8f	CF_3	0.6 ± 0.1	+0.53

When 4-Fluorophenol is used as the ligand, the plot of $-\ln[(4\text{-methoxyacetophenone})_t/(4\text{-methoxyacetophenone})_0]$ vs time yielded a straight line with

the slop of $1.10 \times 10^{-6} \text{ s}^{-1}$ when H_2 used and $1.12 \times 10^{-6} \text{ s}^{-1}$ when D_2 is used. The experimentally determined kinetic isotope value ($k_{\text{H}}/k_{\text{D}}$) within experimental error, is 1.0 ± 0.1 which is inverse kinetic isotopic effect (Figure 4.7). The $k_{\text{H}}/k_{\text{D}}$ values for the hydrogenolysis reaction catalyzed by 4/*p*-X- $\text{C}_6\text{H}_4\text{OH}$ (X = OMe, Et, F, Cl, CF_3) are listed in Table 4.4. Normal deuterium isotope effect was observed for the reaction catalyzed by phenol with electron-releasing group (X = OMe, Et), and inverse isotope effect was measured for the phenols with electron-withdrawing group (X = Cl, CF_3). A negligible small isotope effect was measured in the case of 4-fluorophenol.

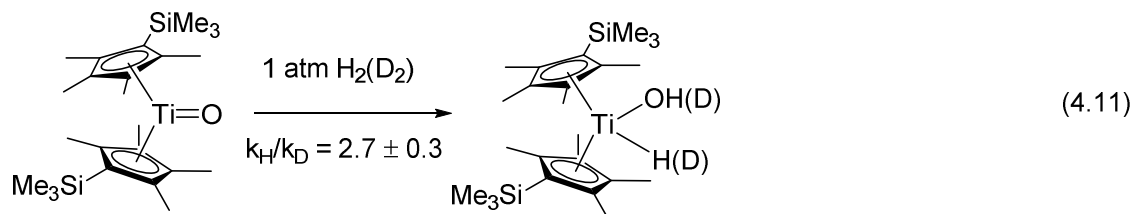
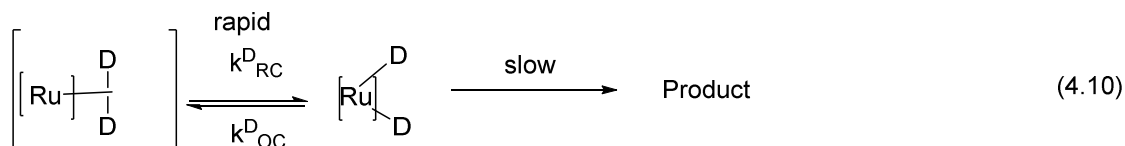
The magnitude of deuterium isotope effect data correlates well with the Hammett σ_{p} values. For the reaction catalyzed by Ru catalyst with an electron-rich phenol ligand, the observation of normal isotope effect is consistent with the notion that the H-H bond activation is intricately intertwined with the turnover-limiting step. Hence, the phenol ligand with an electron-releasing group should facilitate the oxidative addition of H_2 . For the reaction catalyzed by phenol with electron-withdrawing group, a relatively electron poor Ru catalyst is expected to have low affinity for oxidative addition of H_2 . Instead, the stepwise reversible coordination of H_2 and the subsequent partitioning of the equilibrium can explain the observation of inverse isotope effect for the electrophilic nature of Ru catalyst.¹⁸⁻²⁰



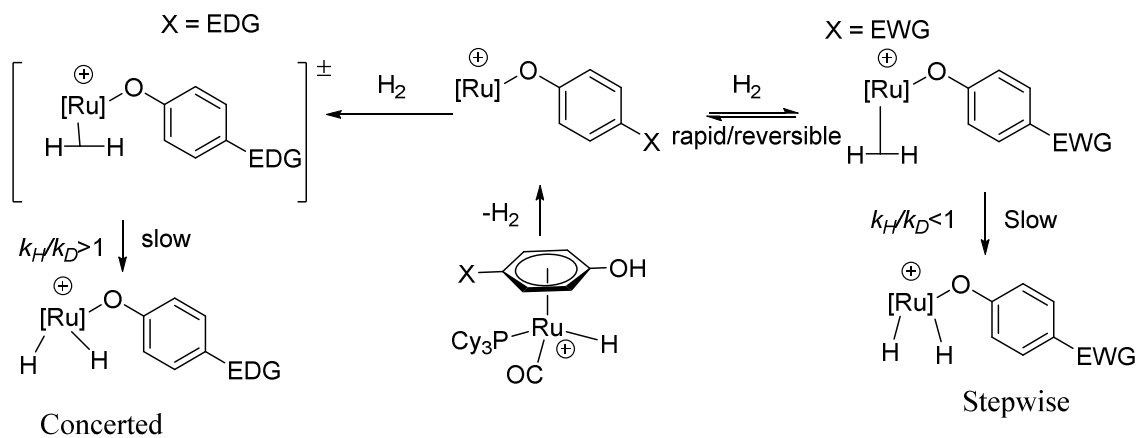
Bergman²¹ explained the inverse KIE in Ir complex mediated C-H activation of hydrocarbons by using equilibrium isotope effect concept [Eq. (4.9)]. In this case, a

stepwise rapid equilibrium between σ -bonded alkyl complex followed by reductive coupled Ir complex and much slower alkyl hydride formation has led to inverse deuterium isotope effect ($k_H/k_D = 0.7$). One explanation for the origin of the inverse equilibrium isotope is that the σ -alkane complex contains an intact, strong C–H or C–D bond, whereas the alkyl hydride complex has a weaker M–H or M–D bond. Furthermore, since this inverse isotope effect is likely to be associated with the C–H/C–D bond-making/bond-breaking step, rather than the alkane dissociation step, the overall isotope effect for alkane loss was attributed to an *inverse equilibrium isotope* effect (i.e., $K_{eq}^{H/D} < 1$) separating the alkyl hydride complex from the σ -alkane complex. Inverse EIE is common for the oxidative addition C–H to a metal center (Scheme 4.1).¹⁸⁻²⁰

We can apply a similar kinetics on the H–H activation catalyzed by Ru–H complex **1**, for the phenols with electron withdrawing groups. We proposed a similar rapid equilibrium in between Ru–H and Ru–H₂ complexes [Eq. (4.10)]. On the other hand, Ru catalyst with phenol with electron-donating group should promote the binding and the activation of H₂. (For X = OMe, k_H/k_D was 2.7).^{17d-e} The normal KIE indicates H–H activation is rate determine step for the hydrogenolysis where weaker H–H bond breaks faster than the strong D–D bond (Scheme 4.1)



Chirik and co-workers reported a similar KIE effect in the addition of $\text{H}_2(\text{D}_2)$ to Ti-oxo complex, which exhibited a normal, primary KIE $k_{\text{H}}/k_{\text{D}} = 2.7 \pm 0.3$ [Eq. (4.11)]. Normal isotope effects of the same direction but with smaller magnitudes were determined for silane addition to the same system [Eq. (4.8)].²² KIE values are consistent with the Hammett data concerted pathway.

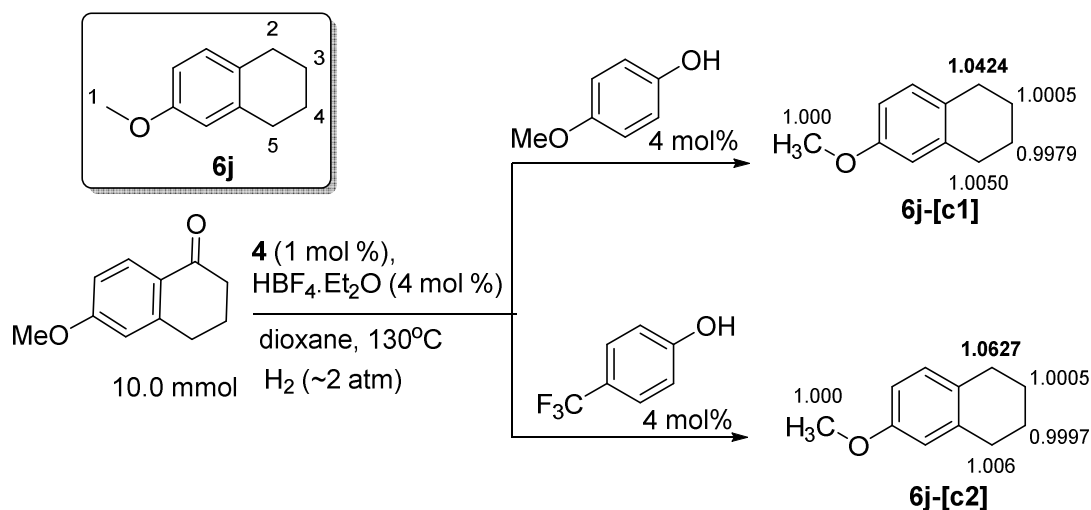


Scheme 4.1: Electronic Effect of Phenol Ligand on Ru-H (**8**) Catalyzed H_2 Activation.

4.4.1.2 Carbon Isotope Effect Study

To further determine the rate determining step of the catalytic reaction, the $^{12}\text{C}/^{13}\text{C}$

kinetic isotope effect (KIE) was successfully measured for the hydrogenolysis reaction by employing Singleton's NMR technique [Eq. (4.12)].²³ To compare the electronic influence of the phenol ligand, we have chosen the phenol ligand with two electronically different substituents *p*-OMe-C₆H₄OH ($\sigma_p = -0.27$) and *p*-CF₃-C₆H₄OH ($\sigma_p = +0.54$). The hydrogenolysis of 6-methoxy-1-tetralone (1.76 g, 10 mmol) was performed with H₂ (3 atm), **4** (1 mol %) and *p*-X-C₆H₄OH (X = OMe or CF₃) (4 mol %) in 1,4-dioxane (8 mL) at 130 °C for 2-3 h. The product 6-methoxytetrahydronaphthalene (**6j**) was isolated by a column chromatography on silica gel (hexanes/Et₂O = 40:1) and analysed by ¹³C NMR. The most pronounced carbon isotope effect on the product **6j** is observed when the ¹³C ratio of the product **6j** at three low conversions (15, 18 and 20 % conversion) was compared with that of the sample obtained at high conversion (95 %).



Scheme 4.2: ¹³C KIE data for the 6-Methoxy-1,2,3,4-tetrahydronaphthalene (A) for the in-situ Generated Catalyst **8a** (B) for the in-situ Generated Catalyst **8f**.

The hydrogenolysis of 6-methoxy-1-tetralone catalyzed by the catalyst **4**/*p*-X-C₆H₄OH resulted in a significant isotope effect on the carbonyl carbon for phenol ligand with both electron-releasing and -withdrawing groups (¹³C at 95 % conversion)/(average of ¹³C at 17

% conversion) at $C(1) = 1.042$ for $X = \text{OMe}$ and $C(1) = 1.063$ for $X = \text{CF}_3$ (Scheme 4.2).

The data indicates that the C-O bond cleavage is the rate-limiting step for the overall hydrogenolysis reaction.

Table 4.5: Average ^{13}C Integration of the Product **13j-[c1]** at High Conversion (Virgin, R_0 ; 96 % conversion), at Low Conversion (R ; avg 18 % conversion) and the Calculated ^{13}C KIE for Catalyst **8a**.

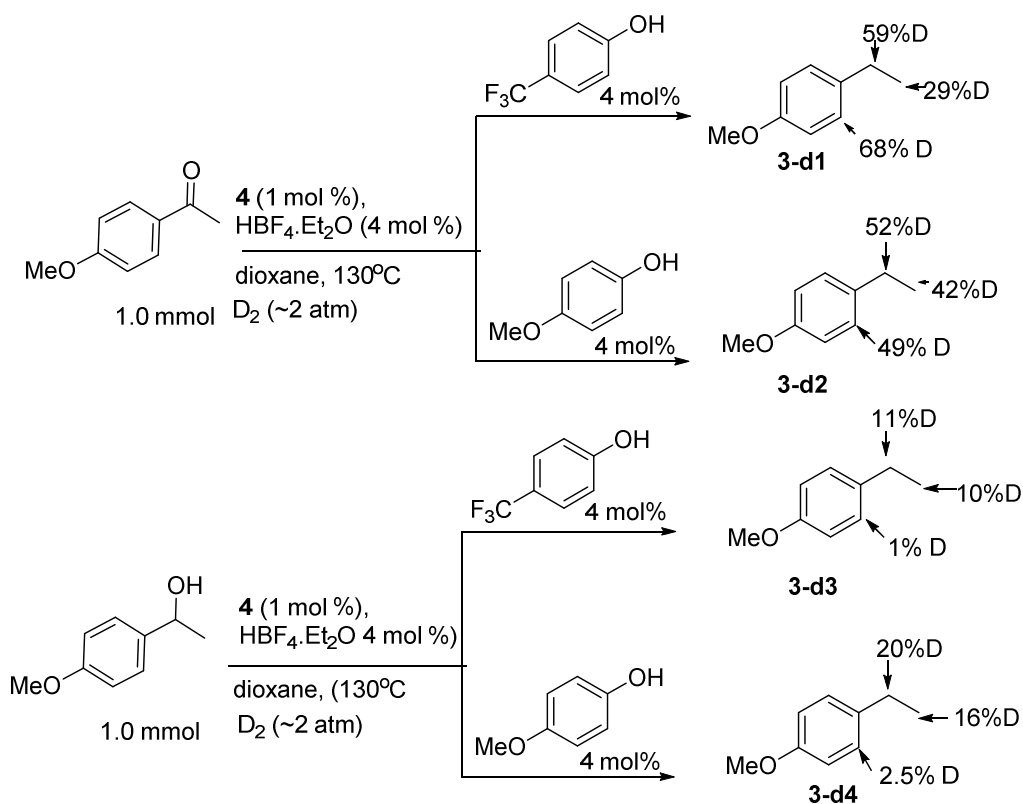
	OMe	C1	C2	C3	C4
Virgin, R_0	1.0000	1.0051	0.9968	1.0000	1.0223
Sample R_1	1.0000	0.9991	0.9868	0.9999	0.9801
Sample R_2	1.0000	1.0050	0.9980	1.0006	0.9811
Sample R_3	1.0000	1.0050	0.9979	1.0005	0.9811
Avg (R)	1.0000	1.0030	0.9942	1.0004	0.9807
R_0/R	1.0000	1.0021	1.0026	0.9996	1.0424

Table 4.6: Average ^{13}C Integration of the Product **13j-[c2]** at High Conversion (Virgin, R_0 ; 96 % conversion), at Low Conversion (R ; avg 18 % conversion) and the Calculated ^{13}C KIE for the Catalyst **8f**.

	OMe	C1	C2	C3	C4
Virgin, R_0	1.0000	1.0051	0.9968	1.0000	1.0223
Sample R_1	1.0000	0.9989	0.9972	0.9990	0.9615
Sample R_2	1.0000	0.9999	0.9969	0.9996	0.9617
Sample R_3	1.0000	0.9990	0.9970	0.9998	0.9627
Avg (R)	1.0000	0.9993	0.9971	0.9995	0.9620
R_0/R	1.0000	1.0058	0.9997	1.0005	1.0627

4.4.1.3 Deuterium Labeling Study

To examine H/D exchange pattern on the products, 4-methoxyacetophenone (1.0 mmol) was reacted with D₂ (2 atm) in dioxane at 130 °C for 4 h (Scheme 4.3). The product **12** was isolated by column chromatography, and its deuterium content was analyzed by ¹H and ²H NMR (Figure 4.8-4.11). The deuterium content of the same product **12a**, which was obtained from the analogous treatment of 1-(4-methoxyphenyl)ethanol (1 mmol) with D₂ (2 atm) and 4/*p*-OMe-C₆H₄OH, was also compared with the product obtained from the ketone. To compare the H/D pattern on the electronic effect of phenol ligand, the same set of experiments was repeated for 4/*p*-CF₃-C₆H₄OH catalytic system (Scheme 4.3).



Scheme 4.3: Deuterium Incorporation pattern of 1-Ethyl-4-methoxybenzene Product: (a) 4-Methoxyacetophenone and 4-(Trifluoromethyl)phenol (b) 1-(4-Methoxyphenyl)ethanol and 4-(Trifluoromethyl)phenol (c) 4-Methoxyacetophenone and 4-Methoxyphenol (d) 1-(4-Methoxyphenyl)ethanol and 4-Methoxyphenol.

As illustrated in Scheme 4.3, a much higher amount of deuterium incorporation was observed in the product **3-d2** obtained from the hydrogenolysis of ketone compared to the product obtained from the alcohol **3-d4**. A 29 % deuterium on the CH₃ group on the product suggests that a facile H/D exchange takes place possibly via a keto-enol tautomerization of the ketone substrate (Scheme 4.3), while 68 % of deuterium on the *ortho*-arene C-H can be explained by the formation of chelate-assisted *ortho*-metallation, which is well-known process in catalytic C-H activation chemistry.²³

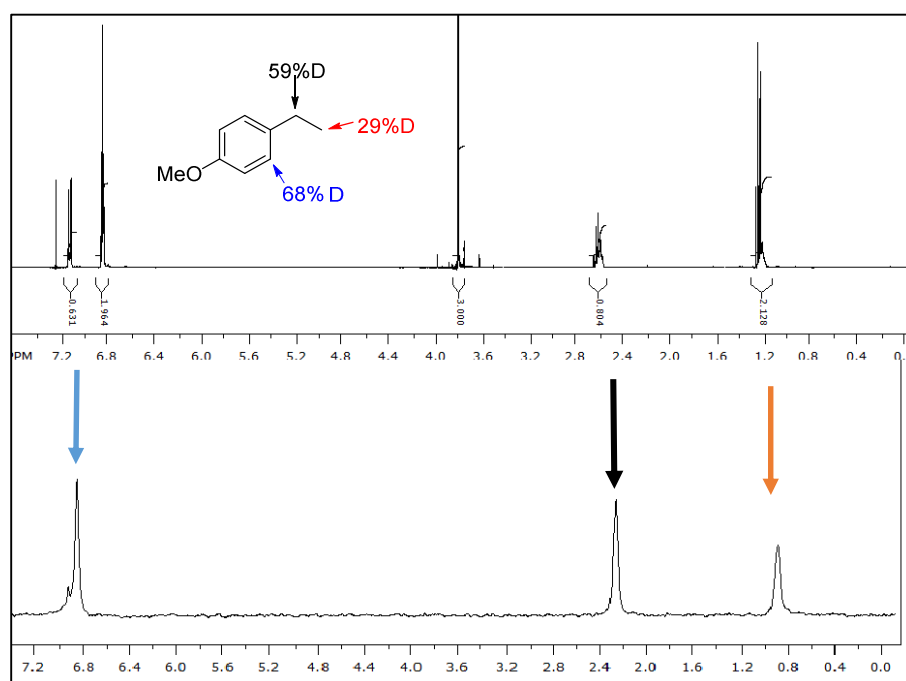


Figure 4.8: ¹H and ²H NMR Spectra for the Hydrogenolysis of 4-Methoxyacetophenone with D₂ Catalyzed by 4/4-CF₃C₆H₄OH.

A 59 % deuterium on the benzylic position supports the notion for rapid and reversible H/D exchange via keto-enol tautomerization and *ortho*-metallation processes. In contrast, only small deuterium incorporation on the product from the hydrogenolysis of 1-

(4-methoxyphenyl)ethanol is consistent with the notion that the C-O hydrogenolysis occurs directly without going through the formation of ketone.

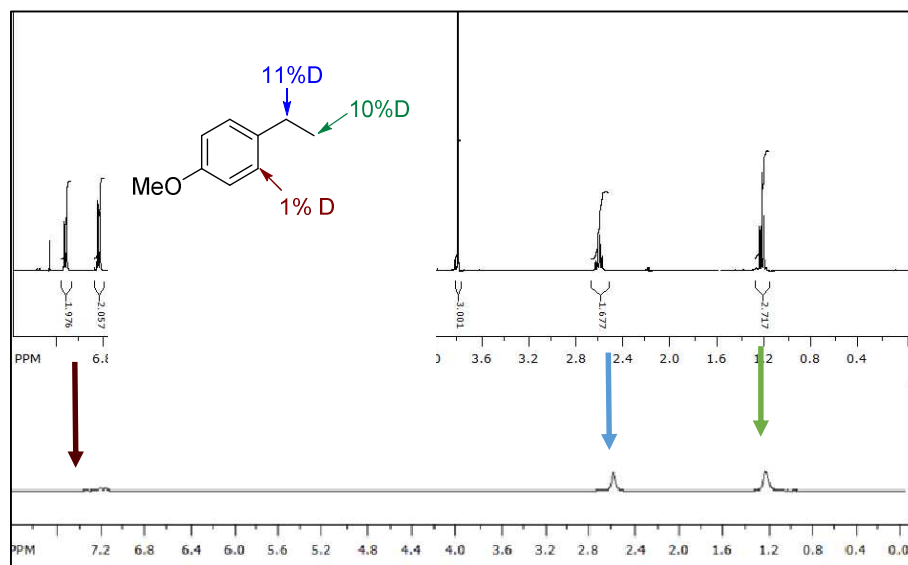


Figure 4.9: ^1H and ^2H NMR Spectra for the Hydrogenolysis of 1-(4-Methoxyphenyl)ethanol with D_2 Catalyzed by 4/4- $\text{CF}_3\text{C}_6\text{H}_4\text{OH}$.

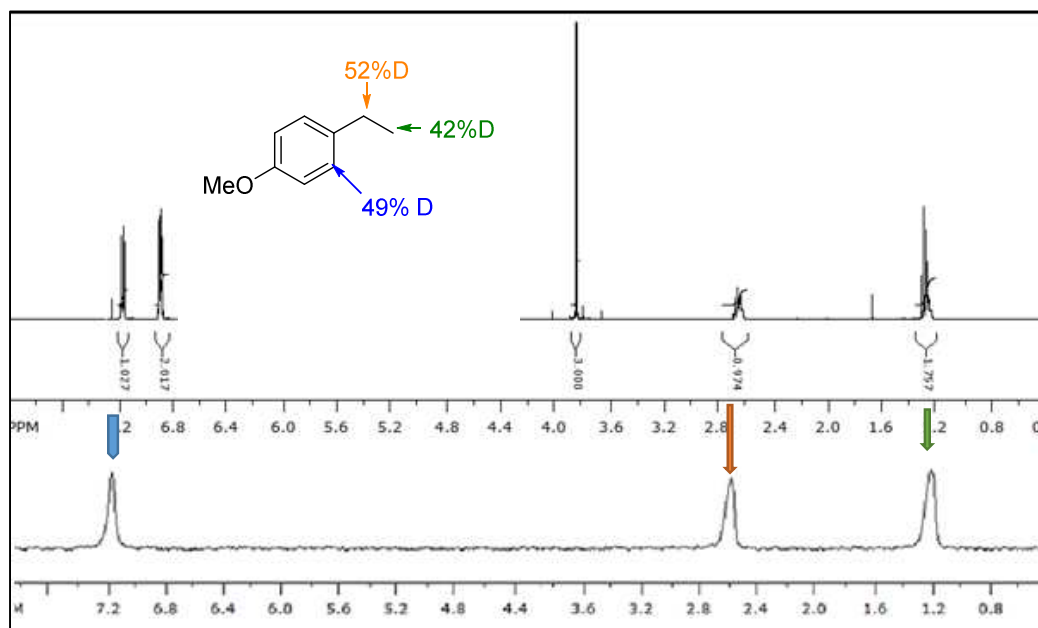


Figure 4.10: ^1H and ^2H NMR Spectra for the Hydrogenolysis of 4-Methoxyacetophenone with D_2 Catalyzed by 4/4- $\text{OMeC}_6\text{H}_4\text{OH}$.

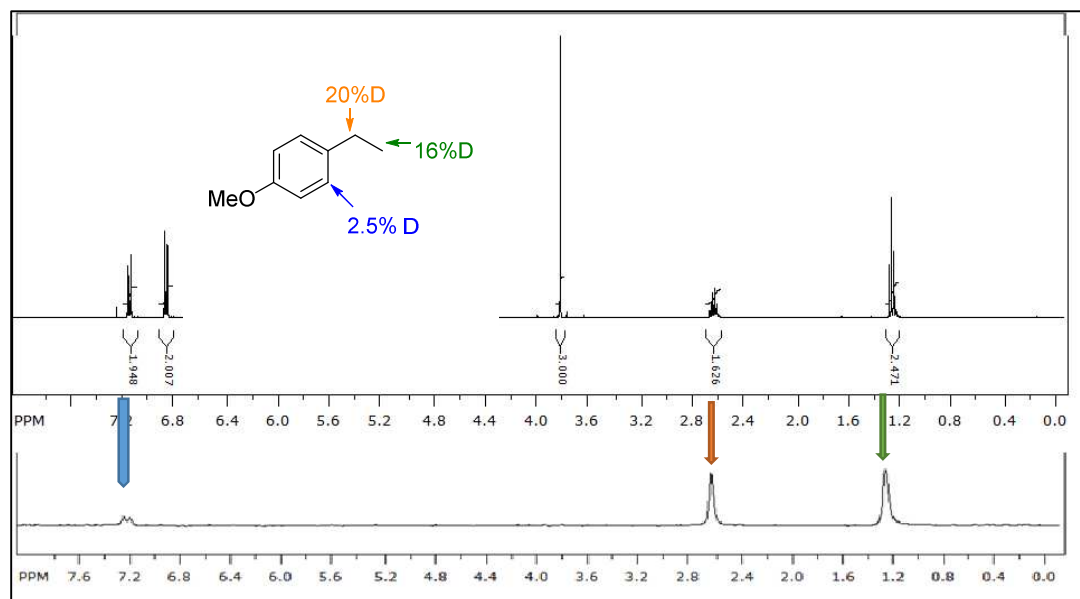
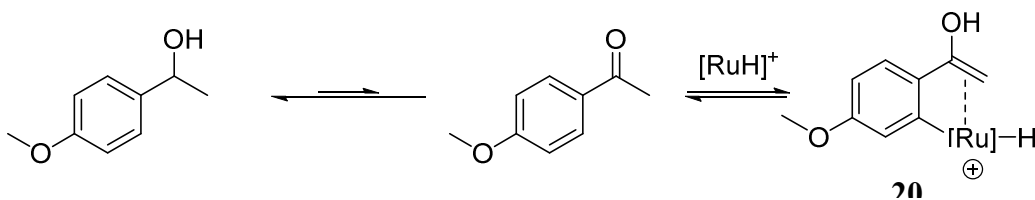


Figure 4.11: ^1H and ^2H NMR Spectra for the Hydrogenolysis of 1-(4-Methoxyphenyl)ethanol with D_2 Catalyzed by 4/4- $\text{OMeC}_6\text{H}_4\text{OH}$.



Scheme 4.4: Keto-Enol Tautomerization and Formation of Ru-enolate Complex

A similar set of H/D exchange pattern was obtained when the analogous hydrogenolysis of 4-methoxyacetophenone was performed with the catalyst 4/*p*- $\text{CF}_3\text{-C}_6\text{H}_4\text{OH}$ having phenol with electron-withdrawing group. But for the hydrogenolysis of 1-(4-methoxyphenyl)ethanol, a much less H/D exchange was observed in *ortho*-C-H of aromatic ring. These results indicate that the reoxidation of alcohol to ketone is not favored

(scheme 4.3, **3-d3**, **3-d4**). High deuterium incorporation on keto and terminal carbon indicate that the keto-enol (scheme 4.3) equilibrium is more favored with 4-methoxyphenol than 4-(trifluoromethyl)phenol.

4.4.2 Determination of Empirical Rate Law

4.4.2.1 Catalyst Concentration Dependence

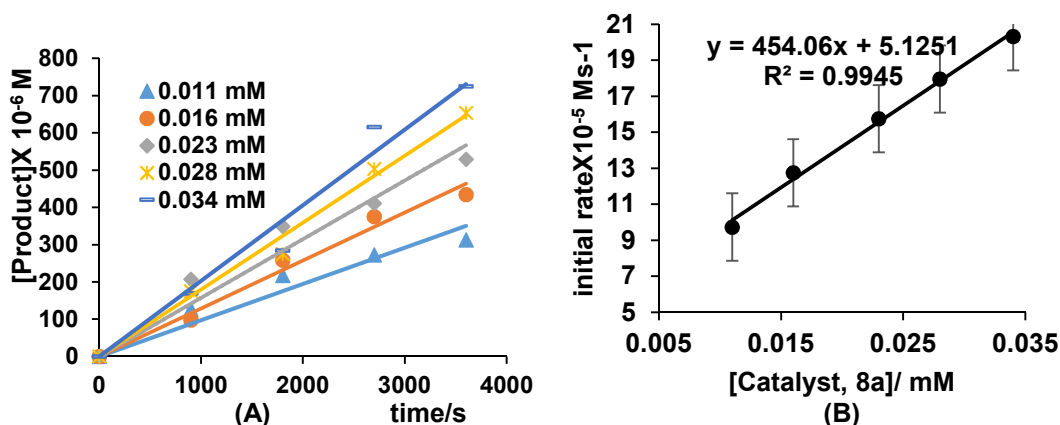


Figure 4.12: (A) The Formation of 1-Ethyl-4-methoxybenzene vs Time. (B) Initial Rate of the Formation 1-Ethyl-4-methoxybenzene vs at Different Catalyst Concentrations of 4/HBF₄·OEt₂/4-OMe-C₆H₄OH (**8a**)

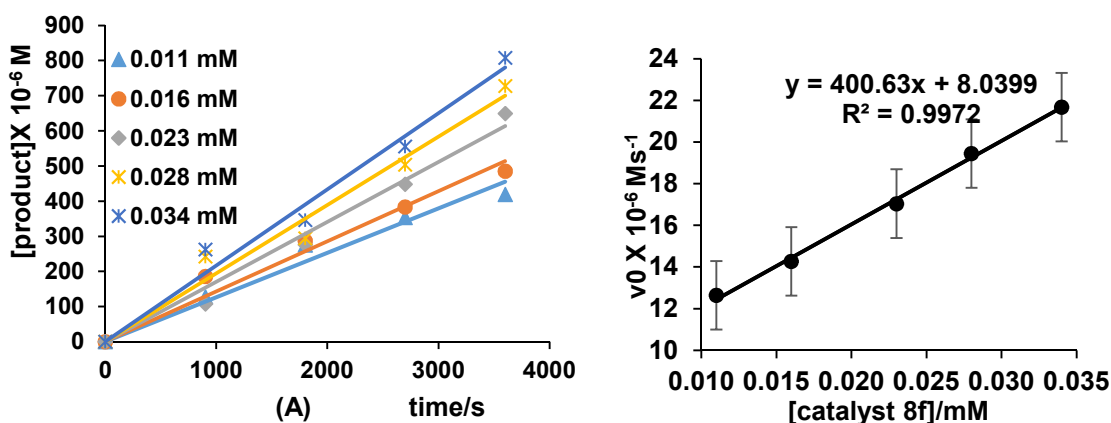


Figure 4.13: (A) The Formation of 1-Ethyl-4-methoxybenzene vs Time. (B) Initial Rate of the Formation 1-Ethyl-4-methoxybenzene vs at Different Catalyst Concentrations of 4/HBF₄·OEt₂/4-CF₃-C₆H₄OH (**8f**).

In an effort to further compare the kinetics of two phenolic ligands, we next determined the empirical rate laws for the hydrogenolysis reaction of 4-methoxyacetophenone mediated by **4/p**-X-C₆H₄OH (X = OMe, CF₃) with opposite electronic environments. First, the rate dependence on the catalyst concentration was measured. From the plot of initial rate (v_0) of formation of 1-ethyl-4-methoxybenzene as a function of [**4/p**-OMe-C₆H₄OH] under pseudo-first-order condition yielded a straight line with the slope of $4.5 \times 10^{-6} \text{ s}^{-1}$ for **4/p**-OMe-C₆H₄OH [**8**] (Figure 4.12). The similar experiment using the catalyst **4/p**-CF₃-C₆H₄OH **8f** also led to the linear dependence on [**4/p**-CF₃-C₆H₄OH] with the slope of $4.0 \times 10^{-6} \text{ s}^{-1}$ (Figure 4.13).

4.4.2.1 Dependence of Substrate Concentration

The analogous method was employed to determine the [ketone] dependence. From the plot of initial rate (v_0) of formation of 1-ethyl-4-methoxybenzene as a function of [4-methoxyacetophenone] under pseudo-first-order condition yielded a straight line for [4-methoxyacetophenone] in the range of 0.3 M-2.0 M for both cases (X = OMe, CF₃). Linear Slopes were obtained for the case of X = OMe (**8a**) was $5.06 \times 10^{-7} \text{ s}^{-1}$ (Figure 4.14), and for the case of X = CF₃ (complex **8f**) was $3.54 \times 10^{-7} \text{ s}^{-1}$ (Figure 4.15).

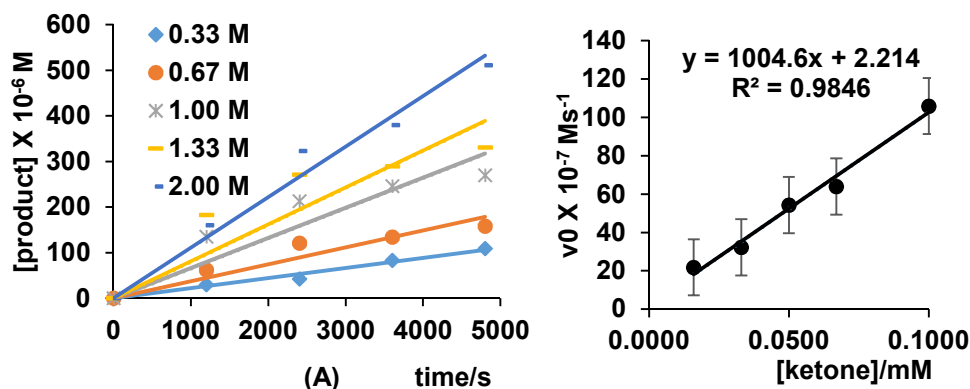


Figure 4.14: (A) The Formation of 1-Ethyl-4-methoxybenzene vs Time. (B) Initial Rate of the Formation 1-Ethyl-4-methoxybenzene vs at Different 4-Methoxyacetophenone Concentrations for the Catalyst **4**/HBF $_4$ ·OEt $_2$ /4-OMe-C $_6$ H $_4$ OH (**8**)

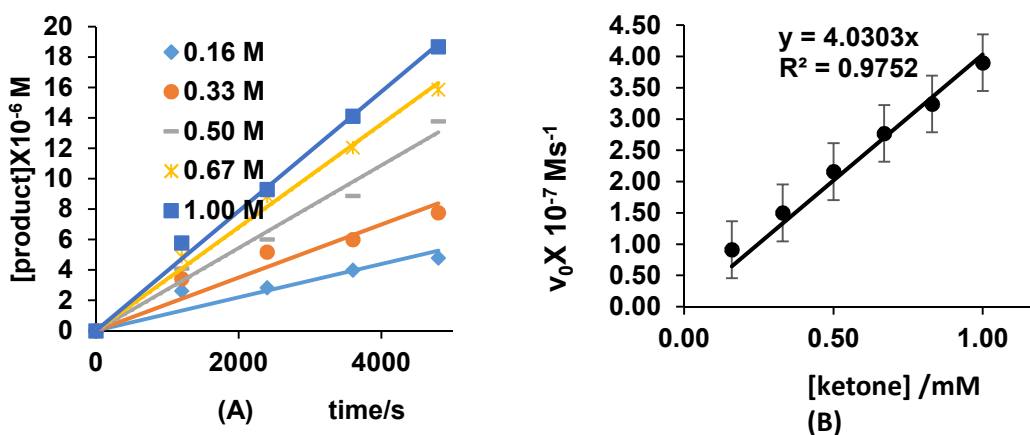


Figure 4.15: (A) The Formation of 1-Ethyl-4-methoxybenzene vs Time. (B) Initial Rate of the Formation 1-Ethyl-4-methoxybenzene vs at Different 4-Methoxyacetophenone Concentrations for the catalyst **4**/HBF $_4$ ·OEt $_2$ /4-CF $_3$ -C $_6$ H $_4$ OH (**8f**)

4.4.2.2 Effect of Hydrogen Pressure

The dependence of [H $_2$] on the rate exhibited distinctly different kinetics between electron-donating and electron-withdrawing group from 4/*p*-X-C $_6$ H $_4$ OH (X = OMe, CF $_3$). Thus, for the hydrogenolysis of 4-methoxyacetophenone, the plot of initial rate (v_0) as a function of [H $_2$] showed that an inverse dependence on hydrogen pressure in the range of

16-55 psi for the reaction catalyzed by 4/*p*-OMe-C₆H₄OH. The plot of H₂ pressure versus initial rate for the formation of 1-ethyl-4-methoxybenzene for 4-methoxyphenol coordinated catalyst **8a** yielded a hyperbola (Fig. 4.16 B) which does not pass through the origin and gave a reaction order of -1.0 on ketone. The plot of p_{H₂} vs 1/*v*₀ gave a linear fit (Fig. 4.16C) which indicate inverse dependence on hydrogen concentration. The inverse dependence on [H₂] for the catalytic hydrogenolysis catalyzed by 4/*p*-OMe-C₆H₄OH indicates that the coordination of second molecule of H₂ inhibits the hydrogenolysis reaction. Since the Ru catalyst with electron-releasing group is expected to have a relatively strong affinity toward H₂, it can effectively inhibit the coordination of the ketone substrate.

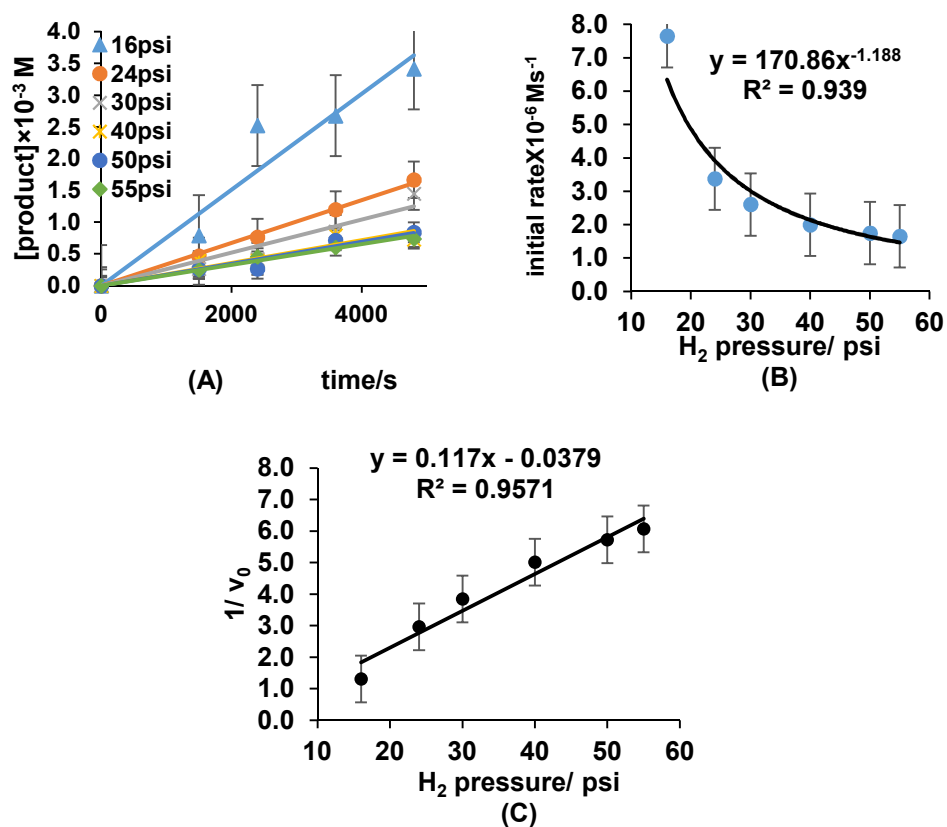


Figure 4.16: (A) The Formation of 1-Ethyl-4-methoxybenzene vs Time. (B) Initial Rate of the Formation 1-Ethyl-4-methoxybenzene vs at Different [H₂] (C) Inverse rate vs [H₂] for the Catalyst 4/HBF₄·OEt₂/4-OMe-C₆H₄OH (**8a**)

In sharp contrast, the plot of initial rate (v_0) for the hydrogenolysis of 4-methoxyacetophenone by phenol with an electron withdrawing group $4/p$ -OMe-C₆H₄OH showed that the reaction rate is independent of [H₂] in the range of 16-55 psi. A straight line parallel to the x-axis was observed for plot of hydrogen pressure versus initial rate for the formation of 1-ethyl-4-methoxybenzene for 4-(trifluoromethyl) phenol coordinated catalyst **8f** (Figure 4.17) which indicates zero order dependence on hydrogen pressure. This is consistent with a rapid and reversible coordination of H₂, in which the electron-poor Ru catalyst has a low affinity toward H₂ compared to the ketone substrate.

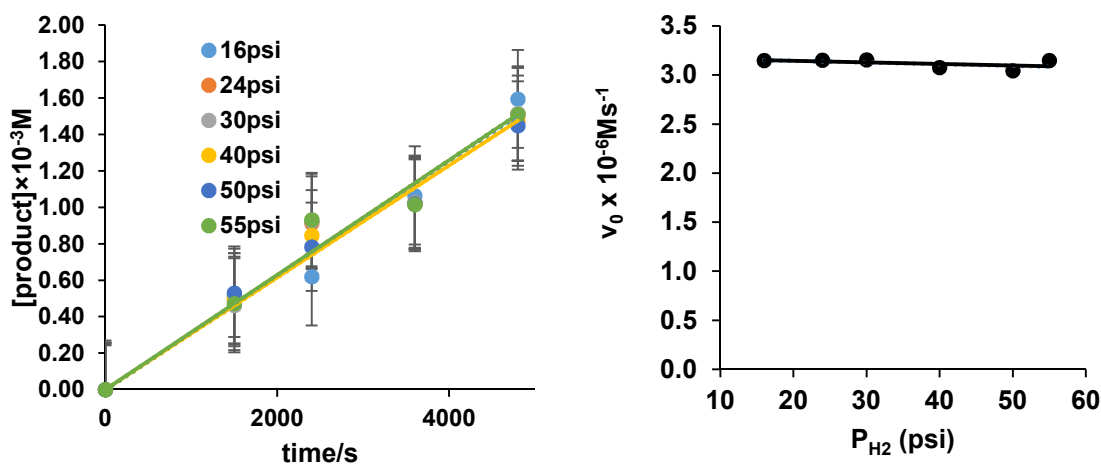


Figure 4.17: (A) The Formation of 1-Ethyl-4-methoxybenzene vs Time. (B) Initial Rate of the Formation 1-Ethyl-4-methoxybenzene vs at Different [H₂] for the Catalyst $4/\text{HBF}_4 \cdot \text{OEt}_2/4\text{-CF}_3\text{-C}_6\text{H}_4\text{OH}$ (**8f**)

Combining these kinetic data, the rate law for the hydrogenolysis of 4-methoxyacetophenone with 4-electron donating group substituted phenol is shown in eq. 4.12.

$$\text{Rate} = k_{\text{obs}}[\text{Ru}][\text{ketone}][\text{H}_2]^{-1} \quad (4.12)$$

Phenols with electron withdrawing group, the rate law is shown in eq. (4.13).

$$\text{Rate} = k_{\text{obs}}[\text{Ru}][\text{ketone}][\text{H}_2]^0 \quad (4.13)$$

4.5 Isolation and Characterization of Catalytically Relevant Ruthenium Complexes.

We explored the reactivity of the complex **1** to gain structural insights on the reactive intermediates. The treatment of **1** with phenol in a NMR tube in CD_2Cl_2 was followed by ^1H and $^{31}\text{P}\{^1\text{H}\}$ NMR. After 2 h of heating at $80\text{ }^\circ\text{C}$, a 1:1 ratio of cationic Ru-H complex **1** and phenol-coordinated complex **8c**, as evidenced by the appearance of new peaks at δ - 10.87 and 70.8 ppm by ^1H and $^{31}\text{P}\{^1\text{H}\}$ NMR, respectively [Eq. (4.14)]. The formation of free benzene molecule at $\delta = 7.4$ ppm was also observed by ^1H NMR, but no evidence for PCy_3 dissociation was detected under these conditions. A series of substituted phenol-coordinated complexes are conveniently synthesized from the reaction of the tetranuclear Ru complex **4** with phenol and $\text{HBF}_4 \cdot \text{Et}_2\text{O}$, by following the similar procedure used to synthesize the complex **1**. The structure of these phenol-coordinated complexes is readily determined by spectroscopic methods, and the solid state structures of **8a**, **8c** and **8e** were also determined by X-ray crystallography (Figure 4.16-4.17).

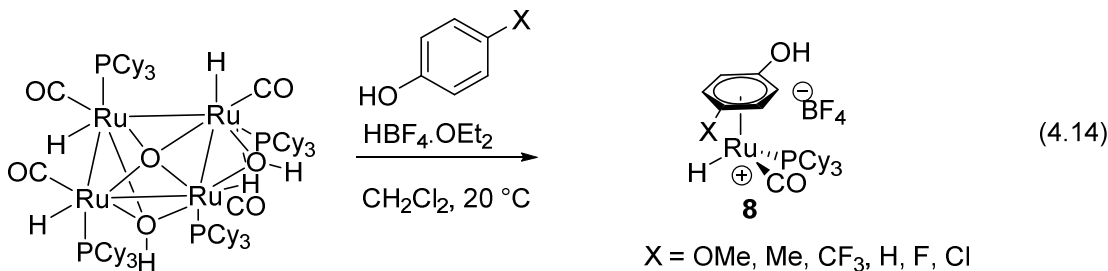
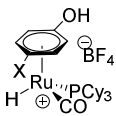
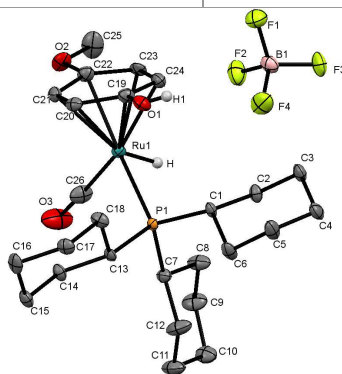


Table 4.7: Selected Spectroscopic Data for Complexes **8a-g**

	¹ H NMR Ru-H/ppm	³¹ P NMR/ppm	FT-IR ν_{CO} / cm^{-1}
X = OMe (8a)	-10.61 (d, $J_{\text{PH}} = 27.0$ Hz)	71.38	1963
X = H (8c)	-10.86 (d, $J_{\text{PH}} = 27.1$ Hz)	70.78	1973
X = F (8d)	-10.29 (d, $J_{\text{PH}} = 26.8$ Hz)	71.71	
X = Cl (8e)	-10.40 (d, $J_{\text{PH}} = 27.4$ Hz)	71.86	1983
X = CF₃ (8f)	-10.55 (d, $J = 26.0$ Hz)	71.38	1947
X = Me (8g)	-10.58 (d, $J_{\text{PH}} = 27.1$ Hz)	71.32	

**Figure 4.18:** ORTEP Diagram of Complex **8a** (H atoms and Solvent Molecules Removed for Clarity)

The complex **8a** has a “piano stool” coordination around the Ru center. The phenolic ligand is stabilized by hydrogen bond with BF_4^- counter ion. The Ru1-P1 bond 2.3349(10) Å and P1-Ru1-C19 bite angle is $98.18(8)^\circ$. Ru1-C19 bond distance is 2.400(3) Å. Ru-H resonance was observed at -10.61 ppm in the H NMR spectrum in CDCl_3 . Ru-P resonance was observed at 71.38 ppm in the $^{31}\text{P}\{\text{H}\}$ NMR spectrum in CDCl_3 . In both cases, Ru-CO and Ru-P bond distances are shorter than that of Ru-H benzene coordinated complex which are 1.8679(5) Å and 2.3207(13) respectively.

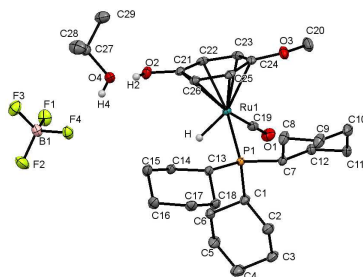


Figure 4.19: ORTEP Diagram of Complex **8a'** (H atoms and Solvent Molecules Removed for Clarity)

The complex **8a'** also has a “piano stool” coordination. The phenolic ligand is stabilized by hydrogen bond with solvate isopropanol molecule, which in turn makes H-bond with BF_4^- counter ion. The Ru1-P1 bond 2.3159(4) Å is lower than that of complex **8a** which is 2.3349(10). P1-Ru1-C19 bite angle $88.66(5)^\circ$ is lower than that of complex **8a'** which $98.18(8)^\circ$. Ru1-C19 bond distance is 1.8460(18) lower than Ru1-C19 bond distance is 2.400(3) Ru-H resonance was observed at -10.61 ppm in the H NMR spectrum in CDCl_3 . Ru-P resonance was observed at 71.38 ppm in the $^{31}\text{P}\{\text{H}\}$ NMR spectrum in CDCl_3 . In both cases Ru-CO and Ru-P bond distances are shorter than that of Ru-H benzene coordinated complex which are 1.8679(5) Å and 2.3207(13) respectively.

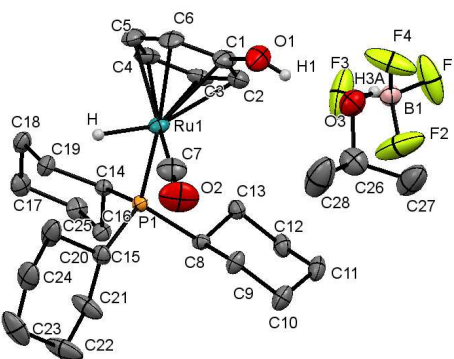
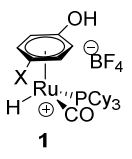
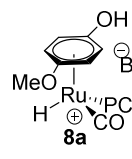
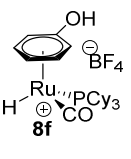


Figure 4.20: ORTEP Diagram of Complex **8c** (H atoms and Solvent Molecules Removed for Clarity)

The complex **8c** shows a similar three legged “piano stool” geometry. The phenolic ligand is stabilized by hydrogen bond with solvate isopropanol molecule, which in turn has H-bond with BF_4^- counter ion. The Ru1-P1 bond 2.3150(7) Å and P1-Ru1-C7 bite angle is 87.04(11)°. Ru1-C7 bond distance is 1.842(4) Å. Ru-H resonance was observed at -10.86 ppm in the ^1H NMR spectrum in CDCl_3 . Ru-P resonance was observed at 70.78 ppm in the $^{31}\text{P}\{\text{H}\}$ NMR spectrum in CDCl_3 .

Table 4.8: Selected Physical Parameters of Complexes **5**, **8a** and **8f**

Parameter			
Ru-CO / Å	1.867(5)	1.8460(18)	1.842(4)
Ru-P / Å	2.3207(13)	2.3159(4)	2.3150(7)
P-Ru-CO/°	88.84(15)	88.66(5)°	87.04(11)
^1H NMR Ru-H/ppm	-10.39	-10.61	-10.86
$^{31}\text{P}\{\text{H}\}$ NMR Ru-P/ppm	72.9	71.38	70.78

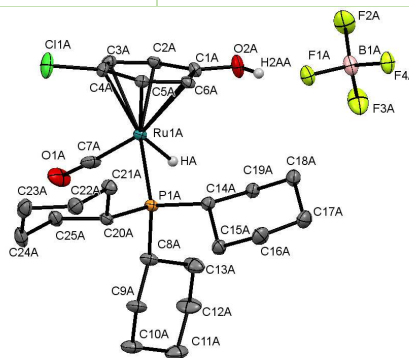
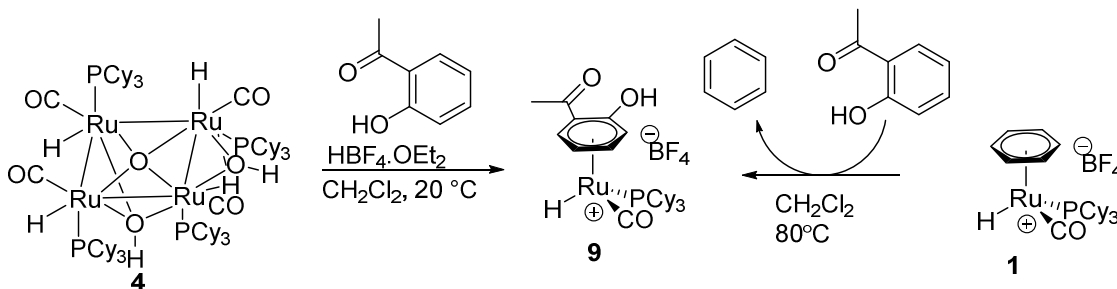


Figure 4.21: ORTEP Diagram of Complex **8e** (H atoms and Solvent Molecules Removed for Clarity)

The complex **8e** shows a three legged “piano stool” geometry. The phenolic ligand is stabilized by hydrogen bond with BF_4^- counter ion. The Ru1-P1 bond 2.3271(6) Å and P1-Ru1-C7 bite angle is 87.96(9)°. Ru1-C7 bond distance is 1.843(3) Å. Ru-H resonance was observed at -10.40 (d, $J_{\text{PH}} = 26.8$ Hz) ppm in the ^1H NMR spectrum in CD_2Cl_2 . Ru-P resonance was observed at 71.86 ppm in the $^{31}\text{P}\{\text{H}\}$ NMR spectrum in CD_2Cl_2 .

In an effort to trap catalytically relevant species, 1:1 ratio of cationic Ru-H complex **1** and 2-hydroxyacetophenone (which is ligand acting also as substrate) were mixed in a J. Young tube using CD_2Cl_2 as the solvent. We observed that initially formed π -coordinated Ru-H complex **9** shows Ru-H resonance at -10.87 ppm and $^{31}\text{P}\{\text{H}\}$ resonance at 70.8 ppm as monitored by ^1H NMR and ^{31}P NMR. The complex **9** was prepared from the analogous treatment of **4** with 2-acetylphenol and $\text{HBF}_4 \cdot \text{Et}_2\text{O}$ in 90 % NMR yield (scheme 4.5).



Scheme 4.5: Synthetic Routes for the Complex **9**

Our attempt to crystallize the complex **9** led to a stable dimeric complex **10**, which is isolated analytically pure complex in 90 % yield [Eq. (4.15)]. Structure of complex **10** was established by spectroscopic methods. The X-ray structure of complex **10** is shown in fig. 4.22

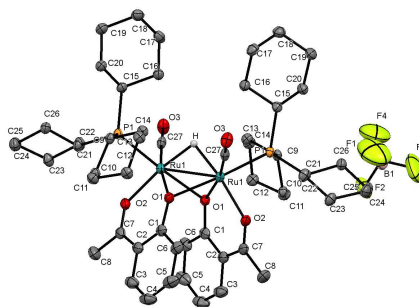
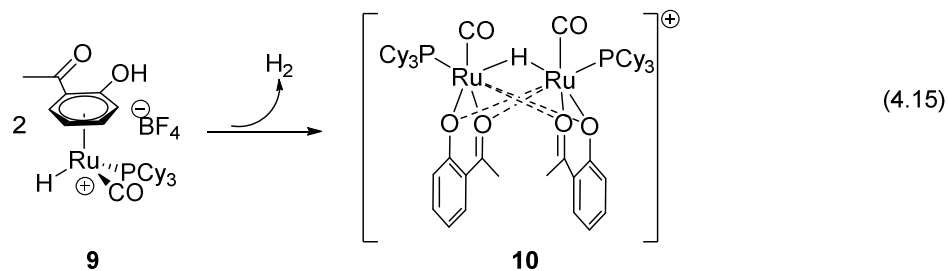


Figure 4.22: ORTEP Diagram of Complex **10** (H atoms and Solvent Molecules Removed for Clarity)

The cationic complex **10** has a dimeric structure with two bridging chelate acetophenolate ligands and bridging hydride. The unit has crystallographic 2-fold symmetry, with octahedral Ru(II) center. Bridging Ru-H resonance was appeared at δ - 28.30 ppm as triplet on ^1H NMR spectrum. Ru-P resonance on $^{31}\text{P}\{\text{H}\}$ NMR spectra found at δ 70.7 ppm. This suggest that initially formed π -coordinated phenolic ruthenium complex is rearranged to more stable Ru-phenoxy complex upon loss of H_2 .

The reaction of binuclear Ru-H complex **10** in wet 1,4-dioxane smoothly converted into the formation of binuclear Ru-hydroxo complex **11**, which is fully characterized by using spectroscopic techniques. Bridging Ru-(μ -OH) resonance was appeared at -3.18 (s, 1H) ppm on ^1H NMR spectrum [Eq. (4.17)] and PCy_3 resonance 66.5 ppm on $^{31}\text{P}\{\text{H}\}$ NMR. The structure of complex **11** was unambiguously characterized by single crystal X-ray diffraction (Figure 4.23). The complex is isostructural with the complex **10**, in that each

Ru(II) core has octahedral coordination containing two bridging acetophenolate ligands. A considerably longer metal-metal distance of 2.948 Å of **11** compared to the hydride complex **10** (2.680 Å) is probably due to a larger ionic radius of the bridging oxygen compared to the hydrogen atom. The dimer has a local 2-fold symmetry but not a crystallographic one, as opposed to complex **10**. Both Ru(II) ions have octahedral coordination. We believe that further reaction with H₂ gas complex **10** produces H₂ coordinated complex **13** via **12** (scheme 4.6) similar to Shvo²⁵ catalyst but the attempt to identify the intermediate was failed due to the fact that those species are highly reactive and readily hydrogenolyses the acetophenolate ligand into 2-ethylphenol.

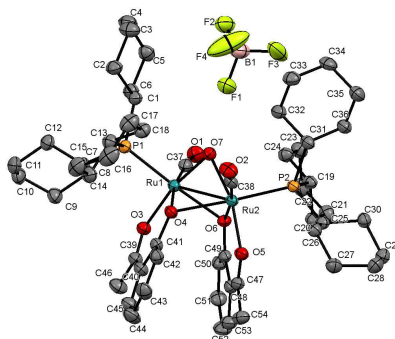
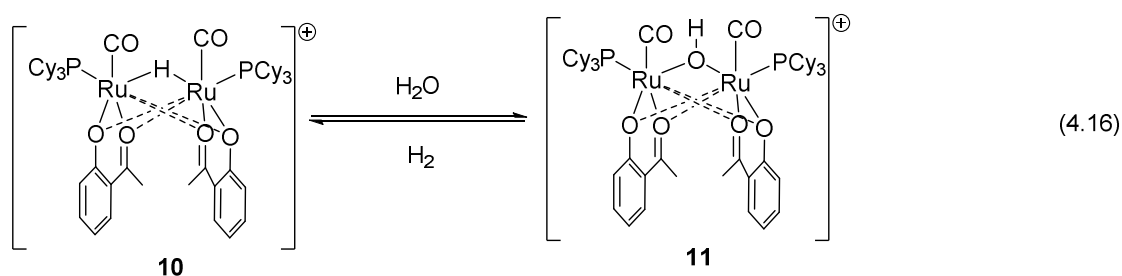
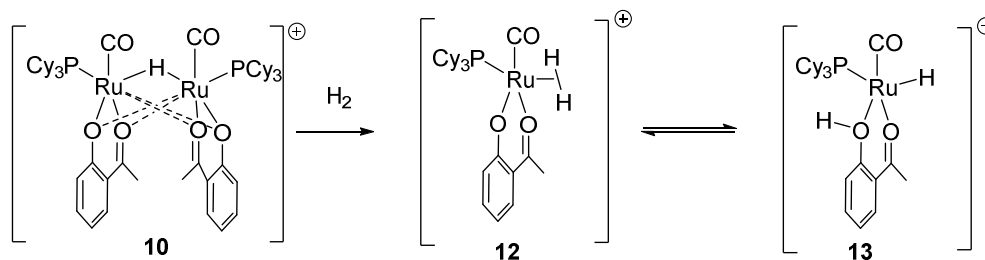


Figure 4.23: ORTEP Diagram of Complex **11** (H atoms and Solvent Molecules Removed for Clarity)



Scheme 4.6: Possible Intermediates from the Reaction of Complex **10** with H₂

4.5.1 Catalyst Concentration Dependence Study.

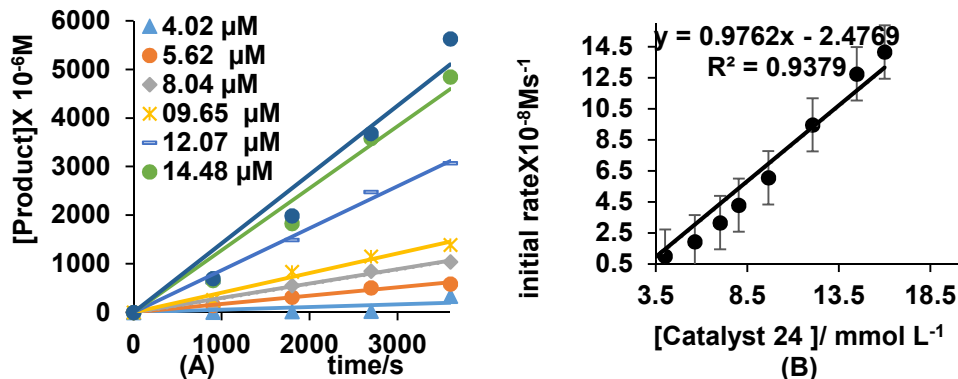
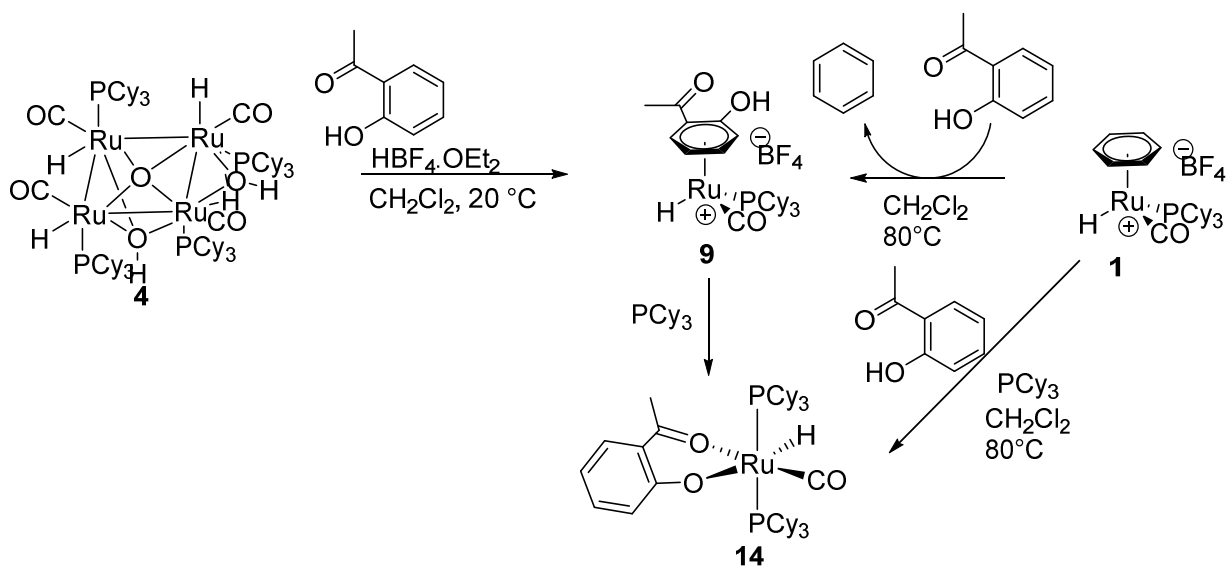


Figure 4.24: A) Plot of [2'-Hydroxyethylbenzene] vs Time at Different Catalyst **10** Concentrations (4 μM-16 μM). B) Initial Rate of Formation 2'-Hydroxyethylbenzene vs Different Catalytic **10** Loading

The hydrogenolysis reaction catalyst concentration dependence on catalyst **10** the reaction rate was studied to prove the active species is monomeric ruthenium complex. Hydrogenolysis of 2-hydroxyacetophenone to 2-ethyl phenol using different amount of catalyst **10** studied under pseudo first order condition in 10 min time interval at 130 °C for 3h in 1,4-dioxane. Concentration of 2-ethylphenol was determined by ¹H NMR using methylbenzoate as the internal standard. From the plot of initial rate (*v*₀) of formation of 2-ethylphenol as a function of [**10**] under pseudo-first-order condition yielded a straight line

for [10] in the range of 4 μM -15 μM has been observed. The procedure was repeated for 8 different catalyst concentrations (4 μM -16 μM). The plot of catalytic concentration vs initial rate of the reaction is shown in Figure 4.24.

From the plot of initial rate of hydrogenolysis of 2-hydroxyacetophenone, the pseudo first order rate constant $9.76 \times 10^{-9} \text{ Ms}^{-1}$ was obtained. The results are consistent with the rapid dimer dissociation into monomers or one of the monomer part is catalytically active or the dimer itself is active for hydrogenolysis. From the similar experiment for the complexes **8a-8f** also we obtained first order of catalyst concentration. Therefore it is inconsistent with the later and consistent with first assumption that is the dimer will dissociate into monomer and formed a catalytically active one part and inactive part.



Scheme 4.7: Synthetic Route for the Complex **14**

All attempts to trap the intermediate **13** by using different ligands and solvents were unsuccessful. Cationic ruthenium hydride complex **1** with 2 equivalence of PCy₃ in CH₂Cl₂ at 80 °C formed neutral Ru-H species **14** and one equivalent of phosphonium salt. In this

case, PCy₃ acted as a base to abstract an acidic proton from phenol ligand. Complex **10** in the presence of PCy₃ exclusively produced complex **14** without dimerization. We can argue that the complex **14** is analogous to complex **13** which replaced ¹H by PCy₃ ligand. We were able to characterize the complex **14** by ¹H NMR and ³¹P{¹H} NMR and X-ray diffraction techniques (Figure 4.25). An alternative way, complex **14** was synthesized from complex (Ch3-3) with the reaction with 2-acetylphenolate in dioxane solvents at 80 °C, 1h reaction time by a single step is shown in eq. 4.17 below.

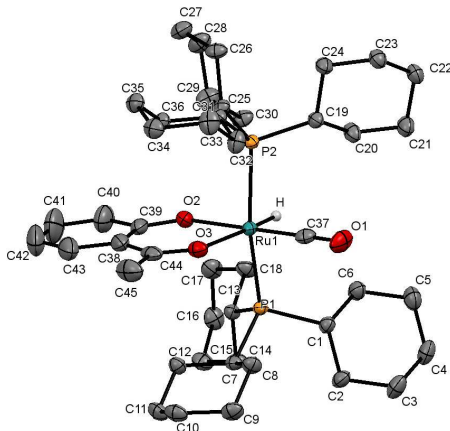
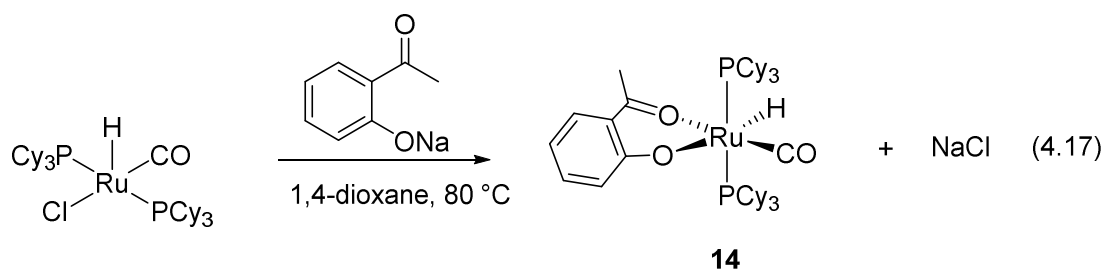


Figure 4.25: ORTEP Diagram of Complex **14** (H atoms and Solvent Molecules Removed for Clarity)

4.6 Determination of pK_a of Ru-H Complexes

Acidity of metal hydride complexes is very important in hydrogenolysis of C-O bonds.

²⁶⁻²⁸ Application of general literature method available for determination of pK_a of metal-

ligand bifunctional catalyst was unsuccessful due to dissociation of phenol ligand. We have surveyed number of different methods to measure the pK_a^{29} of Ru-H catalyst, but we failed due to de-coordination of benzene ligand in the experimental conditions. Finally pK_a of Ru-H complex **1** was determined by measuring pH of different concentration of Ru-H in aqueous medium in the range of 1×10^{-4} - 1×10^{-6} M. pK_a was calculated by extrapolating the plot of the plot of pH vs $\log([A^-]/[HA])$ to get y intercept (which $A^- = \mathbf{15}$ and $HA = \mathbf{16}$) Figure 4.26, [Eq. (4.18)].³⁰

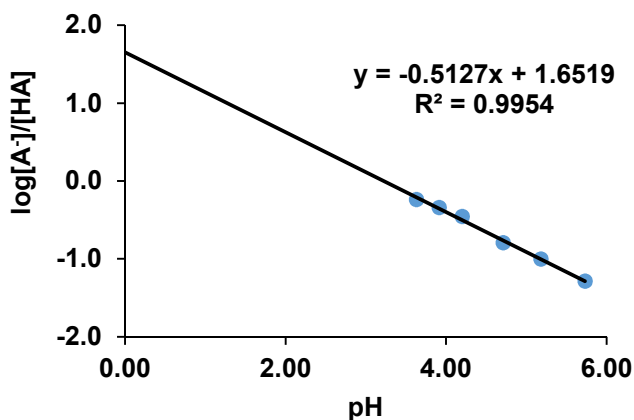
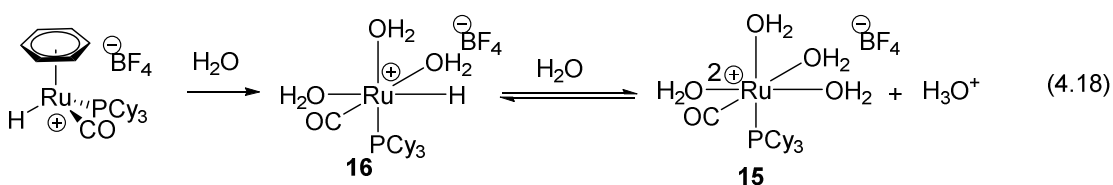


Figure 4.26: The Plot of pH vs $\text{Log}([A^-]/[HA])$

Since the displacement of benzene from the cationic ruthenium hydride is feasible. We measured the pK_a of Ru-aqua complex **16**, from which $pK_a = 1.65$ calculated. According to the bifunctional catalytic system it is very important to be phenol H much more acidic than this value (Figure 4.27).

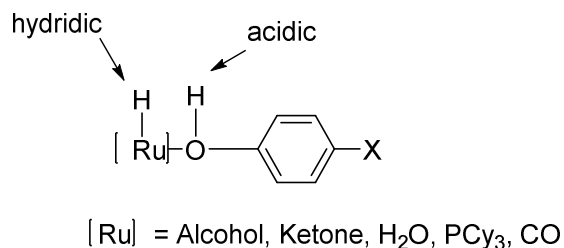


Figure 4.27: Acidic and Hydridic Nature of Ruthenium Phenol Bifunctional Catalyst

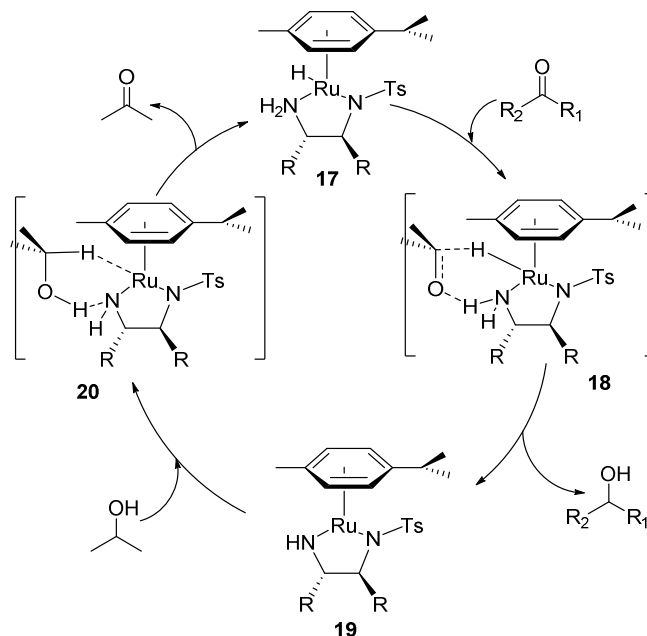
4.7 Proposed Mechanism

We propose that the hydrogenolysis reaction of ketones has two stages. The first stage is the hydrogenation of ketone C=O double bond into alcohols. The mechanism of hydrogenolysis of ketone to alcohols should be similar to outer-sphere mechanism catalyzed by Noyori type bifunctional catalyst.³¹

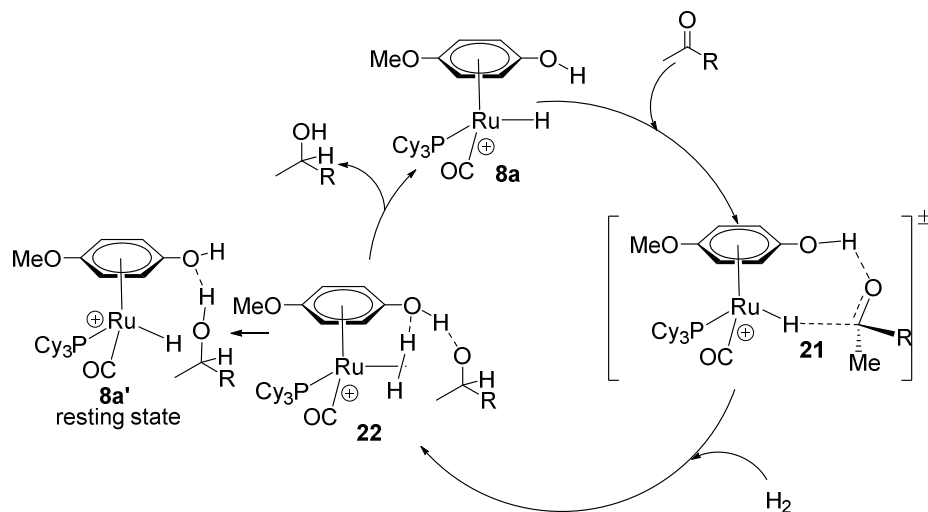
Noyori³¹ and Morris³² proposed that the active species **17** is generated from the precursor chloride complexes (η^6 -arene) RuCl((S,S)-H₂NCHRCHRNTs) by reaction with a reductant (formic acid or 2-propanol) and base. For imines, the reactions are conducted in a formic acid-triethylamine azeotropic 5:2 mixture with or without an additional solvent. Chiral alcohols derived from aryl alkyl ketones and a variety of chiral amines from prochiral imines are obtained in very high ee. They proposed mechanism for the transfer hydrogenation of ketones (Scheme 4.8) via a concerted transfer of the proton and the hydride from **18** to the substrate in a six-membered cyclic transition state to give the alcohol and **19**. The proton and the hydride from 2-propanol are then delivered to the ligand and the metal, respectively, forming **20** and acetone. The reaction is proposed to proceed via outer-sphere mechanism without coordination of either alcohol or ketone (aldehyde) to the

metal. Casey proposed a similar mechanism for the hydrogenation of ketone using outer-sphere mechanism.³³

By adopting their mechanism, we explain first stage of hydrogenolysis of ketone catalyzed by Ru-H complex **8a** (Scheme 4.9). Complex **8a** reacts with ketones to form similar complex **21** as **17**, proton and hydride transfer to ketone in concerted fashion (complex **21**). Hydride transfer to carbonyl carbon and phenolic hydrogen transfer to carbonyl oxygen to form alcohol. Then H₂ gas reacts with Ru center with hydride transfer to electrophilic carbonyl carbon and the proton transfer to oxygen making alcohols which is stabilized by hydrogen bonding (**8a'**). Decoordination of alcohol make active ruthenium catalyst by reacting with H₂ gas via the intermediate **22**. The catalyst **8a** and the resting state **8a'** which was generated by 4-OMeC₆H₄OH was characterized by X-ray crystallography shown in Figure 4.20.



Scheme 4.8: Catalytic Cycle of Noyori Catalyst via a Concerted Six-membered Transition State



Scheme 4.9: Outer-sphere Mechanism for the Hydrogenation of Ketones to Alcohols.

In contrast to ketone hydrogenolysis reaction, the mechanism of the second stage of hydrogenolysis of alcohol C-O bond to methylene compounds has not been studied extensively. According to our kinetic data, two different mechanistic pathways operate between phenol ligands with electron donating group and electron withdrawing group contained. From ¹³C KIE data, we observed that the C-O cleavage is the rate limiting step of the mechanism for both cases.

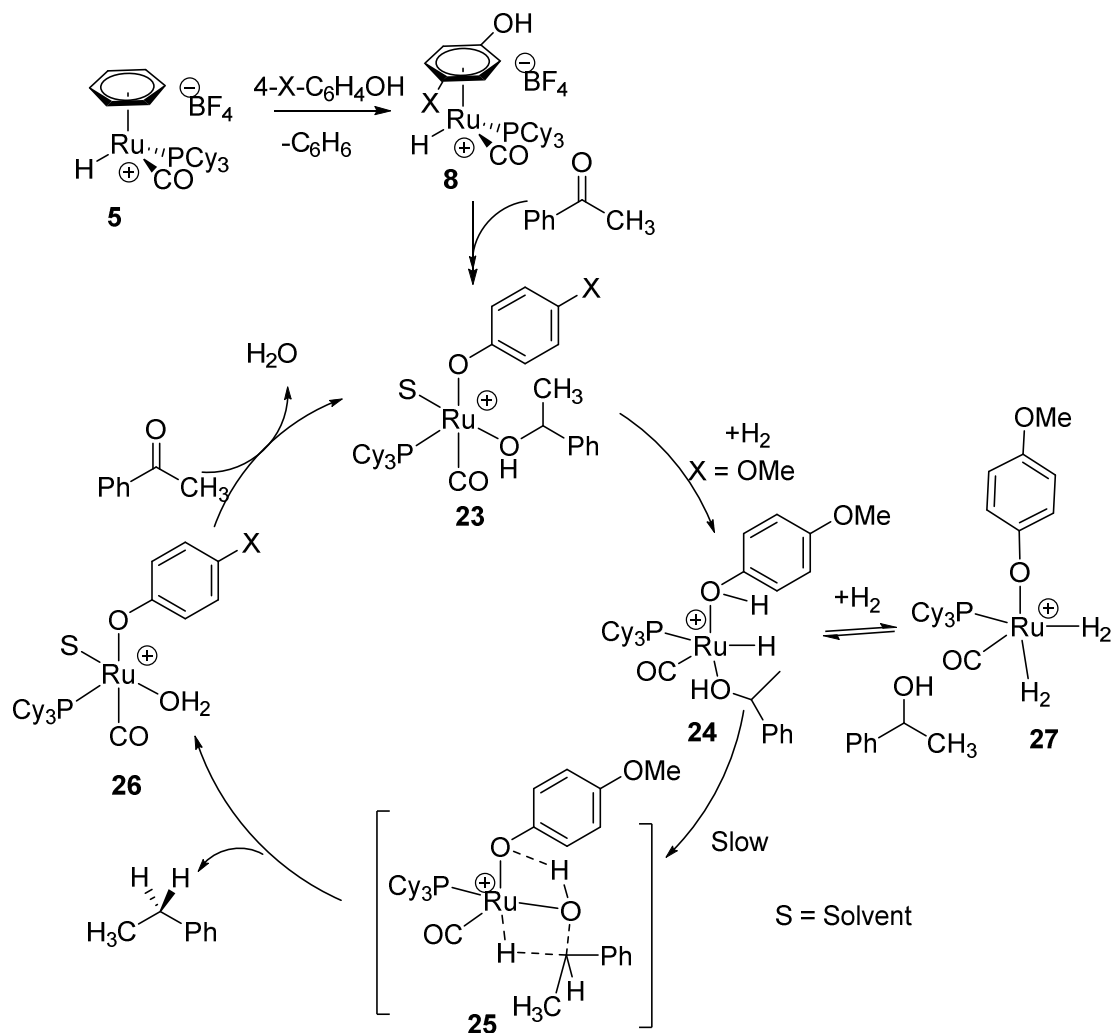
Table 4.9: Summary of Kinetic Parameters for the Hydrogenolysis of Aryl ketone Catalyzed by 4/*p*-X-C₆H₄OH (X = OMe, CF₃).

Kinetic parameter	X = OMe	X = CF ₃
Hammett ρ	-3.3	+1.5
k_H/k_D	2.7	0.6
rate dependence on [H ₂]	1/[H ₂]	[H ₂] ⁰
k_{12C}/k_{13C}^a	1.04	1.06

^a The carbon isotope effect of **6j** obtained from singleton method.

The kinetic data for the catalytic hydrogenolysis are summarized in Table 4.9. On the basis of these kinetics as well as spectroscopic observations, we compiled two plausible mechanistic pathways for the selective hydrogenolysis of a ketone substrate to the aliphatic product based on the electronic nature of ligands (Scheme 4.10 and Scheme 4.11). Based on the ^1H NMR studies³⁴ and available X-ray data, we proposed that the ligand displacement of cationic Ru-H complex **1** with phenol ligand would generate the complex **8**. Phenol ligand switched the coordination mode from $\eta^6\pi$ -mode to $\eta^1\text{O}$ - by deprotonation, and alcohol molecule coordinates as shown in complex **23**. The complex **23** is stabilized by coordination of 1,4-dioxane solvent molecules. This is supported by the formation of complex **10** in the presence of 2-hydroxyacetophenone as the ligand, which is fully characterized by spectroscopic techniques. The complex **10** shows the same catalytic activity for the hydrogenolysis reaction. We proposed the intermediate **23** is the key intermediate species for the hydrogenolysis reaction for both pathways.

For the Ru catalyst with electron-rich phenol ligand ($\text{X} = \text{OMe}$), ^{13}C KIE (1.04) and high negative Hammett value ($\rho = -3.3$) indicate that the C-O bond cleavage is the rate limiting step of the hydrogenolysis reaction. The magnitude of deuterium isotope effect data correlates well with the Hammett σ_p values. High $k_{\text{H}}/k_{\text{D}}$ normal isotope effect indicates that the concerted addition of H_2 is rate limiting step for the H-H activation. We proposed that the complex **23** reacts with H_2 to generate H-H bond cleave product **24** which is analogous to metal ligand bifunctional catalyst evidence for concerted H-H addition.²⁶ The complex **24** could be in equilibrium with π -coordinated complex.



Concerted H₂ addition and C-O cleavage
 $r = [\text{H}_2]^{-1}[\text{ketone}][\text{Ru-H}]$, ¹³C KIE = 1.063

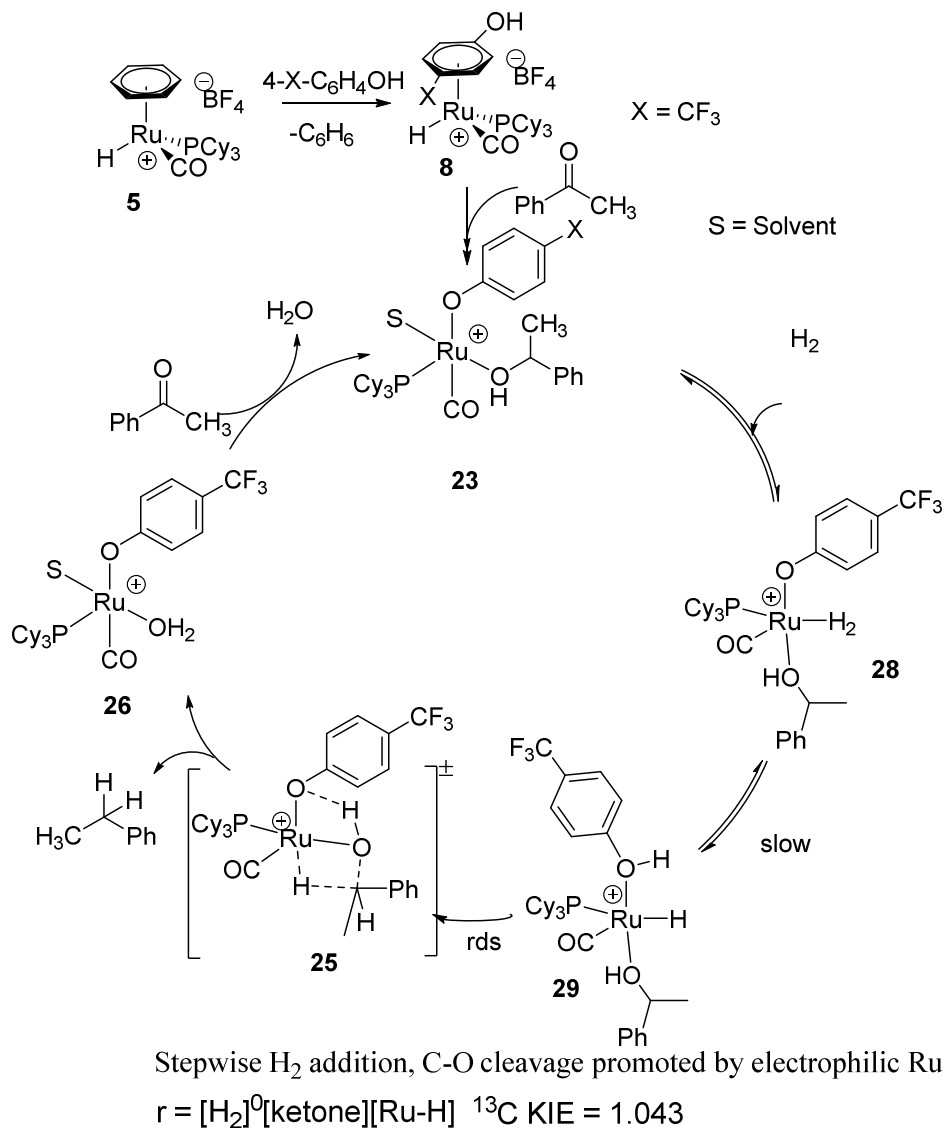
Scheme 4.10: Proposed Mechanism of Ruthenium Catalyzed Hydrogenolysis of 1-Phenethanol to Ethyl Benzene for the Catalyst **8a** (X = OMe).

The inverse dependence on hydrogen pressure suggests that the hydrogenolysis reaction is inhibited by addition of second hydrogen molecule to generate complex **27**. This will compete for the alcohol substrate coordination. For the reaction catalyzed by the phenol ligand with an electron-donating group, the observation of normal isotope effect is consistent with the H-H bond activation is intricately intertwined with the rate determine

step. Hence, the phenol ligand with an electron-releasing group should facilitate the oxidative addition of H₂. High negative Hammett value indicate a relatively electron rich Ru catalyst containing phenol with electron-donating group should promote the binding and the activation of H₂. Based on high negative Hammett value and ¹³C KIE, we suggest that the cleavage of C-O bond of alcohol is mediated by hydrogen coordinated species **25** in concerted fashion.

The production of aliphatic product from the complex **25** and coordination of a H₂O molecule to ruthenium center generates intermediate **26**. We were able to trap analogous intermediate (complex **11**) by using 2-hydroxyacetophenone. The analyses data of complex **11** described in this chapter suggested that the chelation of 2-hydroxyacetophenone lead to generate more stable adduct by reacting a neutral intermediate. Interestingly, this complex **11** also catalytically active for the hydrogenolysis reaction. Another molecule of ketone react with complex **26** to regenerate the active catalytic intermediate **23**.

On the other hand, for the Ru catalyst with electron-poor phenol ligand (X = CF₃), electrophilic nature of the ketone substrates seems to be important in promoting the hydrogenolysis. The generation of active intermediate **23** is same for both mechanisms. The independent kinetics of hydrogen pressure indicate that there is a higher affinity of alcohol substrate than H₂ to stabilize the electrophilic ruthenium center. The independence of [H₂] on the rate suggests that the dative coordination of alcohol is preferred over the H₂ binding to electrophilic Ru center.



Scheme 4.11: Proposed Mechanism of Ruthenium Catalyzed Hydrogenolysis of 1-Phenethanol to Ethyl Benzene for the Catalyst **8f** (X = CF_3).

To explain the rate independent of hydrogen pressure, we proposed that the addition of molecular hydrogen to complex **23** is rapid and reversible step of the reaction. Inverse k_H/k_D indicates that hydrogen addition is η^2 fashion and then oxidative cleavage occurs stepwise as described earlier in this chapter. Inverse k_H/k_D indicates stepwise rapid and reversible formation of dihydrogen coordinated Ru species (**28**) and complex **29**. Based on

the high value of ^{13}C KIE, we proposed that the C-O bond cleavage is the overall rate limiting step of hydrogenolysis of C-O bond of catalyst contained electron withdrawing ligand. Relatively high positive Hammett value indicates a relatively electron-poor Ru catalyst should promote the binding of ketone and alcohol substrates, and the rate-enhancement by phenol with electron withdrawing group may be associated with a strong coordination of these oxygenated substrates. Both mechanisms have the same intermediate **25** as shown in Scheme 4.11. Then the catalytically active complex **23** will regenerate in the same pathway described for the electron donating group.

4.8 Conclusions

We have developed a highly selective catalytic hydrogenolysis method for carbonyl compounds and alcohols by using a well-defined cationic ruthenium-hydride catalyst with tunable phenol ligands. The catalytic method employs cheaply available H_2 , and exhibits high chemoselectivity toward the reduction of aldehydes and ketones to corresponding aliphatic compounds under environmentally sustainable conditions. The detailed kinetic and mechanistic analyses revealed strong electronic effects of phenol ligand on promoting the hydrogenolysis reaction. The ruthenium catalyst with electron-rich phenolic ligand facilitates the H_2 addition step, while the electron poor ruthenium catalyst promotes the hydrogenolysis through strong coordination of the ketone substrate. These kinetic and structural studies provide new mechanistic insights on the rational design of catalyst for the hydrogenolysis of oxygenated compounds.

CHAPTER 5

SYNTHETIC AND MECHANISTIC STUDIES OF RUTHENIUM CATALYZED REDUCTIVE ETHERIFICATION OF CARBONYL COMPOUNDS AND ALCOHOLS

5.0 Introduction

Ethers represent an important class of compounds in nature and play a pivotal role in biochemistry. In addition, they are used as solvents, fuels, fragrances, pharmaceuticals, insecticides, and fumigants in the bulk and fine-chemical industries. To date, the general strategy for constructing ethers strongly relies on either the Williamson reaction, which was discovered in 1850, or the Ullmann ether synthesis.¹ The two methods suffer from drawbacks such as the use of a strong base and organohalide substrates. From an environmental and economic point of view, modern organic synthesis has to avoid the formation of stoichiometric amounts of problematic waste products.² However, for a benign preparation of ethers novel methodologies are rather underdeveloped despite the fast development of organic synthesis.³ Developments in transition metal catalysis have made available many convenient methods for synthesizing various strategic C-O bonds.

Alkyl ether is one of the most important functional groups for organic synthesis, because it is included in many organic chemicals. Further, it is widely used as a protective group of the hydroxy function.⁴ The synthesis of unsymmetrical ethers from carbonyl compounds silyl ethers has also been achieved in the presence of a variety of Lewis acid catalysts.⁵ However, the more direct approach for the synthesis of unsymmetrical ethers from carbonyl compounds and unprotected alcohols with the aid of catalytic methods has

been only moderately investigated and has so far only been achieved by employment either of large amounts of BiCl_3 (>20 mol %)³ or of catalytic amounts of FeCl_3 .⁶ None of the described methods has included study of the impact of additional functionalization of the alcohol coupling partner or attempts to introduce nucleophiles based on different heteroatoms or direct coupling between alcohol and carbonyl compounds without silanes.

Cheaper and greener ways to synthesize ethers by reductive etherification of ketones/aldehydes and alcohols have been studied intensively.⁷ As described in Chapter 1, synthetic routes of unsymmetrical ethers have been developed over the years. There were significant improvements on etherification such as Williamson ether synthesis, Mitsunobu reaction, the Ullmann condensation, and other catalytic methods. These methods showed pre-functionalized substrates, formed copious amounts of byproducts, and exhibited a relatively limited range of substrate scope and functional group tolerance in forming unsymmetrical ether products.

We recently discovered that a well-defined cationic ruthenium hydride complex $[(\text{C}_6\text{H}_6)(\text{PCy}_3)(\text{CO})\text{RuH}]^+\text{BF}_4^-$ (**1**) is a highly selective catalyst precursor for the etherification of two different alcohols in order to form unsymmetrically substituted ethers.⁸ While the etherification reaction directly forms unsymmetrical ethers without forming any wasteful byproducts, it was not effective for the coupling between electronically similar and sterically demanding aliphatic alcohols, as it gave a mixture of symmetrical and unsymmetrical ethers. In an effort to extend the scope of the etherification reaction, we explored the analogous reductive coupling reaction of carbonyl compounds with alcohols. Herein, we report a highly chemoselective formation of unsymmetrically substituted ether products from the reductive coupling of alcohols with aldehydes and

ketones. The “green” features of the catalytic method are that it employs cheaply available molecular hydrogen as the reducing agent, tolerates a number of common functional groups, and uses environmentally benign water as the solvent.

5.1 Result and Discussion

5.1.1 Optimization Studies

5.1.1.1 Catalyst Screening

We initially screened the catalyst activity of the ruthenium complex **1** for the reductive coupling reaction of 2-butanol with 4-methoxybenzaldehyde [Eq. (1)]. While searching for a suitable set of conditions, we discovered that H₂ (1-2 atm) can be used as the reducing agent and water as the solvent. Under the optimized set of conditions, complex **1** was found to exhibit distinctively high activity and selectivity in forming the ether product **2** among screened ruthenium and acid catalysts, as analyzed by both GC and NMR spectroscopic methods (Table 5.1). It should be emphasized that molecular H₂ is rarely used as the reductive etherification reaction, as it typically requires silane as the reducing agent.⁷

We initially screened the catalytic activity of **1** with the etherification of 4-methoxybenzaldehyde and 1-butanol. 4-methoxybenzaldehyde (136 mg, 1.0 mmol), 2-butanol (185 mg, 2.5 mmol) and a catalyst **1** (2.0 mol %) were dissolved in 1:1 mixture Toluene/H₂O (1 mL) in a 25 mL Schlenk tube [Eq. (5.1)]. The tube was for 12 h in an oil bath which was preset at 110 °C. The reaction mixture was analyzed by GC and GC-MS. The results are summarized in Table 5.1. Among the surveyed ruthenium catalysts, complex **1** exhibited a uniquely high activity for the reductive coupling reaction.

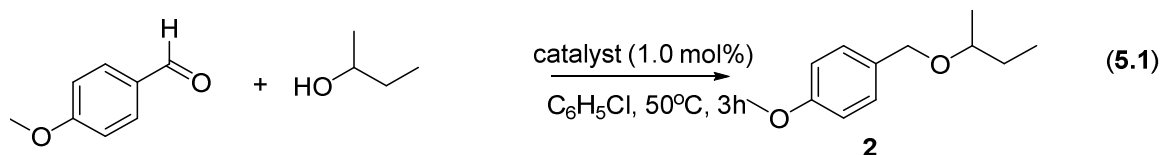


Table 5.1: Catalyst Survey for the Reaction of 4-Methoxybenzaldehyde with 1-Butanol^a

Entry	Catalyst	Additive	Yield (%)
1	$[(C_6H_6)(PCy_3)(CO)RuH]^+BF_4^-$ (1)		95
2	$HBf_4 \cdot OEt_2$		6
3	$[RuH(CO)(PCy_3)]_4(O)(OH)_2$		0
4	$[RuH(CO)(PCy_3)]_4(O)(OH)_2$	$HBf_4 \cdot OEt_2$	72
5	$RuCl_3 \cdot 3H_2O$	$HBf_4 \cdot OEt_2$	0
6	$RuCl_2(PPh_3)_3$		0
7	$RuCl_2(PPh_3)_3$	$HBf_4 \cdot OEt_2$	0
8	$RuH_2(CO)(PPh_3)_3$		3
9	$RuH_2(CO)(PPh_3)_3$	$HBf_4 \cdot OEt_2$	10
10	$[RuCl_2(COD)]_x$	$HBf_4 \cdot OEt_2$	0
11	$[RuH(CO)(PCy_3)_2(CH_3CN)_2]^+BF_4^-$		20
12	$[(p\text{-cymene})RuCl_2]_2$		0
13	$Ru_3(CO)_{12}$	NH_4PF_6	0
14	CF_3SO_3H		trace
15	$BF_3 \cdot OEt_2$		trace
16	$Cy_3PH^+BF_4^-$		trace
17	$AlCl_3$		7
18	$FeCl_3 \cdot H_2O$		<5

^aReaction conditions: 4-methoxybenzaldehyde (136 mg, 1.0 mmol), 1-butanol (185 mg, 2.5 mmol), catalyst (2.0 mol %), additive (1.0 equivalent to Ru), toluene/H₂O (1:1 mL), 110 °C, 12 h. The product yield was determined by GC and GC-MS.

5.1.1.2 Solvent and Temperature Effects

Table 5.2: Solvent Effect on the Reaction of 4-methoxybenzaldehyde with 1-butanol.^a

Entry	Solvent	Temp/°C	Yield(%) ^b
1	Toluene	110	63
2	Chlorobenzene	110	82
3	Dioxane	110	45
4	H ₂ O	110	85
5	H ₂ O/Toluene	110	90
6	Chlorobenzene	120	90
7	H ₂ O	120	95
8	H ₂ O/Toluene	120	95

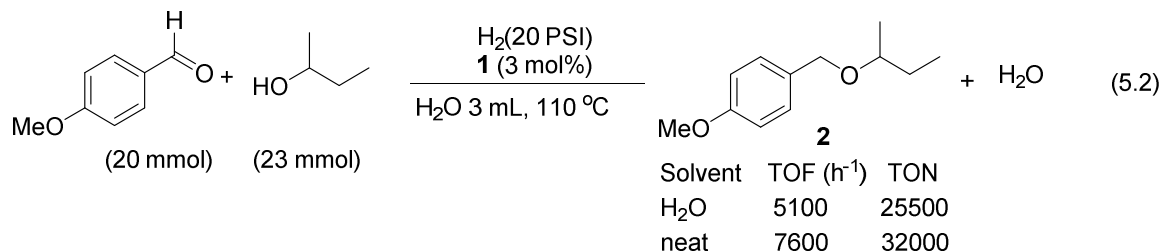
^aReaction conditions: 4-methoxybenzaldehyde (122 mg, 1.0 mmol), 1-butanol (122 mg, 1.2mmol), catalyst 1 (1.0 mol %), in solvent (1 mL) at different temperatures °C, 3h. ^b the yield was determined by GCMS analysis using C₆Me₆ as an internal standard

A number of different solvents were examined for the optimization of the unsymmetrical etherification reaction (Table 5.2). The reactions of 4-methoxybenzaldehyde (136 mg, 1.0 mmol), 1-butanol (185 mg, 1.2 mmol) and a catalyst **1** (2.0 mol %) with different solvents at 60 °C were analyzed by GC-MS after 3h of reaction time. The solvents affected the activity of the unsymmetrical etherification reaction.

Chlorobenzene or H₂O was found to be the most effective solvent for unsymmetrical etherification reaction among screened solvents (entry 1- 6). Polar solvents chlorobenzene, H₂O at 120 °C exhibited with higher conversion (>95 %) of unsymmetrical ethers based on 4-methoxybenzaldehyde. Among those solvents H₂O is the greenest solvent but most organic compounds insoluble in H₂O therefore a H₂O/Toluene mixture

was used as the solvent, at higher temperature of 110-120 °C, higher conversion (> 90 %) of unsymmetrical ethers was achieved in chlorobenzene or H₂O.

5.1.2 Optimization of Turnover Number (TON) and Turnover Frequency (TOF)

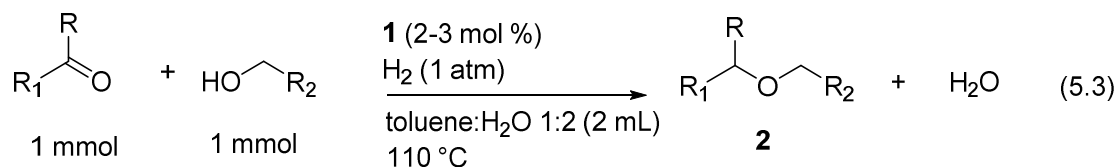


The turn over number (TON) of reductive etherification reaction was explored under the optimized reaction condition. The reaction between 4-methoxybenzaldehyde (20 mmol) and 2-butanol (23 mmol) mixed with ruthenium complex **1**, 0.2 μg (0.0017 mol %) in a fisher-porter-bottle and degassed and filled with pressure of 20 PSI H₂ gas. The fisher-porter-bottle was stirred in an oil bath at 110 °C and aliquot of reaction mixture were analyzed by GC and NMR spectroscopic methods after 1h and after 18h. The same experiment was repeat in the presence of 3 mL of water as the solvent. This reaction resulted in the selective formation of the 2-(4'-methoxybenzyloxy)butane and 338 of TON and 7648 h⁻¹ of TOF as measured by ¹H NMR and GC for neat condition and 25500 of TON and 5099 h⁻¹ of TOF in H₂O solvent (Fig. 4). The most salient feature of the catalytic method from an environmental point of view is that it employs cheaply available H₂ as the reducing agent and water as the solvent.

5.2 Reaction Scope

5.2.1 Reaction Scope of Synthesis of unsymmetrical Ether by Ruthenium Catalyzed Reductive Etherification of Carbonyl Compounds and Alcohols

The substrate scope on the etherification reaction was explored by using the catalyst (Table 5.3). The reductive coupling reaction of carbonyl compound and alcohols gave very high selectivity toward the formation of unsymmetrical ether products over that of symmetrical ether products [Eq. (5.3)].



The coupling reaction between aliphatic secondary alcohols such as 2-butanol and benzaldehyde substrate produced unsymmetrical ether selectively in high yield (Table 5.3, entry 1-5). Reaction between 2-butanol with different *para*-substituted benzaldehyde contained electron withdrawing group such as Cl (Table 5.3, entry 4) has low reactivity and slightly lower yield when compare with electron donating groups such as OMe, OBn (Table 5.3, entry 2-3) for the etherification with 2-butanol. Primary alcohols such as *n*-hexanol with benzaldehyde gave the unsymmetrical ether in high yield (Table 5.3, entry 6). Cyclic alcohols such as cyclopentanol coupling with benzaldehyde produced ether 95 % ((Table 5.3, entry 7). Alcohols contained remote chiral center reacted with benzylic aldehydes to produce unsymmetrical chiral alcohol without affecting the chirality (Table 5.3, entry 8). 1,2-hexanediol and 1,3-butanediol reacts with *para*-methoxybenzaldehyde to produced only selectively reactive towards primary alcohol over the secondary (Table 5.3, entry 9-10).

Table 5.3: Synthesis of Unsymmetrical Ethers from the Dehydrative Coupling of Alcohols^a

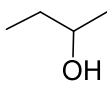
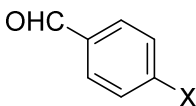
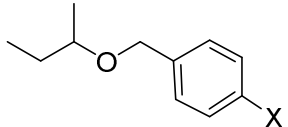
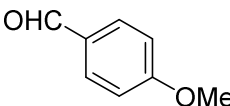
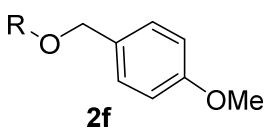
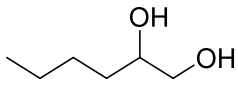
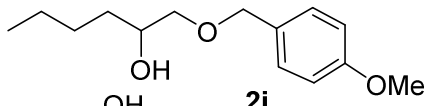
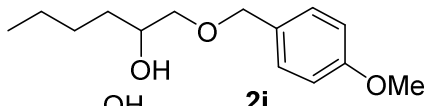
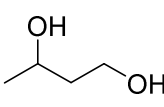
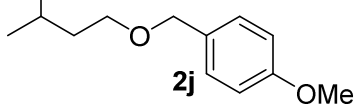
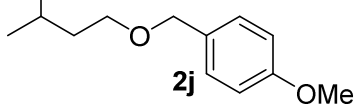
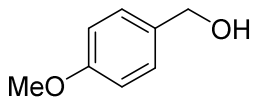
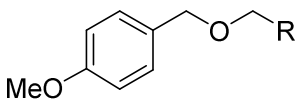
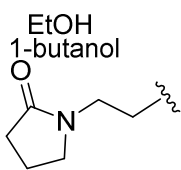
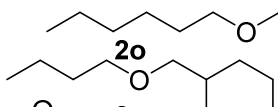
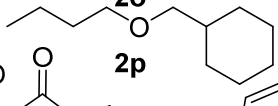
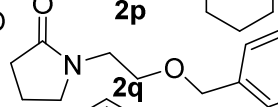
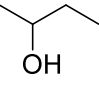
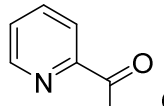
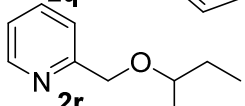
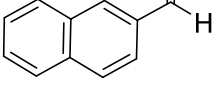
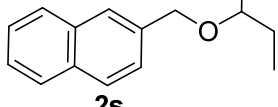
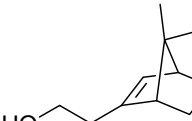
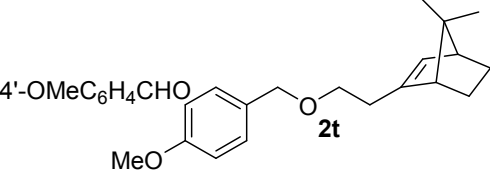
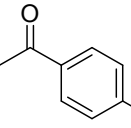
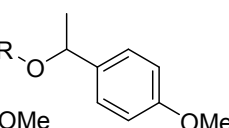
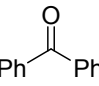
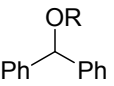
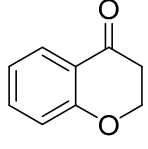
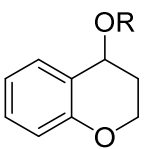
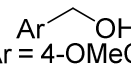
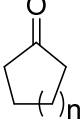
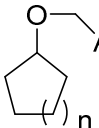
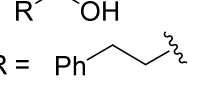
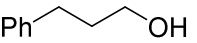
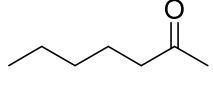
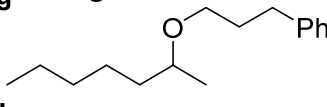
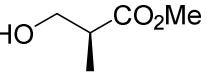
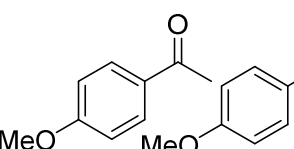
entry	alcohol	carbonyl compd	product(s)	time (h)	yield (%)
1				12	82
2		X = H	2a	12	95
3		X = OMe	2b	12	97
4		X = OBn	2c	12	68
5		X = Cl	2d	12	85
		X = NHCOMe	2e		
6	R-OH R = n-butyl			12	98
7	R = Cyclopentyl		2f	16	95
8	R = (R)-CH ₂ CHMeCO ₂ Me		2g 2h	16	91
9				16	91
			2i		
10				12	89
			2j		
11		R-CHO		12	89
12		R = n-hexyl	2k	12	86
13		R = i-butyl	2l	12	88
14		R = cyclohexyl	2m	12	71
15		R = bezyl	2n	12	
16		n-HexylCHO		12	76
		c-C ₆ H ₁₁ CHO		16	96
		4'-OMeC ₆ H ₄ CHO		12	95
17			2o		
18				12	67
			2p		
19				12	76
			2q		
			2r		
			2s		

Table 5.3: Cont..

entry	alcohol	carbonyl compd	product(s)	time (h)	yield (%)
20		4'-OMeC ₆ H ₄ CHO		12	90
21	R-OH			16	88
22	R = n-butyl		2u	16	93
23	R = cyclopentyl		2v	16	93
23	R = Bn		2w	16	55
24	R-OH			16	94
25	R = 1-butyl		2x	16	92
25	R = cyclopentyl		2y	16	92
26	R = benzyl		2z	16	65
27	R = 1-butyl			16	88
28	R = cyclopentyl		2ab	16	88
29	R = 2-propyl		2ac	16	91
30				16	88
31	Ar = 4-OMeC ₆ H ₄	n = 1	2ad	16	90
31		n = 2	2ae	16	90
32	R = 	n = 1	2af	16	98
32	n-Butyl	n = 2	2ag	16	78
33				16	58
34			2ai (1:1 dr)	16	78

^a Reaction conditions: R₁OH (1.0 mmol), R₂OH (1.2 mmol), chloroform (2 mL), **5** (0.5-1 mol %). ^b Isolated yield of the products with > 95 % purity. ^c The product yield is determined by GC.

p-methoxy benzylic alcohols reacted with different aldehydes such as hexanal, isobutyl aldehyde, cyclohexylcarboxyaldehyde, and also benzaldehyde to produce product **2k**, **2l**, **2m** and **2n** respectively in high yield (Table 5.3, entry 11-14). Primary aliphatic alcohols

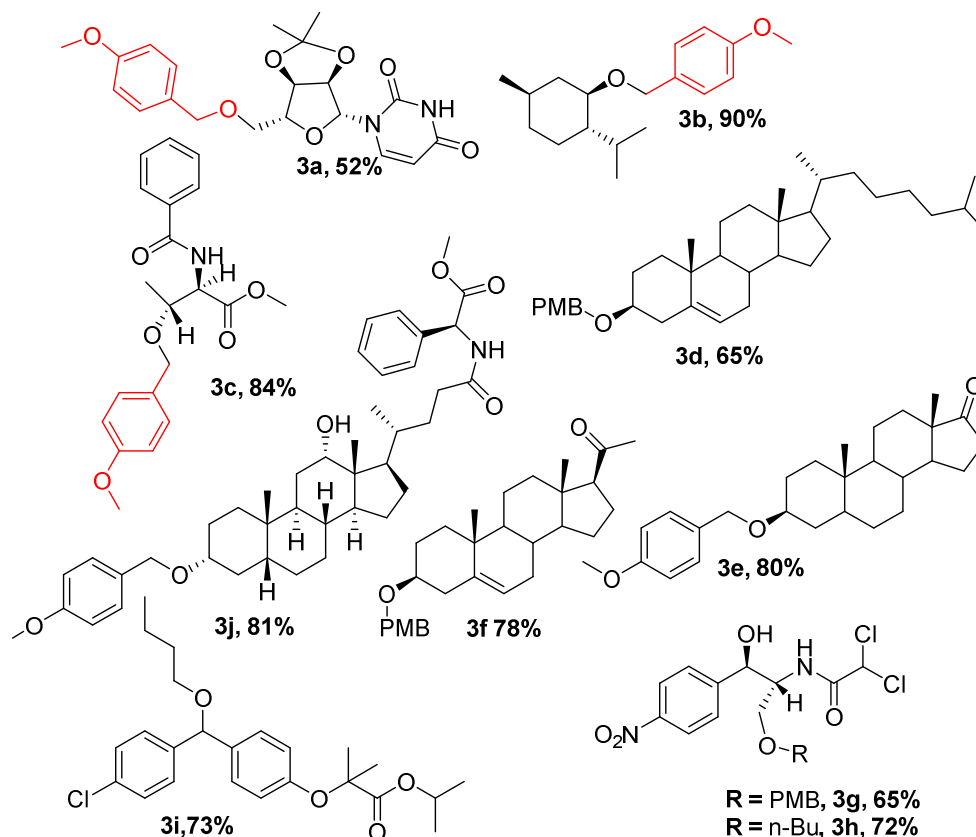
such as ethanol and 1-hexanol reacted with aliphatic aldehydes such as 1-hexanal and cyclohexyl carboxyaldehyde to produce corresponding ether **2o** and **2p** in moderately high yield (Table 5.3, entry 15-16). Amide contain alcohol such as 1-(2-Hydroxyethyl)-2-pyrrolidone reacted with benzylic alcohols producing ether **2q** in high yield showing that amide group tolerance for the reaction (Table 5.3, entry 17). 2-pyridyl aldehyde and 1-naphthaldehyde also reacted with 2-butanol to produce ether **2r** and **2s** in high yield (Table 5.3, entry 18-19). (R)-nopol reacted with 4-mthoxybenzyldehyde to produce optically active ether **2t** in 90 % yield. Aliphatic and benzylic alcohols such as 1-butanol, cyclopentanol, and benzylalcohol produced ether compound **2u-2w** reacting with benzylic ketone substrate, 4-methoxyacetopheone (Table 5.3, entry 21-23).

Next we examined the coupling between different alcohols with benzophenone. Primary aliphatic alcohol such as 1-butanol, cyclic aliphatic alcohol such as cyclopentyl alcohol and benzyl alcohol exclusively reacted with benzophenone giving high yield ether products **2x**, **2y** and **2z** respectively (Table 5.3, entry 24-26). Chromanone also coupled with 1-butyl, cyclopentyl and 2-proyl alcohols to produce high yield of ether products **2aa**, **2ab**, and **2ac** in high yield (Table 5.3, entry 27-29). 4-methoxybenzyl alcohol reacted with cyclohexanone and cyclopentanone to produce **2ad** and **2ae** in 85 % and 90 % yield respectively (Table 5.3, entry 30-31). Aliphatic alcohols such as 3-phenylpropanol reacted with aliphatic cyclic ketone such as cyclopentanone to produce ether product **2af** in 98 % yield. Aliphatic linear ketone such as 2-heptanone produced ether product **2ag** in 55 % yield. Alcohol bearing ester functionality and remote chiral group reacted with 4-methoxy acetophene to produce 1:1 mixture of diastereomeric products **2ai** in 78 % yield (Table 5.3, entry 34) without affecting ester functional group.

5.2.2 Reaction Scope of Synthesis of Unsymmetrical Ethers from the Dehydrative Coupling of Highly Functionalized Bioactive Alcohols

To further illustrate synthetic versatility of the catalytic coupling method, we next surveyed the etherification reaction of functionalized alcohol substrates of biological importance (Table 5.4). First we examined the coupling between 4'-methoxybenzaldehyde with nucleotide 2',3'-isopropylidenedeoxyuridine in the presence of 1 atm H₂ at 90 °C. This reaction produced 52 % ether product **3a** without affecting any other functional group. Next we examined the reaction of 4-methoxybenzaldehyde with (1R, 2S, 5R)-(-)-Menthol in same condition. This reaction produced the ether product **3b** in 90 % yield without racemization. The reductive coupling of 4-methoxybenzaldehyde with different steroidal compounds were tested. Cholesterol, *trans*-Androsterone produced ether products **3d** and **3e** respectively in 65 % and 80 % yield selectively. 3 β -Hydroxy-5-pregnen-20-one produced ether product **3f** in 78 % yield without racemization of 3 β C-O bond. Same aldehyde with (N-benzoyl) threonine methyl ester produced ether **3c** in 84 % yield without racemization of alcohol. Deoxycholic amide of L-phenylglycine methyl ester produced selectively β -benzyloxy ether **3j**, in 81 % yield. Broad spectrum antibiotic and antifungal agent chloroamphenicol selectively produced primary alcohol protected ether **3g** in 65 % yield also with aliphatic aldehyde such as butaldehyde produced product **3h**. The bioactive molecule fenfubrate reacted with aliphatic alcohol such as butanol produces ether **3i**.

Table 5.4: Synthesis of Unsymmetrical Ethers from the Reductive Coupling of Carbonyl Compounds with Alcohols^a



^a Reaction conditions: alcohol (1.0 mmol), alcohol (1.0 mmol), toluene (2 mL)/Chlorobenzene (2 mL), **5** (1-5 mol %), 70 - 110 °C.

5.3 Determination of X-ray Crystallography

Analysis of the X-ray single crystal structure of product **3d**, **3e** and **3f** confirmed the stereocenter remained same as starting material. Single crystals of **3d**, **3e** and **3f** suitable for X-ray crystallographic analysis were obtained from slow evaporation of CH₂Cl₂. Single crystals of **3d**, **3e** and **3f** were colorless needles type. The absolute configuration of single crystal was established objectively.

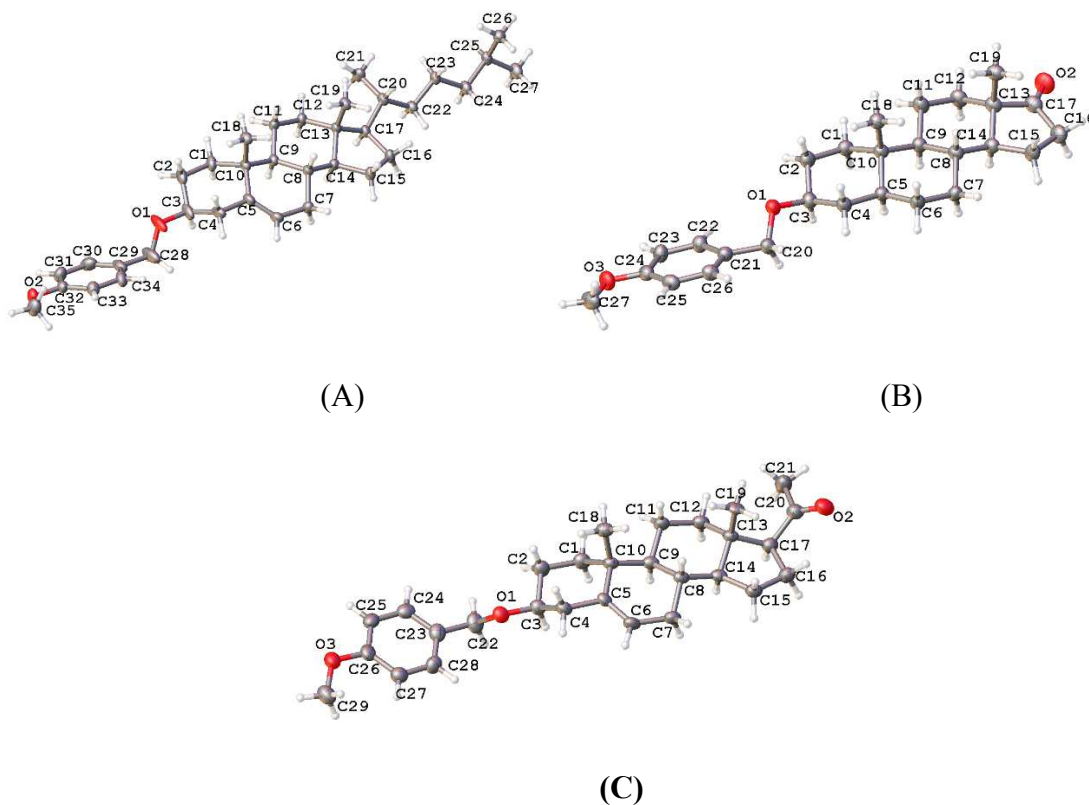
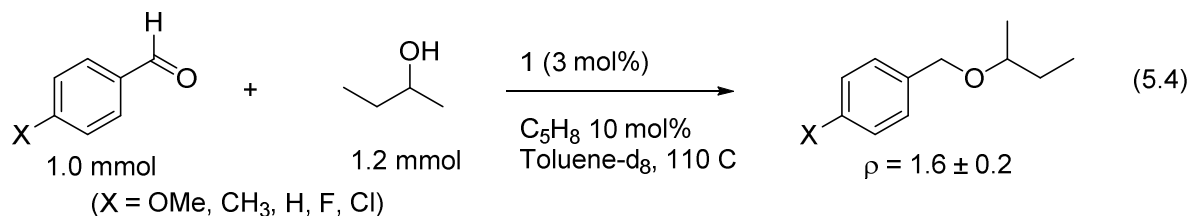


Figure 5.1: X-ray Crystal Structure of (A) **3d** (B) **3e** (C) **3f**.

5.4 Mechanistic Studies



5.4.1 Hammett Study.

To probe electronic influence on the aldehyde substrate, we constructed a Hammett plot from measuring the rate of a series of *para*-substituted benzaldehydes *p*-X-C₆H₄CHO (X = OMe, Me, H, F, Cl) with 2-butanol [Eq. (5.4)]. *Para*-substituted benzylaldehyde, *p*-X-C₆H₅CHO (X = OCH₃, CH₃, H, Cl, F) (0.25 mmol), 2-butanol (0.75 mmol), H₂O (0.05 mmol) and complex 1 (3 mol %) were dissolved in toluene-*d*₈ (0.5 mL) in six separate J-

Yong tubes. The tubes were brought out of the box, and stirred in an oil bath set at 110 °C. Each reaction tube was taken out of the oil bath in 20 minute intervals, and was immediately cooled and analyzed by ^1H NMR. The k_{obs} was determined from a first-order plot of $-\ln([p\text{-X-C}_6\text{H}_5\text{CHO}]_t/p\text{-X-C}_6\text{H}_5\text{CHO}]_0)$ vs. time. The Hammett plot of $\log(k_X/k_H)$ vs. σ_p is shown in fig. 37. A linear correlation from the relative rate vs Hammett σ_p led to a relatively high negative ρ value of -1.6 ± 0.1 (Figure 5.2). This result is consistent with the C-O bond cleavage and the hydrogenolysis step is likely promoted by the by electron-releasing group, but not expected during the formation of hemiacetal species. Similar Hammett ρ values have been observed in the catalytic coupling reactions of arenes.⁹

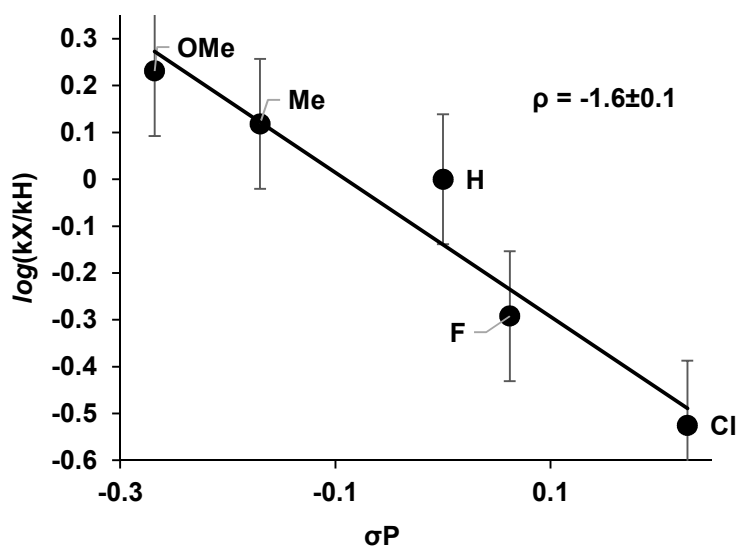


Figure 5.2: Hammett Plot from the Reaction of $p\text{-X-C}_6\text{H}_4\text{CHO}$ (X = OMe, Me, H, F, Cl) with 2-Butanol.

5.4.2 Solvent Isotope Effect

The solvent isotope effect was measured to probe the solvent influence on the etherification reaction. The initial rates of the reaction between 4-methoxybenzaldehyde with 2-butanol (2 equivalence) were separately measured in H_2O and D_2O . Briefly, 4-

methoxybenzaldehyde, *p*-OMe-C₆H₅CHO (340 mg, 1.5 mmol), 2-butanol (462.5 mg, 6.25 mmol) and complex 1 (40 mg, 2 mol %) were mixed in a vial and divided into five separate 25 mL Schlenk tubes. 0.5 mL of H₂O or D₂O was added to each tube and degassed under vacuum. The tubes were stirred in an oil bath set at 110 °C. Each reaction tube was taken out of the oil bath in 15 minute intervals, analysed by ¹H NMR using 10 mg hexamethyl benzene as the internal standard. The *k*_{H₂O} or *k*_{D₂O} was determined from a first-order plot of $-\ln([p\text{-OMe-C}_6\text{H}_5\text{CHO}]_t/[p\text{-OMe-C}_6\text{H}_5\text{CHO}]_0)$ vs. time. The first order plots showed a relatively high normal isotope effect of *k*_{H₂O}/*k*_{D₂O} = 2.9 ± 0.2 (Figure 5.3). Similar value of solvent isotope effect was obtained from 2-propanol/2-propanol-*d*₈ (*k*_{PrOH}/*k*_{PrOD} = 2.0 ± 0.2, Figure 5.4). A relatively large solvent isotope effect value suggests that the water molecules are intricately involved in C–O bond cleavage and hydrogenolysis steps via extensive hydrogen bonding network interactions.¹⁰

Essentially, there are three factors that lead to kinetic solvent isotope effects: (1) Solvent molecules participate as reactants in the reaction. Depending on the other preconditions, actual primary or secondary kinetic isotope effects then appear. (2) The transition state of the reaction can be stabilized by interactions between the reactants and solvent molecules. The extent of these interactions in isotope-substituted solvents can differ from that in the original solvent. As a result, the transition state's energy and thus, the activation energy *E*_a of the respective reaction step (elementary reaction) are altered. If this particular reaction step is the rate-determining step, the result is a kinetic isotope effect. The positively charged transition state of the ether formation, for example, interacts with the polar water molecules to a considerable degree with cationic ruthenium species. (3) Especially in acidic, deuterated solvents (e.g. D₂O or 2-butanol-OD), an H/D exchange or a D transfer

between the solvent molecules and the reactants can occur. Consequently, an actual primary or secondary kinetic isotope effect is obtained. After it has been transferred to ether, D could cause a secondary kinetic isotope effect if the rate-determining step still follows

Data about the rate-determining step and the structure of the transition state, as well as the participation of solvent molecules in the reaction by either solvating the transition state or acting as reactants can be inferred from kinetic solvent isotope effects and not only from pure and obvious primary or secondary kinetic isotope effects. It should be taken into consideration that the formerly mentioned causes of kinetic isotope effects can occur simultaneously and can enhance each other, as is the case in the ether formation.

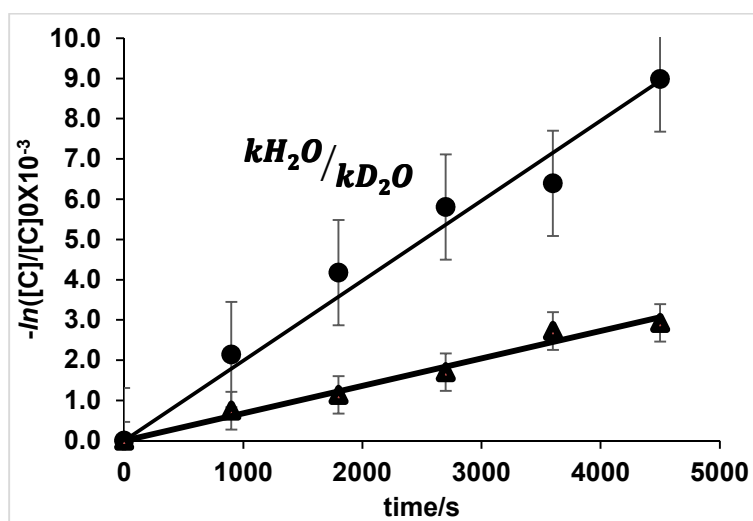


Figure 5.3: First Order Plot of the 4-Methoxybenzaldehyde (S) with 2-Butanol in H_2O (circle) and in D_2O (triangle).

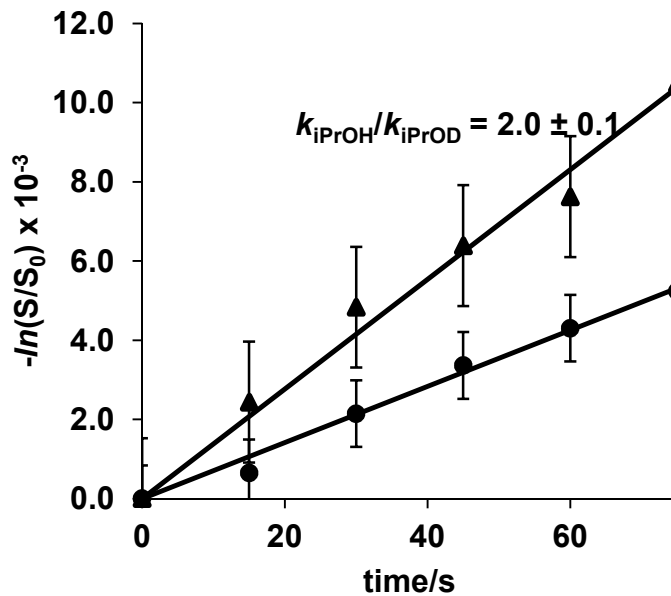


Figure 5.4: First Order Plot of the 4-Methoxybenzaldehyde with 2-Propanol (triangle) and in 2-Propanol- d_1 (circle).

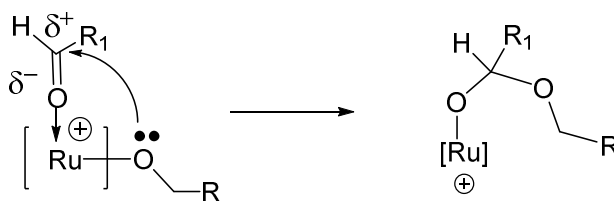


Figure 5.5: Transition State of Ruthenium Alkoxy Species

5.4.3 H/D Exchange Experiment

A series of kinetic experiments were performed to gain mechanistic insights for the etherification reaction. First, the H/D exchange pattern on the coupling reaction was examined.

5.4.3.1 H/D Exchange Reaction of 4-methoxybenzaldehyde with 1-butanol in D₂O.

The treatment of 4-methoxybenzaldehyde with 1-butanol (2 equivalence) in the presence of complex **1** (3 mol %) in D₂O at 110 °C led to the selective deuterium incorporation to benzylic position of the product **2f** [Eq. (5.5)]. The products were completely characterized by ¹H and ²H NMR spectroscopic methods. The ¹H and ²H NMR of **2f**-[D] are shown in Figure 5.6.

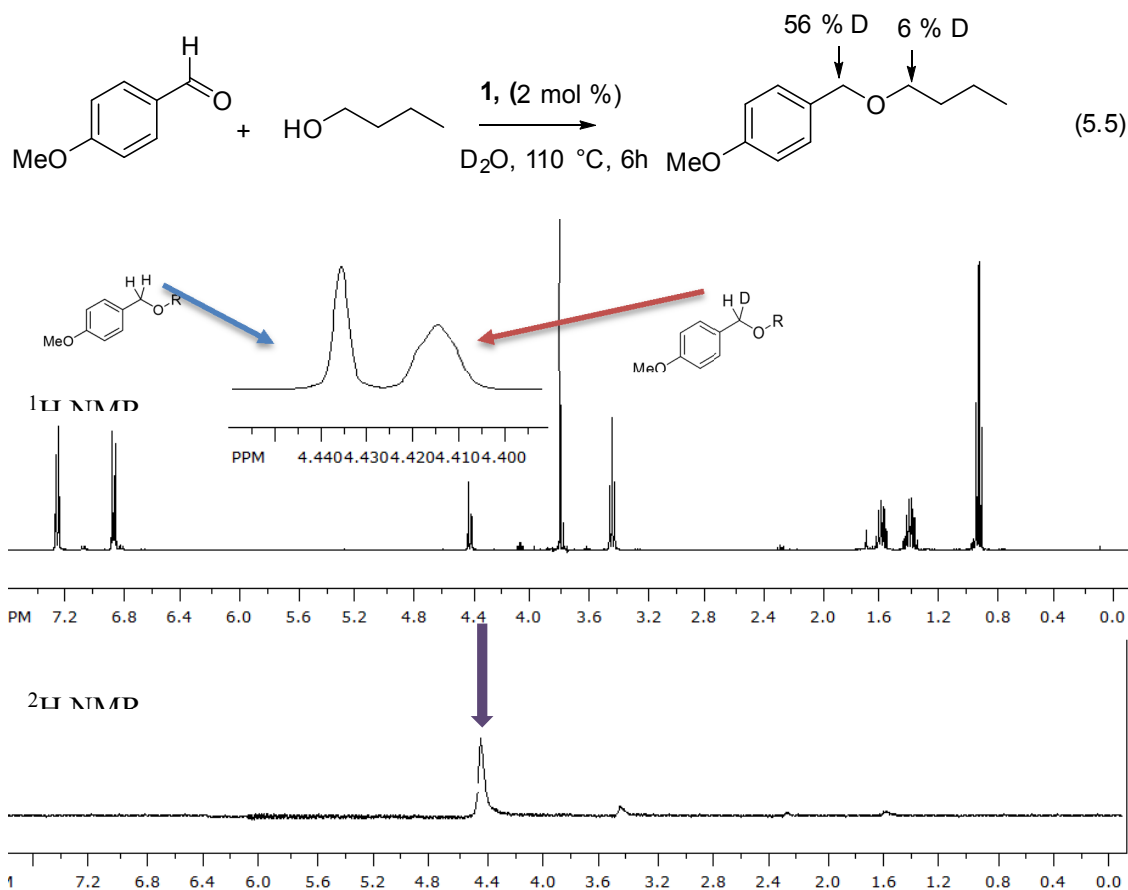


Figure 5.6: ¹H and ²H NMR Spectra of the Product **2f** Isolated from the Reaction of 4-Methoxybenzaldehyde with 1-Butanol in D₂O.

5.4.3.2 H/D Exchange Reaction of 4-methoxybenzaldehyde with iPrOH-*d*₈ in H₂O.

Conversely, 4-methoxybenzaldehyde with 2-propanol-*d*₈ (2 equiv.) in H₂O under

the similar conditions above gave the product with ~50 % protons on benzylic position [Eq. (5.6)]. The ^1H and ^2H NMR of **5-[D]** are shown in Figure 5.7. In a control experiment, the treatment of 2-propanol with D_2O in the presence of **1** (2 mol %) led to a rapid H/D exchange to form $(\text{CH}_3)_2\text{CHOD}$ at room temperature (Figure 5.7). These results suggest an extensive H/D exchange between the solvent and alcohol substrate, and further implicate strong involvement of solvent molecules during the C=O hydrogenolysis step.

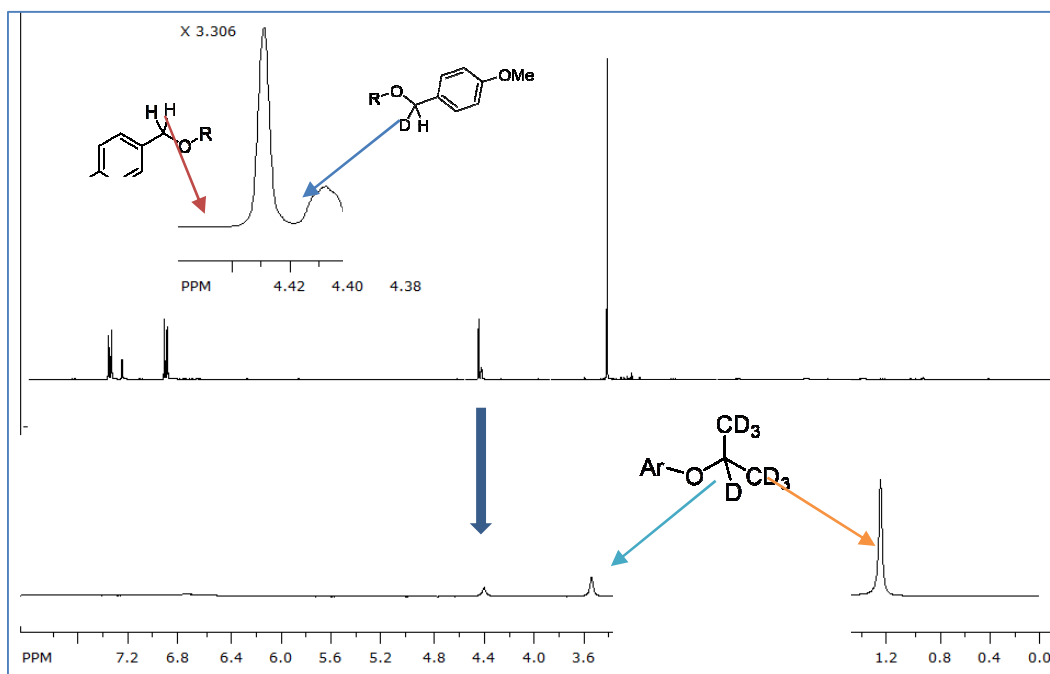
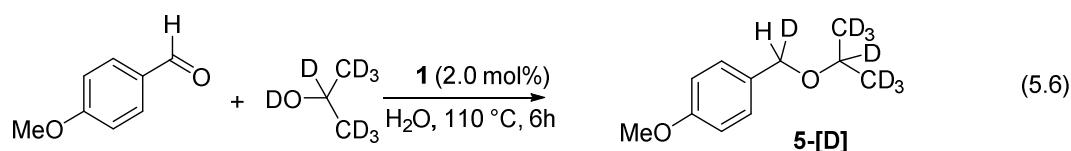
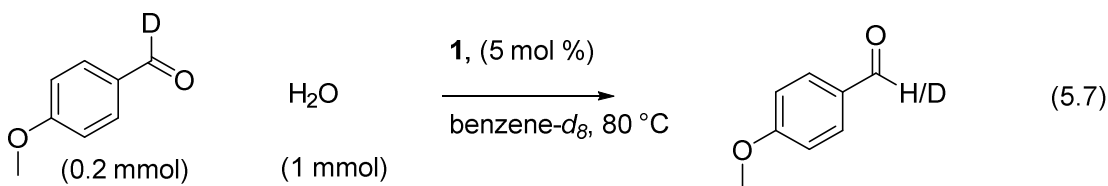


Figure 5.7: ^1H and ^2H NMR Spectra of the Product **5-[D]** Isolated from the Reaction of 4-Methoxybenzaldehyde with 2-propanol- d_8 in H_2O .

The following kinetic experiments were performed to gain mechanistic insights into catalytic C-O bond cleavage of alcohol. To examine H/D exchange pattern of 4-methoxybenzaldehyde- d_1 , the reaction of 4-methoxybenzaldehyde- d_1 (0.2 mmol) with

H₂O (1 mmol) in the presence of **1** (4 mg, 3 mol %) in benzene-*d*₆ (0.4 mL) at 110 °C was stopped after 12h [Eq. (5.7)], and was monitored by both ¹H and ²H NMR (Fig. 5.8).



A negligible amount of proton incorporation to the aldehydic deuterium (< 0.05 %) was observed (Figure 5.8). The results indicate that the carbonyl oxygen is coordinates to metal center and aldehyde alcohol functional group transfer is impossible for benzaldehyde substrate.

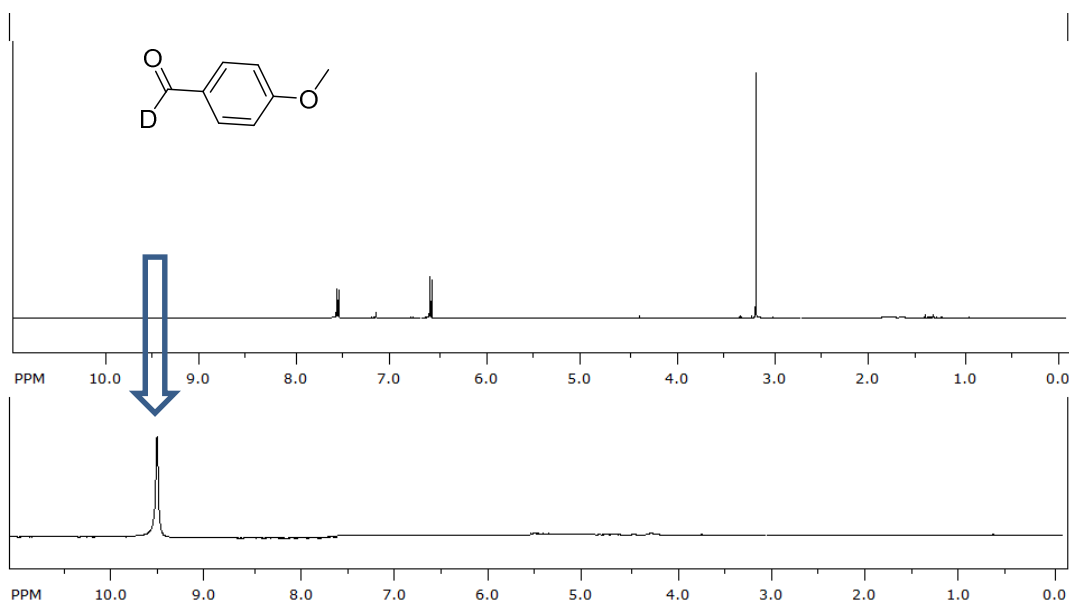


Figure 5.8: ¹H and ²H NMR Spectra of the Reaction Mixture of 4-methoxybenzaldehyde-*d*₁ with H₂O at 110 °C.

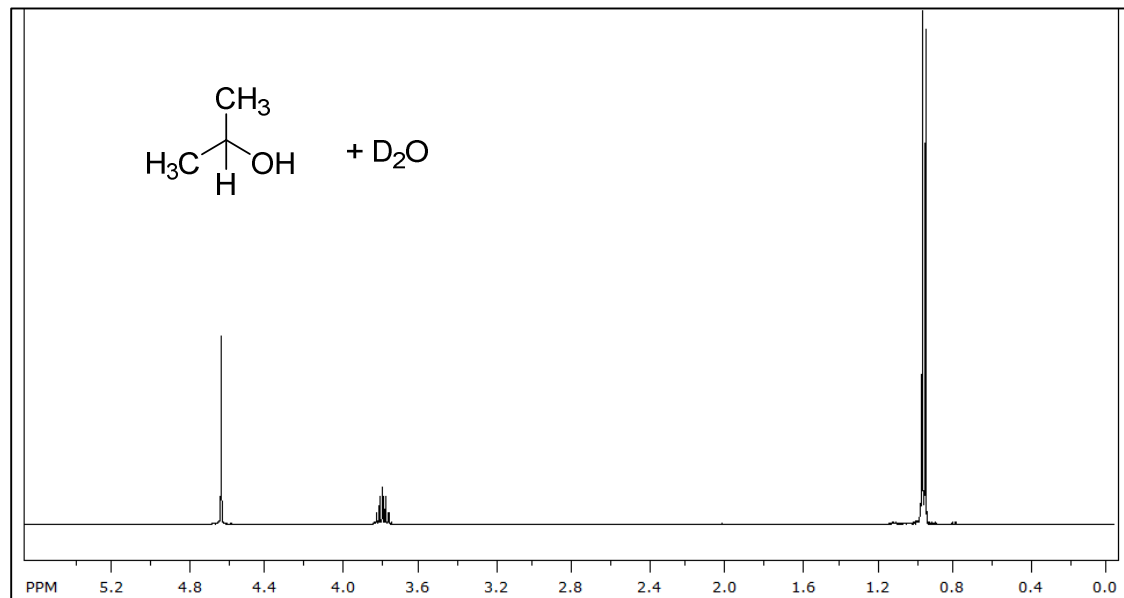
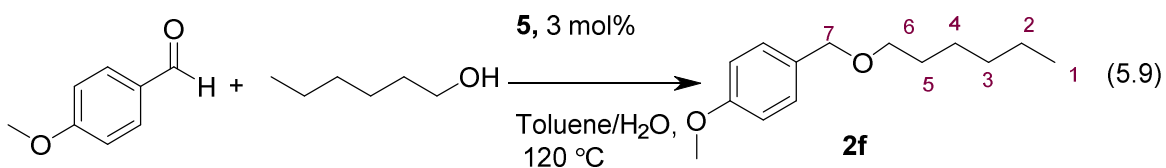
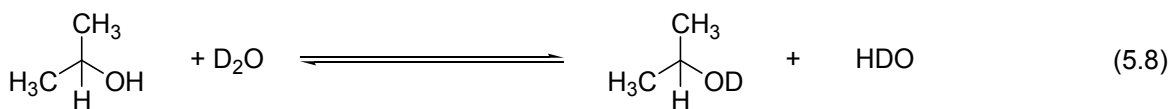


Figure 5.9: ¹H NMR Spectra of the Reaction Mixture of iPrOH with D₂O at 20 °C.

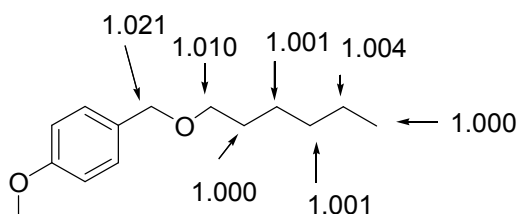
But in H/D exchange experiment all D exchange was observed at alcoholic OH of 2-propanol that is well known process (Fig. 5.9, eq. (5.8)).



5.4.4 Carbon Isotope Effect

In order to obtain a detailed picture of rate determine step of etherification reaction, ¹³C KIE experiment was carried out. By following the general protocol complex 1 (3 mol %) 4-methoxybenzaldehyde (1.36 g, 10.0 mmol), 1-hexanol (0.255 g, 2.5 mmol), water (10 mL) and in toluene (5 mL) was reacted in a 100 mL Fisher-porto-bottle [Eq.

(5.9)].

**Table 5.5:** Calculated Average ^{13}C KIE from Virgin (R_o) and Recovered (R) Samples of **2f**.

Carbon no.	virgin (R_o)	Recovered (R) (18 % conv.)	R_o/R	^{13}C KIE
1 (ref)	1.0000	0.9999	1.0001	0.999
2	1.0068	1.0068	0.9995	1.004
3	1.0036	1.0024	1.0001	1.001
4	1.0010	1.0009	1.0001	1.001
5	1.0029	1.0030	0.9999	1.000
6	1.0087	0.9992	1.0096	1.010
7	1.0071	0.9860	1.0215	1.021

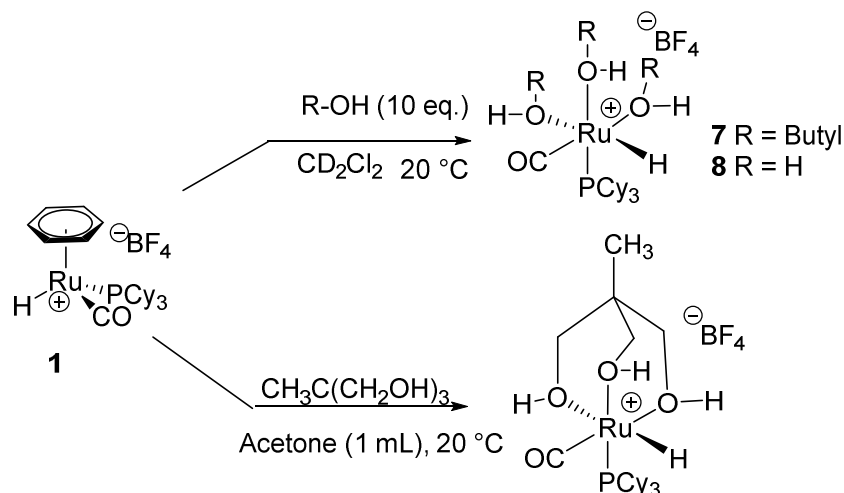
Three reactions were run separately and each reaction was stirred in an oil bath set at 110 °C for 2h, 2.5h, and 3 h respectively. Compound 1-[1-(hexyloxy)methyl]-4-methoxybenzene (**2f**) was isolated by a column chromatography on silica gel (hexanes/EtOAc = 40:1) separately after filtering through a short silica gel column eluting with CH_2Cl_2 (20 mL), and each solution was analyzed by GC (15, 18 and 20 % conversion). The recovered and virgin samples of 1-[1-(hexyloxy)methyl]-4-methoxybenzene were prepared by following same procedure for 16h.

The $^{13}\text{C}\{^1\text{H}\}$ NMR analysis of the recovered and virgin samples of 1-[1-(hexyloxy)methyl]-4-methoxybenzene was performed by following Singleton's ^{13}C NMR

measurement technique. The NMR sample of virgin and recovered 1-[1-(hexyloxy)methyl]-4-methoxybenzene was prepared identically by dissolving (100 mg) in CDCl_3 (0.5 mL) in a 5 mm high precision NMR tube. The $^{13}\text{C}\{^1\text{H}\}$ NMR spectrum was recorded with H-decoupling and 45 degree pulse. A 60 s delay between pulses was imposed to minimize T_1 variations (d1 = 60 s, at = 5.0 s, np = 245098, nt = 704). The data are summarized in Table 5.5.

The most pronounced carbon isotope effect on the product **2f** is observed when the ^{13}C ratio of the product **2f** at three low conversions (15, 18 and 20 % conversion) was compared with the sample obtained at high conversion (98 %). The reductive etherification reaction catalyzed by the catalyst **1** resulted in the significant isotope effect on the 7-carbon of the product **2f** for (^{13}C at 98 % conversion)/(average of ^{13}C at 18 % conversion) at C(7) = 1.021. According to the ^{13}C -KIE data aldehydic carbon has the most pronounced KIE which indicates the C-O cleavage of hemiacetal type intermediate is the rate limiting step. But according to Hammett value nucleophilic attack to carbonyl carbon cannot be rate limiting step. The rate limiting step could be the C-O cleavage of intermediate hemiacetal type compound.

5.4.5 Identification of Catalytic Active Intermediates



Scheme 5.1: Synthesis of Complex **7**, **8** and **9**

To discern the structure of catalytically relevant species, we explored the reactions of **1** with alcohols and water. The treatment of the complex **1** (0.07 mmol) with excess 1-butanol (0.7 mmol) in CD_2Cl_2 (0.6 mL) led to the formation of a new Ru-H species within 30 min at room temperature (Scheme 5.1). The appearance of a new set of peaks was observed along with the formation of free benzene molecule as monitored by NMR (^1H NMR: δ -18.8 (d, $J_{\text{PH}} = 31.3$ Hz) ppm; $^{31}\text{P}\{^1\text{H}\}$ NMR: δ 76.0 ppm) (Fig. 5.10). We tentatively assign the new species to the alcohol-coordinated complex $[(1\text{-butanol})_3(\text{PCy}_3)(\text{CO})\text{RuH}]^+\text{BF}_4^-$ (**7**), in light of the previously observed arene exchange reaction of **1**.¹² The analogous reaction with excess water also formed the water-coordinated complex **8** (^1H NMR: δ -17.7 (d, $J_{\text{PH}} = 30.3$ Hz) ppm; $^{31}\text{P}\{^1\text{H}\}$ NMR: δ 73.0 ppm) (Fig. 5.11). Both complexes **7** and **8** slowly decomposed within 12 h at room temperature. The catalytic activity of complex **7** was found to be identical to **1** for the

etherification of 4-methoxybenzaldehyde with 2-butanol under the conditions described in Eq. (5.1).

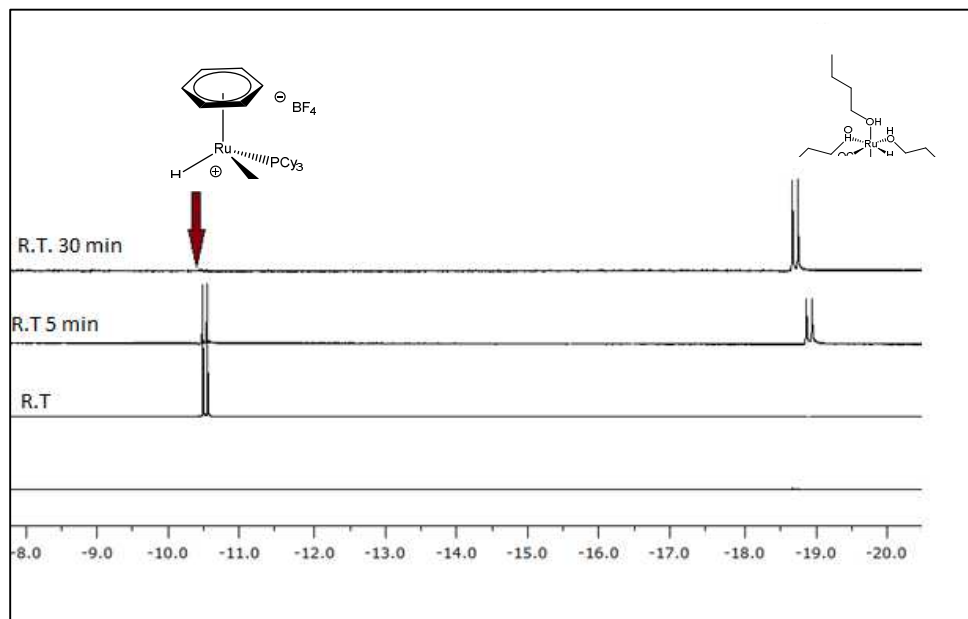


Figure 5.10: ^1H NMR Spectra of the Reaction of **1** with 1-Butanol.

Since the alcohol-coordinated complex is not stable at room temperature, we next examined the reaction of complex **1** with diols and triols as a way to form stable complex. Thus, the treatment of **1** with 1,1,1-tris(hydroxymethyl)ethane in acetone at room temperature led to the triol-coordinated complex **9**, which was isolated in 80 % after crystallization in acetone/pentane. The X-ray crystal structure of **9** showed (Fig. 5.12) a distorted octahedral geometry with a facial arrangement between the triol and the ancillary ligands. A number of ruthenium-hydride complexes have been successfully utilized as catalysts for the alcohol coupling reactions.¹⁰

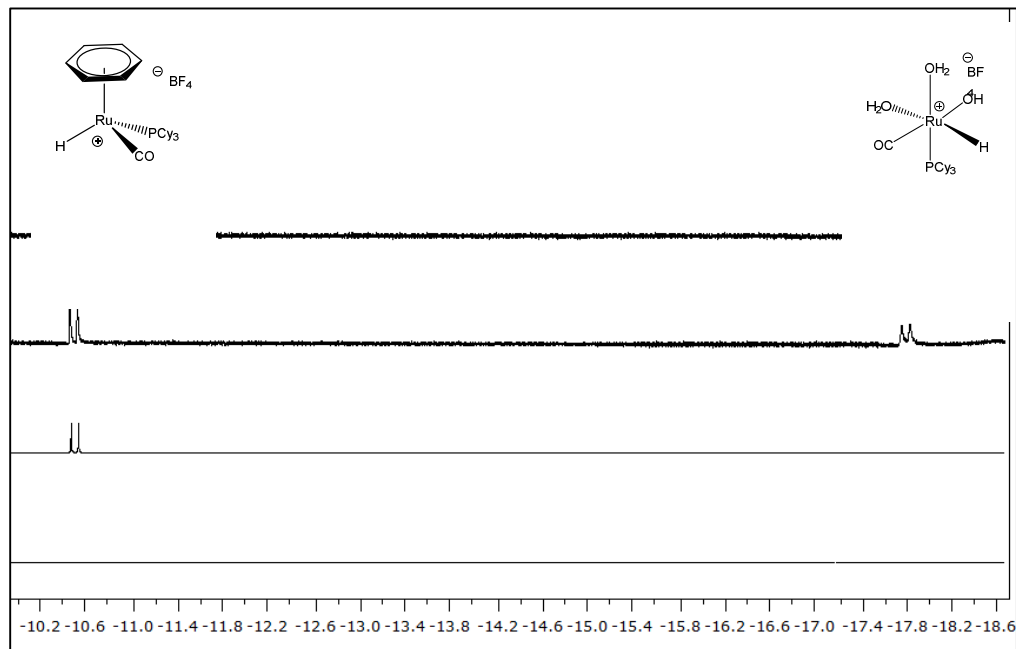


Figure 5.11: ^1H NMR Spectra of the Reaction of **5** with H_2O .

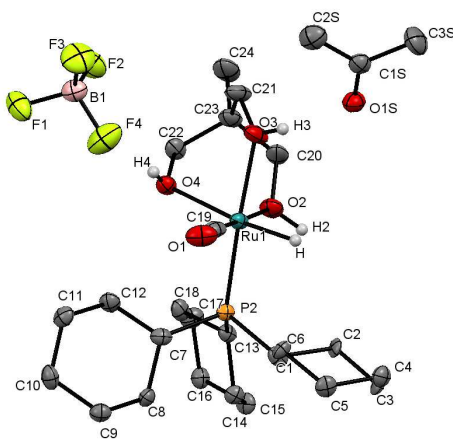


Figure 5.12: ORTEP Diagram of Complex **9** (H Atoms Removed for Clarity)

Under similar experimental conditions cationic ruthenium hydride complex **1**, dissolved in acetone to generate complex **10** as ketone coordinated complex which evidence that ketone also coordinate to the ruthenium center in etherification conditions.

The complex **10** was isolated in 80 % after crystallization in acetone/pentane. The X-ray crystal structure of **10** Ru(II) has an octahedral coordination and the complex represents a cis-isomer. Positions of hydride ligand and H atoms of the aqua ligand are trans-positioned to carbonyl. It contained one H₂O molecule due to acetone solvent contained H₂O as the impurity (Fig. 5.13).

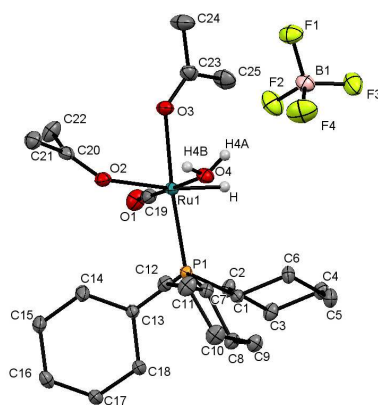
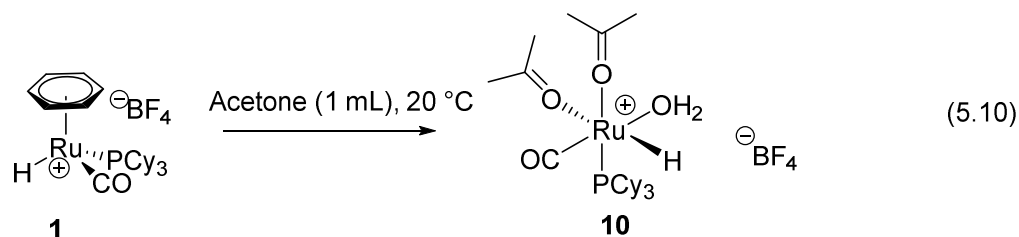


Figure 5.13: ORTEP Diagram of Complex **10** (H Atoms Removed for Clarity)

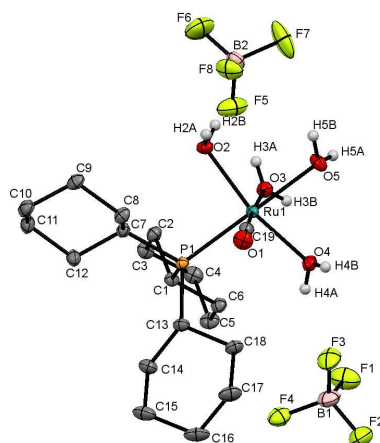
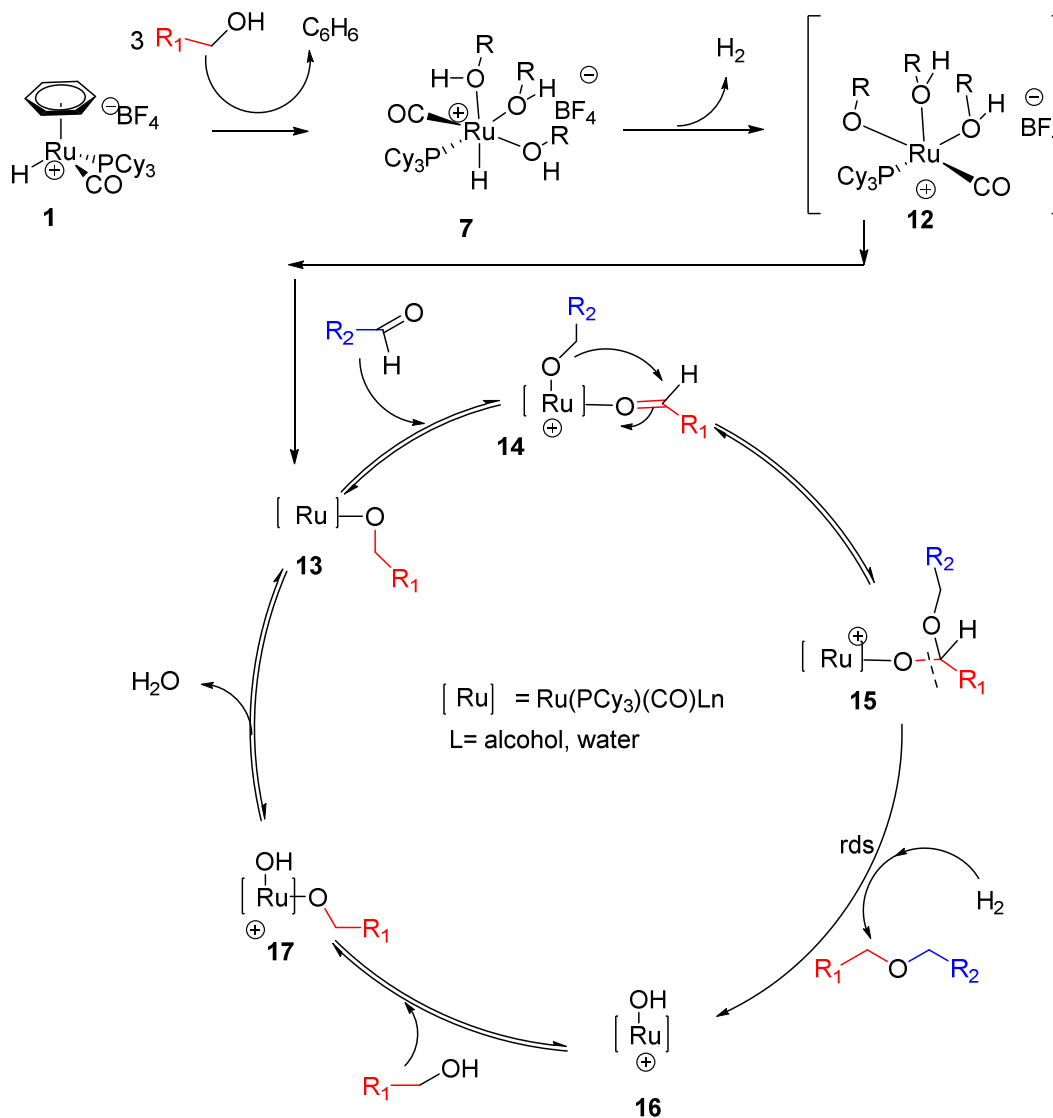


Figure 5.14: ORTEP Diagram of Complex **11** (H Atoms Removed for Clarity)

We observed that the complex **8**, in the presence of HBF_4 in et dioxane undergo rearrangement to tetraqua coordinated dicationic complex **11** which is confirm by X-defraction technique and ^1H NMR and ^{31}P NMR technique. X-ray structure of complex **11** is shown in figure 5.14.

5.5 Proposed Mechanism

On the basis of these results, we present a possible mechanism of the catalytic reaction for the selective formation of unsymmetrical ethers (Scheme 5.2). We propose that an alcohols coordinated cationic Ru-H species **7** initiate the reaction based on the intermediate observed. Complex **7** is initially generated from the benzene ligand displacement and the dehydrogenation steps. In support of this notion, we have been able to detect/isolate the formation of alcohol-coordinated cationic Ru-H complex **7** from the reaction of **5** with alcohols and water. Formation of H_2 gas molecule by deprotonation of alcohol open up an empty coordinate site (intermediate **12**) for carbonyl compound with Ru-alkoxy species **13**. It is the key intermediate species for the etherification reaction.



Scheme 5.2: Proposed Mechanism for the Catalytic Reductive Coupling of Carbonyl Compound with Alcohols.

Then the nucleophilic addition of alkoxide to carbonyl carbon which is promoted by hydrogen bonding found from solvent kinetic isotope effect generates hemiacetal type intermediate **14**. The observed H/D exchange pattern on the α -carbon of the ether product **2** as well as a normal solvent isotope effect indicates that the solvent molecules are intricately involved in the C–O bond hydrogenolysis step. Hammett data and

^{13}C KIE indicates the electron donating group promotes the reactivity and due to hydronolysis of C-O bond of hemiacetal intermediate is the rate limiting step of the mechanism. C-O cleavage of complex **15** by H_2 or solvent promoted hydride transfer produced ether and Ru-OH species **17**. The coordination of another alcohol substrate and the liberation of water byproduct would facilitate the regeneration of the alkoxy species **13**.

Part of this work was published in Nishantha Kalutharage and Chae S. Yi *Org. Lett.*, **2015**, *17* (7), pp 1778-1781; doi: 10.1021/acs.orglett.5b00553.

5.6 Conclusion:

In conclusion, we successfully developed a highly chemoselective catalytic etherification method of aldehydes and ketones with alcohols. The ruthenium-hydride catalyst exhibits a uniquely high activity as well as broad substrate scope in promoting the reductive etherification reaction of carbonyl compounds in an aqueous solution without using any reactive reagents or forming wasteful byproducts. We anticipate that the catalytic etherification method provides an environmentally sustainable and cost effective protocol for forming unsymmetrical ether compounds.

CHAPTER 6

EXPERIMENTAL SECTION

6.0 General Information.

All operations were carried out in a nitrogen-filled glove box or by using standard high vacuum and Schlenk techniques unless otherwise noted. Solvents were freshly distilled over the appropriate drying reagents. Tetrahydrofuran, 1,4-dioxane, benzene, toluene, hexanes and ether were distilled from purple solutions of sodium and benzophenone immediately prior to use. Toluene and chlorobenzene (C_6H_5Cl) were dried over calcium hydride. The 1H , ^{13}C and ^{31}P NMR spectra were recorded on a Varian 300 or 400 or 600 MHz FT-NMR spectrometer, and the data are reported as: s = singlet, d = doublet, t = triplet, q = quartet, p = pentet, m = multiplet, br = broad, app = apparent; coupling constant(s) in Hz; integration. Mass spectra were recorded from an Agilent 6850 GC-MS spectrometer with a HP-5 (5% phenylmethylpolysiloxane) column (30 m, 0.32 mm, 0.25 μ m). The conversion of organic products was measured from a Hewlett-Packard HP 6890 GC spectrometer. High resolution mass spectra were obtained at the Center of Mass Spectrometry, MO and at the Mass Spectrometry/ICP Lab, Department of Chemistry and Biochemistry, University of Wisconsin-Milwaukee, Milwaukee, WI. Optical rotation were measured by using a 1 mL cell with 1 dm path length on a Perkin-Elmer 341 polarimeter with a sodium lamp, and are reported as follows: $[\alpha]_D^{25}$ (c = g/100 mL, solvent). Element analyses were performed at the Midwest Microlab, Indianapolis, IN.

6.1. Synthesis and Mechanistic Studies of Deaminative Coupling Reactions of Amines with Alcohols

6.1.1 General Procedure for the Coupling Reaction of an Amine with an Alcohol.

In a glove box, an amine (1.0 mmol), an alcohol (1 mmol), cyclopentene (1.2 mmol) and complex **1** (17 mg, 3 mol %) were dissolved in toluene (2 mL) in a 25 mL Schlenk tube equipped with a Teflon stopcock and a magnetic stirring bar. The tube was brought out of the glove box, and was stirred in an oil bath set at 130 °C for 6-12h. The reaction tube was taken out of the oil bath, and was immediately cooled in a dry ice/acetone bath. After the tube was open to air, the solution was filtered through a short silica gel column by eluting with CH₂Cl₂ (10 mL), and the filtrate was analyzed by GC and GC-MS. Analytically pure product was isolated by a simple column chromatography on silica gel (280-400 mesh, hexanes/EtOAc = 100:1 to 1:1). The products were completely characterized by NMR and GC-MS spectroscopic methods.

6.1.2 Synthesis of Ru catalysts

The tetrametallic complex **5** was synthesized in two steps from the ruthenium-hydride complex (PCy₃)₂(CO)RuHCl (**2**) (Scheme 3.2). Thus, the reaction of **2** with KOH in 2-propanol produced the bimetallic complex **3**, which was isolated in 85% yield after recrystallization in hexanes.

6.1.3 Synthesis of [(η⁶-C₆H₆)RuH(CO)(PCy₃)]⁺BF₄⁻ (**2**).

In a glove box, complex **5** (200 mg, 0.12 mmol) was dissolved in benzene (10 mL) in a 25 mL Schlenk tube equipped with a Teflon screw-cap stopcock and a magnetic stirring bar. The tube was brought out of the box, and HBF₄·OEt₂ (64 μL, 0.48 mmol) was added via syringe under N₂ stream. The color of the solution was changed from dark red to pale

yellow immediately. After stirring for 1 h at room temperature, the solvent was removed under vacuum, and the residue was crashed by adding hexanes (10 mL). Filtering the resulting solid through a fritted funnel and recrystallization from CH₂Cl₂/hexanes yielded the product as an ivory color powder (262 mg, 95% yield). Single crystals of **2** suitable for X-ray crystallography were obtained from a slow evaporation of benzene and hexanes solution.

For **2**: ¹H NMR (CD₂Cl₂, 400 MHz) δ 6.53 (s, C₆H₆), 2.0-1.2 (m, PCy₃), -10.39 (d, *J*_{PH} = 25.9 Hz, Ru-H); ¹³C {¹H} NMR (CD₂Cl₂, 100 MHz), δ 196.4 (d, *J*_{C-P} = 19.3 Hz, CO), 100.0 (C₆H₆), 38.4, 38.2, 30.2, 29.9, 27.4, 27.3 and 26.2 (PCy₃); ³¹P {¹H} NMR (CD₂Cl₂, 162 MHz) δ 72.9 (PCy₃); IR (KBr) *ν*_{CO} = 1991 cm⁻¹; Anal. Calcd for **2** C₂₅H₄₀BF₄OPRu: C, 52.18; H, 7.01. Found: C, 51.73; H, 6.91.

6.1.4 Catalyst Screening for the Alkylation of 2-Butanol with 3-methoxybenzylamine.

In a glove box, an amine (1.0 mmol), an alcohol (1 mmol), cyclopentene (0.05 mmol) and complex **2** (17 mg, 3 mol %) were dissolved in toluene (2 mL) in a 25 mL Schlenk tube equipped with a Teflon stopcock and a magnetic stirring bar. The tube was brought out of the glove box, and was stirred in an oil bath set at 100-130 °C for 6-12 h. The reaction tube was taken out of the oil bath, and was immediately cooled in a dry ice/acetone bath. After the tube was open to air, the solution was filtered through a short silica gel column by eluting with CH₂Cl₂ (10 mL), and the filtrate was analyzed by GC and GC-MS. Analytically pure product was isolated by a simple column chromatography on silica gel (280-400 mesh, hexanes/EtOAc = 100:1 to 1:1). The products were completely characterized by NMR and GC-MS spectroscopic methods. The results are summarized in

Table 3.1.

6.1.5 Deuterium Labeling Study.

In a glove box, 3-methoxybenzyl amine (0.2 mmol), 2-propanol-*d*₈ (0.4 mmol, 99 % D) and **5** (6 mg, 5 mol %) were dissolved in toluene-*d*₈ (0.4 mL) in a J-Young NMR tube with a Teflon screw cap stopcock (Wilmad). The tube was brought out of the box, and the reaction progress was monitored by both ¹H and ²H NMR at 80 °C. After 1 h, the 3-methoxybenzyl amine substrate was found to contain 34% deuterium on the C(2) position, was also detected as analyzed by both ¹H and ²H NMR. Figure 3.3 shows the ¹H and ²H NMR spectra of the reaction mixture after 1 h of the reaction time.

6.1.6. Carbon Isotope Effect Study.

In a glove box, 1-phenylethanol (1.5 g, 10 mmol), 1-hexylamine (1.6 g, 12 mmol), cyclopentene (70 mg, 1 mmol) and complex **2** (180 mg, 3 mol %) were dissolved in toluene (30 mL) in a 100 mL Schlenk tube equipped with a Teflon screw cap stopcock and a magnetic stirring bar. The tube was brought out of the box, and stirred for 4h, 4.5h, and 5 h respectively, in an oil bath which was preset at 130 °C. Compound Octanophenone (**7d**) was isolated by a column chromatography on silica gel (hexanes/EtOAc = 40:1 to 10:1) separately after filtering through a short silica gel column eluting with CH₂Cl₂ (20 mL), and each solution was analyzed by GC (15, 18 and 20 % conversion). Commercially available Octanophenone was used as the virgin samples.

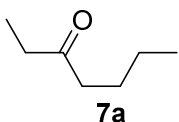
The ¹³C {¹H} NMR analysis of the recovered and virgin samples of Octanophenone was performed by following Singleton's ¹³C NMR measurement technique (chapter 4, ref. 22). The NMR sample of virgin and recovered octanophenone was prepared identically by

dissolving (100 mg) in CDCl_3 (0.5 mL) in a 5 mm high precision NMR tube. The $^{13}\text{C}\{^1\text{H}\}$ NMR spectrum was recorded with H-decoupling and 45 degree pulse. A 60 s delay between pulses was imposed to minimize T_1 variations ($d1 = 60$ s, $at = 5.0$ s, $np = 245098$, $nt = 704$). The data are summarized in Table 3.5.

6.1.7 Hammett Study.

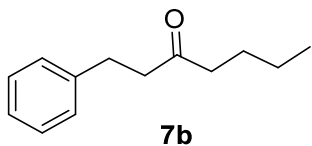
Hammett studies of *para*-substituted benzylamine substrates were performed to determine the electronic effects on arylalketone substrate during C-N bond cleavage reaction. *Para*-substituted benzylamines, $p\text{-X-C}_6\text{H}_5\text{CH}_2\text{NH}_2$ ($\text{X} = \text{OCH}_3, \text{CH}_3, \text{H}, \text{Cl}$) (1.0 mmol), 1-phenylethanol (1.5 mmol), cyclopentene (0.05 mmol) and complex **2** (3 mol %) were dissolved in toluene (2 mL) in six separate 25 mL Schlenk tubes. The tubes were brought out of the box, and stirred in an oil bath set at 130 °C. Each reaction tube was taken out of the oil bath in 30 minute intervals, and was immediately cooled and analyzed by ^1H NMR. The k_{obs} was determined from a first-order plot of $-\ln([p\text{-X-C}_6\text{H}_5\text{CH}_2\text{NH}_2]_t/p\text{-X-C}_6\text{H}_5\text{CH}_2\text{NH}_2]_0)$ vs. time. The Hammett plot of $\log(k_X/k_H)$ vs. σ_p is shown in Fig. 3.2. The Hammett correlation of *para*-substituted benzylamine substrates ($p\text{-X-C}_6\text{H}_4\text{CH}_2\text{NH}_2$ ($\text{X} = \text{OMe}, \text{CH}_3, \text{H}, \text{F}, \text{Cl}$)) was $\rho = -1.2 \pm 0.1$ calculated from slope of the plot (Figure 3.2).

6.1.8 Characterization of Organic Products

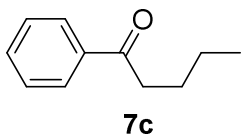


Data for Table 3.3, Compound **7a**: ^1H NMR (400 MHz, CDCl_3) δ 3.32-3.43 (m, 4H), 1.51 (p, $J = 7.3$ Hz, 2H), 1.27 (sextet, $J = 7.4$ Hz, 2H), 1.01 (t, $J = 7.4$ Hz, 3H), 1.01 (t, $J = 7.3$ Hz, 3H) ppm; ^{13}C NMR (400 MHz, CDCl_3) δ 210.1, 41.9, 35.6, 25.8, 22.2, 13.6, 9.9 ppm; GC-

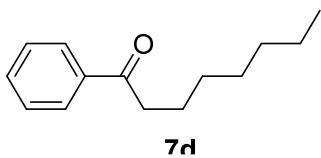
MS $m/z = 114$ (M^+). ^1H and ^{13}C NMR spectral data are in good agreement with the literature data.¹



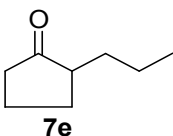
Data for Table 3.3, Compound **7b**: ^1H NMR (400 MHz, CDCl_3) δ 7.02–7.22 (m, 5H), 2.79 (t, $J = 8.1$ Hz, 2H), 2.62 (t, $J = 8.1$ Hz, 2H), 2.28 (t, $J = 7.5$ Hz, 2H), 1.44 (p, $J = 7.5$ Hz, 2H), 1.18 (sextet, $J = 7.5$ Hz, 2H), 0.78 (t, $J = 7.5$ Hz, 1H) ppm; ^{13}C NMR (400 MHz, CDCl_3) δ 210.7, 141.6, 128.9, 128.8, 126.5, 44.7, 43.2, 30.2, 26.3, 22.7, 14.3 ppm; GC-MS $m/z = 162$ (M^+). ^1H and ^{13}C NMR spectral data are in good agreement with the literature data.²



Data for Table 3.3, Compound **7c**: ^1H NMR (400 MHz, CDCl_3) δ 7.85–7.91 (m, 2H), 7.45–7.51 (m, 1H), 7.35–7.42 (m, 2H), 2.90 (t, $J = 7.2$ Hz, 2H), 1.65 (p, $J = 8.6$ Hz, 2H), 1.34 (sextet, $J = 8.0$ Hz, 2H), 0.88 (t, $J = 7.5$ Hz, 3H), ppm; ^{13}C NMR (400 MHz, CDCl_3) δ 200.6, 137.1, 132.8, 128.5, 128.0, 38.3, 26.5, 22.5, 14.0 ppm; GC-MS $m/z = 162$ (M^+). ^1H and ^{13}C NMR spectral data are in good agreement with the literature data.³

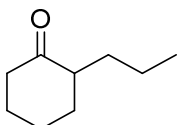
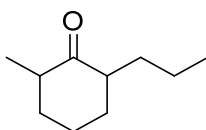


Data for Table 3.3, Compound **7d**: ^1H NMR (400 MHz, CDCl_3) δ 7.96 (dt, $J = 7.0, 1.4$ Hz, 2H), 7.55 (tt, $J = 7.5, 2.1$ Hz, 1H), 7.45 (tt, $J = 7.5, 1.4$ Hz, 2H), 2.96 (t, $J = 7.8$ Hz, 2H), 1.73 (p, $J = 7.3$ Hz, 2H), 1.20–1.45 (m, 8H) 0.88 (t, $J = 7.1$ Hz, 3H), ppm; ^{13}C NMR (400 MHz, CDCl_3) δ 200.6, 137.1, 132.8, 128.5, 128.0, 38.3, 26.5, 22.5, 14.0 ppm; GC-MS $m/z = 204$ (M^+). ^1H and ^{13}C NMR spectral data are in good



agreement with the literature data.⁴

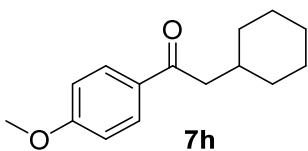
Data for Table 3.3, Compound **7e**: ^1H NMR (400 MHz, CDCl_3) 2.33-1.92 (m, 5H), 1.85-1.65 (m, 2H), 1.56-1.15 (m, 4H), 0.89 (t, $J = 7.2$ Hz, 3H) ppm; ^{13}C NMR (400 MHz, CDCl_3) δ 221.2, 48.7, 37.9, 31.7, 29.4, 20.6, 20.5, 13.8 ppm; GC-MS $m/z = 126$ (M^+). ^1H and ^{13}C NMR spectral data are in good agreement with the literature data.⁵

**7f****7g**

Data for Table 3.3, Compound **7f**: ^1H NMR (400 MHz, CDCl_3) 2.39 (dddd, $J = 13.5, 4.4, 4.3, 1.4$ Hz, 1H), 2.23-2.33 (m, 2H), 2.06-2.14 (m, 1H), 1.96-2.06 (m, 1H), 1.81-1.89 (m, 1H), 1.59-1.81 (m, 3H), 1.34-1.44 (m, 1H), 1.24-1.35 (m, 2H), 1.13-1.24 (m, 1H), 0.89 (t, $J = 7.2$ Hz, 3H) ppm; ^{13}C NMR (400 MHz, CDCl_3) δ 213.6, 50.4, 41.8, 33.7, 31.4, 27.9, 24.7, 20.2, 14.1 ppm; GC-MS $m/z = 140$ (M^+). ^1H and ^{13}C NMR spectral data are in good agreement with the

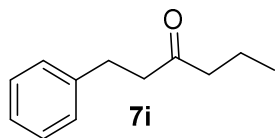
literature data.⁶

Data for Table 3.3, Compound **7g**: ^1H NMR (400 MHz, CDCl_3) *trans*-**7g**: 2.56 (ddd, $J = 10.0, 6.5, 5.2$ Hz, 1H), 2.24-2.52 (m, 1H), 1.60-2.10 (m, 6H), 1.16-1.56 (m, 4H), 1.05 (d, $J = 6.5$ Hz, 3H), 0.89 (t, $J = 6.5$ Hz, 3H). *cis*-**7g**: 2.42 (ddd, $J = 12.8, 6.0, 5.6$ Hz, 1H), 2.24 (m, 1H), 2.03-2.38 (2H, m), 1.62-1.92 (m, 3H), 1.06-1.48 (m, 5H), 1.00 (d, $J = 6.0$ Hz, 3H), 0.89 ($J = 6.5$ Hz, 3H) ppm; ^{13}C NMR (400 MHz, CDCl_3) δ 213.5, 47.4, 41.0, 34.2, 31.0, 27.4, 24.5, 20.0, 14.1 ppm; GC-MS $m/z = 154$ (M^+). ^1H and ^{13}C NMR spectral data are in good agreement with the literature data.⁷

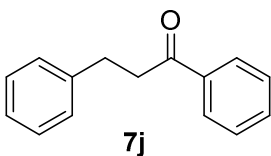
**7h**

Data for Table 3.3, Compound **7h**: ^1H NMR (400 MHz, CDCl_3) δ 7.93 (d, $J = 8.8$ Hz, 2H), 6.92 (δ 7.93d, $J = 8.8$ Hz, 2H), 3.86 (s, 3H), 2.76 (d, $J = 6.8$ Hz, 2H), 1.99-1.64 (m, 6H), 1.32-0.96 (m, 5H) ppm; ^{13}C NMR (400 MHz, CDCl_3) δ 198.9, 163.2, 130.6, 130.4,

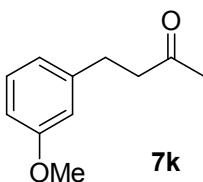
113.6, 55.4, 45.9, 34.8, 33.4, 26.2, 26.1 ppm; GC-MS $m/z = 232$ (M^+). ^1H and ^{13}C NMR spectral data are in good agreement with the literature data.⁸



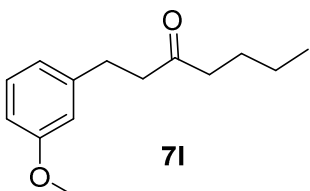
Data for Table 3.3, Compound **7i**: ^1H NMR (400 MHz, CDCl_3) δ 7.16-7.30 (m, 5H) 2.90 (t, $J = 7.6$ Hz, 2H), 2.71 (t, $J = 7.6$ Hz, 2H), 2.36 (t, $J = 7.5$ Hz, 2H), 1.56 (sextet, $J = 7.5$ Hz, 2H), 0.88 (t, $J = 7.5$ Hz, 3H) ppm; ^{13}C NMR (400 MHz, CDCl_3) 210.51, 141.3, 128.5, 127.9, 125.5, 45.0, 44.4, 29.9, 17.3, 3.8 ppm; GC-MS $m/z = 192$ (M^+); ^1H and ^{13}C NMR spectral data are in good agreement with the literature data.⁹



Data for Table 3.3, Compound **7j**: ^1H NMR (400 MHz, CDCl_3) δ 7.95 (d, $J = 6.9$ Hz, 2H), 7.56 (t, $J = 7.3$ Hz, 1H), 7.46 (t, $J = 7.3$ Hz, 2H), 7.20-7.32 (m, 5H), 3.31 (m, 2H), 3.08 (m, 2H) ppm; ^{13}C NMR (400 MHz, CDCl_3) 199.4, 141.4, 137.0, 133.2, 128.7, 128.7, 128.6, 128.2, 126.3, 40.6, 30.3 ppm; GC-MS $m/z = 240$ (M^+); ^1H and ^{13}C NMR spectral data are in good agreement with the literature data.¹⁰

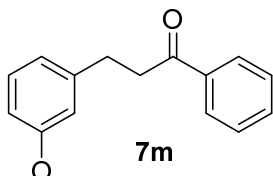


Data for Table 3.3, Compound **7k**: ^1H -NMR (CDCl_3 , 400MHz), δ 7.17-7.22 (m, 1H), 6.73-6.78 (m, 3H), 3.79 (s, 3H), 2.87 (t, $J = 7.6$ Hz, 2H), 2.75 (t, $J = 7.6$ Hz, 2H), 2.14 (s, 3H) ppm; GC-MS $m/z = 178$ (M^+); ^1H and ^{13}C NMR spectral data are in good agreement with the literature data.¹¹

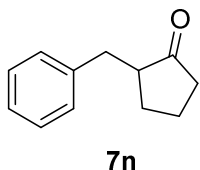


Data for Table 3.3, Compound **7l**: ^1H NMR (400 MHz, CDCl_3) δ 7.16-7.22 (m, 1H), 6.70-6.79 (m, 3H), 3.78 (s, 3H), 2.86 (t, $J = 7.9$ Hz, 2H), 2.72 (t, $J = 8.0$ Hz, 2H), 2.38 (t, $J = 7.6$ Hz, 2H), 1.54 (p, $J = 7.5$ Hz, 2H), 1.28 (sextet, $J =$

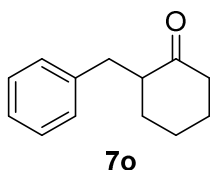
7.5 Hz, 2H), 0.88 (t, $J = 7.5$ Hz, 1H) ppm; ^{13}C NMR (400 MHz, CDCl_3) δ 210.4, 159.7, 142.8, 129.5, 120.7, 114.1, 111.3, 55.1, 44.2, 42.8, 29.8, 25.9, 22.3, 13.9 ppm; GC-MS $m/z = 220$ (M^+); Anal. Calcd for $\text{C}_{14}\text{H}_{20}\text{O}_2$: C, 76.33; H, 9.15. Found: C, 76.10; H, 8.98.



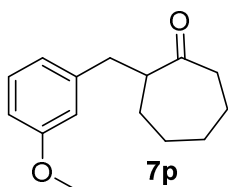
Data for Table 3.3, Compound **7m**: ^1H NMR (400 MHz, CDCl_3) δ 7.94-7.98 (m, 2H), 7.56 (tt, $J = 7.5, 2.0$ Hz, 1H), 7.45 (tt, $J = 7.9, 1.3$ Hz, 2H), 7.22 (t, $J = 8.2$ Hz, 1H), 6.74-6.88 (m, 3H), 3.79 (s, 3H), 3.30 (t, $J = 8.3$ Hz, 2H), 3.05 (t, $J = 8.3$ Hz, 2H) ppm; ^{13}C NMR (400 MHz, CDCl_3) δ 199.2, 159.7, 142.9, 136.8, 133.1, 129.5, 128.6, 128.0, 120.7, 114.2, 111.4, 55.2, 40.3, 30.1 ppm; GC-MS $m/z = 240$ (M^+); ^1H and ^{13}C NMR spectral data are in good agreement with the literature data.¹²



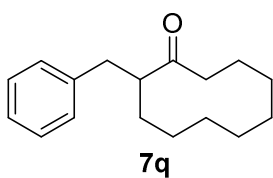
Data for Table 3.3, Compound **7n**: ^1H NMR (400 MHz, CDCl_3) δ 7.00-7.40 (m, 5H), 3.18 (dd, $J = 13.5, 3.5$ Hz, 1H), 1.2-2.7 (m, 8H) ppm; ^{13}C NMR (400 MHz, CDCl_3) δ 207.4, 159.4, 128.9, 127.9, 126.1, 51.1, 39.8, 32.6, 25.2, 20.5 ppm; GC-MS $m/z = 174$ (M^+); ^1H and ^{13}C NMR spectral data are in good agreement with the literature data.¹³



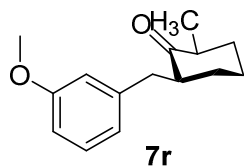
Data for Table 3.3, Compound **7o**: ^1H NMR (400 MHz, CDCl_3) δ 7.02-7.23 (m, 5H), 3.16 (dd, $J = 13.6, 5.1$ Hz, 1H), 2.43-2.55 (m, 1H), 2.32-2.41 (m, 2H), 2.20-2.32 (m, 1H), 1.90-2.06 (m, 2H), 1.69-1.80 (m, 1H), 1.57-1.68 (m, 1H), 1.46-1.58 (m, 1H), 1.17-1.33 (m, 1H) ppm; ^{13}C NMR (400 MHz, CDCl_3) δ 201.6, 140.3, 129.1, 128.2, 125.9, 52.4, 42.1, 35.4, 33.4, 28.0, 25.0 ppm; GC-MS $m/z = 188$ (M^+); ^1H and ^{13}C NMR spectral data are in good agreement with the literature data.¹⁴



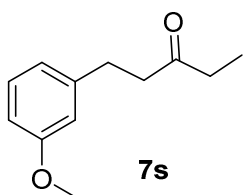
Data for Table 3.3, Compound **7p**: ^1H NMR (400 MHz, CDCl_3) δ 7.17 (t, $J = 7.3$ Hz, 1H), 6.67-6.77 (m, 3H), 3.78 (s, 3H), 3.05 (dd, $J = 14.0, 5.6$ Hz, 1H), 2.76-2.88 (m, 1H), 2.52 (dd, $J = 14.0, 5.6$ Hz, 1H), 2.42-2.48 (m, 2H), 1.70-1.90 (m, 4H), 1.55-1.70 (m, 1H), 1.22-1.40 (m, 3H) ppm; ^{13}C NMR (400 MHz, CDCl_3) δ 215.7, 159.5, 141.6, 129.2, 121.5, 114.9, 111.2, 55.1, 53.4, 43.2, 37.8, 30.3, 29.3, 28.6, 24.2 ppm; GC-MS $m/z = 232$ (M^+); ^1H and ^{13}C NMR spectral data are in good agreement with the literature data.¹⁵



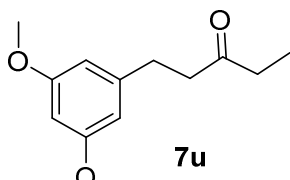
Data for Table 3.3, Compound **7q**: ^1H NMR (400 MHz, CDCl_3) δ 7.14-7.40 (m, 5H), 2.96-3.04 (m, 1H), 2.73 (dd, $J = 13.3, 8.0$ Hz, 1H), 2.56 (dd, $J = 13.4, 7.0$ Hz, 2H), 2.30 (ddd, $J = 16.3, 9.4, 3.1$ Hz, 1H), 1.96 (2.30 (ddd, $J = 16.3, 8.8, 3.1$ Hz, 1H), 1.10-1.90 (m, 13H) ppm; ^{13}C NMR (400 MHz, CDCl_3) δ 203.5, 139.6, 128.7, 128.1, 126.8, 57.9, 54.3, 42.7, 40.6, 30.9, 25.3, 25.2, 25.1, 24.1, 23.7, 23.1 ppm; GC-MS $m/z = 244$ (M^+); ^1H and ^{13}C NMR spectral data are in good agreement with the literature data.¹⁶



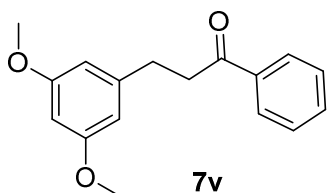
Data for Table 3.3, Compound **7r**: ^1H NMR (400 MHz, CDCl_3) δ 7.16-7.22 (m, 1H), 6.70-6.79 (m, 3H), 3.78 (s, 3H), 3.20 (dd, $J = 13.9, 5.0$ Hz, 1H), 2.49-2.60 (m, 1H), 2.40-2.48 (m, 1H), 2.36 (dd, $J = 13.9, 8.6$, 1H), 2.00-2.14 (m, 2H), 1.60-1.90 (m, 1H), 1.20-1.50 (m, 2H), 1.02 (d, $J = 6.5$ Hz, 3H) ppm; ^{13}C NMR (400 MHz, CDCl_3) δ 213.7, 159.5, 142.4, 129.2, 121.6, 112.0, 111.0, 55.1, 52.5, 45.6, 35.5, 34.7, 25.4, 14.6 ppm; GC-MS $m/z = 232$ (M^+); Anal. Calcd for $\text{C}_{15}\text{H}_{20}\text{O}_2$: C, 77.55; H, 8.68. Found: C, 77.35; H, 8.89.



Data for Table 3.3, Compound **7s**: ^1H NMR (400 MHz, CDCl_3) δ 7.16–7.22 (m, 1H), 6.70–6.79 (m, 3H), 3.78 (s, 3H), 2.78 (t, $J = 8.0$ Hz, 2H), 2.72 (t, $J = 8.0$ Hz, 2H), 2.41 (q, $J = 7.3$ Hz, 2H), 1.04 (t, $J = 7.3$ Hz, 1H) ppm; ^{13}C NMR (400 MHz, CDCl_3) δ 210.7, 159.7, 142.8, 129.5, 120.6, 114.1, 111.3, 55.1, 43.8, 36.1, 29.9, 7.8 ppm; GC-MS $m/z = 192$ (M^+); 192 (M^+); ^1H and ^{13}C NMR spectral data are in good agreement with the literature data.¹⁶

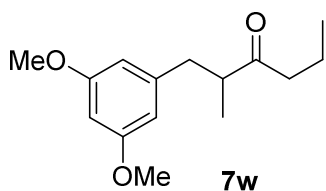


Data for Table 3.3, Compound **7u**: ^1H NMR (400 MHz, CDCl_3) δ 6.33 (d, $J = 2.3$ Hz, 2H), 6.30 (t, $J = 2.4$ Hz, 1H), 3.77 (s, 6H), 2.84 (t, $J = 8.2$ Hz, 2H), 2.71 (t, $J = 8.2$ Hz, 2H), 2.41 (q, $J = 7.5$ Hz, 2H), 1.04 (t, $J = 7.3$ Hz, 1H) ppm; ^{13}C NMR (400 MHz, CDCl_3) δ 210.7, 160.8, 143.6, 106.3, 98.0, 55.3, 43.7, 36.1, 30.1, 7.8 ppm; GC-MS $m/z = 222$ (M^+); ^1H and ^{13}C NMR spectral data are in good agreement with the literature data.¹⁷



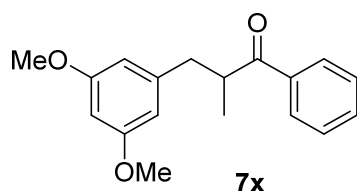
Data for Table 3.3, Compound **7v**: ^1H NMR (400 MHz, CDCl_3) δ 7.96 (m, 2H), 7.53–7.58 (m, 1H), 7.41–7.48 (m, 2H), 6.41 (d, $J = 2.3$ Hz, 2H), 6.32 (t, $J = 2.4$ Hz, 1H), 3.77 (s, 6H), 3.29 (t, $J = 8.2$ Hz, 2H), 3.00 (t, $J = 8.2$ Hz, 2H), ppm; ^{13}C NMR (400 MHz, CDCl_3) δ 199.2, 160.9, 143.7, 136.8, 143.8, 133.1, 128.6, 128.0, 106.4, 98.0, 55.3, 40.3, 30.4 ppm; GC-MS $m/z = 270$ (M^+); ^1H and ^{13}C NMR spectral data are in good agreement with the literature data.¹⁸

Data for Table 3.3, Compound **7w**: ^1H NMR (400 MHz, CDCl_3) δ 7.01 (s, 1H),



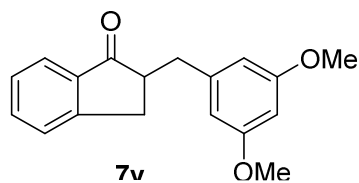
6.29 (s, 2H), 3.84 (s, 3H), 3.76 (s, 3H), 2.91 (dd, $J = 13.1$, 7.3 Hz, 2H), 2.81 (sextet, 2H), 2.47 (dd, $J = 13.1$, 7.3 Hz, 1H), 2.45–2.20 (m, 2H), 1.53 (sextet, $J = 7.6$ Hz, 2H), 1.07 (d, $J = 6.8$ Hz, 3H) 0.85 (t, $J = 8.0$ Hz, 3H) ppm; ^{13}C NMR (400 MHz, CDCl_3) δ 214.2, 191.9, 160.7, 142.3, 106.9, 98.1, 55.6, 55.2, 47.8, 43.8, 39.3, 16.9, 16.5, 13.7 ppm; GC-MS $m/z = 250$ (M^+); Anal. Calcd for $\text{C}_{15}\text{H}_{22}\text{O}_3$: C, 71.97; H, 8.86. Found: C, 71.48; H, 8.62.

Data for Table 3.3, Compound 7x: ^1H NMR (400

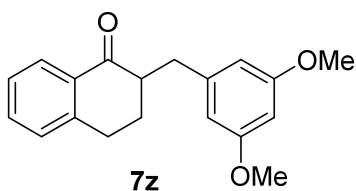


MHz, CDCl_3) δ 7.96 (m, 2H), 7.53–7.58 (m, 1H), 7.41–7.48 (m, 2H), 6.4 (d, $J = 2.3$ Hz, 2H), 6.32 (t, $J = 2.4$ Hz, 1H), 3.77 (s, 6H), 3.10 (dd, $J = 13.9$, 6.5 Hz, 2H), 2.62 (dd, $J = 13.7$, 8.0 Hz, 2H), 1.20 (d, 3H) ppm; ^{13}C NMR (400 MHz, CDCl_3) δ 199.2, 160.9, 143.7, 136.8, 143.8, 133.1, 128.6, 128.0, 106.4, 98.0, 55.3, 40.3, 30.4 ppm; GC-MS $m/z = 284$ (M^+); ^1H and ^{13}C NMR spectral data are in good agreement with the literature data.¹⁹

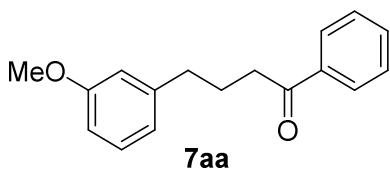
Data for Table 3.3, Compound 7y: ^1H NMR (400



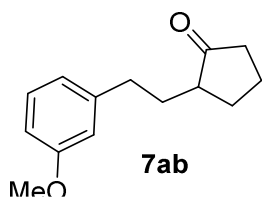
MHz, CDCl_3) δ 7.77 (d, $J = 7.7$ Hz, 1H), 7.57 (td, $J = 7.3$, 1.2 Hz, 1H), 7.34–7.42 (m, 2H), 6.4 (m, 2H), 6.32 (m, 1H), 3.77 (s, 6H), 3.34 (dd, $J = 13.7$, 4.2 Hz, 1H), 3.18 (dd, $J = 17.0$, 7.8 Hz, 1H), 2.98 (dddd, $J = 11.8$, 10.5, 8.2, 4.1 Hz, 1H), 2.86 (dd, $J = 17.3$, 4.2 Hz, 1H), 2.58 (dd, $J = 13.7$, 10.4 Hz, 1H) ppm; ^{13}C NMR (400 MHz, CDCl_3) δ 207.8, 160.8, 153.7, 142.0, 136.5, 134.8, 127.4, 126.6, 124.0, 106.9, 98.2, 55.3, 48.8, 37.3, 32.2 ppm; GC-MS $m/z = 282$ (M^+); ^1H and ^{13}C NMR spectral data are in good agreement with the literature data.²⁰



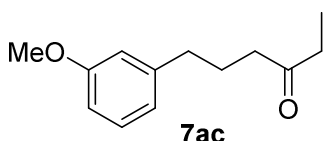
Data for Table 3.3, Compound **7z**: ^1H NMR (400 MHz, CDCl_3) δ 8.08 (d, $J = 7.8$ Hz, 1H), 7.76-7.86 (m, 1H), 7.41-7.49 (m, 1H), 7.28-7.36 (m, 1H), 6.39 (m, 2H), 6.33 (m, 1H), 3.78 (s, 6H), 3.45 (dd, $J = 13.8, 3.8$ Hz, 1H), 2.88-2.97 (m, 2H), 2.75 (m, 1H), 2.55 (dd, $J = 13.8, 10.0$ Hz, 1H), 2.12 (m, 1H), 1.80 (m, 2H) ppm; ^{13}C NMR (400 MHz, CDCl_3) δ 201.7, 163.4, 133.3, 128.7, 127.5, 126.6, 107.2, 107.1, 105.5, 55.7, 49.5, 35.7, 28.6, 27.6 ppm; GC-MS $m/z = 236$ (M^+); ^1H and ^{13}C NMR spectral data are in good agreement with the literature data.²¹



Data for Table 3.3, Compound **7aa**: ^1H NMR (400 MHz, CDCl_3) δ 6.82-7.13 (m, 1H), 6.39-6.75 (m, 3H), 3.72 (m, 3H), 2.54 (t, $J = 7.4$ Hz, 2H), 2.33 (t, $J = 6.3$ Hz, 2H), 2.02 (s, 3H), 1.65-2.13 (m, 2H), ppm; ^{13}C NMR (400 MHz, CDCl_3) δ 200.1, 160.8, 139.1, 136.8, 133.2, 129.9, 128.8, 128.7, 120.5, 112.2, 55.9, 38.4, 35.8, 24.5, 11.6 ppm; Anal. Calcd for $\text{C}_{17}\text{H}_{18}\text{O}_2$: C, 80.28; H, 7.13. Found: C, 79.02; H, 7.22.; ^1H and ^{13}C NMR spectral data are in good agreement with the literature data.²²

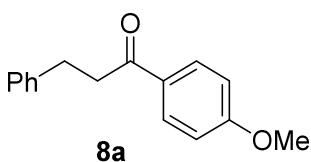


Data for Table 3.3, Compound **7ab**: ^1H NMR (400 MHz, CDCl_3) δ 7.17 (t, $J = 7.3$ Hz, 1H), 6.70-6.81 (m, 3H), 3.78 (s, 3H), 2.57-2.75 (m, 2H), 2.00-2.35 (m, 2H), 2.06-2.18 (m, 2H), 1.96-2.06 (m, 2H), 1.70-1.82 (m, 1H), 1.48-1.59 (m, 2H) ppm; ^{13}C NMR (400 MHz, CDCl_3) δ 221.3, 159.6, 143.2, 129.3, 120.8, 114.1, 111.2, 55.1, 48.3, 38.1, 33.6, 31.2, 29.7, 20.7 ppm; GC-MS $m/z = 218$ (M^+); Anal. Calcd for $\text{C}_{14}\text{H}_{18}\text{O}_2$: C, 77.03; H, 8.31. Found: C, 77.48; H, 8.42.



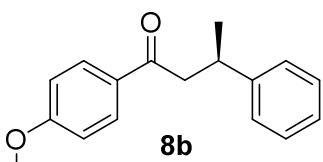
Data for Table 3.3, Compound **7ac**: ^1H NMR (400 MHz, CDCl_3) δ 7.20 (t, $J = 7.7$ Hz, 1H), 6.79-6.70 (m, 3H), 3.79 (s, 3H), 2.59 (t, $J = 7.8$ Hz, 2H), 2.44-2.36 (m, 4H),

1.91 (p, $J = 7.8$ Hz, 2H) 1.04 (t, $J = 7.3$ Hz, 3H) ppm; ^{13}C NMR (400 MHz, CDCl_3) δ 211.8, 159.9, 143.6, 129.6, 121.1, 114.4, 111.5, 55.4, 41.7, 36.2, 35.4, 25.4, 8.1 ppm; GC-MS $m/z = 206$ (M^+); Anal. Calcd for $\text{C}_{13}\text{H}_{18}\text{O}_2$: C, 75.69; H, 8.80. Found: C, 75.48; H, 8.61.



Data for Table 3.4, Compound **8a**: ^1H NMR (400 MHz, CDCl_3) δ 7.94 (d, $J = 9.0$ Hz, 2H), 7.32-7.18 (m, 5H), 6.92 (d, $J = 9.0$ Hz, 2H), 3.86 (s, 3H), 3.27-3.23 (m, 2H), 3.06

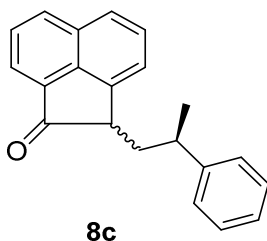
(t, $J = 7.8$ Hz, 2H); ^{13}C NMR (400 MHz, CDCl_3) δ 198.2, 163.6, 141.9, 130.7, 130.4, 128.9, 128.8, 126.5, 114.1, 55.9, 40.5, 30.7 ppm; GC-MS $m/z = 240$ (M^+). ^1H and ^{13}C NMR spectral data are in good agreement with the literature data.²³



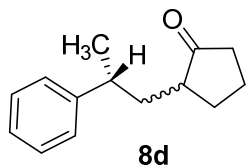
Data for Table 3.4, Compound **8b**: ^1H NMR (400 MHz, CDCl_3) δ 7.92 (d, $J = 8.9$ Hz, 2H), 7.32-7.26 (m, 4H), 7.21-7.17 (m, 1H), 6.91 (d, $J = 8.9$ Hz, 2H), 3.86 (s,

3H), 3.53-3.45 (m, 1H), 3.24 (dd, $J = 16.2, 5.7$ Hz, 1H), 3.13 (dd, $J = 16.2, 8.4$ Hz, 1H), 1.33 (d, $J = 7.0$ Hz, 3H); ^{13}C NMR (400 MHz, CDCl_3) δ 198.1, 163.8, 147.1, 130.8, 130.7, 128.9, 127.3, 126.6, 114.1, 55.9, 47.1, 36.2, 22.3 ppm; GC-MS $m/z = 254$ (M^+); ^1H and ^{13}C NMR spectral data are in good agreement with the literature data.²⁴

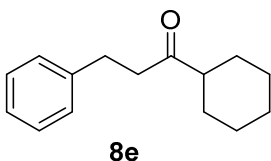
Data for Table 3.4, Compound **8c 3:2 diastereomeric mixture (Major)**: ^1H NMR (400 MHz, CDCl_3) δ 8.06 (t, $J = 9.3$ Hz, 1H), 7.80 (t, $J = 9.3$ Hz, 1H), 7.66 (t, $J = 7.2$ Hz, 1H), 7.29-7.37 (m, 2H), 7.14-7.24 (m, 2H), 3.62 (t, $J = 7.0$ Hz, 1H), 3.32-3.40 (m, 1H),



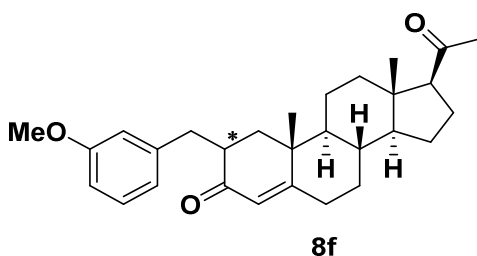
2.49-2.53 (m, 2H), 2.27 (ddd, $J = 13.9, 7.9, 6.4$ Hz, 1H), 2.20 (ddd, $J = 13.9, 9.1, 6.2$ Hz, 1H), 2.04 (ddd, $J = 13.9, 9.3, 5.7$ Hz, 1H), 1.37 (t, $J = 7.0$ Hz, 3H). GC-MS $m/z = 286$ (M^+); **Minor diastereomer** : 7.90 (d, $J = 6.7$ Hz, 1H), 7.84 (d, $J = 7.2$ Hz, 1H), 7.70 (d, $J = 7.6$ Hz, 1H), 7.58 (t, $J = 7.2$ Hz, 1H), 7.29-7.37 (m, 2H), 7.14-7.24 (m, 2H), 3.57 (dd, $J = 9.3, 4.9$ Hz, 1H), 3.22-3.31 (m, 1H), 2.49-2.53 (m, 2H), 2.20 (ddd, $J = 13.9, 9.1, 6.2$ Hz, 1H), 2.04 (ddd, $J = 13.9, 9.3, 5.7$ Hz, 1H), 1.31 (t, $J = 7.0$ Hz, 3H) ppm; GC-MS $m/z = 286$ (M^+); ^1H and ^{13}C NMR spectral data are in good agreement with the literature data.²⁵



Data for Table 3.4, Compound **8d** (**10:1 diastereomer mixture**): **Major diastereomer** ^1H NMR (400 MHz, CDCl_3) δ 7.08-7.24 (m, 5H), 2.61-2.72 (m, 1H), 1.80-2.40 (m, 5H), 1.40-1.80 (m, 4H), 1.20 (d, $J = 7.0$ Hz, 3H), 1.17 (d, $J = 6.8$ Hz, 3H) ppm; ^{13}C NMR (400 MHz, CDCl_3) δ 221.4, 159.6, 143.3, 129.3, 120.8, 114.1, 111.2, 55.1, 48.4, 38.2, 33.7, 31.3, 29.7, 20.7 ppm; GC-MS $m/z = 218$ (M^+); Anal. Calcd for $\text{C}_{14}\text{H}_{18}\text{O}$: C, 83.12; H, 8.97. Found: C, 83.40; H, 8.62.



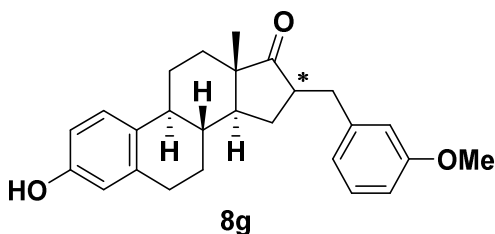
Data for Table 3.4, Compound **8e**: ^1H NMR (400 MHz, CDCl_3) δ 7.24-7.30 (m, 3H), 7.15-7.22 (m, 3H), 2.91-2.96 (m, 1H), 2.87 (t, $J = 7.9$ Hz, 2H), 2.75 (t, $J = 7.9$ Hz, 2H), 2.17-2.36 (m, 2H), 1.70-1.87 (m, 4H), 1.56-1.69 (m, 2H), 1.10-1.40 (m, 5H) ppm; ^{13}C NMR (400 MHz, CDCl_3) δ 213.1, 141.5, 128.4, 128.4, 126.0, 51.0, 42.2, 29.7, 28.4, 25.8, 25.6 ppm; GC-MS $m/z = 216$ (M^+); ^1H and ^{13}C NMR spectral data are in good agreement with the literature data.²⁶



Data for Table 3.4, Compound **8f**, Major

diastereomer(α): ^1H NMR (400 MHz, CDCl_3) δ 7.14-7.20 (m, 1H), 6.67-6.75 (m, 3H), 5.08 (s, 1H), 3.78 (s, 3H), 3.36 (dd, $J = 14.2, 5.6$ Hz, 1H),

2.56-2.68 (m, 1H), 2.44-2.53 (m, 3H), 2.26-2.40 (m, 3H), 2.09 (s, 3H), 1.00-2.05 (brm, 12H), 0.97(s, 3H), 0.6-0.95 (brm, 4H), 0.58 (s, 3H) ppm; ^{13}C NMR (400 MHz, CDCl_3) δ 211.9, 209.6, 159.5, 142.1, 129.2, 121.4, 114.8, 111.0, 63.7, 56.4, 55.1, 53.7, 48.2, 48.0, 45.8, 44.9, 44.2, 38.9, 36.4, 35.3, 35.2, 31.6, 31.5, 28.5, 24.4, 22.8, 21.5, 13.4, 12.4 ppm; GC-MS $m/z = 433$ (M^+); Anal. Calcd for $\text{C}_{29}\text{H}_{38}\text{O}_3$: C, 80.14; H, 8.81. Found: C, 80.40; H, 8.62; **Minor diastereomer (2β):** ^1H NMR (400 MHz, CDCl_3) δ 7.14-7.20 (m, 1H), 6.67-6.75 (m, 3H), 5.73 (s, 1H), 3.78 (s, 3H), 3.42 (dd, $J = 13.4, 3.6$ Hz, 1H), 2.45-2.74 (m, 6H), 2.25-2.44 (m, 5H), 2.09 (s, 3H), 1.00-2.05 (brm, 12H), 1.01 (s, 3H), 0.6-0.95 (brm, 4H), 0.61 (s, 3H) ppm; ^{13}C NMR (400 MHz, CDCl_3) δ 211.9, 209.6, 159.5, 142.1, 129.2, 121.4, 114.8, 111.0, 63.7, 56.4, 55.1, 53.7, 48.2, 48.0, 45.8, 44.9, 44.2, 38.9, 36.4, 35.3, 35.2, 31.6, 31.5, 28.5, 24.4, 22.8, 21.5, 13.4, 12.4 ppm; GC-MS $m/z = 433$ (M^+); Anal. Calcd for $\text{C}_{29}\text{H}_{38}\text{O}_3$: C, 80.14; H, 8.81. Found: C, 80.40; H, 8.62



Data for Table 3.4, Compound **8g**

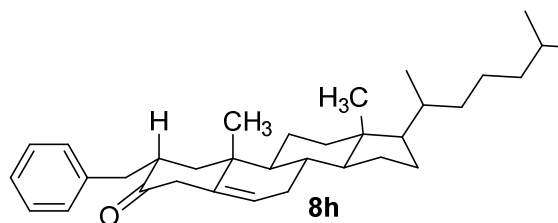
(16α : 16β 2:1 Diastereomeric mixture):Major

Diastereomer **16 α** : ^1H NMR (400 MHz, CDCl_3) δ 7.20 (t, $J = 7.9$ Hz, 1H), 7.14 (t, $J = 8.4$ Hz, 1H), 6.72-6.80 (m, 3H), 6.60-6.66 (m,

1H), 6.54-6.60 (m, 1H), 4.96 (bs, 1H), 3.79 (s, 3H), 3.12 (dd, $J = 13.9, 4.1$ Hz, 1H), 2.77-2.90 (m, 2H), 3.12 (dd, $J = 13.6, 10.2$ Hz, 1H), 1.22-2.44 (brm, 14H), 0.95(s, 3H) ppm; ^{13}C

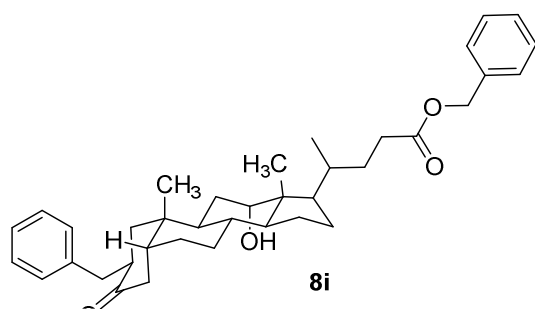
NMR (400 MHz, CDCl₃) δ 229.1, 168.6, 162.5, 150.9, 147.0, 140.8, 138.1, 135.2, 130.1, 123.9, 123.4, 121.4, 120.3 ppm; (rest of the carbons not assigned) GC-MS m/z = 390 (M⁺); Minor Diastereomer **16 β** : ¹H NMR (400 MHz, CDCl₃) δ 7.20 (t, J = 7.9 Hz, 1H), 7.14 (t, J = 8.4 Hz, 1H), 6.72-6.80 (m, 3H), 6.60-6.66 (m, 1H), 6.54-6.60 (m, 1H), 4.96 (bs, 1H), 3.79 (s, 3H), 3.21 (dd, J = 13.4, 3.9 Hz, 1H), 2.60 (dd, J = 13.5, 10 Hz, 1H), 1.22-2.44 (brm, 14H), 0.91 (s, 3H) ppm; δ 229.1, 168.6, 162.5, 150.9, 147.0, 140.8, 138.1, 135.2, 130.1, 123.9, 123.4, 121.4, 120.3 ppm (rest of the carbons not assigned) GC-MS m/z = 390 (M⁺); ¹H and ¹³C NMR spectral data are in good agreement with the literature data.²⁷

Data for Table 3.4, Compound **8h**: ¹H NMR (400 MHz, CDCl₃) δ 7.30-7.10 (m, 5H), 5.73 (d, J = 2.0 Hz, 1H), 3.46 (dd, J = 14.2, 4.0 Hz, 1H), 2.60 (dddd, J = 13.4, 9.1,



4.7, 3.8 Hz, 1H), 2.42 (dd, J = 14.0, 9.1 Hz, 1H), 2.35-2.20 (m, 2H), 2.10-1.93 (m, 3H), 1.90 (dd, J = 13.2, 4.7 Hz, 1H), 1.85-0.80 (br m, 19H), 1.06 (s, 3H), 0.86 (s, 3H), 0.85

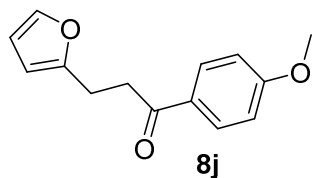
(s, 3H), 0.65 (s, 3H) ppm; ¹³C {¹H} NMR (400 MHz, CDCl₃) δ 200.3, 170.6, 140.3, 129.1, 128.3, 125.8, 123.4, 56.1, 55.8, 54.1, 43.7, 42.2, 41.3, 39.5, 39.1, 36.1, 35.7, 35.4, 35.0, 32.5, 31.9, 28.1, 28.0, 24.1, 23.8, 22.8, 22.6, 20.8, 18.6, 17.3, 11.9 ppm; GC-MS m/z = 474 (M⁺); [α]_D²⁰ = +10.8 (c = 2 in CH₂Cl₂); Anal. Calcd for C₃₄H₅₀O: C, 86.01; H, 10.62. Found: C, 86.51; H, 10.12.



Data for Table 3.4, Compound **8i**:

^1H NMR (600 MHz, CDCl_3) δ 7.41-6.99 (m, 10H), 5.02 (d, $J = 6.6$ Hz, 2H), 3.79 (s, 1H), 3.15 (dd, $J = 14.1, 4.2$ Hz, 1H), 2.72 (t, $J = 13.4$ Hz, 1H), 2.64 (dddd, $J = 13.9,$

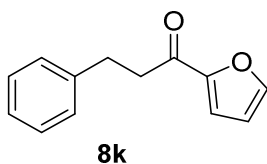
9.1, 4.4, 4.4 Hz, 1H), 2.38-2.28 (m, 2H), 2.26-2.11 (m, 3H), 2.00 (dd, $J = 14.2, 4.2$ Hz, 1H), 1.89-0.91 (br m, 19H), 0.87 (d, $J = 6.0$ Hz, 3H), 0.83 (s, 3H), 0.54 (s, 3H) ppm; $^{13}\text{C}\{^1\text{H}\}$ NMR (400 MHz, CDCl_3) δ 213.3, 174.0, 140.5, 136.1, 129.0, 128.5, 128.3, 128.2, 126.0, 66.1, 48.1, 47.2, 46.9, 46.4, 45.8, 43.5, 42.9, 35.6, 35.2, 35.0, 34.7, 34.4, 31.3, 30.8, 28.9, 27.4, 26.5, 23.5, 22.3, 17.4, 12.7 ppm; muldi $m/z = 570$ (M^+); $[\alpha]_D^{20} = +12.8$ ($c = 2$ in CH_2Cl_2); Anal. Calcd for $\text{C}_{38}\text{H}_{50}\text{O}_4$: C, 79.96; H, 8.83. Found: C, 79.37; H, 8.57.



Data for Table 3.4, Compound **8j**: ^1H NMR (400

MHz, CDCl_3) δ 7.95 (d, $J = 8.8$ Hz, 2H), 7.30 (dd, $J = 1.8, 0.7$ Hz, 1H), δ 6.93 (d, $J = 8.8$ Hz, 2H), 6.27 (dd, $J = 3.1, 1.8$ Hz, 1H), 6.04 (dd, $J = 3.1, 0.7$ Hz, 1H), 3.86 (s, 3H), 3.28

(t, $J = 7.9$ Hz, 2H), 3.07 (t, $J = 7.9$ Hz, 2H) ppm; ^{13}C NMR (400 MHz, CDCl_3) δ 197.2, 163.4, 154.9, 141.0, 130.3, 129.8, 113.7, 110.2, 105.2, 55.4, 36.5, 22.6 ppm; GC-MS $m/z = 230$ (M^+). ^1H and ^{13}C NMR spectral data are in good agreement with the literature data.²⁸



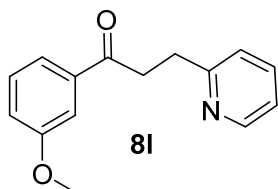
Data for Table 3.4, Compound **8k**: ^1H NMR (400 MHz,

CDCl_3) δ 7.56 (dd, $J = 1.7, 0.7$ Hz, 1H), 7.18-7.32 (m, 5H), 7.17 (dd, $J = 3.5, 0.7$ Hz, 1H), 6.51 (dd, $J = 3.5, 1.7$ Hz, 1H), 3.15 (t, $J = 7.5$ Hz, 2H), 3.04 (t, $J = 7.5$ Hz, 2H) ppm; ^{13}C NMR (400

MHz, CDCl_3) δ 188.6, 152.6, 146.5, 141.0, 128.6, 128.5, 126.2, 117.2, 112.3, 40.2, 20.0

ppm; GC-MS $m/z = 200$ (M^+); Anal. Calcd for $C_{13}H_{12}O_2$: C, 77.98; H, 6.04. Found: C, 77.80; H, 6.02.

Data for Table 3.4, Compound **8I**: 1H NMR (400 MHz, $CDCl_3$) δ 8.54–8.48 (m,



1H) 7.64–7.55 (m, 2H), 7.51–7.48 (m, 1H), 7.34 (t, $J = 8.1$ Hz,

1H), 7.29–7.25 (m, 1H), 7.14–7.06 (m, 2H), 3.83 (s, 3H), 3.50

(t, $J = 7.3$ Hz, 2H), 3.23 (t, $J = 7.3$ Hz, 2H) ppm; ^{13}C NMR (400

MHz, $CDCl_3$) δ 199.0, 160.5, 159.7, 148.8, 138.1, 136.6, 129.5,

123.5, 121.3, 120.7, 119.6, 112.0, 55.3, 37.9, 31.8 ppm; GC-MS $m/z = 241$ (M^+); Anal.

Calcd for $C_{15}H_{15}NO_2$: C, 74.67; H, 6.27. Found: C, 74.20; H, 6.52.

6.2 Synthesis and Mechanistic studies of Decarboxylative and Deaminative Coupling Reactions of Amino Acids with Ketones

6.2.1 Catalyst Screening for the Alkylation of 4-methoxyacetophenone with L-leucine.

In a glove box, 4-methoxyacetophenone (150 mg, 1.0 mmol), L-leucine (157 mg, 1.2 mmol), cyclopentene (7 mg, 10 mol %) and a catalyst (3 mol %) were dissolved in toluene (2 mL) in a 25 mL Schlenk tube equipped with a Teflon stopcock and a magnetic stirring bar. The tube was brought out of the glove box, and was stirred in an oil bath set at 120 °C for 8 h. The reaction tube was taken out of the oil bath, and cooled to room temperature. After filtering through a short silica gel column (280–400 mesh; CH_2Cl_2 , 10 mL), the resulting solution was analyzed by GC and GC-MS. The results are summarized in Table 3.9.

6.2.2. General Procedure for the Coupling Reaction of an Amino Acid with a Ketone.

In a glove box, an amino acid (1.2 mmol), a ketone (1.0 mmol), cyclopentene (0.1 mmol) and **complex 1** (17 mg, 3 mol %) were dissolved in toluene (2 mL) in a 25 mL

Schlenk tube equipped with a Teflon stopcock and a magnetic stirring bar. The tube was brought out of the glove box, and was stirred in an oil bath set at 120 °C for 6-12 h. The reaction tube was taken out of the oil bath, and was cooled to room temperature. After the tube was open to air, the solution was filtered through a short silica gel column by eluting with CH₂Cl₂ (10 mL), and the filtrate was analyzed by GC and GC-MS. Analytically pure product was isolated by a simple column chromatography on silica gel (280-400 mesh, hexanes/EtOAc = 40:1 to 1:1). The products were completely characterized by NMR and GC-MS spectroscopic methods.

6.2.3. H/D Exchange Reaction of Acetophenone-*d*₈ with (*S*)-Leucine.

In a glove box, C₆D₅COCD₃ (1.0 mmol), (*S*)-leucine (1.2 mmol), cyclopentene (0.1 mmol) and **complex 1** (18 mg, 3 mol %) were dissolved in toluene (2 mL) in a 25 mL Schlenk tube equipped with a Teflon stopcock and a magnetic stirring bar. The tube was brought out of the glove box, and was stirred in an oil bath set at 120 °C for 8 h. The reaction tube was taken out of the oil bath, and was immediately cooled in a dry ice/acetone bath. After the tube was open to air, the solution was filtered through a short silica gel column by eluting with CH₂Cl₂ (10 mL), and the filtrate was analyzed by GC and GC-MS. Analytically pure product **14m-d** and unreacted acetophenone substrate were isolated by a simple column chromatography on silica gel (280-400 mesh, hexanes/EtOAc = 40:1). The ¹H and ²H NMR of **14m-d** showed extensive H/D exchange at *ortho*-arene C-H (δ 7.95) as well as α-CH₂ (δ 2.93) and β-CH₂ (δ 1.24) positions (Figure 3.6).

6.2.4 Carbon Isotope Effect Study.

In a glove box, acetophenone (1.5 g, 10 mmol), (*S*)-leucine (1.6 g, 12 mmol), cyclopentene (70 mg, 1 mmol) and **complex 1** (180 mg, 3 mol %) were dissolved in toluene

(20 mL) in a 100 mL Schlenk tubes equipped with a Teflon screw cap stopcock and a magnetic stirring bar. The tube was brought out of the box, and were stirred for 4 h (4.5 h and 5 h for the repeated runs), in an oil bath which was set at 120 °C. The product 1-(4-methoxyphenyl)-5-methyl-1-hexanone (**14m**) was isolated by a column chromatography on silica gel (hexanes/EtOAc = 40:1 to 10:1). The product conversion was determined separately by GC after filtering the crude mixture through a short silica gel column and eluting with CH₂Cl₂ (20 mL) (15, 18 and 20% conversions).

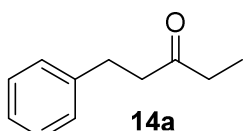
The ¹³C{¹H} NMR analysis of the isolated product **14m** was performed by following Singleton's NMR method.^{S1} The sample was prepared identically by dissolving 100 mg of the isolated **14m** in CDCl₃ (0.5 mL) in a 5 mm high precision NMR tube. The ¹³C{¹H} NMR spectra were recorded with H-decoupling and 45 degree pulses. A 60 s delay between pulses was imposed to minimize *T*₁ variations (d1 = 60 s, at = 5.0 s, np = 245098, nt = 704). The data are summarized in Table 3.12

6.2.5 . Hammett Study.

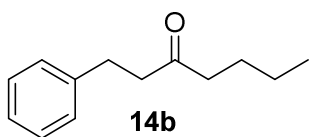
In a glove box, *p*-X-C₆H₄COCH₃ (X = NH₂, CH₃, H, Cl, Br, CN) (0.25 mmol), (*S*)-leucine (0.30 mmol), cyclopentene (10 mol %) and **complex 1** (5 mg, 3 mol %) were dissolved in toluene-*d*₈ (0.5 mL) in six separate J-Young NMR tubes, each equipped with a Teflon screw cap stopcock. The tubes were brought out of the box, and immersed in an oil bath preset at 120 °C. The reaction rate was measured by monitoring the appearance of product signals on ¹H NMR, which were normalized against the internal standard (C₆Me₆) in 30 min intervals for 2-4 h of the reaction time. The *k*_{obs} was determined from a first-

order plot of $-\ln([p\text{-X-C}_6\text{H}_4\text{COCH}_3]_t/[p\text{-X-C}_6\text{H}_4\text{COCH}_3]_0)$ vs time. The Hammett plot of $\log(k_X/k_H)$ versus σ_p is shown in Figure 3.4.

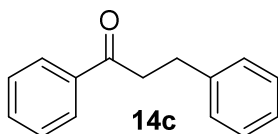
6.2.6 . Characterization Data of the Products.



Data for **14a**: ^1H NMR (400 MHz, CDCl_3) δ 7.31-7.28 (m, 2H), 7.20-7.17 (m, 3H), 2.92 (t, $J = 7.6$ Hz, 2H), 2.73 (t, $J = 7.6$ Hz, 2H), 2.40 (q, $J = 7.5$ Hz, 2H), 1.06 (t, $J = 7.5$ Hz, 3H) ppm; $^{13}\text{C}\{^1\text{H}\}$ NMR (400 MHz, CDCl_3) δ 208.0, 134.3, 129.3, 128.4, 126.7, 35.9, 31.9, 30.6, 22.7 ppm; GC-MS $m/z = 162$ (M^+). The ^1H and ^{13}C spectroscopic data are in good agreement with the literature data.²⁴



Data for **14b**: ^1H NMR (400 MHz, CDCl_3) δ 7.22-7.02 (m, 5H), 2.79 (t, $J = 8.1$ Hz, 2H), 2.62 (t, $J = 8.1$ Hz, 2H), 2.28 (t, $J = 7.5$ Hz, 2H), 1.44 (p, $J = 7.5$ Hz, 2H), 1.18 (sextet, $J = 7.5$ Hz, 2H), 0.78 (t, $J = 7.5$ Hz, 1H) ppm; $^{13}\text{C}\{^1\text{H}\}$ NMR (400 MHz, CDCl_3) δ 210.7, 141.6, 128.9, 128.8, 126.5, 44.7, 43.2, 30.2, 26.3, 22.8, 14.3 ppm; GC-MS $m/z = 190$ (M^+). The ^1H and ^{13}C spectroscopic data are in good agreement with the literature data.²⁴



Data for **14c**: ^1H NMR (400 MHz, CDCl_3) δ 7.95 (d, $J = 7.9$ Hz, 2H), 7.55 (t, $J = 7.4$ Hz, 1H), 7.45 (t, $J = 7.7$ Hz, 2H), 7.31-7.18 (m, 5H), 3.30 (t, $J = 7.7$ Hz, 2H), 3.07 (t, $J = 7.7$ Hz, 2H) ppm; $^{13}\text{C}\{^1\text{H}\}$ NMR (400 MHz, CDCl_3) δ 196.9, 138.8, 134.3, 130.7, 126.2, 126.1, 126.0, 125.6, 123.7, 27.6, 27.5 ppm; GC-MS $m/z = 210$ (M^+). The ^1H and ^{13}C spectroscopic data are in good agreement with the literature data.²⁵

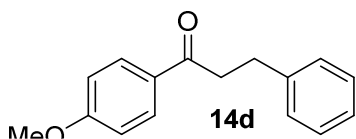


Table 3.9 Compound **14d**: ^1H NMR (400 MHz, CDCl_3) δ 7.88 (d, $J = 9.0$ Hz, 2H), 7.26-7.11 (m, 5H), 6.86 (d, $J = 9.0$ Hz, 2H), 3.79 (s, 3H), 3.30 (t, $J = 8.0$ Hz, 2H),

2.99 (t, $J = 8.0$ Hz, 2H) ppm; $^{13}\text{C}\{^1\text{H}\}$ NMR (400 MHz, CDCl_3) δ 197.8, 163.4, 141.5, 130.3, 129.9, 128.5, 128.4, 126.1, 113.7, 55.5, 40.1, 30.3 ppm; GC-MS $m/z = 240$ (M^+); The ^1H and ^{13}C spectroscopic data are in good agreement with the literature data.²⁶

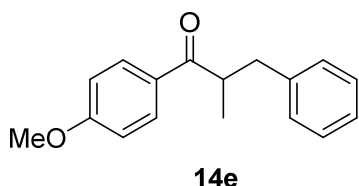


Table 3.9 Compound **14e**: ^1H NMR (400 MHz, CDCl_3) δ 7.92 (d, $J = 8.9$ Hz, 2H), 7.31-7.14 (m, 5H), 6.91 (d, $J = 8.9$ Hz, 2H), 3.86 (s, 3H), 3.75-3.65 (m, 1H), 3.15 (dd, $J = 13.7, 6.5$ Hz, 1H), 2.68 (dd, $J = 13.7, 6.5$ Hz, 1H),

1.19 (d, $J = 6.7$ Hz, 3H) ppm; $^{13}\text{C}\{^1\text{H}\}$ NMR (400 MHz, CDCl_3) δ 202.2, 163.3, 140.1, 130.6, 129.3, 129.0, 128.3, 126.1, 113.7, 55.5, 42.3, 39.4, 17.6 ppm; GC-MS $m/z = 254$ (M^+). The ^1H and ^{13}C spectroscopic data are in good agreement with the literature data.²⁶

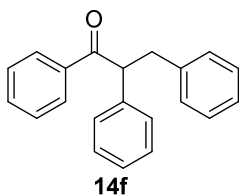
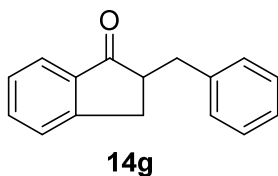
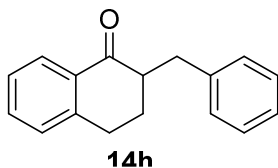


Table 3.9 Compound **14f**: ^1H NMR (400 MHz, CDCl_3) δ 7.85-7.30 (m, 6H), 7.21-6.96 (m, 9H), 4.73 (t, $J = 7.4$ Hz, 1H), 3.49 (dd, $J = 13.8, 7.8$ Hz, 1H), 2.99 (dd, $J = 13.8, 7.8$ Hz, 1H) ppm; $^{13}\text{C}\{^1\text{H}\}$ NMR (400 MHz, CDCl_3) δ 199.3, 139.7, 139.0, 132.8, 129.1, 129.0, 128.8, 128.6, 128.4, 128.2, 128.2, 127.1, 126.1, 55.9, 40.1 ppm; GC-MS $m/z = 286$ (M^+). The ^1H and ^{13}C spectroscopic

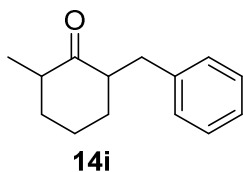
data are in good agreement with the literature data.²⁷

Table 3.9 Compound **7g**: ^1H NMR (400 MHz, CDCl_3)

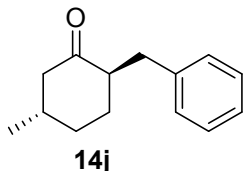
δ 7.79 (d, $J = 7.7$ Hz, 1H), 7.42-7.27 (m, 7H), 3.41 (dd, $J = 14.0$, 4.4 Hz, 1H), 3.17 (dd, $J = 17.2$, 7.7 Hz, 1H), 3.01 (dddd, $J = 10.5$, 7.7, 4.4, 4.0 Hz, 1H), 2.86 (dd, $J = 17.2$, 4.0 Hz, 1H), 2.66 (dd, $J = 14.0$, 10.5 Hz, 1H) ppm; $^{13}\text{C}\{^1\text{H}\}$ NMR (400 MHz, CDCl_3) δ 207.8, 153.6, 139.6, 136.5, 134.8, 128.9, 128.5, 127.4, 126.6, 126.3, 124.0, 48.9, 37.0, 32.1 ppm; GC-MS $m/z = 222$ (M^+). The ^1H and ^{13}C spectroscopic data are in good agreement with the literature data.²⁸

Table 3.9 Compound **14h**: ^1H NMR (400 MHz, CDCl_3)

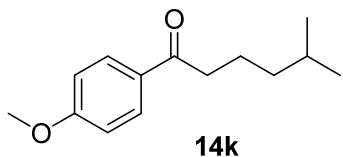
δ 8.05 (d, $J = 7.8$ Hz, 1H), 7.45 (dt, $J = 7.1$, 1.2 Hz, 1H), 7.32-7.19 (m, 7H), 3.48 (dd, $J = 13.4$, 3.7 Hz, 1H), 2.95-2.89 (m, 2H), 2.74-2.59 (m, 1H), 2.62 (dd, $J = 13.4$, 9.6 Hz, 1H), 2.09 (dq, $J = 13.4$, 4.4 Hz, 1H), 1.84-1.70 (m, 1H) ppm; ^{13}C NMR (400 MHz, CDCl_3) δ 201.7, 144.0, 140.1, 133.2, 129.7, 128.7, 128.4, 127.5, 126.5, 126.1, 103.6, 49.5, 35.7, 28.6, 27.6 ppm; GC-MS $m/z = 236$ (M^+). The ^1H and ^{13}C spectroscopic data are in good agreement with the literature data.²⁸

Table 3.9 Compound **14i**: ^1H NMR (600 MHz, CDCl_3) δ 

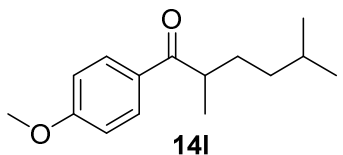
7.30-7.23 (m, 2H), 7.21-7.13 (m, 3H), 3.23 (dd, $J = 13.9$, 5.0 Hz, 1H), 2.55 (dddd, $J = 13.9$, 12.9, 8.6, 5.1, 5.0, 1.3 Hz, 1H), 2.48-2.35 (m, 2H), 1.84-1.75 (m, 1H), 1.66 (qt, $J = 13.8$, 3.8 Hz, 1H), 1.34 (pt, $J = 12.9$, 3.8 Hz, 2H), 1.03 (d, $J = 6.3$ Hz, 3H) ppm; $^{13}\text{C}\{^1\text{H}\}$ NMR (600 MHz, CDCl_3) δ 213.8, 140.8, 129.1, 128.2, 125.9, 52.7, 45.7, 37.4, 35.5, 34.7, 25.6, 25.5 ppm; GC-MS $m/z = 202$ (M^+). The ^1H and ^{13}C spectroscopic data are in good agreement with the literature data.^{29,30}

Table 3.9 Compound **14j**: ^1H NMR (600 MHz, CDCl_3) δ 

7.30-7.23 (m, 2H), 7.21-7.13 (m, 3H), 3.24 (dd, $J = 14.0, 4.6$ Hz, 1H), 2.47 (dddd, $J = 12.9, 9.0, 4.6, 1.4, 1.3$ Hz, 1H), 2.43-2.33 (m, 2H), 2.09-1.96 (m, 1H), 1.93-1.76 (m, 1H), 1.38-1.22 (m, 2H), 1.01 (d, $J = 6.3$ Hz, 3H) ppm; $^{13}\text{C}\{^1\text{H}\}$ NMR (400 MHz, CDCl_3) δ 212.0, 140.5, 129.1, 128.2, 125.9, 51.6, 50.5, 35.7, 35.2, 33.9, 32.4, 22.3 ppm; GC-MS $m/z = 202$ (M^+). The ^1H and ^{13}C spectroscopic data are in good agreement with the literature data.³¹

Table 3.9 Compound **14k**: ^1H NMR (400 MHz,

CDCl_3) δ 7.94 (d, $J = 9.0$ Hz, 2H), 6.93 (d, $J = 9.0$ Hz, 2H), 3.86 (s, 3H), 2.88 (t, $J = 7.6$ Hz, 2H), 1.76-1.66 (m, 2H), 1.62-1.52 (m, 1H), 1.30-1.21 (m, 2H), 0.89 (d, $J = 6.5$ Hz, 6H) ppm; $^{13}\text{C}\{^1\text{H}\}$ NMR (400 MHz, CDCl_3) δ 199.2, 163.2, 130.3, 130.1, 113.6, 55.4, 38.6, 38.5, 27.9, 22.5, 22.4 ppm; GC-MS $m/z = 220$ (M^+); Anal. Calcd for $\text{C}_{14}\text{H}_{20}\text{O}_2$: C, 76.33; H, 9.15. Found: C, 76.70; H, 9.38.

Table 3.9 Compound **14l**: ^1H NMR (400 MHz,

CDCl_3) δ 7.94 (d, $J = 9.0$ Hz, 2H), 6.93 (d, $J = 9.0$ Hz, 2H), 3.86 (s, 3H), 3.47-3.31 (m, 1H), 1.61-1.35 (m, 5H), 1.17 (d, $J = 6.6$ Hz, 3H), 0.86 (d, $J = 6.6$ Hz, 3H), 0.84 (d, $J = 6.6$ Hz, 3H) ppm; $^{13}\text{C}\{^1\text{H}\}$ NMR (400 MHz, CDCl_3) δ 203.2, 163.3, 130.5, 128.9, 113.7, 55.4, 40.4, 36.7, 31.7, 22.6, 22.4, 17.5 ppm; GC-MS $m/z = 234$ (M^+); Anal. Calcd for $\text{C}_{15}\text{H}_{22}\text{O}_2$: C, 76.88; H, 9.46. Found: C, 76.58; H, 9.04.

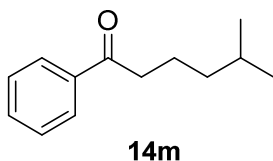


Table 3.9 Compound **14m**: ^1H NMR (400 MHz, CDCl_3) δ 7.96 (dd, $J = 8.3, 1.4$ Hz, 2H), 7.54 (t, $J = 7.3$ Hz, 1H), 7.46 (t, $J = 7.4$ Hz, 2H), 2.95 (t, $J = 7.3$ Hz, 2H), 1.80-1.70 (m, 2H), 1.64-1.54 (m, 1H), 1.33-1.23 (m, 2H), 0.80 (t, $J = 6.4$ Hz, 6H); $^{13}\text{C}\{^1\text{H}\}$ NMR (400 MHz, CDCl_3) δ 200.8, 137.2, 133.0, 128.7, 128.2, 39.0, 38.8, 28.1, 22.7, 22.4 ppm; GC-MS $m/z = 190$ (M^+). The ^1H and ^{13}C spectroscopic data are in good agreement with the literature data.²⁴

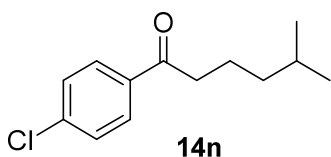


Table 3.9 Compound **14n**: ^1H NMR (400 MHz, CDCl_3) δ 7.89 (d, $J = 8.7$ Hz, 2H), 7.42 (d, $J = 8.7$ Hz, 2H), 2.91 (t, $J = 7.4$ Hz, 2H), 1.58 (septet, $J = 7.0$ Hz, 1H), 1.28-1.21 (m, 2H), 0.89 (d, $J = 6.6$ Hz, 6H) ppm; $^{13}\text{C}\{^1\text{H}\}$ NMR (400 MHz, CDCl_3) δ 199.3, 139.2, 135.3, 129.5, 128.9, 38.8, 38.5, 27.9, 22.5, 22.1 ppm; GC-MS $m/z = 224$ (M^+); Anal. Calcd for $\text{C}_{13}\text{H}_{17}\text{ClO}$: C, 69.48; H, 7.62. Found: C, 69.07; H, 7.20.

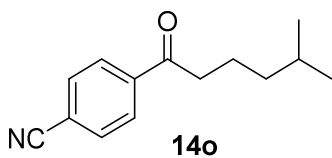


Table 3.9 Compound **14o**: ^1H NMR (400 MHz, CDCl_3) δ 8.03 (d, $J = 8.8$ Hz, 2H), 7.76 (d, $J = 8.8$ Hz, 2H), 3.0 (t, $J = 7.2$ Hz, 2H), 1.79-1.68 (m, 2H), 1.64-1.53 (m, 1H), 1.30-1.21 (m, 2H), 0.88 (d, $J = 6.7$ Hz, 6H) ppm; $^{13}\text{C}\{^1\text{H}\}$ NMR (400 MHz, CDCl_3) δ 199.1, 134.0, 132.5, 128.4, 118.0, 116.2, 39.1, 38.4, 27.9, 22.5, 21.9 ppm; GC-MS $m/z = 215$ (M^+); Anal. Calcd for $\text{C}_{14}\text{H}_{17}\text{NO}$: C, 78.10; H, 7.96. Found: C, 77.79; H, 8.03.

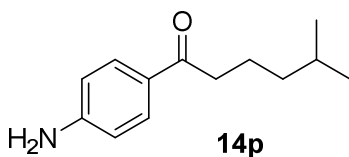


Table 3.9 Compound **14p**: ^1H NMR (400 MHz, CDCl_3) δ 7.81 (d, $J = 8.8$ Hz, 2H), 6.64 (d, $J = 8.8$ Hz, 2H), 4.10 (br s, 1H), 2.83 (t, $J = 7.5$ Hz, 2H), 1.75-1.51 (m,

3H), 1.28-1.19 (m, 2H), 0.88 (d, $J = 3.5$ Hz, 6H) ppm; $^{13}\text{C}\{^1\text{H}\}$ NMR (400 MHz, CDCl_3) δ 199.0, 150.9, 130.5, 127.7, 113.8, 38.7, 38.2, 27.9, 22.7, 22.6 ppm; GC-MS $m/z = 205$ (M^+); Anal. Calcd for $\text{C}_{13}\text{H}_{19}\text{NO}$: C, 76.06; H, 9.33. Found: C, 75.72; H, 8.99.

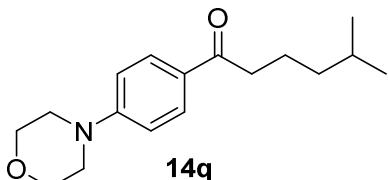


Table 3.9 Compound **14q**: ^1H NMR (400

MHz, CDCl_3) δ 7.89 (d, $J = 9.0$ Hz, 2H), 6.86 (d, $J = 9.0$ Hz, 2H), 3.84 (t, $J = 5.0$ Hz, 4H), 3.29 (t, $J = 5.0$ Hz, 4H), 2.85 (t, $J = 7.7$ Hz, 2H), 1.75-1.65 (m, 2H),

1.57 (nonet, $J = 6.8$ Hz, 1H), 1.28-1.20 (m, 2H), 0.88 (d, $J = 6.8$ Hz, 6H) ppm; $^{13}\text{C}\{^1\text{H}\}$ NMR (400 MHz, CDCl_3) δ 199.1, 154.1, 130.1, 120.0, 113.3, 66.6, 47.6, 38.7, 38.3, 27.9, 22.7, 22.6 ppm; GC-MS $m/z = 275$ (M^+); Anal. Calcd for $\text{C}_{17}\text{H}_{25}\text{NO}_2$: C, 74.14; H, 9.15. Found: C, 74.59; H, 8.79.

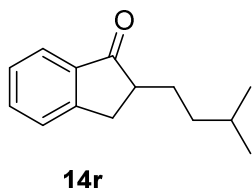


Table 3.9 Compound **14r**: ^1H NMR (400 MHz,

CDCl_3) δ 7.74 (d, $J = 8.3$ Hz, 1H), 7.57 (t, $J = 7.5$ Hz, 1H), 7.44 (d, $J = 7.6$ Hz, 1H), 7.35 (t, $J = 7.6$ Hz, 1H), 3.31 (dd, $J = 17.2, 7.9$ Hz, 1H), 2.80 (dd, $J = 17.2, 3.9$ Hz, 1H), 2.62

(dddd, $J = 11.0, 8.0, 4.5, 4.0$ Hz, 1H), 1.96 (dddd, $J = 13.2, 10.0, 7.0, 4.4$ Hz, 1H), 1.56 (septet, $J = 6.6$ Hz, 1H), 1.43 (dddd, $J = 13.2, 10.0, 8.8, 5.7$ Hz, 1H), 1.29 (m, 2H), 0.90 (d, $J = 6.0$ Hz, 3H), 0.88 (d, $J = 6.3$ Hz, 3H) ppm; $^{13}\text{C}\{^1\text{H}\}$ NMR (400 MHz, CDCl_3) δ 209.1, 153.8, 136.9, 134.6, 127.3, 126.5, 123.9, 47.6, 36.6, 32.9, 29.3, 28.2, 22.7, 22.5 ppm; GC-MS $m/z = 202$ (M^+). The ^1H and ^{13}C spectroscopic data are in good agreement with the literature data.²³

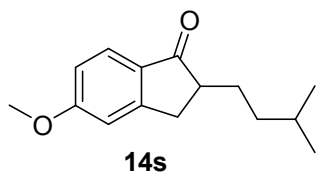


Table 3.9 Compound **14s**: ^1H NMR (400 MHz, CDCl_3) δ 7.68 (d, $J = 8.4$ Hz, 1H), 6.91-6.81 (m, 2H), 3.88 (s, 3H), 3.25 (dd, $J = 17.3, 7.8$ Hz, 1H), 2.74 (dd, $J = 17.3, 3.9$ Hz, 1H), 2.61 (dddd, $J = 11.8, 9.4, 7.9, 3.9$ Hz, 1H), 1.94 (dddd, $J = 13.2, 10.0, 7.0, 4.2$ Hz, 1H), 1.48-1.35 (m, 1H), 1.32-1.22 (dddd, $J = 15.0, 13.2, 10.1, 4.2$ Hz, 1H), 0.90 (d, $J = 6.0$ Hz, 3H), 0.88 (t, $J = 6.4$ Hz, 3H) ppm; $^{13}\text{C}\{^1\text{H}\}$ NMR (400 MHz, CDCl_3) δ 207.3, 165.2, 156.7, 130.1, 125.5, 115.2, 109.6, 55.6, 47.7, 36.5, 32.9, 29.5, 28.1, 22.6, 22.5 ppm; GC-MS $m/z = 232$ (M^+); Anal. Calcd for $\text{C}_{15}\text{H}_{20}\text{O}_2$: C, 77.55; H, 8.68. Found: C, 77.77; H, 8.86.

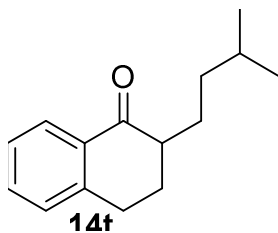


Table 3.9 Compound **14t**: ^1H NMR (400 MHz, CDCl_3) δ 8.10 (dd, $J = 7.5, 1.6$ Hz, 1H), 7.57 (td, $J = 7.4, 1.6$ Hz, 1H), 7.33 (td, $J = 7.5, 1.6$ Hz, 1H), 7.25-7.21 (m, 1H), 3.33 (dd, $J = 17.2, 8.0$ Hz, 1H), 2.79 (dd, $J = 17.2, 4.6$ Hz, 1H), 2.74-2.65 (m, 1H), 1.90-1.74 (m, 2H), 1.37-1.23 (m, 1H), 0.97 (d, $J = 6.4$ Hz, 6H) ppm; $^{13}\text{C}\{^1\text{H}\}$ NMR (400 MHz, CDCl_3) δ 209.4, 153.7, 136.7, 134.6, 127.3, 126.5, 123.9, 45.5, 40.6, 33.3, 26.6, 23.5, 21.7 ppm; GC-MS $m/z = 216$ (M^+); Anal. Calcd for $\text{C}_{15}\text{H}_{20}\text{O}$: C, 83.28; H, 9.32. Found: C, 83.00; H, 8.95.

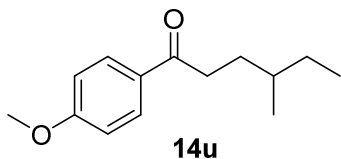


Table 3.9 Compound **14u**: ^1H NMR (400 MHz, CDCl_3) δ 7.94 (d, $J = 9.2$ Hz, 2H), 6.93 (d, $J = 9.2$ Hz, 2H), 3.86 (s, 3H), 2.99-2.83 (m, 2H), 1.80-1.70 (m, 1H), 1.58-1.47 (m, 1H), 1.47-1.33 (m, 2H), 1.27-1.13 (m, 1H), 1.92 (d, $J = 6.5$ Hz, 3H), 0.89 (t, $J = 7.2$ Hz, 3H) ppm; $^{13}\text{C}\{^1\text{H}\}$ NMR (400 MHz, CDCl_3) δ 201.6, 163.3, 130.3, 130.1, 113.7, 55.5, 36.1, 31.2, 29.3, 19.1, 11.4 ppm; GC-MS $m/z =$

220 (M^+). The 1H and ^{13}C spectroscopic data are in good agreement with the literature data.³³

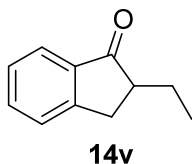


Table 3.9 Compound **14v**: 1H NMR (400 MHz, $CDCl_3$) δ 7.74

(dsextet, $J = 7.7$, 0.6 Hz, 1H), 7.58 (td, $J = 7.7$, 1.3 Hz, 1H), 7.46 (dp, $J = 7.7$, 1.0 Hz, 1H), 7.35 (tq, $J = 7.3$, 1.0 Hz, 1H), 3.32 (dd, $J = 17.3$,

7.8 Hz, 1H), 2.82 (dd, $J = 17.3$, 4.0 Hz, 1H), 2.62 (dddd, $J = 9.0$, 7.8, 4.4, 4.0 Hz, 1H), 1.97 (ddq, $J = 16.5$, 9.0, 7.4 Hz, 1H), 1.54 (ddq, $J = 16.5$, 7.6, 7.4 Hz, 1H), 0.94 (t, $J = 7.4$, 3H) ppm; $^{13}C\{^1H\}$ NMR (400 MHz, $CDCl_3$) δ 209.1, 153.8, 136.8, 134.6, 127.3, 126.6, 123.8, 48.7, 32.3, 24.5, 11.6 ppm; GC-MS $m/z = 160$ (M^+). The 1H and ^{13}C spectroscopic data are in good agreement with the literature data.³⁴

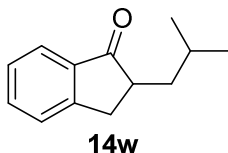


Table 3.9 Compound **14w**: 1H NMR (400 MHz, $CDCl_3$) δ

7.75 (dq, $J = 7.7$, 0.8 Hz, 1H), 7.57 (td, $J = 7.4$, 1.2 Hz, 1H), 7.45 (dp, $J = 7.7$, 1.2 Hz, 1H), 7.36 (tq, $J = 7.4$, 0.8 Hz, 1H) 3.33 (dd, $J = 17.2$,

8.0 Hz, 1H), 2.79 (dd, $J = 17.2$, 4.0 Hz, 1H), 2.70 (dddd, $J = 9.0$, 8.1, 8.0, 4.0 Hz, 1H), 1.90-1.74 (m, 2H), 1.31 (dd, $J = 10.8$, 8.1 Hz, 1H), 0.97 (d, $J = 6.4$, 6H) ppm; ^{13}C NMR (400 MHz, $CDCl_3$) δ 209.4, 153.7, 136.7, 134.6, 127.3, 126.5, 123.9, 45.5, 40.6, 33.3, 26.6, 23.5, 21.8 ppm; GC-MS $m/z = 188$ (M^+). The 1H and ^{13}C spectroscopic data are in good agreement with the literature data.³²

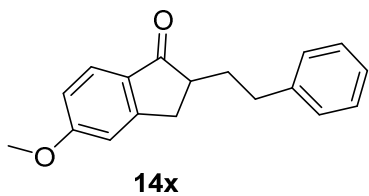


Table 3.9 Compound **14x**: 1H NMR (400 MHz,

$CDCl_3$) δ 7.68 (d, $J = 8.1$ Hz, 1H), 7.33-7.15 (m, 5H), 6.91-6.87 (m, 2H), 3.88 (s, 3H), 3.28 (dd, $J = 17.3$, 7.8 Hz, 1H), 2.85-2.70 (m, 3H), 2.66 (dddd, $J = 12.5$, 8.2,

7.8, 3.6 Hz, 1H), 2.28 (dddd, $J = 13.4$, 9.7, 6.9, 4.6 Hz, 1H), 1.75 (dddd, $J = 13.4$, 9.7, 9.3,

5.7 Hz, 1H) ppm; $^{13}\text{C}\{^1\text{H}\}$ NMR (400 MHz, CDCl_3) δ 206.9, 165.3, 156.5, 141.6, 130.1, 128.5, 128.4, 126.0, 125.5, 115.3, 109.6, 55.6, 46.8, 33.6, 33.4, 33.0 ppm; GC-MS m/z = 266 (M^+); Anal. Calcd for $\text{C}_{18}\text{H}_{18}\text{O}_2$: C, 81.17; H, 6.81. Found: C, 81.61; H, 7.60.

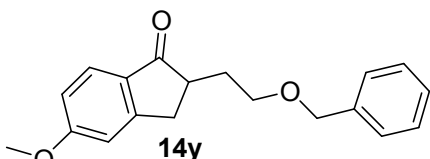
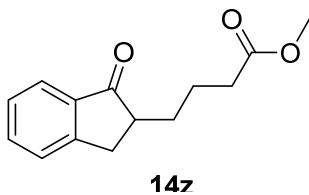


Table 3.9 Compound **14y**: ^1H NMR (400

MHz, CDCl_3) δ 7.66-7.59 (m, 1H), 7.25-7.08 (m, 5H), 6.85-6.79 (m, 1H), 6.75 (m, 1H), 3.81 (s, 2H),

3.79 (s, 3H), 3.38 (dd, J = 14.0, 4.2 Hz, 1H), 3.26 (dd, J = 17.6, 7.9 Hz, 1H), 3.10 (dd, J = 17.3, 7.9 Hz, 1H), 2.99 (dddd, J = 10.3, 7.9, 7.9, 3.9 Hz, 1H), 2.84-2.73 (m, 1H), 2.57 (dd, J = 14.0, 10.7 Hz, 1H), 1.96 (dddd, J = 13.6, 12.0, 7.5, 4.4 Hz, 1H), 1.49-1.30 (m, 1H) ppm; $^{13}\text{C}\{^1\text{H}\}$ NMR (400 MHz, CDCl_3) δ 206.0, 165.4, 139.8, 129.8, 128.9, 128.5, 126.3, 125.7, 125.5, 115.3, 109.6, 55.6, 49.0, 48.9, 37.2, 32.4, 32.2 ppm; GC-MS m/z = 296 (M^+); Anal. Calcd for $\text{C}_{19}\text{H}_{20}\text{O}_3$: C, 77.00; H, 6.80. Found: C, 77.28; H, 7.04.

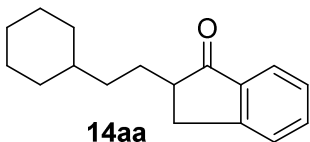
Table 3.9 Compound **14z**: ^1H NMR (400 MHz, CDCl_3)



δ 8.22 (d, J = 7.9 Hz, 1H), 7.72 (t, J = 7.4 Hz, 1H), 7.57 (d, J = 7.9 Hz, 1H), 7.45 (t, J = 7.4 Hz, 1H), 3.66 (s, 3H), 3.34 (dd, J = 17.3, 7.9 Hz, 1H), 2.84 (dd, J = 17.3, 4.1 Hz, 1H), 2.72-2.62

(m, 1H), 2.45-2.30 (m, 2H), 2.02-1.91 (m, 1H), 1.82-1.72 (m, 1H), 1.56-1.43 (m, 2H) ppm; $^{13}\text{C}\{^1\text{H}\}$ NMR (400 MHz, CDCl_3) δ 208.4, 173.8, 153.6, 143.5, 134.8, 127.4, 126.6, 123.9, 51.6, 47.1, 32.8, 30.8, 26.1, 22.8 ppm; GC-MS m/z = 232 (M^+); Anal. Calcd for $\text{C}_{14}\text{H}_{16}\text{O}_3$: C, 72.39; H, 6.94. Found: C, 72.20; H, 6.87.

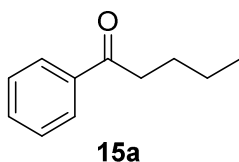
Table 3.9 Compound **14aa**: ^1H NMR (400 MHz,



CDCl_3) δ 7.68 (d, J = 7.6 Hz, 1H), 7.50 (t, J = 7.4 Hz, 1H), 7.38 (d, J = 7.8 Hz, 1H), 7.28 (t, J = 7.5 Hz, 1H), 3.24 (dd, J

= 17.2, 8.0 Hz, 1H), 2.72 (dd, $J = 17.3, 3.6$ Hz, 1H), 2.50 (dddd, $J = 12.7, 8.2, 3.7, 3.7$ Hz, 1H) 2.00-0.80 (m, 15H) ppm; $^{13}\text{C}\{^1\text{H}\}$ NMR (400 MHz, CDCl_3) δ 209.2, 153.8, 136.9, 134.6, 127.3, 126.5, 123.9, 47.7, 37.7, 35.1, 33.4, 33.1, 32.8, 28.8, 26.6, 26.4, 26.3 ppm; GC-MS $m/z = 242$ (M^+); Anal. Calcd for $\text{C}_{17}\text{H}_{22}\text{O}$: C, 84.25; H, 9.15. Found: C, 84.26; H, 8.65.

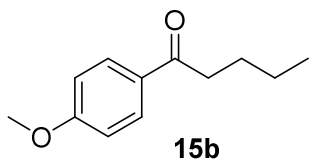
Table 3.10 Compound **15a**: ^1H NMR (400 MHz, CDCl_3)



δ 7.98-7.92 (m, 2H), 7.58-7.51 (m, 1H), 7.47-7.41 (m, 2H), 2.96 (t, $J = 7.6$ Hz, 2H), 1.71 (p, $J = 7.6$ Hz, 2H), 1.41 (sextet, $J = 7.5$ Hz, 2H), 0.95 (t, $J = 7.5$ Hz, 3H); $^{13}\text{C}\{^1\text{H}\}$ NMR (400 MHz,

CDCl_3) δ 199.5, 163.7, 130.7, 130.6, 114.1, 55.8, 40.6, 18.4, 14.3 ppm; GC-MS $m/z = 148$; Anal. Calcd for $\text{C}_{11}\text{H}_{14}\text{O}_2$: C, 74.13; H, 7.92. Found: C, 74.44; H, 8.09. The ^1H and ^{13}C spectroscopic data are in good agreement with the literature data.²⁴

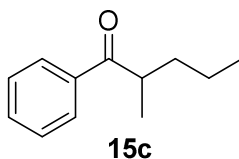
Table 3.10 Compound **15b**: ^1H NMR (400 MHz,



CDCl_3) δ 7.94 (d, $J = 9.3$ Hz, 2H), 6.93 (d, $J = 9.0$ Hz, 2H), 3.86 (s, 3H), 2.91 (t, $J = 7.6$ Hz, 2H), 1.70 (p, $J = 7.4$ Hz, 2H), 1.40 (sextet, $J = 7.7$ Hz, 2H), 0.94 (t, $J = 7.4$ Hz, 3H) ppm;

$^{13}\text{C}\{^1\text{H}\}$ NMR (400 MHz, CDCl_3) δ 201.7, 163.3, 130.3, 130.2, 113.6, 55.4, 38.0, 26.7, 22.5, 13.9 ppm; GC-MS $m/z = 192$ (M^+). The ^1H and ^{13}C spectroscopic data are in good agreement with the literature data.²⁴

Table 3.10 Compound **15c**: ^1H NMR (400 MHz, CDCl_3)



δ 7.96 (m, 2H), 7.55 (m, 1H), 7.46 (m, 2H), 3.49 (sextet, $J = 6.9$ Hz, 1H), 1.78 (m, 1H), 1.36 (m, 3H), 1.19 (d, $J = 6.9$ Hz, 3H), 0.90 (d, $J = 7.2$ Hz, 3H) ppm; $^{13}\text{C}\{^1\text{H}\}$ NMR (400 MHz, CDCl_3) δ

204.8, 136.7, 133.0, 128.8, 128.5, 40.5, 36.1, 20.8, 17.4, 14.4 ppm; GC-MS m/z = 176 (M^+). The ^1H and ^{13}C spectroscopic data are in good agreement with the literature data.³⁵

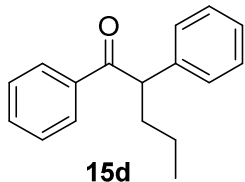
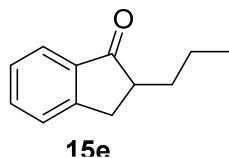


Table 3.10 Compound **15d**: ^1H NMR (400 MHz, CDCl_3)

δ 7.92 (m, 2H), 7.54-7.22 (m, 8H), 4.56 (t, J = 7.3 Hz, 1H), 2.15 (dddd, J = 13.5, 9.9, 7.3, 6.0 Hz, 1H), 1.28 (dddd, J = 13.4, 10.0, 7.3, 5.6 Hz, 1H), 0.92 (t, J = 7.4 Hz, 3H) ppm; $^{13}\text{C}\{^1\text{H}\}$ NMR (400

MHz, CDCl_3) δ 200.1, 139.8, 137.0, 132.8, 128.8, 128.6, 128.4, 128.2, 127.0, 53.4, 36.2, 20.9, 14.1 ppm; GC-MS m/z = 238 (M^+). The ^1H and ^{13}C spectroscopic data are in good agreement with the literature data.³⁶



Compound **15e**: ^1H NMR (400 MHz, CDCl_3) δ 7.74 (d, J =

7.8 Hz, 1H), 7.57 (t, J = 7.4 Hz, 1H), 7.45 (d, J = 7.8 Hz, 1H), 7.36 (t, J = 7.4 Hz, 1H), 3.32 (dd, J = 17.4, 8.0 Hz, 1H), 2.81 (dd, J =

17.4, 4.0 Hz, 1H), 2.67 (dddd, J = 8.0, 7.9, 4.0, 2.7 Hz, 1H), 1.98-1.85 (m, 1H), 1.55-1.37 (m, 3H), 0.95 (t, J = 7.2 Hz, 3H) ppm; $^{13}\text{C}\{^1\text{H}\}$ NMR (400 MHz, CDCl_3) δ 201.6, 134.6, 127.3, 160.4, 136.6, 126.5, 123.8, 47.3, 33.6, 32.9, 20.7, 14.1 ppm; GC-MS m/z = 266 (M^+). The ^1H and ^{13}C spectroscopic data are in good agreement with the literature data.³⁷

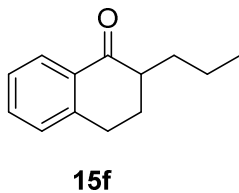
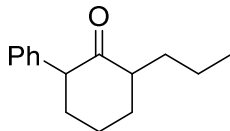


Table 3.10 Compound **15f**: ^1H NMR (400 MHz, CDCl_3) δ

8.04 (dd, J = 7.7, 1.2 Hz, 1H), 7.46 (ddd, J = 7.4, 7.4, 1.5 Hz, 1H), 7.32 (dd, J = 8.0, 7.7 Hz, 1H), 7.24 (d, J = 7.6 Hz, 1H), 3.03-2.98 (m, 2H), 2.49-2.35 (m, 1H), 2.26 (ddd, J = 13.2, 9.5, 4.6 Hz, 1H),

2.06-1.84 (m, 2H), 1.54-1.33 (m, 3H), 0.96 (t, J = 7.5 Hz, 3H) ppm; $^{13}\text{C}\{^1\text{H}\}$ NMR (400 MHz, CDCl_3) δ 200.4, 143.9, 133.0, 132.5, 128.6, 127.4, 126.5, 47.2, 31.5, 28.2, 28.1, 20.2,

14.2 ppm; GC-MS $m/z = 188$ (M^+). The ^1H and ^{13}C spectroscopic data are in good agreement with the literature data.³⁸



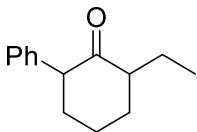
15g dr(10:1)

Table 3.10 Compound **15g(cis)** : ^1H NMR (400 MHz,

CDCl_3) δ 7.49-7.06 (m, 5H), 3.77 (dd, $J = 8.5, 5.6$ Hz, 1H), 2.52-2.44 (m, 1H), 2.32-2.20 (m, 1H), 2.20-2.10 (m, 1H), 2.04-1.95 (m, 1H), 1.94-1.68 (m, 4H), 1.45-1.20 (m, 3H), 0.90 (t, $J = 7.2$

Hz, 3H) ppm; $^{13}\text{C}\{^1\text{H}\}$ NMR (400 MHz, CDCl_3) δ 213.6, 138.5, 128.5, 127.9, 126.7, 54.0, 49.1, 33.1, 32.9, 32.7, 21.1, 20.4, 14.1 ppm; GC-MS $m/z = 216$ (M^+); Anal. Calcd for $\text{C}_{15}\text{H}_{20}\text{O}$: C, 83.28; H, 9.32. Found: C, 83.11; H, 9.66.

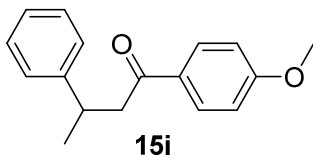
Table 3.10 Compound **15h Major Diastereomer (Cis)**:



15h dr(3:2)

^1H NMR (400 MHz, CDCl_3) δ 3.77 (dd, $J = 8.3, 5.6$ Hz, 1H), 0.90 (t, $J = 7.5$ Hz, 3H) ppm; $^{13}\text{C}\{^1\text{H}\}$ NMR (400 MHz, CDCl_3) δ 213.5, 138.5, 128.5, 127.9, 126.7, 54.0, 51.0, 33.1, 32.5, 23.5, 21.1, 11.7

ppm; GC-MS $m/z = 216$ (M^+). **15h Minor Diastereomer (Trans)**: ^1H NMR (400 MHz, CDCl_3) δ 3.62 (dd, $J = 12.5, 4.8$ Hz, 1H), 0.89 (t, $J = 7.4$ Hz, 3H) ppm; $^{13}\text{C}\{^1\text{H}\}$ NMR (400 MHz, CDCl_3) δ 211.0, 138.7, 128.7, 128.2, 126.8, 58.0, 52.9, 36.7, 34.8, 25.8, 22.3, 11.8 ppm. The ^1H and ^{13}C spectroscopic data are in good agreement with the literature data.³⁹



15i

Table 3.10 Compound **15j**: ^1H NMR (400 MHz,

CDCl_3) δ 7.94 (d, $J = 9.0$ Hz, 2H), 6.92, 7.17-7.34 (m, 5H), (d, $J = 9.0$ Hz, 2H), 3.86 (s, 3H), 3.44 (m, 1H), 3.25 (dd, $J =$

16.4, 5.9 Hz, 1H), 3.14 (dd, $J = 16.4, 8.5$ Hz, 1H), 1.34 (d, $J = 6.9$ Hz, 3H) ppm; $^{13}\text{C}\{^1\text{H}\}$ NMR (400 MHz, CDCl_3) δ 197.7, 163.4, 146.7, 130.4, 130.3, 128.6, 126.9, 126.2, 113.6,

55.6, 46.7, 35.7, 21.9 ppm; GC-MS $m/z = 254$ (M^+). The ^1H and ^{13}C spectroscopic data are in good agreement with the literature data.⁴⁰

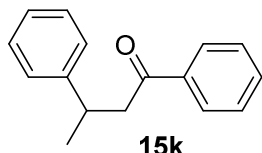


Table 3.10 Compound **15k**: ^1H NMR (400 MHz, CDCl_3)

δ 7.88 (m, 2H), 7.50 (m, 1H), 7.40 (t, 2H, $J = 7.6$ Hz), 7.27-7.21 (m, 4H), 7.15 (m, 1H), 3.49-3.44 (m, 1H), 3.26 (dd, $J = 16.5, 5.5$

Hz, 1H), 3.17-3.13 (m, 1H), 1.31 (d, 3H, $J = 6.9$ Hz) ppm; $^{13}\text{C}\{^1\text{H}\}$ NMR (400 MHz, CDCl_3) δ 199.0, 146.6, 137.3, 132.9, 128.5, 128.5, 128.1, 126.8, 126.3, 47.0, 35.6, 21.8 ppm; GC-MS $m/z = 224$ (M^+). The ^1H and ^{13}C spectroscopic data are in good agreement with the literature data.⁴¹

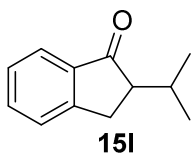


Table 3.10 Compound **15l**: ^1H NMR (400 MHz, CDCl_3) δ 7.73

(dsextet, $J = 7.8, 0.6$ Hz, 1H), 7.57 (td, $J = 7.6, 1.3$ Hz, 1H), 7.47 (td, $J = 7.6, 0.9$ Hz, 1H), 7.35 (dt, $J = 7.6, 0.8$ Hz, 1H), 3.14 (dd, $J = 17.4,$

8.0 Hz, 1H), 2.93 (dd, $J = 17.4, 4.0$ Hz, 1H), 2.67 (ddd, $J = 8.3, 4.3, 4.0$ Hz, 1H), 2.42 (dseptet, $J = 7.0, 4.3$ Hz, 1H), 1.05 (d, $J = 7.0$ Hz, 3H), 0.78 (d, $J = 6.8$ Hz, 3H) ppm; $^{13}\text{C}\{^1\text{H}\}$ NMR (400 MHz, CDCl_3) δ 208.9, 154.2, 137.9, 134.5, 127.2, 126.5, 123.6, 53.1, 29.0, 28.2, 20.9, 17.3 ppm; GC-MS $m/z = 174$ (M^+). The ^1H and ^{13}C spectroscopic data are in good agreement with the literature data.⁴²

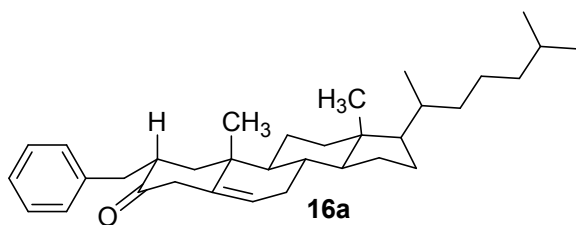


Table 3.11 Compound **16a**: ^1H

NMR (400 MHz, CDCl_3) δ 7.30-7.10 (m, 5H), 5.73 (d, $J = 2.0$ Hz, 1H), 3.46 (dd, $J = 14.2, 4.0$ Hz, 1H), 2.60 (dddd, $J = 13.4, 9.1, 4.7, 3.8$ Hz, 1H), 2.42 (dd, $J = 14.0, 9.1$ Hz, 1H), 2.35-2.20 (m, 2H),

2.10-1.93 (m, 3H), 1.90 (dd, $J = 13.2, 4.7$ Hz, 1H), 1.85-0.80 (br m, 19H), 1.06 (s, 3H), 0.86 (s, 3H), 0.85 (s, 3H), 0.65 (s, 3H) ppm; $^{13}\text{C}\{^1\text{H}\}$ NMR (400 MHz, CDCl_3) δ 200.3, 170.6, 140.3, 129.1, 128.3, 125.8, 123.4, 56.1, 55.8, 54.1, 43.7, 42.2, 41.3, 39.5, 39.1, 36.1, 35.7, 35.4, 35.0, 32.5, 31.9, 28.1, 28.0, 24.1, 23.8, 22.8, 22.6, 20.8, 18.6, 17.3, 11.9 ppm; GC-MS $m/z = 474$ (M^+); $[\alpha]^{20}_{\text{D}} = +10.8$ ($c = 2$ in CH_2Cl_2); Anal. Calcd for $\text{C}_{34}\text{H}_{50}\text{O}$: C, 86.01; H, 10.62. Found: C, 86.51; H, 10.12.

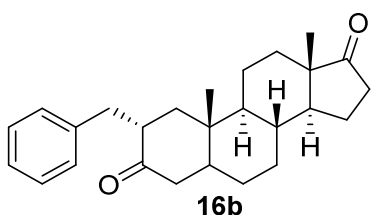


Table 3.11 Compound **16b (2 β)**: ^1H NMR (400

MHz, CDCl_3) δ 7.38-7.10 (m, 5H), 3.31 (dd, $J = 14.2, 5.0$ Hz, 1H), 2.68-2.56 (m, 1H), 2.44 (dd, $J = 18.7, 8.1$ Hz, 1H), 2.39-2.31 (m, 2H), 2.15 (dd, $J = 14.0, 3.9$ Hz,

1H), 1.74-2.10 (br m, 6H), 1.00-1.63 (br m, 14H), 1.01 (s, 3H), 0.84 (s, 3H) ppm; $^{13}\text{C}\{^1\text{H}\}$ NMR (400 MHz, CDCl_3) δ 221.0, 211.6, 140.4, 129.0, 126.9, 125.9, 53.9, 53.1, 51.1, 48.2, 47.7, 45.7, 44.9, 36.6, 35.8, 35.2, 34.7, 31.4, 30.6, 28.4, 21.8, 20.8, 13.8, 12.4 ppm; GC-MS $m/z = 378$ (M^+); $[\alpha]^{20}_{\text{D}} = +36.0$ ($c = 2$ in CH_2Cl_2); Anal. Calcd for $\text{C}_{26}\text{H}_{34}\text{O}_2$: C, 82.49; H, 9.05. Found: C, 82.20; H, 9.07.

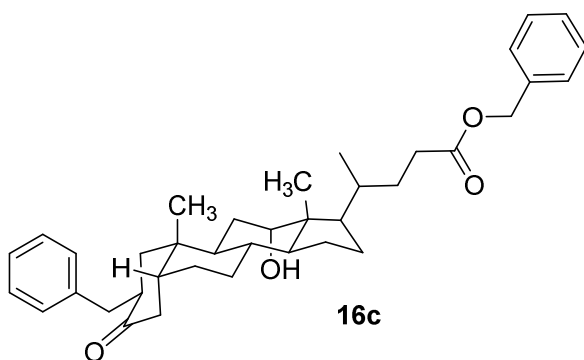


Table 3.11 Compound **16c**: ^1H

NMR (600 MHz, CDCl_3) δ 7.41-6.99 (m, 10H), 5.02 (d, $J = 6.6$ Hz, 2H), 3.79 (s, 1H), 3.15 (dd, $J = 14.1, 4.2$ Hz, 1H), 2.72 (t, $J = 13.4$ Hz, 1H), 2.64 (dddd, $J = 13.9, 9.1, 4.4, 4.4$ Hz, 1H), 2.38-2.28

(m, 2H), 2.26-2.11 (m, 3H), 2.00 (dd, $J = 14.2, 4.2$ Hz, 1H), 1.89-0.91 (br m, 19H), 0.87 (d, $J = 6.0$ Hz, 3H), 0.83 (s, 3H), 0.54 (s, 3H) ppm; $^{13}\text{C}\{^1\text{H}\}$ NMR (400 MHz, CDCl_3) δ

213.3, 174.0, 140.5, 136.1, 129.0, 128.5, 128.3, 128.2, 126.0, 66.1, 48.1, 47.2, 46.9, 46.4, 45.8, 43.5, 42.9, 35.6, 35.2, 35.0, 34.7, 34.4, 31.3, 30.8, 28.9, 27.4, 26.5, 23.5, 22.3, 17.4, 12.7 ppm; muldi $m/z = 570$ (M^+); $[\alpha]^{20}_D = +12.8$ ($c = 2$ in CH_2Cl_2); Anal. Calcd for $C_{38}H_{50}O_4$: C, 79.96; H, 8.83. Found: C, 79.37; H, 8.57.

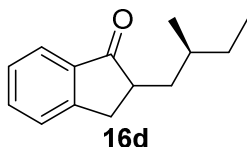


Table 3.11 Compound **16d** (2:1 diastereomeric mixture)

Major isomer: 1H NMR (400 MHz, $CDCl_3$) δ 7.95 (d, $J = 8.0$ Hz, 1H), 7.57 (t, $J = 7.4$ Hz, 1H), 7.45 (d, $J = 8.0$ Hz, 1H), 7.36 (t, $J = 7.4$ Hz, 1H), 3.39-3.27 (m, 1H), 2.95-2.87 (m, 2H), 2.85-2.67 (m, 2H), 1.96 (ddd, $J = 12.7, 8.0, 4.8$ Hz, 1H), 1.78 (ddd, $J = 13.7, 10.0, 4.0$ Hz, 1H), 1.70-1.10 (m, 4H), 0.95 (t, $J = 6.3$ Hz, 3H), 0.90 (d, $J = 8.2$ Hz, 3H) ppm; ^{13}C $\{^1H\}$ NMR (400 MHz, $CDCl_3$) δ 201.6, 134.6, 127.3, 127.2, 126.5, 126.4, 123.8, 45.6, 38.3, 33.2, 30.3, 28.5, 18.5, 11.5 ppm; GC-MS $m/z = 202$ (M^+); Anal. Calcd for $C_{14}H_{18}O$: C, 83.12; H, 8.97. Found: C, 83.50; H, 8.46. **Minor isomer:** 1H NMR (400 MHz, $CDCl_3$) δ 7.95 (d, $J = 8.0$ Hz, 1H), 7.57 (t, $J = 7.4$ Hz, 1H), 7.45 (d, $J = 8.0$ Hz, 1H), 7.36 (t, $J = 7.4$ Hz, 1H), 3.34 (dd, $J = 16.7, 7.9$ Hz, 1H), 2.80 (dd, $J = 16.7, 4.1$ Hz, 1H), 2.67-2.85 (m, 1H), 1.96 (ddd, $J = 13.7, 7.9, 4.7$ Hz, 1H), 1.70-1.58 (m, 1H), 1.43-1.10 (m, 4H), 0.95 (d, $J = 6.3$ Hz, 3H), 0.91 (t, $J = 8.2$ Hz, 3H) ppm; ^{13}C $\{^1H\}$ NMR (400 MHz, $CDCl_3$) δ 209.4, 153.7, 136.6, 134.6, 127.2, 126.4, 123.8, 45.7, 38.8, 33.7, 32.8, 28.5, 19.8, 11.2 ppm; GC-MS $m/z = 202$ (M^+).

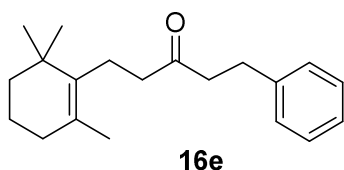


Table 3.11 Compound **16e:** 1H NMR (400 MHz, $CDCl_3$) δ 7.77-7.08 (m, 5H), 2.83 (t, $J = 7.5$ Hz, 2H), 2.64 (t, $J = 7.5$ Hz, 2H), 2.36 (t, $J = 9.4$ Hz, 2H), 2.16 (t, $J = 9.4$ Hz, 2H), 1.80 (t, $J = 6.2$ Hz, 2H), 1.50 (m, 2H), 1.31 (t, $J = 6.2$ Hz, 2H), 0.99 (s, 3H), 0.87 (s, 6H) ppm; ^{13}C $\{^1H\}$ NMR

(400 MHz, CDCl₃) δ 210.4, 141.1, 128.9, 128.5, 128.3, 127.1, 126.1, 43.8, 39.9, 39.7, 35.0, 32.7, 28.7, 22.2, 20.0, 19.7, 19.6, 19.4 ppm; GC-MS m/z = 266 (M⁺); Anal. Calcd for C₁₈H₁₈O₂: C, 81.17; H, 6.81. Found: C, 81.69; H, 6.57.

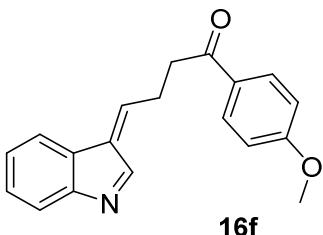


Table 3.11 Compound **16f**: ¹H NMR (400 MHz, CDCl₃) δ 7.34 (d, J = 8.4 Hz, 1H), 7.26 (t, J = 8.4 Hz, 4H), 7.17 (t, J = 7.4 Hz, 1H), 7.05 (t, J = 7.2 Hz, 1H), 6.70 (d, J = 9.0 Hz, 1H), 6.81-6.70 (m, 2H), 6.20-6.13 (m, 1H), 4.18

(t, J = 8.1 Hz, 3H), 3.84 (s, 3H), 3.06 (t, J = 8.1 Hz, 3H) ppm; ¹³C {¹H} NMR (400 MHz, CDCl₃) δ 201.7, 163.0, 130.4, 127.1, 122.0, 121.9, 121.4, 119.3, 118.5, 113.7, 112.5, 111.1, 108.2, 107.6, 55.3, 47.7, 27.6 ppm; GC-MS m/z = 291 (M⁺); Anal. Calcd for C₁₉H₁₇NO₂: C, 78.33; H, 5.88; Found: C, 78.68; H, 5.61.

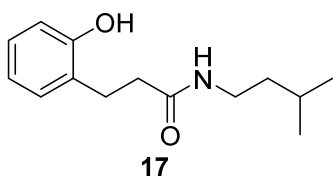


Table 3.9 Compound **17**: ¹H NMR (400 MHz, CDCl₃) δ 9.20 (s, 1H), 7.08 (dt, J = 7.4, 1.8 Hz, 1H), 7.03 (dd, J = 7.5, 1.7 Hz, 1H), 6.89 (dd, J = 8.0, 1.2 Hz, 1H), 6.81 (dt, J = 7.4, 1.4 Hz, 1H), 6.16 (t, 5.7 Hz, 1H), 3.24 - 3.16 (m, 2H), 2.89 (t, J = 6.6 Hz, 2H), 2.58 (t, J =

6.6 Hz, 2H), 1.49 (septet, J = 6.8 Hz, 1H), 1.23 (q, J = 7.5 Hz, 2H), 0.78 (d, J = 6.6 Hz, 6H) ppm; ¹³C {¹H} NMR (400 MHz, CDCl₃) δ 174.1, 154.7, 130.4, 127.8, 127.7, 120.1, 117.2, 38.0, 37.9, 36.8, 25.5, 25.0, 22.2 ppm; GC-MS m/z = 216(M⁺); Anal. Calcd for C₁₄H₂₁NO₂: C, 71.46; H, 8.99. Found: C, 71.55; H, 8.47.

6.3. Scope and Mechanistic Analysis for Chemoselective Hydrogenolysis of Carbonyl Compounds Catalyzed by a Cationic Ruthenium-Hydride Complex with Tunable Phenol Ligands

6.3.1. Experimental Procedures.

General Procedure for the Hydrogenolysis. Method A: In a glove box, carbonyl substrate (1.0 mmol), complex **1** (18 mg, 3 mol %) and phenol (10 mg, 10 mol %) were dissolved in 1,4-dioxane (2 mL) in a 25 mL Schlenk tube equipped with a Teflon stopcock and a magnetic stirring bar. The tube was brought out of the glove box, and cooled in a liquid N₂ bath and evacuated *in vacuo*. [**Alternative Procedure for the In-situ Generation of the Active Ru-H Catalyst 8.** Complex **4** (17 mg, 1 mol %) and phenol (4 mg, 4 mol %) were dissolved in CH₂Cl₂ (1 mL) in a 25 mL Schlenk tube equipped with a Teflon stopcock and a magnetic stirring bar. HBF₄·OEt₂ (7 μL, 4 mol %) was added under a stream of N₂ gas. The mixture was stirred about 15 min at room temperature.] The tube was filled with H₂ (2 atm) via a vacuum line. The tube was stirred in an oil bath set at 130 °C for 8-16 h. The reaction tube was taken out of the oil bath, and was cooled to room temperature. After the tube was open to air, the solution was filtered through a short silica gel column by eluting with CH₂Cl₂ (10 mL), and the filtrate was analyzed by GC-MS. Analytically pure product was isolated by a simple column chromatography on silica gel (280-400 mesh, hexanes/EtOAc).

Method B: In a glove box, carbonyl substrate (1.0 mmol), complex **1** (18 mg, 3 mol %) and phenol (10 mg, 10 mol %) were dissolved in 2-propanol/1,4-dioxane (2 mL, 1:1 v/v) in a 25 mL Schlenk tube equipped with a Teflon stopcock and a magnetic stirring bar. The tube was brought out of the glove box, and stirred in an oil bath set at 130 °C for

8-16 h. The reaction tube was taken out of the oil bath, and was cooled to room temperature. After the tube was open to air, the solution was filtered through a short silica gel column by eluting with CH_2Cl_2 (10 mL), and the filtrate was analyzed by GC-MS. Analytically pure product was isolated by a simple column chromatography on silica gel (280-400 mesh, hexanes/EtOAc).

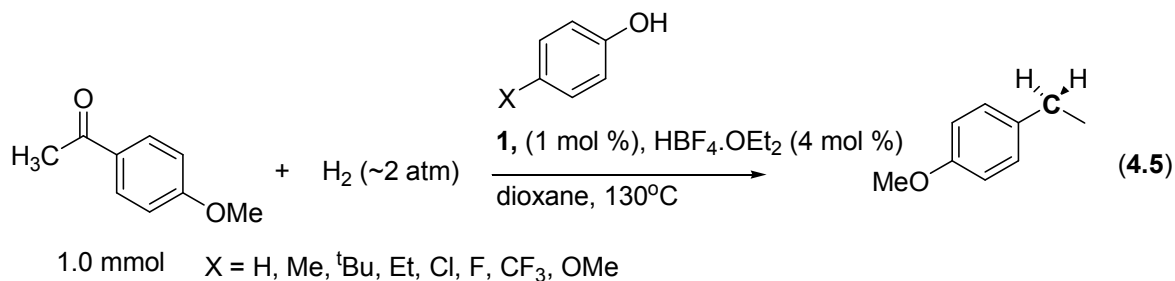
6.3.2 Ligand Screening and Optimization Study.

In a glove box, 4-methoxyacetophenone (160 mg, 1 mmol), complex **1** (18 mg, 3 mol %) and ligand (10 mol %) were dissolved in 1,4-dioxane (2 mL) in a 25 mL Schlenk tube equipped with a Teflon stopcock and a magnetic stirring bar. The tube was brought out of the glove box, cooled in liquid N_2 bath and degased under a high vacuum. The tube was filled with H_2 (2 atm) via a vacuum line. The tube was stirred in an oil bath set at 130 °C for 8-16 h. The reaction tube was taken out of the oil bath, and was cooled to room temperature. After the tube was open to air, the solution was filtered through a short silica gel column by eluting with CH_2Cl_2 (10 mL), and the filtrate was analyzed by ^1H NMR.

Table 6.1: Ligand Screening for the Hydrogenolysis Reaction of 4-Methoxyacetophenone.^a

	Catalyst	Ligand	Solvent	Yield
1	5	phenol	dioxane	>95
2	5	phenol	PhCl	89
3	5	aniline	PhCl	<5
4	5	2-NH ₂ PhCOMe	PhCl	35
5	5	benzamide	PhCl	<5
6	5	1,2-catechol	toluene	73
7	5	1,1'-BINOL	toluene	54
8	5	1,2-C ₆ H ₄ (NH ₂) ₂	toluene	<5
9	4	phenol	dioxane	<5
10	4/H⁺	phenol	dioxane	95
11	[Ru(cod)Cl ₂] _x	phenol	dioxane	0
12	RuCl ₃ ·3H ₂ O	phenol	dioxane	0
13	Ru ₃ (CO) ₁₂	phenol	dioxane	0
14	(PPh ₃) ₃ (CO)RuH ₂	phenol	dioxane	0
15	[(PCy ₃) ₂ (CO)(CH ₃ CN) ₂ RuH]BF ₄	phenol	dioxane	30

^a Reaction conditions: 4-methoxyacetophenone (160 mg, 1 mmol), solvent (2 mL), catalyst (3 mol %), ligand (10 mol %), H₂ (2 atm), 130 °C, 12 h. ^b The product yield of **12** was determined by ¹H NMR using methyl benzoate as an internal standard.



6.3.2 Hammett Study

In a glove box, complex **4** (40 mg, 1 mol %) and *p*-X-C₆H₄OH (4 mol %) were dissolved in CH₂Cl₂ (2 mL) in 25 mL Schlenk tube equipped with a Teflon screw cap stopcock. The tubes were brought out of the box, and HBF₄·OEt₂ (15 μL, 4 mol %) was added under a nitrogen stream. After the mixture was stirred 15 min at room temperature, the solvent was removed *in vacuo*. 4-Methoxyacetophenone (240 mg) was added, and the residue was dissolved in 1,4-dioxane (8 mL). The resulting solution was divided into four equal portions, and each portion was transferred to a 25 mL Schlenk tube. The tubes were cooled in liquid N₂ bath, evacuated under high vacuum, and were filled with H₂ (1 atm) via a vacuum line. The tubes were stirred in an oil bath set at 130 °C. Each tube was taken out from the oil bath at 30 min intervals. The tube was cooled in ice water bath, and the solvent was removed under low vacuum. Methyl benzoate (10 mg, internal standard) in CDCl₃ (1 mL) was added, and the conversion of ketone to methylene was analyzed by ¹H NMR spectroscopy. The reaction rate was measured by monitoring the appearance of the product signals on ¹H NMR, which was normalized against the internal standard peak. The *k*_{obs} was determined from a first-order plot of $-\ln[(4\text{-methoxyacetophenone})_t/(4\text{-methoxyacetophenone})_0]$ vs time. The Hammett plot of $\log(k_X/k_H)$ vs σ_p is shown in Figure 6.2.

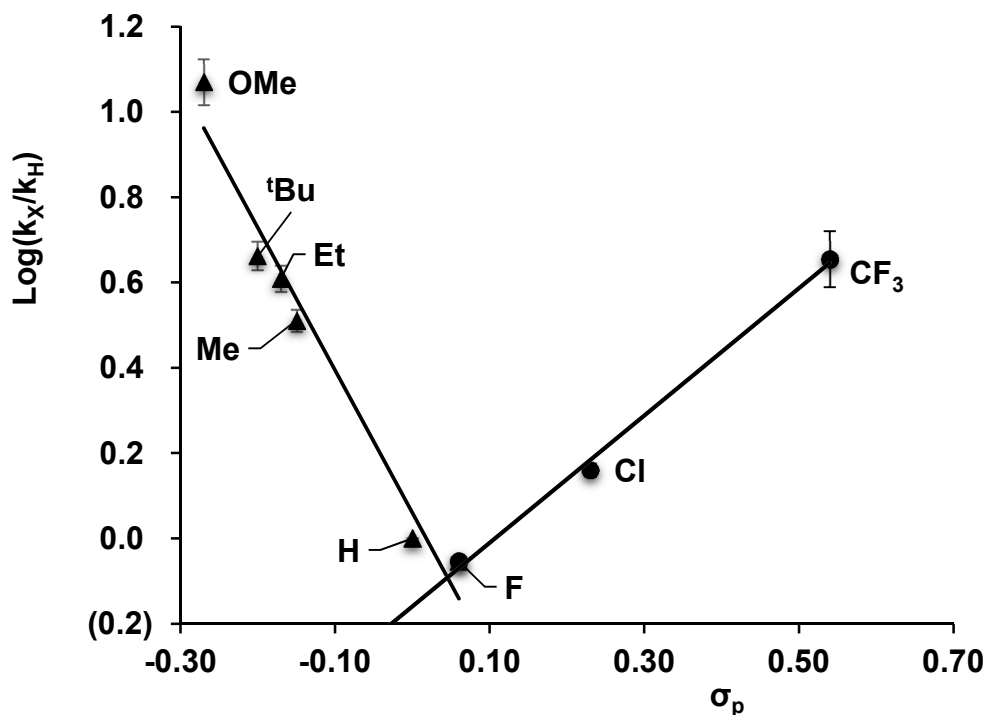


Figure 6.1. Hammett Plot of 4-Methoxyacetophenone with p -X-C₆H₄OH (X = OMe, *t*-Bu, Me, Et, H, F, Cl, CF₃).

6.3.3 Deuterium Isotope Effect Study.

In a glove box, **4** (50 mg, 1 mol %) and p -X-C₆H₄OH (4 mol %) (X = OMe, Et, Cl, CF₃) were dissolved in CH₂Cl₂ (2 mL) 25 mL Schlenk tubes equipped with a Teflon screw cap stopcock. The tubes were brought out of the box, and HBF₄·OEt₂ (20 μL, 4 mol %) was added under nitrogen stream. The mixture was stirred about 15 min at room temperature, and solvent was removed under high vacuum. The tube was brought into the glove box, and 4-methoxyacetophenone (300 mg) was dissolved in dioxane (8 mL). The resulting solution was divided into five equal portions, and placed into five separate 25 mL Schlenk tubes.

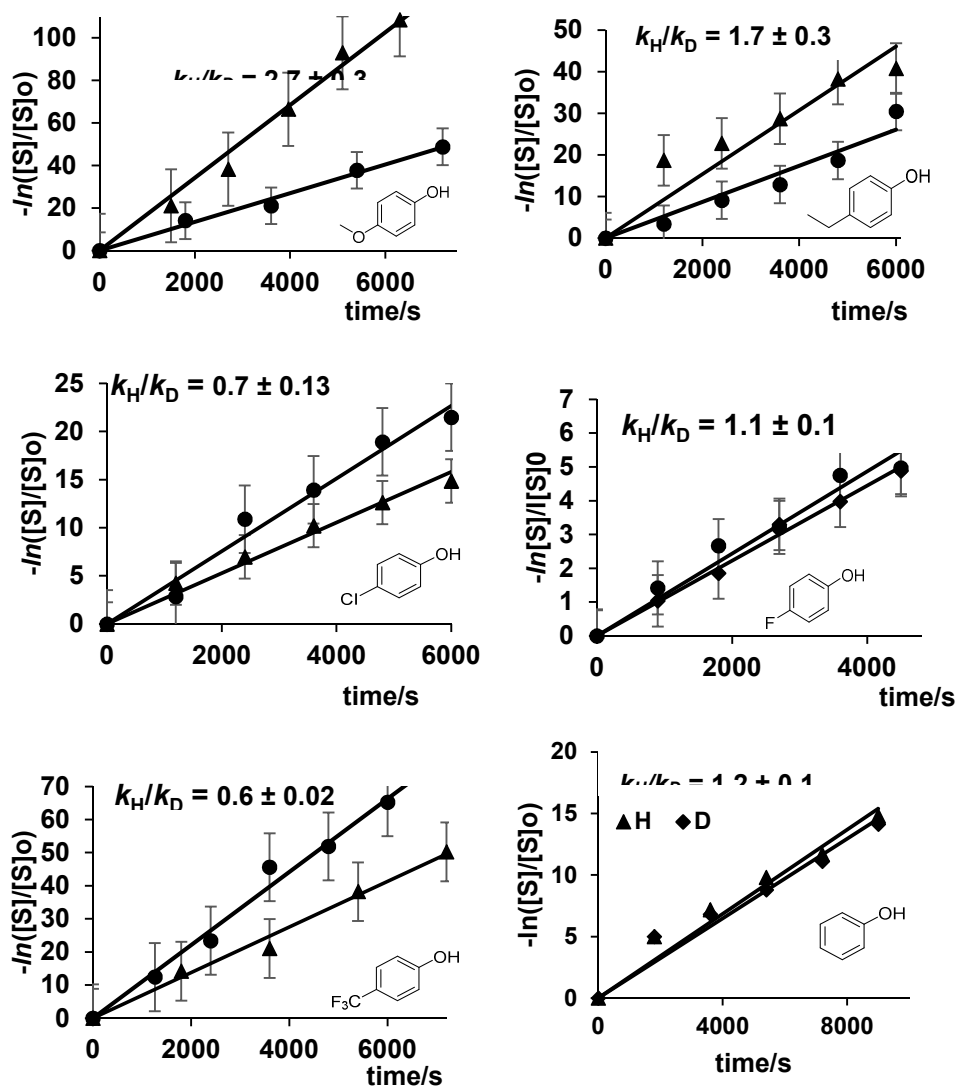
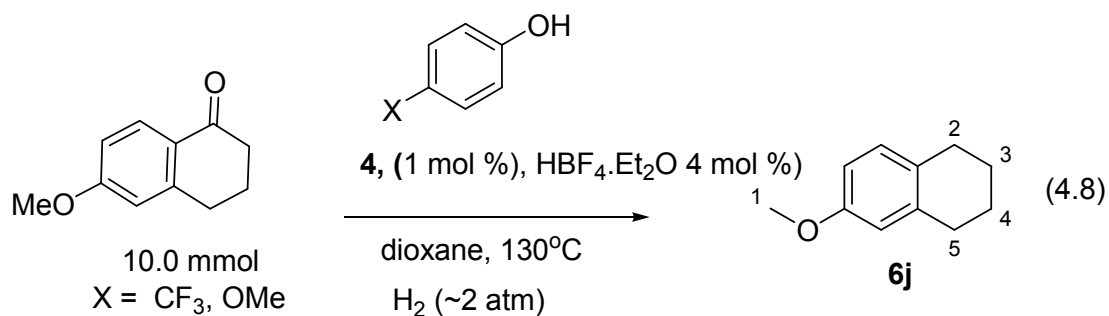


Figure 6.2. First Order Plots from the Hydrogenolysis Reaction of 4-Methoxyacetophenone with H₂ (triangle) and D₂ (circle) Catalyzed by 4/4-X-C₆H₄OH (X = OMe, Et, Cl, H, F, CF₃).

The tubes were brought out of the glove box, cooled in liquid nitrogen bath, and degassed under high vacuum. The tubes were filled with H₂ or D₂ (2 atm) via a vacuum line, and were stirred in an oil bath set at 130 °C. Each tube was taken out from the oil bath in 30 min intervals for analysis. After the tube was cooled to room temperature, the solvent was removed under vacuum, and methyl benzoate (10 mg, internal standard) was added. The

mixture was dissolved in CDCl_3 (1 mL), and was analyzed by ^1H NMR and ^2H NMR. The reaction rate was measured by monitoring the appearance of the product signals on ^1H NMR, which were normalized against an internal standard (methyl benzoate). The k_{obs} was determined from a first-order plot of $-\ln[(4\text{-methoxyacetophenone})_t/(4\text{-methoxyacetophenone})_0]$ vs time. Using the plot of $-\ln[(4\text{-methoxyacetophenone})_t/(4\text{-methoxyacetophenone})_0]$ vs time $k_{\text{H}}/k_{\text{D}}$ was calculated for each phenol ligands (Figure 6.2).



6.3.4 Carbon Isotope Effect Study.

In a glove box, **4** (400 mg, 1 mol %) and $p\text{-X-C}_6\text{H}_4\text{OH}$ (4 mol %), ($\text{X} = \text{OMe}$ or CF_3) were dissolved in CH_2Cl_2 (5 mL) in a 100 mL Schlenk tube equipped with a Teflon screw cap stopcock. The tube was brought out of the box, and $\text{HBF}_4\cdot\text{OEt}_2$ (60 μL , 4 mol %) was added under nitrogen stream. After the mixture was stirred 15 min at room temperature, the solvent was removed under high vacuum. The tube was brought into the glove box, 6-methoxy-1-tetralone (1.76 g, 10 mmol) was added and the mixture was dissolved in dioxane (8 mL). After the tube was brought out of the glove box, it was cooled in liquid nitrogen and was degassed under high vacuum. The tube was filled with H_2 (1 atm) via a vacuum line. The tube was stirred in an oil bath set at 130 $^\circ\text{C}$ for 2 h (2.5 h and 3 h for the repeated runs). The conversion was determined separately by GC after filtering a small sample of the crude mixture through a short silica gel column and eluting with CH_2Cl_2 (20 mL) (15, 18 and 20 % conversions). The product **6j** was isolated by a column

chromatography on silica gel (hexaness/Et₂O = 40:1).

Table 6.2: Average ¹³C Integration of the Product **6j** at High Conversion (Virgin, *R*₀; 96 % conversion), at Low Conversion (*R*; avg 18 % conversion) and the Calculated ¹³C KIE using 4-OMeC₆H₄OH as the ligand.

	OMe	C1	C2	C3	C4
<i>R</i> ₀	1.0000	1.0051	0.9968	1.0000	1.0223
<i>R</i> 1	1.0000	0.9991	0.9868	0.9999	0.9801
<i>R</i> 2	1.0000	1.0050	0.9980	1.0006	0.9811
<i>R</i> 3	1.0000	1.0050	0.9979	1.0005	0.9811
<i>R</i>	1.0000	1.0030	0.9942	1.0004	0.9807
<i>R</i> ₀ / <i>R</i>	1.0000	1.0021	1.0026	0.9996	1.0424

Table 6.3: Average ¹³C Integration of the Product **6j** at High Conversion (Virgin, *R*₀; 96 % conversion), at Low Conversion (*R*; avg 18 % conversion) and the Calculated ¹³C KIE using 4-CF₃-C₆H₄OH as the ligand

	OMe	C1	C2	C3	C4
<i>R</i> ₀	1.0000	1.0051	0.9968	1.0000	1.0223
<i>R</i> 1	1.0000	0.9989	0.9972	0.9990	0.9615
<i>R</i> 2	1.0000	0.9999	0.9969	0.9996	0.9617
<i>R</i> 3	1.0000	0.9990	0.9970	0.9998	0.9627
<i>R</i>	1.0000	0.9993	0.9971	0.9995	0.9620
<i>R</i> ₀ / <i>R</i>	1.0000	1.0058	0.9997	1.0005	1.0627

The $^{13}\text{C}\{^1\text{H}\}$ NMR analysis of the isolated product **6j** was performed by following Singleton's NMR method.²² The sample was prepared identically by dissolving 200 mg of the isolated **6j** in CDCl_3 (0.5 mL) in a 5 mm high precision NMR tube. The $^{13}\text{C}\{^1\text{H}\}$ NMR spectra were recorded with H-decoupling and 45 degree pulses. A 120 s delay between pulses was imposed to minimize T_1 variations (d1 = 120 s, at = 5.0 s, np = 245098, nt = 736). The data are summarized in Table 6.2 and 6.3.

6.3.5 Deuterium Labeling Study.

In a glove box, complex **4** (17 mg, 1 mol %) and 4-trifluoromethylphenol (8 mg, 4 mol %) were dissolved in CH_2Cl_2 (1 mL) in a 25 mL Schlenk tube equipped with a Teflon stopcock and a magnetic stirring bar. The tube was brought out of the glove box, and $\text{HBF}_4\cdot\text{OEt}_2$ (6.6 μL , 4 mol %) was added via a syringe under stream of N_2 . After the mixture was stirred for 15 min at room temperature, the solvent was removed under vacuum. The tube was brought into the glove box, and 4-methoxyacetophenone (150 mg, 1.0 mmol) and dioxane (2 mL) were added. The tube was brought out of the glove box, was cooled in liquid nitrogen, and was evacuated under high vacuum. The tube was filled with D_2 (2 atm) via a vacuum line. The tube was stirred in an oil bath set at 130 °C for 4 h. The reaction tube was taken out of the oil bath, and was cooled to room temperature. After the tube was open to air, the solution was filtered through a short silica gel column by eluting with CH_2Cl_2 (10 mL), and the analytically pure product was isolated by a simple column chromatography on silica gel (280-400 mesh, hexanes/EtOAc = 100:1). The products were completely characterized by ^1H NMR and ^2H NMR spectroscopic methods (Figure 6.3).

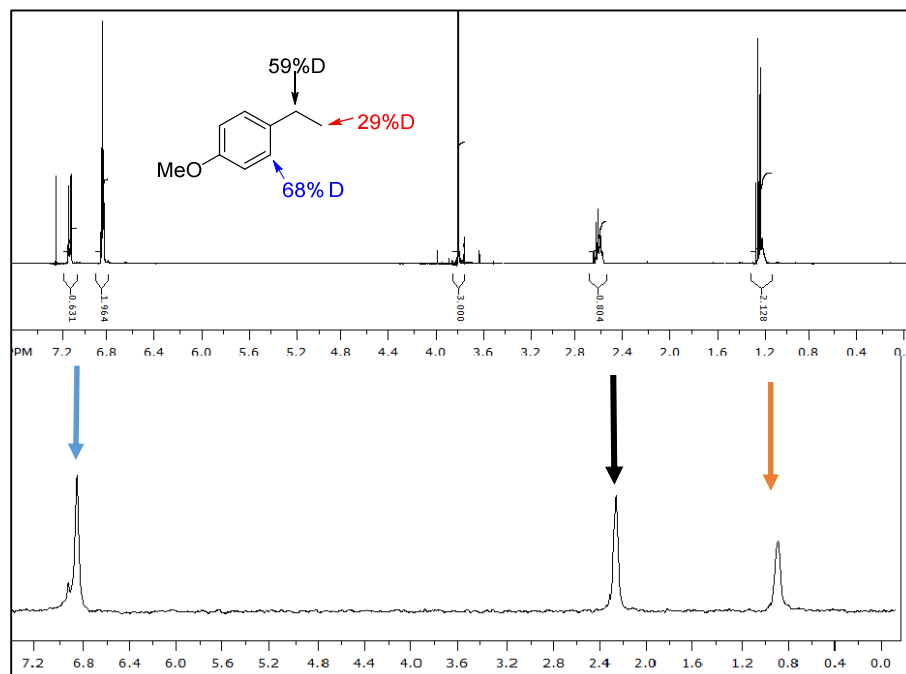


Figure 6.3. ^1H and ^2H NMR spectra for the Hydrogenolysis of 4-Methoxyacetophenone with D_2 Catalyzed by 4/4- $\text{CF}_3\text{C}_6\text{H}_4\text{OH}$.

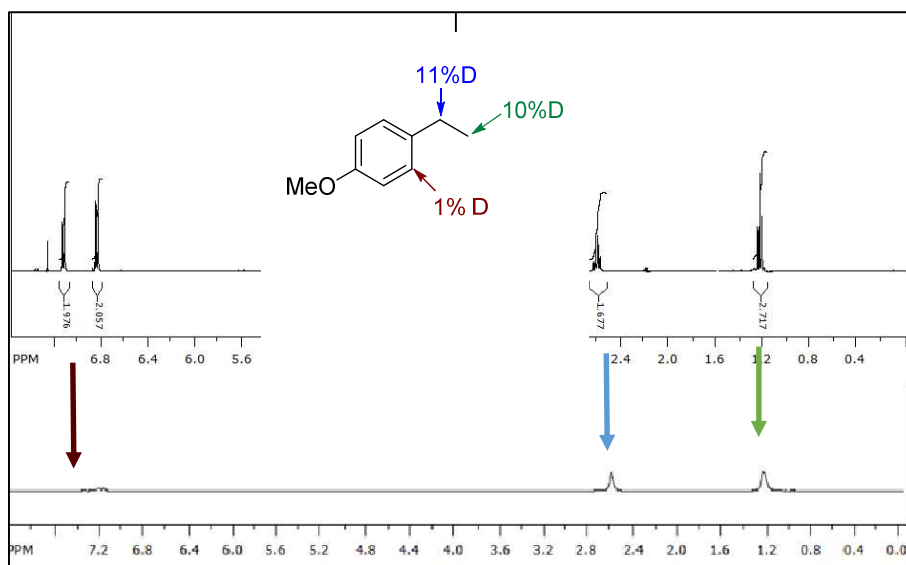


Figure 6.4. ^1H and ^2H NMR spectra for the Hydrogenolysis of 1-(4-Methoxyphenyl)ethanol with D_2 Catalyzed by 4/4- $\text{CF}_3\text{C}_6\text{H}_4\text{OH}$.

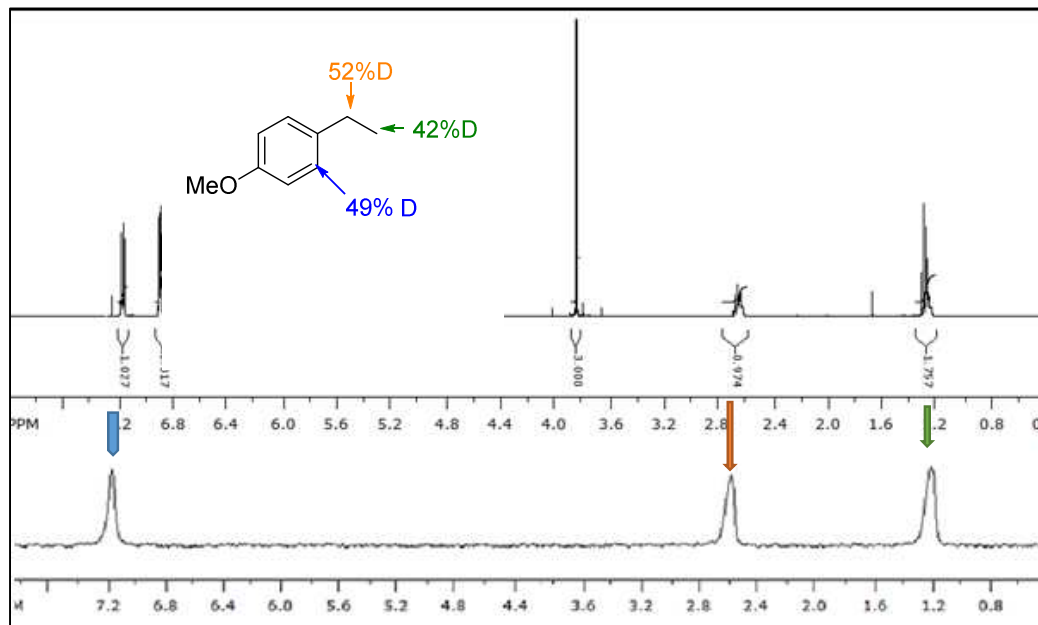


Figure 6.5. ^1H and ^2H NMR spectra for the Hydrogenolysis of 4-Methoxyacetophenone with D_2 Catalyzed by 4/4- $\text{OMeC}_6\text{H}_4\text{OH}$.

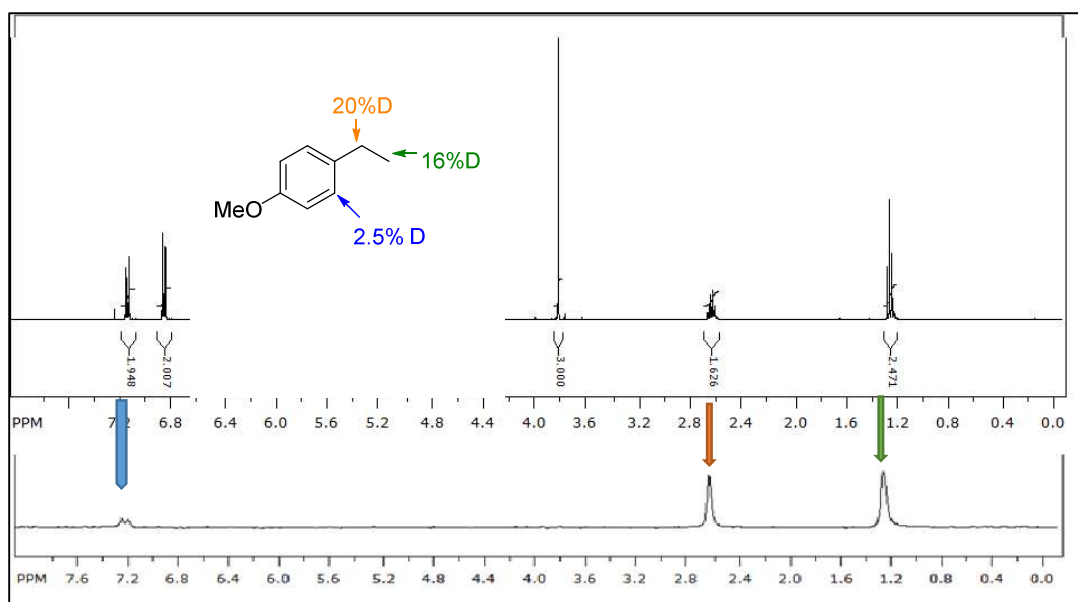


Figure 6.6. ^1H and ^2H NMR spectra for the Hydrogenolysis of 1-(4-Methoxyphenyl)ethanol with D_2 Catalyzed by 4/4- $\text{OMeC}_6\text{H}_4\text{OH}$.

The same procedure was used for: the hydrogenolysis of 1-(4-methoxyphenyl)ethanol with D_2 using 4/4- $\text{CF}_3\text{-C}_6\text{H}_4\text{OH}$ (Figure 6.4), the hydrogenolysis

of 4-methoxyacetophenone with D₂ using 4/4-OMe-C₆H₄OH (Figure 6.5), and for the hydrogenolysis of 1-(4-methoxyphenyl)ethanol with D₂ using 4/4-OMe-C₆H₄OH (Figure 6.6).

6.3.6 Empirical Rate Measurements: Catalyst Concentration Dependence.

In a glove box, **4** (20 mg, 0.01 mmol) and *p*-X-C₆H₄OH (4.0 equivalence, X = CF₃, OMe) were dissolved in CH₂Cl₂ (2.0 mL) in a 25 mL Schlenk tubes equipped with a Teflon screw cap stopcock. The tubes were brought out of the box, and HBF₄·OEt₂ (15 μL, 4 equiv) was added under nitrogen stream. The mixture was stirred about 15 min at room temperature and solvent was removed under vacuum and filled with nitrogen. Solvent removed under vacuum and 300 mg of 4-methoxyacetophenone was added. The mixture was dissolved in 4 mL of 1,4-dioxane and transferred into 4 different 25 mL Schlenk tubes each contained equal portions. Tubes were cooled in liquid nitrogen and degassed under vacuum. The tube was filled with hydrogen gas connected to vacuumed line. The tube was tightly closed when hydrogen gas bubbles through the mercury manometer. This was stirred in an oil bath set at 130 °C. Each tube was taken out from the oil bath at 20 min intervals. Cooled with liq. nitrogen and removed solvent under low vacuum and methyl benzoate (internal standard, 10 μL) and CDCl₃ (1 mL) was added and the conversion of ketone to methylene was analyzed by ¹H NMR spectroscopy. The reaction rate was measured by monitoring the appearance of the product signals on ¹H NMR, which were normalized against the internal standard methylbenzoate. The initial rate of the reaction was determined from a first-order plot of [1-Ethyl-4-methoxybenzene] vs time. This procedure was repeated for 5 different concentrations of catalyst. The plot of catalytic concentration vs initial rate of the reaction is shown in Figure 6.7-6.10.

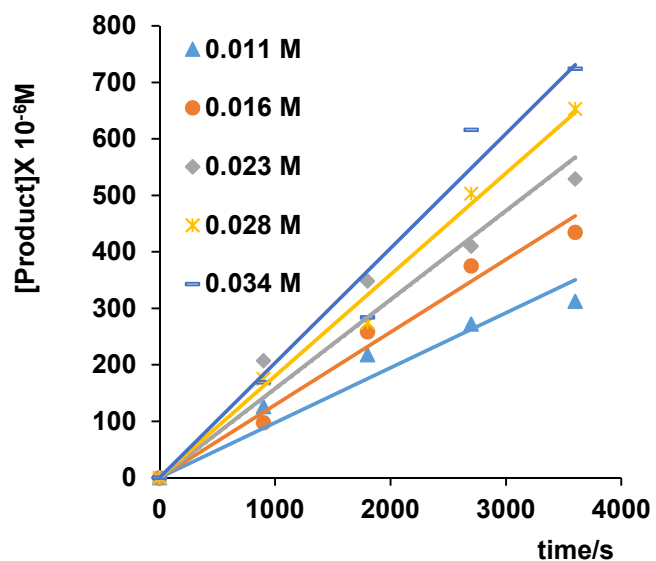


Figure 6.7: The Formation of 1-Ethyl-4-methoxybenzene vs Time at Different Catalyst Concentrations of $4/\text{HBF}_4 \cdot \text{OEt}_2/4\text{-OMe-C}_6\text{H}_4\text{OH}$.

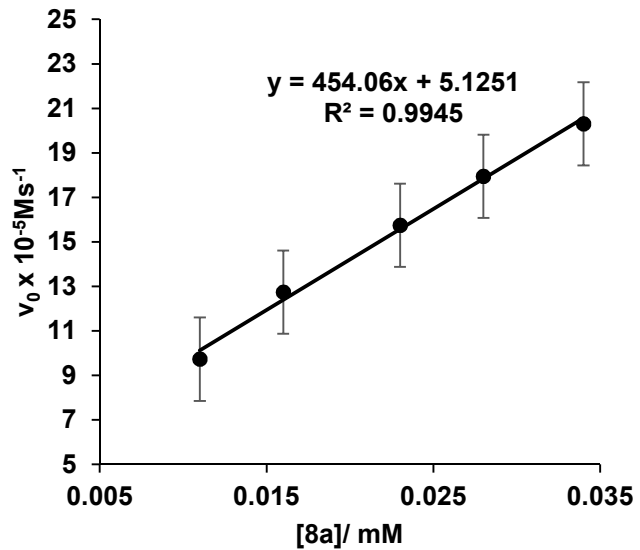


Figure 6.8: Initial Rate of the Formation 1-Ethyl-4-methoxybenzene vs Catalyst Concentration of $4/\text{HBF}_4 \cdot \text{OEt}_2/4\text{-OMe-C}_6\text{H}_4\text{OH}$.

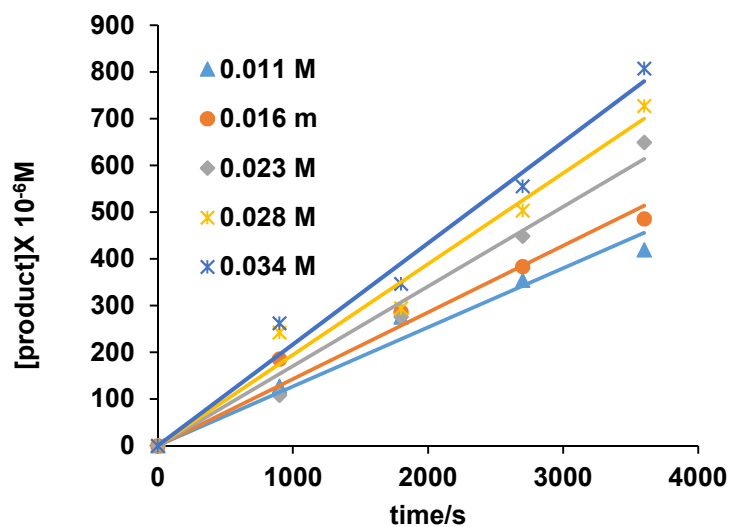


Figure 6.9: The Formation of 1-Ethyl-4-methoxybenzene vs Time at Different Catalyst Concentrations of $4/\text{HBF}_4 \cdot \text{OEt}_2/4\text{-CF}_3\text{-C}_6\text{H}_4\text{OH}$.

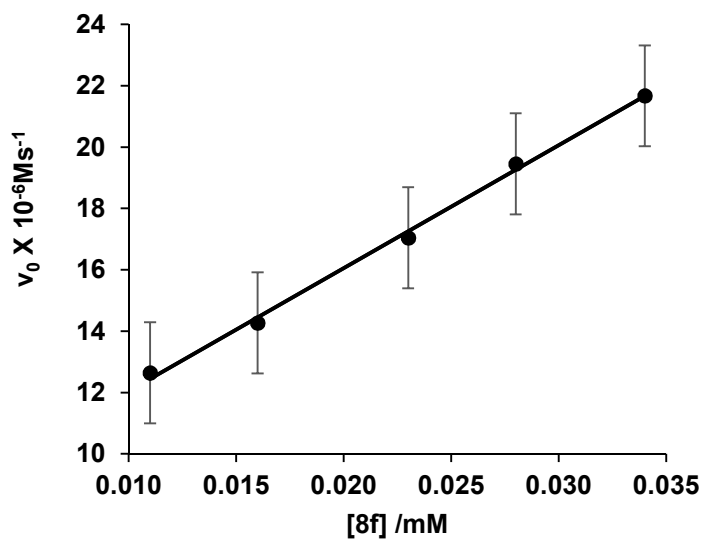


Figure 6.10: Initial Rate of the Formation 1-Ethyl-4-methoxybenzene vs Catalyst Concentration of $4/\text{HBF}_4 \cdot \text{OEt}_2/4\text{-CF}_3\text{-C}_6\text{H}_4\text{OH}$.

6.3.7 Catalyst Dependence Study.

In a glove box, complex **10** (20 mg, 16 μM) and 2'-hydroxyacetophenone (136 mg, 1 mmol) were dissolved in 1,4-dioxane (4 mL) in a vial equipped with a screw cap and a magnetic stirring bar. After the solution was stirred for 10 min at room temperature, it was divided into four equal portions and each portion was transferred into four separate 25 mL Schlenk tubes. The tubes were brought out of the glove box, were cooled in liquid nitrogen bath, and were evacuated under vacuum. The tube was filled with H_2 (2 atm) via vacuum line. The tubes were stirred in an oil bath set at 130 $^\circ\text{C}$. Each tube was taken out from the oil bath at 20 min intervals. Cooled in a liquid nitrogen bath, and the solvent was removed in vacuo. Methyl benzoate (10 μL , internal standard) in CDCl_3 (1 mL) was added, and the product conversion was analyzed by ^1H NMR spectroscopy. The initial rate of the reaction was determined from a first-order plot of [2'-hydroxyacetophenone] vs time. The procedure was repeated for 8 different concentration of the catalyst (4 μM -16 μM). The plot of catalytic concentration vs initial rate of the reaction is shown in Figure 6.11-6.12.

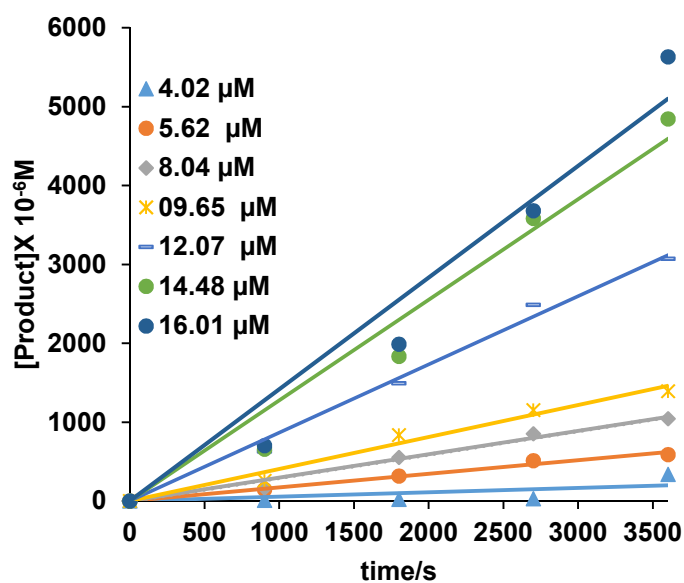


Figure 6.11: The Formation of 2'-hydroxyethylbenzene vs Time at Different Catalyst Concentrations of **10** (4 μM -16 μM).

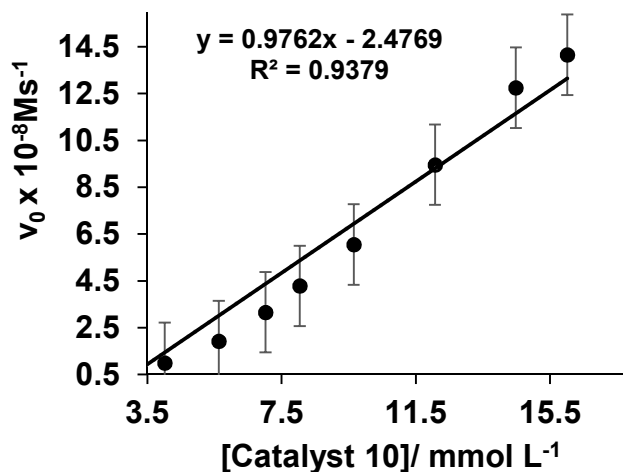


Figure 6.12: Initial Rate of the Formation 2'-Hydroxyethylbenzene Vs Catalyst Concentration of 10.

6.3.8 Ketone Substrate Dependence Study.

The same experimental procedure was used for the hydrogenolysis of 4-methoxyacetophenone at different concentrations of 4-methoxyacetophenone (0.33M-2M) at 0.04 mM catalyst concentration. The data obtained are shown in following Fig. 6.13.

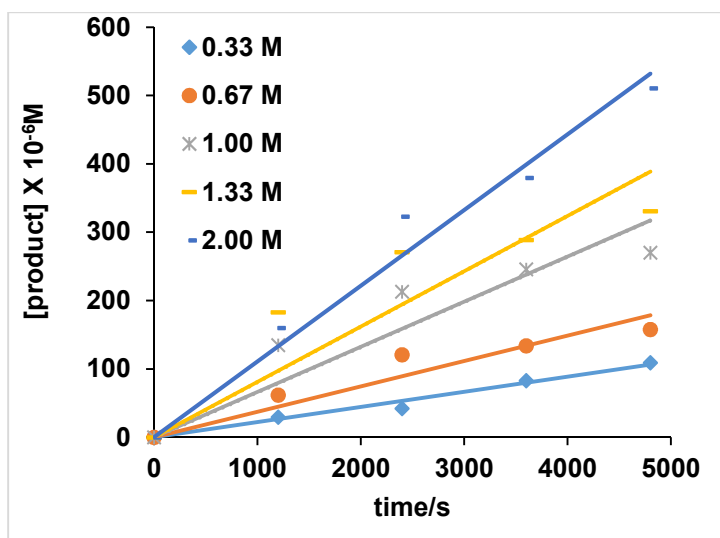


Figure 6.13: The Formation of 1-Ethyl-4-Methoxybenzene Vs Time at Different Concentration of 4-Methoxyacetophenone for the Catalyst 4/HBF₄·OEt₂/4-OMe-C₆H₄OH.

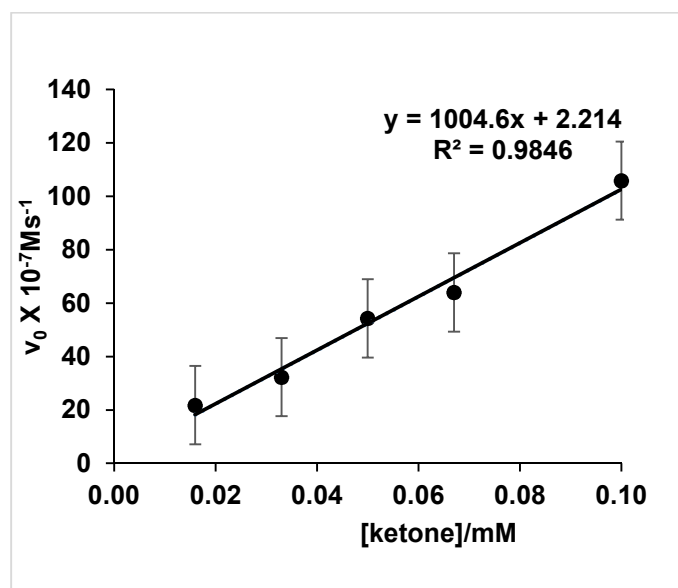


Figure 6.14: Initial Rate of Formation 1-Ethyl-4-Methoxybenzene Vs Concentration of 4-Methoxyacetophenone for the Catalyst $4/\text{HBF}_4 \cdot \text{OEt}_2/4\text{-OMe-C}_6\text{H}_4\text{OH}$.

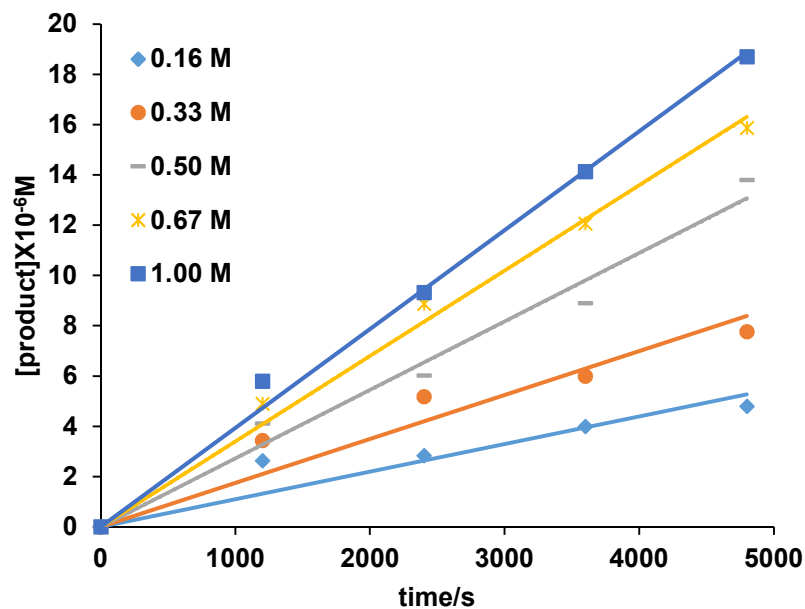


Figure 6.15: The Formation of 1-Ethyl-4-Methoxybenzene Vs Time at Different Concentration of 4-Methoxyacetophenone for the Catalyst $4/\text{HBF}_4 \cdot \text{OEt}_2/4\text{-CF}_3\text{-C}_6\text{H}_4\text{OH}$.

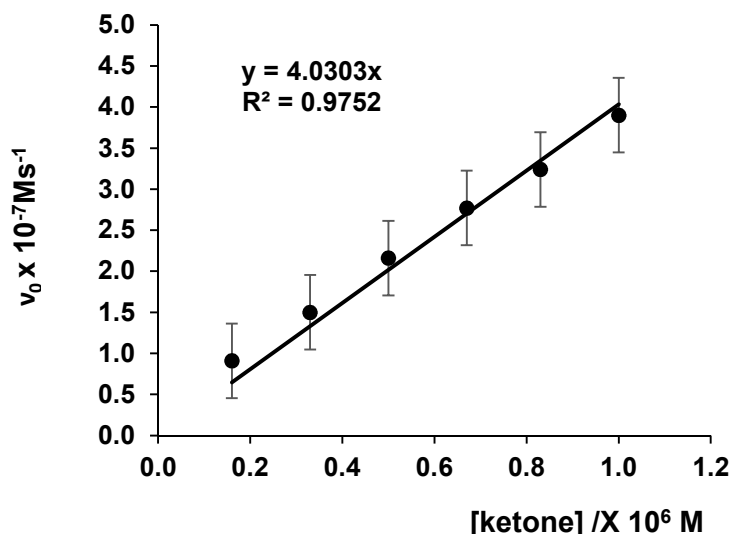


Figure 6.16: Initial Rate of Formation 1-Ethyl-4-Methoxybenzene Vs Concentration of 4-Methoxyacetophenone for the Catalyst **4**/HBF₄·OEt₂/4-CF₃-C₆H₄OH.

6.3.9 Hydrogen Pressure Dependence.

In a glove box, **4** (20 mg, 1 mol %) and *p*-X-C₆H₄OH (4.0 equivalent, X = CF₃, OMe) were dissolved in CH₂Cl₂ (2.0 mL) in a 25 mL Schlenk tube equipped with a Teflon screw cap stopcock. The tube was brought out of the box, and HBF₄·OEt₂ (15 μL, 4 equiv) was added under nitrogen stream. After the mixture was stirred about 15 min at room temperature, the solvent was removed under vacuum, and 4-methoxyacetophenone (300 mg, 2 mmol) was added. The mixture was dissolved in 1,4-dioxane (4 mL), and the solution was divided into four equal portions, and each portion was transferred into four separate 100 mL Fisher-Porter tubes. The tubes were cooled in liquid nitrogen and was evacuated under high vacuum. Each tubes was connected to a hydrogen gas cylinder filled with H₂ (1-5 atm). The tube was stirred in an oil bath set at 130 °C. Each tube was taken out from the oil bath at 20 min intervals, cooled in a liquid N₂ bath and the solvent was removed in vacuo. Methyl benzoate (10 μL, internal standard) and CDCl₃ (1 mL) was added and the

product conversion of ketone was analyzed by ^1H NMR spectroscopy. The initial rate of the reaction was determined from a first-order plot of pressure of H_2 vs time as shown in Figure 6.17-6.22.

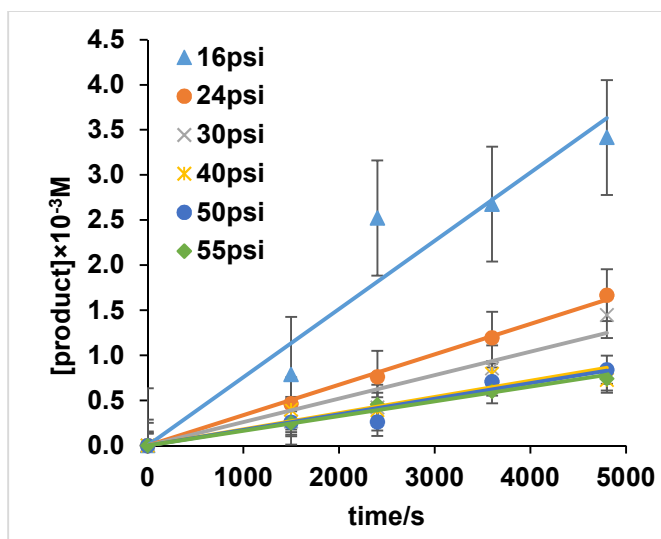


Figure 6.17: The Formation of 1-Ethyl-4-Methoxybenzene Vs Time at Different Hydrogen Pressure for the Catalyst $4/\text{HBF}_4 \cdot \text{OEt}_2/4\text{-OMe-C}_6\text{H}_4\text{OH}$.

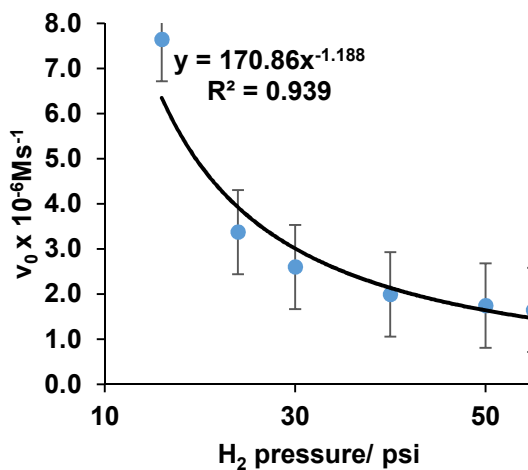


Figure 6.18: Initial Rate of the Formation 1-Ethyl-4-Methoxybenzene vs Time at Different Hydrogen Pressure for the Catalyst $4/\text{HBF}_4 \cdot \text{OEt}_2/4\text{-OMe-C}_6\text{H}_4\text{OH}$.

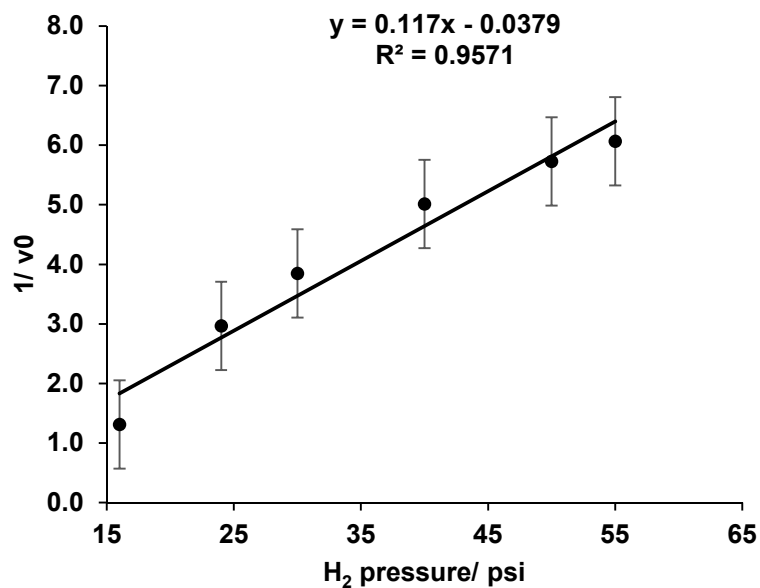


Figure 6.19: Initial Rate of the Formation 1-Ethyl-4-Methoxybenzene ($1/v_0$) vs Time at Different Hydrogen Pressure for the Catalyst $4/HBF_4 \cdot OEt_2/4-OMe-C_6H_4OH$.

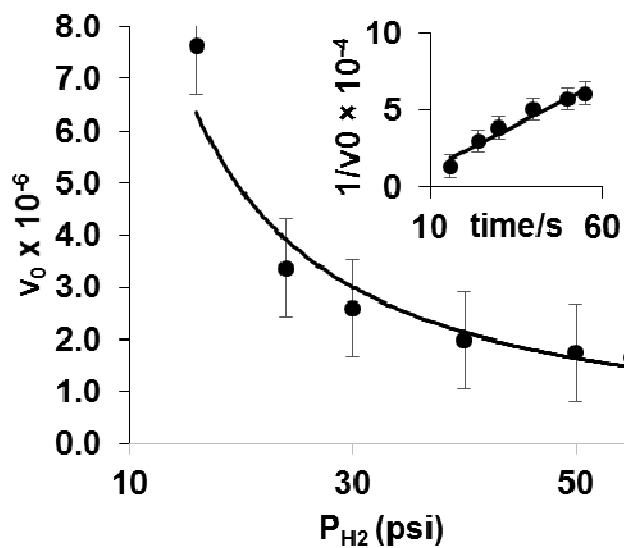


Figure 6.20: (A) Plot of Initial Rate of Formation 1-Ethyl-4-Methoxybenzene Vs Time at Different Hydrogen Pressure when 4-Methoxyphenol is used. (Inset) ($1/v_0$) Vs Time at Different Hydrogen Pressure for the Catalyst $4/HBF_4 \cdot OEt_2/4-OMe-C_6H_4OH$

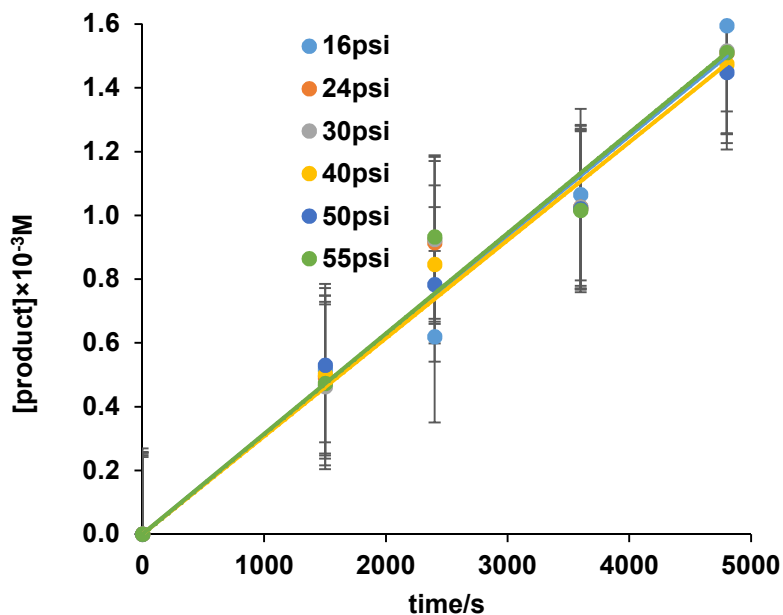


Figure 6.21: The Formation of 1-Ethyl-4-methoxybenzene vs Time at different hydrogen pressure for the catalyst $4/\text{HBF}_4 \cdot \text{OEt}_2/4\text{-CF}_3\text{-C}_6\text{H}_4\text{OH}$.

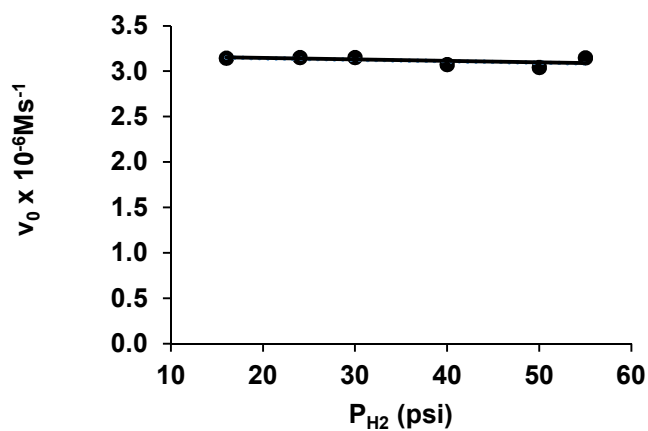
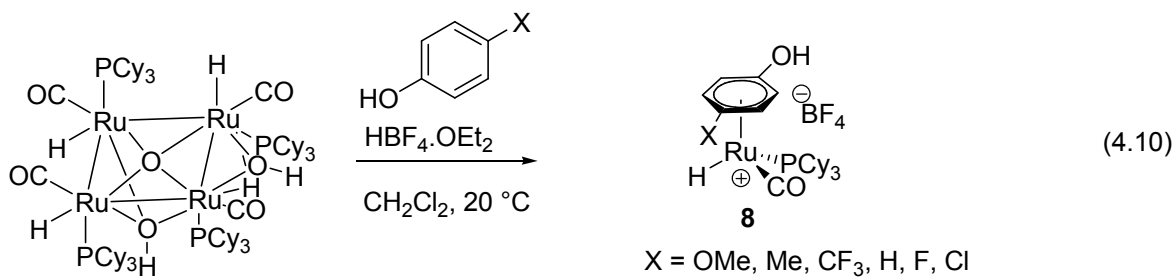


Figure 6.22: Initial Rate of the Formation 1-Ethyl-4-methoxybenzene vs time at different hydrogen pressure for the catalyst $4/\text{HBF}_4 \cdot \text{OEt}_2/4\text{-CF}_3\text{-C}_6\text{H}_4\text{OH}$.

6.3.10 Isolation and Characterization of Catalytically Relevant Ruthenium Complexes.

The treatment of **5** with phenol in a NMR tube in CD_2Cl_2 was followed by ^1H and $^{31}\text{P}\{^1\text{H}\}$ NMR. After 2 h of heating at $80\text{ }^\circ\text{C}$, a 1:1 ratio of cationic Ru-H **complex 1** and phenol-coordinated complex **8**, as evidenced by the appearance of new peaks at δ -10.87 and 70.8 ppm by ^1H and $^{31}\text{P}\{^1\text{H}\}$ NMR, respectively. The formation of free benzene molecule at $\delta = 7.4$ ppm was also observed by ^1H NMR. A series of substituted phenol-coordinated complexes are conveniently synthesized from the reaction of the tetranuclear Ru complex **4**, with phenol and $\text{HBF}_4\cdot\text{Et}_2\text{O}$. The structure of these phenol-coordinated complexes is readily determined by spectroscopic methods, and the solid state structures of **8a** and **8c** were also determined by X-ray crystallography (Figure 4.16-4.17).



6.3.10.1 Synthesis of phenol Coordinated Complexes:

In a glove box, tetrameric complex **4**, 100 mg 1 mol% and phenol 4 mol % were dissolved in CH_2Cl_2 (1 mL) in a 25 mL Schlenk tube equipped with a Teflon stopcock and a magnetic stirring bar. $\text{HBF}_4\cdot\text{OEt}_2$ (38 μL , 4 mol %) was added under stream of nitrogen. The mixture was stirred about 15 min at room temperature and solvent was removed under vacuum and filled with nitrogen. The schlenk tube was brought into glove box and solvent (Acetone or CH_2Cl_2) (2 mL) was added. Recrystallized by adding hexanes and the resultant

solid was filtered to obtain the pure phenol coordinated ruthenium complex in 70-95% yield.

To synthesize pure complex **9**, also prepared from the analogous treatment of **4** with 2-acetylphenol and $\text{HBF}_4 \cdot \text{Et}_2\text{O}$. Crude ^1H NMR shows > 95 % complex **9**.

Our attempt to crystallize the complex **9** led to a stable dimeric complex **10** which was **recrystallized** from $\text{CH}_2\text{Cl}_2/\text{n-pentane}$ solvent (scheme 4.5). It is isolated analytically pure complex **10** in 90 % yield. Structure of complex **10** also characterized by spectroscopic methods. The X-ray structure of complex **10** is shown in Fig. 6.23. Bridging Ru-H resonance was appeared at -28.30 ppm as triplet on ^1H NMR spectrum. Ru-P resonance on $^{31}\text{P}\{\text{H}\}$ NMR spectra found at 70.7 ppm.

6.3.10.2 Synthesis of Binuclear Bridging Hydroxyl Coordinated Ru complex **10**

100 mg of binuclear Ru-H complex **10** dissolved in 1 mL of wet 1,4-dioxane in inert atmosphere. The red colour solution was crystallized from hexanes to obtain pure binuclear Ru-hydroxo complex **11** in >95 % yield. The complex **11** was characterized using spectroscopic techniques. Bridging Ru-(μ -OH) resonance was appeared at -3.18 (s, 1H) ppm on ^1H NMR spectrum. Ru-P resonance on $^{31}\text{P}\{\text{H}\}$ NMR spectra found at 66.5 ppm. The structure of complex **11** was unambiguously characterized by single crystal X-ray diffraction (Figure 4.19).

Synthesis of Neutral Ru complex **14**;

Route 1: In a J-Young tube cationic ruthenium hydride **complex 1** (20 mg), mixed with 2 equivalence of PCy_3 (19 mg) in CH_2Cl_2 at 80 °C neutral Ru-H species **14** was formed in >95 % yield and at the same time 1 equivalence of H^+PCy_3 .

Route 2: 20 mg of complex **10** was mixed with 1 equivalence of PCy_3 in CH_2Cl_2 exclusively produces complex **14** without dimerization.

We were able to characterized the complex **14** by X-ray diffraction techniques and also by ^1H NMR and $^{31}\text{P}\{\text{H}\}$ NMR technique.

Route 3: 20 mg of copund **2**, chapter **3** was mixed with 1 quivalce of 2-acetylphenolate in dioxane solvents and heated at $80\text{ }^\circ\text{C}$ for 1h. The resultand uspension was filter under nitrogen atmosphere and the filtrate was crystalized with hexanes to obtained the complex **14** in $>95\%$ yield as an orange crystals.

6.3.11 X-Ray Crystallographic Determination of **8a**, **8a'**, **8c**, **8e**, **10** and **11**.

For **8a**: Colorless single crystals of **8a** were grown in acetone/n-pentane at room temperature. A suitable crystal with the dimension of $0.376 \times 0.2569 \times 0.1911\text{ mm}^3$ was selected and mounted on an Oxford SuperNova diffractometer equipped with dual microfocus Cu/Mo X-ray sources, X-ray mirror optics, and Atlas CCD area detector. A total of 35933 reflection data were collected by using $\text{MoK}\alpha$ ($\lambda = 0.71073$) radiation while the crystal sample was cooled at $100.00(10\text{ K})\text{ K}$ during the data collection. Using Olex2, the molecular structure was solved with the ShelXS structure solution program by using Direct Methods, and the data was refined with the XL refinement package using Least Squares minimization. The molecular structure of **8a** is shown in Figure 6.22.

For **8a'**: Colorless single crystals of **8a'** were grown in acetone/n-pentane at room temperature. A suitable crystal with the dimension of $0.4122 \times 0.143 \times 0.1397\text{ mm}^3$ was selected and mounted on an Oxford SuperNova diffractometer equipped with dual microfocus Cu/Mo X-ray sources, X-ray mirror optics, and Atlas CCD area detector. A total of 13359 reflection data were collected by using $\text{MoK}\alpha$ ($\lambda = 0.71073$) radiation while

the crystal sample was cooled at 100.00(10 K) K during the data collection. Using Olex2, the molecular structure was solved with the ShelXS structure solution program by using Direct Methods, and the data was refined with the XL refinement package using Least Squares minimization. The molecular structure of **8a'** is shown in Figure 6.23.

For **8c**: Colorless single crystals of **8c** were grown in acetone/n-pentane at room temperature. A suitable crystal with the dimension of $0.2975 \times 0.1164 \times 0.0395 \text{ mm}^3$ was selected and mounted on an Oxford SuperNova diffractometer equipped with dual microfocus Cu/Mo X-ray sources, X-ray mirror optics, and Atlas CCD area detector. A total of 30380 reflection data were collected by using MoK α ($\lambda = 0.71073$) radiation while the crystal sample was cooled at 100.00(10 K) K during the data collection. Using Olex2, the molecular structure was solved with the ShelXS structure solution program by using Direct Methods, and the data was refined with the XL refinement package using Least Squares minimization. The molecular structure of **8c** is shown in Figure 6.24.

For **8e**: Colorless single crystals of **8e** were grown in acetone/n-pentane at room temperature. A suitable crystal with the dimension of $0.3138 \times 0.2705 \times 0.1982 \text{ mm}^3$ was selected and mounted on an Oxford SuperNova diffractometer equipped with dual microfocus Cu/Mo X-ray sources, X-ray mirror optics, and Atlas CCD area detector. A total of 30380 reflection data were collected by using CuK α ($\lambda = 1.54184$) radiation while the crystal sample was cooled at 100.00(10 K) K during the data collection. Using Olex2, the molecular structure was solved with the ShelXS structure solution program by using Direct Methods, and the data was refined with the XL refinement package using Least Squares minimization. The molecular structure of **8e** is shown in Figure 6.25.

For **10**: Colorless single crystals of **10** were grown in acetone/n-pentane at room temperature. A suitable crystal with the dimension of $0.6545 \times 0.082 \times 0.0667 \text{ mm}^3$ was selected and mounted on an Oxford SuperNova diffractometer equipped with dual microfocus Cu/Mo X-ray sources, X-ray mirror optics, and Atlas CCD area detector. A total of 32469 reflection data were collected by using MoK α ($\lambda = 0.71073$) radiation while the crystal sample was cooled at 100.00(10 K) K during the data collection. Using Olex2, the molecular structure was solved with the ShelXS structure solution program by using Direct Methods, and the data was refined with the XL refinement package using Least Squares minimization. The molecular structure of **10** is shown in Figure 6.26.

For **11**: Colorless single crystals of **11** were grown in acetone/n-pentane at room temperature. A suitable crystal with the dimension of $0.2265 \times 0.1198 \times 0.0692 \text{ mm}^3$ was selected and mounted on an Oxford SuperNova diffractometer equipped with dual microfocus Cu/Mo X-ray sources, X-ray mirror optics, and Atlas CCD area detector. A total of 22228 reflection data were collected by using MoK α ($\lambda = 0.71073$) radiation while the crystal sample was cooled at 100.00(10 K) K during the data collection. Using Olex2, the molecular structure was solved with the ShelXS structure solution program by using Direct Methods, and the data was refined with the XL refinement package using Least Squares minimization. The molecular structure of **11** is shown in Figure 6.25.

For **14**: Colorless single crystals of **14** were grown in CH₂Cl₂/n-pentane at room temperature. A suitable crystal with the dimension of $0.1903 \times 0.0959 \times 0.044 \text{ mm}^3$ was selected and mounted on an Oxford SuperNova diffractometer equipped with dual microfocus Cu/Mo X-ray sources, X-ray mirror optics, and Atlas CCD area detector. A total of 32322 reflection data were collected by using CuK α ($\lambda = 1.54184$) radiation while

the crystal sample was cooled at 100.00(10 K) K during the data collection. Using Olex2, the molecular structure was solved with the ShelXS structure solution program by using Direct Methods, and the data was refined with the XL refinement package using Least Squares minimization. The molecular structure of **14** is shown in Figure 6.27.

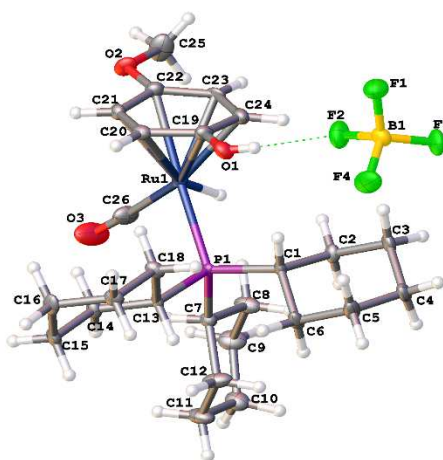


Figure 6.23. Molecular Structure of **8a**.

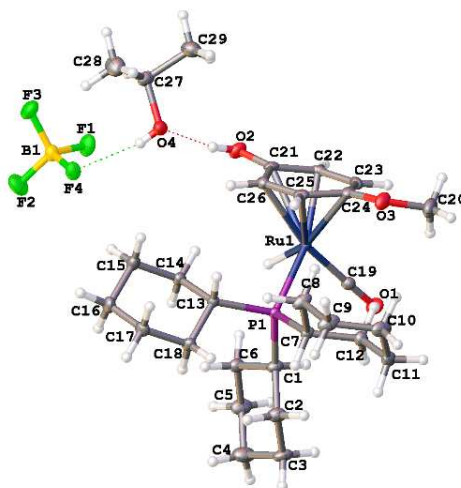


Figure 6.24: X-ray Structure of Complex **8a'**

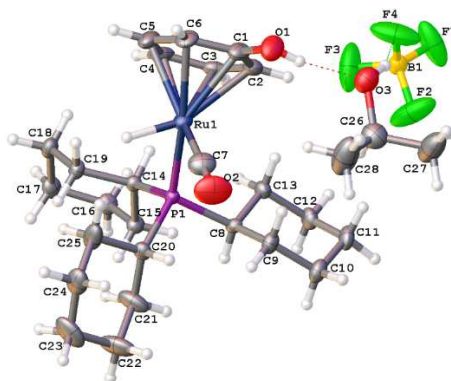


Figure 6.25. Molecular Structure of **8c**.

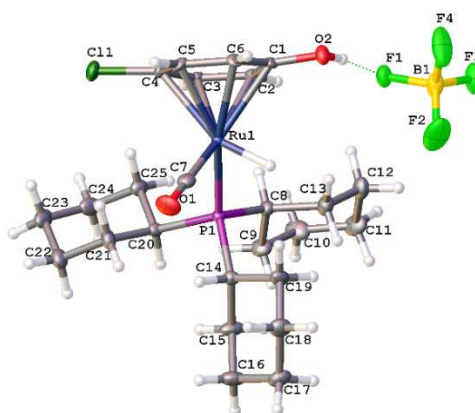


Figure 6.26. Molecular Structure of **8e**.

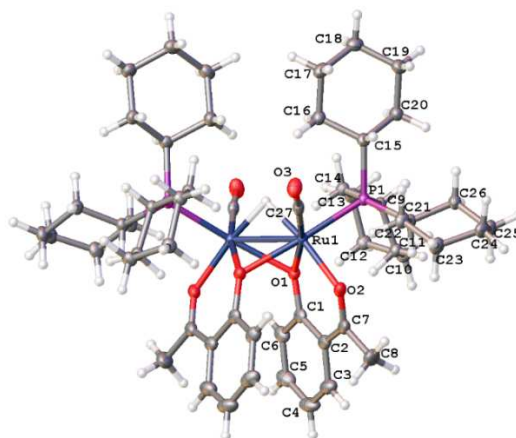


Figure 6.27. Molecular Structure of **10**.

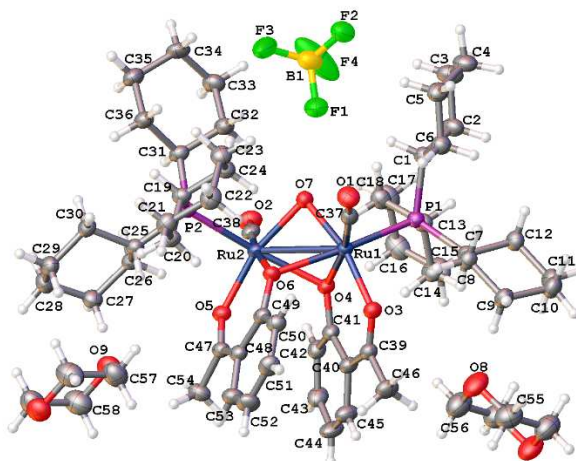


Figure 6.28. Molecular Structure of 11.

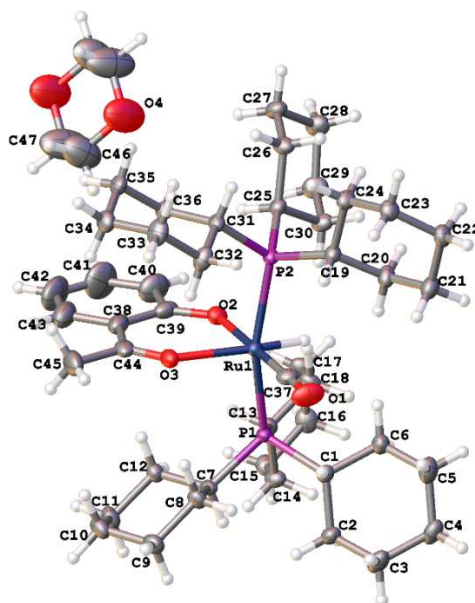


Figure 6.29: X-ray structure of complex 14

6.3.12 Characterization Data of the Products.

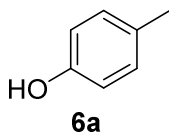


Table 4.2, Compound **6a**: Method A at 130 °C for 12 h. Analytically pure product **6a** was isolated by a column chromatography on silica gel (hexanes/EtOAc = 100:1). Yield: 97 mg, 90 %. Data for **6a**: ^1H NMR (400 MHz, CDCl_3) δ 7.02 (d, $J = 7.9$ Hz, 2H), 6.72 (d, $J = 7.9$ Hz, 2H), 5.0 (br s, 1H), 2.31 (s, 3H) ppm; $^{13}\text{C}\{^1\text{H}\}$ NMR (100 MHz, CDCl_3) δ 153.2, 130.2, 130.1, 115.2, 20.6 ppm; GC-MS $m/z = 108$ (M^+); ^1H and ^{13}C NMR spectral data are in good agreement with the literature data.⁴³

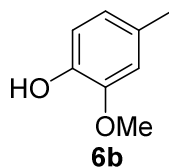


Table 4.2, Compound **6b**. Method A at 130 °C for 12 h. Analytically pure product **6b** was isolated by a column chromatography on silica gel (hexanes/EtOAc = 100:1). Yield: 131 mg, 95 %. Data for **6b**: ^1H NMR (400 MHz, CDCl_3) δ 6.85 (d, $J = 7.4$ Hz, 1H), 6.77-6.62 (m, 2H), 5.55 (s, 1H), 3.84 (s, 3H), 2.34 (s, 3H) ppm; $^{13}\text{C}\{^1\text{H}\}$ NMR (100 MHz, CDCl_3) δ 146.2, 143.3, 129.6, 121.5, 114.2, 111.7, 55.8, 21.0 ppm; GC-MS $m/z = 138$ (M^+); ^1H and ^{13}C NMR spectral data are in good agreement with the literature data.⁴⁴

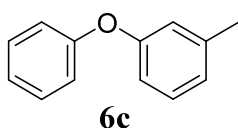


Table 4.2, Compound **6c**. Method A at 130 °C for 8 h. Analytically pure product **6c** was isolated by a column chromatography on silica gel (hexanes/EtOAc = 100:1). Yield: 169 mg, 92 %. Data for **6c**: ^1H NMR (400 MHz, CDCl_3) δ 7.33 (dd, $J = 8.5, 7.3$ Hz, 2H), 7.21 (dd, $J = 7.8, 7.6$ Hz, 1H), 7.09 (t, $J = 7.3$ Hz, 1H), 7.00 (d, $J = 8.5$ Hz, 2H), 6.92 (d, $J = 7.6$ Hz, 1H), 6.83 (s, 1H), 6.81 (d, $J = 7.8$ Hz, 1H), 2.33 (s, 3H) ppm; $^{13}\text{C}\{^1\text{H}\}$ NMR (100 MHz, CDCl_3) 157.6, 157.4, 140.2, 129.9,

129.7, 124.3, 123.3, 119.8, 119.1, 116.1, 21.6 ppm; GC-MS $m/z = 184$ (M^+); ^1H and ^{13}C NMR spectral data are in good agreement with the literature data.⁴⁵

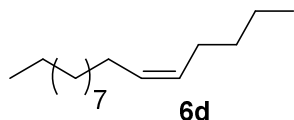


Table 4.2 Compound **6d**. Method A at 130 °C for 12 h. Analytically pure product **6d** was isolated by a column chromatography on silica gel (hexanes). Yield: 161 mg, 72 %. Data for **6d**: ^1H NMR (400 MHz, CDCl_3) δ 5.58-5.27 (m, 2H), 2.12-1.89 (m, 4H), 1.31-1.22 (m,

20H), 0.89 (t, $J = 7.0$ Hz, 6H) ppm; $^{13}\text{C}\{^1\text{H}\}$ NMR (100 MHz, CDCl_3) δ 130.4, 129.9, 77.4, 32.6, 32.3, 31.9, 31.6, 29.72, 29.71, 29.5, 29.4, 29.2, 29.2, 29.1, 22.7, 14.1 ppm; GC-MS $m/z = 224$ (M^+); ^1H and ^{13}C NMR spectral data are in good agreement with the literature data.⁴⁶

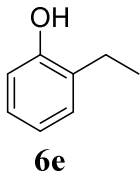


Table 4.2 Compound **6e**. Method A at 120 °C for 8 h. Analytically pure product **6e** was isolated by a column chromatography on silica gel (hexanes/EtOAc = 100:1). Yield: 122 mg, 94 %. Data for **6e**: ^1H NMR (400 MHz, CDCl_3) δ 7.14 (d, $J = 7.2$ Hz, 1H), 7.83 (t, $J = 7.9$ Hz, 1H), 6.89 (t, $J = 7.6$ Hz, 1H), 6.76 (d, $J =$

7.6 Hz, 1H), 4.76 (br s, 1H), 2.75 (q, $J = 7.2$ Hz, 2H), 1.25 (t, $J = 7.2$ Hz, 3H) ppm; $^{13}\text{C}\{^1\text{H}\}$ NMR (100 MHz, CDCl_3) δ 129.4, 127.1, 121.0, 115.2, 23.0, 14.1 ppm; GC-MS $m/z = 122$ (M^+); ^1H and ^{13}C NMR spectral data are in good agreement with the literature data.⁴⁷

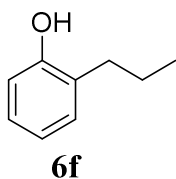


Table 4.2 Compound **6f**. Method A at 130 °C for 8 h. Analytically pure product **6f** was isolated by a column chromatography on silica gel (hexanes/EtOAc = 10:1). Yield: 151 mg, 91 %. Data for **6f**: ^1H NMR (400 MHz, CDCl_3) δ 1.08 (t, J = 9.0 Hz, 3H), 1.70-1.82 (m, 2H), 2.71 (m, 2H), 5.73 (s, 1H), 6.84-7.24 (m, 4H) ppm; $^{13}\text{C}\{^1\text{H}\}$ NMR (100 MHz, CDCl_3) δ 154.0, 130.8, 129.2, 127.5, 115.8, 121.1, 32.5, 23.4, 14.5 ppm; GC-MS m/z = 136 (M^+); ^1H and ^{13}C NMR spectral data are in good agreement with the literature data.⁴⁸

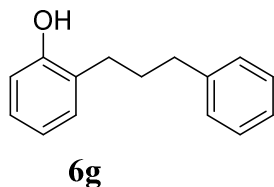


Table 4.2 Compound **6g**. Method A at 130 °C for 8 h. Analytically pure product **6g** was isolated by a column chromatography on silica gel (hexanes/EtOAc = 20:1). Yield: 196 mg, 92 %. Data for **6g**: ^1H NMR (400 MHz, CDCl_3) δ 7.28-7.19 (m, 3H), 7.38-7.28 (m, 2H), 7.19-7.09 (m, 2H), 6.95-6.87 (m, 1H), 6.77 (d, J = 8.2 Hz, 1H), 4.82 (s, 1H), 2.71 (dt, J = 15.7, 7.8 Hz, 4H), 2.00 (quintet, J = 7.8 Hz, 2H) ppm; $^{13}\text{C}\{^1\text{H}\}$ NMR (100 MHz, CDCl_3) δ 153.4, 142.2, 130.1, 128.4, 128.3, 128.1, 127.1, 125.7, 120.7, 115.2, 35.5, 31.2, 29.4 ppm; GC-MS m/z = 214 (M^+); ^1H and ^{13}C NMR spectral data are in good agreement with the literature data.⁴⁹

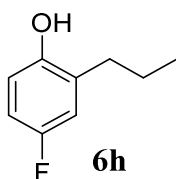
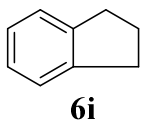


Table 4.2 Compound **6h**. Method A at 130 °C for 8 h. Analytically pure product **6h** was isolated by a column chromatography on silica gel (hexanes/EtOAc = 20:1). Yield: 140 mg, 91 %. Data for **6h**: ^1H NMR (400 MHz, CDCl_3) δ 6.86-6.67 (m, 3H), 5.18 (s, 1H), 2.53 (t, J = 7.7 Hz, 2H), 1.62 (m, 2H),

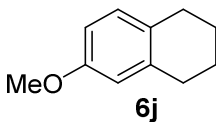
0.92 (t, $J = 7.4$ Hz, 3H) ppm; $^{13}\text{C}\{^1\text{H}\}$ NMR (100 MHz, CDCl_3) δ 157.2 (d, $J_{\text{C-F}} = 236.0$ Hz), 149.5, 130.3 (d, $J_{\text{C-F}} = 7.6$ Hz), 116.4 (d, $J_{\text{C-F}} = 22.9$ Hz), 115.7 (d, $J_{\text{C-F}} = 25.0$ Hz), 112.9 (d, $J_{\text{C-F}} = 25.0$ Hz), 32.0, 22.7, 13.9 ppm; GC-MS $m/z = 154$ (M^+); ^1H and ^{13}C NMR spectral data are in good agreement with the literature data.⁵⁰

Table 4.2 Compound **6i** Method A at 130 °C for 16 h.



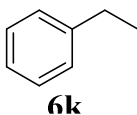
Analytically pure product **6i** was isolated by a column chromatography on silica gel (hexanes). Yield: 165 mg, 90 %. Data for **6i**: ^1H NMR (400 MHz, CDCl_3) δ 7.29-7.24 (m, 2H), 7.18-7.15 (m, 2H), 2.95 (t, $J = 7.5$ Hz, 4H), 2.10 (quintet, $J = 7.4$ Hz, 2H) ppm; $^{13}\text{C}\{^1\text{H}\}$ NMR (100 MHz, CDCl_3) δ 144.1, 125.9, 124.3, 32.8, 25.3 ppm; GC-MS $m/z = 106$ (M^+); ^1H and ^{13}C NMR spectral data are in good agreement with the literature data.⁵¹

Table 4.2 Compound **6j**. Method A at 120 °C for 16 h.



Analytically pure product **6j** was isolated by a column chromatography on silica gel (hexanes/diethylether = 100:1). Yield: 150 mg, 93 %. Data for **6j**: ^1H NMR (400 MHz, CDCl_3) δ 6.98 (d, $J = 8.4$ Hz, 1H), 6.68 (dd, $J = 8.4, 2.8$ Hz, 1H), 6.61 (d, $J = 2.8$ Hz, 1H), 3.75 (s, 3H), 2.68 - 2.78 (m, 4H), 1.76-1.80 (m, 4H) ppm; $^{13}\text{C}\{^1\text{H}\}$ NMR (100 MHz, CDCl_3) δ 157.5, 138.3, 130.1, 129.4, 113.8, 111.9, 55.4, 29.9, 28.7, 23.6, 23.3 ppm; GC-MS $m/z = 162$ (M^+); ^1H and ^{13}C NMR spectral data are in good agreement with the literature data.⁵²

Table 4.2 Compound **6k**. Method A at 130 °C for 12 h.



Analytically pure product **6k** was isolated by a column chromatography

on silica gel (hexanes). Yield: 101 mg, 79 %. Data for **6k**: ^1H NMR (400 MHz, CDCl_3) δ 7.24-7.27 (m, 2H), 7.13-7.18 (m, 3H), 2.60-2.65 (q, 2H), 1.20-1.24 (t, 3H) ppm; $^{13}\text{C}\{^1\text{H}\}$ NMR (100 MHz, CDCl_3) δ 144.4, 128.4, 128.0, 125.7, 29.0, 16.0 ppm; GC-MS m/z = 128 (M^+). ^1H and ^{13}C NMR spectral data are in good agreement with the literature data.⁵³

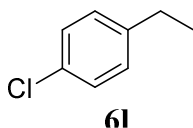


Table 4.2 Compound **6l**. Method A at 130 °C for 12 h.

Analytically pure product **6l** was isolated by a column chromatography on silica gel (hexanes/EtOAc = 100:1). Yield: 113 mg, 82 %. Data for **6l**: ^1H NMR (400 MHz, CDCl_3) δ 7.25 (d, J = 8.8 Hz, 2H), 7.13 (d, J = 8.6 Hz, 2H), 2.63 (q, J = 7.6 Hz, 2H), 1.23 (t, J = 7.6 Hz, 3H); $^{13}\text{C}\{^1\text{H}\}$ NMR (100 MHz, CDCl_3) δ 142.7, 131.3, 129.8, 128.5, 28.4, 15.7 ppm; GC-MS m/z = 140 (M^+). ^1H and ^{13}C NMR spectral data are in good agreement with the literature data.⁵⁴

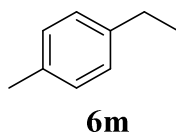


Table 4.2 Compound **6m**. Method A 130 °C for 12 h.

Analytically pure product **6m** was isolated by a column chromatography on silica gel (hexanes/ Et_2O = 100:1); Yield: 110 mg, 92 %. Data for **6m**: ^1H NMR (400 MHz, CDCl_3) δ 7.08-6.98 (m, 4H); 3.40 (q, J = 7.0 Hz, 2H), 2.15 (s, 3H), 1.13 (t, J = 7.0 Hz, 3H) ppm; $^{13}\text{C}\{^1\text{H}\}$ NMR (100 MHz, CDCl_3) δ 141.2, 138.1, 131.2, 127.4, 29.1, 21.2, 16.9 ppm; GC-MS m/z = 120 (M^+). ^1H and ^{13}C NMR spectral data are in good agreement with the literature data.⁵⁵

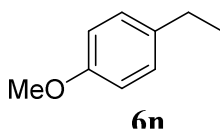


Table 4.2 Compound **6n**. Method A and B at 130 °C for 12

h. Analytically pure product **6n** was isolated by a column chromatography on silica gel (hexanes/EtOAc = 40:1). Yield: 132 mg, 95 %. Data for **6n**: ^1H NMR (400 MHz, CDCl_3) δ 7.14 (d, J = 8.7 Hz, 2H), 6.85 (d, J = 8.7 Hz, 2H), 3.81 (s, 3H), 2.61 (q, J = 7.5 Hz, 2H), 1.23 (t, J = 7.5 Hz, 3H) ppm;

$^{13}\text{C}\{^1\text{H}\}$ NMR (100 MHz, CDCl_3) δ 157.5, 136.3, 128.7, 113.7, 55.2, 27.9, 15.9 ppm; GC-MS m/z = 136 (M^+). ^1H and ^{13}C NMR spectral data are in good agreement with the literature data.⁵⁶

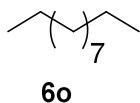


Table 4.2 Compound **6o**. Method A at 130 °C for 24 h.

Analytically pure product **6o** was isolated by a column chromatography on silica gel (hexanes). Yield: 65 % (GC). Data for

6o: ^1H NMR (400 MHz, CDCl_3) δ 1.21-1.44 (m, 18H), 0.91 (t, J = 6.8 Hz, 6H) ppm; $^{13}\text{C}\{^1\text{H}\}$ NMR (100 MHz, CDCl_3) δ 32.0, 29.8, 29.8, 29.47, 22.8, 14.1 ppm; GC-MS m/z = 156 (M^+). ^1H and ^{13}C NMR spectral data are in good agreement with the literature data.⁵⁷

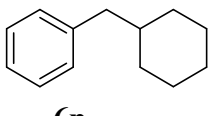


Table 4.2 Compound **6p**. Method A at 130 °C for 24 h.

Analytically pure product **6p** was isolated by a column chromatography on silica gel (hexanes/EtOAc = 20:1). Yield: 94 mg,

54 %. Data for **6p**: ^1H NMR (400 MHz, CDCl_3) δ 7.26-7.20 (m, 3H), 7.05-6.92 (m, 2H), 2.39 (d, J = 6.2 Hz, 2H), 1.80-1.66 (m, 5H), 1.46-1.33 (m, 1H), 1.21-1.12 (m, 3H), 0.88-0.71 (m, 2H) ppm; $^{13}\text{C}\{^1\text{H}\}$ NMR (100 MHz, CDCl_3) δ 138.7, 128.6, 128.2, 126.0, 41.0, 38.9, 33.2, 28.3, 25.8 ppm; GC-MS m/z = 174 (M^+); ^1H and ^{13}C NMR spectral data are in good agreement with the literature data.⁵⁸

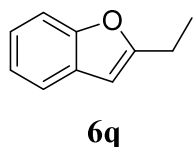


Table 4.2 Compound **6q**. Method A at 130 °C for 12 h.

Analytically pure product **6q** was isolated by a column chromatography on silica gel (hexanes/EtOAc = 20:1). Colorless

liquid; Yield: 144 mg, 95 %. Data for **6q**: ^1H NMR (400 MHz, CDCl_3) δ 7.48 (m, 1H), 7.40 (m, 1H), 7.18 (m, 2H), 6.37 (d, J = 1.2 Hz, 1H), 2.81 (q, J = 7.6 Hz, 2H), 1.34 (t, J = 7.6 Hz, 3H) ppm; $^{13}\text{C}\{^1\text{H}\}$ NMR (100 MHz, CDCl_3) δ 158.5, 154.9, 129.0,

123.0, 122.3, 120.2, 110.7, 101.1, 21.9, 11.9 ppm; GC-MS $m/z = 146$ (M^+); ^1H and ^{13}C NMR spectral data are in good agreement with the literature data.⁵⁹

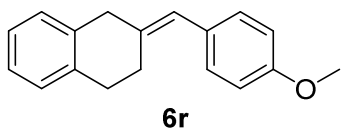


Table 4.2 Compound **6r** Method B at 130 °C for 24 h. Analytically pure product **6r** was isolated by a column chromatography on silica gel (hexanes/EtOAc = 100:1). Yield: 212 mg, 85 %; Data for **6r**: ^1H NMR (400 MHz, CDCl_3) δ 7.18-7.10 (m, 3H), 7.10-7.07 (m, 2H), 7.00 (d, $J = 7.0$ Hz, 1H), 6.85 (d, $J = 8.7$ Hz, 2H), 6.25 (s, 1H), 3.81 (s, 3H) 3.46 (s, 1H), 2.78 (t, $J = 8.2$ Hz, 2H), 2.19 (t, $J = 8.2$ Hz, 2H) ppm; $^{13}\text{C}\{^1\text{H}\}$ NMR (100 MHz, CDCl_3) δ 158.1, 141.2, 134.8, 134.4, 131.4, 130.0, 127.2, 126.4, 126.3, 125.6, 123.6, 113.8, 55.3, 42.9, 28.2, 27.0 ppm; GC-MS $m/z = 250$ (M^+); Anal. Calcd for $\text{C}_{18}\text{H}_{18}\text{O}$: C, 86.36; H, 7.25. Found: C, 86.29; H, 7.19.

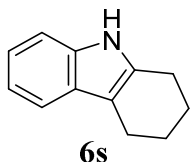


Table 4.2 Compound **6s**. Method A at 130 °C for 24 h. Analytically pure product **6s** was isolated by a column chromatography on silica gel (hexanes/EtOAc = 20:1). Yield: 94 mg, 55 %. Data for **6s**: ^1H NMR (400 MHz, CDCl_3) δ 7.66 (br s, 1H), 7.46 (d, $J = 7.0$ Hz, 1H), 7.29-7.27 (m, 1H), 7.13-7.05 (m, 2H), 2.75-2.70 (m, 4H), 1.95-1.84 (m, 4H) ppm; $^{13}\text{C}\{^1\text{H}\}$ NMR (100 MHz, CDCl_3) δ 135.6, 134.0, 127.8, 120.9, 119.1, 117.7, 110.3 (2C), 23.3, 23.2, 23.2, 20.9 ppm; GC-MS $m/z = 171$ (M^+). ^1H and ^{13}C NMR spectral data are in good agreement with the literature data.⁶⁰

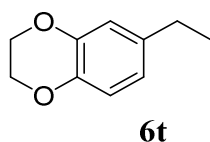


Table 4.2 Compound **6t**. Method A at 130 °C for 12 h. Analytically pure product **6t** was isolated by a column chromatography on silica gel (hexanes/EtOAc = 20:1; Yield: 147

mg, 90 %. Data for **6t**: ^1H NMR (400 MHz, CDCl_3) δ 6.81-6.67 (m, 1H), 6.74-6.66 (m, 2H), 4.25 (s, 4H), 2.56 (q, $J = 7.6$ Hz, 2H), 1.21 (t, $J = 7.6$ Hz, 3H) ppm; $^{13}\text{C}\{^1\text{H}\}$ NMR (100 MHz, CDCl_3) δ 143.2, 141.4, 137.6, 120.1, 116.9, 116.4, 64.4, 64.3, 28.1, 15.7 ppm; GC-MS $m/z = 164$ (M^+); Anal. Calcd for $\text{C}_{10}\text{H}_{12}\text{O}_2$: C, 73.15; H, 7.37. Found: C, 73.20; H, 7.34.

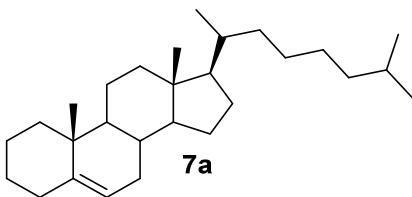


Table 4.2 Compound **7a**. Method B at 130 °C for 12 h. Analytically pure product **7a** was isolated by a column chromatography on silica gel (hexanes/EtOAc = 100:1). Yield: 215 mg, 56 %.

Data for **7a**: ^1H NMR (400 MHz, CDCl_3) δ 5.30-5.28 (m, 1H), 2.32-2.18 (m, 1H), 2.10-1.93 (m, 3H), 1.90-1.81 (m, 2H), 1.79-1.69 (m, 1H), 1.63-0.92 (m, 23H), 1.00 (s, 3H), 0.92 (d, $J = 6.4$ Hz, 3H), 0.90 (d, $J = 1.3$ Hz, 3H), 0.88 (d, $J = 1.3$ Hz, 3H), 0.70 (s, 3H) ppm; $^{13}\text{C}\{^1\text{H}\}$ NMR (100 MHz, CDCl_3) δ 143.7, 119.0, 56.8, 56.1, 50.6, 42.31, 39.9, 39.8, 39.5, 37.5, 36.2, 35.8, 32.9, 31.9, 31.8, 28.2, 28.0, 28.0, 24.3, 23.8, 22.8, 22.5, 20.7, 19.5, 18.7, 11.8 ppm; GC-MS $m/z = 370$ (M^+); ^1H and ^{13}C NMR spectral data are in good agreement with the literature data.⁶¹

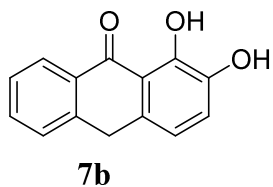


Table 4.2 Compound **7b**. Method A at 130 °C for 24 h. Analytically pure product **7b** was isolated by a column chromatography on silica gel (CH_2Cl_2 /methanol = 100:1). Orange solid; Yield: 151 mg, 67%. Data for **7b**:

^1H NMR (400 MHz, CDCl_3) δ 12.76 (s, 1H), 7.99 (dd, $J = 8.0, 1.2$ Hz, 1H), 7.22-7.40 (m, 1H), 7.06-7.21 (m, 2H), 6.87 (d, $J = 8.0$ Hz, 2H), 6.53 (dt, $J = 8.2, 1.1$ Hz, 2H), 5.41 (br.s, 1H), 3.97 (s, 2H) ppm; $^{13}\text{C}\{^1\text{H}\}$ NMR (100 MHz, CDCl_3) δ 190.1, 149.3, 142.8, 142.6,

133.7, 133.5, 132.2, 130.8, 128.5, 127.0, 120.7, 118.2, 31.8 ppm; GC-MS $m/z = 226$ (M^+).

^1H and ^{13}C NMR spectral data are in good agreement with the literature data.⁶³

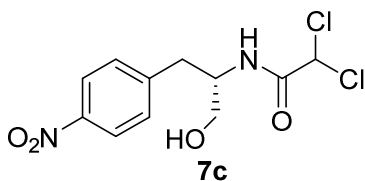


Table 4.2 Compound **7c**. Method B at 150 °C for 12 h. Analytically pure product **7c** was isolated by a column chromatography on silica gel (hexanes/EtOAc = 4:1). Yield: 137 mg, 45%. Data for **7c**: ^1H NMR (400

MHz, CDCl_3) δ 8.13 (d, $J = 8.5$ Hz, 2H), 7.50 (d, $J = 8.8$ Hz, 2H), 7.03 (d, $J = 9.0$ Hz, 1H), 5.74 (s, 1H), 5.26 (t, $J = 3.3$ Hz, 1H), 4.22 (tdd, $J = 8.4, 8.4, 5.2, 2.9$ Hz, 1H), 3.73 (dd, $J = 11.1, 8.0$ Hz, 1H), 3.57-3.51 (m, 2H) ppm; $^{13}\text{C}\{^1\text{H}\}$ NMR (100 MHz, CDCl_3) δ 164.4, 147.7, 126.7, 126.7, 123.7, 70.3, 65.9, 56.5, 42.7 ppm; GC-MS $m/z = 306$ (M^+); ^1H and ^{13}C NMR spectral data are in good agreement with the literature data.⁶²

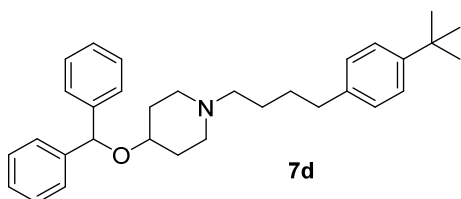


Table 4.2 Compound **7d**. Method B at 150 °C for 12 h. Analytically pure product **7d** was isolated by a column chromatography on silica gel (hexanes/EtOAc = 4:1). White solid; Yield:

382 mg, 84 %. Data for **7d**: ^1H NMR (400 MHz, CDCl_3) δ 7.31-7.11 (m, 12H), 7.02 (d, $J = 8.1$ Hz, 2H), 5.44 (s, 1H), 3.40-3.29 (m, 1H), 2.70-2.59 (m, 2H), 2.50 (t, $J = 7.5$ Hz, 2H), 2.27-2.18 (m, 2H), 2.09-1.93 (m, 2H), 1.86-1.74 (m, 2H), 1.71-1.59 (m, 2H), 1.57-1.37 (m, 5H), 1.25-1.19 (m, 9H) ppm; $^{13}\text{C}\{^1\text{H}\}$ NMR (100 MHz, CDCl_3) δ 148.3, 142.8, 139.4, 128.3, 128.0, 127.2, 127.1, 125.1, 79.9, 58.6, 51.19, 51.18, 51.17, 35.2, 34.3, 31.4, 29.5, 26.9 ppm; GC-MS $m/z = 455$ (M^+); HRMS (ESI) Calcd for $[\text{M}+\text{H}]^+$ $\text{C}_{32}\text{H}_{41}\text{NO}$: 456.3251 Found: 456.3266.

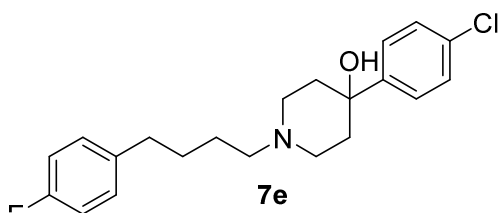


Table 4.2 Compound **7e**. Method B at 150 °C for 12 h. Analytically pure product **7e** was isolated by a column chromatography on silica gel (CH₂Cl₂/MeOH = 80:1). White

solid; Yield: 220 mg, 68 %. Data for **7e**: ¹H NMR (400 MHz, CDCl₃) δ 6.76-7.03 (m, 8H), 3.43 - 3.47 (m, 1H), 2.67-2.80 (m, 2H), 2.27-2.39 (m, 2H), 2.10-2.23 (m, 1H), 2.02-2.10 (m, 2H), 1.64-1.76 (m, 2H), 1.39-1.57 (m, 3H), 1.18-1.39 (m, 4H) ppm; ¹³C {¹H} NMR (100 MHz, CDCl₃) δ 144.8(d, J_{C-F} = 249 Hz), 129.6 (d, J_{C-F} = 7.8 Hz), 128.4 (d, J_{C-F} = 6.9 Hz), 128.2 (d, J_{C-F} = 5.9 Hz), 126.8, 125.6, 115.0, 114.8, 58.9, 54.3, 42.1, 35.8, 33.4, 29.5, 26.9 ppm; GC-MS *m/z* = 361 (M⁺); HRMS (ESI) Calcd for [M+H]⁺ C₂₁H₂₅ClFNO: 362.8934 Found: 362.8938

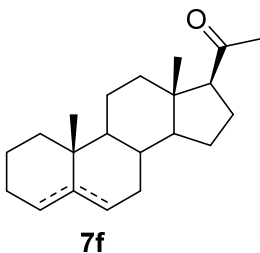


Table 4.2 Compound **7f**. Method B at 130 °C for 12 h. Analytically pure product was isolated by The product **7f** was isolated by a column chromatography on silica gel (hexanes/EtOAc = 100:1). White solid; Yield: 156 mg, 52 %.(two isomer were not separated assign by comparing literature data) Data for **7f**: ¹H NMR (400 MHz, CDCl₃) δ 5.28 (br. s, 1H),

5.24 (dt, *J* = 5.4, 1.9 Hz, 1H), 2.51 (td, *J* = 8.9, 6.5 Hz, 2H), 2.11-2.26 (m, 4H), 2.09 (s, 6H), 1.05-2.04 (m, 40 H), 0.90 (s, 3H), 0.76 (d, *J* = 0.4 Hz, 3H), 0.57 (s, 3H), 0.56 (s, 3H) ppm; ¹³C {¹H} NMR (100 MHz, CDCl₃) δ 209.6, 209.6, 144.5, 143.5, 119.2, 118.6, 63.9, 63.8, 56.8, 56.77, 54.5, 46.9, 44.3, 43.5, 40.4, 39.3, 39.1, 38.6, 37.5, 36.2, 35.8, 35.4, 32.0, 28.9, 28.8, 27.3, 27.1, 26.9, 26.7, 26.5, 24.4, 24.3, 24.1, 22.8, 22.6, 22.1, 21.2, 20.7, 20.75,

13.4, 13.36, 12.1 ppm; GC-MS $m/z = 300$ (M^+); ^1H and ^{13}C NMR spectral data are in good agreement with the literature data.⁶¹

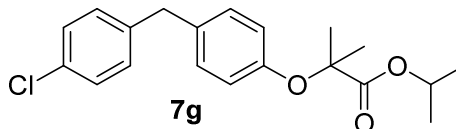
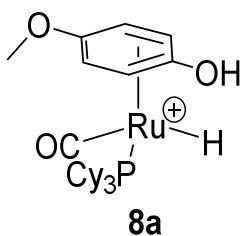
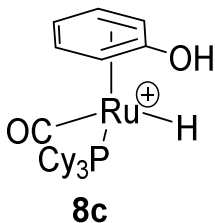


Table 4.2 Compound **7g**. Method B at 130 °C for 12 h. Analytically pure product was isolated by The product **7g** was isolated by a column chromatography on silica gel (hexanes/EtOAc = 100:1). White solid; Yield: 249 mg, 72 %. Data for **7g**: ^1H NMR (400 MHz, CDCl_3) δ 6.90-6.97 (m, 2H), 6.76-6.81 (m, 2H), 6.68-6.74 (m, 2H), 6.45-6.53 (m, 2H), 4.78 (spt, $J = 6.90$ Hz, 1H), 3.57 (s, 2H), 1.28 (s, 6H), 0.92 (d, $J = 6.28$ Hz, 6H) ppm; $^{13}\text{C}\{^1\text{H}\}$ NMR (100 MHz, CDCl_3) δ 173.7, 154.0, 139.8, 134.0, 131.8, 130.2, 129.4, 128.5, 119.1, 79.1, 68.9, 40.4, 25.4, 21.6 ppm; GC-MS $m/z = 346$ (M^+); HRMS (ESI) Calcd for $[\text{M}+\text{H}]^+ \text{C}_{20}\text{H}_{24}\text{ClO}_3$:.347.1414 Found: 347.1412.

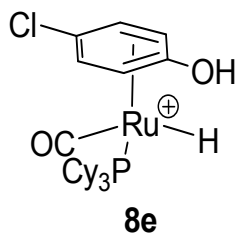


Synthesis of Complex 8a. Same procedure as **8c** was repeated using 4-methoxyphenol (60 mg, 0.48 mmol) as the phenol ligand. Kept in glove box for 3 days for crystallization and filtered the resulting solid through a fritted funnel yielded the product as a white crystals (198 mg, ca. 76 % yield). Single crystals of **8a** suitable for X-ray crystallography were obtained from acetone/*n*-pentane solution. Data for **8a**: ^1H NMR (400 MHz, CDCl_3) δ 6.44 (dd, $J = 7.2, 2.3$ Hz, 1H), 6.36 (dd, $J = 7.4, 2.6$ Hz, 1H), 3.79 (s, 3H) 6.00-6.15 (m, 2H), 1.79-2.06 (m, 15H), 2.18 (s, 2H), 1.63-1.79 (m, 3H), 1.22-1.51 (m, 16H), -10.61 (d, $J_{\text{PH}} = 27.0$ Hz, 1H) ppm; $^{13}\text{C}\{^1\text{H}\}$ NMR (100 MHz, CDCl_3) δ 198.6 (d, $J_{\text{C-P}} = 18.8$ Hz) 87.6, 87.5, 85.0, 84.2, 57.8, 37.7, 37.5, 30.8, 30.1, 27.9, 27.8, 26.7 ppm; FT-IR (Solid) $\nu_{\text{CO}} = 1963 \text{ cm}^{-1}$; $^{31}\text{P}\{^1\text{H}\}$ NMR (400 MHz,

CDCl_3) δ 71.38 ppm; HRMS (ESI) Calcd for $[\text{M}]^+$ $\text{C}_{26}\text{H}_{42}\text{O}_3\text{PRu}$: 535.1912 Found: 535.1917.

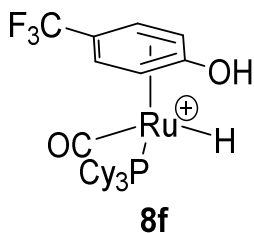


Synthesis of Complex 8c. In a glove box, the tetrameric ruthenium complex $\{[(\text{PCy}_3)(\text{CO})\text{RuH}]_4(\mu\text{-O})(\mu\text{-OH})_2\}$ (**4**) (200 mg, 0.12 mmol) and Phenol (44 mg, 0.48 mmol) were dissolved in CH_2Cl_2 (5 mL) in a 25 mL Schlenk tube equipped with a teflon screw cap stopcock and a magnetic stirring bar. The tube was brought out of the box, and $\text{HBF}_4 \cdot \text{OEt}_2$ (64 μL , 0.48 mmol) was added under N_2 stream. The color of the solution was changed from dark red to light yellow immediately. After stirring for 1 h at room temperature, the solvent was removed under vacuum, and the residue was transferred to glove box. Then the residue washed with hexanes and dried. It was dissolved in acetone (2 mL) and layered with *n*-pentane (2 mL). Kept in glove box for 3 days for crystallization and filtered the resulting solid through a fritted funnel yielded the product as a white crystals (210 mg, ca. 76 % yield). Single crystals of **8c** suitable for X-ray crystallography were obtained from acetone/*n*-pentane solution. Data for **8c**: ^1H NMR (400 MHz, CDCl_3) δ 9.11 (br. s, 1H), 6.62-6.70 (m, 1H), 6.54-6.62 (m, 1H), 6.33 (d, $J = 7.0$ Hz, 1H), 5.91 (d, $J = 5.5$ Hz, 1H), 5.69 (t, $J = 5.9$ Hz, 1H), 0.76-2.45 (m, 33H), -10.86 (d, $J_{\text{PH}} = 27.1$ Hz, 1H) ppm; $^{13}\text{C}\{^1\text{H}\}$ NMR (100 MHz, CDCl_3) δ 197.6 (d, $J_{\text{C-P}} = 18.1$ Hz), 148.8, 103.8, 103.6, 88.1, 85.4, 84.8, 38.3, 37.9, 30.7, 30.1, 30.1, 27.9, 27.7, 26.7 ppm; $^{31}\text{P}\{^1\text{H}\}$ NMR (400 MHz, CDCl_3) δ 70.78 ppm; FT-IR (Solid) $\nu_{\text{CO}} = 1973$ cm^{-1} ; HRMS (ESI) Calcd for $[\text{M}]^+$ $\text{C}_{25}\text{H}_{40}\text{O}_2\text{PRu}$: 505.1902 Found: 505.1911.

Synthesis of Complex 8e. Same procedure as **8a** was

repeated using 4-chlorophenol (60 mg, 0.48 mmol) as the phenol ligand. Crushed out with hexane and the solid filtered the resulting solid through a fritted funnel yielded the product as a white solid (180 mg, ca. 72 % yield). Growing single

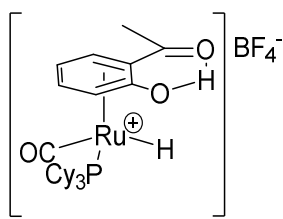
crystal was unsuccessful. Data for **8e**: ^1H NMR (400 MHz, CDCl_3) δ 6.75-6.85 (m, 1H), 6.68 (d, $J = 7.00$ Hz, 1H), 6.17 (d, $J = 5.44$ Hz, 1H), 5.98 (d, $J = 6.70$ Hz, 1H), 0.98 - 2.04 (m, 33H), -10.40 (d, $J = 27.4$ Hz, 1H) ppm; FT-IR (Solid) $\nu_{\text{CO}} = 1983$ cm^{-1} ; $^{13}\text{C}\{^1\text{H}\}$ NMR (100 MHz, CDCl_3) δ 196.2 (d, $J_{\text{CP}} = 18.0$ Hz) 104.1, 101.8, 85.7, 82.9, 37.9, 37.6, 30.6, 39.9, 27.8, 27.6, 26.5 ppm; $^{31}\text{P}\{^1\text{H}\}$ NMR (400 MHz, CDCl_3) δ 71.86 ppm; HRMS (ESI) Calcd for $[\text{M}]^+$ $\text{C}_{25}\text{H}_{39}\text{ClO}_2\text{PRu}$: 539.1420 Found: 539.1417.

Synthesis of Complex 8f. Same procedure as **8a** was

repeated using 4-(trifluoromethyl)phenol (78 mg, 0.48 mmol) as the phenol ligand. Crushed out with hexane and the solid filtered the resulting solid through a fritted funnel yielded the product as a white solid (198 mg, ca. 76 % yield).

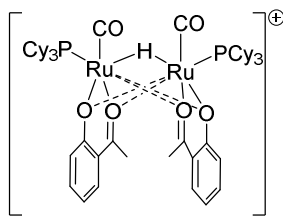
Growing single crystal was unsuccessful. Data for **8f**: ^1H NMR (400 MHz, CDCl_3) δ 9.68 (br.s., 1H), 7.01 (d, $J = 6.60$ Hz, 1H), 6.81 (d, $J = 6.97$ Hz, 1H), 6.64 (d, $J = 6.24$ Hz, 1H), 5.64 (d, $J = 6.60$ Hz, 1H), 1.76-1.95 (m, 22H), 1.17-1.32 (m, 18H), -10.55 (d, $J = 26.00$ Hz, 1 H) ppm; FT-IR (Solid) $\nu_{\text{CO}} = 1947$ cm^{-1} ; $^{31}\text{P}\{^1\text{H}\}$ NMR (400 MHz, CDCl_3) δ 71.38 ppm;

Synthesis of 9. In a glove box, the tetrameric ruthenium complex $\{[(\text{PCy}_3)(\text{CO})\text{RuH}]_4(\mu\text{-O})(\mu\text{-OH})_2\}$ (**4**) (200 mg, 0.12 mmol) and 2-hydroxyacetophenone

**9**

(64 mg, 0.48 mmol) were dissolved in CH_2Cl_2 (5 mL) in a 25 mL Schlenk tube equipped with a teflon screw cap stopcock and a magnetic stirring bar. The tube was brought out of the box, and $\text{HBF}_4 \cdot \text{OEt}_2$ (64 μL , 0.48 mmol) was added under N_2 stream.

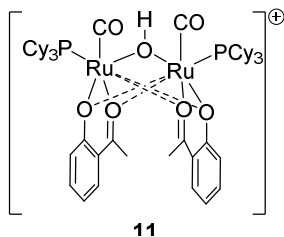
The color of the solution was changed from dark red to light red immediately. After stirring for 1 h at room temperature, the solvent was removed under vacuum, and *n*-hexane (10 mL) was added to the residue. The resulting solid was filtered through a fritted funnel. Then the residue washed with hexanes and dried to yield the product as an orange residue (281 mg, 82% yield). The product was analyzed by NMR. Spectroscopic Data for **9**: ^1H NMR (400 MHz, CDCl_3) δ 8.98 (br. s, 1H), 6.57 (t, $J = 6.4$ Hz, 1H), 6.23 (d, $J = 6.6$ Hz, 1H), 5.91 (d, $J = 6.1$ Hz, 1H), 5.68 (t, $J = 5.9$ Hz, 1H), 2.07-1.61 (m, 20H), 1.46-1.14 (m, 17H), -10.87 (d, $J_{\text{PH}} = 26.8$ Hz, 1H) ppm; $^{13}\text{C}\{^1\text{H}\}$ NMR (100 MHz, CDCl_3) this compound is not stable at 13C acquisition time scale; $^{31}\text{P}\{^1\text{H}\}$ NMR (400 MHz, CDCl_3) δ 70.8 ppm;

**10**

Synthesis of Complex 10.

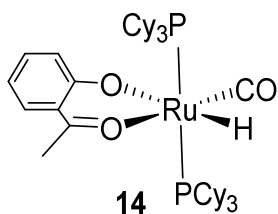
The product **4** (200 mg, 0.27 mmol) was dissolved in CH_2Cl_2 (2 mL) and layered with *n*-pentane (2 mL). Kept in glove box for 3 days for crystallization and filtered the resulting solid through a fritted funnel yielded the product as a bright orange crystals (160 mg, ca. 90 % yield). Single crystals of **10** suitable for X-ray crystallography were obtained from $\text{CH}_2\text{Cl}_2/n$ -pentane solution. Data for **10**: ^1H NMR (400 MHz, CDCl_3) δ 7.16-7.30 (m, 4H), 6.45-6.56 (m, 4H), 5.12-5.21 (m, 1H), 2.40 (s, 6H), 0.90-1.92 (m, 112H), -28.30 (t, $J_{\text{PH}} = 9.54$ Hz, 1H) ppm; selected $^{13}\text{C}\{^1\text{H}\}$ NMR (100 MHz, CDCl_3) δ 201.1 (d, $J_{\text{C-P}} = 17.1$ Hz), 204.5; $^{31}\text{P}\{^1\text{H}\}$

NMR (400 MHz, CDCl₃) δ 70.7 ppm; FT-IR (Solid) ν_{CO} = 1929 cm⁻¹, 1944 cm⁻¹. HRMS (ESI) Calcd for [M]⁺ C₅₄H₈₁O₆P₂Ru₂:.1091.3595 Found: 1091.3605.



Synthesis of Complex 11. The product **11** (20 mg, 0.027 mmol) was dissolved in dioxane (2 mL) and H₂O (5 μ L, 0.027 mmol). The resulting solution was heated to 80 °C about an hour. Kept in glove box for 1 days for crystallization a bright

orange crystals was obtained. Single crystals of **11** suitable for X-ray crystallography were obtained from dioxane/*n*-pentane solution. Data for **11**: ¹H NMR (400 MHz, CDCl₃) δ 7.40-7.30 (m, 4H), 7.00 (dd, *J* = 8.7, 1.1 Hz, 2H), 6.71-6.62 (m, 2H), 2.17-2.05 (m, 6H), 1.84-1.50 (m, 33H), 1.28-0.92 (m, 33H), -3.18 (s, 1H) ppm; selected ¹³C {¹H} NMR (100 MHz, CDCl₃) δ 205.9 (d, *J*_{C-P} = 17.8 Hz), 205.2; ³¹P {¹H} NMR (400 MHz, CDCl₃) δ 66.5 ppm; HRMS (ESI) Calcd for [M]⁺ C₅₄H₈₁O₇P₂Ru₂:.1107.3539 Found: 1107.3530.



Synthesis of Complex 14. In a glove box, **Complex**

1 (100 mg, 0.2 mmol), 2-hydroxyacetophenone (23 mg, 0.2 mmol) and PCy₃ (100mg, 0.4 mmol) was dissolved in 1,4-dioxane (3 mL) in 25 mL Schlenk tube. The tube was taken out and heat about 1h at 80 °C. The resulting orange color solution was crushed out with hexane and the resulting solid filtered through a fritted funnel yielded the product as a orange solid (129 mg, ca. 90 % yield). Growing single crystal was unsuccessful. Data for **14**: ¹H NMR (400 MHz, CD₂Cl₂) δ 6.90-7.01 (m, 1H), 6.44 (dd, *J* = 8.7, 1.1 Hz, 1H), 6.17 (ddd, *J* = 8.2, 6.7, 1.2 Hz, 1H), 5.24-5.38 (m, 1H), 2.41 (s, 3H), 0.96-2.11 (m, 66H), -15.73 (t, *J* = 20.5 Hz, 1H) ppm; ³¹P {¹H} NMR (400 MHz, CDCl₃) δ 44.07 ppm.

6.3.13 X-Ray Data:

Table 6.4: Crystal data and structure refinement for 8a.	
Identification code	8a
Empirical formula	C ₂₉ H ₅₀ BO ₄ F ₄ PRu
Formula weight	681.54
Temperature/K	100.00(10)
Crystal system	monoclinic
Space group	P2 ₁ /n
a/Å	10.51406(15)
b/Å	12.03200(16)
c/Å	24.8572(3)
α /°	90.00
β /°	92.3407(12)
γ /°	90.00
Volume/Å ³	3141.94(7)
Z	4
ρ_{calc} /mg/mm ³	1.441
m/mm ⁻¹	0.606
F(000)	1424.0
Crystal size/mm ³	0.376 × 0.2569 × 0.1911
Radiation	MoK α (λ = 0.71073)
2 Θ range for data collection	5.98 to 58.98°
Index ranges	-13 ≤ h ≤ 14, -16 ≤ k ≤ 15, -33 ≤ l ≤ 33
Reflections collected	35933
Independent reflections	7944 [R _{int} = 0.0327, R _{sigma} = 0.0301]
Data/restraints/parameters	7944/0/376
Goodness-of-fit on F ²	1.056
Final R indexes [I ≥ 2 σ (I)]	R ₁ = 0.0283, wR ₂ = 0.0606
Final R indexes [all data]	R ₁ = 0.0359, wR ₂ = 0.0643
Largest diff. peak/hole / e Å ⁻³	1.07/-0.54

Table 6.5: Crystal data and structure refinement for 8a'	
Identification code	8a'
Empirical formula	C ₂₆ H ₄₂ BF ₄ O ₃ PRu
Formula weight	621.45
Temperature/K	100.00(10)
Crystal system	monoclinic
Space group	Pn
a/Å	10.2651(3)
b/Å	13.2515(3)
c/Å	10.5887(3)
α /°	90.00
β /°	104.080(3)
γ /°	90.00
Volume/Å ³	1397.09(7)
Z	2
ρ_{calc} /cm ³	1.477
μ /mm ⁻¹	0.671
F(000)	644.0
Crystal size/mm ³	0.4122 × 0.143 × 0.1397
Radiation	MoK α (λ = 0.71073)
2 Θ range for data collection/°	6.14 to 58.92
Index ranges	-13 ≤ h ≤ 13, -18 ≤ k ≤ 17, -13 ≤ l ≤ 13
Reflections collected	13359
Independent reflections	13359 [R _{int} = 0.0000, R _{sigma} = 0.0470]
Data/restraints/parameters	13359/2/335
Goodness-of-fit on F ²	0.995
Final R indexes [I ≥ 2 σ (I)]	R ₁ = 0.0499, wR ₂ = 0.1265
Final R indexes [all data]	R ₁ = 0.0609, wR ₂ = 0.1313
Largest diff. peak/hole / e Å ⁻³	1.56/-1.15
Flack parameter	-0.01(3)

Table 6.6: Crystal data and structure refinement for 8c.	
Identification code	8c
Empirical formula	C ₂₈ H ₄₈ BF ₄ O ₃ PRu
Formula weight	651.51
Temperature/K	100.00(10)
Crystal system	orthorhombic
Space group	Pbca
a/Å	10.29093(13)
b/Å	18.5770(3)
c/Å	31.9420(4)
α /°	90.00
β /°	90.00
γ /°	90.00
Volume/Å ³	6106.51(14)
Z	8
ρ_{calc} mg/mm ³	1.417
m/mm ⁻¹	5.093
F(000)	2720.0
Crystal size/mm ³	0.2975 × 0.1164 × 0.0395
Radiation	CuK α (λ = 1.54184)
2 Θ range for data collection	9.52 to 147.3°
Index ranges	-12 ≤ h ≤ 12, -22 ≤ k ≤ 15, -38 ≤ l ≤ 38
Reflections collected	30380
Independent reflections	6048 [R _{int} = 0.0287, R _{sigma} = 0.0198]
Data/restraints/parameters	6048/0/357
Goodness-of-fit on F ²	1.093
Final R indexes [I ≥ 2 σ (I)]	R ₁ = 0.0404, wR ₂ = 0.0943
Final R indexes [all data]	R ₁ = 0.0443, wR ₂ = 0.0966
Largest diff. peak/hole / e Å ⁻³	1.14/-0.69

Table 6.7: Crystal data and structure refinement for 8e.	
Identification code	8e
Empirical formula	C ₂₅ H ₃₉ BClF ₄ O ₂ PRu
Formula weight	625.86
Temperature/K	100.00(10)
Crystal system	monoclinic
Space group	P2 ₁
a/Å	10.38368(11)
b/Å	11.82238(9)
c/Å	23.1436(2)
α/°	90.00
β/°	102.7232(10)
γ/°	90.00
Volume/Å ³	2771.34(4)
Z	4
ρ _{calc} /cm ³	1.500
μ/mm ⁻¹	6.428
F(000)	1288.0
Crystal size/mm ³	0.3138 × 0.2705 × 0.1982
Radiation	CuKα (λ = 1.54184)
2θ range for data collection/°	7.84 to 148.04
Index ranges	-12 ≤ h ≤ 11, -14 ≤ k ≤ 14, -27 ≤ l ≤ 28
Reflections collected	27608
Independent reflections	10695 [R _{int} = 0.0213, R _{sigma} = 0.0240]
Data/restraints/parameters	10695/1/663
Goodness-of-fit on F ²	1.037
Final R indexes [I ≥ 2σ (I)]	R ₁ = 0.0217, wR ₂ = 0.0540
Final R indexes [all data]	R ₁ = 0.0222, wR ₂ = 0.0544

Largest diff. peak/hole / e Å ⁻³	0.47/-0.51
Flack parameter	0.000(5)

Table 6.8: Crystal data and structure refinement for 10.	
Identification code	10
Empirical formula	C ₅₄ H ₈₁ BF ₄ O ₆ P ₂ Ru ₂
Formula weight	1177.13
Temperature/K	100.00(10)
Crystal system	monoclinic
Space group	C2/c
a/Å	19.8500(4)
b/Å	17.9759(3)
c/Å	16.6953(3)
α/°	90.00
β/°	107.1132(19)
γ/°	90.00
Volume/Å ³	5693.49(17)
Z	4
ρ _{calc} /mg/mm ³	1.451
m/mm ⁻¹	0.720
F(000)	49.0
Crystal size/mm ³	0.6545 × 0.082 × 0.0667
Radiation	MoKα (λ = 0.71073)
2θ range for data collection	5.62 to 58.94°
Index ranges	-26 ≤ h ≤ 25, -23 ≤ k ≤ 23, -23 ≤ l ≤ 21
Reflections collected	32469
Independent reflections	7101 [R _{int} = 0.0353, R _{sigma} = 0.0322]
Data/restraints/parameters	7101/24/389
Goodness-of-fit on F ²	1.090
Final R indexes [I ≥ 2σ (I)]	R ₁ = 0.0324, wR ₂ = 0.0730
Final R indexes [all data]	R ₁ = 0.0401, wR ₂ = 0.0766

Largest diff. peak/hole / e Å ⁻³	0.85/-0.60
---	------------

Table 6.9: Crystal data and structure refinement for 11.

Identification code	11
Empirical formula	C ₅₄ H ₈₁ O ₇ BF ₄ P ₂ Ru ₂
Formula weight	1193.13
Temperature/K	100.00(10)
Crystal system	triclinic
Space group	P-1
a/Å	11.44999(18)
b/Å	11.75213(19)
c/Å	23.6747(2)
α/°	96.5819(10)
β/°	100.9333(10)
γ/°	111.4618(15)
Volume/Å ³	141.36(7)
Z	2
ρ _{calc} /mg/mm ³	1.491
m/mm ⁻¹	5.387
F(000)	1334.0
Crystal size/mm ³	0.2265 × 0.1198 × 0.0692
Radiation	CuKα (λ = 1.54184)
2θ range for data collection	7.76 to 147.42°
Index ranges	-14 ≤ h ≤ 14, -14 ≤ k ≤ 14, -29 ≤ l ≤ 29
Reflections collected	22228
Independent reflections	22228 [R _{int} = 0.0000, R _{sigma} = 0.0144]
Data/restraints/parameters	22228/0/688
Goodness-of-fit on F ²	1.080
Final R indexes [I ≥ 2σ (I)]	R ₁ = 0.0433, wR ₂ = 0.1299
Final R indexes [all data]	R ₁ = 0.0470, wR ₂ = 0.1342
Largest diff. peak/hole / e Å ⁻³	1.04/-0.92

Empirical formula	C ₄₇ H ₇₈ O ₄ P ₂ Ru
Formula weight	870.10
Temperature/K	100.00(10)
Crystal system	monoclinic
Space group	C2/c
a/Å	37.7836(5)
b/Å	9.91950(11)
c/Å	24.3603(3)
α /°	90.00
β /°	90.9411(11)
γ /°	90.00
Volume/Å ³	9128.90(18)
Z	8
ρ_{calc} /cm ³	1.266
μ /mm ⁻¹	3.747
F(000)	3728.0
Crystal size/mm ³	0.1903 × 0.0959 × 0.044
Radiation	CuK α (λ = 1.54184)
2 Θ range for data collection/°	7.26 to 147.28
Index ranges	-46 ≤ h ≤ 46, -12 ≤ k ≤ 10, -30 ≤ l ≤ 30
Reflections collected	32322
Independent reflections	9049 [R _{int} = 0.0309, R _{sigma} = 0.0278]
Data/restraints/parameters	9049/0/492
Goodness-of-fit on F ²	1.033
Final R indexes [I ≥ 2 σ (I)]	R ₁ = 0.0367, wR ₂ = 0.0940
Final R indexes [all data]	R ₁ = 0.0421, wR ₂ = 0.0980
Largest diff. peak/hole / e Å ⁻³	1.54/-0.87

6.4 Synthetic and Mechanistic Studies of Ruthenium Catalyzed Reductive Etherification of Carbonyl Compounds and Alcohols

6.4.2 Experimental Procedures

General Procedure for the Catalytic Reaction. Method A: In a glove box, **complex 1** (17 mg, 3 mol %), carbonyl compound (1.0 mmol) and an alcohol (2.5 mmol) were dissolved in C_6H_5Cl (1 mL) in a 25 mL Schlenk tube equipped with a Teflon stopcock and a magnetic stirring bar. The tube was brought out of the box, and was stirred for 8-16 h in an oil bath which was preset at 110 °C. The reaction tube was taken out of the oil bath, and was cooled to room temperature. After the tube was open to air, the solution was filtered through a short silica gel column (CH_2Cl_2), and the filtrate was analyzed by GC and GC-MS. Analytically pure product was isolated by a simple column chromatography on silica gel (280-400 mesh, hexanes/ Et_2O or hexanes/ $EtOAc$).

Method B: In a glove box, **complex 1** (17 mg, 3 mol %), carbonyl compound (1.0 mmol) and an alcohol (1.3 mmol) were added into a 25 mL Schlenk tube equipped with a Teflon stopcock and a magnetic stirring bar. The tube was brought out of the box, and H_2O (1 mL) was added (0.5 mL of toluene was added for water insoluble substrates). N_2 gas was removed under vacuum, was filled with H_2 (1 atm) and the tube was stirred for 8-16 h in an oil bath which was preset at 110 °C. The reaction tube was taken out of the oil bath, and was cooled to room temperature. After the tube was open to air, the solution was filtered through a short silica gel column (CH_2Cl_2), and the filtrate was analyzed by GC and GC-MS. Analytically pure product was isolated by a simple column chromatography on silica gel (280-400 mesh, hexanes/ Et_2O or hexanes/ $EtOAc$).

6.4.3 Catalyst Screening Study.

Table 6.11. Catalyst Survey for the Coupling Reaction of 4-Methoxybenzaldehyde with 1-Butanol.^a

Entry	Catalyst	Additive	Yield (%)
1	$[(C_6H_6)(PCy_3)(CO)RuH]BF_4$ (4)		95
2	$[RuH(CO)(PCy_3)]_4(O)(OH)_2$		0
3	$[RuH(CO)(PCy_3)]_4(O)(OH)_2$	$HBF_4 \cdot OEt_2$	72
4	$RuCl_3 \cdot 3H_2O$	$HBF_4 \cdot OEt_2$	0
5	$RuCl_2(PPh_3)_3$	$HBF_4 \cdot OEt_2$	trace
6	$RuH_2(CO)(PPh_3)_3$		3
7	$RuH_2(CO)(PPh_3)_3$	$HBF_4 \cdot OEt_2$	10
8	$[RuCl_2(COD)]_x$	$HBF_4 \cdot OEt_2$	0
9	$[RuH(CO)(PCy_3)_2(CH_3CN)_2]^+ BF_4^-$		20
10	$[(COD)RuCl_2]_x$	$HBF_4 \cdot OEt_2$	0
11	$Ru_3(CO)_{12}$	NH_4PF_6	0
12	$Cy_3PH^+ BF_4^-$		trace
13	$BF_3 \cdot OEt_2$		trace
14	$AlCl_3$		7
15	$FeCl_3 \cdot H_2O$		trace
16	$HBF_4 \cdot OEt_2$		6
17	CF_3SO_3H		trace

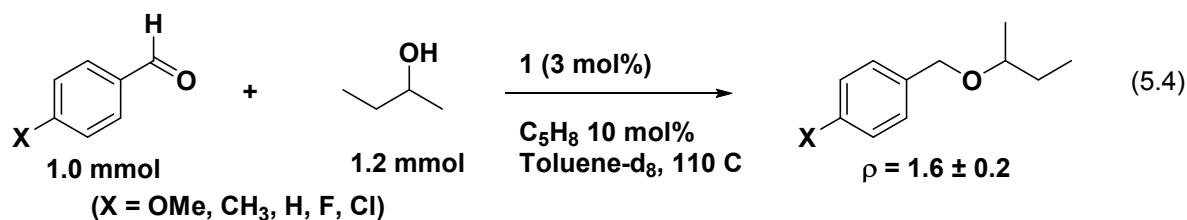
^aReaction conditions: 4-methoxybenzaldehyde (1.0 mmol), 1-butanol (2.5 mmol), catalyst (2 mol %), additive (1.0 equiv to catalyst), toluene/H₂O (1 mL, 1:1), 12 h, 110 °C. The product yield was determined by GC and GC-MS.

In a glove box, 4-methoxybenzaldehyde (136 mg, 1.0 mmol), 1-butanol (185 mg, 2.5 mmol) and a catalyst (2 mol %) were dissolved in toluene/H₂O (1:1, 1 mL) in a 25 mL Schlenk tube equipped with a Teflon stopcock and a magnetic stirring bar. The tube was brought out of the box, and was stirred for 12 h in an oil bath which was preset at 110 °C.

The reaction tube was taken out of the oil bath and the solution mixture was analyzed by GC and GC-MS. The results are summarized in Table 6.10.

6.4.4 Determination of TON.

In a glove box, 4-methoxybenzaldehyde (2.72 g, 20 mmol), 2-butanol (1.48 g, 23 mmol) and the ruthenium catalyst **1** (0.2 μg , 1.7×10^{-3} mol %) were dissolved in water (3 mL) in a 100 mL Fisher-Porter pressure tube. The reaction tube was brought out of the box, and H_2 (20 psi) was added. The tube was stirred in an oil bath at 110 °C. A small aliquot was drawn from the reaction mixture after 1 h and after 18 h, and was analyzed by GC and NMR spectroscopic methods.



6.4.5 Hammett Study.

In a glove box, *para*-substituted benzaldehyde $p\text{-X-C}_6\text{H}_5\text{CHO}$ ($\text{X} = \text{OCH}_3, \text{CH}_3, \text{H}, \text{Cl}, \text{F}$) (0.25 mmol), 2-butanol (0.75 mmol), H_2O (0.05 mmol) and **complex 1** (3 mol %) were dissolved in toluene- d_8 (0.5 mL) in six separate J-Young NMR tubes. The tubes were brought out of the box, and stirred in an oil bath set at 110 °C. Each reaction tube was taken out of the oil bath in 20 min intervals, was immediately cooled in an ice water bath, and was analyzed by ^1H NMR. The k_{obs} was determined from a first-order plot of $-\ln([p\text{-X-C}_6\text{H}_5\text{CHO}]_t/[p\text{-X-C}_6\text{H}_5\text{CHO}]_0)$ vs. time.

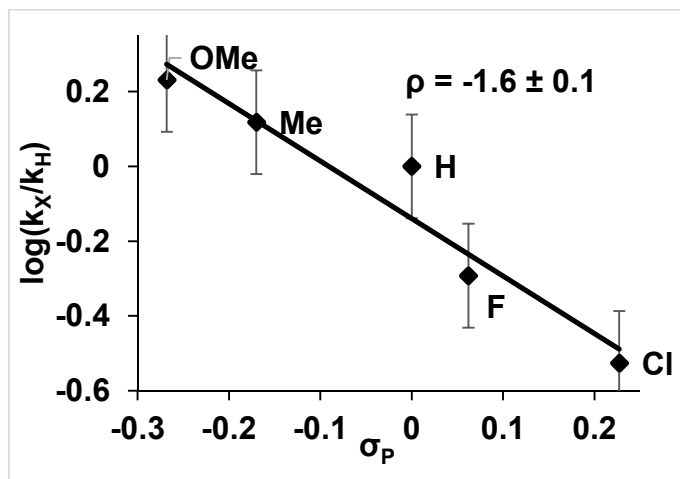


Figure 6.30: Hammett Plot from the Reaction of p -X-C₆H₄CHO (X = OMe, Me, H, F, Cl) with 2-Butanol. Rearrange Y-axis

6.4.6 Solvent Isotope Effect Study.

In a glove box, 4-methoxybenzaldehyde (340 mg, 1.5 mmol), 2-butanol (463 mg, 6.6 mmol) and **complex 1** (40 mg, 2 mol %) were mixed in a vial and divided into five separate 25 mL Schelenk tubes equipped with magnetic stirring bar. After adding H₂O (0.5 mL), each tube was evacuated, and refilled with N₂ gas. The tubes were stirred in an oil bath set at 110 °C. Each reaction tube was taken out of the oil bath in 15 min intervals, was immediately cooled in liquid N₂ bath, and hexamethylbenzene (10 mg, internal standard) dissolved in CDCl₃ (1 mL) was added. After shaking the reaction tube for 5 min, CDCl₃ layer was separated and was analyzed by ¹H NMR. The k_{H_2O} was determined from a first-order plot of $-\ln([p\text{-OMe-C}_6\text{H}_5\text{CHO}]_t/p\text{-OMe-C}_6\text{H}_5\text{CHO}]_0)$ vs. time. The k_{D_2O} was determined from the experiment using D₂O as the solvent. The k_{H_2O}/k_{D_2O} was calculated from the ratio of slopes (Figure 6.31).

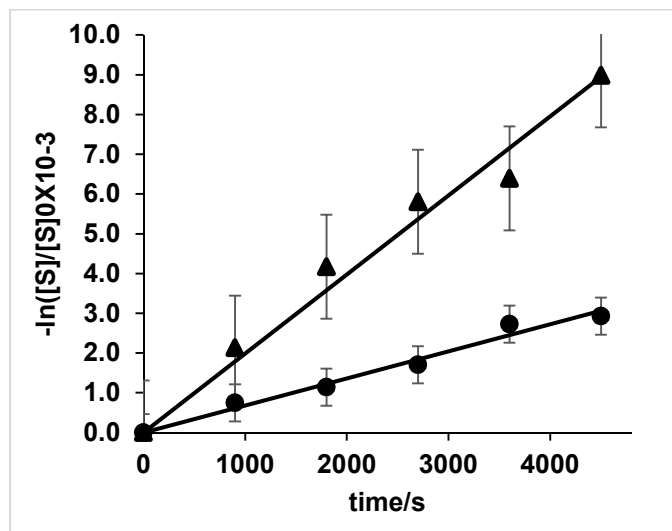


Figure 6.31: First Order Plot of the 4-Methoxybenzaldehyde with 2-Butanol in H₂O (triangle) and in D₂O (circle).

In a glove box, 4-methoxybenzaldehyde (340 mg, 1.5 mmol), 2-propanol (0.5 mL) and **complex 1** (50 mg, 2 mol %) were mixed in a vial and divided into five separate 25 mL Schelenk tubes equipped with magnetic stirring bar. The tubes were degassed under vacuum line and filled with N₂ gas. The tubes were stirred in an oil bath set at 110 °C. Each reaction tube was taken out of the oil bath in 15 min intervals, was immediately cooled in liquid N₂ and hexamethylbenzene (10 mg, internal standard) was dissolved in benzene-*d*₆ (0.5 mL) and analysed by ¹H NMR. The k_{PrOH} was determined from a first-order plot of $-\ln([p\text{-OMe-C}_6\text{H}_5\text{CHO}]_t/[p\text{-OMe-C}_6\text{H}_5\text{CHO}]_0)$ vs. time. The same experiment was repeated by using 2-propanol-*d* as the solvent to determine k_{PrOD} . The $k_{\text{PrOH}}/k_{\text{PrOD}}$ was calculated from the ratio of slopes.

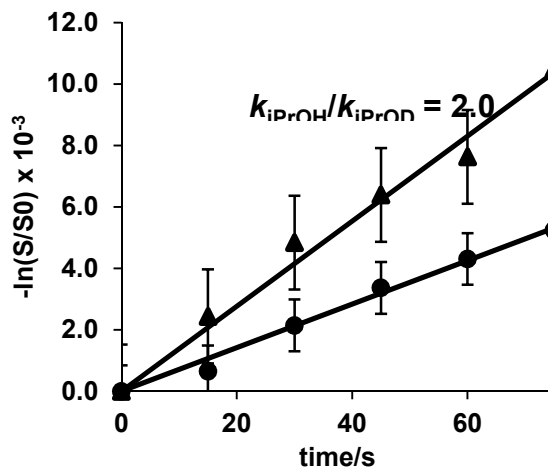


Figure 6.32. First Order Plot of the 4-Methoxybenzaldehyde with 2-Propanol (triangle) and in 2-Propanol- d_1 (circle).

6.4.7 H/D Exchange Reaction of 4-Methoxybenzaldehyde with 1-Butanol in D_2O .

In a glove box, **complex 1** (17 mg, 3 mol %) was placed into a 25 mL Schlenk tube equipped with a Teflon stopcock and a magnetic stirring bar. The tube was brought out of the glove box, and 4-methoxybenzaldehyde (0.136 g, 1.0 mmol), 1-butanol (0.185 g, 2.5 mmol) and D_2O (99% D, 1 mL) were added to the tube. The tube was filled with N_2 , and was stirred in an oil bath set at 110 °C for 12 h. The reaction tube was taken out of the oil bath, and was cooled to room temperature. After the tube was open to air, CH_2Cl_2 (2 mL) was added and the organic layer was extracted. The organic layer was filtered through a short silica gel column by eluting with CH_2Cl_2 (10 mL), and the filtrate was analyzed by GC and GC-MS. Analytically pure product was isolated by a simple column chromatography on silica gel (280-400 mesh, hexanes/ Et_2O = 40:1). The deuterium content of the product **2f** was determined by 1H and 2H NMR spectroscopic methods (Figure 6.33).

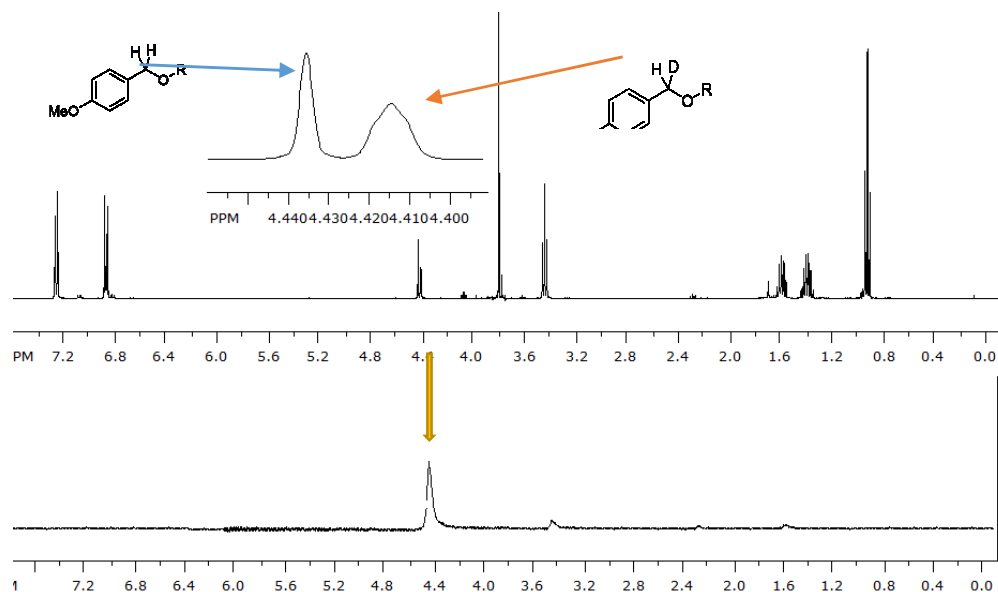
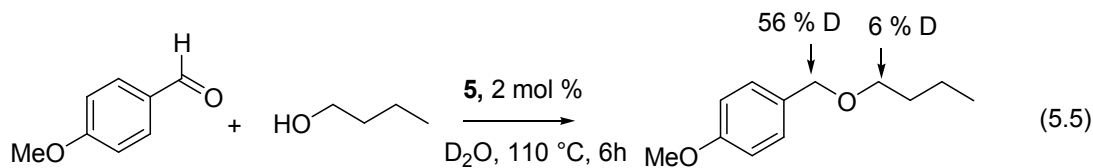


Figure 6.33: ^1H and ^2H NMR Spectra of the Product **2f** Isolated from the Reaction of 4-Methoxybenzaldehyde with 1-Butanol in D_2O .

6.4.8 Carbon Isotope Effect Study.

In a glove box, complex **1** (170 mg, 3 mol %) was placed into a 100 mL Schlenk tube equipped with a Teflon stopcock and a magnetic stirring bar. The tube was brought out of the glove box, and 4-Methoxybenzaldehyde (1.36 g, 10 mmol), 1-hexanol (0.255 g, 2.5 mmol), H_2O (10 mL) and toluene (5 mL) were added to the tube. Three samples were prepared separately and each tube was degassed under vacuum, filled with nitrogen, and was stirred in an oil bath set at 110 °C for 2 h, 2.5 h, and 3 h respectively. Compound **2k** was isolated by a column chromatography on silica gel (hexanes/EtOAc = 40:1) separately after filtering through a short silica gel column eluting with CH_2Cl_2 (20 mL), and each solution was analyzed by GC (15 % conversion). The experiment was repeated two more

times, and the product was isolated after 2.5 h, and 3 h of the reaction time (18 and 20 % conversion).

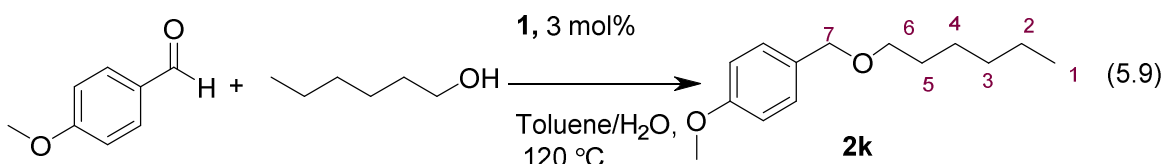


Table 6.12. Calculated Average ^{13}C KIE from Virgin (R_0) and Recovered (R) Samples of **2k**.

Carbon No.	Virgin (R_0)	Recovered (R) (18% conv.)	R_0/R	^{13}C KIE
1 (ref)	1.0000	0.9999	1.0001	0.999
2	1.0068	1.0068	0.9995	1.004
3	1.0036	1.0024	1.0001	1.001
4	1.0010	1.0009	1.0001	1.001
5	1.0029	1.0030	0.9999	1.000
6	1.0087	0.9992	1.0096	1.010
7	1.0071	0.9860	1.0021	1.021

The $^{13}\text{C}\{^1\text{H}\}$ NMR analysis of the recovered and virgin samples of **2k** was performed by following Singleton's ^{13}C NMR measurement technique. The NMR sample of virgin and recovered **2k** (100 mg) was prepared identically by dissolving them in CDCl_3 (0.5 mL) in a 5 mm high precision NMR tube. The $^{13}\text{C}\{^1\text{H}\}$ NMR spectrum was recorded with H-decoupling and 45 degree pulse. A 60 s delay between pulses was imposed to minimize T_1 variations ($d_1 = 60$ s, $at = 5.0$ s, $np = 245098$, $nt = 704$). The data are summarized in Table 6.11.

6.4.9 Generation and Synthesis of the Alcohol and Aqua Complexes **7**, **8** and **9**.

In a glove box, complex **1** (40 mg, 0.07 mmol) was dissolved in CD₂Cl₂ (1 mL) in a NMR tube. 1-Butanol (0.052 mg, 10 equiv) was added via syringe and the tube was shaken for 10 min at room temperature. The reaction progress was monitored by ¹H NMR and ³¹P NMR at 50 °C. After 10 min, the appearance of new ruthenium hydride species and free benzene molecule (δ 7.26 ppm on ¹H NMR), as indicated by a new Ru–H signal (¹H NMR: δ -18.8 (d, *J* = 31.3 Hz, 1H) ppm) as shown in the Figure 6.34.

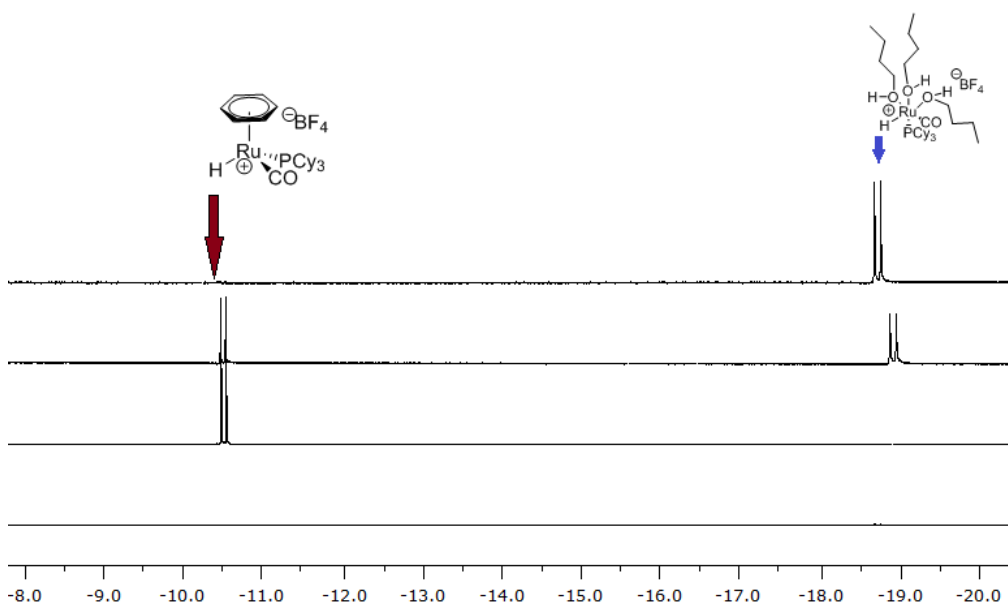


Figure 6.34. ¹H NMR Spectra of the Reaction of **1** with 1-Butanol. Indicate Time and Temp For Each Spectrum

Generation of **8**: Complex **1** (40 mg) with H₂O (13 mg, 10 equiv) at room temperature. After 5 min, the appearance of **8** was detected by ¹H NMR and ³¹P NMR. Because the complex decomposes within 1 h at room temperature, both ¹H NMR and ³¹P NMR spectra were recorded at -10 °C in this case (¹H NMR: δ -17.7 (d, *J*_{H-P} = 30.3 Hz) ppm, ³¹P NMR: δ 73.0 ppm).

Synthesis of **9**. The analogous treatment of complex **1** (115 mg, 0.2 mmol) with 1,1,1-tris(hydroxymethyl)ethane (24 mg, 0.2 mmol) in acetone (2 mL), and the mixture was stirred for 30 min at room temperature. The solution was layered with *n*-pentane (5 mL) to obtain single crystals of **9** as white color crystals in 80 % yield.

6.4.10 X-Ray Crystallographic Determination of **3d**, **3e**, **3f**, **9**, **10** and **11**.

For **3d**: Colorless single crystals of **3d** were grown in CH₂Cl₂ at room temperature. A suitable crystal with the dimension of 0.6896 × 0.1863 × 0.0598 mm³ was selected and mounted on an Oxford SuperNova diffractometer equipped with dual microfocus Cu/Mo X-ray sources, X-ray mirror optics, and Atlas CCD area detector. A total of 15140 reflection data were collected by using CuKα (λ = 1.54184) radiation while the crystal sample was cooled at 100.00 K during the data collection. Using Olex2, the molecular structure was solved with the ShelXS structure solution program by using Direct Methods, and the data was refined with the XL refinement package using Least Squares minimization. The molecular structure of **3d** is shown in Figure 6.35.

For **3e**: Colorless single crystals of **3e** were grown in CH₂Cl₂ at room temperature. A suitable crystal with the dimension of 0.28 × 0.27 × 0.22 mm³ was selected and mounted on an Oxford SuperNova diffractometer equipped with dual microfocus Cu/Mo X-ray sources, X-ray mirror optics, and Atlas CCD area detector. A total of 9989 reflection data were collected by using CuKα (λ = 1.54184) radiation while the crystal sample was cooled at 100.00 K during the data collection. Using Olex2, the molecular structure was solved with the ShelXS structure solution program by using Direct Methods, and the data was

refined with the XL refinement package using Least Squares minimization. The molecular structure of **3e** is shown in Figure 6.36.

For **3f**: Colorless single crystals of **3f** were grown in CH₂Cl₂ at room temperature. A suitable crystal with the dimension of 0.42 × 0.12 × 0.05 mm³ was selected and mounted on an Oxford SuperNova diffractometer equipped with dual microfocus Cu/Mo X-ray sources, X-ray mirror optics, and Atlas CCD area detector. A total of 11497 reflection data were collected by using MoK α ($\lambda = 1.54184$) radiation while the crystal sample was cooled at 100.00 K during the data collection. Using Olex2, the molecular structure was solved with the ShelXS structure solution program by using Direct Methods, and the data was refined with the XL refinement package using Least Squares minimization. The molecular structure of **3f** is shown in Figure 6.37.

For **9**: Colorless single crystals of **9** were grown in acetone/*n*-pentane at room temperature. A suitable crystal with the dimension of 0.3068 × 0.2254 × 0.0989 mm³ was selected and mounted on an Oxford SuperNova diffractometer equipped with dual microfocus Cu/Mo X-ray sources, X-ray mirror optics, and Atlas CCD area detector. A total of 55980 reflection data were collected by using MoK α ($\lambda = 1.54184$) radiation while the crystal sample was cooled at 100.00 K during the data collection. Using Olex2, the molecular structure was solved with the ShelXS structure solution program by using Direct Methods, and the data was refined with the XL refinement package using Least Squares minimization. The molecular structure of **9** is shown in Figure 6.38.

For **10**: yellow single crystals of **10** were grown in acetone/*n*-pentane at room temperature. A suitable crystal with the dimension of 0.7044 × 0.0647 × 0.0498mm³ was selected and mounted on an Oxford SuperNova diffractometer equipped with dual

microfocus Cu/Mo X-ray sources, X-ray mirror optics, and Atlas CCD area detector. A total of 66389 reflection data were collected by using MoK α ($\lambda = 0.71073$) radiation while the crystal sample was cooled at 99.9(2) K during the data collection. Using Olex2, the molecular structure was solved with the ShelXS structure solution program by using Direct Methods, and the data was refined with the XL refinement package using Least Squares minimization. The molecular structure of **10** is shown in Figure 6.39.

For **11**: yellow single crystals of **11** were grown in acetone/*n*-pentane at room temperature. A suitable crystal with the dimension of $0.3672 \times 0.3351 \times 0.2841$ mm³ was selected and mounted on an Oxford SuperNova diffractometer equipped with dual microfocus Cu/Mo X-ray sources, X-ray mirror optics, and Atlas CCD area detector. A total of 40501 reflection data were collected by using MoK α ($\lambda = 0.71073$) radiation while the crystal sample was cooled at 100.00 K during the data collection. Using Olex2, the molecular structure was solved with the ShelXS structure solution program by using Direct Methods, and the data was refined with the XL refinement package using Least Squares minimization. The molecular structure of **11** is shown in Figure 6.40.

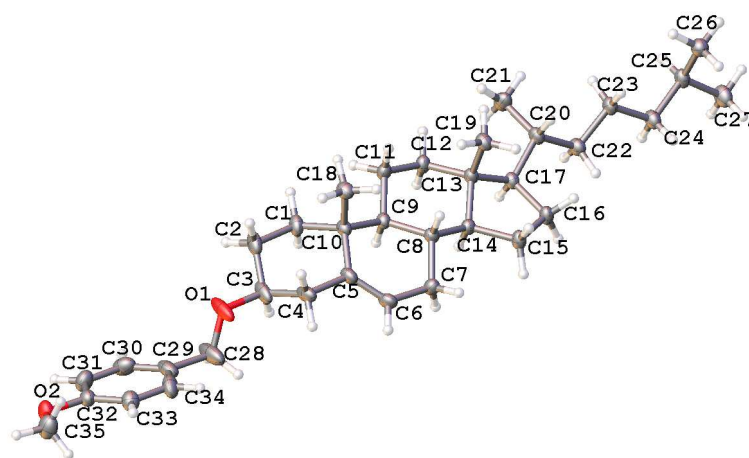


Figure 6.35: X-ray Crystal Structure of **3d**.

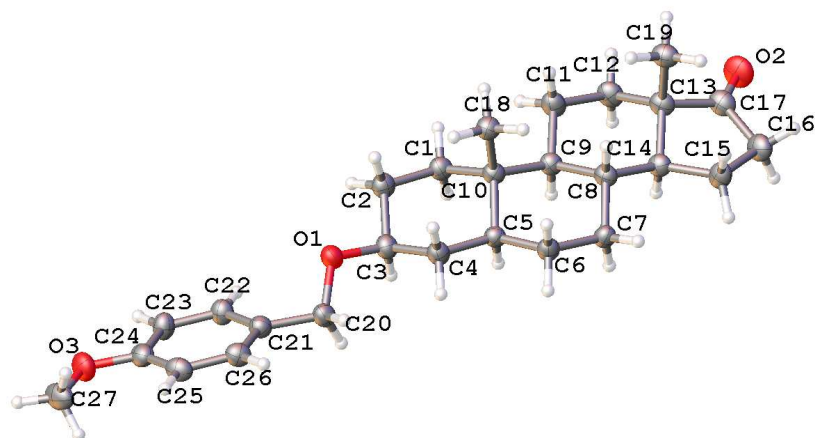


Figure 6.36: X-ray Crystal Structure of **3e**.

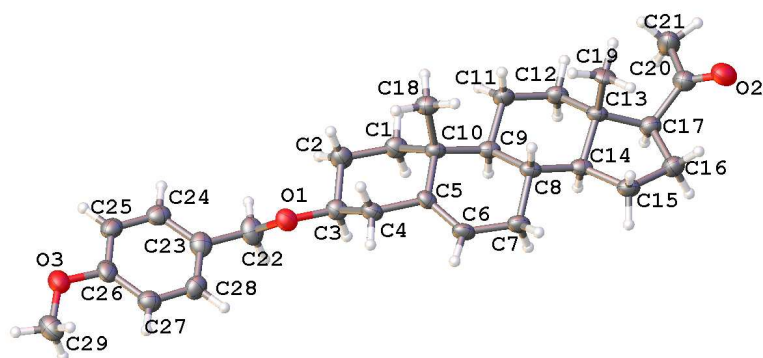


Figure 6.37: X-ray Crystal Structure of **3f**.

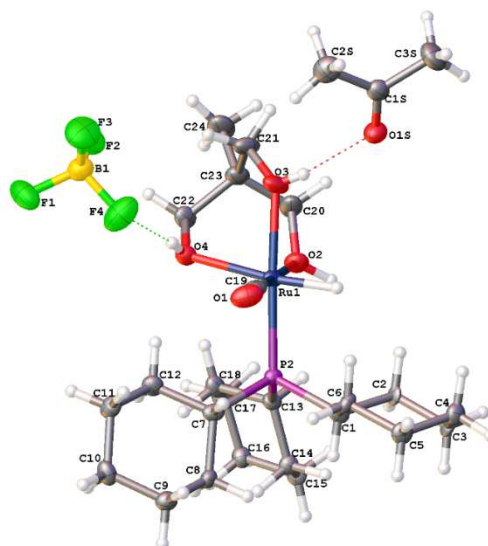


Figure 6.38: Molecular Structure of **9**.

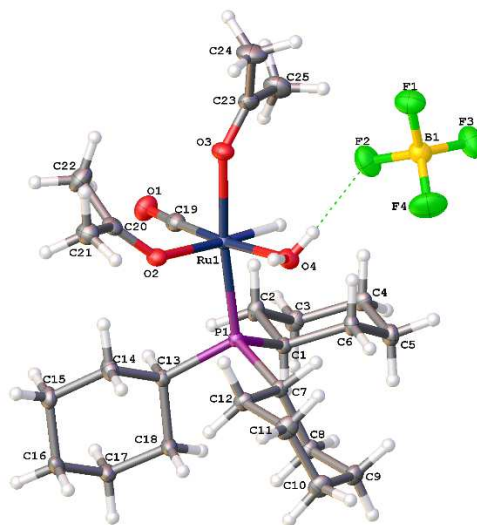


Figure 6.39: X-ray structure of complex 10 (H atoms removed for clarity)

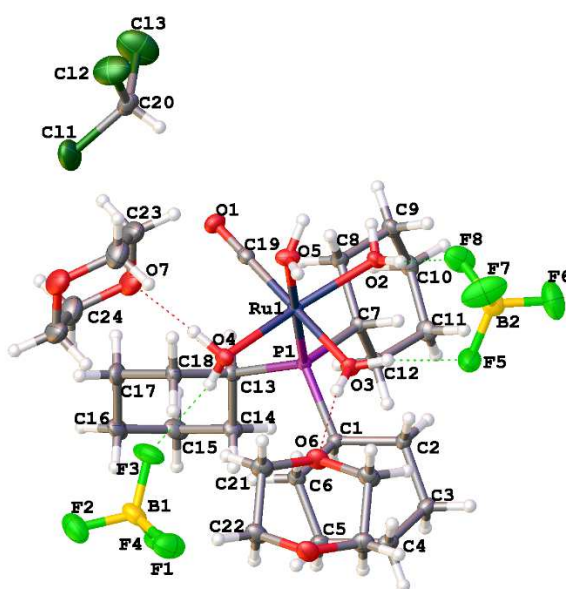
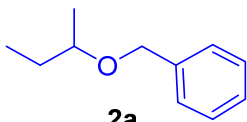


Figure 6.40: X-ray structure of complex 11

6.4.10 Characterization Data of the Products.

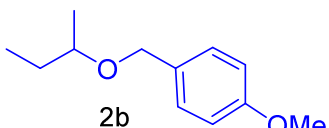
Data for **Table 5.3, Compound 2a**: ^1H NMR (400 MHz,



CDCl_3) δ 7.77-7.95 (m, 3H), 7.42-7.59 (m, 2H), 4.57 (d, $J = 11.9$ Hz, 1H), 4.49 (d, $J = 11.9$ Hz, 1H), 3.52 (sextet, $J = 6.1$ Hz, 1H),

1.63-1.74 (m, 1H), 1.47-1.61 (m, 1H), 1.25 (d, $J = 6.1$ Hz, 3H), 0.97 (t, $J = 7.4$ Hz, 3H) ppm; $^{13}\text{C}\{^1\text{H}\}$ NMR (100 MHz, CDCl_3) δ 138.2, 128.4, 127.8, 127.6, 72.1, 70.2, 29.2, 19.2, 9.8 ppm; GC-MS $m/z = 164$ (M^+). ^1H and ^{13}C NMR spectral data are in good agreement with the literature data.⁶⁴

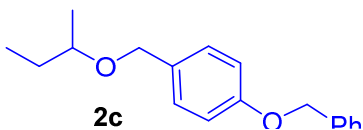
Data for **Table 5.3, Compound 2b**: ^1H NMR (400



MHz, CDCl_3) δ 7.29 (d, $J = 8.3$ Hz, 2H), 6.89 (d, $J = 8.3$ Hz, 2H), 4.51 (d, $J = 11.7$ Hz, 1H), 4.42 (d, $J = 11.7$ Hz, 1

H), 3.81 (s, 3H), 3.44 (sextet, $J = 7.0$ Hz, 1H), 1.61 (dq, $J = 14.7, 7.9$ Hz, 1H), 1.49 (qd, $J = 14.0, 7.9$ Hz, 1H), 1.19 (d, $J = 6.1$ Hz, 3H), 0.93 (t, $J = 7.9$ Hz, 3H) ppm; $^{13}\text{C}\{^1\text{H}\}$ NMR (100 MHz, CDCl_3) δ 158.9, 131.2, 129.1, 113.7, 75.8, 69.9, 55.2, 29.2, 19.2, 9.8 ppm; GC-MS $m/z = 194$ (M^+). ^1H and ^{13}C NMR spectral data are in good agreement with the literature data.⁶⁵

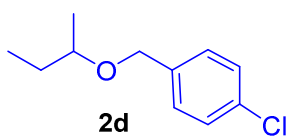
Data for **Table 5.3, Compound 2c**: ^1H NMR



(400 MHz, CDCl_3) δ 7.27-7.47 (m, 7H), 6.95-6.99 (m, 2H), 5.09 (s, 2H), 4.52 (d, $J = 11.3$ Hz, 1H), 4.43 (d, $J =$

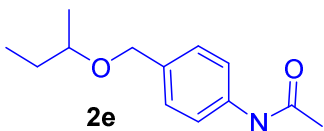
11.3 Hz, 1H), 3.46 (sextet, $J = 5.9$ Hz, 1H), 1.58-1.74 (m, 1H), 1.45-1.56 (m, 1H), 1.20 (d, $J = 6.3$ Hz, 3H), 0.94 (t, $J = 7.4$ Hz, 3H) ppm; $^{13}\text{C}\{^1\text{H}\}$ NMR (100 MHz, CDCl_3) δ 158.1, 137.0, 131.5, 129.1, 128.5, 127.8, 127.4, 114.6, 75.9, 69.9, 69.9, 29.2, 19.2, 9.8 ppm; GC-MS $m/z = 16$ (M^+); Anal. Calcd for $\text{C}_{18}\text{H}_{22}\text{O}_2$: C, 79.96; H, 8.20. Found: C, 79.88; H, 8.31.

Data for **Table 5.3, Compound 2d**: ^1H NMR (400



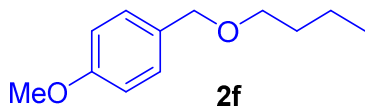
MHz, CDCl_3) δ 7.20-7.23 (m, 4H), 4.45 (d, $J = 12.2$ Hz, 1H), 4.36 (d, $J = 12.2$ Hz, 1H), 3.36 (sextet, $J = 6.1$ Hz, 1H), 1.51-1.61 (m, 1H), 1.35-1.47 (m, 1H), 1.11 (d, $J = 6.4$ Hz, 3H), 0.85 (t, $J = 7.5$ Hz, 3H) ppm; $^{13}\text{C}\{^1\text{H}\}$ NMR (100 MHz, CDCl_3) δ 137.7, 133.0, 128.8, 128.4, 76.4, 69.5, 29.2, 19.1, 9.8 ppm; GC-MS $m/z = 198$ (M^+); Anal. Calcd for $\text{C}_{11}\text{H}_{15}\text{ClO}$: C, 66.50; H, 7.61. Found: C, 66.48; H, 7.52.

Data for **Table 5.3, Compound 2e**: ^1H NMR (400

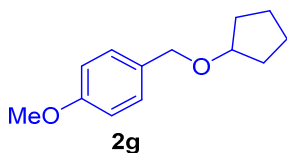


MHz, CDCl_3) δ 7.55 (br s, 1H), 7.47 (d, $J = 8.61$ Hz, 2H), 7.30 (d, $J = 8.2$ Hz, 2H), 4.52 (d, $J = 11.7$ Hz, 1H), 4.43 (d, $J = 11.7$ Hz, 1H), 3.44 (sextet, $J = 6.1$ Hz, 1H), 2.16 (s, 3H), 1.61 (ddd, $J = 13.7, 7.4, 6.3$ Hz, 1H), 1.48 (ddd, $J = 13.7, 7.4, 5.8$ Hz, 1H), 1.18 (d, $J = 6.3$ Hz, 3H), 0.92 (t, $J = 7.4$ Hz, 3H) ppm; $^{13}\text{C}\{^1\text{H}\}$ NMR (100 MHz, CDCl_3) δ 168.4, 137.0, 135.0, 128.3, 199.8, 76.1, 69.8, 29.1, 24.5, 19.1, 9.8 ppm; GC-MS $m/z = 221$ (M^+); Anal. Calcd for $\text{C}_{13}\text{H}_{19}\text{NO}_2$: C, 70.56; H, 8.65. Found: C, 70.48; H, 8.61.

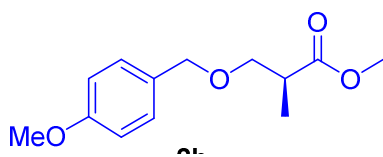
Data for **Table 5.3, Compound 2f**: ^1H NMR



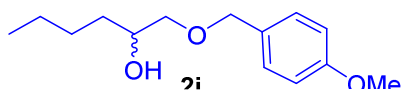
(400 MHz, CDCl_3) δ 7.28 (d, $J = 8.5$ Hz, 2H), 6.90 (d, $J = 8.5$ Hz, 2H), 4.45 (s, 2H), 3.81 (s, 3H), 3.46 (t, $J = 6.6$ Hz, 2H), 1.60 (quin, $J = 6.2$ Hz, 2H), 1.41 (sextet, $J = 7.4$ Hz, 2H), 0.93 (t, $J = 7.4$ Hz, 3H) ppm; $^{13}\text{C}\{^1\text{H}\}$ NMR (100 MHz, CDCl_3) δ 159.0, 130.7, 129.1, 113.6, 72.4, 69.8, 55.1, 31.8, 19.3, 13.9 ppm; GC-MS $m/z = 194$ (M^+); ^1H and ^{13}C NMR spectral data are in good agreement with the literature data.⁶⁵



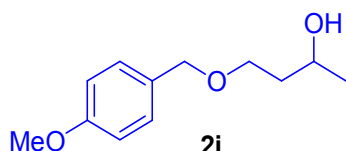
Data for **Table 5.3, Compound 2g**: ^1H NMR (400 MHz, CDCl_3) δ 7.16-7.22 (m, 2H), 6.77-6.82 (m, 2H), 4.33 (s, 2H), 3.87-3.94 (m, 1H), 3.72 (s, 3H), 1.59-1.71 (m, 6H), 1.39-1.49 (m, 2H) ppm; $^{13}\text{C}\{^1\text{H}\}$ NMR (100 MHz, CDCl_3) δ 158.9, 131.0, 129.2, 129.1, 113.7, 80.5, 70.3, 55.2, 32.3, 23.6, 23.5 ppm; GC-MS $m/z = 206$ (M^+); ^1H and ^{13}C NMR spectral data are in good agreement with the literature data.⁶⁶



Data for **Table 5.3, Compound 2h**: ^1H NMR (400 MHz, CDCl_3) δ 7.14-7.18 (m, 2H), 6.77-6.81 (m, 2H), 4.37 (dd, $J = 14.0, 12.0$ Hz, 2H), 3.71 (s, 3H), 3.60 (s, 3H), 3.54 (dd, $J = 9.0, 7.4$ Hz, 1H), 3.37 (dd, $J = 9.2, 6.1$ Hz, 1H), 2.68 (qt, $J = 7.5, 6.1$ Hz, 1H), 1.08 (d, $J = 7.0$ Hz, 3H) ppm; $^{13}\text{C}\{^1\text{H}\}$ NMR (100 MHz, CDCl_3) δ 175.2, 159.2, 130.1, 129.1, 113.6, 72.6, 71.5, 55.1, 51.6, 40.1, 13.9 ppm; GC-MS $m/z = 238$ (M^+); ^1H and ^{13}C NMR spectral data are in good agreement with the literature data.⁶⁷

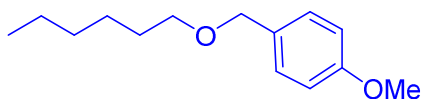


Data for **Table 5.3, Compound 2i**: ^1H NMR (400 MHz, CDCl_3) δ 7.24-7.30 (m, 2H), 6.87-6.92 (m, 2H), 4.49 (s, 2H), 3.81 (s, 3H), 3.49 (dd, $J = 9.4, 3.1$ Hz, 1H), 3.3 (dd, $J = 9.4, 7.8$ Hz, 1H), 2.39 (br s, 1H), 1.26-1.51 (m, 7H), 0.90 (t, $J = 7.4$ Hz, 3H) ppm; $^{13}\text{C}\{^1\text{H}\}$ NMR (100 MHz, CDCl_3) δ 159.2, 130.0, 129.4, 113.8, 74.3, 72.9, 70.4, 55.2, 32.8, 27.7, 22.7, 14.0 ppm; GC-MS $m/z = 238$ (M^+); ^1H and ^{13}C NMR spectral data are in good agreement with the literature data.⁶⁸



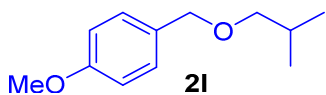
Data for **Table 5.3, Compound 2j**: ^1H NMR (400 MHz, CDCl_3) δ 7.15-7.21 (m, 2H), 6.78-6.83 (m, 2H), 4.38 (s, 2H), 3.87-3.96 (m,

1H), 3.73 (s, 3 H), 3.50-3.63 (m, 2H), 2.89 (br. s, 1H), 1.58-1.73 (m, 3H), 1.11 (d, $J = 6.3$ Hz, 3H) ppm; ^{13}C NMR (400 MHz, CDCl_3) δ 159.2, 123.0, 129.3, 113.8, 72.9, 68.8, 67.6, 55.2, 38.0, 23.3 ppm; GC-MS $m/z = 210$ (M^+); ^1H and ^{13}C NMR spectral data are in good agreement with the literature data.⁶⁹



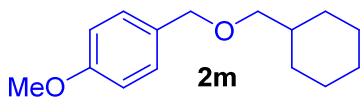
Data for **Table 5.3, Compound 2k**: ^1H NMR

(400 MHz, CDCl_3) δ 7.23-7.32 (m, 2H), 6.85-6.93 (m, 2H), 4.44 (s, 2 H), 3.80 (s, 3H), 3.44 (t, $J = 6.7$ Hz, 2H), 1.55-1.66 (m, 2H), 1.23-1.42 (m, 6H), 0.89 (t, $J = 7.0$ Hz, 3H) ppm; $^{13}\text{C}\{^1\text{H}\}$ NMR (400 MHz, CDCl_3) δ 159.0, 130.7, 129.1, 113.6, 72.4, 70.2, 55.1, 31.6, 29.7, 25.8, 22.6, 14.0 ppm; GC-MS $m/z = 222$ (M^+); ^1H and ^{13}C NMR spectral data are in good agreement with the literature data.⁶⁶



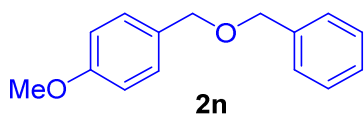
Data for **Table 5.3, Compound 2l**: ^1H NMR (400

MHz, CDCl_3) δ 7.28 (d, $J = 8.4$ Hz, 2H), 6.90 (d, $J = 8.7$ Hz, 2H), 4.45 (s, 2H), 3.82 (s, 3H), 3.49 (t, $J = 6.8$ Hz, 2H), 1.74 (dt, $J = 13.4, 6.7$ Hz, 1H), 1.52 (qd, $J = 6.8, 0.9$ Hz, 2H), 0.92 (d, $J = 7.7$ Hz, 6H) ppm; $^{13}\text{C}\{^1\text{H}\}$ NMR (100 MHz, CDCl_3) δ 159.0, 130.7, 129.2, 113.7, 72.5, 68.5, 55.2, 38.5, 22.6 ppm; GC-MS $m/z = 194$ (M^+); ^1H and ^{13}C NMR spectral data are in good agreement with the literature data.⁷⁰



Data for **Table 5.3, Compound 2m**: ^1H NMR

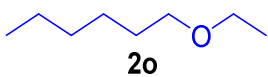
(400 MHz, CDCl_3) δ 7.13 (d, $J = 8.7$ Hz, 2H), 6.9 (d, $J = 8.6$ Hz, 2H), 4.47 (s, 2H), 3.80 (s, 3H), 3.29 (d, $J = 6.5$ Hz, 2H), 1.62-1.95 (m, 5H), 1.15-1.49 (m, 4H), 0.92-1.05 (m, 2H) ppm; $^{13}\text{C}\{^1\text{H}\}$ NMR (100 MHz, CDCl_3) δ 157.8, 133.6, 129.6, 113.7, 75.9, 72.5, 55.1, 55.1, 40.0, 38.0, 30.1, 26.6, 25.8 ppm; GC-MS $m/z = 234$ (M^+); Anal. Calcd for $\text{C}_{15}\text{H}_{22}\text{O}_2$: C, 76.88; H, 9.46. Found: C, 76.48; H, 9.51.



Data for **Table 5.3, Compound 2n**: ^1H NMR

(400 MHz, CDCl_3) δ 7.49-7.30 (m, 7H), 6.99-6.92 (m, 2H), 4.59 (s, 2H), 4.55 (s, 2H), 3.85 (s, 3H) ppm;

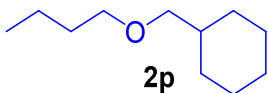
$^{13}\text{C}\{^1\text{H}\}$ NMR (100 MHz, CDCl_3) δ 159.3, 138.5, 130.4, 129.5, 128.5, 127.9, 127.7, 113.9, 71.9, 71.8, 55.3 ppm; GC-MS $m/z = 228$ (M^+). ^1H and ^{13}C NMR spectral data are in good agreement with the literature data.⁷¹



Data for **Table 5.3, Compound 2o**: ^1H NMR (400 MHz,

CDCl_3) δ 3.37 (t, $J = 6.5$ Hz, 2H), 3.50 (q, $J = 11.9$ Hz, 2H),

1.31-1.51 (m, 8H), 1.10 (t, $J = 6.5$ Hz, 3H), 0.88 (t, $J = 6.5$ Hz,



3H) ppm; $^{13}\text{C}\{^1\text{H}\}$ NMR (100 MHz, CDCl_3) δ 70.4, 66.6, 31.8,

30.0, 22.7, 22.6, 15.2, 14.1 ppm; GC-MS $m/z = 130$ (M^+); ^1H and

^{13}C NMR spectral data are in good agreement with the literature data.⁷²

Data for **Table 5.3, Compound 2p**: ^1H NMR (400 MHz, CDCl_3) δ 3.29 (t, $J = 6.6$

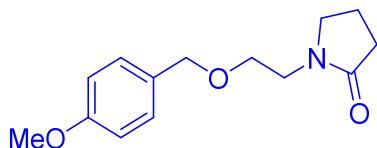
Hz, 2H), 3.08 (d, $J = 6.0$ Hz, 2H), 1.52-1.71 (m, 5H), 1.41-1.52 (m, 2H), 1.22-1.34 (m,

2H), 0.98-1.22 (m, 4H), 0.73-0.89 (m, 5H) ppm; $^{13}\text{C}\{^1\text{H}\}$ NMR (100 MHz, CDCl_3) δ 76.8,

70.8, 38.0, 31.8, 30.1, 26.7, 25.9, 19.3, 13.9 ppm; GC-MS $m/z = 170$ (M^+). ^1H and ^{13}C

NMR spectral data are in good agreement with the literature data.⁷²

Data for **Table 5.3, Compound 2q**: ^1H



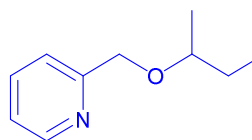
NMR (400 MHz, CDCl_3) δ 7.18 - 7.24 (m, 2H),

6.82 - 6.87 (m, 2H), 4.41 (s, 2H), 3.75 - 3.80 (m,

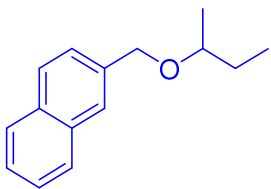
2H), 3.55 (t, $J = 5.1$ Hz, 2H), 3.42 - 3.48 (m, 2H), 2.34 (t, $J = 7.8$ Hz, 2H), 1.98 (tt, $J =$

15.7, 7.8 Hz, 2H) ppm; ^{13}C NMR (400 MHz, CDCl_3) δ 175.0, 159.0, 130.0, 129.1, 113.6,

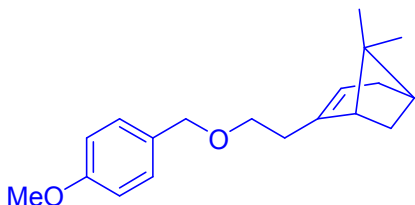
72.3, 67.8, 55.1, 48.3, 42.3, 30.8, 17.9 ppm; GC-MS m/z = 249 (M^+); Anal. Calcd for $C_{14}H_{19}NO_3$: C, 67.45; H, 7.68. Found: C, 75.48; H, 8.61.



Data for **Table 5.3, Compound 2r**: 1H NMR (400 MHz, $CDCl_3$) δ 8.18 (dq, J = 4.9, 1.4 Hz, 1H), 7.37 (td, J = 7.8, 1.7 Hz, 1H), 7.28 (dq, J = 7.9, 1.1 Hz, 1H), 6.87 (ddd, J = 8.0, 4.8, 1.3 Hz, 1H), 5.17 (t, J = 2.3 Hz, 1H), 3.40 (sxt, J = 6.2 Hz, 1H), 1.14 - 1.33 (m, 2H), 0.74 (d, J = 6.4 Hz, 3H), 0.60 (t, J = 7.5 Hz, 3H) ppm; ^{13}C NMR (400 MHz, $CDCl_3$) 160.0, 148.2, 136.7, 123.2, 121.1, 73.9, 73.6, 29.8, 20.0, 9.9 ppm; GC-MS m/z = 165 (M^+); Anal. Calcd for $C_{10}H_{15}NO$: C, 72.69; H, 9.15. Found: C, 75.48; H, 8.61.

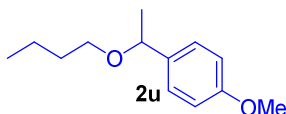


Data for **Table 5.3, Compound 2s**: 1H NMR (400 MHz, $CDCl_3$) δ 7.77-7.95 (m, 4H), 7.42-7.59 (m, 3H), 4.72 (dd, J = 35.6, 12.1 Hz, 2H), 3.52 (sxt, J = 6.1 Hz, 1H), 1.63-1.74 (m, 1H), 1.47-1.61 (m, 1H), 1.25 (d, J = 6.1 Hz, 3H), 0.97 (t, J = 7.4 Hz, 3H) ppm; ^{13}C NMR (400 MHz, $CDCl_3$) δ 136.7, 133.3, 132.9, 128.0, 127.8, 127.7, 126.1, 126.0, 125.87, 125.86, 125.85, 125.7, 76.2, 70.4, 29.3, 19.2, 9.9 ppm; GC-MS m/z = 165 (M^+); Anal. Calcd for $C_{10}H_{15}NO$: C, 72.69; H, 9.15. Found: C, 75.48; H, 8.61.



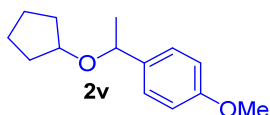
Data for **Table 5.3, Compound 2t**: 1H NMR (400 MHz, $CDCl_3$) δ 7.14-7.21 (m, 2H), 6.76-6.83 (m, 2H), 5.18 (ddd, J = 4.3, 2.9, 1.4 Hz, 1H), 4.35 (s, 2H), 3.71 (s, 3H), 3.33-3.42 (m, 2H), 1.91-2.32 (m, 9H), 1.15-1.22 (m, 3H), 0.71-0.78 (m, 3H) ppm; ^{13}C NMR (400 MHz, $CDCl_3$) δ 159.0, 145.1, 130.6, 129.2, 117.7, 113.6, 72.4, 68.5, 55.2, 45.7, 40.7, 37.9, 37.1, 31.6,

31.3, 26.3, 21.1 ppm; GC-MS $m/z = 286$ (M^+); ^1H and ^{13}C NMR spectral data are in good agreement with the literature data.⁷²



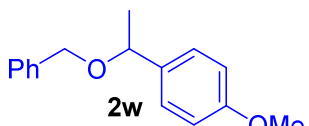
Data for **2u**: ^1H NMR (400 MHz, CDCl_3) δ 6.93 (d, $J = 8.7$ Hz, 2H), 6.57 (d, $J = 8.8$ Hz, 2H), 4.03 (q, $J = 6.4$ Hz, 1H), 3.49 (s, 3H), 2.96 (t, $J = 6.6$ Hz, 2H), 1.18-1.28 (m, 2H), 1.11 (d, $J = 6.4$ Hz, 3H), 0.98-1.09 (m, 2H), 0.58 (t, $J = 7.4$ Hz, 3H)

ppm; $^{13}\text{C}\{^1\text{H}\}$ NMR (100 MHz, CDCl_3) δ 158.8, 136.3, 127.2, 113.6, 77.3, 68.1, 55.1, 32.0, 24.1, 19.3, 13.9 ppm; GC-MS $m/z = 208$ (M^+). ^1H and ^{13}C NMR spectral data are in good agreement with the literature data.⁷³



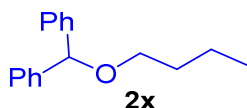
Data for **2v**: ^1H NMR (400 MHz, CDCl_3) δ 7.26 (d, $J = 8.4$ Hz, 2H), 6.89 (d, $J = 8.5$ Hz, 2H), 4.43 (q, $J = 6.5$ Hz, 1H), 3.82 (s, 3H), 1.41-1.77 (m, 9H), 1.39 (d, $J = 6.5$ Hz, 3H) ppm; $^{13}\text{C}\{^1\text{H}\}$ NMR (100 MHz, CDCl_3) δ 158.7, 136.7, 127.4, 113.6,

78.3, 74.9, 55.2, 33.0, 31.8, 24.6, 23.5, 23.4 ppm; GC-MS $m/z = 220$ (M^+). ^1H and ^{13}C NMR spectral data are in good agreement with the literature data.⁷⁴



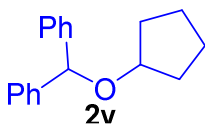
Data for **2w**: ^1H NMR (400 MHz, CDCl_3) δ 7.10-7.33 (m, 7H), 6.72-6.87 (m, 2H), 4.38 (q, $J = 6.5$ Hz, 1H), 4.35 (d, $J = 11.9$ Hz, 1H), 4.19 (d, $J = 11.9$ Hz, 1H), 3.75 (s, 3H), 1.39

(d, $J = 6.5$ Hz, 3H) ppm; $^{13}\text{C}\{^1\text{H}\}$ NMR (100 MHz, CDCl_3) δ 159.0, 138.9, 135.7, 128.3, 127.7, 127.6, 127.4, 113.8, 76.7, 70.0, 55.3, 24.1 ppm; GC-MS $m/z = 242$ (M^+); ^1H and ^{13}C NMR spectral data are in good agreement with the literature data.⁷⁵



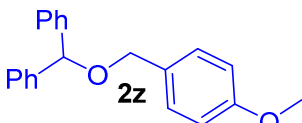
Data for **2x**: ^1H NMR (400 MHz, CDCl_3) δ 7.27-7.48 (m, 10H), 5.44 (s, 1H), 3.56 (t, $J = 6.5$ Hz, 2H), 1.69-1.79 (m, 2H),

1.48-1.62 (m, 2H), 1.02 (t, $J = 7.4$ Hz, 3H) ppm; $^{13}\text{C}\{^1\text{H}\}$ NMR (100 MHz, CDCl_3) δ 142.6, 128.3, 128.3, 128.2, 128.2, 127.2, 126.9, 126.9, 126.9, 126.8, 83.5, 68.9, 32.0, 19.4, 13.9 ppm; GC-MS $m/z = 240$ (M^+); ^1H and ^{13}C NMR spectral data are in good agreement with the literature data.⁷⁶



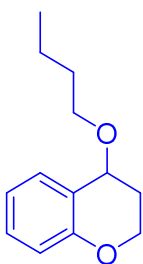
Data for **2y**: ^1H NMR (400 MHz, CDCl_3) δ 7.23-7.52 (m, 10H), 5.54 (s, 1H), 4.05-4.16 (m, 1H), 1.74-1.96 (m, 6H), 1.54-1.70 (m, 2H) ppm; $^{13}\text{C}\{^1\text{H}\}$ NMR (100 MHz, CDCl_3) δ 142.8, 128.2,

127.2, 127.1, 80.9, 78.9, 32.5, 23.5 ppm; GC-MS $m/z = 252$ (M^+); Anal. Calcd for $\text{C}_{18}\text{H}_{20}\text{O}$: C, 85.67; H, 7.99. Found: C, 75.48; H, 8.61.



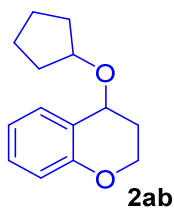
Data for **2z**: ^1H NMR (400 MHz, CDCl_3) δ 7.13-7.34 (m, 12H), 6.78-6.85 (m, 2H), 5.35 (s, 1H), 4.40 (s, 2H), 3.74 (s, 3H) ppm; $^{13}\text{C}\{^1\text{H}\}$ NMR (100 MHz, CDCl_3) δ 159.1,

142.2, 130.4, 129.4, 128.4, 127.4, 127.1, 113.7, 82.0, 70.1, 55.3 ppm; GC-MS $m/z = 304$ (M^+); ^1H and ^{13}C NMR spectral data are in good agreement with the literature data.⁷⁸

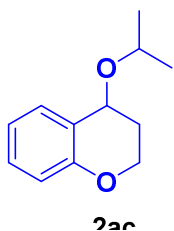


Data for **2aa**: ^1H NMR (400 MHz, CDCl_3) δ 7.27 (dd, $J = 7.6$, 1.8 Hz, 1 H), 7.20 (ddd, $J = 8.4$, 7.0, 1.8 Hz, 1H), 6.91 (td, $J = 7.4$, 1.2 Hz, 1H), 6.85 (dd, $J = 8.2$, 1.2 Hz, 1H), 4.38 (t, $J = 3.7$ Hz, 1H), 4.32 (td, $J = 11.0$, 3.1 Hz, 1H), 4.25 (dtd, $J = 11.0$, 4.1, 0.8 Hz, 1H), 3.59 (ttt, $J = 15.7$, 12.9, 6.3 Hz, 2H), 2.10-2.18 (m, 1H), 2.01-2.10 (m, 1H), 1.57-

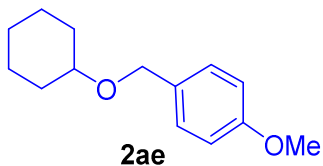
1.66 (m, 2H), 1.37-1.48 (m, 2H), 0.95 (t, $J = 7.4$ Hz, 3H) ppm; $^{13}\text{C}\{^1\text{H}\}$ NMR (100 MHz, CDCl_3) δ 154.7, 130.5, 129.4, 122.2, 119.9, 116.8, 70.3, 68.0, 62.2, 32.1, 27.6, 19.4, 13.9 ppm; GC-MS $m/z = 206$ (M^+); Anal. Calcd for $\text{C}_{13}\text{H}_{18}\text{O}_2$: C, 75.69; H, 8.80. Found: C, 75.48; H, 8.61.



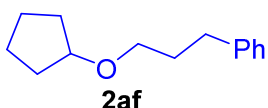
Data for **2ab**: ^1H NMR (400 MHz, CDCl_3) δ 7.24 (dd, $J = 1.6$, 7.5 Hz, 1H), 7.17 (dt, $J = 1.8$, 7.8 Hz, 1H), 6.87-6.92 (m, 1H), 6.79-6.83 (m, 1H), 4.43 (t, $J = 4.0$ Hz, 1H), 4.41-4.45 (m, 1H), 4.16-4.36 (m, 2H), 1.93-2.12 (m, 2H), 1.67-1.67 (m, 1H), 1.63-1.88 (m, 5H), 1.51-1.63 (m, 2H) ppm; $^{13}\text{C}\{^1\text{H}\}$ NMR (100 MHz, CDCl_3) δ 154.8, 130.3, 129.2, 122.8, 120.1, 116.8, 78.5, 68.0, 62.4, 33.0, 32.8, 28.1, 23.6, 23.4 ppm; GC-MS $m/z = 192$ (M^+); Anal. Calcd for $\text{C}_{12}\text{H}_{16}\text{O}_2$: C, 74.97; H, 8.39. Found: C, 75.48; H, 8.61.



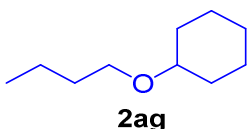
Data for **2ac**: ^1H NMR (400 MHz, CDCl_3) δ 7.24-7.27 (m, 1H), 7.16-7.21 (m, 1H), 6.91 (td, $J = 7.43$, 1.21 Hz, 1H), 6.81-6.85 (m, 1H), 4.48 (t, $J = 3.9$ Hz, 1H), 4.28-4.35 (m, 1H), 4.22-4.28 (m, 1H), 4.16-4.22 (m, 1H), 3.88 (spt, $J = 6.1$ Hz, 1H), 2.04-2.08 (m, 2H), 1.27 (d, $J = 6.0$ Hz, 3H), 1.25 (d, $J = 6.2$ Hz, 3H) ppm; ^{13}C NMR (400 MHz, CDCl_3) δ 154.8, 130.2, 129.2, 122.8, 120.2, 116.8, 68.9, 67.4, 62.3, 28.4, 23.3, 22.4 ppm; GC-MS $m/z = 192$ (M^+); Anal. Calcd for $\text{C}_{12}\text{H}_{16}\text{O}_2$: C, 74.97; H, 8.39. Found: C, 74.48; H, 8.41.



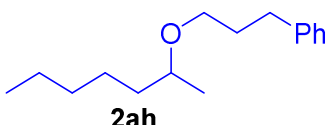
Data for **2ae**: ^1H NMR (400 MHz, CDCl_3) δ 7.24 (dd, $J = 7.5$, 1.6 Hz, 1H), 7.17 (td, $J = 7.8$, 1.8 Hz, 1H), 6.87-6.92 (m, 1H), 6.79-6.83 (m, 1H), 4.43 (t, $J = 4.0$ Hz, 1H), 4.41-4.45 (m, 1H), 4.36-4.16 (m, 4H), 1.93-2.12 (m, 2H), 1.67 (m, 1H), 1.63-1.88 (m, 5H), 1.51-1.63 (m, 2H) ppm; $^{13}\text{C}\{^1\text{H}\}$ NMR (100 MHz, CDCl_3) δ 154.8, 130.3, 129.2, 122.8, 120.1, 116.8, 78.5, 77.4, 68.0, 62.4, 33.0, 32.8, 28.1, 23.6, 23.4 ppm; GC-MS $m/z = 218$ (M^+); Anal. Calcd for $\text{C}_{14}\text{H}_{20}\text{O}_2$: C, 76.33; H, 9.15. Found: C, 76.38; H, 9.13.



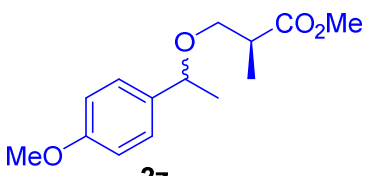
Data for **2af**: ^1H NMR (400 MHz, CDCl_3) δ 7.25-7.32 (m, 2H), 7.17-7.23 (m, 3H), 4.28-4.35 (m, 1H), 3.65 (t, $J = 6.8$ Hz, 2H), 2.70 (t, $J = 7.7$ Hz, 2H), 1.94-2.04 (m, 2H), 1.84-1.93 (m, 2H), 1.68-1.82 (m, 4H), 1.48-1.65 (m, 2H) ppm; $^{13}\text{C}\{^1\text{H}\}$ NMR (100 MHz, CDCl_3) δ 141.8, 128.4, 128.4, 128.4, 128.3, 128.3, 128.3, 125.8, 73.9, 62.1, 35.4, 34.1, 32.0, 23.2 ppm; GC-MS $m/z = 234$ (M^+); ^1H and ^{13}C NMR spectral data are in good agreement with the literature data.⁸⁰



Data for **2ag**: ^1H NMR (400 MHz, CDCl_3) δ 3.43 (t, $J = 6.7$ Hz, 2H), 3.13-3.23 (m, 1H), 1.80-1.95 (m, 3H), 1.66-1.77 (m, 3H), 1.47-1.57 (m, 3H), 1.31-1.42 (m, 2H), 1.14-1.31 (m, 6H), 0.91 (t, $J = 7.4$ Hz, 3H) ppm; $^{13}\text{C}\{^1\text{H}\}$ NMR (100 MHz, CDCl_3) δ 77.4, 67.5, 32.3, 32.3, 25.8, 25.8, 24.2, 19.4, 13.9 ppm; GC-MS $m/z = 156$ (M^+); ^1H and ^{13}C NMR spectral data are in good agreement with the literature data.⁷²



Data for **2ah**: ^1H NMR (400 MHz, CDCl_3) 7.17-7.24 (m, 3H), 7.08-7.15 (m, 2H), 3.42 (dt, $J = 9.1, 6.4$ Hz, 2H), 3.23-3.31 (m, 2H), 2.63 (td, $J = 7.8, 1.8$ Hz, 2H), 1.76-1.85 (m, 2H), 1.39-1.52 (m, 1H), 1.16-1.35 (m, 6H), 1.05 (d, $J = 5.9$ Hz, 3H), 0.82 (t, $J = 6.8$ Hz, 3H) ppm; $^{13}\text{C}\{^1\text{H}\}$ NMR (100 MHz, CDCl_3) δ 142.2, 128.5, 128.3, 125.7, 75.4, 67.43, 36.7, 32.5, 32.0, 31.7, 25.3, 22.7, 19.7, 14.1 ppm; GC-MS $m/z = 234$ (M^+); Anal. Calcd for $\text{C}_{16}\text{H}_{26}\text{O}$: C, 81.99; H, 11.18. Found: C, 75.48; H, 8.61.



Data for **2ai** (1:1 diastereomers): Isomer **A**: ^1H NMR (400 MHz, CDCl_3) δ 7.21 (d, $J = 8.8$ Hz, 2H), 6.87 (d, $J = 8.8$ Hz, 2H), 4.35 (q, $J = 6.3$ Hz, 1H), 3.80 (s, 3H),

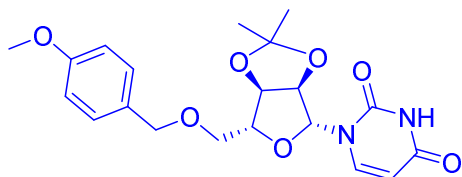
3.67 (s, 3H), 3.46 (t, $J = 9.3$ Hz, 1H), 3.28 (t, $J = 6.4$ Hz, 1H), 2.78-2.66 (m, 1H), 1.38 (d, $J = 6.3$ Hz, 3H), 1.14 (d, $J = 7.0$ Hz, 3H) ppm; $^{13}\text{C}\{^1\text{H}\}$ NMR (100 MHz, CDCl_3) δ 175.5, 143.7, 128.3, 127.4, 126.1, 78.5, 70.5, 51.7, 40.3, 24.1, 14.0 ppm. Isomer **B**: ^1H NMR (100 MHz, CDCl_3) δ 7.20 (d, $J = 8.8$ Hz, 2H), 6.87 (d, $J = 8.8$ Hz, 2H), 4.34 (q, $J = 6.3$ Hz, 1H),

3.80 (s, 3H), 3.68 (s, 3H), 3.48 (t, $J = 9.3$ Hz, 1H),

3.30 (t, $J = 6.4$ Hz, 1H), 2.78-2.66 (m, 1H), 1.39

(d, $J = 6.3$ Hz, 3H), 1.12 (d, $J = 7.0$ Hz, 3H) ppm;

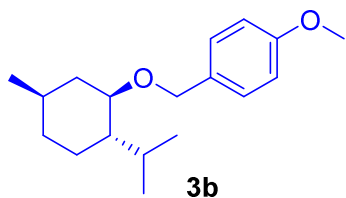
$^{13}\text{C}\{^1\text{H}\}$ NMR (100 MHz, CDCl_3) δ 175.3, 143.7,



3a

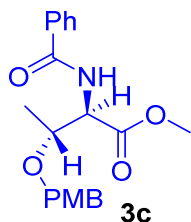
128.4, 127.4, 126.1, 78.2, 70.4, 51.7, 40.3, 24.1, 14.0 ppm; GC-MS $m/z = 252$ (M^+); ^1H and ^{13}C NMR spectral data are in good agreement with the literature data.⁸¹

Data for **3a**: ^1H NMR (400 MHz, CDCl_3) δ 8.79 (br s, 1H), 7.59 (d, $J = 8.1$ Hz, 1H), 7.23 (d, $J = 8.9$ Hz, 2H), 6.90 (d, $J = 8.7$ Hz, 2H), 5.96 (d, $J = 2.8$ Hz, 1H), 5.52 (dd, $J = 8.1, 2.3$ Hz, 1H), 4.81 (dd, $J = 6.2, 2.9$ Hz, 1H), 4.7 (dd, $J = 6.2, 2.8$ Hz, 1H), 4.47 (dd, $J = 14.3, 11.1$ Hz, 2H), 4.40 (dd, $J = 5.6, 2.9$ Hz, 1H), 3.82 (s, 3H), 3.76 (dd, $J = 10.5, 2.6$ Hz, 1H), 3.65 (dd, $J = 10.5, 3.4$ Hz, 1H), 1.59 (s, 3H), 1.35 (s, 3H) ppm; ^{13}C NMR (100 MHz, CDCl_3) 163.5, 159.4, 150.2, 141.1, 129.5, 129.1, 114.0, 113.8, 102.1, 92.3, 85.5, 84.9, 80.8, 73.2, 69.7, 55.2, 27.1, 25.2 ppm; HRMS (ESI): calcd for $\text{C}_{20}\text{H}_{24}\text{N}_2\text{O}_7$ ($[\text{M}+\text{H}]^+$) 405.1656, found 405.1658. ^1H and ^{13}C NMR spectral data are in good agreement with the literature data.⁸²



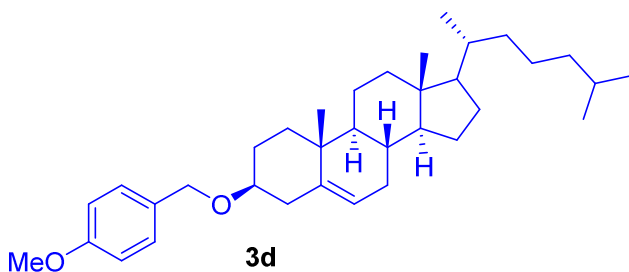
Data for **3b**: ^1H NMR (400 MHz, CDCl_3) δ 7.26-7.33 (m, 2H), 6.87-6.92 (m, 2H), 4.61 (d, $J = 11.0$ Hz, 1H), 4.35 (d, $J = 11.0$ Hz, 1H), 3.81 (s, 3H), 3.17 (td, $J = 10.5$, 4.2 Hz, 1H), 2.31 (m, $J = 2.7$ Hz, 1H), 2.20 (m, $J = 1.7$ Hz, 1H), 1.60-1.71 (m, 2H), 1.39 (s, 2H), 0.95-0.98 (m, 6H), 0.92 (d, $J = 7.1$ Hz, 3H), 0.73 (d, $J = 6.9$ Hz, 3H) ppm;

$^{13}\text{C}\{^1\text{H}\}$ NMR (100 MHz, CDCl_3) δ 158.9, 131.2, 129.3, 113.6, 78.3, 70.0, 55.1, 48.2, 40.2, 34.5, 31.5, 25.4, 23.2, 22.3, 21.0, 14.0 ppm; GC-MS $m/z = 276$ (M^+); ^1H and ^{13}C NMR spectral data are in good agreement with the literature data.⁸³



Data for **3c**: ^1H NMR (400 MHz, CDCl_3) δ 7.79-7.86 (m, 2H), 7.46-7.52 (m, 1H), 7.38-7.45 (m, 2H), 7.17-7.22 (m, 2H), 6.84-6.89 (m, 3H), 4.87 (dd, $J = 9.1$, 2.4 Hz, 1H), 4.54 (d, $J = 11.5$ Hz, 1H), 4.34 (d, $J = 11.5$ Hz, 1H), 4.20 (ddd, $J = 12.6$, 6.3, 2.4 Hz, 1H), 3.78 (d, $J = 0.4$ Hz, 3H), 3.68 (s, 3H), 1.26 (d, $J = 6.2$ Hz, 3H) ppm;

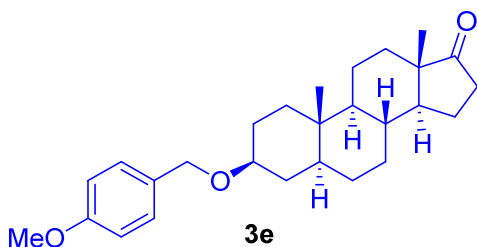
$^{13}\text{C}\{^1\text{H}\}$ NMR (100 MHz, CDCl_3) δ 171.0, 167.5, 159.2, 133.7, 131.6, 129.7, 129.3, 128.4, 127.0, 113.6, 73.7, 70.3, 56.9, 55.1, 52.2, 16.2 ppm; HRMS (ESI): calcd for $\text{C}_{20}\text{H}_{23}\text{NO}_5$ ($[\text{M}+\text{Na}]^+$) 380.1668, found 380.1669.



Data for **3d**: ^1H NMR (400 MHz, CDCl_3) δ 7.27 (d, $J = 8.9$ Hz, 2H), 6.87 (d, $J = 8.9$ Hz, 2H), 5.34 (d, $J = 5.3$ Hz, 1H), 4.49 (s, 2H), 3.80 (s, 3H), 3.26 (tt, $J = 11.1$, 4.60

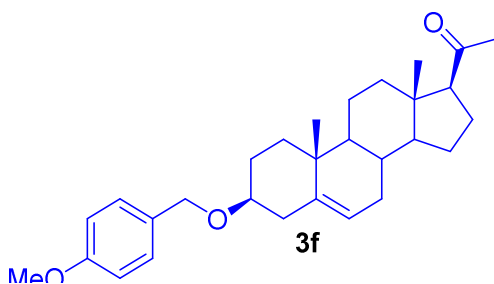
Hz, 1H), 2.40-0.84 (m, 40H), 0.67 (s, 3H) ppm; $^{13}\text{C}\{^1\text{H}\}$ NMR (100 MHz, CDCl_3) δ 159.0,

141.0, 131.1, 129.1, 121.5, 113.8, 78.3, 69.6, 56.8, 56.1, 55.3, 50.2, 42.3, 39.8, 39.5, 39.2, 37.3, 36.9, 36.2, 35.8, 31.9, 31.9, 28.4, 28.2, 28.0, 24.3, 23.8, 22.8, 22.6, 21.1, 19.4, 18.7, 11.9 ppm; HRMS (ESI-TOF) $m/z = 506.41$ (M^+); Anal. Calcd for $C_{35}H_{54}O_2$: C, 82.95; H, 10.74. Found: C, 82.57; H, 10.52.



Data for **3e**: 1H NMR (400 MHz, $CDCl_3$) δ 7.22 - 7.27 (m, 2H), 6.82 - 6.88 (m, 2H), 4.46 (s, 2 H), 3.77 (s, 3H), 3.25 - 3.35 (m, 1H), 2.41 (dd, $J=19.1, 8.6$ Hz, 1H), 2.03 (td, $J=18.3, 8.8$ Hz, 1H), 1.90 (ddd, $J=13.7, 8.4, 5.5$

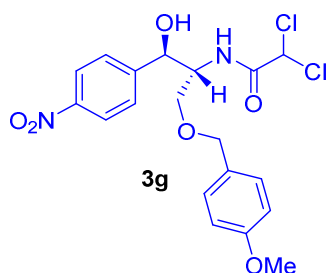
Hz, 2H), 1.59 - 1.81 (m, 5H), 1.15 - 1.58 (m, 10H), 0.86 - 1.11 (m, 3H), 0.83 (d, $J=7.8$ Hz, 6H), 0.66 (td, $J=11.8, 4.3$ Hz, 1H) ppm; ^{13}C NMR (400 MHz, $CDCl_3$) 221.1, 158.8, 131.0, 128.9, 113.5, 77.30, 69.3, 55.1, 54.3, 51.2, 47.6, 44.7, 36.8, 35.8, 35.7, 34.8, 34.6, 31.4, 30.7, 28.4, 28.0, 21.6, 20.3, 13.6, 12.1 ppm; GC-MS $m/z = 276$ (M^+); Anal. Calcd for $C_{27}H_{38}O_2$: C, 78.98; H, 9.33. Found: C, 78.48; H, 9.61.⁸⁵



Data for **3f**: 1H NMR (400 MHz, $CDCl_3$) δ 7.22-7.30 (m, 2H), 6.81-6.90 (m, 2H), 5.29-5.37 (m, 1H), 4.48 (s, 2H), 3.78 (s, 3H), 3.19-3.31 (m, 1H), 2.47-2.56 (m, 1H), 2.35-2.45 (m, 1H), 2.12-2.30 (m, 2H), 2.11 (s,

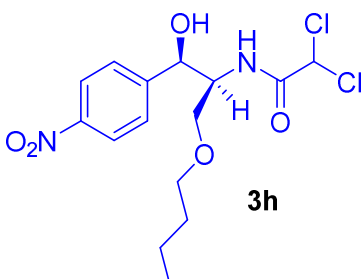
3H), 1.77-2.06 (m, 4H), 1.37-1.72 (m, 9H), 1.01 - 1.31 (m, 3H), 1.00 (s, 3H), 0.61 (s, 3H) ppm; ^{13}C NMR (100 MHz, $CDCl_3$) 209.4, 58.9, 140.9, 131.0, 129.0, 121.1, 113.7, 78.0, 69.5, 63.6, 56.8, 55.2, 49.9, 43.9, 39.0, 38.7, 37.2, 36.8, 31.7, 31.7, 31.5, 28.3, 24.4, 22.7,

21.0, 19.3, 13.1 ppm; GC-MS $m/z = 276$. ^1H and ^{13}C NMR spectral data are in good agreement with the literature data.⁸⁴



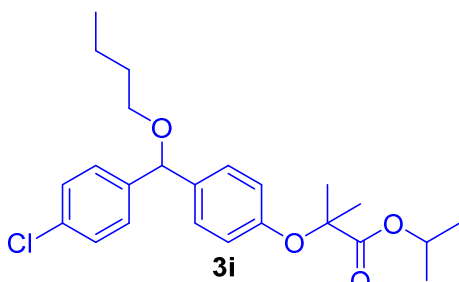
Data for **3g**: ^1H NMR (400 MHz, CDCl_3) δ 8.02-8.13 (m, 2 H), 7.42 (d, $J = 8.7$ Hz, 2H), 7.18 (d, $J = 8.7$ Hz, 2H), 7.09 (d, $J = 9.0$ Hz, 1H), 6.83 (d, $J = 8.5$ Hz, 2H), 5.70 (s, 1H), 5.13 (d, $J = 2.4$ Hz, 1H), 4.44 (s, 2H), 4.12-4.19 (m, 1H), 3.73 (s, 3H), 3.60-3.69 (m, 3H) ppm; $^{13}\text{C}\{^1\text{H}\}$ NMR

(100 MHz, CDCl_3) δ 164.1, 159.6, 147.5, 129.6, 128.7, 126.7, 123.5, 114.0, 73.5, 73.3, 70.4, 66.1, 55.3, 54.4 ppm; GC-MS $m/z = 443$ (M^+); HRMS (APCI): calcd for $\text{C}_{19}\text{H}_{22}\text{Cl}_2\text{N}_2\text{O}_6$ ($[\text{M}+\text{H}]^+$) 443.0777; found. 443.0779.



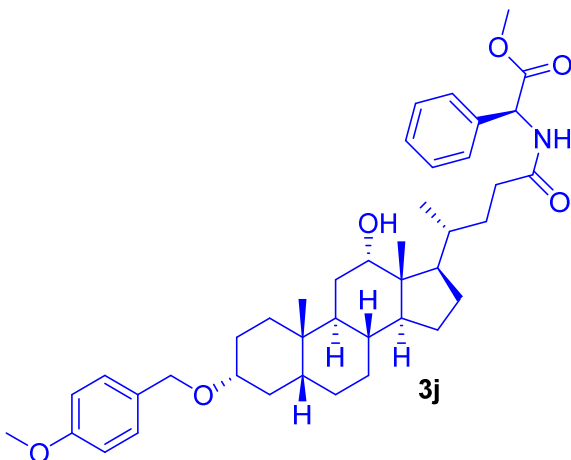
Data for **3h**: ^1H NMR (400 MHz, CDCl_3) δ 8.17-8.23 (m, 2H), 7.50-7.55 (m, 2H), 7.08 (d, $J = 9.7$ Hz, 1H), 5.68 (s, 1H), 5.08-5.13 (m, 1H), 4.88 (t, $J = 5.0$ Hz, 1H), 4.32 (dq, $J = 9.7, 1.8$ Hz, 1H), 4.08-4.20 (m, 3H), 1.76-1.85 (m, 3H), 1.49-1.61 (m, 2H), 1.01 (t, $J = 7.3$ Hz, 3H)

ppm; $^{13}\text{C}\{^1\text{H}\}$ NMR (100 MHz, CDCl_3) δ 163.5, 147.5, 144.4, 126.4, 126.4, 123.5, 123.4, 102.9, 78.4, 77.4, 77.3, 76.7, 76.6, 70.2, 65.9, 47.6, 36.7, 17.0, 14.0 ppm; GC-MS $m/z = 379$ (M^+); HRMS (APCI): calcd for $\text{C}_{15}\text{H}_{21}\text{Cl}_2\text{N}_2\text{O}_5$ ($[\text{M}+\text{H}]^+$) 379.0828; found. 379.0825.



Data for **3i**: ^1H NMR (400 MHz, CDCl_3) δ 7.23-7.31 (m, 4H), 7.12-7.20 (m, 2H), 6.77-6.85 (m, 2H), 5.25 (s, 1H), 5.08 (spt, $J = 6.2$ Hz, 1H), 3.60 (dt, $J = 9.3, 6.6$ Hz, 1H), 1.52-1.66 (m, 9H), 1.34-1.47 (m, 2H), 1.20 (d, $J = 6.5$ Hz, 6H), 0.93

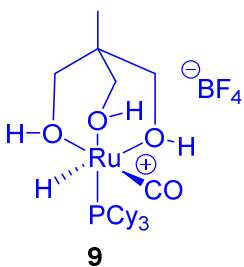
(t, $J = 7.8$ Hz, 3H) ppm; ^{13}C NMR (100 MHz, CDCl_3) 173.6, 154.9, 141.3, 135.4, 128.3, 128.2, 127.7, 118.6, 102.8, 82.3, 78.9, 68.8, 65.0, 35.5, 31.9, 25.3, 21.4, 19.4, 18.0, 13.8 ppm; GC-MS $m/z = 418$; HRMS (APCI): calcd for $\text{C}_{24}\text{H}_{31}\text{ClO}_4$ ($[\text{M}+\text{H}]^+$) 419.1989, found 419.1991.



Data for **3j**: ^1H NMR (400 MHz, CDCl_3) δ 7.33-7.42 (m, 5H), 7.30 (d, $J = 8.9$ Hz, 2H), 6.90 (d, $J = 7.8$ Hz, 2H), 6.69 (d, $J = 7.24$ Hz, 1H), 5.65 (d, $J = 6.7$ Hz, 1H), 4.50-4.53 (m, 2H), 3.97 (br s, 1H), 3.83 (s, 3H), 3.75 (s, 3H), 3.39 (tt, $J = 11.0, 4.4$ Hz, 1H), 2.30-2.42 (m,

1H), 1.04-1.94 (m, 24H), 0.95-1.02 (m, 4H), 0.94 (s, 3H), 0.68 (s, 3H) ppm; $^{13}\text{C}\{^1\text{H}\}$ NMR (100 MHz, CDCl_3) δ 172.8, 171.4, 158.8, 136.5, 131.0, 128.9, 128.8, 128.3, 127.1, 113.6, 78.1, 72.9, 69.2, 56.12, 55.1, 52.6, 48.0, 46.9, 46.3, 41.9, 35.9, 35.1, 34.9, 34.3, 33.4, 33.0, 32.8, 31.1, 28.5, 27.3, 27.1, 26.9, 25.9, 23.5, 23.1, 17.2, 12.6 ppm; HRMS (ESI): calcd for $\text{C}_{41}\text{H}_{57}\text{NO}_6$ ($[\text{M}+\text{H}]^+$) 660.4259, found 660.4262.

Synthesis of Complex **9**: In the glove box **complex 1** (115

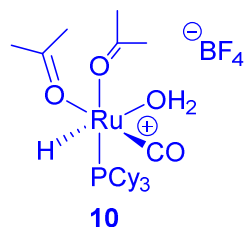


mg, 0.2 mmol) was mixed with 1,1,1-tris(hydroxymethyl)ethane (24 mg, 0.2 mmol) in acetone (2 mL) solvent and stirred 30 min at room temperature. Crystallization in acetone/*n*-pentane to obtain the complex as white crystals in 80% yield. ^1H NMR (400 MHz,

acetone- d_6) δ 3.64 (m, 3H), 3.48-3.55 (m, 6H), 1.17-1.39 (m, 33H), 0.82 (s, 3H), -17.76 (d, $J_{\text{PH}} = 34.2$ Hz, 1H) ppm; $^{13}\text{C}\{^1\text{H}\}$ NMR (100 MHz, CDCl_3) δ 216.1 (d, $J_{\text{CP}} = 18.3$ Hz),

72.0, 65.7, 64.5, 37.5, 30.8, 30.1, 27.9, 27.8, 26.7 ppm; ^{31}P NMR (100 MHz, CDCl_3) δ 76.4 ppm; IR (pure solid) $\nu_{\text{CO}} = 1915 \text{ cm}^{-1}$.

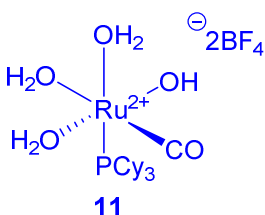
Synthesis of Complex **10**: In the glove box **complex 1** (50



mg, 0.1 mmol) was dissolved acetone (1 mL) as solvent and stirred 10 min at room temperature. Crystallization in acetone/*n*-pentane to obtain the complex as yellow crystals in 80% yield. ^1H NMR

(400 MHz, acetone- d_6) δ 4.48 (br.s, 2H), 2.63-2.74 (br.s, 12H), 1.17-1.39 (m, 33H), -17.51 (d, $J_{\text{PH}} = 31.1 \text{ Hz}$, 1H) ppm; ^{31}P NMR (100 MHz, CDCl_3) δ 73.4 ppm.

Synthesis of Complex **11**: In the glove box **complex 4** (50



mg, 0.03 mmol) was dissolved dioxane (1 mL) as solvent and $\text{HBF}_4 \cdot \text{Et}_2\text{O}$ (19 μL , 0.12 mmol) was added stirred 3 h at room temperature. Crystallization in dioxane/*n*-pentane to obtain the complex as yellow crystals in 75 % yield. ^1H NMR (400 MHz, CD_2Cl_2) δ 4.48 (br.s, 8H), 0.99-2.15 (m, 33H) ppm; ^{31}P NMR

(100 MHz, CDCl_3) δ 55.09 ppm.

6.4.11 X-Ray Data:

Table 6.13: Crystal data and structure refinement for 9.	
Identification code	9
Empirical formula	C ₂₇ H ₅₂ BO ₅ F ₄ PRu
Formula weight	675.54
Temperature/K	100.00(10)
Crystal system	monoclinic
Space group	I2/a
a/Å	16.7775(4)
b/Å	9.6540(2)
c/Å	39.1720(11)
α /°	90.00
β /°	93.7(2)
γ /°	90.00
Volume/Å ³	6334.4(3)
Z	8
$\rho_{\text{calc}}/\text{cm}^3$	1.417
μ/mm^{-1}	4.975
F(000)	2832.0
Crystal size/mm ³	0.3068 × 0.2254 × 0.0989
Radiation	CuK α ($\lambda = 1.54184$)
2 θ range for data collection/°	9.04 to 149.48
Index ranges	-20 ≤ h ≤ 20, -11 ≤ k ≤ 11, -48 ≤ l ≤ 48
Reflections collected	55980
Independent reflections	6382 [R _{int} = 0.0867, R _{sigma} = 0.0312]
Data/restraints/parameters	6382/0/372
Goodness-of-fit on F ²	1.320
Final R indexes [I ≥ 2 σ (I)]	R ₁ = 0.0927, wR ₂ = 0.2173
Final R indexes [all data]	R ₁ = 0.0933, wR ₂ = 0.2175
Largest diff. peak/hole / e Å ⁻³	2.01/-3.04

Table 6.14: Crystal data and structure refinement for 3e.	
Identification code	3e
Empirical formula	C ₂₇ H ₃₈ O ₃
Formula weight	410.57
Temperature/K	100.00(10)
Crystal system	triclinic
Space group	P1
a/Å	7.0758(5)
b/Å	9.5647(10)
c/Å	10.1305(8)
α /°	63.457(9)
β /°	69.879(7)
γ /°	82.885(7)
Volume/Å ³	575.55(8)
Z	1
ρ_{calc} /mm ³	1.185
m/mm ⁻¹	0.585
F(000)	224.0
Crystal size/mm ³	0.28 × 0.27 × 0.22
Radiation	CuK α (λ = 1.54184)
2 θ range for data collection	10.32 to 147.22°
Index ranges	-8 ≤ h ≤ 8, -11 ≤ k ≤ 11, -12 ≤ l ≤ 12
Reflections collected	9989
Independent reflections	4060 [R _{int} = 0.0650, R _{sigma} = 0.0444]
Data/restraints/parameters	4060/3/274
Goodness-of-fit on F ²	1.037
Final R indexes [I ≥ 2 σ (I)]	R ₁ = 0.0488, wR ₂ = 0.1352
Final R indexes [all data]	R ₁ = 0.0510, wR ₂ = 0.1389
Largest diff. peak/hole / e Å ⁻³	0.29/-0.23
Flack parameter	-0.1(2)

Table 6.15: Crystal data and structure refinement for 3f.

Identification code	3f
Empirical formula	C ₂₉ H ₄₀ O ₃
Formula weight	436.61
Temperature/K	100.00(10)
Crystal system	trigonal
Space group	P3 ₂
a/Å	13.48807(18)
b/Å	13.48807(18)
c/Å	11.6705(2)
α/°	90.00
β/°	90.00
γ/°	120.00
Volume/Å ³	1838.73(5)
Z	3
ρ _{calc} /mm ³	1.183
m/mm ⁻¹	0.578
F(000)	714.0
Crystal size/mm ³	0.42 × 0.12 × 0.05
Radiation	CuKα (λ = 1.54184)
2θ range for data collection	7.56 to 147.18°
Index ranges	-16 ≤ h ≤ 16, -16 ≤ k ≤ 16, -10 ≤ l ≤ 14
Reflections collected	11497
Independent reflections	4347 [R _{int} = 0.0231, R _{sigma} = 0.0230]
Data/restraints/parameters	4347/274/587
Goodness-of-fit on F ²	1.053
Final R indexes [I ≥ 2σ (I)]	R ₁ = 0.0281, wR ₂ = 0.0734
Final R indexes [all data]	R ₁ = 0.0282, wR ₂ = 0.0736
Largest diff. peak/hole / e Å ⁻³	0.08/-0.10
Flack parameter	-0.09(18)

Table 6.16: Crystal data and structure refinement for 11.

Identification code	11
Empirical formula	$C_{23.78}H_{49.78}B_2Cl_{2.34}F_8O_7PRu$
Formula weight	836.39
Temperature/K	99.8(5)
Crystal system	triclinic
Space group	P-1
a/Å	9.5104(2)
b/Å	13.8626(3)
c/Å	14.6984(2)
$\alpha/^\circ$	88.4724(15)
$\beta/^\circ$	86.0834(15)
$\gamma/^\circ$	70.824(2)
Volume/Å ³	1826.01(6)
Z	2
$\rho_{\text{calc}}/\text{cm}^3$	1.521
μ/mm^{-1}	0.722
F(000)	858.0
Crystal size/mm ³	0.3672 × 0.3351 × 0.131
Radiation	MoK α ($\lambda = 0.71073$)
2 Θ range for data collection/ $^\circ$	5.48 to 59.08
Index ranges	-13 ≤ h ≤ 12, -19 ≤ k ≤ 18, -20 ≤ l ≤ 20
Reflections collected	40501
Independent reflections	9261 [$R_{\text{int}} = 0.0210$, $R_{\text{sigma}} = 0.0188$]
Data/restraints/parameters	9261/0/452
Goodness-of-fit on F ²	1.077
Final R indexes [$I \geq 2\sigma(I)$]	$R_1 = 0.0396$, $wR_2 = 0.1113$
Final R indexes [all data]	$R_1 = 0.0418$, $wR_2 = 0.1129$
Largest diff. peak/hole / e Å ⁻³	2.47/-0.90

Table 6.17: Crystal data and structure refinement for 10.

Identification code	10
Empirical formula	C ₂₅ H ₄₈ BF ₄ O ₄ PRu
Formula weight	631.48
Temperature/K	99.9(2)
Crystal system	orthorhombic
Space group	Pbca
a/Å	9.2302(3)
b/Å	17.0701(4)
c/Å	37.3811(10)
α /°	90.00
β /°	90.00
γ /°	90.00
Volume/Å ³	5889.8(3)
Z	8
ρ_{calc} /cm ³	1.424
μ /mm ⁻¹	0.640
F(000)	2640.0
Crystal size/mm ³	0.7044 × 0.0647 × 0.0498
Radiation	MoK α (λ = 0.71073)
2 Θ range for data collection/°	5.48 to 59.04
Index ranges	-10 ≤ h ≤ 11, -22 ≤ k ≤ 23, -47 ≤ l ≤ 48
Reflections collected	66389
Independent reflections	7652 [R _{int} = 0.0534, R _{sigma} = 0.0334]
Data/restraints/parameters	7652/0/341
Goodness-of-fit on F ²	1.065
Final R indexes [I ≥ 2 σ (I)]	R ₁ = 0.0317, wR ₂ = 0.0664
Final R indexes [all data]	R ₁ = 0.0431, wR ₂ = 0.0725
Largest diff. peak/hole / e Å ⁻³	0.71/-0.58

BIBLIOGRAPHY

CHAPTER 1:

- 1) Reviews on the transition metal catalyzed C-C activation reactions: (a) Murakami, M.; Ito, Y. In *Topics in Organometallic Chemistry* Murai, S. Ed.; Springer: New York, 1999. (b) Rybtchinski, B.; Milstein, D. *Angew. Chem., Int. Ed.* **1999**, *38*, 871-883. (c) Jun, C.-H. *Chem. Soc. Rev.* **2004**, *33*, 610-618; (d) Slagt, V. F.; de Vries, A. H. M.; de Vries, J. G.; Kellogg, R. M. *Org. Process Res. Dev.*, **2010**, *14* (1), 30-47; Chen, F.; Wang, T.; Jiao, N. *Chem. Rev.*, **2014**, *114* (17), 8613-8661

- 2) For catalytic C-N activation reaction: (a) Kuninobu, Y.; Nishi, M.; Takai, K. *Chem. Commun.* **2010**, 8860-8862. (b) Kruger, K.; Tillack, A.; Beller, M. *Chem. Sus. Chem* **2009**, *2*, 715-719. (c) Ueno, S.; Chatani, N.; Kakiuchi, F. *J. Am. Chem. Soc.* **2007**, *129*, 6098-6099. (d) Zou, B.; Jiang, H.-F.; Wang, Z.-Y. *Eur. J. Org. Chem.* **2007**, 4600-4604. (e) Trzeciak, A. M.; Ciunik, Z.; Zioikowski, J. *J. Organometallics* **2002**, *21*, 132-137. (f) Gandelman, M.; Milstein, D. *Chem. Commun.* **2000**, 1603-1604. (g) Hosokawa, T.; Kamiike, T.; Murahashi, S.-I.; Shimada, M.; Sugafuji, T. *Tetrahedron Lett.* **2002**, *43*, 9323-9325. (h) Laine, R. M.; Thomas, D. W.; Cary, L. *J. Am. Chem. Soc.* **1982**, *104*, 1763-1765. (i) Takano, K.; Inagaki, A.; Akita, M. *Chem. Lett.* **2006**, *35*, 434-435. (j) Burling, S.; Mahon, M. F.; Powell, R. E.; Whittlesey, M. K.; Williams, J. M. *J. Am. Chem. Soc.* **2006**, *128*, 13702-13703. (k) Caddick, S.; Cloke, F. G. N.; Hitchcock, P. B.; de K. Lewis, A. K. *Angew. Chem., Int. Ed.* **2004**, *43*, 5824-5827. (l) Katritzky, A. R.; Yao, J.; Bao, W.; Qi, M.; Steel, P. *J. J. Org. Chem.* **1999**, *64*, 346-350; (m) Shen, H.; Xie, Z. *J. Organomet. Chem.* **2009**, 694, 1652-1657; (n) Shen, H.; Wang, Y.; Xie, Z. *Org. Lett.* **2011**, *13*, 4562-4565; (o) Jin, Y. H.; Fang, F.; Zhang, X.; Liu, Q. Z.; Wang, H. B.; Tian, S. K. *J. Org. Chem.* **2011**, *76*, 4163-4167.

- 3) Olah, G. A.; Molnár, A. *Hydrocarbon Chemistry*, 2nd revised ed., Wiley: New York, 2003.

- 4) de Lasa, H.; Salaiques, E.; Mazumder, J.; Lucky, R. *Chem. Rev.* **2011**, *111*, 5404-5433.

- 5) Huber, G. W.; Iborra, S.; Corma, A. *Chem. Rev.* **2006**, *106*, 4044-4098.

- 6) (a) Jun, C.-H.; Park, J.-W. *Top. Organomet. Chem.*, Chatani, N. Ed.; Springer: Berlin, Germany, 2007, 24. (b) Park, Y. J.; Park, J.-W.; Jun, C.-H. *Acc. Chem. Res.* **2008**, *41*, 222-234.
- 7) Periana, R. A.; Bergman R. G. *J. Am. Chem. Soc.* **1984**, *106*, 7272-7273.
- 8) (a) Gozin, M.; Weisman, A.; Ben-David, Y.; Milstein, D. *Nature* **1993**, *364*, 699-701. (b) Rybtchinski, B.; Vigalok, A.; Ben-David, Y.; Milstein, D. *J. Am. Chem. Soc.* **1996**, *118*, 12406-12415.
- 9) Crabtree, R. H.; Dion R. P.; Gibboni, D. J.; McGrath, D. V.; Holt E. M. *J. Am. Chem. Soc.* **1986**, *108*, 7222-7227.
- 10) Bart, S. C.; Chirik, P. J. *J. Am. Chem. Soc.* **2003**, *125*, 886-887.
- 11) Murakami, M.; Amii H.; Shigeto K.; Ito Y. *J. Am. Chem. Soc.* **1996**, *118*, 8285-8290.
- 12) Matsumura, S.; Maeda, Y.; Nishimura, T.; Uemura, S. *J. Am. Chem. Soc.* **2003**, *125*, 8862-8869.
- 13) Nishimura, T.; Uemura, S. *J. Am. Chem. Soc.* **2000**, *122*, 12049-12050.
- 14) (a) Kim, S.; Takeuchi, D.; Osakada, K. *J. Am. Chem. Soc.* **2002**, *124*, 762-763 (b) Murakami, M.; Takahashi, K.; Amii, H.; Ito, Y. *J. Am. Chem. Soc.* **1997**, *119*, 9307-9308.
- 15) Kondo, T.; Kodoi, K.; Nishinaga, E.; Okada, T.; Morisaki, Y.; Watanabe, Y.; Mitsudo, T. *J. Am. Chem. Soc.* **1998**, *120*, 5587-5588.
- 16) Suggs, J. W.; Jun, C.-H. *J. Am. Chem. Soc.* **1984**, *106*, 3054-3056.
- 17) Chatani, N.; Kakiuchi, Y. Ie, F.; Murai, S. *J. Am. Chem. Soc.* **1999**, *121*, 8645-8646.
- 18) (a) Jun, C.-H.; Lee, H. *J. Am. Chem. Soc.* **1999**, *121*, 880-881 (b) Jun, C.-H.; Lee, D.-Y.; Kim, Y.-H.; Lee, H. *Organometallics* **2001**, *20*, 2928-2931. (c) Jun, C.-H.; Lee, H.; Lim, S.-G. *J. Am. Chem. Soc.* **2001**, *123*, 751-752. (d) Jun, C.-H.; Hong, J.-

- B. Org. Lett.* **1999**, *1*, 887-889. (e) Lee, D.-Y.; Kim, I.-J.; Jun, C.-H. *Angew. Chem., Int. Ed.* **2002**, *41*, 3031-3033. (f) Jun, C.-H.; Moon, C. W.; Lim, S.-G.; Lee, H. *Org. Lett.* **2002**, *4*, 1595-1597.
- 19) Li H.; Li Y.; Zhang X.; Chen K.; Wang X.; Shi Z. *J. Am. Chem. Soc.* **2011**, *133*, 15244-15247
- 20) (a) Murakami, M.; Itahashi, T.; Ito, Y. *J. Am. Chem. Soc.* **2002**, *124*, 13976-13977. (b) Matsuda, T.; Fujimoto, A.; Ishibashi, M.; Murakami, M. *Chem. Lett.* **2004**, *33*, 876-877
- 21) Murakami, M.; Ashida, S.; Matsuda, T. *J. Am. Chem. Soc.* **2005**, *127*, 6932-6933
- 22) (a) He, C.; Guo, S.; Huang, L.; Lei, A. *J. Am. Chem. Soc.* **2010**, *132*, 8273-8275. (b) Chen, K.; Li, H.; Li, Y.; Zhang, X.-S.; Lei, Z.-Q.; Shi, Z.-J. *Chem. Sci.* **2012**, *3*, 1645-1649. (d) Tobisu M.; Kinuta, H.; Kita, Y.; Rémond, E.; Chatani, N. *J. Am. Chem. Soc.* **2012**, *134*, 115-118.
- 23) a) Weaver, J. D.; Recio, III, A.; Grenning, A. J.; Tunge, J. A. *Chem. Rev.* **2011**, *111*, 1846-1913. (b) Wang, C.; Piel, I.; Glorius, F. *J. Am. Chem. Soc.* **2009**, *131*, 4194-4195. (c) Wang, C.; Rakshit, S.; Glorius, F. *J. Am. Chem. Soc.* **2010**, *132*, 14006-14008.
- 24) (a) Jones, W. D. *Nature* **1993**, *364*, 676-677. (b) Goldman, A. S. *Nature* **2010**, *463*, 435-436.
- 25) Hartwig, J. *Organotransition Metal Chemistry from Bonding to Catalysis*, University Science Books: Sausalito, CA, 2010, pp. 289-292.
- 26) For Hydrodenitrogenation in heterogeneous phase (a) Lia, S.; Leea, J. S.; Hyeon, T.; Suslick, K. S. *Applied Catalysis A: General.* **1999**, *184* 1-9 (b) Furimsky, E.; Massoth, F. E. *Cat. Rev. : Sci. and Eng.* **2005**, *47:3*, 297-489 (c) Nagai, M.; Masunaga, T.; Hana-oka, N. *Energy & Fuels* **1988**, *5*, 645-651 (d) Egorova, M.; Prins, R. *Fuel Chemistry Division Preprints* **2003**, *48*, 34 (e) Gong, J. *Chem. Rev.* **2012**, *112*, 2987-3054 (f) Suresh, C.; Santharaj, D.; Gurulakshmi, M.; Deepa, G.; Selvaraj, M.; Rekha, N. R. S; Shanthi, K. *ACS Catal.* **2012**, *2*, 127-134 (g) Nagai, M.; Masunaga, T.; Hana-oka, N. *Energy & Fuels* **1988**, *2*, 645-651.
- 27) For Hydrodenitrogenation in homogeneous phase (a) Weller, K. J.; Fox, P. A.; Grays, S. D.; Wigley, D. E. *Polyhedron.* **1997**, *16*, 3139-3163 (b) Valencia, D.;

- Klimova, T.; García-Cruz, I. *Fuel* **2012**, *100*, 177-185 (c) Kleckley, T. S.; Bennett, J. L.; Wolczanski, P. T.; Lobkovsky, E. B. *J. Am. Chem. Soc.* **1997**, *119*, 247-248 (d) Gray S. D.; Weller, K. J.; Bruck, M. A.; Briggs, P. M.; Wigley, D. E. *J. Am. Chem. Soc.* **1995**, *117*, 10678-10693, (e) Zhu, G.; Tanski, J. M.; Churchill, D. G; Janak, K. E.; Parkin, G. *J. Am. Chem. Soc.* **2002**, *124*, 13658-13659 (f) Sattler, A.; Zhu, G.; Parkin, G. *J. Am. Chem. Soc.* **2009**, *131*, 7828-7838, (g) Bianchini, C.; Meli, A.; Vizza, F. *Eur. J. Chem.* **2001**, 43-68.
- 28) Ho, T. C. *Catal. Rev.-Sci. Engng.* **1988**, *30*, 117-160.
- 29) (a) Harvey, T. G; Matheson, T. W. *J. Catal.* **1986**, *101*, 253-261. (b) de Los Reyes, J. A.; Vrinat, M.; Geantet, C. and Breyse, M. *Catal. Today* **1991**, *10*, 645-664.
- 30) Spies, G. H. and Angelici, R. J. *Organometallics* **1987**, *6*, 1897-1903.
- 31) Bonanno, J. B.; Henry, T. P; Neithamer, D. R; Wolczanski, P. T.; Lobkovsky, E. B. *J. Am. Chem. Soc.* **1996**, *118*, 5132-5133.
- 32) Shen, H.; Lu X.; Jiang, K-Z.; Yang K-F.; Lu, Y.; Zheng, Z-J.; Lai G.-Q.; Xu, Li-W. *Tetrahedron* **2012**, *68*, 8916-8923.
- 33) (a) Chan, Y. W.; Renner, M.W.; Balch, A. L. *Organometallics* **1983**, *2*, 1888-1889 (b) Chan, P. Y. W.; Wood, F. E.; Renner, M. W.; Hope, H.; Balch, A. L. *J. Am. Chem. Soc.* **1984**, *106*, 3380-3381 (c) Balch, A. L.; Wai, Y.; Chan, Olmstead M. M.; Renner, M. W.; Wood, F. E. *J. Am. Chem. Soc.* **1988**, *110*, 3897-3902
- 34) (a) Lei, Y.; Wroblewski, A.D.; Golden, J.E.; Powell, D.R.; Aubé, J. *J. Am. Chem. Soc.* **2005**, *127*, 4552-4553, (b) Jones, W.D. *Organometallics* **1986**, *5*, 1823-1829 (c) Calafat, A.M.; MarzilliInorg, L.G. *Chem. Commun.* **1993**, *32*, 2906-2911 (d) Yamamoto, Y. ; Seta, J; Murooka, H.; HanInorg, X.H. *Chem. Commun.* **2003**, *6*, 202-205 (e) Ardura, D.; López, R.; Sordo, T.L. *J. Org. Chem.* **2006**, *71*, 7315-7321
- 35) (a) Chung, K.H.; Kim, J.N.; Ryu, E.K. *Tetrahedron Lett.* **1994**, *35*, 2913-2914 (b) Seong, M.R.; Lee, H.J.; Kim, J.N. *Tetrahedron Lett.* **1998**, *39*, 6219-6222 (c) Lee H.J.; Seong, M.R.; Kim, J.N. *Tetrahedron Lett.* **1998**, *39*, 6223-6226 (d) Liu C.-R.; Li M.-B.; Cheng, D.-J.; Yang, C.-F.; Tian, S.-K. *Org. Lett.* **2009**, *11*, 2543-2545 (e) He, Q.-L.; Sun F.-L.; Zheng, X.-J.; You, S.-L. *Synlett.* **2009**, 1111-1114 (f) Yang B.-L.; Tian S.-K. *Chem. Commun.* **2010**, 6180-6182.

- 36) (a) Stamm, H.; Onistschenko, A.; Buchholz, B.; Mall T. *J. Org. Chem.* **1989**, *54*, 193-199 (b) Esquivias, J.; Gómez-Arrayás, R.; Carretero, J.C. *Angew. Chem., Int. Ed.* **2006**, *45*, 629-633 (c) Alonso, I.; Esquivias, J.; Gómez-Arrayás, R.; Carretero, J.C. *J. Org. Chem.* **2008**, *73*, 6401-6404 (d) Liu, C.-R.; Li, M.-B.; Yang, C.-F.; Tian, S.-K. *Chem.-Eur. J.* **2009**, *15*, 793-797 (e) Liu, C.-R.; Yang, F.-L.; Jin, Y.-Z.; Ma, X.-T.; Cheng, D.-J.; Li N.; Tian, S.-K. *Org. Lett.*, **2010**, *12*, 3832-3835 (f) Jiang, Z.-Y.; Zhang, C.-H.; Gu, F.-L.; Yang, K.-F.; Lai G.-Q.; Xu, L.-W.; Xia, C.-G. *Synlett.* **2010**, 1251-1254 (g) Yang, C.F.; Wang, J.Y.; Tian, S.K. *Chem. Commun.* **2011**, 8343-8345
- 37) Zhao, X.; Liu D.; Guo, H; Liu, Y.; Zhang, W. *J. Am. Chem. Soc.* **2011**, *133*, 19354-19357
- 38) (a) Hirao, T.; Yamada, N.; Ohshiro, Y.; Agawa, T. *J. Organomet. Chem.* **1982**, *236*, 409-414. (b) Yamamoto, T.; Akimoto, M.; Saito, O.; Yamamoto, A. *Organometallics* **1986**, *5*, 1559-1567.
- 39) (a) Dubovyk, I.; Pichugin, D.; Yudin, A. K. *Angew. Chem., Int. Ed.* **2011**, *50*, 5924-5926 (b) Lowe, M. A.; Ostovar, M.; Ferrini, S.; Chen, C. C.; Lawrence, P. G.; Fontana, F.; Calabrese, A. A.; Aggarwal, V. K. *Angew. Chem., Int. Ed.* **2011**, *50*, 6370-6374.
- 40) Li, M.-B; Wang, Y.; Tian, S,-K. *Angew. Chem. Int. Ed.* **2012**, *51*, 2968-2971.
- 41) Trost, B. M. ; Osipov, M.; Dong G. *J. Am. Chem. Soc.*, **2010**, *132* (44), 15800-15807
- 42) Dubovyk, I; Pichugin, D.; Yudin, A. -K. *Angew. Chem. Int. Ed.* **2011**, *50*, 5924-5926.
- 43) Koreeda, T; Kochi, T; Kakiuchi, F. *J. Am. Chem. Soc.* **2009**, *131*, 7238-7239.
- 44) Blakey, S. -B; MacMillan, D. W. C. *J. Am. Chem. Soc.* **2003**, *125*, 6046-6047.
- 45) Liu, C.-R., Li M.-B.; Cheng, D.J.; Yang, C. F; Tian, S. -K. *Org. Lett.* **2009**, *11*, 2543-2545.
- 46) Weng, Z. -T; Li Y., Tian S. K., *J. Org. Chem.* **2011**, *76*, 8095-8099.

- 47) Liu, C. -R; Fu-Lai F. -L.; Jin, Y.-Z.; Ma, X. -T; Cheng, D. J; Li N; Tian, S.-K. *Org. Lett.* **2010**, *12*, 3832-3835.
- 48) Li, B. J; Wang, H. -Y; Zhu, Q.-L.; Shi, Z.-J, *Angew. Chem. Int. Ed.* **2012**, *51*, 3948 - 3952.
- 49) Cheng, C.; Sun, J.; Xing, L.; Xu J.; Wang, X.; Hu, Y. *J. Org. Chem.* **2009**, *74*, 5671-5674.
- 50) Lei, Y; Wroblewski, A.D; Golden, J. E; Powell, D. R; Aube, J. *J. Am. Chem. Soc.* **2005**, *127*, 4552-4553.
- 51) Horton, H. R.; Moran, L. A.; Scrimgeour, K. G.; Perry, M. D.; Rawn J. D., *Principles of Biochemistry*, 2006, Pearson Education, Inc., New Jersey.
- 52) (a) Turner. N. *J. Chem. Rev.* **2011**, *111*, 4073-4087 (b) Steiner, R. A.; Kalk, K. H.; Dijkstra, B. W. *PNAS* **2002**, *99*, 16625-16630 (c) Al-Mjeni, F.; Ju, T.; Pochapsky, T.C.; Maroney, M. J. *Biochemistry* **2002**, *41*, 6761-6769 (d) Johnson-Winters, K.; Purpero, V. M.; Kavana, M.; Nelson, T.; Moran, G. R. *Biochemistry* **2003**, *42*, 2072-2080 (e) de Villiers, M.; Veetil, V. P.; Raj H.; de Villiers, J.; Poelarends, G. J. *ACS Chem. Biol.* **2012**, *7*, 618-1628 (f) Paine, T.K.; Zheng, H.; Que, L. *Inorg. Chem.* **2005**, *44*, 474-476 (g) Straganz, G.D.; Nidetzky, B., *J. Am. Chem. Soc.* **2005**, *127*, 12306-12314 (h) Straganz, G. D.; Hofer H.; Steiner, W.; Nidetzky, B. *J. Am. Chem. Soc.* **2004**, *126*, 12202-12203 (i) Sedgwick, B. *Nature Rev. Molecular Cell Biol.* **2004**, *5*, 148-157.
- 53) Karki, S. B.; Dinnocenzo, J. P; Jones J. P; Korzekwag, K. R. *J. Am. Chem. Soc.*, **1995**, *117*, 3657-3664
- 54) Chiavarino, B.; Cipollini, R.; Crestoni, M. E.; Fornarini, S.; Lanucara, F.; Lapi, A. *J. Am. Chem. Soc.* **2008**, *130*, 3208-3217
- 55) Lee, D. -H; Lippard, S. J. *J. Am. Chem. Soc.* **2001**, *123*, 4611-4612
- 56) Yi, C.; Yang, C-G.; He, C. *Acc. Chem. Res.* **2009**, *42*, 4, 519-529
- 57) Koskinen, M; Hemminki, K. *Org. Lett.* **1999**, *1* (8), 1233-1235

- 58) S.; Raushel, F. L. *Biochemistry* **2010**, *49*, 4374-4382
- 59) Kamat, S. S.; Fan, H.; Sauder, J. M.; Burley, S. K.; Shoichet, B. K.; Sali, A.; Raushel, F. M. *J. Am. Chem. Soc.* **2011**, *133*, 2080-2083
- 60) Hitchcock, D.; Fwdorov, A. A.; Fedorov, E. V.; Dangott, L. J.; Almo, S. C.; Raushel, F. M. *Biochemistry* **2011**, *50*, 5555-5557.
- 61) Goble, A. M.; Zhang, Z.; Sauder, J. M.; Burley, S. K.; Swaminathan, S.; Raushel, F. M. *Biochemistry* **2011**, *50*, 6589-6597.

CHAPTER 2:

- 1) Clemmensen, E. *Chem. Ber.* **1914**, *47*, 51, 681-687. (b) Vedejs, E. *Org. React.* **1975**, *22*, 401-422.
- 2) Kishner, J. *J. Russ. Phys. Chem. Soc.* **1911**, *43*, 582-595. (b) Wolff, C. *Liebigs Ann.* **1912**, *394*, 86-108. (c) Todd, D. *Org. React.* **1948**, *4*, 378-422. (d) Minlon, H. *J. Am. Chem. Soc.* **1949**, *71*, 3301-3303.
- 3) Gates M.;Tschudi, G., *J. Org. Chem.* **1956**, *78*, 1380-1393.
- 4) Marino, J. P.; Rubio, M. B.; Cao, G.; De Dios, A. , *J. Am. Chem. Soc.* **2002**, *124* (45), 13398-13399
- 5) Kawano, M.; Kiuchi, T.; Negishi, S.; Tanaka, H.; Hoshikawa, T.; Matsuo, J. I.; Ishibashi, H., *Angew. Chem. Int. Ed.* **2013**, *52* (3), 906-910.
- 6) Miyaoka, H.; Kajiwara, Y.; Hara, Y.; Yamada, Y., *J. Org. Chem.* **2001**, *66* (4), 1429-1435.
- 7) (a) Huang-Minlon, *J. Am. Chem. Soc.* **1946**, *68*(12), 2487-2488 (b) Huang-Minlon, *J. Am. Chem. Soc.* **1949**, *71* (10), 3301-3303.
- 8) Cram, D. J.; Sahyun, M. R. V., *J. Am. Chem. Soc.* **1962**, *84* (9): 1734-1735.

- 9) Caglioti, L.; Magi, M., *Tetrahedron* 1963, 19 (7): 1127; Caglioti, L., *Tetrahedron* **1966**, 22 (2), 487-493.
- 10) Furrow, M. E.; Myers, A. G. , *J. Am. Chem. Soc.* **2004**, 126 (17), 5436-5445
- 11) Zhou, L.; Liu, Z.; Liu, Y.; Zhang, Y.; Wang, J., *Tetrahedron* **2013**, 69,6083-6087
- 12) Yamamura, S.; Toda, M.; Hirata, Y., *Org. Synth.* **1988**, 6, 289 ; Yamamura, S.; Toda, M.; Hirata, Y., *Org. Synth.* **1973**, 53, 86 .
- 13) (a) Xu, S.; Toyama, T.; Nakamura, J.; Arimoto, H., *Tetrahedron Lett.* **2010**, 4534-4537; (b) Godinez, C. E.; Zepeda, G.; Mortko, C. J.; Dang, H.; G.-Garibay M. A., *J. Org. Chem.* **2004**, 69 (5), 1652-1662; (c) Génisson, Y.; Tyler, P. C.; Ball, R. G.; Young, R. N., *J. Am. Chem. Soc.* **2001**, 123, 11381-11387; (d) Pakush, J.; Rùchardt, C. *Chem. Ber.* **1990**, 123, 2147-2151 (e) Meyer, K. H. *Org.Syn.*, Coll.Vol.1, 1941, 60-61
- 14) Ishimoto, K.; Mitoma, Y.; Nagashima, S.; Tashiro, H.; Prakash, G. K. S.; Olah G. A.; Tashiro M., *Chem. Comm.* **2003**, 514-515.
- 15) Zieger, H.E.; Dixon, J.A., *J. Am. Chem. Soc.* **1960**, 82 (14), 3702-3705.
- 16) J. J.; Eisch, Liu, Z.-R.; Boleslawski M. P., *J. Org. Chem.* **1992**, 57, 2143-2141.
- 17) silane articles (a) Gevorgyan, V.; Rubin, M.; Liu, J.-X.; Yamamoto, Y., *J. Org. Chem.* **2001**, 66, 1672-1675 (b) Chandrasekhar , S.; Reddy , Ch. R.; Babu, B. N., *J. Org. Chem.* **2002**, 67, 9080-9082
- 18) Dal Zotto C., Virieux D., Campagne J.-M. , *Synlett.* **2009**, 2, 0276-0278.;
- 19) Surya-Prakash, G. K.; Do, C.; Mathew, T.; Olah, G.A, *Catal. Lett.* **2011**, 141, 507-511.
- 20) Fagan P.J.; Voges M.H.; Bullock R.M., *Organometallics* **2010**, 29, 1045-1048
- 21) Rahaim, R. J., Jr.; Maleczka, R. E., Jr., *Org. Lett.* **2011**,13,4,584-587

- 22) Deoxygenation of ester: (a) Baldwin, S. W.; Haut, S. A. *J. Org. Chem.* **1975**, *40* (26), 3885-3887; b) Lam, K.; Markó I. E., *Org. Lett.* **2008**, *10*, 2919-2922; c) Sakai, N.; Moriya T.; Konakahara, T., *J. Org. Chem.* **2007**, *72*, 5920-5922
- 23) Deoxygenation Amide: Sakai N.; Fujii, K.; Konakahara, T., *Tetrahedron Lett.* **2008**, *49*, 6873-6875. b) Igarashi M.; Fuchikami, T., *Tetrahedron Lett.* **2001**, *42*, 1945-1947., (c) Kuwano, R.; Takahashi, M.; Ito, Y., *Tetrahedron Lett.* **1998**, *39*, 1017-1020.
- 24) **Deoxygenation of carboxylic acid:** a) Das, S.; Addis, D.; Zhou, S.; Junge, K.; Beller, M., *J. Am. Chem. Soc.* **2010**, *132*, 1770-1771; (b) Hanada, S.; Yuasa, A.; Kuroiwa, H.; Motoyama, Y.; Nagashima, H.; *Eur. J. Org. Chem.* **2010**, 1021-1025 (c) Sunada, Y.; Kawakami, H.; Imaoka, T.; Motoyama, Y.; Nagashima, H., *Angew. Chem. Int. Ed.* **2009**, *48*, 9511-9514; (d) Inagaki, T.; Yamada, Y.; Phong, L. T.; Furuta, A.; Ito, J.-I.; Nishiyama, H., *Synlett* **2009**, 253-256 (e) Hanada, S.; Motoyama, Y.; Nagashima, H., *Eur. J. Org. Chem.* **2008**, 4097-4100. (f) Sassaman, M. B.; Kotian, K. D.; Prakash, G. K. S.; Olah, G. A., *J. Org. Chem.* **1987**, *52*, 4314-4319. (g) Yadav, J. S.; Antony, A.; George, J.; Subba Reddy, B. V., *Eur. J. Org. Chem.* **2010**, 591-605. (h) Augé, J.; Lubin-Germain, N.; Uziel, J., *Synthesis* **2007**, 1739-1764.
- 25) Moriya, T.; Yoneda, S.; Kawana, K.; Ikeda, R.; Konakahara, T.; Sakai, N., *J. Org. Chem.* **2013**, *78*, 10642-10650
- 26) (a) Grey, R. A.; Pez, G. P.; Wallo, A. *J. Am. Chem. Soc.* **1981**, *103*, 7536. (b) Matteoli, U.; Menchi, G.; Bianchi, M.; Piacenti, F. *J. Mol. Catal.* **1988**, *44*, 347. (c) Hara, Y.; Inagaki, H.; Nishimura, S.; Wada, K. *Chem. Lett.* **1992**, *21*, 1983. (d) T. Teunissen, H. *Chem. Commun.* 1998, 1367. (e) van Engelen, M. C.; Teunissen, H. T.; de Vries, J. G.; Elsevier, C. J. *J. Mol. Catal. A: Chem.* **2003**, *206*, 185.
- 27) (a) Zhang, J.; Leitus, G.; Ben-David, Y.; Milstein, D. *Angew. Chem., Int. Ed.* **2006**, *45*, 1113. (b) Balaraman, E.; Gunanathan, C.; Zhang, J.; Shimon, L. J. W.; Milstein, D. *Nat. Chem.* **2011**, *3*, 609. (c) Fogler, E.; Balaraman, E.; Ben-David, Y.; Leitus, G.; Shimon, L. J. W.; Milstein, D. *Organometallics* **2011**, *30*, 3826. (d) Gunanathan, C.; Milstein, D. *Acc. Chem. Res.* **2011**, *44*, 588. (e) Fogler, E.; Garg, J. A.; Hu, P.; Leitus, G.; Shimon, L. J. W.; Milstein, D. *Chem. Eur. J.* **2014**, *20*, 15727.
- 28) (a) Saudan, L. A.; Saudan, C. M.; Debieux, C.; Wyss, P. *Angew. Chem., Int. Ed.* **2007**, *46*, 7473. (b) Saudan, L.; Dupau, P.; Riedhauser, J.-J.; Wyss, P.; Firmenich S. A. Swiss Patent WO2006106483A1, **2006**; p 40. (c) Saudan, L.; Dupau, P.; Riedhauser, J.-J.; Wyss, P.; Firmenich S. A. Swiss Patent WO2006106484A1, **2006**; p 29. (d) Saudan, C.; Saudan, L.; Firmenich S. A. Swiss Patent WO2010061350A1, **2010**; p 55.

- 29) (a) Kuriyama, W.; Ino, Y.; Ogata, O.; Sayo, N.; Saito, T. *Adv. Synth. Catal.* **2010**, 352, 92. (b) Ino, Y.; Kuriyama, W.; Ogata, O.; Matsumoto, T. *Top. Catal.* **2010**, 53, 1019. (c) Kuriyama, W.; Matsumoto, T.; Ino, Y.; Ogata, O. Takasago International Corporation, Japan. Patent WO2011048727A1, **2011**; p 62. (d) Kuriyama, W.; Matsumoto, T.; Ogata, O.; Ino, Y.; Aoki, K.; Tanaka, S.; Ishida, K.; Kobayashi, T.; Sayo, N.; Saito, T. *Org. Process Res. Dev.* **2012**, 16, 166.
- 30) (a) Acosta-Ramirez, A.; Bertoli, M.; Gusev, D. G.; Schlaf, M. *Green Chem.* **2012**, 14, 1178. (b) Spasyuk, D.; Smith, S.; Gusev, D. G. *Angew. Chem., Int. Ed.* **2012**, 51, 2772. (c) Spasyuk, D.; Gusev, D. G. *Organometallics* **2012**, 31, 5239. (d) Spasyuk, D.; Smith, S.; Gusev, D. G. *Angew. Chem., Int. Ed.* **2013**, 52, 2538.
- 31) (a) W. W. N, O.; Lough, A. J.; Morris, R. H. *Chem. Commun.* **2010**, 46, 8240. (b) Ito, M.; Ootsuka, T.; Watari, R.; Shiibashi, A.; Himizu, A.; Ikariya, T. *J. Am. Chem. Soc.* **2011**, 133, 4240. (c) Touge, T.; Hakamata, T.; Nara, H.; Kobayashi, T.; Sayo, N.; Saito, T.; Kayaki, Y.; Ikariya, T. *J. Am. Chem. Soc.* **2011**, 133, 14960. (d) Junge, K.; Wendt, B.; Westerhaus, F. A.; Spannenberg, A.; Jiao, H.; Beller, M. *Chem. Eur. J.* **2012**, 18, 9011. (e) Otsuka, T.; Ishii, A.; Dub, P. A.; Ikariya, T. *J. Am. Chem. Soc.* **2013**, 135, 9600. (f) Chakraborty, S.; Dai, H.; Bhattacharya, P.; Fairweather, N. T.; Gibson, M. S.; Krause, J. A.; Guan, H. *J. Am. Chem. Soc.* **2014**, 136, 7869.
- 32) Tan, X.; Wang, Y.; Liu, Y.; Wang, F.; Shi, L.; Lee, K.-H.; Lin, Z.; Lv, H.; Zhang, X., *Org. Lett.* **2015**, 17, 454-457.
- 33) (a) Brown, H.C.; Helm, P. *J. Org. Chem.* **1973**, 38, 912-914. (b) Prasa, A.S.B.; Kanth, J.V.B.; Periasamy, M. *Tetrahedron*, **1992**, 48, 4623-4627 (c) Giannis, A.; Sandoff, K. *Angew. Chem. Int. Ed. Engl.*, **1989**, 28, 218-220 (d) Akabori, S.; Takanohashi, Y. *J. Chem. Soc.; Perkin Trans 1*, **1991**, 479-482 (e) Wann, S.R.; Thorsen, P.T.; Kreevoy, M.M. *J. Org. Chem.* **1981**, 46, 2579-2581 (f) Kabno, S.; Tanaka, Y.; Sugino, E.; Hibino, S. *Synthesis* **1980**, 695.
- 34) Narasimhan, S.; Madhavan, S.; Balakumar, R.; Swarnalakshmi, S. *Synth. Commun.* **1997**, 27, 391-394.
- 35) Chakraborty, S.; Dai, H.; Bhattacharya, P.; Fairweather, N. T.; Gibson, M. S.; Krause, J. A.; Guan, H., *J. Am. Chem. Soc.* **2014**, 136, 7869-7872.
- 36) Das, S.; Addis, D.; Zhou, S.; Junge, K., Beller, M., *J. Am. Chem. Soc.* **2010**, 132, 1770-1771.

- 37) Mikami, Y.; Noujima, A.; Mitsudome, T.; Mizugaki, T.; Jitsukawa, K.; Kaneda, K., *Chem. Eur. J.*, **2011**, 17, 1768.
- 38) Cheng, C.; Brookhart, M., *J. Am. Chem. Soc.* **2012**, 134, 11304-11307
- 39) (a) Furimsky, E., *Appl. Catal. A*. **2000**, 199, 147-190 .b) Zakzeski, J.; Bruijninx, P. C. A.; Jongorius, A. L; Weckhuysen, B. M., *Chem. Rev.* **2010**, 110, 3552-3599 c). Huber, G. W.; Iborra, S.; Corma, A., *Chem. Rev.* **2006**, 106, 4044-4098 d) Marshall, A. L.; Alaimo, P. J., *Chem. Eur. J.* **2010**, 16, 4970-4980 e) Pu, Y.; Zhang, D.; Singh, P. M.; Ragauskas, A. J., *Biofuels Bioprod. Bioref.* **2008**, 2, 58-73.
- 40) Maercker, A., *Angew. Chem. Int. Ed. Engl.* **1987**, 26, 972-989.
- 41) van der Boom, M.E., Liou, S., Ben-David, Y., Shimon, L.J.W., Milstein, D., *J. Am. Chem. Soc.*, **1998**, 120,6531-6541.
- 42) Dyson, P. J., *Dalton Trans.* **2003**, 2964-2974.
- 43) a) Wenkert, E.; Michelotti, E. L.; Swindell, C. S., *J. Am. Chem. Soc.* **1979**. 101, 2246-2247. b). Wenkert, E.; Michelotti, E. L.; Swindell, C. S.; Tingoli, M., *J. Org. Chem.* **1984**, 49, 4894-4899. c). Dankwardt, J. W., *Angew. Chem. Int. Ed.* **2004**, 43, 2428-2432. d) Guan B.T.; Xiang S.K.; Wu T.; Sun Z.P.; Wang B.Q.; Zhao K.Q.; Shi Z.J., *Chem. Commun. (Camb.)* **2008**, 12, 1437-1439. e) Tobisu, M.; Shimasaki, T.; Chatani, N., *Angew. Chem. Int. Ed.* **2008**, 47, 4866-4869.
- 44) Widegren, J. A.; Finke, R. G., *J. Mol. Catal. A* **2003**, 198, 317-341.
- 45) Tobisu, M.; Shimasaki, T.; Chatani N., *Chem. Lett*, **2009**, 38, 7, 710-711.
- 46) He, L.; Wang, Q.; Zhou, G.-C.; Guo, L.; Yu X.-Q., *Arkivoc*, **2008**, 103-108
- 47) Nichols, J. M.; Bishop, L. M.; Bergman, R. G.; Ellman, J. A., *J. Am. Chem. Soc.*, **2010**, 132 (36), 12554-12555
- 48) Sergeev A. G.; Hartwig, J. F., *Science* **2011**, 332, 439.
- 49) Sergeev, A.G.; Webb, J.D.; Hartwig, J.F., *J. Am. Chem. Soc.* **2012**, 134, 20226–20229

- 50) Hanson, S.K.; Wu, R.; Louis, A., *Angew. Chem. Int. Ed.* **2012**, 51, 3410-3413
- 51) Rao, H.; Li, C.-J. *Angew. Chem. Int. Ed.* **2011**, 50, 8936-8939
- 52) a) Elliott, M. C., *J. Chem. Soc.-Perkin Trans. I* **1998**, 4175-4200. (b) Elliott, M. C.; Williams, E., *J. Chem. Soc., Perkin Trans. I* **2001**, 2303-2340. (c) Buckingham, J. *Dictionary of Natural Products*; University Press: Cambridge, MA, 1994 (d) Hiroki F.; Yuki H.; Yuji M., *Org. Lett.* **2009**, 11, 4382
- 53) Williamson, W. A., *J. Chem. Soc.* **1852**, 4, 229-239.
- 54) (a) Baggett, N. In *Comprehensive Organic Chemistry*; Stoddart, J. F., Ed.; Pergamon Press: New York, 1979, Vol. 1, pp 799-850. (b) Feuer, H.; Hooz, J. In *The Chemistry of Ether Linkage*; Patai, S., Ed.; Interscience Publishers: London, UK, 1967; pp 445-449 and 460-468.
- 55) (a) Mitsunobu, O.; Yamada, M. *Bull. Chem. Soc. Jpn.* **1967**, 40, 2380-2382 (b) Mitsunobu, O. *Synthesis*. **1981**, 1-28.
- 56) Shi Y. J.; Hughes, D. L.; McNamara, J. M. *Tetrahedron Lett.* **2003**, 44, 3609-3611.
- 57) Kashman Y. *J. Org. Chem.* **1972**, 37, 912-914.
- 58) (a) Kato, J.-I.; Iwasawa, N.; Mukaiyama, T., *Chem. Lett.* **1985**, 743-746. b) Sassaman, M. B.; Kotian, K. D.; Prakash, G. K. S.; Olah, G. A. *J. Org. Chem.* **1987**, 52, 4314-4319. c) Hatakeyama, S.; Mori, H.; Kitano, K.; Yamada, H.; Nishizawa, M., *Tetrahedron Lett.* **1994**, 35, 4367-4370. d) Komatsu, N.; Ishida, J.; Suzuki, H., *Tetrahedron Lett.* **1997**, 38, 7219-7222. e) Bajwa, J. S.; Jiang, X.; Slade, J.; Prasad, K.; Repic, O.; Blacklock, T. J., *Tetrahedron Lett.* **2002**, 43, 6709-6713. f) Yang, W.-C.; Lu, X.-A.; Kulkarni, S. S.; Hung, S.-C., *Tetrahedron Lett.* **2003**, 44, 7837-7840. g) Chandrasekhar, S.; Chandrashekar, G.; Babu, B. N.; Vijeender, K.; Reddy K. V., *Tetrahedron Lett.* **2004**, 45, 5497-5499.
- 59) Ullmann, F. *Ber. Dtsch. Chem. Ges.* **1903**, 36, 2389-2391; Hassan, J.; Sévignon, M.; Gozzi, C.; Schulz, E. *et al. Chem. Rev.* **2002**, 102, 1359-1470; Beletskaya, I. P.; Cheprakov, A. V. *Coord. Chem. Rev.* **2004**, 248, 2337-2364; Monnier, F.; Taillefer, M. *Angew. Chem. Int. Ed.* **2008**, 47, 3096-3099; Monnier, F.; Taillefer, M. *Angew. Chem. Int. Ed.* **2009**, 48, 6954-6971; Evano, G.; Blanchard, N.; Toumi, M. *Chem. Rev.* **2008**, 108, 3054-3131

- 60) Gulevskaya, A. V.; Pozharskii, A. F. In *Advances in Heterocyclic Chemistry, Vol 93* **2007**; Vol. 93, p 57-115. (9) Buncel, E.; Dust, J. M.; Terrier, F. *Chem. Rev.* **1995**, *95*, 2261-2280. (10) Bunnett, J. F.; Zahler, R. E. *Chem. Rev.* **1951**, *49*, 273-412. (b) hersulettone B synthesis *Org. Lett.*, **2011**, *13* (23), 6268-6271
- 61) Boger, D. L.; Patane, M. A.; Zhou, J. C. *J. Am. Chem. Soc.* **1994**, *116*, 8544-8556.
- 62) Altman, R. A.; Shafir, A.; Lichtor, P. A.; Buchwald, S. L., *J. Org. Chem.* **2008**, *73*, 284-286.
- 63) Zhang, Q.; Wang, D.; Wang, X.; Ding, K., *J. Org. Chem.*, **2009**, *74*, 7187-7190.
- 64) Liu, Y.; Jua, R.; Sun H. B.; Qiu, X. *Organometallic*, **2005**, *24*, 2819-2821.
- 65) Sakai, N., Hirasawa, M, Konakahara, T. *Tetrahedron Lett.* **2005**, *46*, 6407-6410, Sakai, N., Moriay, T., Konakahra, T. *J. Org. Chem.*, **2007**, *72*, 5920-5922.
- 66) Prades, A.; Corberan, R.; Poyatos, M.; Peris, E. *Eurpoean J. Chem.*, **2008**, *14*, 11474-11479.
- 67) (a) Davies, T. E.; Kean, J. R.; Apperley, D. C.; Taylor, S. H.; Graham, A. E., *ACS Sustainable Chem. Eng.* **2014**, *2*, 860-866. (b) Sharma, G. V. M; Mahalingam, A. K., *J. Org. Chem.* **1999**, *64*, 8943-8944.
- 68) Uenishi, J.; Ohmi, M.; Ueda, A. *Tetrahedron: Asymmetry*, **2005**, *16*, 1299-1303.
- 69) Kim, J.; Lee, D.-H.; Kalutharage, N.; Yi, C. S., *ACS Catal.* **2014**, *4* (11), 3881-3885.
- 70) Brase, S.; de Meijere, A. In *Metal-catalyzed Cross-coupling Reactions*; Diederich, F. and Stang, P. J., Ed.; Wiley-VCH: Weinheim, Germany, 1998, pp 99-166 and references therein
- 71) Tietze, L. F.; Ila, H.; Bell, H. P. *Chem. Rev.* **2004**, *104*, 3453-3516.
- 72) Uenishi, J.; Ohmi, M. *Angew. Chem.-Int. Ed.* **2005**, *44*, 2756-2760.
- 73) Takacs, J. M.; Jiang, X. T. *Curr. Org. Chem.* **2003**, *7*, 369-396.

- 74) (a) Trost, B. M.; Toste, F. D. *J. Am. Chem. Soc.* **1999**, 121, 4545-4554. (b) Muci, A. R.; Buchwald, S. L. *Top. Curr. Chem.* **2002**, 219, 131-209. (c) López, F.; Ohmura, T.; Hartwig, J. F. *J. Am. Chem. Soc.* **2003**, 125, 3426-3427. (d) Beletskaya, I. P.; Cheprakov, A. V. *Coord. Chem. Rev.* **2004**, 248, 2337-2364. (e) Onitsuka, K.; Okuda, H.; Sasai, H. *Angew. Chem., Int. Ed.* **2008**, 47, 1454-1457.
- 75) Smith, M. B.; March, J. *March's Advanced Organic Chemistry*, 5th ed.; Wiley: New York, 2001; p 996.
- 76) (a) Ronchin, L.; Quartarone, G.; Vavasori, A. *J. Mol. Catal. A: Chem.* **2012**, 353, 192-203. (b) Ronchin, L.; Vavasori, A.; Toniolo, L. *J. Mol. Catal. A: Chem.* **2012**, 355, 134-141.
- 77) Sevov, C.S.; Hartwig, J.F. *J. Am. Chem. Soc.* **2013**, 135, 9303-9306.
- 78) Yu, J. L.; Wang, H.; Zhang, J. R.; Gao, X.; Zhang, D. W. *Tetrahedron*, **2013**, 69, 310-315.
- 79) Wada, M.; Nagayama, S.; Mizutani, K.; Hiroi, R.; Miyoshi, N. *Chem. Lett.* **2002**, 4, 245-248.
- 80) Doyle, M. P. ; DeBruyn, D. J.; Kooistra, D. A. *J. Am. Chem. Soc.* **1972**, 94, 3659.
- 81) Nicolaou, K. C. ; Hwang, C.-K.; Nugiel, D. A. *J. Am. Chem. Soc.* **1989**, 111, 4136-4137.
- 82) Izumi, M.; Fukase, K. *Chem. Lett.* **2005**, 34, 594-595.
- 83) a) Watahiki T.; Oriyama, T., *Tetrahedron Lett.* **2002**, 43, 8959-8962. b) Watahiki, T.; Akabane, Y.; Mori, S.; Oriyama, T., *Org. Lett.* **2003**, 5, 3045-3048. c) Iwanami, K.; Oriyama, T., *Chem. Lett.* **2004**, 33, 1324-1325. d) Iwanami, K.; Aoyagi, M.; Oriyama, T., *Tetrahedron Lett.* **2005**, 46, 7487-7490. e) Iwanami, K.; Aoyagi, M.; Oriyama, T., *Tetrahedron Lett.* **2006**, 47, 4741-4744.
- 84) Iwanami K.; Seo, H.; Tobita, Y.; Oriyama, T. *Synthesis*, **2005**, 183-186. b) Iwanami, K.; Yano, K.; Oriyama, T. *Synthesis*, **2005**, 2669-2672., *Chemistry Letters* Vol.36, No.1 (2007), 38-39. (c) Gooßen, L. J.; Linder, C. *Synlett*, **2006**, 3489-3491

- 85) Gellert, B. A.; Kahlcke, N.; Feurer, M.; Roth, S., *Chem. Eur. J.* **2011**, *17*, 12203- 12209.
- 86) **(a)** Gharpure, S. J. and Prasad, J. V. K., *Eur. J. Org. Chem.* **2013**, 2076-2079; **(b)** Gharpure, S. J.; Prasad, J. V. K., *J. Org. Chem.*, **2011**, *76* (24), 10325-10331; Evans, P.A.; Cui, J.; Gharpure, S.J.; Hinkle, R.J. *J. Am. Chem. Soc.* **2003** 11456-11457; Evans, P. A.; Cui, J.; Gharpure, S. J.; Polosukhin, A.; Zhang, H.-R. , *J. Am. Chem. Soc.* **2003** 14702-14703; Lee,T.; Gong, Y.D., *Molecules* **2012**, *17*, 5467-5496; Curran, D. P.; Ko, S. B.; Josien, H. *Angew. Chem., Int. Ed. Engl.* **1996**, *34*, 2683; Evans, P. A.; Cui, J.; Gharpure, S. J, *Org. Lett.* **2003**, 3883-3885; Lim H.S.; Choi Y.L.; Heo J.N., *Org. Lett.* *15*(18), **2013**, 4718-4721.
- 87) Reddy, C.R.; Rao, N.N., *RSC Adv.* **2012**, *2*, 7724-7734;
- 88) Sakai, N.; Nonomura, Y.; Ikeda, R.; Konakahara, T., *Chem. Lett.* **2013**, *42*, 489-491.

CHAPTER 3

- 1) Trost, B. M.; Spagnol, M. D. *J. Chem. Soc., Perkin. Trans. 1* **1995**, *17*, 2083-2096,
- 2) Liu, C.-R.; Li, M.-B.; Yang, C.-F.; Tian S.-K. *Chem. Eur. J.* **2009** , *15* , 793-797
- 3) Yang, C. -F.; Wang, J.-Y.; Tian, S.-K. *Chem. Commun.* **2011**, *47*, 8343–8345
- 4) Zhao, X.; Liu D.; Guo, H; Liu, Y.; Zhang, W. *J. Am. Chem. Soc.* **2011**, *133*, 19354-19357
- 5) Cheng, C.; Sun, J.; Xing, L.; Xu J.; Wang, X.; Hu, Y. *J. Org. Chem.* **2009**, *74*, 5671-5674.
- 6) Li, M.-B; Wang, Y.; Tian, S,-K. *Angew. Chem. Int. Ed.* **2012**, *51*, 2968-2971
- 7) Petroff, O.A.C, Book Review: *Neuroscientist* December **2002**, *8*, 562-573
- 8) Hylin, J. W. *J. Agric. Food Chem.* **1969**, *17* , 492-496
- 9) Borthwick, A. D., *Chem. Rev.* **2012**, *112*, 3641-3716.

- 10) Ager, D. J.; Prakash I. ; Schaad D. R., *Chem. Rev.* **1996**, *96*, 835-875.
- 11) Han, S.-Y.; Kim, Y.-A., *Tetrahedron* **2004**, *60*, 2447-2467
- 12) Michael, J. D.; Richard, F.W. J. *Tetrahedron*, **1997** , *53*, 13905-13914
- 13) Jurczak, J.; Gokpiowski, A. *Chem. Rev.* **1989**. *89*, 149-164
- 14) Myers, A. G.; Zhong, B.; Movassaghi, M.; Kung, D. W.; Lanman, B. A.; Kwon, S., *Tetrahedron Letters* **2000**, *41*, 1359-1362
- 15) Ottenheijm, H. C. J.; Herscheid, J. D. M, *Chem. Rev.* **1986**, *86*, 697-707
- 16) For some recent examples of decarboxylative reaction, see: (a) Knight, J. G.; Ainge, S. W.; Harm, A. M.; Harwood, S. J.; Maughan, H. I.; Armour, D. R.; Hollinshead, D. M.; Jaxa-Chamiec, A. A. *J. Am. Chem. Soc.* **2000**, *122*, 2944-2945. (b) Lalic, G.; Aloise, A. D.; Shair, M. D. *J. Am. Chem. Soc.* **2003**, *125*, 2852-2853. (c) Lou, S.; Westbrook, J. A.; Schaus, S. E. *J. Am. Chem. Soc.* **2004**, *126*, 11440-11441. (d) Trost, B. M.; Xu, J. *J. Am. Chem. Soc.* **2005**, *127*, 17180-17181. (e) Bourgeois, D.; Craig, D.; King, N. P.; Mountford, D. M. *Angew. Chem., Int. Ed.* **2005**, *44*, 618-621. (f) Craig, D.; Grellepois, F. *Org. Lett.* **2005**, *7*, 463-465. (g) Mohr, J. T.; Nishimata, T.; Behenna, D. C.; Stoltz, B. M. *J. Am. Chem. Soc.* **2006**, *128*, 11348-11349. (h) Patil, N. T.; Huo, Z.; Yamamoto, Y. *J. Org. Chem.* **2006**, *71*, 6991-6995. (i) Yeagley, A. A.; Chruma, J. J. *Org. Lett.* **2007**, *9*, 2879-2882. (j) Sim, S. H.; Park, H.-J.; Lee, S. I.; Chung, Y. K. *Org. Lett.* **2008**, *10*, 433-436. (k) Shang, R.; Fu, Y.; Li, J.-B.; Zhang, S.-L.; Guo, Q.-X.; Liu, L. *J. Am. Chem. Soc.* **2009**, *131*, 5738-5739.
- 17) For a review, see: Goossen, L. J.; Rodriguez, N.; Goossen, K. *Angew. Chem., Int. Ed.* **2008**, *47*, 3100-3120.
- 18) (a) Goossen, L. J.; Deng, G.; Levy, L. M. *Science* **2006**, *313*, 662-664. (b) Goossen, L. J.; Rodriguez, N.; Melzer, B.; Linder, C.; Deng, G.; Levy, L. M. *J. Am. Chem. Soc.* **2007**, *129*, 4824-4833. (c) Goossen, L. J.; Rudolphi, F.; Opperl, C.; Rodriguez, N. *Angew. Chem., Int. Ed.* **2008**, *47*, 3043-3045. (d) Goossen, L. J.; Zimmermann, B.; Knauber, T. *Angew. Chem., Int. Ed.* **2008**, *47*, 7103-7106.
- 19) (a) Myers, A. G.; Tanaka, D.; Mannion, M. R. *J. Am. Chem. Soc.* **2002**, *124*, 11250-11251. (b) Tanaka, D.; Myers, A. G. *Org. Lett.* **2004**, *6*, 433-436. (c) Tanaka, D.; Romeril, S. P.; Myers, A. G. *J. Am. Chem. Soc.* **2005**, *127*, 10323-10333.

- 20) (a) Rayabarapu, D. K.; Tunge, J. A. *J. Am. Chem. Soc.* **2005**, *127*, 13510-13511. (b) Waetzig, S. R.; Rayabarapu, D. K.; Weaver, J. D.; Tunge, J. A. *Angew. Chem., Int. Ed.* **2006**, *45*, 4977-4980. (c) Burger, E. C.; Tunge, J. A. *J. Am. Chem. Soc.* **2006**, *128*, 10002-10003. (d) Waetzig, S. R.; Tunge, J. A. *J. Am. Chem. Soc.* **2007**, *129*, 4138-4139. (e) Waetzig, S. R.; Tunge, J. A. *J. Am. Chem. Soc.* **2007**, *129*, 14860-14861. (f) Weaver, J. D.; Tunge, J. A. *Org. Lett.* **2008**, *10*, 4657-4660.
- 21) Hashimoto M.; Eda, Y.; Osanai, Y.; Iwai, T.; Aoki S., *Chem. Lett.* **1986**, 893-896.
- 22) Cid S. B; Miguélez-Arrizado M. J.; Becker B.; Holzapfel W. H.; Vidal-Carou M. C., *Food Microbiology* **2008**, *25*, 269-77.
- 23) Laval,G; Golding B. T., *Synlett.* **2003**, *4*, 542-546
- 24) Bi, H.-P.; Chen, W.-W.; Liang, Y.-M.; Li, C.-J., *Org. Lett.* **2009**, *11*, 3246-3249.
- 25) Yang, D.; Zhao,D.; Mao,L.; Wang,L.; Wang R., *J. Org. Chem.* **2011**, *76*, 6426-6431.
- 26) Das, D.; Richers, T.R.; Ma L.; Seidel, D.; *Org. Lett.* **2011**, *13*, 6584-6587.
- 27) Hu, J.; Zhao, N.; Yang, B.; Wang, G.; Guo, L. N.; Liang, Y. M.; Yang, S. D. *Chem.-Eur. J.* **2011**, *17*, 5516 and 6281.
- 28) Zhang, C.; Seidel, D. *J. Am. Chem. Soc.* **2010**, *132*, 1798-1799.
- 29) (a) Turner. N. *J. Chem. Rev.* **2011**, *111*, 4073-4087 (b) Steiner, R. A.; Kalk, K. H.; Dijkstra, B. W. *PNAS* **2002**, *99*, 16625-16630 (c) Al-Mjeni, F.; Ju, T.; Pochapsky, T.C.; Maroney, M. J. *Biochemistry* **2002**, *41*, 6761-6769 (d) Johnson-Winters, K.; Purpero, V. M.; Kavana, M.; Nelson, T.; Moran, G. R. *Biochemistry* **2003**, *42*, 2072-2080 (e) de Villiers, M.; Veetil, V. P.; Raj H.; de Villiers, J.; Poelarends, G. J. *ACS Chem. Biol.* **2012**, *7*, 618-1628 (f) Paine, T.K.; Zheng, H.; Que, L. *Inorg. Chem.* **2005**, *44*, 474-476 (g) Straganz, G.D.; Nidetzky, B., *J. Am. Chem. Soc.* **2005**, *127*, 12306-12314 (h) Straganz, G. D.; Hofer H.; Steiner, W.; Nidetzky, B. *J. Am. Chem. Soc.* **2004**, *126*, 12202-12203 (i) Sedgwick, B. *Nature Rev. Molecular Cell Biol.* **2004**, *5*, 148-157.
- 30) Casas, J.S.; Castineiras, C.; Condori, F.; Couce, M. D.; Russo, U.; Sínche, A.; Seoane, R.; Sordo, J.; Varela, J. M., *Polyhedron* **2003**, *22*, 53-65.

- 31) Shanbbag, V.M.; Martell, A. E., *J. Am. Chem. Soc.* **1991**, *113*, 6479-6487.
- 32) For recent reviews, see: (a) Nixon, T. D.; Whittlesey, M. K.; Williams, J. M. J. *Dalton Trans.* **2009**, 753-762. (b) Guillena, G.; Ramon, D. J.; Yus, M. *Angew. Chem., Int. Ed.* **2007**, *46*, 2358-2364. (c) Shibahara, F.; Krische, M. *J. Chem. Lett.* **2008**, *37*, 1102-1107.
- 33) For recent reviews, see: (a) Nixon, T. D.; Whittlesey, M. K.; Williams, J. M. J. *Dalton Trans.* **2009**, 753-762. (b) Guillena, G.; Ramon, D. J.; Yus, M. *Angew. Chem., Int. Ed.* **2007**, *46*, 2358-2364. (c) Shibahara, F.; Krische, M. *J. Chem. Lett.* **2008**, *37*, 1102-1107.
- 34) Cho, C. S.; Kim, B. T.; Kim, T. -J.; Shim, S. C. *Tetrahedron Lett.* **2002**, *43*, 7987-7989.
- 35) Taguchi, K.; Nakagawa, H.; Hirabayashi, T.; Sakaguchi, S.; Ishii, Y. *J. Am. Chem. Soc.* **2004**, *126*, 72-73
- 36) Kuwahara, T.; Fukuyama, T.; Ryu I. *Org. Lett.*, **2012**, *14*, 4703-4705
- 37) (a) Yi, C. S.; Lee, D. W. *Organometallics* **2009**, *28*, 4266-4268. (b) Yi, C. S.; Lee, D. W. *Organometallics*, **2010**, *29*, 1883-1885. (c) Kwon, K.-H.; Lee, D. W.; Yi, C. S. *Organometallics*, **2010**, *29*, 5748-5750. (d) Kwon, K.-H.; Lee, D. W.; Yi, C. S. *Angew. Chem., Int. Ed.* **2011**, *50*, 1692-1695.
- 38) (a) Yi, C. S.; Lee, D.-H.; Kwon, K.-H. *Science* **2011**, *333*, 1613-1616 (b) Yi, C. S.; Lee, D.-H.; Kwon, K.-H. *J. Am. Chem. Soc.* **2012**, *134*, 7325-7328 (c) Stoutland, P. O.; Bergman, R. G. *J. Am. Chem. Soc.* **1985**, *107*, 4581-4582. (d) Renkema, K. B.; Kissin, Y. V.; Goldman, A. S. *J. Am. Chem. Soc.* **2003**, *125*, 7770-7771.
- 39) Yi, C. S.; Lee, D. W. *Organometallics* **2009**, *28*, 947-949.
- 40) Singleton method: Singleton DA, Thomas AA. *J. Am. Chem. Soc.* 1995, *117*, 9357-9358; Frantz DE, Singleton DA, Snyder JP. *J. Am. Chem. Soc.* 1997, *119*, 3383-3384; Singleton, D. A.; Schulmeier, B. E. *J. Am. Chem. Soc.* 1999, *121*, 9313-9317; D. A. Singleton ; M. J. Szymanski, *J. Am. Chem. Soc.*, **1999**, *121* (40), 9455-9456; J. S. Hirschi, T. Takeya, C. Hang, and D. A. Singleton, *J. Am. Chem. Soc.* **2009**, *131*, 2397-2403; B. R. Ussing, C. Hang, and D. A. Singleton, *J. Am. Chem. Soc.* **2006**, *128*, 7594-7607; Singleton, D. A.; Hang, C.; Szymanski, M. J.; Meyer, M. P.; Leach, A. G.; Kuwata, K. T.; Chen, J. S.; Greer, A.; Foote, C. S.; Houk, K. N. *J. Am. Chem. Soc.*

- 2003**, *125*, 1319-1328.; Singleton, D. A.; Nowlan, D. T., III; Jahed, N.; Matyjaszewski, K. *Macromolecules* **2003**, *36*, 8609-8616. Singleton, D. A.; Hang, C.; Szymanski, M. J.; Greenwald, E. E. *J. Am. Chem. Soc.* **2003**, *125*, 1176-1177; Saettel, N. J.; Wiest, O.; Singleton, D. A.; Meyer, M. P. *J. Am. Chem. Soc.* **2002**, *124*, 11552-11559.; Singleton, D. A.; Merrigan, S. R.; Kim, B. J.; Beak, P.; Phillips, L. M.; Lee, J. K., *J. Am. Chem. Soc.* **2000**, *122*, 3296-3300; Singleton, D. A.; Merrigan, S. R. *J. Am. Chem. Soc.* **2000**, *122*, 11035-11036; Frantz, D. E.; Singleton, D. A. *J. Am. Chem. Soc.* **2000**, *122*, 3288-3295.
- 41) Melander, L.; Saunders, W. H., Jr. *Reaction Rates of Isotopic Molecules*; Wiley: New York, 1980, pp 95-102.
- 42) Barton, D. H. R.; McCombie, S. W. *J. Chem. Soc., Perkin Trans. 1* **1975**, 1574- 1585
- 43) Similar ruthenium enolate complexes have been observed, see articles for recent reviews, see:(a) Casiraghi, G.; Battistini, L.; Curti, C.; Rassa, G.; Zanardi, F. *Chem. Rev.* **2011**, *111*, 3076-3154. (b) Palomo, C.; Oiarbide, M.; Garcí'a, J. M. *Chem. Soc. Rev.* **2004**, *33*, 65-75. (c) Arya, P.; Qin, H. *Tetrahedron* **2000**, *56*, 917-947. (d) Burkhardt, E. R.; Doney, J. J.; Berman R. G.; Heathcock C. H., *J. Am. Chem. Soc.*, **1987**, *109*, 2022-2039 (e) Rasley, B. T.; Rapta M.; Kulawiec, R. J. *Organometallics*, **1996**, *15*, 2852-2854 , (f) Bartoszewicz, A., Jeżowska, M. M.; Laymand, K.; Möbus, J. ; Martín-Matute, B. , *Eur. J. Inorg. Chem.*, **2012**, *9*, 1517-1530 (g) Hartwig, J. F.; Bergman, R. G.; Andersen, R. A. *J. Am. Chem.Soc.* **1990**, *112*, 5670-5671. (h) Hartwig, J. F.; Bergman, R. G.; Andersen, R. A. *Organometallics* **1991**, *10*, 3326-3344 (i) Tasley, B. T.; Rapta, M.; Kulawiec, R. J. *Organometallics* **1996**, *15*, 2852-2854
- 44) For similar example see (a) Trost, B. M.; Portnoy, M.; Kurihara, H. *J. Am. Chem. Soc.* **1997**, *119*, 836-837
- 45) J. Mendham, R. C. Denney, J. D. Barnes, M. J. K. Thomas, *Vogel's Quantitative Chemical Analysis*, 6th ed., Prentice Hall, New York, 2000.
- 46) T. Michałowski, A. G. Asuero, S. Wybraniec, *J. Chem. Educ.* 2013, *90*, 191-197.
- 47) Weaver, J. D.; Recio III, A.; Grenning, A. J.; Tunge, J. A., *Chem. Rev.* **2011**, *111*, 1846-1913.
- 48) We have not been able to detect any ruthenium enolate species when we monitored a C₆D₆ solution of **258** with acetophenone by VT NMR spectroscopy within the temperature range of 20-80°C.

CHAPTER 4

- 1) Selective reviews bio fuel : (a) van Putten, R.-J.; van der Waal, J. C.; de Jong, E.; Rasrendra, C. B.; Heeres, H. J.; de Vries, J. G. *Chem. Rev.* **2013**, 113, 1499-1597. (b) Alonso, D. M.; Wettstein, S. G.; Dumesic, J. A. *Green Chem.* **2013**, 15, 584-595. (c) Gallezot, P. *Chem. Soc. Rev.* **2012**, 41, 1538-1558. (d) Lange, J.-P.; Van der Heide, E.; Van Buijtenen, J.; Price, R. *ChemSusChem* **2012**, 5, 150-166. (e) Gallezot, P. *Chem. Soc. Rev.* **2012**, 41, 1538-1558. (f) Lange, J.-P.; Van der Heide, E.; Van Buijtenen, J.; Price, R. *ChemSusChem.* **2012**, 5, 150-166.

- 2) a). Lee, W. Y; Park, C. H.; Kim, H.-J.; Kim, S. *J. Org. Chem.* **1994**, 59, 878-884; b) Baumann, K.; Knapp, H.; Strnadt, G.; Schulz, G.; Grassberger, M. A. *Tetrahedron Lett.* **1999**, 40, 7761-7764.

- 3) a) Furimsky, E., *Appl. Catal. A* **2000**, 199, 147-190; b) Ruppert, A. M.; Weinberg, K.; Palkovits, R. *Angew. Chem. Int. Ed.* **2012**, 51, 2564- 2601; *Angew. Chem.* **2012**, 124, 2614-2654; c) Bozell, J. J.; Petersen, G. R. *Green Chem.* **2010**, 12, 539-554; d) Vennestrøm, P. N. R.; Osmundsen, C. M.; Christensen, C. H.; Taarning, E. *Angew. Chem.* **2011**, 123, 10686-10694.

- 4) Clive, D. L. J.; Wang, J. *J. Org. Chem.* **2002**, 67, 1192-1198.

- 5) a) Clemmensen, E. *Ber. Dtsch. Chem. Ges.* **1914**, 47, 681; b) Clemmensen, E. *Chem. Ber.* **1914**, 47, 51, 681-687. (b) Vedejs, E. *Org. React.* **1975**, 22, 401-422.

- 6) a) Kishner, J. J. *Russ. Phys. Chem. Soc.* **1911**, 43, 582; b) Wolff, C. *Justus Liebigs Ann.* **1912**, 394, 86; c) Todd, D. *Org. React.* **1948**, 4, 378; d) Minlon, H. *J. Am. Chem. Soc.* **1949**, 71, 3301

- 7) Marino, J. P.; Rubio, M. B.; Gao, G.; de Dios, A. *J. Am. Chem. Soc.* **2002**, 124, 13398-13399.

- 8) (c) Miyaoka, H.; Kajiwara, Y.; Hara, Y.; Yamada, Y. *J. Org. Chem.* **2001**, 66, 1429-1435.

- 9) Miyaoka, H.; Kajiwara, Y.; Hara, Y.; Yamada, Y., *J. Org. Chem.*, **2001**, 66 (4): 1429-1435.

- 10) Kursanov, D.N.; Parnes, Z.N.; Bassova, G.I.; Loim, N.M.; Zdanovich, V.I., *Tetrahedron*, **1967**, 23, 2235.
- 11) Nishiyama, Y.; Hamanaka, S.; Ogawa, A.; Kambe, N.; Sonoda, N., *J. Org. Chem.*, **1988**, 53, 1326-1329.
- 12) Kawai, A.; Hara, O.; Hamada, Y.; Shiara, T., *Tetrahedron Lett.* **2003**, 44, 6331-6334.
- 13) Lau, C. K.; Dufresne, C.; Belanger, P. C.; Pietre, S.; Scheigetz, J., *J. Org. Chem.* **1986**, 51, 3038-3043.
- 14) Studer, M.; Burkhardt, S.; Indolese, A. F.; Blaser, H.-U. *Chem. Commun.* **2000**, 1327-1328.
- 15) (a) Yi, C. S.; Lee, D.-H.; Kwon, K.-H. *Science* **2011**, 333, 1613-1616 (b) Yi, C. S.; Lee, D.-H.; Kwon, K.-H. *J. Am. Chem. Soc.* **2012**, 134, 7325-7328 (c) Stoutland, P. O.; Bergman, R. G. *J. Am. Chem. Soc.* **1985**, 107, 4581-4582. (d) Renkema, K. B.; Kissin, Y. V.; Goldman, A. S. *J. Am. Chem. Soc.* **2003**, 125, 7770-7771.
- 16) Kim, J.; Lee, D.-H.; Kalutharage, N.; Yi, C. S., *ACS Catal.* **2014**, 4 (11), 3881-3885.
- 17) U- or V-shaped Hammett plots have been interpreted as evidence for dual reaction mechanisms. For leading reports, see: (a) Fuchs, R.; Carlton, D. M. *J. Am. Chem. Soc.* **1963**, 85, 104 (b) Buckley, N.; Oppenheimer, N. J. *J. Org. Chem.* **1996**, 61, 7360-7372; (c) Tanner, D. D.; Koppula, S.; Kandanarachchi, P. *J. Org. Chem.* **1997**, 62, 4210-4215; (d) Ohshiro, H.; Mitsui, K.; Ando, N.; Ohsawa, Y.; Koinuma, W.; Takahashi, H.; Kondo, S. i.; Nabeshima, T.; Yano, Y. *J. Am. Chem. Soc.* **2001**, 123, 2478-2486; (e) Moss, R. A.; Ma, Y.; Sauers, R. R. *J. Am. Chem. Soc.* **2002**, 124, 13968-13969; (f) Zdilla, M. J.; Dexheimer, J. L.; Abu-Omar, M. M. *J. Am. Chem. Soc.* **2007**, 129, 11505-11511.
- 18) **KIE ketone hydrogenation**: Sandoval, C. A.; Ohkuma, T.; Muniz, K.; Noyori, R. *J. Am. Chem. Soc.* **2003**, 125, 13490-13503; Kass, M.; Friedrich, A.; Drees, M.; Schneider, S. *Angew. Chem., Int. Ed.* **2009**, 48, 905-907; Zimmer-De Iuliis, M.; Morris, R. H. *J. Am. Chem. Soc.* **2009**, 131, 11263-11269.
- 19) Examples of normal k_H/k_D : (a) Abis, L.; Sen, A.; Halpern, J. *J. Am. Chem. Soc.* **1978**, 100, 2915-2916; (b) Michelin, R. A.; Faglia, S.; Uguagliati, P. *Inorg. Chem.* **1983**, 22, 1831-1834; (c) Janowicz, A. H.; Bergman, R. G. *J. Am. Chem. Soc.* **1983**, 105, 3929-3939; (d) Moravskiy, A.; Stille, J. K. *J. Am. Chem. Soc.* **1981**, 103, 4182-4186; (e)

- McCarthy, T. J.; Nuzzo, R. G.; Whitesides, G. M. *J. Am. Chem. Soc.* **1981**, 103, 3396-3403. (f) Hackett, M.; Ibers, J. A.; Whitesides, G. M., *J. Am. Chem. Soc.* **1988**, 110, 1436-1448.
- 20) **Inverse primary KIE:** Buchanan, J. M.; Stryker, J. M.; Bergman, R. G. *J. Am. Chem. Soc.* **1986**, 108, 1537-1550; Periana, R. A.; Bergman, R. G. *J. Am. Chem. Soc.* **1986**, 108, 7332-7346; Bullock, R. M.; Headford, C. E. L.; Hennessy, K. M.; Kegley, S. E.; Norton, J. R. *J. Am. Chem. Soc.* **1989**, 111, 3897-3908; Parkin, G.; Bercaw, J. E. *Organometallics* **1989**, 8, 1172-1179; Gould, G. L.; Heinekey, D. M. *J. Am. Chem. Soc.* **1989**, 111, 5502-5504; Wang, C.; Ziller, J. W.; Flood, T. C. *J. Am. Chem. Soc.* **1995**, 117, 1647-1648; Howart, O. W.; McAteer, C. H.; Moore, P.; Morris, G. E. *J. Chem. Soc., Dalton Trans.* **1984**, 1171-1180; Jones, W. D.; Feher, F. J. *J. Am. Chem. Soc.* **1985**, 107, 620-626; Wick, D. D.; Reynolds, K. A.; Jones, W. D. *J. Am. Chem. Soc.* **1999**, 121, 3974-3983; Jensen, M. P.; Wick, D. D.; Reinartz, S.; White, P. S.; Templeton, J. L.; Goldberg, K. I. *J. Am. Chem. Soc.* **2003**, 125, 8614-8624; Bullock, R. M.; Headford, C. E. L.; Kegley, S. E.; Norton, J. R. *J. Am. Chem. Soc.* **1985**, 107, 727-729; Bengali, A. A.; Amdtsen, B. A.; Burger, P. M.; Schultz, R. H.; Weiller, B. H.; Kyle, K. R.; Moore, C. B.; Bergman, R. G. *Pure Appl. Chem.* **1995**, 67, 281-288; Jones, W. D.; Hessell, E. T. *J. Am. Chem. Soc.* **1992**, 114, 6087-6095; (f) Stahl, S. S.; Labinger, J. A.; Bercaw, J. E. *J. Am. Chem. Soc.* **1996**, 118, 5961-5976. (g) Wang, C.; Ziller, J. W.; Flood, T. C. *J. Am. Chem. Soc.* **1995**, 117, 1647-1648.
- 21) Janowicz, A. H.; Bergman, R. G. *J. Am. Chem. Soc.* **1982**, 104, 352-354.
- 22) Hanna, T. A.; Lobkovsky, E.; Chirik, P. *J. Inorg. Chem.* **2007**, 46, 2359.
- 23) See Chapter 3: reference number 40
- 24) (a) Macklin, T.; Snieckus V. in *Handbook of C-H Transformations* (Ed.: G. Dyker), Wiley-VCH, Weinheim, 2005, pp.106-119; (b) Clayden J., in *the Chemistry of Organolithium Compounds* (Eds.: Z. Rappoport, I. Marek), Wiley, New York, 2004, pp. 497-648; (c) Anctil, E. J.-G.; Snieckus V., in *Metal-Catalyzed Cross-Coupling Reactions* (Eds.: A. de Meijere, F. Diederich), Wiley-VCH, Weinheim, 2004, pp. 761-814; (d) Whisler, M. C.; MacNeil S.; Snieckus, V.; Beak, P. *Angew. Chem.* **2004**, 116, 2256-2276; *Angew. Chem. Int. Ed.* **2004**, 43, 2206-2225; (e) Hartung, C. G.; Snieckus V. in *Modern Arene Chemistry* (Ed.: D. Astruc), Wiley-VCH, Weinheim, **2002**, pp. 330-367; Snieckus, V., *Chem. Rev.* **1990**, 90, 879-933.
- 25) Shvo catalyst : (a) Casey C.P.; Beetner S.E.; Johnson J.B., *J. Am. Chem. Soc.* **2008**, 130, 2285-2295, (b) Yuki, Y.; Takahashi, K.; Tanaka, Y.; Nozaki, K., *J. Am. Chem. Soc.* 2013, 135, 17393-17400; (c) Casey, C. P.; Johnson, J. B.; Singer, S. W.; Cui, Q.

- J. Am. Chem. Soc.* **2005**, 127, 3100-3109; (d) Casey C.P.; Johnson J. B., *J. Am. Chem. Soc.*, **2005**, 127 (6), 1883-1894.
- 26) (e) *Bifunctional Molecular Catalysis*: (a) Grotjahn, D. *Top. Catal.* **2010**, 53, 1009–1014, (b) Kuwata, S.; Ikariya, T. *Dalton Trans.* **2010**, 39, 2984-2992, (c) Ikariya, T.; Gridnev, I. *Top. Catal.* **2010**, 53, 894-901, (d) Milstein, D. *Top. Catal.* **2010**, 53, 915-923; (e) Ikariya, T.; Shibasaki, M., Eds.; Springer: Berlin/Heidelberg, **2011**; Vol. 37, (f) Askevold, B.; Roesky, H. W.; Schneider, S. *Chem. Cat. Chem* **2012**, 4, 307–320.;(g) Muniz, K. *Angew. Chem., Int. Ed.* **2005**, 44, 6622–6627. (h) Ito, M.; Ikariya, T. *J. Synth. Org. Chem. Jpn.* **2008**, 66, 1042–1048. ; (i) Grützmacher, H. *Angew. Chem., Int. Ed.* **2008**, 47, 1814-1818; (j) Ikariya, T.; Murata, K.; Noyori, R. *Org. Biomol. Chem.* **2006**, 4, 393-406.
- 28) Tan, X.; Wang, Y.; Liu, Y.; Wang, F.; Shi, L.; Lee, K.-H.; Lin, Z.; Lv, H.; Zhang, X., *Org. Lett.* **2015**, 17, 454-457.
- 29) (a) Raebiger, J. W.; Miedaner, A.; Curtis, C. J.; Miller, S. M.; Anderson, O. P.; DuBois, D. L. *J. Am. Chem. Soc.* **2004**, 126, 5502. (b) Miedaner, A.; Raebiger, J. W.; Curtis, C. J.; Miller, S. M.; DuBois, D. L. *Organometallics* **2004**, 23, 2670. (c) Raebiger, J. W.; DuBois, D. L. *Organometallics* **2005**, 24, 110. (d) Guan, H.; Iimura, M.; Magee, M. P.; Norton, J. R.; Janak, K. E. *Organometallics* **2003**, 22, 4084. (e) Guan, H. R.; Iimura, M.; Magee, M. P.; Norton, J. R.; Zhu, G. *J. Am. Chem. Soc.* **2005**, 127, 7805. (f) Roberts, J.A.S.; Appel, A.M.; DuBois, D.L.; Bullock, R.M. *J. Am. Chem. Soc.* **2011**, 133, 14604–14613 (g) *J. Am. Chem. Soc.* **2009**, 131, 2794-2795. (h) *J. Am. Chem. Soc.* **2012**, 134, 15743-15757
- 30) Braun, R. D. *Introduction to Chemical Analysis*; McGraw-Hill; New York, 1982, pp. 197-199; Patterson, G. S. *J. Chem. Educ.*, **1999**, 76, 395–398.
- 31) **Outer-sphere Mechanisms**: (a) Noyori, R.; Ohkuma, T. *Angew. Chem., Int. Ed.* **2001**, 40, 40-73 (b) Ma, G. B.; McDonald, R.; Ferguson, M.; Cavell, R. G.; Patrick, B. O.; James, B. R.; Hu, T. Q. *Organometallics* **2007**, 26, 846-854;(c) Baratta, W.; Ballico, M.; Esposito, G.; Rigo, P. *Chem. Eur. J.* **2008**, 14, 5588-5595 (d) Sandoval, C. A.; Shi, Q. X.; Liu, S. S.; Noyori, R. *Chem. Asian J.* **2009**, 4, 1221-1224; Ito, M.; Hirakawa, M.; Murata, K.; Ikariya, T. *Organometallics* **2001**, 20, 379-381.
- 32) O, W.W. N.; Lough, A.J. ; Morris R. H., *Organometallics* **2012**, 31 (6), 2152–2165.
- 33) Casey, C. P.; Singer, S.; Powell, D. R.; Hayashi, R. K.; Kavana, M. *J. Am. Chem. Soc.* **2001**, 123, 1090

34) Free benzene was observed at δ 7.26 ppm in ^1H NMR and GC-MS analyses

CHAPTER 5:

- 1) a) Feuer, H.; Hooz, J., in *The Chemistry of Ether Linkage* (Ed.: S. Patai), Interscience, London, **1967**; b) Cakmak, M.; Mayer, P.; Trauner, D., *Nat. Chem.* **2011**, 3, 543-545.
- 2) a). Trost, B. M., *Science* **1991**, 254, 1471-1477; b) Sanderson, K., *Nature* **2011**, 474, S12-S14; c) Gunanathan, C.; Ben-David, Y.; Milstein, D., *Science* **2007**, 317, 790-792.
- 3) a) Schmoyer, L. F.; Case, L. C., *Nature* **1960**, 187, 592; b) Young, P. C.; Schopf, N. A.; Lee, A.-L., *Chem. Commun.* **2013**, 49, 4262-4264.
- 4) T. W. Greene, P. G. M. Wuts, in *Protective Groups in Organic Synthesis*, 3rd ed., Wiley-Interscience, New York, **1999**, Chap. 2
- 5) For selected examples, see: a) Hatakeyama, S.; Mori, H.; Kitano, K.; Yamada, H.; Nishizawa, M., *Tetrahedron Lett.* **1994**, 35, 4367-4370; b) Komatsu, N.; Ishida, J.-Y.; Suzuki, H., *Tetrahedron Lett.* **1997**, 38, 7219-7222; c) Jiang, X.; Bajwa, J. S.; Slade, J.; Prasad, K.; Repic, O.; Blacklock, T. J., *Tetrahedron Lett.* **2002**, 43, 9225-9227; d) Yang, W.-C.; Lu, X.-A.; Kulkarnia, S. S.; Hung, S.-C., *Tetrahedron Lett.* **2003**, 44, 7837-7840; e) Iwanami, K.; Seo, H.; Tobita, Y.; Oriyama, T., *Synthesis* **2005**, 183-186.
- 6) M. Wada, S. Nagayama, K. Mizutani, R. Hiroi, N. Miyoshi, *Chem. Lett.* **2002**, 248-249.
- 7) K. Iwanami, K. Yano, T. Oriyama, *Chem. Lett.* **2007**, 36, 38-39.
- 8) Kim, J.; Lee, D.-H.; Kalutharage, N.; Yi, C. S. *ACS Catal.* **2014**, 4, 3881-3885.
- 9) Similar Hammett values: (a) Nakagawa, Y.; Mizuno, N. *Inorg. Chem.* **2007**, 46, 1727-1736. (b) Fedorov, A.; Chen, P. *Organometallics* **2010**, 29, 2994-3000. (c) Chakraborty, S.; Blacque, O.; Fox, T.; Berke, H. *ACS Catal.* **2013**, 3, 2208-2217. (d) Ball, L. T.; Lloyd-Jones, G. C.; Russell, C. A. *J. Am. Chem. Soc.* **2014**, 136, 254-264.
- 10) Selected recent examples: (a) Gómez-Gallego, M.; Sierra, M. A. *Chem. Rev.* **2011**, 111, 4857-4963. (b) Gregory, M. C.; Denisov, I. G.; Grinkova, Y. V.; Khatri, Y.; Sligar, S. G. *J. Am. Chem. Soc.* **2013**, 135, 16245-16247. (c) Waugh, M. W.; Marsh, E. N. G.

- Biochemistry* **2014**, 53, 5537-5543. Solvent KIE: (a) *J. Am. Chem. Soc.* **2001**, 123, 10889-10898 (b) *Environ. Sci. Technol.* **1995**, 29, 1646-1654 (c) Chang, W.; Sun, C.; Pang, X.; Sheng, H.; Li, Y.; Ji, H.; Song, W.; Chen, C.; Ma, W.; Zhao, J., *Angew. Chem. Int. Ed.*, **2015**, 54, 2052 -2056 (d) S. A. Adediran, S. A. Deraniyagala, Yang Xu, and R. F. Pratt, *Biochemistry* **1996**, 35, 3604-3613 (e) Karsten, W. E., Lai, C.-J., & Cook, P. F. *J. Am. Chem. Soc.* **1995**, 117, 5914-5918 (f) Koo, I. S., Lee, J. S., Yang, K., Kang, K., and Lee, I., *Bull. Korean Chem. Soc.* **1999**, 20, 573.
- 11) (a) Sieffert, N.; Buehl, M. *J. Am. Chem. Soc.* **2010**, 132, 8056-8070. (b) Denichoux, A.; Fukuyama, T.; Doi, T.; Horiguchi, J.; Ryu, I. *Org. Lett.* **2010**, 12, 1-3. (c) Fogler, E.; Balaraman, E.; Ben-David, Y.; Leitun, G.; Shimon, L. J. W.; Milstein, D. *Organometallics* **2011**, 30, 3826-3833. (d) Kang, B.; Fu, Z.; Hong, S. H. *J. Am. Chem. Soc.* **2013**, 135, 11704-11707. (e) Tseng, K.-N. T.; Kampf, J. W.; Szymczak, N. K. *Organometallics* **2013**, 32, 2046-2049. (f) Pinggen, D.; Lutz, M.; Vogt, D. *Organometallics* **2014**, 33, 1623-1629.

CHAPTER 6:

- 1) Liu, P. N.; Ju, K. D.; Lau, C. P., *Adv. Syn. & Cat.* **2011**, 353(2+3), 275-280.
- 2) Genna D. T.; Posner G. H., *Org. Lett.* **2011**, 13, 5358-5361.
- 3) Sheng W. B.; Jiang Q.; Luo W.-P.; Guo C., *J. Org. Chem.* **2013**, 78, 5691-5693.
- 4) Kuwahara T.; Fukuyama T.; Ryu I., *Org. Lett.* **2012**, 14, 4703-4705.
- 5) Ajoy K. ; Erich N.; Guy T. G. ; Philippe R., *J. Am. Chem. Soc.* **2009**, 131 (49), 17746-17747.
- 6) Corrie, J. E. T. *Tetrahedron* **1998**, 54, 5407-5416.
- 7) Babu S. A.; Yasuda M.; Baba A., *Org. Lett.* **2007** 9 (3), 405-408.
- 8) Pennell, M. N.; Turner, P. G.; Sheppard, T. D., *Chem. Eur. J.* **2012**, 18: 4748-4758.
- 9) Chidara, V. K.; Du, G. *Organometallics* **2013**, 32, 5034-5037.

- 10) Shang, J.-Y., Li, F., Bai, X.-F., Jiang, J.-X., Yang, K.-F., Lai, G.-Q. ; Xu, L.-W. , *Eur. J. Org. Chem.* **2012**: 02809–2815.
- 11) Muratake, H.; Natsume, M.; Nakai, H. *Tetrahedron* **2004**, 60(51), 11783-11803.
- 12) Cerichelli, G.; Cerritelli, S.; Chiarini, M.; De Maria, P.; Fontana, A., *Chem. –Euro. J.* **2002**, 8(22), 5204-5210.
- 13) Taniguchi, K.; Hattori, K.; Tsubaki, K.; Okitsu, O.; Tabuchi, S. *PCT Int. Appl.* **1997**, WO 9703973 A1 19970206.
- 14) Gary A. G.; Daniel E. P., *Org. Lett.* **2008**, 10, 1795-1798.
- 15) Corrie, J. E. T. *Tetrahedron* **1998**, 54, 5407-5416.
- 16) Molander, G. A.; Jean-Gerard, L. *J. Org. Chem.* **2009**, 74(3), 1297-1303.
- 17) Hsieh J.-C.; Chen Y.-C.; An-Yi Cheng A.-Y.; Tseng H.-C., *Org. Lett.* **2012**, 1282-1285.
- 18) Ding, B.; Zhang, Z.; Liu, Y.; Sugiya, M.; Imamoto, T.; Zhang, W. *Org. Lett.* **2013**, 15, 3690-3693.
- 19) Colbon, P.; Ruan, J.; Purdie, M.; Xiao, J. *Org. Lett.*, **2010**, 12, 3670-3673.
- 20) Sharma, K. S.; Taneja, K. L.; Mukherji, S. M. *Ind. J. Chem. Section B*: **1982**, 21B, 572-573.
- 21) Kose, O.; Saito, S., *Org. Biool. Chem.* **2010**, 8, 896-900.
- 22) Boivin, R. P.; Luu-The, V.; Lachance, R.; Labrie, F.; Poirier, D. *J. Med. Chem.* **2000**, 43, 4465-4478.
- 23) Sharma, A.J; Kumar, V.; Sinha, A. K, *Adv. Synth. Cata.* **2006**, 348, 354-360.
- 24) Mattson, M. N.; Rapoport, H. *J. Org. Chem.* **1996**, 61, 6071-6074.

- 25) Genna D. T.; Posner, G. H. *Org. Lett.* **2011**, *13*, 5358-5361.
- 26) Vellakkaran, M.; Andappan, M. M. S.; Kommu, N. *Eur. J. Org. Chem.* **2012**, 4694-4698.
- 27) Samanta, S.; Samanta, S.; Mishra, B. K.; Pace, T. C. S.; Sathyamurthy, N.; Bohne, C.; Moorthy, J. N. *J. Org. Chem.* **2006**, *71*, 4453-4459.
- 28) Bugarin, A.; Connell, B. T. *Chem. Commun.* **2011**, *47*, 7218-7220.
- 29) Poisson, T.; Dalla, V.; Marsais, F.; Dupas, G.; Oudeyer, S.; Levacher, V. *Angew. Chem., Int. Ed.* **2007**, *46*, 7090-7093.
- 30) Kosal, A. D.; Ashfeld, B. L. *Org. Lett.* **2010**, *12*, 44-47.
- 31) Kuwajima, I.; Nakamura, E.; Shimizu, M. *J. Am. Chem. Soc.* **1982**, *104*, 1025.
- 32) Noyori, R.; Nishida, I.; Sakata, J. *J. Am. Chem. Soc.* **1983**, *105*, 1598-1608.
- 33) Cho, C. S.; Kim, B. T.; Lee, M. J.; Kim, T.-J.; Shim, S. C. *Angew. Chem. Int. Ed.* **2001**, *40*, 958-960.
- 34) Lipshutz, B. H.; Huang, S.; Leong, W. W. Y.; Zhong, G.; Isley, N. A. *J. Am. Chem. Soc.* **2012**, *134*, 19985-19988.
- 35) Beletskiy, E. V.; Sudheer, C.; Douglas, C. J. *J. Org. Chem.* **2012**, *77*, 5884-5893.
- 36) Trost, B. M.; Xu, J.; Schmidt, T. *J. Am. Chem. Soc.* **2009**, *131*, 18343-18357.
- 37) Kulasekharan, R.; Maddipatla, M. V. S. N.; Parthasarathy, A.; Ramamurthy, V. *J. Org. Chem.* **2013**, *78*, 942-949.
- 38) Hussain, Z.; Hopf, H.; Pohl, L.; Oeser, T.; Fischer, A. K.; Jones, P. G. *Eur. J. Org. Chem.* **2006**, 5555-5569.

- 39) Putignano, E.; Bossi, G.; Rigo, P.; Baratta, W. *Organometallics* **2012**, *31*, 1133-1142.
- 40) Kamal, A.; Qureshi, A.; Ali, A. *Tetrahedron* **1963**, *19*, 513-520.
- 41) Matsuda, T.; Makino, M.; Murakami, M. *Org. Lett.* **2004**, *6*, 1257-1259.
- 42) Yasukawa, T.; Miyamura, H.; Kobayashi, S. *J. Am. Chem. Soc.* **2012**, *134*, 16963-16966.
- 43) Malosh, C. F.; Ready, J. M. *J. Am. Chem. Soc.* **2004**, *126*, 10240-10241.
- 44) Inamoto, K.; Nozawa, K.; Yonemto, M.; Kondo, Y., *Chem. Comm.* **2011**, 47(42), 11775-11777.
- 45) Vickery, E. H.; Pahler, L. F.; Eisenbraun E. J., *J. Org. Chem.* **1979**, *44*(24), 4444-4446.
- 46) Furrow, M. E.; Myers, A.G. *J. Am. Chem. Soc.* **2004**, *126* (17), 5436-5445.
- 47) Yang, D. S.; Fu H., *Chem. Eur J.* **2010**, *16*(8), 2366-2370.
- 48) Brunel, J. M., *Tetrahedron*, **2007**, *63*(18), 3899-3906.
- 49) Tanaka, N.; Goto, R.; Ito, R.; Hayakawa, M.; Ogawa, T.; Fujimoto, K., *Chem. Pharm. Bull.* **1998**, *46*(4), 639-646.
- 50) Suzuki, Y.; Hiraoka, S.; Yokoyama, A.; Yokozawa, T., *Macromolecules* **2003**, *36* (13), 4756-4765
- 51) Hisaki, I., *J. Org. Chem.* **2005**, *70*(5), 1853-1864.
- 52) Kiren, S; Padwa, A. *J. Org. Chem.* **2009** *74* (20), 7781-7789.
- 53) Venugopal K.; Kumar, R.; Gopidas K. R. *Tetrahedron Lett.* **2011**, *52*(24), 3102-3105.

- 54) Sloan, M. E.; Staubitz, A., Lee, K.; Manners, I. *Eur. J. Org. Chem.* **2011**, 672-675.
- 55) Krueger, T.; Vorndran, K.; Linker, T. *Eur. J. Chem.* **2009**, *15*, 12082-12091.
- 56) Wang, B.; Sun, H.-X.; Sun, Z.-H., *Eur. J. Org. Chem.* **2009**, 3688-3692.
- 57) (a) Yadav, J. S.; Reddy, P. S.; Joshi, B. V. *Tetrahedron* **1988**, *44*, 7243-7254. (b) Hillier, J. L.; Fletcher, T.J.; Solum, M. S.; Pugmire, R. J., *Ind. Eng. Chem. Res.* **2013**, *52*, 15522-15532.
- 58) Liu, G.-B.; Zhao, H.-Y.; Zhu, J.-D.; He, H.-J.; Yang, H.-J.; Thiemann, T.; Tashiro H.; Tashiro, M., *Syn. Comm.* **2008**, *38*(10), 1651-1661.
- 59) Lee, D.-H., Kwon, K.-H., Yi, C. S., *J. Am. Chem. Soc.* **2012**, *134* (17), 7325-7328 .
- 60) Leogane, O.; Lebel, H., *Angew. Chem. Int. Ed.* **2008**, *47*: 350-352.
- 61) McDonald, C. E.; Ramsey, J. R.; Sampsell, D. G.; Anderson, L. A.; Krebs, J. E.; Smith, S. N., *Tetrahedron* **2013**, *69*(14), 2947-2953.
- 62) Murray, I. A.; Lewendon, A.; Williams, J. A.; Cullis, P. M.; Shaw, William V.; Leslie, A. G. W. , *Biochemistry* **1991**, *30*(15), 3763-3770
- 63) Prinz, H.; Wiegrebe, W.; Müller, K., *J. Org. Chem.* **1996** *61* (8), 2853-2856
- 64) Dimitriadis, E.; Massy-Westropp R. A. *Aust. J. Chem.* **1984**, *37*, 619-627.
- 65) Yu, J.-L.; Wang, H.; Zou, K.-F.; Zhang, J.-R.; Gao, X.; Zhang, D.-W.; Li, Z.-T. *Tetrahedron* **2013**, *69*, 310-315.
- 66) Molander, G. A.; Canturk, B. *Org. Lett.* **2008**, *10*, 2135-2138.
- 67) Burke, C. P.; Haq, N.; Boger, D. L, *J. Am. Chem. Soc.* **2010**, *132*, 2157-2159.
- 68) Joseph, M.; Jacobsen, E. N. *J. Am. Chem. Soc.* **2001**, *123*, 2687-2688.

- 69) Chakraborty, T.K.; *Tetrahedron* **2003**, 59(46), 9127-9135
- 70) Shah, S. T. A.; Singh, P. S.; Guiry J. *J. Org. Chem.* **2009**, 74, 2179-2182.
- 71) Molander, G. A.; Canturk, B. *Org. Lett.* **2008**, 10, 2135
- 72) Radhakrishnan, S.; Franken, J.; Martens, J. A. *Green Chem.* **2012**, 14, 1475-1479
- 73) Sassaman, M. B.; Kotian, K. D.; Prakash, G. K. S.; Olah, G. A. *J. Org. Chem.* **1987**, 52, 4314-4319.
- 74) Wang, H. *Chinese J. Chem.* **2011**, 29, 1180-1184.
- 75) Sharma, G. V. M.; *Org. Prep. Proced. Int.* **2004**, 36(6), 581-586
- 76) Zaccheria, F.; Psaro, R.; Ravasio, N. *Tetrahedron Lett.* **2009**, 50, 5221-5224.
- 77) Talluri, S. K.; Sudalai, A. *Org. Lett.* **2005**, 7, 855-857.
- 78) Davies, T. E.; Kean, J. R.; Apperley, D. C.; Taylor, S. H.; Graham, A. E. *ACS Sust. Chem. Eng.* **2014**, 2, 860-866.
- 79) Yadav, J. S.; Meshram, H. M.; Reddy, G. S.; Sumithra, G. *Tetrahedron Lett.* **1998**, 39, 3043-3046.
- 80) Shen, Z.; Sheng, L.; Zhang, X.; Mo, W.; Hu, B.; Sun, N.; Hu, X. *Tetrahedron Lett.* **2013**, 54, 1579-1583.
- 81) Huang, H.; Nelson, C. G.; Taber, D. F. *Tetrahedron Lett.* **2010**, 51, 3545-3546.
- 82) Kim, J.; Lee, D.-H.; Kalutharage, N.; Yi, C. S. *ACS Catal.* **2014**, 4, 3881-3885.
- 83) Shintou, T.; Mukaiyama, T. *J. Am. Chem. Soc.* **2004**, 126, 7359-7367.
- 84) Blank, H.U.; Pfeleiderer, W. *Justus Liebigs Ann. Chem.* **1970**, 742, 1-15.

- 85) Piazza, P. V.; Vallee, M.; Felpin, F.-X.; Revest, J.-M.; Fabre, S. *PCT Int. Appl.* **2014**, WO2014083068 A1 20140605.